

Computational Studies on Interstellar Molecular Species: From Formation to Detection

A Thesis
Submitted for the Degree of
DOCTOR OF PHILOSOPHY
In the Faculty of Science

by

Emmanuel Edet Etim



Department of Inorganic and Physical Chemistry
INDIAN INSTITUTE OF SCIENCE
BANGALORE - 560012, INDIA

July, 2016

DEDICATED TO THE ALMIGHTY GOD

Declaration

I hereby declare that the work presented in this Thesis entitled "*Computational Studies on Interstellar Molecular Species: From Formation to Detection*" has been carried out by me at the Department of Inorganic and Physical Chemistry, Indian Institute of Science Bangalore - 560012, India, under the supervision of Professor E. Arunan.

Date

Emmanuel Edet Etim

Certificate

I hereby certify that the work presented in this Thesis entitled **"Computational Studies on Interstellar Molecular Species: From Formation to Detection"** has been carried out by Mr. Emmanuel Edet Etim at the Department of Inorganic and Physical Chemistry, Indian Institute of Science Bangalore - 560012, India, under my supervision.

Date

Prof. E. Arunan
(Research Supervisor)

Acknowledgments

I am not one of the self-made people in the world. I am who I am because of God and the contributions of individuals, institutions and organizations that He has brought my way. It is almost an impossible task to adequately acknowledge, appreciate and thank to the right measure all the contributions, efforts, help and assistance of individuals, institutions and organizations that have led to the successful completion of my PhD program. Be it as it may, I want to sincerely thank and appreciate everyone that has contributed in one way or the other for the successful completion of this course. I cannot thank you enough but I remain indebted to you all. I want to specifically thank my Thesis supervisor, Prof. E. Arunan for all his contributions, the Indian Institute of Science, Bangalore for the research fellowship and the Royal Society of Chemistry, UK for travel grant. For the time, energy and resources of individuals, institutions and organizations, I cannot pay you back. I pray may the almighty God reward you all abundantly beyond what you can ever imagined. I love you all. Thank you and God bless.

Emmanuel E. Etim

Table of Contents

Synopsis	i
List of Tables	v
List of Figures	xi

CHAPTER 1: INTRODUCTION

1.0 In the Beginning	2
1.1 The Interstellar Medium	3
1.2 Interstellar Molecular Species	4
1.3 Molecular Spectroscopy: An Indispensable Tool in Interstellar Chemistry	6
1.3.1. Rotational Spectroscopy in Interstellar Chemistry	7
1.3.2 Vibrational Spectroscopy in Interstellar Chemistry	9
1.3.3 Electronic Spectroscopy in Interstellar Chemistry	10
1.4 Formation of Interstellar Molecules	10
1.5. Hydrogen Bonding	12
1.6 Definition of Terms	12
1.6.1 Standard Enthalpy of formation	12
1.6.2 Column Density, Column Amount or Column Abundance, N	12
1.6.3 Fractional or Abundance Ratio	12
1.6.4 Atomization Energy	13
1.6.5 Electron Affinity	13
1.6.6 Proton Affinity	13
1.6.7 Ionization Potential	13
1.6.8 Dipole moment	13
1.7 Present Investigations	13
1.8 References	13

Chapter 2: METHODOLOGY

2.0 Introduction: Computational Chemistry in Interstellar Chemistry	17
2.1 Gaussian Software	17
2.2 Electronic Structure Methods	17
2.2.1 Semi-empirical Methods	18
2.2.2 Ab Initio Methods	18
2.2.3 Density Functional Theory (DFT)	18
2.3 Compound Methods	19
2.4 Basis Sets	20

2.4.1 Minimal Basis Sets	20
2.4.2 Split Valence Basis Sets	20
2.4.3 Correlation-Consistent Basis Set	21
2.5 Basis Set Superposition Error (BSSE)	21
2.6 Major Calculations Using Gaussian Software	21
2.6.1 Geometry Optimization	22
2.6.2 Frequency Calculation	22
2.6.3 Stability Check	22
2.7 Atoms in Molecule Theory (AIM)	23
2.7.2 Types of Critical Points	23
2.8 Pulsed Nozzle Fourier Transform Microwave (PN-FTMW) Spectrometer	24
2.9 Summary	24
2.10 References	24

Chapter 3: INTERSTELLAR ISOMERS: ENERGY, STABILITY AND ABUNDANCE (ESA) RELATIONSHIP AMONG INTERSTELLAR MOLECULES

Setting the stage	27
3.0 Introduction	28
3.1 Computational Methods	29
3.1.1 Atomization energies and enthalpy of formation	30
3.2 Result and Discussion	31
3.2.1 Isomers with 3 atoms	32
3.2.2 Isomers with 4 atoms	34
3.2.3 Isomers with 5 atoms	36
3.2.4 Isomers with 6 atoms	38
3.2.5 Isomers with 7 atoms	40
3.2.6 Isomers with 8 atoms	42
3.2.7 Isomers with 9 atoms	45
3.2.8 Isomers with 10 atoms	47
3.2.9 Isomers with 11 atoms	49
3.2.10 Isomers with 12 atoms	51
3.3 Immediate Consequences of ESA Relationship	53
3.3.1 Where are Cyclic Interstellar Molecules?	54
3.3.2 What are the possible candidates for astronomical observation?	54
3.3.3 Why are more Interstellar Cyanides than isocyanides?	55
3.4 ESA Relationship Summary	55
3.5 Other Applications of the ESA Relationship	56
3.6 Is ESA Relationship the Tool in Searching for Interstellar Heterocycles?	56
3.6.1 Introduction	56
3.6.2 Computational details	57

3.6.3 Results and Discussion	57
3.7 Summary on the Searches for Interstellar Heterocycles with ESA Relationship as the Tool	68
3.8. C₅H₉N Isomers: Pointers to Possible Branched Chain Interstellar Molecules	69
3.8.1 Introduction	69
3.8.2 Computational Details	71
3.8.3 Results and Discussion	71
3.8.4 Summary on C ₅ H ₉ N Isomers ad Pointers to Possible Branched Chain Interstellar Molecules	75
3.9 Is C-C-O Bonding Backbone Truly Elusive?	75
3.9.1 Introduction	75
3.9.2 Computational methods	76
3.9.3 Results and Discussion	76
3.9.4 Summary on C-C-O Bonding Backbone	82
3.10 Partition Function And Astronomical Observation Of Molecules: Is There A Link?	82
3.10.1 Introduction	82
3.10.2 Methodology	83
3.10.3 Results and Discussion	85
3.10.4 Summar on Partition Function and Astronomical Observation Of Molecules	95
3.11 ESA Relationship and Other related Studies	96
3.12 Conclusions on Interstellar Isomers: Energy, Stability and Abundance (ESA) Relationship among Interstellar Molecules	97
3.13 References	97

Chapter 4: INTERSTELLAR HYDROGEN BONDING: DETECTING WEAKLY BOUND COMPLEXES IN SPACE

Preamble	103
4.0 Introduction	104
4.1 Computational details	105
4.2 Result and Discussion	105
4.2.1 Deviations from thermodynamically controlled processes	106
4.2.2 Delayed observation of the most stable isomers	108
4. 2. 3 Unsuccessful observations: Amino acids	110
4. 2. 4 What could be searched for? Ketenes!!!	111
4.2.5: Interstellar Aldehydes and their Corresponding Reduced Alcohols: Interstellar Propanol?	113
4.2.6 Detecting Weakly Bound complexes in the ISM?	114

4.2 7. Summary on Interstellar Hydrogen Bonding	115
4. 3 Other Aspect of Interstellar Hydrogen Bonding	116

4.4 Interstellar chemistry of sulphur and oxygen containing species: S/O abundance ratio, interstellar hydrogen bonding and detectable analogues	116
4.4.1 Introduction	116
4.4.2 Computational details	118
4.4.3 Results and discussion	118
4.4.4 Summary on Interstellar Sulphur and Oxygen Containing Species:	124
4.5 Conclusions on Interstellar Hydrogen Bonding: Detecting Weakly Bound Complexes in Space	125
4.6 References	125
4.7 Supporting Information	129

Chapter 5: LINEAR INTERSTELLAR CARBON CHAINS: THE DOMINANT THEME IN INTERSTELLAR CHEMISTRY

Setting the stage	170
Accurate Rotational Constants for linear Interstellar Carbon Chains: Achieving Experimental Accuracy	171
5.0 Introduction	171
5.1 Methodology	173
5.2 Results and Discussion	173
5.2.1 HC_{2n+1}N linear carbon chains	174
5.2.2 DC_{2n+1}N linear carbon chains	176
5.2.3 HC_{2n}N linear chains	177
5.2.4 HC_{2n}NC linear carbon chains	179
5.2.5 $\text{CH}_3(\text{C}\equiv\text{C})_n\text{CN}$ Linear Carbon Chains	180
5.2.6 C_nO , C_nS and HC_nS Interstellar Linear Carbon Chains	181
5.2.7 C_{2n}H^+ and C_nN^+ Linear Carbon Chains	188
5.2.8 C_nH and C_nN Linear Carbon Chains	190
5.2.9 C_nSi and $\text{CH}_3(\text{CC})_n\text{H}$ Linear Carbon Chains	194
5.3 Astrophysical Implications: Towards 'U' Lines Reduction	198
5.4 Summary on Accurate Rotational Constants for linear Interstellar Carbon Chains	202
Linear Interstellar Carbon Chains: Is Thermodynamics the key?	203
5. 5 Introduction	203
5.6 Computational Details	204
5.7 Results and Discussion	204
5.7.1 C_n Chains	204
5.7.2 C_nO Chains	205

5.7.3 C _n S Chains	207
5.7.4 C _n N Chains	208
5.7.5 C _n Si Chains	209
5.7.6 HC _n N Chains	210
5.7.7 C _n H Chains	211
5.7.8 C _n P Chains	212
5.7.9 H ₂ C _n Chains	213
5.7.10 C _n N ⁻ Chains	214
5.7.11 C _n H ⁻ Chains	215
5.8 Effect of Kinetics on the Formation of Carbon Chains	217
5.9 Summary on Linear Interstellar Carbon Chains and Thermodynamics	218
5.10 Conclusions on Linear Interstellar Carbon Chains: The Dominant Theme in Interstellar Chemistry	218
5.11 References	219

Chapter 6: INTERSTELLAR IONS AND ISOTOPLOGUES: KNOWN AND POTENTIAL

Preamble	224
 Interstellar Protonated Molecular Species	
6.0 Introduction	225
6.1 Computational Details	226
6.2 Results and Discussion	227
6.2.1 Neutral Species and Their Corresponding Known Protonated Analogues	227
6.2.2 Neutral Species and Their Corresponding Detectable Protonated Analogues	230
6.3 Summary on Interstellar Protonated Molecular Species	237
 Detectable Interstellar Anions: Examining the Key Factors	
6.4 Introduction	238
6.5 Computational Method	239
6.6 Results and discussion	240
6.6.1 Carbon Chains with Corresponding Known Interstellar Anions	240
6.6.2 Carbon Chains with Potential Interstellar Anions	242
6.6.3 Summary on Detectable Interstellar Anions	249
 Deuterated Interstellar and Circumstellar Molecules: D/H Ratio and Dominant Formation Processes	
6.7 Introduction	250
6.7.1 Methodology	252

6.8 Results and Discussion	252
6.9 Summary on Deuterated Interstellar and Circumstellar Molecules	267

Optimizing the Searches for Interstellar Heterocycles	267
6.10 Introduction	267
6.11 Methodology	269
6.12 Results and Discussion	270
6.12.1 Imidazole and Its Isomers	270
6.12.2 Pyridine and Its Isomers	272
6.12.3 Pyrimidine and Its Isomers	274
6.12.4 Pyrrole and Its Isomers	276
6.12.5 Quinoline, Isoquinoline and their Isomers	278
6.12.6 Furan and Its Isomers	281
6.13 Summary on Optimizing the Searches for Interstellar Heterocycles	283
6.14 Conclusions on Interstellar Ions and Isotopologues: Known and Potential	283
6.15 References	284

Chapter 7: BENCHMARK STUDIES ON THE ISOMERIZATION ENTHALPIES FOR INTERSTELLAR MOLECULES

Setting the stage	289
7.0 Introduction	290
7.1 Computational Details	291
7.2 Result and Discussion	291
7.2.1 Isomers with 3 atoms	292
7.2.2 Isomers with 4 atoms	294
7.2.3 Isomers with 5 atoms	295
7.2.4 Isomers with 6 atoms	296
7.2.5 Isomers with 7 atoms	299
7.2.6 Isomers with 8 atoms	301
7.2.7 Isomers with 9 atoms	303
7.2.8 Isomers with 10 atoms	305
7.2.9 Isomers with 11 atoms	306
7.2.10 Isomers with 12 atoms	307
7.3 Potential Interstellar Molecules	309
7.4 Conclusion	311
7.5 References	312
7.6 Supporting information	315

Chapter 8: CONCLUSIONS AND FUTURE DIRECTIONS

8.0 Conclusions	319
8.1 Future Directions	321

8.2.1 Bending the linear carbon chains: Potential Interstellar Cyclic Molecules	321
8.2.2 Spectroscopy of Linear Interstellar Carbon Chain Isotopologues	323
Appendices	327
Appendix1: APPENDIX PRELIMINARY INVESTIGATIONS ON ISOPRENE...AR COMPLEX	
A1.1 Introduction	328
A1.2 Search for the Isoprene Monomer and Isoprene...Argon Rotational Spectra	329
A1.3 Conclusion	329
A1.4 References	329
Appendix2: INTERSTELLAR C₃S: DIFFERENT DIPOLE MOMENT, DIFFERENT COLUMN DENSITY, SAME ASTRONOMICAL SOURCE	
A2.1 Introduction	331
A2.2 Computational details	333
A2.3 Results and discussion	333
A2.4 Conclusion	336
A2.5 References	336
A2.6 Supporting information	337

Synopsis

Initiated with the purpose of assigning the Fraunhofer lines in the solar spectrum to atomic transitions in the 18th century, the collaboration between spectroscopists and astrophysicists has remained fruitful, successful and ever fascinating. This collaboration has resulted in the unique detection of over 200 different molecular species in the interstellar medium (ISM). These interstellar molecular species play significant roles in diverse fields such as atmospheric chemistry, astrochemistry, prebiotic chemistry, astrophysics, astronomy, astrobiology, etc, and in our understanding of the solar system "the world around us". This Thesis work focuses on understanding of the different aspects of the chemistry of the various classes of these molecular species.

Chapter one starts with an historical perspective of what is now regarded as Molecular Astrophysics or Astrochemistry and discusses the interstellar medium and its properties; interstellar molecular species and their importance; molecular spectroscopy as an indispensable tool in interstellar chemistry and the different formation routes of these molecular species. It also discusses hydrogen bonding which is one of the most important of all the intermolecular interactions. The chapter ends by setting the stage for the present investigations.

The chapter two of the Thesis saddled with the task of describing the methodology employed in this Thesis begins by setting the stage on the importance of computational chemistry in interstellar chemistry. It discusses the Gaussian 09 suite of programs and the various theoretical methods used in all the quantum chemical calculations reported in this Thesis. The chapter ends with a brief summary on the homebuilt Pulsed Nozzle Fourier Transform Microwave (PN-FTMW) spectrometer used for the preliminary studies on Isoprene...Argon weakly bound complex reported in the appendix.

After the introductory chapters, chapter three begins with what is unarguably one of the most important classes of interstellar molecular species - 'interstellar isomers'. In this chapter, the Energy, Stability and Abundance (ESA) relationship existing among interstellar molecular species has been firmly established using accurate thermochemical parameters obtained with the composite models and reported observational data. From the relationship, "*Interstellar abundances of related species are directly proportional to their stabilities in the absence of the effect of interstellar hydrogen bonding*". The immediate consequences of the relationship in addressing some of the questions in interstellar chemistry such as: *Where are Cyclic Interstellar Molecules? What are the possible candidates for astronomical observation? Why are more Interstellar Cyanides than isocyanides?* among others are briefly discussed. Following the ESA relationship, other studies addressing some of the whys and wherefores in interstellar chemistry are discussed in details. From ESA relationship, though there has not been any successful astronomical observation of any heterocycle, the ones so far searched remain the best candidates for astronomical observation in their respective isomeric groups. The observation of the first branched chain molecule in ISM is in agreement with the ESA

relationship and the C_5H_9N isomers have been shown to contain potential branched chain interstellar molecules. That molecules with the C-C-O backbone have less potential of formation in ISM as compared to their counterparts with the C-O-C backbone has been demonstrated not to be true following the ESA relationship. A detailed investigation on the relationship between molecular partition function and astronomical detection of isomeric species (or related molecules) shows that there is no direct correlation between the two rather there is a direct link between the thermodynamic stability of the isomeric species (or related molecules) and their interstellar abundances which influences the astronomical observation of some isomers at the expense of others.

Chapter four presents an interesting and a fascinating phenomenon among the interstellar molecular species as it discusses for the first time, the existence and effects of Interstellar Hydrogen Bonding. This interstellar hydrogen bonding is shown to be responsible for the deviations from thermodynamically controlled processes, delayed observation of the most stable isomers, unsuccessful observations of amino acids among other happenings in interstellar chemistry and related areas. On the prediction that ketenes are the right candidates for astronomical searches among their respective isomers, a ketenyl radical; HCCO has recently been detected in line with this prediction. The deviation from the rule that the ratio of an interstellar sulphur molecule to its oxygen analogue is close to the cosmic S/O ratio is well accounted for on the basis of hydrogen bonding on the surface of the dust grains. Detecting weakly bound complexes in ISM has not been a major interest in the field so far but the detectability of weakly bound complexes in ISM is very possible as discussed in this chapter. Following the conditions in which these complexes are observed in the terrestrial laboratory as compared to the ISM conditions; it suffices to say that weakly bound complexes are present and are detectable in ISM. They could even account for some of the 'U' lines.

Chapter five of the Thesis discusses the Linear Interstellar Carbon Chains which are the dominant theme in interstellar chemistry accounting for over 20% of all the known interstellar and circumstellar molecular species. Accurate spectroscopic parameters within experimental accuracy of few kHz which are the indispensable tools for the astronomical observation of these molecular species; are obtained for over 200 different species from the various chains using an inexpensive combined experimental and theoretical approach. With the availability of the spectroscopic parameters; thermodynamics is utilized in accounting for the known systems and in examining the right candidates for astronomical searches. These molecular species are shown to also obey the ESA relationship observed for the isomeric species discussed in chapter three of this work. The effect of kinetics on the formation processes of these molecular species is well controlled by thermodynamics as discussed in this chapter. Finally, the application of these studies in reducing the 'U' lines and probing new molecular species has been briefly summarized.

Chapter six discusses Interstellar Ions and Isotopologues which are two unique classes of interstellar molecular species. Different studies on interstellar ions and isotopologues are presented. From the studies on interstellar protonated species with over 100 molecular species; protonated species resulting from a high proton affinity prefers to remain protonated

rather than transferring a proton and returning to its neutral form as compared to its analogue that gives rise to a lower proton affinity from the same neutral species. The studies on detectable interstellar anions account for the known interstellar anions and predict members of the $C_{2n}O^-$, $C_{2n}S^-$, $C_{2n-1}Si^-$, $HC_{2n}N^-$, C_nP^- , and C_{2n} chains as outstanding candidates for astronomical observation including the higher members of the $C_{2n}H^-$ and $C_{2n-1}N^-$ groups whose lower members have been observed. From high level ab initio quantum chemical calculations; ZPE and Boltzmann factor have been used to explain the observed deuterium enhancement and the possibility of detecting more deuterated species in ISM. Though all the heterocycles that have so far been searched for in ISM have been shown to be the right candidates for astronomical observation as discussed in the ESA relationship, they have also been shown to be strongly bonded to the surface of the interstellar dust grains thereby reducing their abundances, thus, contributing to their unsuccessful detection except for furan which is less affected by hydrogen bonding. The D-analogues of the heterocycles are shown from the computed Boltzmann factor to be formed under the dense molecular cloud conditions where major deuterium fractionation dominates implying very high D/H ratio above the cosmic D/H ratio which suggests the detectability of these deuterated species.

Chapter seven examines the isomerization of the most stable isomer (which is probably the most abundant) to the less stable isomer(s) as one of the plausible formation routes for interstellar molecular species. An extensive investigation on the isomerization enthalpies of 243 molecular species from 64 isomeric groups is reported. From the results, the high abundances of the most stable isomers coupled with the energy sources in interstellar medium drive the isomerization process even for relative enthalpy difference as high as 67.4 kcal/mol. Specifically, the cyanides and their corresponding isocyanides pairs appear to be effectively synthesized via this process. The following potential interstellar molecules; CNC, NCCP, c- C_5H , methylene ketene, methyl Ketene, CH_3SCH_3 , C_5O , 1,1-ethanediol, propanoic acid, propan-2-ol and propanol are identified and discussed. In all the isomeric groups, isomerization appears to be an effective route for the formation of the less stable isomers (which are probably less abundant) from the most stable ones.

Chapter eight summarizes the conclusions drawn from the different studies presented in this Thesis and also highlights some of the future directions of these studies. The first appendix presents the preliminary study on Isoprene...Ar weakly bound complex while the second appendix contains a study on interstellar C_3S describing the importance of accurate dipole moment in calculating interstellar abundances of molecular species and in astrophysical and astronomical models.

List of Tables

Table 1.1: Different components of the interstellar matter and their characteristics

Table 1.2: Interstellar molecules between 2 and 7 atoms

Table 1.3: Interstellar molecules between 2 and 7 atoms

Table 2.1: Different methods for different calculations in compound methods

Table 3.1: Known interstellar isomeric pairs, triads and their isomeric groups.

Table 3.2: Experimental $\Delta_f H^0$ (0K), of elements and H^0 (298K) – H^0 (0K)

Table 3.3: $\Delta_f H^0$ for isomers with 3 atoms and current astronomical status

Table 3.4: $\Delta_f H^0$ for isomers with 4 atoms and current astronomical status

Table 3.5: $\Delta_f H^0$ for isomers with 5 atoms and current astronomical status

Table 3.6: $\Delta_f H^0$ for isomers with 6 atoms and current astronomical status

Table 3.7: $\Delta_f H^0$ for isomers with 7 atoms and current astronomical status

Table 3.8: $\Delta_f H^0$ for isomers with 8 atoms and current astronomical status

Table 3.9: $\Delta_f H^0$ for isomers with 9 atoms and current astronomical status

Table 3.10: $\Delta_f H^0$ for isomers with 10 atoms and current astronomical status

Table 3.11: $\Delta_f H^0$ for isomers with 11 atoms and current astronomical status

Table 3.12: $\Delta_f H^0$ for isomers with 12 atoms and current astronomical status

Table 3.13: $\Delta_f H^0$ for $C_3H_4N_2$ isomers

Table 3.14: $\Delta_f H^0$ for C_5H_5N isomers

Table 3.15: $\Delta_f H^0$ for $C_4H_4N_2$ isomers

Table 3.16: $\Delta_f H^0$ for C_4H_5N isomers

Table 3.17: $\Delta_f H^0$ for C_9H_7N isomers

Table 3.18: $\Delta_f H^0$ for C_4H_4O Isomers

Table 3.19: $\Delta_f H^0$ for C_4H_7N isomers and current astronomical status

Table 3.20: $\Delta_f H^0$, structures and dipole moments for C_5H_9N isomers

Table 3.21: C_2H_2O isomers, enthalpies of formation and astronomical status

Table 3.22: C_2H_4O isomers, enthalpies of formation and astronomical status

Table 3.23: $C_2H_4O_2$ isomers, enthalpies of formation and astronomical status

Table 3.24: C_2H_6O isomers, enthalpies of formation and astronomical status

Table 3.25: Molecular partition function, enthalpy of formation and current astronomical status of isomers with 3 atoms

Table 3.26: Molecular partition function, enthalpy of formation and current astronomical status of isomers with 4 atoms

Table 3.27: Molecular partition function, enthalpy of formation and current astronomical status of isomers with 5 atoms

Table 3.28: Molecular partition function, enthalpy of formation and current astronomical status of isomers with 6 atoms

Table 3.29: Molecular partition function, enthalpy of formation and current astronomical status of isomers with 7 atoms

Table 3.30: Molecular partition function, enthalpy of formation and current astronomical status of isomers with 8 atoms

Table 3.31: Molecular partition function, enthalpy of formation and current astronomical status of isomers with 9 atoms

Table 3.32: Molecular partition function, enthalpy of formation and current astronomical status of isomers with 10 atoms

Table 3.33: Molecular partition function, enthalpy of formation and current astronomical status of isomers with 11 atoms

Table 3.34: Molecular partition function, enthalpy of formation and current astronomical status of isomers with 12 atoms

Table 4.1: Optimized geometry (\AA , deg) parameters of the water monomer

Table 4.2: Binding energies for $\text{C}_2\text{H}_4\text{O}_2$ isomer complexes with water

Table 4.3: Binding energies for $\text{C}_2\text{H}_6\text{O}$ isomer complexes with water

Table 4.4: Binding energies for $\text{C}_3\text{H}_6\text{O}_2$ isomer complexes with water

Table 4.5: Binding energies for $\text{C}_3\text{H}_8\text{O}$ isomer complexes with water

Table 4.6: Binding energies for $\text{C}_2\text{H}_5\text{NO}_2$ isomer complexes with water

Table 4.7: Binding energies for propenal and methyl ketene-water complexes

Table 4.8: Binding energies for propynal and methylene ketene-water complexes

Table 4.9: Binding energies for ethynol and ketene-water complexes

Table 4.10: S and O-containing species, their B.E with water and S/O ratio

Table 4.11: Deviation from cosmic S/O ratio as a function of binding energy (B.E)

Table 4.12: Parameters for Known O- and detectable S-containing molecules

Table 4.13: Enthalpy of formation for O-containing isomers and their detectable S-analogues

Table 4.14: Parameters for Known S- and detectable O-containing molecules

Table 5.1: Experimental rotational constants and moments of inertia for $\text{H}-(\text{C}\equiv\text{C})_n\text{-CN}$ linear carbon chains

Table 5.2: Calculated parameters for $\text{H}-(\text{C}\equiv\text{C})_n\text{-CN}$ linear carbon chains

Table 5.3: Equilibrium rotational constants for $\text{H}-(\text{C}\equiv\text{C})_n\text{-CN}$ linear carbon chains obtained from HF/6-311++G**

Table 5.4: Experimental rotational constants and moments of inertia for DC_{2n+1}N linear carbon chains

Table 5.5: Calculated parameters for DC_{2n+1}N linear carbon chains

Table 5.6: Equilibrium rotational constants for DC_{2n+1}N linear carbon chains obtained from HF/6-311++G**

Table 5.7: Experimental rotational constants and moments of inertia for HC_{2n}N linear carbon chains

Table 5.8: Calculated parameters for HC_{2n}N linear carbon chains

Table 5.9: Equilibrium rotational constants for HC_{2n}N linear carbon chains obtained from HF/6-311++G**

Table 5.10: Experimental rotational constants and moments of inertia for HC_{2n}NC linear carbon chains

Table 5.11: Calculated parameters for HC_{2n}NC linear carbon chains

Table 5.12: Equilibrium rotational constants for HC_{2n}NC linear carbon chains obtained from HF/6-311++G**

Table 5.13: Experimental rotational constants and moments of inertia for $\text{CH}_3(\text{C}\equiv\text{C})_n\text{CN}$ linear carbon chains

Table 5.14: Calculated parameters for $\text{CH}_3(\text{C}\equiv\text{C})_n\text{CN}$ linear carbon chains

Table 5.15: Equilibrium rotational constants for $\text{CH}_3(\text{C}\equiv\text{C})_n\text{CN}$ linear carbon chains obtained from HF/6-311++G**

Table 5.16: Experimental rotational constants and moments of inertia for C_nO linear carbon chains

Table 5.17: Calculated parameters for C_nO linear carbon chains

Table 5.18: Equilibrium rotational constants for C_nO linear carbon chains obtained from HF/6-311++G**

Table 5.19: Experimental rotational constants and moments of inertia for C_nS linear carbon chains

Table 5.20: Calculated parameters for C_nS linear carbon chains

Table 5.21: Equilibrium rotational constants for C_nS linear carbon chains obtained from HF/6-311++G**

Table 5.22: Experimental rotational constants and moments of inertia for HC_nS linear carbon chains

Table 5.23: Calculated parameters for HC_nS linear carbon chains

Table 5.24: Equilibrium rotational constants for HC_nS linear carbon chains obtained from HF/6-311++G**

Table 5.25: Experimental rotational constants and moments of inertia for C_{2n}H^- linear carbon chains

Table 5.26: Calculated parameters for C_{2n}H^- linear carbon chains

Table 5.27: Equilibrium rotational constants for C_nH^- linear carbon chains obtained from HF/6-311++G**

Table 5.28: Experimental rotational constants and moments of inertia for $\text{C}_{2n-1}\text{N}^-$ linear carbon chains

Table 5.29: Calculated parameters for $\text{C}_{2n-1}\text{N}^-$ linear carbon chains

Table 5.30: Equilibrium rotational constants for C_nN^- linear carbon chains obtained from HF/6-311++G**

Table 5.31: Experimental rotational constants and moments of inertia for C_nH linear carbon chains

Table 5.32: Calculated parameters for C_nH linear carbon chains

Table 5.33: Equilibrium rotational constants for C_nH linear carbon chains obtained from HF/6-311++G**

Table 5.34: Experimental rotational constants and moments of inertia for C_nN linear carbon chains

Table 5.35: Calculated parameters for C_nN linear carbon chains

Table 5.36: Equilibrium rotational constants for C_nN linear carbon chains obtained from HF/6-311++G**

Table 5.37: Experimental rotational constants and moments of inertia for C_nSi linear carbon chains

Table 5.38: Calculated parameters for C_nSi linear carbon chains

Table 5.39: Equilibrium rotational constants for C_nSi linear carbon chains obtained from HF/6-311++G**

Table 5.40: Experimental rotational constants and moments of inertia for $CH_3(CC)_nH$ linear carbon chains

Table 5.41: Calculated parameters for $CH_3(CC)_nH$ linear carbon chains

Table 5.42: Equilibrium rotational constants for $CH_3(CC)_nH$ linear carbon chains obtained from HF/6-311++G**

Table 5.43: Δ_fH^0 for C_n chains and current astronomical status

Table 5.44: Δ_fH^0 for C_nO chains and current astronomical status

Table 5.45: Δ_fH^0 for C_nS chains and current astronomical status

Table 5.46: Δ_fH^0 for C_nN chains and current astronomical status

Table 5.47: Δ_fH^0 for C_nSi chains and current astronomical status

Table 5.48: Δ_fH^0 for HC_nN chains and current astronomical status

Table 5.49: Δ_fH^0 for C_nH chains and current astronomical status

Table 5.50: Δ_fH^0 for C_nP chains and current astronomical status

Table 5.51: Δ_fH^0 for H_2C_n chains and current astronomical status

Table 5.52: Δ_fH^0 for C_nN^- chains and current astronomical status

Table 5.53: Δ_fH^0 for C_nH^- chains and current astronomical status

Table 5.54: Carbon chains that have been considered in this study

Table 6.1 Known protonated species and their corresponding neutral analogues

Table 6.2: Proton affinity for known neutral species with 2 atoms

Table 6.3: Proton affinity for known neutral species with 3 atoms

Table 6.4: Proton affinity for known neutral species with 4 atoms

Table 6.5: Proton affinity for known neutral species with 5 atoms

Table 6.6: Proton affinity for known neutral species with 6 atoms

Table 6.7: Proton affinity for known neutral species with 7 atoms

Table 6.8: Proton affinity for known neutral species with 8 atoms

Table 6.9: Electron affinity (eV) for C_nN chains and dipole moment for both C_nN and C_nN^- chains

Table 6.10: Electron affinity (eV) for C_nH chains and dipole moment for both C_nH and C_nH^- chains

Table 6.11: Electron affinity (eV) for C_nO chains and dipole moment for both C_nO and C_nO^- chains

Table 6.12: Electron affinity (eV) for C_nS chains and dipole moment for both C_nS and C_nS^- chains

Table 6.13: Electron affinity (eV) for pure C_n chains

Table 6.14: Electron affinity (eV) for C_nSi chains and dipole moment for both C_nSi and C_nSi^- chains

Table 6.15: Electron affinity (eV) for C_nP chains and dipole moment for both C_nP and C_nP^- chains

Table 6.16: Electron affinity (eV) for C_nP chains and dipole moment for both C_nP and C_nP^- chains

Table 6.17: Known D-molecules, their excitation temperature, Boltzmann factor (E/kT) and D/H ratio

Table 6.18: Boltzmann factor (E/kT) for D-analogues of H-containing diatomic species and the corresponding ZPE

Table 6.19: Boltzmann factor (E/kT) for D-analogues of H-containing triatomic species and the corresponding ZPE

Table 6.20: Boltzmann factor (E/kT) for D-analogues of H-containing tetra-atomic species and the corresponding ZPE

Table 6.21: Boltzmann factor (E/kT) for D-analogues of H-containing penta-atomic species and the corresponding ZPE

Table 6.22: Boltzmann factor (E/kT) for D-analogues of H-containing hexa-atomic species and the corresponding ZPE

Table 6.23: Boltzmann factor (E/kT) for D-analogues of H-containing hepta-atomic species and the corresponding ZPE

Table 6.24: Boltzmann factor (E/kT) for D-analogues of H-containing octa-atomic species and the corresponding ZPE

Table 6.25: Boltzmann factor (E/kT) for D-analogues of H-containing nona-atomic species and the corresponding ZPE

Table 6.26: Boltzmann factor (E/kT) for D-analogues of H-containing deca-atomic species and the corresponding ZPE

Table 6.27: Boltzmann factor (E/kT) for D-analogues of H-containing undeca-atomic species and the corresponding ZPE

Table 6.28: Boltzmann factor (E/kT) for D-analogues of H-containing dodeca-atomic species and the corresponding ZPE

Table 6.29: Boltzmann factor (E/kT) for D-analogues of H-containing trideca-atomic species and the corresponding ZPE

Table 6.30: The dependence of D/H ration on Boltzmann factor

Table 6.31: $C_3H_4N_2$ Isomers, Binding Energy with water, ΔH°_f and Dipole moment

Table 6.32: ZPE and Boltzmann factor (E/kT) for Imidazole and its D-analogues

Table 6.33: C_5H_5N isomers, Binding Energy with water, ΔH°_f and Dipole moment

Table 6.44: ZPE and Boltzmann factor (E/kT) for Pyridine and its D-analogues

Table 6.35: $C_4H_4N_2$ Isomers, Binding Energy with water, ΔH°_f and Dipole moment

Table 6.36: ZPE and Boltzmann factor (E/kT) for Pyrimidine and its D-analogues

Table 6.37: C_4H_5NI isomers, Binding Energy with water, ΔH°_f and Dipole moment

Table 6.38: ZPE and Boltzmann factor (E/kT) for Pyrrole and its D-analogues

Table 6.39: C_9H_7NI isomers, Binding Energy with water, ΔH°_f and Dipole moment

Table 6.40: ZPE and Boltzmann factor (E/kT) for Quinoline and its D-analogues

Table 6.41: ZPE and Boltzmann factor (E/kT) for Isoquinoline and its D-analogues

Table 6.42: C_4H_4O Isomers, Binding Energy with water, ΔH°_f and Dipole moment

Table 6.43: ZPE and Boltzmann factor (E/kT) for Furan and its D-analogues

Table 7.1: Isomerization enthalpies for isomers with 3 atoms
 Table 7.2: Isomerization enthalpies for isomers with 4 atoms
 Table 7.3: Isomerization enthalpies for isomers with 5 atoms
 Table 7.4: Isomerization enthalpies for isomers with 6 atoms
 Table 7.5: Isomerization enthalpies for isomers with 7 atoms
 Table 7.6: Isomerization enthalpies for isomers with 8 atoms
 Table 7.7: Isomerization enthalpies for isomers with 9 atoms
 Table 7.8: Isomerization enthalpies for isomers with 10 atoms
 Table 7.9: Isomerization enthalpies for isomers with 11 atoms
 Table 7.10: Isomerization enthalpies for isomers with 12 atoms
 Table 7.11: Relative energies of CNC and CCN
 Table 7.12: Relative energies of linear and cyclic stable isomers of C₅H

Table 8.1: Relative energy for C₄O linear and cyclic isomers
 Table 8.2: Relative energy for C₄S linear and cyclic isomers
 Table 8.3: Relative energy for C₄P linear and cyclic isomers
 Table 8.4: C_nO systems and their isotopologues
 Table 8.5: C_nH⁺ systems and their isotopologues
 Table 8.6: C_nSi systems and their isotopologues
 Table 8.7: HC_nN systems and their isotopologues

Table A1.1: Rotational constants and dipole moment components along the three principle axes for the isoprene...argon complex
 Table A1.2: Observed transitions of isoprene monomer.

Table A2.1: Chronological listing of interstellar S-containing molecules and their O-analogues.
 Table A2.2: Dipole moment of C₃S from different levels of theory and basis set.
 Table A2.3: Column density of C₃S estimated with different dipole moment values.
 Table A2.4: Dipole moment of C₃S from different levels of theory and basis set.

List of Figures

Fig. 1.1: Known interstellar Molecular Species

Fig. 1.2: Key reactions in astrochemistry (Reproduced with permission from Reference 28)

Figure 3.1: Plot showing the $\Delta_f H^\circ$ for molecules with 3 atoms

Figure 3.2: Plot showing the $\Delta_f H^\circ$ for molecules with 4 atoms

Figure 3.3: Plot showing the $\Delta_f H^\circ$ for molecules with 5 atoms

Figure 4: Plot showing the $\Delta_f H^\circ$ for molecules with 6 atoms

Figure 3.5: Plot showing the $\Delta_f H^\circ$ for molecules with 7 atoms.

Figure 3.6: Plot showing the $\Delta_f H^\circ$ for molecules with 8 atoms

Figure 3.7: Optimized structures of methyl formate (A), acetic acid (B), methyl ketene (C) and propenal (D) at G4 level of theory.

Figure 3.8: Plot showing the $\Delta_f H^\circ$ for molecules with 9 atoms

Figure 3.9: Plot showing the $\Delta_f H^\circ$ for molecules with 10 atoms.

Figure 3.10: Plot showing the $\Delta_f H^\circ$ for molecules with 11 atoms.

Figure 3.11: Optimized structures of propanoic acid (A), ethylformate (B), propanol (C), propan-2-ol (D) and ethyl methyl ether (E) at G4 level of theory.

Figure 3.12: Plot showing the $\Delta_f H^\circ$ for molecules with 12 atoms

Figure 3.13: Optimized Structures of $C_3H_4N_2$ isomers

Figure 3.14: Plot showing the $\Delta_f H^\circ$ for $C_3H_4N_2$ isomers

Figure 3.15: Optimized Structures of C_5H_5N isomers

Figure 3.16: Plot showing the $\Delta_f H^\circ$ for C_5H_5N isomers

Figure 3.17: Optimized Structures of $C_4H_4N_2$ isomers

Figure 3.18: Plot showing the $\Delta_f H^\circ$ for $C_4H_4N_2$ isomers

Figure 3.19: Optimized Structures of C_4H_5N isomers

Figure 3.20: Plot showing the $\Delta_f H^\circ$ for C_4H_5N isomers

Figure 3.21: Optimized Structures of C_9H_7N isomers

Figure 3.22: Plot showing the $\Delta_f H^\circ$ for C_9H_7N Isomers

Figure 3.23: Optimized Structures of C_4H_4O isomers

Figure 3.24: Plot showing the $\Delta_f H^\circ$ for C_4H_4O Isomers

Figure 3.25: Plot showing the $\Delta_f H^\circ$ for C_4H_7N isomers

Figure 3.36: Optimized structures of the C_5H_9N isomers .

Figure 3.27: Plot showing the $\Delta_f H^\circ$ for C_4H_7N isomers.

Figure 3.28: Plot of the enthalpy of formation for C_2H_2O isomers.

Figure 3.29: Plot of the enthalpy of formation for C_2H_4O isomers.

Figure 3.30: Plot of the enthalpy of formation for $C_2H_4O_2$ isomers.

Figure 4.1: Optimized structures of the hydrogen bonded $C_2H_4O_2$ and C_2H_6O isomer complexes with water.

Figure 4.2: Optimized structures of the hydrogen bonded $C_3H_6O_2$ and C_3H_8O isomer complexes with water.

Figure 4.3: Optimized structures of the hydrogen bonded $\text{C}_2\text{H}_5\text{NO}_2$ complexes with water.
Figure 4.4: Optimized structures of the hydrogen bonded $\text{C}_2\text{H}_2\text{O}$, $\text{C}_3\text{H}_2\text{O}$ and $\text{C}_3\text{H}_4\text{O}$ complexes with water.
Figure 4.5: Successive hydrogen additions for the formation of alcohols.
Figure 4.6: Schematic picture of the effect of interstellar hydrogen bonding.
Figure 4.7: Correlation between B.E and S/O abundance ratio.
Figure 4.8: Dependence of column density on enthalpy of formation for CHNO and CHNS systems.

Figure 5.1a: Parts of the 3 mm line survey of IRC +10216 showing the assigned and unassigned lines ('U' lines in red oval shape).
Figure 5.1b: Parts of the 3 mm line survey of IRC +10216 showing the assigned and unassigned lines ('U' lines in red oval shape).
Figure 5.1c: Parts of the 3 mm line survey of IRC +10216 showing the assigned and unassigned lines ('U' lines in red oval shape).
Figure 5.1d: Parts of the 3 mm line survey of IRC +10216 showing the assigned and unassigned lines ('U' lines in red oval shape).
Figure 5.2: Plot showing the $\Delta_f\text{H}^\circ$ for C_n chain molecules
Figure 5.3: Plot showing the $\Delta_f\text{H}^\circ$ for C_nO chain molecules
Figure 5.4: Plot showing the $\Delta_f\text{H}^\circ$ for C_nS chain molecules
Figure 5.5: Plot showing the $\Delta_f\text{H}^\circ$ for C_nN chain molecules
Figure 5.6: Experimental (A) and theoretical geometry (B) of c-SiC₃ molecule
Figure 5.7: Plot showing the $\Delta_f\text{H}^\circ$ for C_nSi chain molecules
Figure 5.8: Plot showing the $\Delta_f\text{H}^\circ$ for HC_nN chain molecules
Figure 5.9: Plot showing the $\Delta_f\text{H}^\circ$ for C_nH chain molecules
Figure 5.10: Plot showing the $\Delta_f\text{H}^\circ$ for C_nP chain molecules
Figure 5.11: Plot showing the $\Delta_f\text{H}^\circ$ for H_2C_n chain molecules
Figure 5.12: Plot showing the $\Delta_f\text{H}^\circ$ for C_nN^- chain molecules
Figure 5.13: Plot showing the $\Delta_f\text{H}^\circ$ for C_nH^- chain molecules
Figure 5.14: Percentage of detected odd and even number carbon chains

Figure 6.1: Relationship between PA and astronomical observation of protonated species.
Figure 6.2: Plot showing electron affinity for C_nN carbon chains
Figure 6.3: Plot showing electron affinity for C_nH carbon chains
Figure 6.4: Plot showing electron affinity for C_nO carbon chains
Figure 6.5: Plot showing electron affinity for C_nS carbon chains
Figure 6.6: Plot showing electron affinity for C_n pure carbon chains
Figure 6.7: Plot showing electron affinity for C_nSi pure carbon chains
Figure 6.8: Plot showing electron affinity for C_nP carbon chains
Figure 6.9: Plot showing electron affinity for HC_nN carbon chains
Figure 6.10: Dependence of D/H ratio on Boltzmann factor
Figure 6.11: Optimized structures of the hydrogen bonded $\text{C}_3\text{H}_4\text{N}_2$ isomer complexes with water
Figure 6.12: Optimized structure of imidazole

Figure 6.13: Optimized structures of the hydrogen bonded C_5H_5N isomer complexes with water

Figure 6.14: Optimized structure of Pyridine

Figure 6.15: Optimized structures of the hydrogen bonded $C_4H_4N_2$ isomer complexes with water

Figure 6.16: Optimized structure of pyrimidine

Figure 6.17: Optimized structures of the hydrogen bonded C_4H_5N isomer complexes with water

Figure 6.18: Optimized structure of pyrrole

Figure 6.19: Optimized structures of the hydrogen bonded C_9H_7N isomer complexes with water

Figure 6.20: Optimized structure of quinoline

Figure 6.21: Optimized structure of isoquinoline

Figure 6.22: Optimized structures of the hydrogen bonded C_4H_4O isomer complexes with water

Figure 6.23: Optimized structure of furan.

Figure 7.1: Optimized structures of cyclic C_5N isomers.

Figure 7.2: Optimized structures of cyclic C_5H isomers.

Figure 7.3: Optimized structures of cyclic C_5S isomers.

Figure 7.4: Optimized structures of cyclic $SiCH_3N$ isomers.

Figure 7.5: Optimized structures of cyclic C_5O isomers.

Figure 7.6: Optimized structures of cyclic C_2H_5N (A) and CH_4N_2O (B) isomers.

Figure 7.7: Optimized structures of cyclic C_5H_4 (A and B) and C_3H_6 (C) isomers.

Figure 7.8: Optimized geometries of CNC and CCN at MP2(full)/6-311++G** level.

Figure 7.9: Optimized structures of C_5H most stable isomers.

Figure 8.1: Relative energy of cyclic and their corresponding linear carbon chains

Figure A1.1: Optimized structure for isoprene...argon complex.

Figure A2.1: plot of experimental dipole moment of C_3S in comparison with theoretically calculated values.

Figure A2.2: Optimized geometry of C_3S from different levels of theory and basis sets.

Chapter 1:

Introduction

CHAPTER 1: Introduction

1.0 In the Beginning

It all started at the dawn of spectroscopy when Joseph von Fraunhofer (1787-1826), a German Physicist and Optician discovered the solar system using the lenses he manufactured and the refractory telescopes he built. He found a large number of fine dark absorption lines (about 700) which he studied in great details, in the solar system. These dark lines in the solar system discovered by Joseph von Fraunhofer are known as the Fraunhofer lines till date. They result from the absorption by elements in the solar chromospheres of some of the wavelengths of visible radiation emitted by the hot interior of the sun. The discovery that both stars and the sun are made up of the same chemical constituents as the earth is widely accepted as one of the earliest and greatest achievements of spectroscopy and its foremost application to astronomical objects.¹⁻³

The interaction initiated in the 18th century (about four decades after Fraunhofer's original discovery of the solar spectrum) between spectroscopists and astrophysicists for the purpose of assigning the Fraunhofer lines in the solar spectrum to atomic transitions marked the beginning of what is now referred to as modern astrophysics. Bunsen and Kirchhoff (professors of chemistry and physics) of the University of Heidelberg used their new methods of spectral analysis in assigning the Fraunhofer lines from which they recognized that every chemical element exhibits a characteristic spectrum which is its unique fingerprint which can be used to detect it in the laboratory and in far astronomical objects. The identification of Fraunhofer lines established spectroscopy as a powerful analytic tool for studying physical and chemical processes both in the terrestrial laboratory and astronomical objects. Thrilled by what they could achieve with spectroscopy, Bunsen and Kirchhoff stated that spectroscopy would open "an entirely untraversed field, stretching far beyond the limits of the earth, or even our solar system".¹⁻³

This collaboration between the spectroscopists and astrophysicists has remained fruitful, successful and ever fascinating. This has led to the successful detection of over 200 different molecular species in the interstellar medium (ISM) and circumstellar envelopes ranging from the simple diatomics like H₂, O₂, OH, CO, etc., to the complex species (those with six atoms and above) including the buckyballs with each molecule telling the story of the chemistry and physics of the environment from where it was observed. Of course molecules are not only limited to the ISM, they are ubiquitous except in the stellar interiors and high temperature diffuse interstellar gas. They are present in protostars, accretion disk, bipolar flows and even in youthful stars known as T.Tauri objects. However, the present work will mainly focus on the interstellar and circumstellar molecules.⁴⁻⁸ The use of these molecular species as probes of the physical and chemical conditions in space has emerged as one of the major driving forces for the increased interest in the fields of astronomy, astrophysics and other related fields. The field of astrobiology thrives on the discoveries of biologically related molecules in space.

The astrophysicists and astronomers are so concerned with the detection of molecules in ISM (obviously because of the information these molecules furnish them regarding the physical

and chemical conditions of the astronomical objects from where they are observed) without paying much attention to the chemistry of these molecular species. This has given birth to Astrochemistry synonymously called Molecular Astrophysics which is concerned with the study of molecules in space and it encompasses observation, theory, modelling and experiments all aimed at interpreting molecular emission patterns in space. Alex Dalgano (1934-2015),⁹ one of the founding fathers in the field, defined it as "*The blending of astronomy and chemistry in which each area enriches the other in a mutually stimulating interaction.*"

This Thesis work focuses on understanding some of the chemistry of the different classes of interstellar molecular species both the known and postulated ones.

1.1 The Interstellar Medium

The space between the stars is not empty. In the early part of the 20th century, the interstellar space was regarded as an empty vacuum dotted with stars, planets, black holes and other celestial formations. This idea or perception was soon laid to rest when it was realized that the regions between the stars contain by far the largest reservoir of chemically bonded matter in nature through the discoveries of different molecular species some of which were not even known in the terrestrial laboratory as at the time of their astronomical observation, e.g HNC, HCS⁺, HOCO⁺,¹⁰⁻¹¹etc. The interstellar medium is simply all the stuff between stars. It is the matter that exists in the space between the stars. The matter in ISM includes gas (in ionic, atomic and molecular forms), dust and cosmic rays. By composition, the ISM is composed of 99% gas and 1% dust. With respect to the gas in ISM, 89% are atoms of hydrogen, 9% are atoms of helium while the remaining 2% are atoms of elements heavier than helium (with atomic number of 3 and above) which are regarded as 'metals' in astrochemistry parlance. The interstellar dust consists preferentially of particles of heavy elements.⁴

The detection of singly ionized calcium (Ca⁺) in the visible spectrum toward the binary star system σ -Orionis marked the beginning of observation of molecular species in the ISM. Interstellar chemistry started actively in the late 1930's with the observations of CH, CN, and CH⁺ in the ISM.¹²⁻¹⁶ Since then, observation of interstellar molecules has become a continuous process with an average of four molecules observed yearly except during the period of 1942 to 1962 with no observation. Table 1.1 summarizes the different components of the ISM.¹⁷ Of all the components of ISM, the molecular clouds are of utmost importance in interstellar chemistry. Molecules are formed in the molecular clouds and are also detected there. A molecular cloud, sometimes referred to as a stellar nursery (if star formation is occurring within) is a type of interstellar cloud whose density and size permit the formation of molecules, most commonly, molecular hydrogen which is of course the most abundant molecular species in ISM.¹

Table 1.1: Different components of the interstellar matter and their characteristics

Component	Number density (cm ⁻³)	Temperature (K)	Major constituents	Main detection technique
Molecular clouds (dark nebulae)	Up to 10 ⁶	10-20	H ₂ , many molecules, ice-coated dust grains.	Radio and infrared emissions and absorptions
Intergalactic coronal gas	≈10 ⁻³	10 ⁶ -10 ⁷	H ⁺ , C ³⁺ , N ⁴⁺ , O ⁺⁵	UV absorption, X-ray emission
Neutral and ionized medium	0.2 – 0.5	6 – 10 × 10 ³	H, H ⁺ , He, He ⁺	21cm emission of H, H α emission
Ionized diffuse clouds (Emission nebulae, HII regions)	10 ² -10 ⁴	8×10 ³	H ⁺ , He ⁺ , O ⁺ , C ⁺ , N ⁺ , CH ⁺ , H ₃ ⁺ , HCO ⁺	H α emission
Neutral diffuse clouds (reflection nebulae, HI regions)	20-50	50-100	H, He, H ₂ , H ₃ ⁺ , C ⁺ , CO, CN, OH, NH, C ₂ , dust	21 cm emission of H atoms

The material within the ISM is not uniformly distributed but it forms clouds of variable size density, temperature and mass as depicted in Table 1.1. It can be said to be 'clumpy' and the clumpiness is due to matter in the clouds gravitating towards each other. The main types of clouds are shown in Table 1.1. The dark clouds are of comparatively high density containing molecular materials and dust grains.¹⁸ They are relatively dense; hence, they are not penetrated by ultraviolet radiation. They are the regions in which most molecules are found in the ISM; thus, they are also referred to as the molecular clouds.

1.2 Interstellar Molecular Species

The strong collaboration between spectroscopists, astrophysicists and astronomers coupled with the advances in astronomical and spectroscopic instruments have led to the successful detection of over 200 different molecular species in the ISM and circumstellar envelopes largely through their rotational transitions.⁴ Figure 1.1 lists the currently (as at February 2016)⁴¹ known interstellar molecular species. These molecular species are typically found in the interstellar molecular clouds with large sizes of 1-100 light years and average gas densities of 10⁻²-10⁺³cm⁻³.¹ Of all the known molecular species in space, less than 20 elements are represented (precisely, 17). These include; H, Li, C, N, O, F, Na, Mg, Al, Si, P, S, Cl, Ar, K, Ti, Fe; with the four most important biogenic elements; C, H, N and O (sometimes referred to as 'CHON') being the most abundant.

With hydrogen being the most abundant constituent of the interstellar molecular clouds, the prevalence of highly unsaturated carbon containing species in the ISM and circumstellar shells remains a surprise. This unsaturation manifests largely in the linear carbon chain species such as the polyynes, cyanopolyyynes, etc. With over 200 known molecular in ISM, only about ten are cyclic; (with the unconfirmed claimed observation of 2H-azirine) c-SiC₂, c-C₃H, c-C₃H₂, c-H₂C₃O, c-C₂H₄O, 2H-azirine, benzene, C₆₀, C₇₀ and C₆₀⁺ while the rest are straight chain molecules with only one currently known branched chain molecule; isopropyl cyanide.¹⁹⁻²⁷ Besides the unsaturated species, a few saturated species have also been detected

in ISM. While some of the saturated molecules like acetic acid, ethylene glycol, ethanol, methylamine, etc are believed to be products of surface chemistry on grains, others like methylformate, acetone, dimethyl ether, etc., are regarded as likely products of gas-phase chemical reactions.¹⁷ Radicals, protonated species, cations and anions are among the known interstellar and circumstellar molecular species. The chemistry of these species is rich and ever fascinating.

2 atoms	3 atoms	4 atoms	5 atoms	6 atoms	7 atoms	8 atoms	9 atoms	10 atoms	11 atoms	12 atoms	>12 atoms
H ₂ , CO, CSi, CP	H ₂ O, H ₂ S, HCN, TiO ₂ , HNC, CO ₂ , SO ₂	NH ₃ , H ₂ CO	CH ₄ , SiH ₄	CH ₃ OH, CH ₃ SH	CH ₂ CHO	CH ₃ COO	(CH ₃) ₂ O	(CH ₃)CO	HC ₉ N	C ₆ H ₆	HC ₁₁ N
CS, NO, NS, SO		H ₂ CS, C ₂ H ₂	CH ₂ NH, NH ₂ CN	C ₂ H ₄ , HC ₃ H	c-C ₂ H ₄ O	HCOOC	CH ₃ CH ₂ C	HOC ₂ H ₄ O	CH ₃ C ₆ H	C ₃ H ₇ CN	C ₆₀
HCl, NaCl, KCl	MgCN, MgNC, NaCN	HNCS	CH ₂ CO, HCOOH	CH ₃ CN, CH ₃ NC	HC(O)CH	HOCH ₂ C	CH ₃ CH ₂ O	H ₃ CCH ₂ C	HCOOC ₂	C ₂ H ₅ OCH	C ₆₀ ⁺
AlCl, AlF, PN	FeCN, KCN,	H ₃ O ⁺ , SiC ₃	H ₃ CCCN, HCCNC	HCONH ₂	H ₃ CCCH	HOCH ₂ C	CH ₃ CH ₂ S	H ₃ CCH ₂ C	CH ₃ C ₄ CN	CH ₃ OCO	C ₇₀
SiN, SiO, SiS	C ₃ S, H ₂ CN	C ₃ S, H ₂ CN	c-C ₃ H ₂ , I-	I-C ₃ H ₂	HC ₂ C(O)	CH ₃ NH ₂	H ₃ C ₃ CN, C ₂ H, (NH ₂) ₂ CO	CH ₃ C ₄ H		branched-C ₃ H ₇ CN	
NH, OH, C ₂	AIOH, H ₂ Cl, H ₂ O ⁺ , H ₂ Cl ⁺ , N ₂ O, NH ₂	H ₂ Cl, H ₃ C ₂	e-C ₃ H, I-C ₃ H ₂	CH ₂ CN, H ₂ COH ⁺	HC ₃ NH ⁺	HC ₄ CN	CH ₂ CHC	H ₂ C ₆	HC ₇ N		
NH, OH, C ₂	OCS				HC ₅ N						
CN, HF, FeO	CH ₂ , HCO, C ₃	C ₂ CN, C ₃ O	C ₅	C ₄ Si	C ₆ H	C ₆ H	H ₂ CCHC	CH ₃ CONH ₂			
LiH, CH, CH ⁺	C ₂ H, C ₂ O, C ₂ S	HCO ⁺ , HOCO ⁺	H ₃ CCN ⁺	H ₃ CCCC	H ₂ C ₄ , H ₂ CCNH			CH ₂ CCH	C ₈ H		
CO ⁺ , SO ⁺ , SH, NO ⁺	AlNC, HNO	C ₂ N, HNCO	C ₄ H	C ₄ H	C ₅ N ⁻			H ₂ NCH ₂ C	CH ₃ CHC		
O ₂ , N ₂ , CF ⁺	SiCN, N ₂ H ⁺	H ₃ SCN, C ₃ N, PH ₃	H ₃ CO, NCCP, MgCCH, HOCH ₂	HCO(O)CN, CH ₃ O, HNCNH, H ₂ NCO ⁺ , NH ₃ D ⁺	H ₃ CHCN, C ₅ S, SiH ₃ CN			H			
PO, HD	SiNC, c-SiC ₂			NCCNH ⁺							
SiH, AlO, ArH ⁺ , OH ⁺ , CN ⁺ , SH ⁺ , HCl ⁺ , TiO, HO ₂	C ₂ N, HCO ⁺ , HOC ⁺ , HCS ⁺ , H ₃ O ⁺	HCO, MgCCH, HOCH ₂	H ₂ O ₂								

Fig. 1.1: Known interstellar Molecular Species

The interstellar molecular species play significant roles in diverse fields such as, astrochemistry, prebiotic chemistry, astrophysics, astronomy, astrobiology, etc, and in our understanding of the solar system "the world around us". Emission from tracer molecules such as NH₃, CS and HC₃N (which are excited at high densities only) can be used to infer the density of interstellar gas. Molecules provide the cooling mechanism for the clouds through their emission. This is important in reducing the temperature of dust cloud, facilitating the gravitational collapse required for star formation. The cooling prevents the cloud that is collapsing from heating up as gravitational potential energy is converted into heat.^{18,28,29} The symmetric rotors like CH₃CN and CH₃CCH are important interstellar thermometers. The metal-bearing species like SiO, AlNC, FeO, etc furnish useful information regarding the depletion of these molecular species into the molecular dust grains. From a prebiotic chemistry point of view, understanding how the simple molecules that were present on the

early earth may have given rise to the complex systems and processes of contemporary biology is widely regarded as one of the unanswered chemistry questions. Interestingly, the biologically important molecules so far detected in the ISM serve as important tools toward addressing this question. Among the $C_2H_4O_2$ isomeric species, acetic acid is considered a precursor for glycine; the simplest biologically important amino acid. This is simply because in the laboratory, a bimolecular synthesis of glycine occurs when acetic acid combines with amidogen cation. Glycolaldehyde (an isomer of acetic acid) is an important biomarker being structurally the simplest member of the monosaccharide sugars.

Interstellar molecules are important probes of the physical conditions in space. They serve as the most important tools for probing deep into the interior of the molecular clouds and the molecular clouds are significant because it is from them that stars and consequently new planets are formed. Every interstellar molecule tells the story of the chemistry and physics of the environment from where it was found. Molecules with a well-understood chemistry in the ISM can be used as probes of astrophysical phenomena. Thus, the better the chemistry of the molecular species is understood; the more their potential can be utilized. Let's go for the chemistry of interstellar molecular species!!!

1.3 Molecular Spectroscopy: An Indispensable Tool in Interstellar Chemistry

Of all the tools that may be at the disposal of an astronomer, spectroscopy which is simply the study of the interaction between matter and light (electromagnetic radiation from radiofrequency to gamma rays), has become an indispensable partner. This is because with spectroscopy, astronomers can study the universe; determine the chemical compositions, physical properties, and radial velocities of astronomical sources. The dark matter content of galaxies, the masses of two stars in orbit about each other, the mass of a cluster of galaxies, the rate of expansion of the Universe have all been measured with the help of spectroscopy. Also, it makes it possible for the astronomer to determine the physical conditions in distant stars and nebulae, including the chemical composition and temperatures, by quantitative analysis of the strengths of spectral features, thus constraining models of chemical enrichment in galaxies and the evolution of the universe.⁴

Molecular species are detected in ISM through their spectroscopic signatures. The fact that each molecule has a characteristic spectrum which is its distinct fingerprint has been found to be very useful for identification of molecules both in the terrestrial laboratory and in ISM. The basic technique in detecting molecules in ISM is the matching of spectroscopic frequencies obtained from a spectrometer that is connected to a radio telescope with those spectral features obtained in the laboratory or via accurate theoretical predictions. Since the atmospheric water vapor can reabsorb microwave radiation from space and interfere with the measurement; earth-bound telescopes are often located at the top of high mountains while in the case of infrared astronomy, the astronomical observation is carried out primarily in space-borne telescopes because the Earth's atmosphere absorbs a great deal of infrared radiation. The spectral lines of atoms and molecules (both ionized and neutral) contain detailed but specific information on the physical and chemical conditions of the sources from which they emanate. The excitation conditions, the temperature of the source, gaseous number-density of the source can all be deduced from these spectral features.^{1,4,30}

The gas which constitutes about 99% of the total composition of ISM readily emits detectable radiation; thus, can easily be studied. The conditions in the ISM (very low density) enable the observation of "forbidden lines" which are spectral lines observed from interstellar gas that are not normally observed in the terrestrial laboratory. Under normal laboratory conditions, spectral lines with low transition probabilities are "forbidden or not-allowed" because the excited states get collisionally de-excited before they can radiate while in the ISM, collisional times are typically much longer than the lifetimes of those excited states with only forbidden transitions. Thus, forbidden transitions are easily observed in ISM and they can even dominate the spectrum in some cases. A molecule can possess rotational energy as a result of the bodily rotation about its centre of gravity; this rotational energy is the origin of radioastronomy. Molecules have vibrational energy because of the periodic displacement of the atoms from their equilibrium position. Vibrational energy of molecules is the bedrock of infrared astronomy. Molecules also possess electronic energy since the electrons associated with each atom or bond are in unceasing motion. The electronic energy of molecules is the foundation of optical astronomy. Molecular species are detected in ISM and circumstellar shells by their characteristic spectral frequencies across the different regions of the electromagnetic spectrum, thus making molecular spectroscopy an indispensable tool in the chemical examination of the interstellar medium.^{30,31} The three key molecular spectroscopic techniques in interstellar chemistry are briefly summarized here.

1.3.1. Rotational Spectroscopy in Interstellar Chemistry

High resolution-spectroscopy is the closest and an indispensable partner to an astronomer. Among the different high resolution-spectroscopic techniques, some are better than others and the most important of these for identifying molecules in ISM is the microwave or rotational spectroscopy. Unlike other spectroscopic techniques with widespread applications in analytical chemistry like NMR, UV-Visible and infrared spectrometers, microwave or rotational spectroscopy has very few but unique applications and one of such is in the chemical examination of the interstellar medium. Rotational spectroscopy involves the measurement of the energies of transitions between quantized rotational states of molecules in the gas phase. These transitions arise from the rotation of the permanent dipole moment that can interact with an electromagnetic field in the microwave region of the spectrum.

Transitions between rotational states are in general the least energetic as compared to the transitions between electronic and vibrational states. Thus, at the low temperature of the ISM where most molecules are in their electronic and vibrational ground states (not excited states), rotational excited states are easily populated. Therefore, the spectrum of the molecular cloud in the radio frequency and microwave regions will consist of sharp lines corresponding to rotational transitions. Rotational spectroscopy has remained the best technique for probing molecules in ISM. From Tables 1.2 and 1.3, it is crystal clear that over 80% of all the known interstellar molecular species have been detected via their rotational spectral features.⁴ From the rotational emission spectra obtained from a spectrometer that is connected to a radio telescope; accurate information regarding the molecular species doing the emitting, the abundances of these species and the physical conditions in the source are obtained.⁸

Table 1.2: Interstellar molecules between 2 and 7 atoms

2 atoms	3 atoms	4 atoms	5 atoms	6 atoms	7 atoms
H_2 , CO , CSi , CP	H_2O , H_2S , HCN , TiO_2 , HNC , CO_2 , SO_2	NH_3 , H_2CO	CH_4 , SiH_4	CH_3OH , CH_3SH	CH_2CHOH
CS , NO , NS , SO	H_2CS , C_2H_2	NH_2CN	C_2H_4 , HC_4H	$\text{c-C}_2\text{H}_4\text{O}$	
HCl , NaCl , KCl	MgCN , MgNC	HNCS	CH_2CO , HCOOH	CH_3CN , CH_3NC	HC(O)CH_3
AlCl , AlF , PN	NaCN , FeCN , KCN	H_3O^+ , SiC_3	C_3S , H_2CN	HCOOH	H_3CCCH
SiN , SiO , SiS	C_3S , H_2CN	$\text{C}_3\text{S}, \text{H}_2\text{CN}$	HCCC , HCCNC	$\text{HC}_2\text{C(O)H}$	CH_3NH_2
NH , OH , C_2	AlOH , H_2Cl , H_2O^+ , H_2Cl^+ , N_2O	HCCN , CH_3	$\text{c-C}_3\text{H}_2$, $\text{l-C}_3\text{H}_2$	HC_3NH^+	CH_2CHCN
CN , HF , FeO	NH_2 , OCS	C_2CN , C_3O	$\text{HC}_2\text{C(O)H}$	HC_4N	HC_4CN
LiH , CH , CH^+	CH_2 , HCO , C_3	HCNH^+ , HOCO^+	C_4Si	C_5N^-	
CO^+ , SO^+ , SH , NO^+	C_2H , C_2O , C_2S , AlNC , HNO	C_3N^- , HNCO	C_5	$\text{c-H}_2\text{C}_3\text{O}$	
O_2 , N_2 , CF^+	HSCN , C_3N , PH_3	HMgNC	HNC	HNCHCN , C_5S , SiH_3CN	
PO , HD	SiCN , N_2H^+	HCCO	C_4H^-		
SiH , AlO ,	SiNC , c-SiC_2	NCCP			
ArH^+ , OH^+ , CN^- , SH^+ , HCl^+ , TiO , HO_2	C_2N , HCO^+ , HOC^+	MgCCH	HC(O)CN		
	HCS^+ , H_3^+	HOCHN	CH_3O		
	OCN^- , HCP		HNCNH		
	CCP , SiCSi	H_2O_2	H_2NCO^+		
			NH_3D^+		
			NCCNH^+		

Rotational (mm/sub-mm); both rotational (mm/sub-mm) and uv-vs (electronic); uv-vs (electronic); infrared (vibrational) (Edited with permission from Reference 4)

Table 1.3: Interstellar molecules with 8 atoms and above

8 atoms	9 atoms	10 atoms	11 atoms	12 atoms	>12 atoms
<chem>CH3COOH</chem>	<chem>(CH3)2O</chem>	<chem>(CH3)CO</chem>	<chem>HC9N</chem>	<chem>C6H6</chem>	<chem>HC11N</chem>
<chem>HCOOCH3</chem>	<chem>CH3CH2CN</chem>	<chem>HOC2H4OH</chem>	<chem>CH3C6H</chem>	<chem>C3H7CN</chem>	<chem>C60</chem>
<chem>HOCH2CHO</chem>	<chem>CH3CH2OH</chem>	<chem>H3CCH2COH</chem>	<chem>HCOOC2H5</chem>	<chem>C2H5OCH3</chem>	<chem>C60+</chem>
<chem>H3C3CN, C7H, (NH2)2CO</chem>	<chem>CH3CH2SH</chem> <chem>CH3C4H</chem>	<chem>CH3C4CN</chem>	<chem>CH3OCOCH3</chem>	<chem>branched-C3H7CN</chem>	<chem>C70</chem>
<chem>H2C6</chem>	<chem>HC7N</chem>				
<chem>H(CC)3H</chem>	<chem>C8H</chem>				
<chem>H2CCHCHO</chem>	<chem>CH3CONH2</chem>				
<chem>CH2CCHCN</chem>	<chem>C8H-</chem>				
<chem>H2NCH2CN, CH3CHNH</chem>	<chem>CH3CHCH2</chem>				

Rotational (mm/sub-mm); **infrared (vibrational)**; (Edited with permission from Reference 4)

1.3.2 Vibrational Spectroscopy in Interstellar Chemistry

One major drawback associated with rotational spectroscopy with respect to the detection of molecules in ISM is the fact that it is only limited to microwave active molecules i.e molecules that possess permanent dipole moment. Thus, non-polar molecular species such as benzene, acetylene, methane, C_n linear carbon chains, etc, cannot be probed via radio astronomy. Apart from the slow quasi-rigid-body motion known as rotation, molecules also undergo much more rapid vibrational motions. For a molecule containing N atoms, there are total of $3N$ degrees of freedom of which three are rotational (for non-linear molecules and 2 for linear molecules) and 3 are translational in origin. The remaining $3N-6$ (for non-linear molecules and $3N-5$ for linear molecules) degrees of freedom are vibrational and are best represented as collective vibrational motions known as normal modes. Thus, there are $3N-6$ and $3N-5$ degrees of vibrational freedom for non-linear and linear molecules respectively.⁸

Vibrational or infrared spectroscopy is the next most useful spectroscopic technique for probing molecules in ISM. From Tables 1.2 and 1.3, the molecules probed in ISM via their infrared transitions are indicated in green. Transitions between vibrational states can produce lines in the infrared region of the electromagnetic spectrum which form the basis of infrared astronomy. Vibrational energy levels are much further apart as compared to the rotational levels; thus, for each vibrational level, a large series of associated rotational levels can be expected. Unlike in rotational or microwave transitions; here transitions between two vibrational states do not require permanent dipole moment but the criterion here is that the

dipole moment change along the periodic motion of the particular normal mode undergoing the transition.

1.3.3 Electronic Spectroscopy in Interstellar Chemistry

With respect to the detection of molecules in the interstellar medium, electronic or optical astronomy is probably the least useful technique. Transitions between electronic states are in general the most energetic and can produce several lines in the optical, ultraviolet and infrared regions of the spectrum. The high energy photons associated with electronic spectroscopy are indicative of electron rearrangement in molecules with the effect of changes in the strength of the chemical bond. This high energy associated with electronic transitions play important role in chemical reactions; electronic excitation adds energy to the system. For example, a reaction may not be possible in the ground electronic state but when the molecule is electronically excited, it becomes highly reactive and the reaction can occur.¹⁶ The use of electronic spectroscopy in astronomy ISM is only limited to the diffuse clouds and stellar atmosphere but cannot be used to probe the dense clouds since external visible and ultraviolet light cannot penetrate the diffuse clouds because of the scattering by the dust particles. As indicated in Tables 1.2 and 1.3, very few molecular species; mostly diatomics like H₂, CH⁺, NH, etc have been detected in ISM via their electronic transitions.^{6,14,16,32, 33}

1.4 Formation of Interstellar Molecules

Hydrogen and helium are considered to be primordial while every other element higher than helium is believed to have been synthesized slowly by the thermonuclear reactions in the hot interior of stars. At the death of star, the star forming elements are ejected into the ISM to form molecules. The energy source for this process is the gravitational pull toward the centre of a star which creates massive amounts of heat and pressure resulting in the nuclear fusion. Through this process of merging, heavier elements are formed.^{1,17} Though there is hardly a consensus as to how molecules are formed in ISM, the rapid advances in science and technology have resulted in an increased depth of knowledge regarding the formation of molecular species in ISM. Gas phase reactions and reactions that occur on the surface of the interstellar dust grains are the main processes by which molecules are formed in ISM. Of these two processes, reactions that occur on the surfaces of interstellar dust particles have been invoked for the formation of molecular hydrogen as well as for the synthesize of larger interstellar molecular species. In any astronomical environment, the processes that convert hydrogen atoms (H) to hydrogen molecules (H₂) are considered the most important ones not only because molecular hydrogen is by far the most abundant molecular species in the universe but also because molecular hydrogen plays important role in the formation of almost every other molecular species in ISM.²⁸ Different studies have shown that the conversion of hydrogen atoms to hydrogen molecule [2H_(g)→H_{2(g)}] occurs through surface catalysis.^{18,34} The dust grains and ice play an important role in the formation of molecular species. Whereas in the thin space between the stars, gas phase reactions relying on three body collisions are very rare, molecules and atoms residing on the solid surfaces can roam around the surfaces

until a reaction occurs. Thus, the dust grains act as a catalyst in the formation of molecular species in ISM.

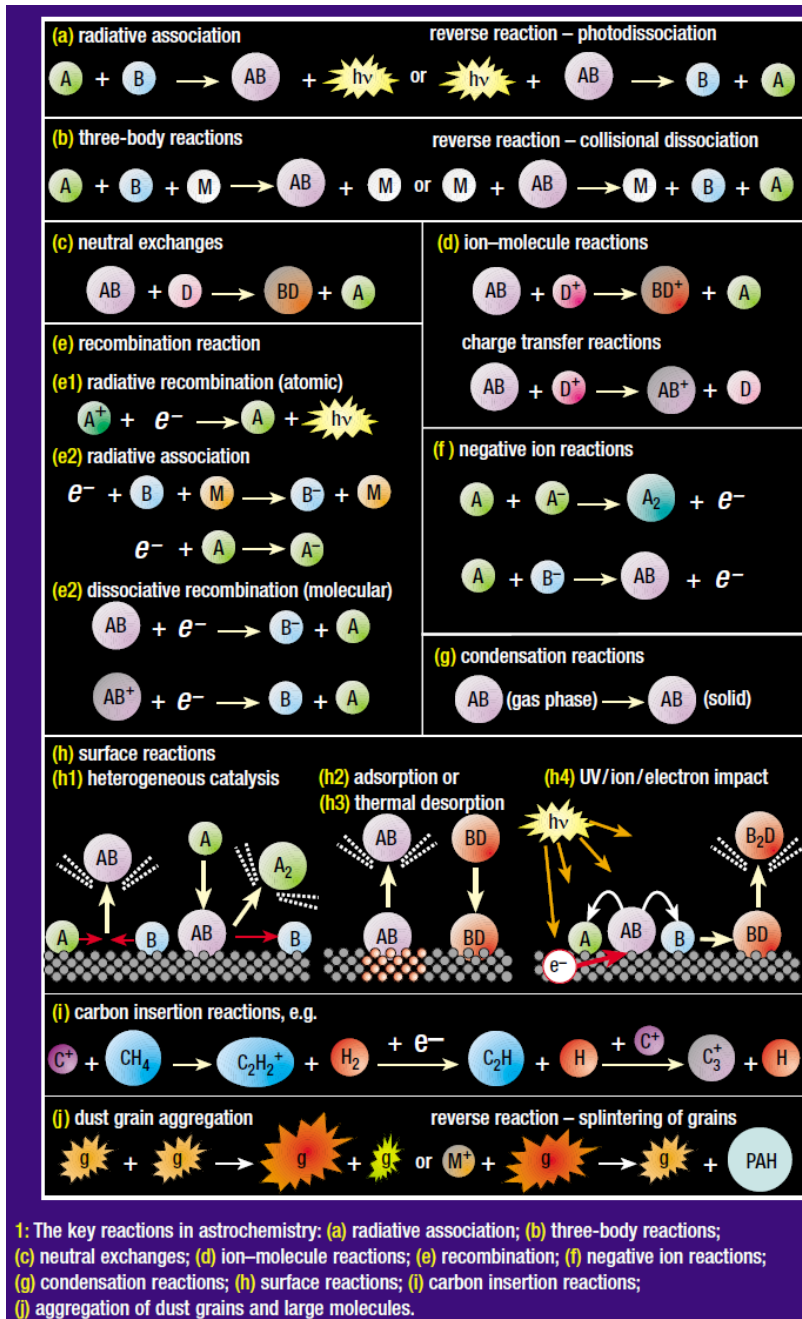


Fig. 1.2: Key reactions in astrochemistry (Reproduced with permission from Reference 28)

Figure 1.2 illustrates the types of reactions that play a role in astrochemistry. Among these reactions; surface reactions (already described above), three-body association and ion-molecule reactions are the main chemical routes via which molecules can be synthesized in ISM. Three-body association are the dominant formation routes in high-density environment such as stellar photosphere and planetary atmosphere.

Ions are known to play significant roles in interstellar formation processes though only a few of them have been detected. Under the conditions of the ISM, neutral atoms and molecules

tend to be unreactive toward molecular hydrogen but in the presence of ions, most of the reactions become very efficient since the ions can easily react without having to overcome the reaction barrier.^{16,28} Shock waves which can arise from the interaction of the Earth's magnetic field with the solar wind, molecular outflows during star formation, supernova blasts and even from galaxies colliding with each other are one of the main sources of energy for chemical reactions in the interstellar medium. The shock waves provide energy for both the formation and distribution of large interstellar species.³⁵ Gas heating caused by shock waves enables neutral-neutral reactions (A+B→C+D) to occur.

1.5. Hydrogen Bonding

Intermolecular interactions are very vital in the elucidation of structure and properties of many biological molecules like water, DNA, proteins, etc. They are embedded in chemical and biological systems by nature. Due to their importance, they are well studied and understood to an extent. Some of these interactions are critical in maintaining the 3-dimensional structure of large molecules such as proteins and nucleic acids. They enable one large molecule to bind specifically but transiently to another, thus making them the basis of many dynamic biological processes. Among the different intermolecular interactions, hydrogen bond is well recognized, studied and understood to a large extent because of its overwhelming impacts in different systems and phenomena. Hydrogen bond underlines the chemical and biological properties of water. It acts as a stabilizing force in macromolecules. The IUPAC task group led by Arunan defined the hydrogen bond as "*The hydrogen bond is an attractive interaction between a hydrogen atom from a molecule or a molecular fragment X-H in which X is more electronegative than H, and an atom or a group of atoms in the same or a different molecule, in which there is evidence of bond formation*".^{36,37} Other intermolecular interactions that have been identified include halogen bonding, lithium bonding, chalcogen bonding, agostic bonding, pnicogen bonding and carbon bonding.^{38,39} Whether hydrogen bonding also exist and play a role in interstellar chemistry will be seen in this Thesis work.

1.6 Definition of Terms

Interstellar chemistry is a multidisciplinary field lying at the interface of Astronomy, Astrophysics, Physics and Chemistry; it therefore becomes pertinent to define some of the keywords used in this Thesis as some of them could be used to mean a different thing in another context. These terms include:

1.6.1 Standard Enthalpy of formation: This is the energy change when one mole of a compound is formed from its constituents' elements in their standard states.⁴⁰ This is represented as ΔH_f^0 .

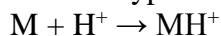
1.6.2 Column Density, Column Amount or Column Abundance, N: This is the number of elementary entities in a vertical column. Specifically, in interstellar chemistry, it is defined as the length of line of sight between observer and a light-emitting (stellar) object. It has the unit of cm^{-2} .¹⁷

1.6.3 Fractional or Abundance Ratio: This is the number of entities X per number of H_2 molecules.¹⁷ This is expressed mathematically as;

1.6.4 Atomization Energy: This is defined as the energy difference between a molecule and its component atoms. For a molecule AB_2 , its atomization energy is computed as: $E(A) + 2(B) - E(AB_2)$. The computed quantity is also synonymously referred to as the total dissociation energy, D_o .⁴⁰

1.6.5 Electron Affinity: This is simply defined as the energy released when an electron is added to a neutral molecule. For a molecule AB_2 , its electron affinity is computed as: $E(AB_2) - E(AB_2^-)$.⁴⁰

1.6.6 Proton Affinity: According to Lias et al.,⁴² the gas phase basicity and proton affinity of a molecule, M are both defined in terms of the hypothetical reaction:



The gas phase basicity is the negative of the free energy change associated with this reaction while the proton affinity is the negative of the corresponding enthalpy change.

1.6.7 Ionization Potential: This is the amount of energy required to remove an electron from a molecule. For a molecule AB_2 , its ionization potential is computed as: $E(AB_2^+) - E(AB_2)$.⁴⁰

1.6.8 Dipole moment: This is a measure of the asymmetry in a molecular charge distribution, and it is given as a vector in three dimensions. It is the first derivative of the energy with respect to an applied electric field.⁴⁰ It is an important parameter in interstellar chemistry because the intensities of rotational transitions scale with the square of the dipole moment, the higher the dipole moment, the higher the intensity of the lines.

1.7 Present Investigations

The focus of this Thesis work is mainly on understanding some of the basic chemistry of the different classes of interstellar molecular species, both the known and postulated species. In Chapter 2, details regarding the methodology employed in this work are presented. Chapter 3 discusses Interstellar Isomers (one of the most conspicuous classes of interstellar molecular species) and the Energy, Stability and Abundance (ESA) relationship which accounts for most of the happenings among interstellar molecules. In Chapter 4, the existence and effect of interstellar hydrogen are reported for the first time. Chapter 5 discusses the Linear Interstellar Carbon Chains which are the dominant theme in interstellar chemistry. In Chapter 6, two unique classes of interstellar molecular species; ions and isotopologues are presented. Future directions and conclusions regarding these studies are presented in Chapter 7. The preliminary report on weakly bound complex of Isoprene...Argon is presented in Appendix I while the study on Interstellar C_3S regarding its dipole moment is reported in Appendix II.

1.8 References

1. Yamada, K. M. T., and Winnewisser, G., in *Interstellar Molecules: Their Laboratory and Interstellar Habitat* (Eds), Yamada, K. M. T., and Winnewisser, G. Springer-Verlag Berlin Heidelberg, 2011.
2. Donati, G. B. *Mon. Not. R. Astron. Soc.*, 1964, 25, 31, 1864.
3. Winnewisser, G., Armstrong, J. T. *The Physics and Chemistry of Interstellar Molecular Clouds*. Lecture Note in Physics 331; Springer, Berlin, 1989.
4. Etim, E. E., Arunan, E. *Planex Newsletter*, 2015, 5(2), 16
5. Weinreb, S., Barrett, A. H., Meeks, M. L., Henry, J. C. *Nature*, 1963, 200, 829
6. Carruthers, G. R. *Astrophys J*, 1970, 161, L81

7. Smith, A. M., Stecher, T. P. *Astrophys J*, 1971, 164,L43
8. Herbst, E., in *Millimeter-Wave Astronomy: Molecular Chemistry and Physics in Space*,(Eds) Wall, W.F., Carramiñana, A., Carrasco, L., Goldsmith, P.F. Kluwer Academic Publishers, 1999.
9. van Dishoeck, E. F, Hartquist, T., Sternberg, A. P. *Natl. Acad. Sci. USA*, 2015, 112(31), 9498
10. Zuckerman, B., Morris, M., Palmer, P., Turner, B. E. *Astrophys J*, 1972, 173,125
11. Thaddeus, P., Guelin, M., Linke, R. A. *Astrophys J*, 1981, 246,L41
12. Swings, P., Rosenfeld, L. *Astrophys J*, 1937, 86,483
13. McKellar, A. *Publ. Astron. Soc. Pac*, 1940, 52,187
14. Douglas, A. E., and Herzberg, G. *Astrophys J*, 1941, 94,381
15. Adams, W. S. *Astrophys J*, 1941, 93,11
16. Shaw, A. M. *Astrochemistry: From Astronomy to Astrobiology*. Wiley, 2006.
17. Rehder, D. *Chemistry in Space: From Interstellar Matter to the Origin of Life*. Wiley- VCH Verlag Co. KGaA, Boschstr. 12, 69469 Weinheim, Germany, 2010.
18. Islam, F. *The Formation of Molecules in the Interstellar Medium*. PhD Thesis. University College London., 2009.
19. Turner, B. E. *Astrophys. J. Suppl. S*, 1991, 76, 617
20. Dickens, J. E., Irvine, W. M.; Ohishi, M., Ikeda, M., Ishikawa, S., Nummelin, A., Hjalmarson, A. *Astrophys J*, 1997, 489,753
21. Cernicharo, J., Heras, A. M.; Tielens, A. G. G. M., Pardo, J. R.; Herpin, F., Guélin, M., Waters, L. B. F. M. *Astrophys J*, 2001, 546, L123
22. Hollis, J. M., Remijan, A. J., Jewell, P. R., Lovas, F. J. *Astrophys J*, 2006, 642, 933
23. Thaddeus, P., Cummins, S. E., Linke, R. A. *Astrophys J*, 1984, 283, 45
24. Thaddeus, P., Vrtilek, J. M., Gottlieb, C. A. *Astrophys J*, 1985, 299, 63
25. Cami, J., Bernard-Salas, J., Peeters, E., Malek, S. E. *Science*, 2010, 329,1180
26. Berné, O., Mulas, G., Joblin, C. *Astron Astrophys*, 2013, 550,L4
27. Belloche, A., Garrod, R. T., Müller, H. S. P.,Menten, K. M. *Science*, 2014, 345, 1584
28. Fraser, H. J., McCoustra., Williams, D. A. *Astron. Geosc*, 2002, 43 (2), 10
29. Tielens, A. G. G.M. *Rev. Mod. Phys*, 2013, 85,1021
30. Atkins, P., and De Paula, J. *Atkins' Physical Chemistry*. Oxford University Press, 9th Edition, 2010.
31. Banwell, C. N., and McCash, E. M. *Fundamentals of Molecular Spectroscopy*. Tata McGraw-Hill, 1995.
32. Meyer, D. M., Roth, K. C. *Astrophys J*, 1991, 376,L49
33. Knauth, D. C., Andersson, B. G., McCandliss, S. R., Moos, H. W. *Natur*, 2004, 409,636
34. Cook, A. H. *Nature*, 1980, 285,359
35. Lovas, F. J., Hollis, J. M., Remijan, A. J., Jewell, P. R. *Astrophys J*, 2006, 645, L137
36. Lodish H, Berk A, Zipursky SL, et al. *Molecular Cell Biology*. 4th edition. New York: W. H. Freeman; 2000.
37. Arunan, E., Desiraju, G. R., Klein, R. A., Sadlej, J., Scheiner, S., Alkorta, I., Clary, D. C., Crabtree, R. H., Dannenberg, J. J., Hobza, P., Kjaergaard, H. G., Legon, A. C., Mennucci, B., Nesbitt, D. *J. Pure Appl. Chem.*, 2011, 83 (8), 1637
38. Mani, D., and Arunan, E. *Phys Chem Chem Phys*, 2013, 15, 14377
39. Shahi, A., and Arunan, E. *Phys Chem Chem Phys*, 2014, 16, 22935
40. Foresman, J. B., and Frish, A. *Exploring Chemistry with Electronic Structure Methods*. Gaussian Inc, Pittsburgh, USA, 2nd ed, 1996.
41. http://www.astrochymist.org/astrochymist_ism.html Accesed in Feb, 2016.
42. Lias, S. G., Liebman, J. F., and Levi, R. D. *J. Phys. Chem. Ref. Data*, 1984, 13(3),695

Chapter 2:

Methodology

Chapter 2: Methodology

2.0 Introduction: Computational Chemistry in Interstellar Chemistry

The advances in science coupled with the developments in computer technology have made it possible for many of the roles played by laboratory work in the field of interstellar chemistry and related areas to be effectively carried out with computational methods with a very high level of accuracy. Besides guiding experimental work in the sequence of events involved from the identification of new molecular species in the interstellar medium (ISM) to the understanding of their chemistry, computational and theoretical methods have been shown to be effective and accurate enough to guide successful detection of new molecular species in ISM and in the understanding of their chemistry.¹⁻⁷ Whereas the conditions in the ISM; low temperature and low pressure, are not easily reproduced in the terrestrial laboratories but these conditions are well suited for computational studies. A number of chemical species that exist in ISM are highly unstable e.g radicals and ions that are very difficult (if not impossible) to synthesize and study in the terrestrial laboratory but studies on such chemical species are well handled computationally.

Quantum chemical calculations play significant role in interstellar chemistry by providing spectroscopic parameters that can guide laboratory detection or astronomical observation of molecules. Understanding of the possible formation routes, kinetics and other properties of interstellar molecular species are well carried out computationally. Computational chemistry involves the simulation of chemical processes and systems numerically based in full or in part on the fundamental laws of physics. Electronic structure theory is one of the main areas under computational chemistry devoted to the study of structure of molecules and their reactivity. Electronic structure methods use the laws of quantum mechanics in predicting the structures and properties of molecules.⁸⁻⁹

2.1 Gaussian Software

Gaussian 09 suite of programs¹⁰ is the main computational software employed for the studies reported in this Thesis. Gaussian computational chemistry program is a general purpose electronic structure package that is capable of computing a wide range of properties such as reaction paths, energies, transition states, vibrational frequencies, excited states, etc. Its use in the scientific community is not only limited to the chemists but physicists, biologists, biochemists, chemical engineers and others in related areas are all beneficiaries of the Gaussian computational software

2.2 Electronic Structure Methods

A theoretical method is a way to model a system using a specific set of approximations. A number of procedures corresponding to different approximations methods/levels of theory are embedded in the Gaussian computational software. In order to compute the properties of interest for any system, these approximations are combined with a calculation algorithm and

are applied to atomic orbitals defined by the basis set. Semi-empirical, ab initio and density functional methods are the main types of electronic structure methods.

2.2.1 Semi-empirical Methods

These methods use a certain number of experimental data to simplify the computation. The use of experimental data dramatically reduces the computational time but in general, these methods are not very accurate. PM3 (Parameterized Model number 3), MINDO (Modified Intermediate Neglect of Differential Overlap), MNDO (Modified Neglect of Diatomic Overlap), AM1 (Austin Model 1) are examples of these methods.¹¹⁻¹³

2.2.2 Ab Initio Methods

Ab initio methods use no experimental data in their computations rather their computations are based only on the laws of quantum mechanics or theoretical principles. They provide very high quality quantitative predictions for a broad range of systems. Hartree-Fock is the basic ab initio method. The limitations associated with Hartree-Fock calculations arise from the fact that Hartree-Fock theory does not involve a full treatment of the effect of electron correlation i.e the energy contribution arising from electrons interacting with one another. The effect of electron correlation is treated in an average sense by Hartree-Fock theory.¹⁴⁻¹⁶

The second order second-order Moller-Plesset perturbation theory, MP2 [and its other variants, MPn (n=2,3,...,6)] start with the Hartree-Fock calculation and include some treatments of the effect of electron correlation. The MP2(full) method which is employed for some of the studies reported in this Thesis explicitly considers inner shell electrons also in estimating the correlation energy. Configuration interaction (CI) methods are ab initio methods oftenly used for excited states. They are found to be very accurate but require expensive computational resources. They include the CID (configuration interaction with all double substitutions), CISD (configuration interaction with all single and double substitutions), QCISD (quadratic configuration interaction calculation with single and double excitations).¹⁷⁻²⁰ The coupled cluster method including singles and doubles and optional triple terms CCSD(T) is widely regarded as the "gold standard" because of its ability in predicting high accurate parameters that are in good agreement with experimental values for a wide range of systems. However, the very high computational time and resources required by this method limit its applications.²¹

2.2.3 Density Functional Theory (DFT)

DFT methods are becoming more and more attractive because they give result that are comparable to the ones obtained using ab initio methods but the computational resources and time are drastically reduced in the case of DFT methods as compared to the ab initio methods. Traditional methods in electronic structure theory like the ab initio methods are based on many-body electronic wave function while in DFT, the many-body electronic wave function

is replaced with electron density as the basic quantity. The Becke, three-parameter, Lee-Yang-Parr (B3LYP) is the most popular and commonly used DFT method. The exchange component of Perdew and Wang's 1991 functional; PW91 (gradient-correlated method) and VWN (a method based on local density approximation) are DFT methods among others.²²⁻²⁶

2.3 Compound Methods

These are general procedures for computing the total energies of molecular species at their equilibrium geometries. Unlike the traditional electronic structure methods described above that consist of a single job, compound methods consist of several component calculations whose results are then combined in a predefined way. They combined both Hartree-Fock and Post-SCF methods. They are used in archiving high accuracy results at less computational cost. The Gaussian theory 4 (G4 and G4MP2) and Weizmann-1 theory (W1 and W1U) and Weizmann-2 theory (W2 and W2U) compound methods have been extensively used in calculating the thermochemical properties for most of the systems reported in this Thesis work.

Even though multiple calculations are carried out, their total computational requirement is still significantly less than that of the single high accuracy method which they are designed to approximate. Table 2.1 shows a brief summary of the different methods used at various steps of calculations in the G4, G4MP2, W1U and W2U compound methods. They are found to estimate thermochemical quantities within chemical accuracy (i.e. the accuracy required to make realistic chemical predictions and is generally considered to be 1 kcal/mol or 4 kJ/mol). This is not true in all cases especially for the radicals, unstable species, etc, as shown in chapter three of this Thesis.²⁷⁻²⁹

Table 2.1: Different methods for different calculations in compound methods

Calculation	G4	G4MP2
Geometry optimization	B3LYP/6-31G(2df,p)	B3LYP/6-31G(2df,p)
ZPE	B3LYP/6-31G(2df,p) Scaled by 0.9854	B3LYP/6-31G(2df,p) Scaled by 0.9854
Single-point calculations	MP4/6-31G(d) modified by corrections from additional cals. (with MP4 and other methods)	CCSD(T)/6-31G(d) modified by corrections from additional cals. (with MP2 and other methods)
Energy	MP4/6-31G(d) and the corrections from previous step.	CCSD(T)/6-31G(d) and the corrections from previous step./6-31G(d)
Core correlation	Higher level correction terms.	Higher level correction terms.
Calculation	W1U	W2U
Geometry optimization	B3LYP/cc-pVTZ	CCSD(T)/cc-pVQZ
ZPE	B3LYP/cc-pVTZ	CCSD(T)/cc-pVTZ
Single-point calculations	CCSD(T)/aug-cc-pVDZ	CCSD(T)/aug-cc-pVQZ
Energy	SCF/aug-pVDZ	SCF/aug-pVQZ
Core correlation	CCSD/MT	CCSD/MT

2.4 Basis Sets

Simply put, a basis set is a mathematical representation of the molecular orbitals within a molecule. The basis set can be interpreted as restricting each electron to a particular region of space. The larger the basis set, the fewer the constraints imposed on the electrons and the more accurate the exact molecular orbital can be approximated. The larger basis set of course will require more computational resources. The main types of basis sets are briefly discussed below:

2.4.1 Minimal Basis Sets

These are the basis sets that contain the minimum number of basis functions needed for the description of each orbital. The most common minimal basis set is the STO-nG, where n is an integer. The value of n represents the number of Gaussian Type Orbitals (GTOs) used in describing one STO (Slater Type Orbital). Minimal basis sets do not give very accurate results; $n < 3$ gives very poor results, thus STO-3G is regarded as the minimal basis set. Minimal basis sets are computationally inexpensive, thus they are still in use today especially for very large molecules.^{30,31}

2.4.2 Split Valence Basis Sets

These are also called Pople basis sets. They allow specific number of GTOs to be used in describing the core and valence electrons separately. The notation for the split valence basis set is typically N-MPXG, where N is the number of Gaussian functions used in describing the inner shell orbitals, - indicates split valence basis set, MP indicates the number of Gaussian functions used in fitting the different size of say 1s orbitals, MPX in the case of p orbitals, G indicates that GTOs are used. The 6-311G basis set which uses 6GTOs for core orbital; 3GTOs for inner valence and 2 different GTOs for outer valence is used alongside the diffuse and polarized basis functions (described below) in most of the calculations reported in this Thesis.⁹

The split valence basis set has a limitation of only allowing the orbitals to change size but not shape. This limitation is removed by polarized functions which are auxiliary functions with one additional node and are denoted by a single asterisk (*) and double asterisk (**). They add orbitals with angular momentum beyond what is required for the ground state to the description of each atom. A single asterisk indicates that polarization function is added to heavy atoms while a double asterisk implies that polarization functions are added to both hydrogen and heavy atoms. The split valence basis sets allow the orbitals to change size, the addition of the polarization functions enables the orbitals to change shape. The split valence basis set can yet be modified through the addition of diffuse functions. Diffuse functions allow the electrons to move far away from the nucleus, creating diffuse orbitals. They are denoted in the Split valence/Pople basis sets by a plus (+) sign and "aug" (augmented) in Dunning-type basis sets/correlation consistent basis set (this is described in section 2.5.3). A

single plus sign indicates that diffuse functions are added to atoms other than hydrogens while a double plus sign (++) entails the addition of diffuse functions to all atoms including hydrogens.^{9,32,33}

2.4.3 Correlation-Consistent Basis Set

All of the basis sets described above are optimized at the Hartree-Fock level. With the doubt that this optimization might not be the best for correlated system computations; Dunning and co-workers created a set of basis sets designed to converge systematically to the complete basis set (CBS) limit using extrapolation techniques. These are denoted as cc-pVXZ where cc stands for correlation consistent; pV indicates that it is a polarized valence basis set and XZ stands for the zeta number (X=D for double, T for triple, Q for quadrupole, 5,6,7). They include successively large shells of polarization (correlating) functions (d,f,g, etc). The prefix 'aug' (augmented) is used in adding diffuse functions. The 6-311++G**, cc-pVXZ and aug-cc-pVXZ (X=D or T) are used in all the calculations reported in this Thesis. All of these basis sets are well studied and are known to give reliable results. The compound methods; G4, G4MP2, W1U and W2U used in some of the computations reported in this Thesis do not require the user to choose the basis set to work with. They use basis sets that are predefined.^{9,34-36}

2.5 Basis Set Superposition Error (BSSE)

The Boys-Bernadi counterpoise procedure is followed in eliminating BSSE for all the quantum chemical calculations involving interaction energies. When finite basis sets are used for estimating interaction energies in a quantum chemical calculation, such calculation is susceptible to BSSE. This is because as the atoms of the interacting molecules or different parts of the same molecule approach one another, their basis function overlap.³⁷ For a dimer A...B formed by the monomers A and B, the BSSE following the Boys-Bernadi counterpoise procedure is calculated as follows:

$$E_{BSSE} = E_A + E_B - [E_A(AB) + E_B(AB)]$$

where E_A and E_B are the energies of the monomers A and B respectively at the same basis set as that of AB. $E_A(AB)$ is the energy of the monomer 'A' calculated by taking its geometry in AB at the same level of theory as that of AB while $E_B(AB)$ is the energy of the monomer 'B' calculated by taking its geometry in AB at the same level of theory as that of AB. The basis set corrected interaction energy ΔE_{BSSE} is calculated as follows

$$\Delta E = E_{AB} - (E_A + E_B)$$

$$\Delta E_{BSSE} = \Delta E + E_{BSSE}$$

2.6 Major Calculations Using Gaussian Software

A number of calculations have been performed using the Gaussian 09 suit of programs for this Thesis work. However, the key calculations that have led to the reported results in this Thesis are briefly summarized below. The Gaussian reference manual (both hard copy and the online version) contains details of all the possible calculations that could be performed with the software.³⁸

2.6.1 Geometry Optimization

This is simply the first derivative of the energy with respect to atomic positions. Every physical system tends to have its shape, position, geometry, arrangement, etc, corresponding to the least energy possible. What geometry optimization does is attempting to find the configuration of minimum energy of the system under investigation. The whole idea in geometry optimization is how to find a minimum of a mathematical function wherein the geometry is dependent on many variables (especially internal or Cartesian coordinates of a molecule). The procedure calculates the wave function and the energy at the starting geometry and thereafter proceeds to search a new geometry of a lower energy. The process is repeated until the lowest energy geometry is found. A successful geometry optimization will give the following key information among others; dipole moment, rotational constants, moments of inertia, atomic distances and angles, HOMO/LUMO eigen values, atomic coordinates for the optimized geometry, Mulliken atomic charges, etc. The keyword for this calculation in Gaussian 09 suit of programs is 'opt'.^{9,39,40}

2.6.2 Frequency Calculation

Unlike geometry optimization, frequency calculation is the second derivative of the energy with respect to the nuclear or atomic positions. By default, every frequency calculation also includes a section for thermochemistry. The keyword 'freq' is used to initiate frequency calculation in the Gaussian software. In order to arrive at accurate predictions that are in good agreement with experimental values (where available), scaling factors have been developed for different theoretical methods and basis sets through detailed benchmarking studies. These scaling factors can be incorporated in frequencies and thermochemistry calculations using the keyword 'Scale=X' where X is the scaling factor.

All the calculations reported in this Thesis are for stable structures with no imaginary frequency. This stability check is one of the main reasons for carrying out frequency calculation. The thermodynamic parameters computed during the vibrational analysis are based on ideal gas assumptions and rigid-rotor harmonic-oscillation approximations. This assumption of non-interacting particles (ideal gas assumption) will introduce some errors depending on the extent that any system being studied is non-ideal. Every successful frequency calculation leaves the researcher with so much properties/data to think about. Besides all the properties that are obtained from geometry optimization, the following are also computed during vibrational analysis; single point energy, IR intensities, force constants, reduced masses, Harmonic frequencies, Raman intensities (on demand) and the thermodynamic properties such as entropy, free energy, enthalpy, temperature, pressure, isotopes used, molecular mass, thermal energy, constant volume molar heat capacity.^{9,38}

2.6.3 Stability Check

A molecule can be stable in more than one electronic state e.g. singlet and triplet in the cases of the C_n , HC_nN , C_nO , C_nS etc linear carbon chains.⁴² The stability check initiated in the

Gaussian suit of programs via the keyword 'stable' determines whether the wave function computed for the molecular system is stable or not. For a stable geometry, the output file will contain the following message "***The wave function is stable under the perturbation considered***" while for unstable geometry, the following message will be found "***The wave function has internal instability***". This procedure has been employed in this study especially for systems with no experimentally determined ground electronic states like some of the linear carbon chains, radical, ions, etc.^{38,42}

2.7 Atoms in Molecule Theory (AIM)

AIM theory developed by Richard F. W. Bader is used in quantifying the strength and nature of inter and intra-molecular bonds. The basic concept of the AIM theory is to understand the topology of electron density (ρ) of the atoms in a molecule. It examines the distribution (variation) of electron density at every point around the nucleus of a molecule. The electron density can be directly estimated from the wave function and from the electron density critical points arising from the analysis; the nature of the bonding within a molecule can be quantified. A critical point is a point in space at which the gradient of the electron density ($\nabla\rho$) vanishes. The second derivative of the electron density is used in deciding the nature of the critical point.^{43,44} The different critical points classified based on the eigen values of the Hessian matrix of electron density are briefly summarized below:

2.7.2 Types of Critical Points

Electron density varies along three different directions, thus in a 3D space, one can write the Hessian for the electron density function. Critical points are classified based on the Hessian matrix of electron density. The critical points are denoted as (r,s) where 'r' is the rank (i.e the number of its non-zero eigen value) and 's' is the signature (the algebraic sum of the signs of non-zero eigen values) of the Hessian matrix. Based on the above information, the different critical points are defined as follows:

Nuclear Attractor: This is denoted as (3,-3) which implies that the electron density is maximum along each of the three directions. Here, all the three eigenvalues are non-zero and the curvatures corresponding to these eigenvalues are maxima (i.e with a negative sign) in all three directions. Generally, this critical point corresponds to the nucleus of atoms in a molecule.

Bond Critical Point (BCP): BCP is denoted as (3,-1) which implies that two curvatures are negative, thus the electron density is minimum in one direction and maximum along the other two directions. BCP appears between two atoms. The presence of BCP between two atoms and the presence of bond paths connecting the two atoms denote bonding between the two atoms.

Ring Critical Point (RCP): This is denoted as (3, +1) implying that the electron density is minimum along two directions and maximum along the third direction. RCP is present at the

centre of cyclic structures like benzene. The distance between RCP and BCP shows the stability of a bond. The longer the distance, the more stable the bond and vice versa.

Cage Critical Point (CCP): CCP is denoted as (3, +3) which means that electron density is minimum in all directions. CCP is found at the centre of cage structures e.g cubane.

2.8 Pulsed Nozzle Fourier Transform Microwave (PN-FTMW) Spectrometer

The homebuilt PN-FTMW spectrometer in our laboratory has been used for the preliminary studies on the Isoprene...Argon weakly bound complex. Details of the working principles and components of this instrument can be found in the review on its advances and application.⁴⁵

2.9 Summary

This chapter dedicated to the methodology employed in this Thesis work begins by setting the stage on the importance of computational chemistry in interstellar chemistry. The Gaussian 09 suit of programs and the various theoretical methods used in all the quantum chemical calculations reported in this Thesis are discussed. The choice of our basis sets which is based on experience, literature reports and the major calculations executed with the Gaussian 09 suit of programs are explained. The AIM theory used in characterizing the nature of bonds (intra and inter-molecular) is briefly summarized. The chapter ends with a brief summary on the homebuilt PN-FTMW spectrometer used for the preliminary studies on Isoprene...Argon weakly bound complex reported in the appendix.

2.10 References

1. Ziurys, L. M., Turner, B. E. *Astrophys J*, 1986, 302,L31
2. Green, S., Montgomery, Jr., J. A., Thaddeus, P. *Astrophys J*, 1974, 193,L89
3. Guélin, M., Thaddeus, P. *Astrophys J*, 1977, 212,L81
4. Buhl, D., Snyder, L. E. *Nature*, 1970, 228,267.
5. Woods, R. C., Gudeman, C. S., Dickman, R. L., et al. *Astrophys J*, 1983, 270,583
6. Zuckerman, B., Morris, M., Palmer, P., Turner, B. E. *Astrophys J*, 1972, 173,L125.
7. Tucker, K. D.; Kutner, M. L.; Thaddeus, P. *Astrophys J*, 1974, 193,L115
8. Puzzarini, C. Reference Module in Chemistry, Molecular Sciences and Chemical Engineering. <http://dx.doi.org/10.1016/B978-0-12-409547-2.10836-4>
9. Foresman, J. B., and Frish, A. Exploring Chemistry with Electronic Structure Methods. Gaussian Inc, Pittsburgh, USA, 2nd ed, 1996.
10. Frisch, M. J.; Trucks, G. W.; Schlegel, H. B.; Scuseria, G. E.; Robb, M. A.; Cheeseman, J. R.; Scalmani, G.; Barone, V.; Mennucci, B.; Petersson, G. A.; Gaussian 09, revision D.01; Gaussian, Inc., Wallingford, CT, 2009.
11. Michael J. S. Dewar and Walter Thiel. *J. Am. Chem. Soc*, 1977, 99 (15),4899
12. Michael J. S. Dewar, Eve G. Zoebisch, Eamonn F. Healy, James J. P. Stewart. *J. Am. Chem. Soc*, 1985, 107 (13), 3902
13. James J. P. Stewart. *J. Comput. Chem*, 1989, 10 (2),209
14. Roothaan, C. C. *J. Rev. Mod. Phys.*, 1951, 23, 69
15. Pople, J. A., and Nesbet, R. K. *J. Chem. Phys*, 1954, 22, 571
16. McWeeny, R., and Dierksen, G. *J. Chem. Phys*, 1968, 4852
17. Møller, N., and Plesset, M. S. *Phys. Rev*, 1934, 46, 0618

18. Head-Gordon, M., Pople, J. A., and Frisch, M. *Chem Phys Lett*, 1988, 153, 503
19. Head-Gordon, M., and Head-Gordon, T. *Chem Phys Lett*, 1994, 220, 122
20. John A. Pople, Martin Head-Gordon, and Krishnan Raghavachari. *J. Chem. Phys*, 1987, 87 (10), 5968
21. Pople, J. A., Head-Gordon, M., and Raghavachari, K. *J. Chem. Phys*, 1987, 87, 5968
22. Parr, G., and Yang, W. *Density-functional theory of atoms and molecules*, Oxford Univ. Press, Oxford, 1989.
23. Becke, A. D. *J. Chem. Phys*, 1996, 104, 1040
24. Perdew, J. P., Chevary, J. A., Vosko, S. H., Jackson, K. A., Pederson, M. R., Singh, D. J., and Fiolhais, C. *Phys Rev B*, 1993, 48, 4978
25. Perdew, J. P., Burke, K., and Wang, Y. *Phys Rev B*, 1996, 54, 16533
26. Vosko, S. H., Wilk, L., and Nusair, M. *Can J Phys*, 1980, 58, 1200
27. Martin, J. M. L; de Oliveira, G. *J. Chem. Phys*, 1999, 111, 1843
28. Curtiss, L. A.; Redfern, P. C.; Raghavachari, K. *J. Chem. Phys*, 2007, 126, 084108
29. Curtiss, L. A.; Redfern, P. C.; Raghavachari, K. *J. Chem. Phys*, 2007, 127, 124105
30. Hehre, W. J., Stewart, R. F., and Pople J. A. *J. Chem. Phys*, 1969, 51, 2657
31. Collins, J. B., Schleyer, P. v. R., Binkley, J. S., and Pople, J. A. *J. Chem. Phys*, 1976, 64, 5142
32. Petersson, G. A., Bennett, A., Tensfeldt, T. G., Al-Laham, M. A., Shirley, W. A., and Mantzaris, J. *J. Chem. Phys*, 1988, 89, 2193
33. Petersson, G. A., and Al-Laham, M. A. *J. Chem. Phys*, 1991, 94, 6081
34. Dunning Jr., T. H. *J. Chem. Phys*, 1989, 90, 1007
35. Kendall, R. A., Dunning Jr., T. H., and Harrison, R. J. *J. Chem. Phys*, 1992, 96, 6796
36. Woon, D. E., and Dunning Jr., T. H. *J. Chem. Phys*, 1993, 98, 1358
37. Boys, S. F., and Bernardi, F. *Mol Phys*, 1970, 19, 553
38. http://www.gaussian.com/g_tech/g_ur/g09help.htm Accessed in Feb, 2016
39. Li, X., and Frisch, M. J. *J. Chem. Theory Comput.*, 2006, 2, 835
40. Baker, J. *J. Comput. Chem*, 1993, 14, 1085
41. Jochnowitz, E. B., and Maier, J. P. *Annu Rev Phys Chem*, 2008, 59, 519
42. Seeger, R., and Pople, J. A. *J. Chem. Phys*, 1977, 66, 3045
43. Bader, R. W (1994). *Atoms in Molecules: A Quantum Theory*. USA: Oxford University Press. ISBN 978-0-19-855865-1.
44. Bader, R. W. *Chem Rev*, 1991, 91, 893
45. Arunan, E., Dev, S., and Mandal, P. K. *Appl. Spectrosc. Rev.*, 2004, 39, 1

Interstellar Isomers: Energy, Stability and Abundance (ESA) Relationship among Interstellar Molecules

Setting the stage: The first main chapter of this Thesis begins with the most important class of interstellar molecular species; '**interstellar isomers**'. The first part of these studies leads to the establishment of the Energy, Stability and Abundance (ESA) relationship existing among the interstellar and circumstellar isomers. After few studies on the immediate consequences of the ESA relationship; detailed studies employing the ESA relationship in addressing some of the whys and wherefores in interstellar chemistry are presented.

3.0 Introduction

The importance of chemistry in the interstellar space cannot be overemphasised. The interstellar space is not just an open vacuum dotted with stars, planets and other celestial formations as it is considered to be in popular perception; rather it consists of a bizarre mixture of both familiar molecules such as water, ammonia etc., and a large number of exotic ones such as radicals, acetylenic carbon chains, highly reactive cationic and anionic species, carbenes and high molecular isomers that are so unfamiliar in the terrestrial laboratory that chemists and astronomers have termed them “non-terrestrial”. The development of radio-astronomical techniques and the close collaboration between laboratory spectroscopists and astrophysicists have resulted in the detection of over 200 different molecular species in the interstellar space largely via their rotational emission spectra during the last few decades. These molecules are used as probes of astrophysical phenomena. The density and temperature of the gas phase species observed in the interstellar medium (ISM) are determined from the observed spectra (rotational and vibrational) of these species. Of course these molecules are exciting clues to the chemical origin of life and serve as powerful tool in addressing the unanswered chemistry question; how the simple molecules present on the early earth may have given rise to the complex systems and processes of contemporary biology.¹⁻⁶

Despite the importance of these molecules, not much is known about how they are formed under the low temperature and low density conditions of the interstellar clouds. This has led to the lack of a consensus on how most of these molecules; especially the complex (those with six atoms and above) ones are formed in ISM. Gas phase reactions and reactions that occur on the surface of the interstellar dust grains are the dominant processes believed to be responsible for the formation of these molecules. The formation of molecular hydrogen is assumed to occur via the reactions on the surface of the interstellar dust grains. Molecular hydrogen plays a pivotal role in the formation of other molecular species in ISM. Among the known interstellar and circumstellar molecular species, some of the common features observed include isomerism, successive hydrogen addition, dominance of carbon containing species, and periodic trends. These serve as pointers towards how these molecules are formed in the interstellar medium^{7,8}

Of all the observed concepts existing among interstellar molecules, the impact of isomerism appears to be very important. Isomerism has now emerged as an important concept in interstellar chemistry as more and larger isomeric species are being detected in the interstellar medium. Excluding the diatomic species, a number of hydrogen saturated species and other special species like the C₃, C₅, which cannot form isomers, about 40% of all interstellar molecules have isomeric counterparts.^{6,7} Table 3.1 lists some of the known interstellar isomeric pairs, triads and their corresponding isomeric groups. The clear existence of isomerism among interstellar molecules suggests that molecular formation routes for isomeric species may have common precursors for their formation processes.^{7,9}

Table 3.1: Known interstellar isomeric pairs, triads and their isomeric groups.

Isomeric Group	Astronomically observed isomers	
CHN	HCN, HNC	
CNMg	MgCN, MgNC	
CNSi	SiCN, SiNC	
CHO ⁺	HOC ⁺ , HCO ⁺	
CHSN	HSCN, HNCS	
HC ₃	c-C ₃ H, l-C ₃ H	
H ₂ C ₃	c-C ₃ H ₂ , l-C ₃ H ₂	
CN ₂ H ₂	NH ₂ CN, HNCNH	
C ₃ H ₂ O	HCCCHO, c-H ₂ C ₃ O	
C ₄ H ₂	H(CC) ₂ H, H ₂ C ₄	
C ₆ H ₂	H ₂ C ₆ , H(CC) ₃ H	
C ₄ H ₃ N	CH ₂ CCHCN, CH ₃ CCCN	
C ₂ H ₆ O	(CH ₃) ₂ O, CH ₃ CH ₂ OH	
C ₃ H ₆ O	(CH ₃) ₂ CO, CH ₃ CH ₂ C(O)H	
C ₃ H ₆ O ₂	HC(O)OCH ₂ CH ₃ , CH ₃ OC(O)CH ₃	
C ₄ H ₇ N	n-CH ₃ CH ₂ CH ₂ CN, b-CH ₃ CH ₂ CH ₂ CN	
CHON	HNCO, HCNO, HOCHN	
C ₂ H ₄ O ₂	CH ₃ COOH, HC(O)OCH ₃ , HOCH ₂ C(O)H	
C ₂ H ₄ O	CH ₂ CH(OH) c-C ₂ H ₄ O, HC(O)CH ₃	
C ₂ H ₃ N	CH ₃ CN, CH ₃ NC, H ₂ CCNH	
C ₃ HN	HC ₂ CN, HC ₂ NC	HNCCC

With the concept of isomerism among interstellar molecules almost becoming an “established” chemistry, it can therefore be explored in unravelling other basic chemistry among the interstellar species. Astronomical searches for isomeric analogues of known interstellar molecular species have been both successful and unsuccessful in many cases. Since interstellar isomeric species are considered to possibly have common precursors for their formation. The question arises “*why are some isomeric species observed in the interstellar space and others not?*”

In addressing this question and other whys and wheresores among the astromolecules, we employ high level quantum chemical calculations with the aim of extensively investigating the relationship; energy (enthalpy of formation), stability and abundance (ESA) among interstellar molecules which could influence the astronomical observation of some molecules at the expense of others. For this investigation, we have considered 130 molecules comprising of 31 isomeric groups (with at least one molecule astronomically observed from each isomeric group considered) and 24 cyanide/isocyanide pairs with atoms ranging from 3 to 12. To the best of our knowledge, the extensive investigation of this relationship under consideration has not been reported in literature until now.

3.1.0 Computational Methods

The Gaussian 09 suite of programs is employed for all the quantum chemical calculations reported in this work.¹⁰ A few of the molecules considered in this study have experimentally measured standard enthalpy of formation ($\Delta_f H^0$) while many of them do not. Theoretical

methods that can predict accurate enthalpies of formation for the molecules with experimentally known Δ_fH^0 values are highly desirable as such methods should by extension be able to predict enthalpies of formation of similar molecules with no experimentally measured values to chemical accuracy. The compound methods which combine both the Hartree-Fock and Post-SCF methods offer high accuracy at less computational cost are used in this study. In this study, the Weizmann 1 and Weizmann 2 theory represented as W1U and W2U respectively and the Gaussian methods; G3, G4 and G4MP2 are employed in determining the standard enthalpies of formation for all the molecules considered in this study.^{11,12,13} While the Weizmann methods (W1U and W2U) employ different levels of theory for geometry optimization, zero-point energy, single point calculations and energy computations, the Gaussian G4 and G4MP2 theories use the same method in their geometry optimization and zero-point energy calculations while different methods are employed in their single point calculations and energy computation. The reported zero-point corrected standard enthalpies of formation of all the molecules considered in this study were calculated from the optimized geometries of the molecules at the levels of theory mentioned above. In characterizing the stationary nature of the structures, harmonic vibrational frequency calculations were used with equilibrium species possessing all real frequencies.

3.1.1 Atomization energies and enthalpy of formation

Considering a wide range molecules with known and unknown enthalpies of formation, the total atomization energies method is more advantageous than methods like isodesmic and Benson group additivity. With a good computational method and accurate experimental values of standard enthalpy of formation of the constituents' elements involved, very high accurate enthalpies of formation can be estimated for different set molecular systems. Atomization energies (sometimes synonymously referred to as the total dissociation energies (D_0)) were evaluated using the calculated values of energies (sum of electronic and zero-point energy corrections) with the methods described in the computational methods above. For a reaction,



The expression for computing the atomization energy of the molecule (A_2B) is given as;

$$\sum D_0(A_2B) = 2E_0(A) + E_0(B) - E_0(A_2B) \quad (2)$$

In calculating the enthalpy of formation (Δ_fH^0) at 0 K for all the molecules reported in this study, the experimental values of standard enthalpy of formation of elements C, H, O, N, Na, Mg, Al, Si and S reported in literature¹⁴ were used. These values are reported in the Table 3.2. Values are given in kcal/mol.

Table 3.2. Experimental $\Delta_f H^0(0K)$, of elements and $H^0(298K) - H^0(0K)$

Element	$\Delta_f H^0(0K)$	$H^0(298K) - H^0(0K)$
H	51.63±0.01	1.01
C	169.98±0.1	0.25
O	58.99±0.02	1.04
N	112.53±0.02	1.04
Na	25.69±0.17	1.54
Mg	34.87±0.2	1.19
Al	78.23±1.0	1.08
Si	106.6±1.9	0.76
S	65.66±0.06	1.05

The enthalpy of formation at 0 K is calculated using the following expression:

$$\Delta H_f^0(A_2B,0K) = 2\Delta H_f^0(A,0K) + \Delta H_f^0(B,0K) - \sum D_0(A_2B) \quad (3)$$

The enthalpy of formation at 298 K is calculated using the following expression:

$$\Delta H_f^0(A_2B,298K) = \Delta H_f^0(A_2B,0K) + (H_{A_2B}^0(298K) - H_{A_2B}^0(0K)) - [2\{H_A^0(298K) - H_A^0(0K)\} + \{H_B^0(298K) - H_B^0(0K)\}] \quad (4)$$

From equation 4, $H_{A_2B}^0(298K) - H_{A_2B}^0(0K)$ is defined as $H_{\text{corr}} - E_{\text{zpe}}$. Where $H_{\text{corr}} = E_{\text{tot}} + k_B T$ and $E_{\text{tot}} = E_t + E_r + E_v + E_e$, where the subscripts refer to translational, rotational, vibrational and electronic, respectively. Thermal energies were calculated using rigid-rotor harmonic-oscillator approximations, in built in Gaussian code.

The above description for calculating enthalpy of formation is only valid for neutral molecules. For ions, this is obtained from the enthalpy of formation of the corresponding neutral species; this value is then added to the ionization potential (if it is a cation) or the electron affinity (if it is an anion).

3.2 Result and Discussion

Experimental values of enthalpy of formation for some of the molecules considered in this study are known. These values were taken from the NIST¹⁵ database (except otherwise stated) and are reported in some of the Tables (as expt). The G3 method gives enthalpy of formation values that are extremely different from the experimentally measured values. This shows how "unreal" theoretical thermochemistry could be with some methods. The values from this method are not used in the following discussion. Among the different high level quantum chemical calculation methods employed in this study, the G4 method gives the best estimate of the enthalpy of formation for the different molecules considered in this study with the difference between the theoretically calculated enthalpy of formation and the experimentally measured enthalpy of formation $\leq \pm 5\text{kcal/mol}$ for molecules whose experimental enthalpy of formation values are known. The calculated enthalpies of formation are also subject to the uncertainties in the experimental values of the standard enthalpy of

formation of the elements used in calculating the enthalpy of formation at 0 k. All the reported enthalpies of formation (from both theory and experiment) in this study are reported in kcal/mol and at 298.15K. The different plots (Figures 3.1-3.6, 3.8-3.10, 3.12) reported in this paper are based on the enthalpy of formation values obtained with the G4 method. The following subsections discuss the results obtained using the various methods employed in this study. The different isomeric groups are grouped according to the number of atoms, starting from 3 to 12.

3.2.1 Isomers with 3 atoms: The zero-point corrected standard enthalpies of formation ($\Delta_f H^0$) for the different isomeric groups with three atoms considered in this study are shown in Table 3.3, with their current astronomical status. The G4 method estimates the enthalpy of formation for both HCN and HNC (whose experimental enthalpy of formation values are known) to chemical accuracy, i.e., the difference between the theoretically calculated values and the experimentally measured values are within ± 1 kcal/mol. The CNO^- isomeric group is the only ion considered in this study. For the OCN^- , the calculated value with the W1U method is in excellent agreement with the experimental value. From Table 3.3, the zero-point corrected standard enthalpies of formation at the G4 and G4MP2 levels of theory are approximately the same while there are slight differences in the values obtained with the W1U and W2U methods.

In all the 6 isomeric groups considered here, the isomers with lower enthalpies of formation have all been observed in the interstellar space while only 3 of the isomers with higher enthalpies of formation have been observed. This implies that the lower the enthalpy of formation, the more stable the molecule, and the higher the stability of a molecule, the higher its abundance in the interstellar medium which makes it easy for the astronomical observation of such molecule.

In almost all the cases considered here, where both isomers have been observed, it is the most stable isomer that was first observed before the less stable one (HCN before HNC, MgNC before MgCN), implying that the most stable isomer, which is likely to be the most abundant, is astronomically easier to be detected than the less stable isomer.¹⁶⁻²⁶ HCN which is more stable than HNC is found to be more abundant than HNC in different molecular clouds^{27,28}. This is also the case for the MgNC/MgCN abundance ratio measured in the asymptotic giant branch (AGB) stars^{21,20}. AlNC also has a lower enthalpy of formation than AlCN and it has been observed while AlCN is yet to be observed.

Figure 3.1 depicts the plot of the $\Delta_f H^0$ for the molecules with 3 atoms considered in this study. It is clear from the plot that the non-observed molecules (indicated with open symbols) are the ones with higher $\Delta_f H^0$ values in their respective isomeric groups compared to the ones that have been astronomically observed (indicated with filled symbols).

Table 3.3: $\Delta_f H^0$ of isomers with 3 atoms and current astronomical status

Molecule	$\Delta_f H^0$ (kcal/mol)						Astronomical status
	W1U	W2U	G3	G4MP2	G4	Expt	
HNC	45.03	44.7	46.0	45.6	45.6	46.5±2.2	Observed
HCN	31.3	31.4	31.3	32.2	32.2	32.30	Observed
NaNC	36.4	45.3	28.4	34.5	37.0		Not observed
NaCN	34.3	43.8	28.4	34.5	34.5	22.5±0.5 ²⁹	Observed
MgCN	67.7	67.3	66.5	69.0	69.0		Observed
MgNC	65.6	65.6	65.7	69.7	65.8		Observed
AlCN	71.8	72.3	68.4	73.1	73.1	71.9±3.3 ³⁰	Not observed
AlNC	65.2	65.2	63.2	65.8	65.8	66.5±3.3 ³⁰	Observed
SiCN	105.1	105.2	105.8	105.9	105.9		Observed
SiNC	105.3	105.3	107.5	105.7	105.7		Observed
ONC ⁻	14.3	14.2	14.3	12.4	12.4		Not observed
OCN ⁻	-53.7	-54.0	-53.4	-54.5	-54.5	-52.8 ³¹	Observed

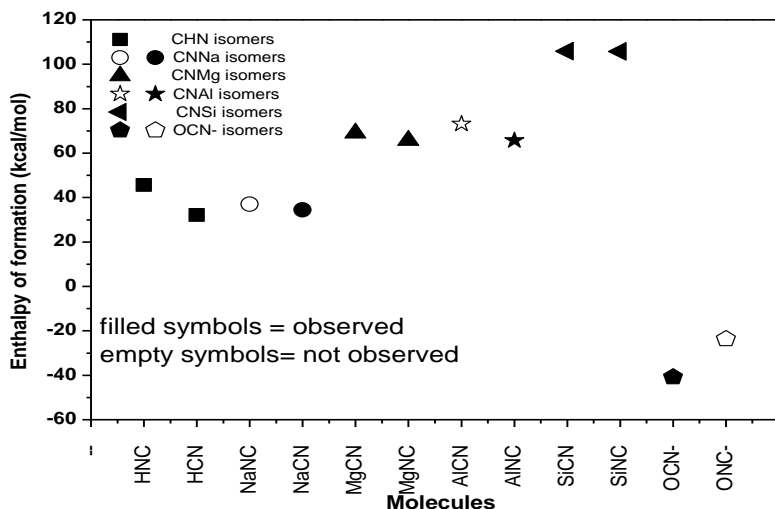


Figure 3.1: Plot showing the $\Delta_f H^0$ for molecules with 3 atoms

3.2.2 Isomers with 4 atoms: Table 3.4 gives the zero-point corrected standard enthalpies of formation, $\Delta_f H^0$ in descending order of magnitude for isomers with 4 atoms considered in this study. There is a dearth of information regarding the experimental standard enthalpy of formation values for some of these molecules. For all the CHNO isomers (isocyanic acid, cyanic acid, fulminic acid and isofulminic acid) shown in Table 3.4, the calculated enthalpies of formation at the G3 level are in good agreement with the experimental values reported by Schuurman and co-workers.¹⁸⁴ The reported¹⁸² enthalpy of formation value of -31.0 kcal/mol for isocyanic acid is in good agreement with the values predicted at the W1U and W2U methods. But there is a marked difference between the experimental $\Delta_f H^0$ value for the same molecule reported in the NIST website¹⁵ (-23±3.1kcal/mol).

Molecules with the empirical formula CHNO are the simplest species which contain the four most important biogenic elements; carbon, hydrogen, nitrogen and oxygen. As a result, their astronomical observations are important from both the astrobiological and prebiotic chemistry perspectives.³²

Table 3.4: $\Delta_f H^0$ for isomers with 4 atoms and current astronomical status

Molecule	$\Delta_f H^0$ (kcal/mol)						Astronomical status
	W1U	W2U	G3	G4MP2	G4	Expt	
Isofulminic acid	55.1	55.5	55.7	52.8	52.8	56.0 ¹⁸⁴	Not observed
Fulminic acid	36.3	36.3	40.0	34.1	34.1	40.4 ¹⁸⁴	Observed
Cyanic acid	-3.0	-2.2	-3.5	-4.4	-4.4	-3.1 ¹⁸⁴	Observed
Isocyanic acid	-31.6	-31.6	-28.8	-33.4	-33.4	-23±3.1 -31.0 ¹⁸² -27.6 ¹⁸⁴	Observed
HCNC	135.9	136.0	139.4	133.5	133.5		Not observed
HCCN	123.9	123.9	126.1	122.6	122.6	126±3.0 ⁴⁰	Observed
HSCN	39.7	39.7	38.3	38.3	38.3		Observed
HNCS	28.2	28.8	29.8	27.1	27.1	25.0 ⁴¹	Observed

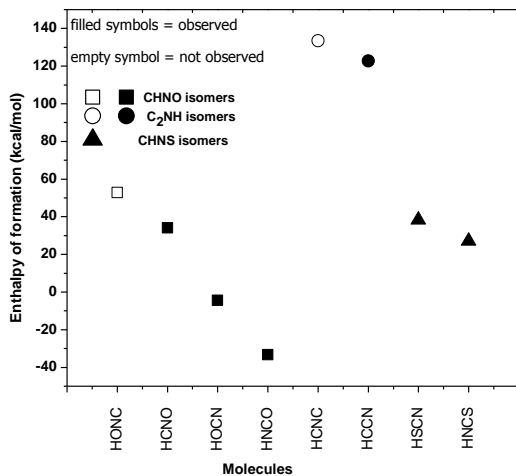


Figure 3.2: Plot showing the $\Delta_f H^0$ for molecules with 4 atoms

Just like in the previous case (isomers with 3 atoms), we observed the energy, stability and abundance (ESA) relationship among the isomers with 4 atoms. From the results presented in Table 3, the isomers with the lower enthalpies of formation; isocyanic acid (HNCO), cyanic acid (HOCN) and fulminic acid (HCNO) have all been observed in different sources in the interstellar space³³⁻³⁶ while isofulminic(HONC) acid with higher enthalpy compared to the previous three isomers has not been observed. As HNCO is more stable than HCNO, it is more abundant than HCNO in the different molecular clouds where it has been observed.³⁸

This trend is also observed for the C₂HN isomeric group, where only HC₂N which has the lowest enthalpy of formation has been astronomically observed.³⁷ Both HSCN and HNCS have been astronomically observed.^{3,39} However, it is interesting to note that the most stable isomer, HNCS, was observed long before (1979) the least stable isomer (2009). This is also the case in the CHNO isomers where the most stable isomer, HNCO, was observed in 1972, almost four decades before the other isomers. The data presented for all the four atom species, summarized in Figure 2, support the ESA relationship.

3.2.3 Isomers with 5 atoms: We present 5 different isomeric groups with 5 atoms considered in this study with their zero-point corrected standard enthalpies of formation and their current astronomical status in Table 3.5. The experimental enthalpy of formation of ketene is in excellent agreement with the theoretically predicted value at the G4 and G4MP2 levels. The experimental $\Delta_f H^0$ values for HCCN and CH₂NN differ from the predicted value at the G4 method with 3.7 and 4.2 kcal/mol respectively.

It is crystal clear from both Table 3.5 and Figure 3 that there is a direct link between stability of molecules and their interstellar abundances which influences their astronomical

observation. The ESA relationship is strictly followed in all the isomeric groups considered here, as only the isomers with lower enthalpies of formation in their respective groups have been astronomically observed.⁴²⁻⁴⁸

Table 3.5: $\Delta_f H^0$ for isomers with 5 atoms and current astronomical status

Molecule	$\Delta_f H^0$ (kcal/mol)						Astronomical status
	W1U	W2U	G3	G4MP2	G4	Expt	
HCNCC	163.0	162.2	167.3	160.9	160.9		Not observed
CC(H)CN	140.2	140.2	139.5	138.8	138.8		Not observed
HNCCC	135.4	135.4	140.1	134.0	133.7		Observed
HCCNC	115.0	115.0	115.7	112.3	112.4		Observed
HCCCN	89.7	89.8	88.8	88.4	88.3	84.6	Observed
HCONC	25.0	25.1	24.8	21.4	21.4		Not observed
HCOCN	13.4	13.4	11.7	10.6	10.6		Observed
Oxirene	68.6	68.6	65.0	66.3	66.3		Not observed
Ethynol	24.8	24.8	22.2	23.2	23.2		Not observed
Ketene	-12.5	-12.5	-12.1	-15.6	-15.6	-14.78	Observed
CH ₂ NC	81.6	81.7	85.7	79.1	79.1		Not observed
CH ₂ CN	58.5	58.6	61.8	56.8	56.8	58±3 ⁵¹	Observed
NH ₂ NC	73.6	73.6	78.2	72.7	72.7		Not observed
CH ₂ NN	56.9	56.9	64.5	55.6	55.6	51.4	Not observed
NH ₂ CN	29.3	29.3	33.0	29.2	29.2		Observed

Among the C₃HN isomeric group, in which more than one isomer has been observed, it is the most stable isomer, HCCCN, which was first observed (1971) before the other isomers

(1992), as seen in previous cases discussed above. The HC_3N , the most stable isomer of the C_3HN isomeric group, is also found to be more abundant than the other two known isomers: HC_2NC and HNC_3 in all the astronomical sources where they have been observed^{42,43,49,50}. HCNCC has received the attention of many investigators. However, even with the available literature about HCNCC , it has not been observed probably due to its high enthalpy of formation as compared to other isomers of C_3NH . This is still in agreement with the ESA relationship among interstellar molecules.

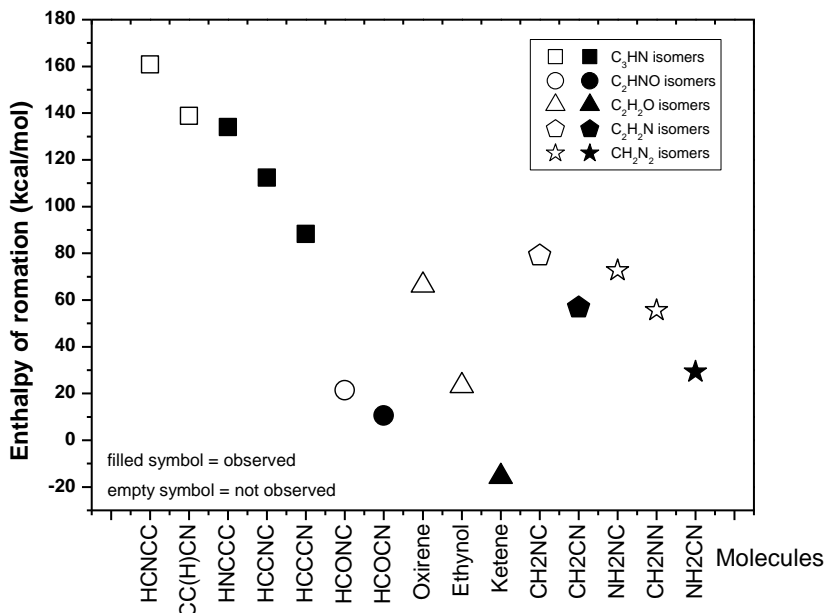


Figure 3.3: Plot showing the $\Delta_f H^\circ$ for molecules with 5 atoms

3.2.4 Isomers with 6 atoms: Both G4 and G4MP2 methods accurately predict the enthalpies of formation of methyl cyanide and methyl isocyanide in good agreement with the reported experimental values while the W2U method does same for formamide (Table 3.6). These accurate predictions of enthalpies of formation for molecules with experimentally known enthalpies of formation are good omens for the desired accuracy for the molecules with no experimental enthalpies of formation.

Of the 4 different isomeric groups (with 6 atoms) presented in Table 3.6 and in Figure 3.4, comprising of 14 molecules, 6 of them have been uniquely detected from different sources in the interstellar medium⁵²⁻⁵⁷ while the remaining 8 have not been astronomically observed (except for 2H-azirine with unconfirmed astronomical observation).

The link between stability and interstellar abundance observed among isomeric species in the previous cases discussed is also noticed here. The only exception to the ESA relationship is methylene ketene which has the lowest enthalpy of formation among the $\text{C}_3\text{H}_2\text{O}$ isomers and it is yet to be astronomically observed. The ESA relationship is followed in all other cases

with 6 atoms considered here. As in the previous cases, where more than one isomer has been observed, it is the most stable isomer that is first observed.

In the C_2H_3N isomeric group, the most stable isomer, methyl cyanide (acetonitrile), was observed first (1971) followed by methyl isocyanide (the second most stable, 1988) and lastly ketenimine (2006). Methyl cyanide, being the most stable isomer of the group is also found to be the most abundant isomer as compared to methyl isocyanide and ketenimine in different molecular clouds and hot cores region where they have been detected.^{53,55,58,83}

Table 3.6: $\Delta_f H^0$ for isomers with 6 atoms and current astronomical status

Molecule	$\Delta_f H^0$ (kcal/mol)						Astronomical status
	W1U	W2U	G3	G4MP ₂	G4	Expt	
1H-azirine	99.4	99.4	99.1	96.7	96.7		Not observed
2H-azirine	66.1	66.1	66.0	62.4	62.4		Not observed
Ethyeamine	58.4	58.4	59.9	58.1	58.1		Not observed
Ketenimine	40.5	40.6	44.7	38.9	38.9		Observed
Methyl isocyanide	41.9	42.0	42.2	38.8	38.8	39±2	Observed
Methyl cyanide	18.2	18.2	17.8	15.8	15.8	15.74	Observed
HC ₃ NC	185.9	185.9	189.7	181.9	181.1		Not observed
HC ₄ N	166.8	166.8	171.0	163.6	163.6		Observed
Cyclopropenone	40.0	40.0	43.2	34.5	35.5		observed
Propynal	35.2	35.2	32.1	32.1	32.1	29.7 ⁶²	Observed
<i>Methylene ketene</i>	29.5	29.5	30.1	24.8	24.8		<i>Not observed</i>
Nitrosomethane	16.7	16.8	17.7	13.5	13.5		Not observed
Hydroxymethylimine	-34.0	-33.9	-33.6	-34.7	-34.7		Not observed
Formamide	-46.7	-46.6	-45.0	-47.3	-47.3	-44.5 (45.1±0.1 ⁶³)	Observed

The recent 'detection' of 2H-azirine in the protostellar environment,⁵⁸ with only one observed transition, has been questioned.⁵⁹ Hence, it is now classified under the "non-detected" interstellar molecules. This could be linked to its low stability and probably low abundance which has resulted in the unsuccessful confirmatory searches. Propynal is about 5 times more abundant than cyclopropenone in the molecular clouds.^{60, 61}

Methylene ketene, as the name suggests, is an unsaturated ketone. However, the chemistry of ketenes resembles that of carboxylic acid anhydrides which makes ketenes remarkably reactive. The high reactivity of ketenes can affect their abundances in the ISM thereby making their astronomical observations difficult. Nevertheless, ketenes remain potential candidates for astronomical observation with more sensitive astronomical instruments.

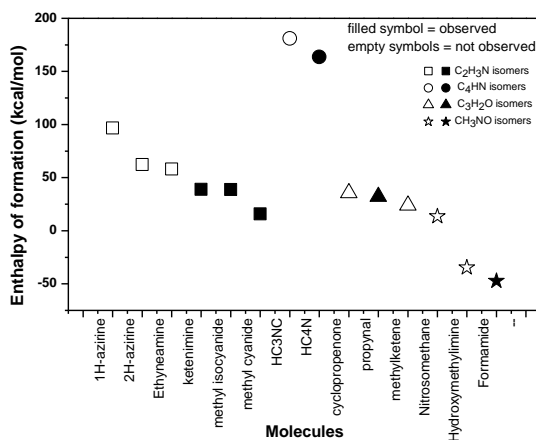


Figure 3.4: Plot showing the Δ_fH° for molecules with 6 atoms

3.2.5 Isomers with 7 atoms: Table 3.7 lists the standard enthalpies of formation and the current astronomical status of the two isomeric groups with 7 atoms examined in this study while Figure 5 shows the plot of the Δ_fH° for these molecules.

Fortunately, almost all (with the exception of isocyanoethene) molecules with 7 atoms considered here have experimentally measured enthalpy of formation; thus, giving ample opportunities to test the accuracy of the theoretical methods. The G4 and G4MP2 methods give excellent predictions of the zero-point corrected enthalpies of formation for the different molecules with known experimental enthalpy of formation values listed in Table 3.7 as compared to the W1U and W2U methods.

Table 3.7: $\Delta_f H^0$ for isomers with 7 atoms and current astronomical status

Molecule	$\Delta_f H^0$ (kcal/mol)						Astronomical status
	W1U	W2U	G3	G4MP2	G4	Expt	
Ethylene oxide	-8.7	-8.7	-5.8	-14.6	-14.6	-12.58	Observed
Vinyl alcohol (anti)	-25.7	-25.7	-28.5	-28.5	-28.5	-29.9±2.0	Observed
Vinyl alcohol (syn)	-27.1	-27.1	-29.5	-30.2	-30.2	-30.6	Observed
Acetaldehyde	-37.5	-37.5	-39.6	-42.4	-42.4	-40.8±0.4	Observed
Isocyanoethene	66.9	66.2	66.7	63.2	63.2		Not observed
Acrylonitrile	46.1	46.1	44.8	43.3	43.3	42.9	Observed

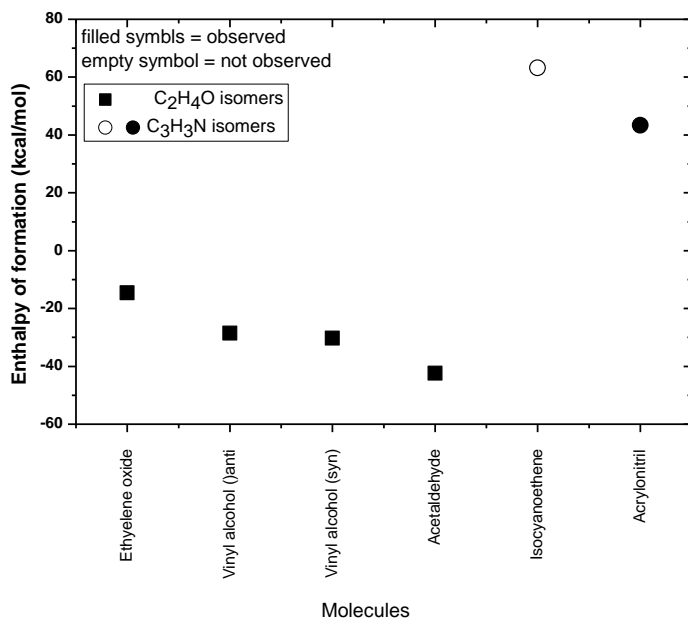


Figure 3.5: Plot showing the $\Delta_f H^0$ for molecules with 7 atoms.

The trend with respect to the observed energy, stability and (interstellar) abundance relationship is nicely followed here. Unlike in other sets of isomers where some are not yet observed in the interstellar space, the 4 stable isomers of the C_2H_4O family (Table 6 and Figure 5) have all been detected in the interstellar medium.^{64,65,66,67} As would be expected, the

most stable isomer of the C₂H₄O family, acetaldehyde was first observed (1973) before the other isomers. Moreover, acetaldehyde has been observed to be present in high abundance in all the astronomical sources where it has been detected as compared to the abundances of vinyl alcohol and ethylene oxides in the same sources.^{67,68,69,70}

It is important to note that the energy difference between the most stable and the least stable molecules should only be considered for species from the same set of isomers and it is not to be compared with the difference in another set of isomers. The only non-observed species here is isocyanoethene, CH₂CHNC, which has higher enthalpy value compared to acrylonitrile, CH₂CHCN that has been observed⁷¹.

3.2.6 Isomers with 8 atoms: Table 3.8 and Figure 6 give the different isomeric groups with 8 atoms considered in this study. Experimental enthalpy of formation values for the molecular species with 8 atoms from the different isomeric groups considered here (Table 7) are scarce with only acetic acid, methyl formate and cyclopropanone having experimentally measured enthalpy of formation values. The G4 and G4MP2 methods predict the enthalpy of formation of acetic acid to a very high accuracy of about 0.2 kcal/mol while that of methyl formate is 2.9kcal/mol. The experimental enthalpy of formation value for cyclopropanone is close to what is predicted by the G3 method. The experimental enthalpy of formation for methyl ketene in the range of -17.1±0.5 to -19.3±0.3¹⁸³ kcal/mol is in good agreement with the G4 value.

The concept of isomerism among interstellar molecules is more pronounced among the interstellar complexes with eight atoms as compared to others. Of the twelve interstellar molecules^{58,72-82} comprising of eight atoms, seven have isomeric (more than 50%) counterparts.

The C₂H₄O₂ family of isomers contains molecules of biological interest. Acetic acid is considered as a precursor for glycine; the simplest biologically important amino acid, because in the laboratory, a biomolecular synthesis of glycine occurs when acetic acid combines with amidogen cation. Glycolaldehyde is an important biomarker since it is structurally the simplest member of the monosaccharide sugars.

With the exception of methyl ketene that is yet to be astronomically observed, the data presented in Table 3.8 and Figure 6 show the influence of interstellar abundance on astronomical observation. The abundance of molecules in ISM has a direct correlation with their stability. The less stable molecules are of course very reactive; this high reactivity has a negative effect on their abundance in ISM as they are being transformed to other molecular species thereby making their astronomical observations difficult as compared to stable molecular species. From Table3.8 and Figure 6, the data are consistent with the ESA relationship discussed in the previous cases with the exception noted above i.e. the non-observation of methyl ketene. The non-observation of methyl ketene could be traced to the same reason as noted for methylene ketene in case of isomers with 6 atoms, i.e, the

carboxylic nature of ketenes which make them to be remarkably reactive as compared to propynal that has been astronomically observed.

Table 3.8: $\Delta_f H^0$ for isomers with 8 atoms and current astronomical status

Molecule	$\Delta_f H^0$ (kcal/mol)						Astronomical status
	W1U	W2U	G3	G4MP2	G4	Expt	
CH ₂ CCHNC	103.5	103.5	104.0	98.8	98.8		Not observed
CH ₃ CCNC	104.4	104.5	108.3	98.6	98.6		Not observed
HCCCH ₂ CN	88.8	88.8	89.1	86.1	86.1		Not observed
CH ₂ CCHCN	80.0	80.0	79.6	76.2	76.2		Observed
CH ₃ CCCN	77.6	77.6	85.8	73.1	73.1		Observed
H ₂ NCH ₂ NC	51.7	50.7	51.5	47.1	47.1		Not observed
H ₂ NCH ₂ CN	30.9	30.9	30.9	28.1	28.1		Observed
1,2-dioxetane	7.7	7.7	1.9	-0.7	-0.7		Not observed
1,3-dioxetane	-42.3	-42.3	-48.6	-50.9	-50.9		Not observed
Glycolaldehyde	-65.3	-65.2	-86.0	-70.5	-70.5		Observed
Methylformate	-82.2	-82.2	-99.6	-89.4	-89.4	-86.5	Observed
Acetic acid	-98.0	-98.6	-95.9	-103.7	-103.7	-103.5±0.7	Observed
Epoxypropene	52.7	52.7	52.4	47.7	47.7		Not observed
2-cyclopropenol	32.0	32.0	26.2	27.4	27.4		Not observed
1-cyclopropenol	31.9	31.9	27.3	25.9	25.9		Not observed
Methoxyethyne	29.8	29.8	26.4	23.9	23.9		Not observed
Propargyl alcohol	20.0	20.0	13.8	17.2	17.2		Not observed
Propynol	17.6	17.1	13.5	12.7	12.7		Not observed
Cyclopropanone	7.8	7.9	4.7	0.7	0.7	3.8±1.0	Not observed
Propenal	-10.5	-10.5	-13.8	-15.8	-15.8		Observed
<i>Methyl ketene</i>	<i>-14.0</i>	<i>-13.9</i>	<i>-15.7</i>	<i>-20.4</i>	<i>-18.1</i>	<i>-17.1±0.5</i> to <i>-19.3±0.3¹⁸³</i>	<i>Not observed</i>

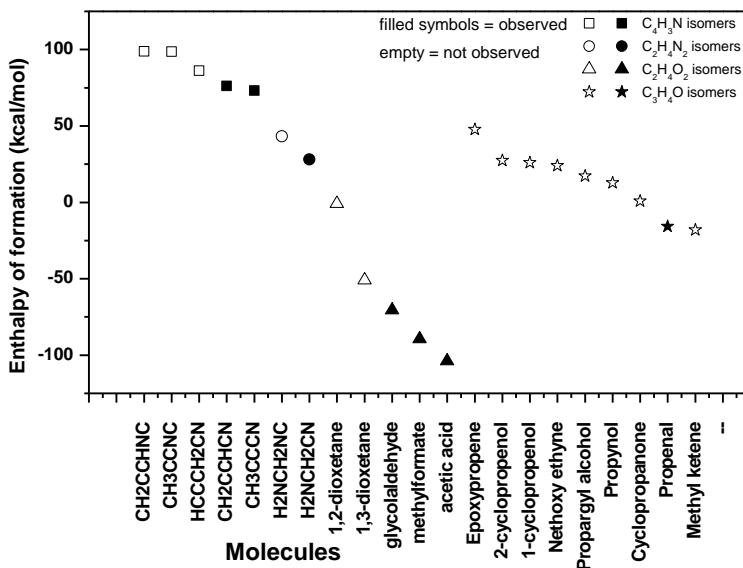


Figure 3.6: Plot showing the $\Delta_f H^\circ$ for molecules with 8 atoms

The order of observation of the $C_2H_4O_2$ isomers follows the order of their abundance, the most abundant isomer, methyl formate, was first observed (1975) followed by the next abundant isomer, acetic acid (1997) and later by the less abundant isomer, glycolaldehyde (2000). This trend of astronomical observation has been noted in the previous cases discussed above still pointing to the fact that the isomers with lower enthalpies of formation are more stable than those with higher enthalpies of formation, the more stable isomers are more abundant in the ISM, and the isomers with higher abundances in the ISM are more easily observed astronomically as compared to those with lower abundances.

From our calculations and the experimentally measured enthalpies of formation, acetic acid is the most stable isomer of the $C_2H_4O_2$ isomeric group and as such it should also be the most abundant species in the interstellar space but this is not the case. Methyl formate is generally regarded as “interstellar weed” as a result of its high abundance and huge number of detectable transitions in the different interstellar sources. The reason for this exception: the low abundance of acetic acid as compared to methyl formate, could be due to interstellar hydrogen bonding on the surface of the interstellar dust grains which causes a greater part of acetic acid to be attached to the surface of the grains (thereby reducing its abundance) because of the presence of the acidic hydrogen (H1 in structure B of Figure 3.7) in the COOH group of acetic acid which is lacking in methyl formate. Of the two types of processes; gas phase chemical reactions and reactions that occur on the surfaces of dust particles, that dominate in the molecular clouds by which molecules are synthesized, the latter mechanism (reactions that occur on the surfaces of dust particles) is invoked for the formation of molecular hydrogen, H_2 ; as well as for the synthesis of larger interstellar molecules. Reactions that occur on the surfaces of dust particles create the platform for interstellar H-bonding. Interstellar hydrogen bonding is discussed in details in chapter 4 of this Thesis.

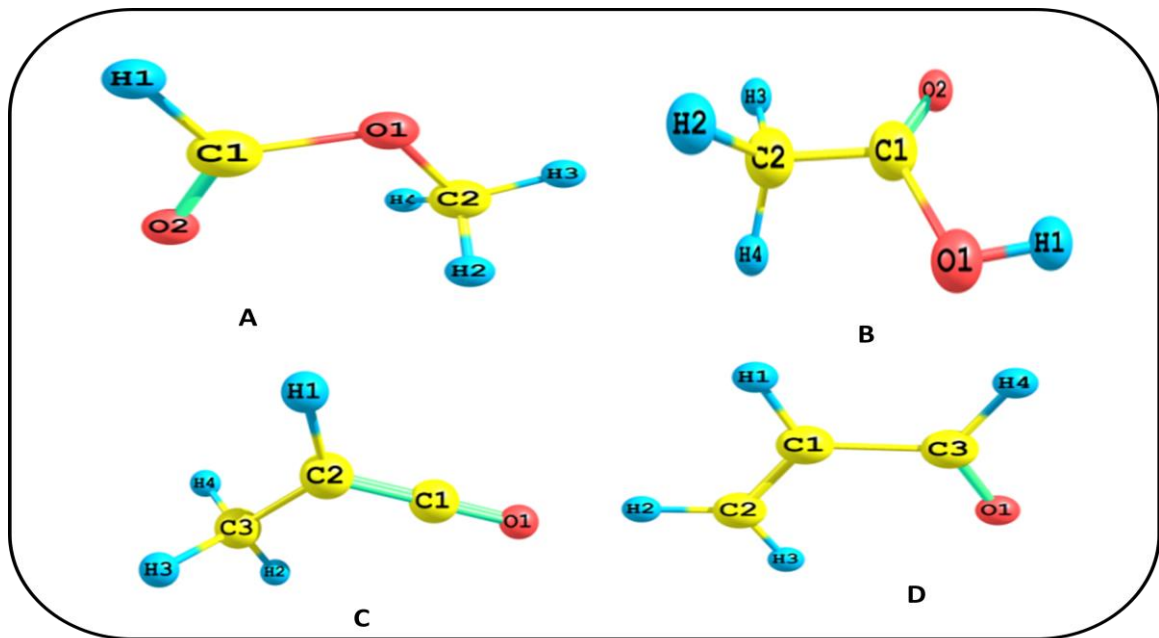


Figure 3.7: Optimized structures of methyl formate (A), acetic acid (B), methyl ketene (C) and propenal (D) at G4 level of theory.

It is also possible that methyl formate and propenal may be formed by more than one formation routes compared to acetic acid and methyl ketene respectively which could account for their high abundances compared to the experimentally/theoretically stable isomers. The low abundance of methyl ketene may require more sensitive instruments for its astronomical detection.

3.2.7 Isomers with 9 atoms: The enthalpies of formation and the current astronomical status of different isomeric groups with 9 atoms considered in this study are summarised in Table 3.9 and Figure 3.8. For the molecules with experimentally known enthalpies of formation, the theoretically predicted enthalpies of formation are in good agreement with results from the G3, G4 and G4MP2 methods.

The two known stable isomers of the C_2H_6O isomeric groups; ethanol and dimethyl ether have been detected in the interstellar medium via their rotational transition spectra.^{83,84,85} The abundance ratio of ethanol and dimethyl ether ranges from around 0.3 to 3.0 in different astronomical sources.^{69,70,86}

Among the isomeric groups with the empirical formulae C_3H_5N and C_2H_5NO , only cyanoethane and acetamide have been observed in the interstellar medium^{62,86,87} from their respective groups. The observed isomers of these sets are also the isomers with the lowest enthalpies of formation (Table 8) compared to other species in their respective groups. This observation is nicely depicted in Figure 8, with the astronomically observed molecules indicated with filled symbols while the non-astronomically observed molecules are marked with open symbols.

Without any exception, the observed the ESA relationship among interstellar isomeric species is strictly followed among the isomers with 9 atoms considered in this study.

Table 3.9: $\Delta_f H^0$ for isomers with 9 atoms and current astronomical status

Molecule	$\Delta_f H^0$ (kcal/mol)						Astronomical status
	W1U	W2U	G3	G4MP2	G4	Expt	
Dimethyl ether	-41.4	-41.4	-44.4	-49.0	-49.0	-44.0±0.1	Observed
Ethanol	-51.3	-51.3	-56.3	-56.7	-56.7	-56.2±0.1 ⁸⁸	Observed
Cyanoethoxyamide	77.7	77.7	76.3	72.5	72.5		Not observed
1-aziridnol	22.3	22.4	19.6	16.0	16.0		Not observed
Nitrosoethane	10.5	10.5	9.0	2.8	2.8		Not observed
N-methylformate	-45.0	-46.0	-45.7	-52.2	-52.2		Not observed
Acetamide	-57.0	57.5	-57.9	-61.9	-61.9	-56.96±0.1 ₉	Observed
1-azabicyclo(1.1.0)butane	72.3	72.331	67.5	64.4	64.4		Not observed
Propargylamine	59.2	59.2	56.6	56.0	56.1		Not observed
Methylazaridine	60.6	60.9	60.8	54.8	54.8		Not observed
Cyclopropanimine	54.3	54.3	52.3	48.2	48.2		Not observed
1-Azetine	50.4	50.5	49.9	43.2	43.2		Not observed
N-methylene ethenamine	42.0	42.1	40.3	36.9	36.9		Not observed
2-propen-1-imine	37.0	37.1	36.5	36.2	36.2		Not observed
Propylenimine	37.9	38.0	37.2	33.0	33.0		Not observed
Isocyanoethane	37.8	37.9	32.8	31.8	31.8	31.7	Not observed
Cyanoethane	16.3	16.3	13.2	11.0	11.0	12.30	Observed

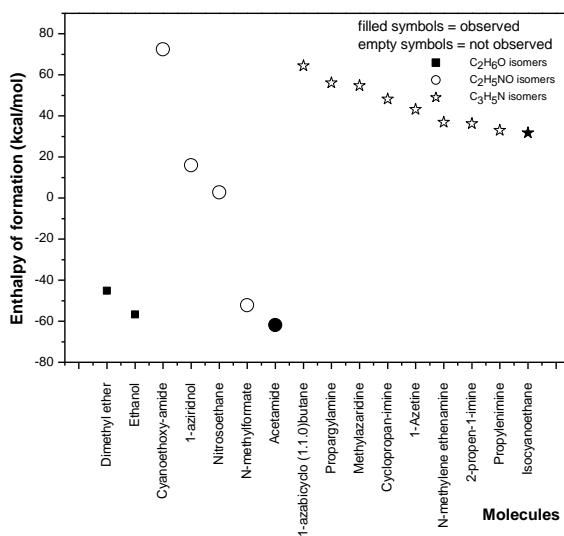


Figure 3.8: Plot showing the $\Delta_f H^\circ$ for molecules with 9 atoms

3.2.8 Isomers with 10 atoms: Table 3.10 lists the isomers consisting of 10 atoms and their corresponding standard enthalpies of formation (theoretically predicted and experimentally measured; where available). Whereas the W1U and W2U methods overestimate the enthalpies of formation of these molecular species, the G3, G4 and G4MP2 methods consistently predict the enthalpies of formation of the molecules with good agreement with the available experimental values.

In all the three different isomeric groups, the observed isomers are the isomers with the lowest enthalpies of formation compared to others in the same isomeric group.^{75,89-92} In the C₃H₆O isomeric group where two isomers have been astronomically observed, the most stable isomer, propanone (acetone) which is probably the most abundant isomer, was first observed (1987) before the next stable isomer, propanal, was observed (2004).

This observation is also clearly pictured in Figure 3.9, where the observed isomers in each group are indicated with filled symbols while the non-observed isomers are indicated with open symbols. This further supports the ESA relationship among interstellar isomeric species.

Table 3.10: $\Delta_f H^0$ for isomers with 10 atoms and current astronomical status

Molecule	$\Delta_f H^0$ (kcal/mol)						Astronomical status
	W1U	W2U	G3	G4MP2	G4	Expt	
Dimethane peroxide	-27.0	-27.6	-29.2	-35.9	-35.9	-30.1	Not observed
Ethylhydroperoxide	-34.0	-33.9	-38.3	-41.7	-41.7		Not observed
Ethylene glycol	-82.2	-82.2	-90.9	-87.5	-87.5	-92.7±0.5	Observed
Oxetane	-12.4	-12.4	-19.1	-21.8	-21.8	-19.25±0.15	Not observed
Cyclopropanol	17.0	-17.0	-24.0	-21.8	-23.8	-28.6±4.0 ⁹³	Not observed
1,2-epoxypropane	-16.3	-16.3	-22.7	-25.0	-25.0	-22.6±0.2	Not observed
2-propene-1-ol	-22.8	-22.8	-29.2	-27.9	-27.9	-29.5.±0.4	Not observed
Methoxyethene	-21.9	-21.6	-26.0	-29.4	-29.4		Not observed
1-propen-1-ol	-30.4	-30.3	-35.4	-36.4	-36.4		Not observed
Propen-2-ol	-35.1	-35.1	-40.5	-41.2	-41.2	-41.1	Not observed
Propanal	-39.2	-39.1	-44.1	-47.0	-47.0	-45.10±0.1	Observed
Propanone	-47.2	-47.8	-47.0	-55.0	-55.0	-52.2±0.1	Observed
CH ₃ (CC) ₂ NC	158.4	158.4	159.1	150.6	150.6		Not observed
CH ₃ (CC) ₂ CN	131.9	131.1	131.7	125.3	125.3		Observed

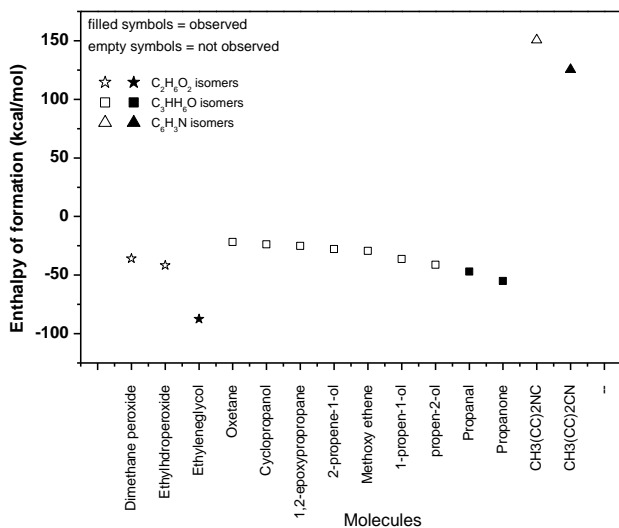


Figure 3.9: Plot showing the $\Delta_f H^\circ$ for molecules with 10 atoms.

3.2.9 Isomers with 11 atoms: Among the different ab initio quantum chemical calculation methods employed in this study for the estimation of the zero-point corrected standard enthalpy of formation, the G4 and G4MP2 are consistently the best as compared to the W1U and W2U methods as shown in Table 10 where the G4 and G4MP2 values are in good agreement with the available experimental values; thus, increasing the reliability in using these methods in estimating enthalpies of formation for molecules with no experimental values.

Table 3.11 shows the isomers of $C_3H_6O_2$ (with 11 atoms) with their corresponding zero-point corrected enthalpies in descending order of magnitude. Figure 3.10 shows the current astronomical status of these molecules, with astronomically observed molecules indicated with filled symbols while the non-astronomically observed molecules are indicated with open symbols.

With the exception of propanoic acid which is the most stable isomer but yet to be astronomically observed, the astronomically observed isomers (methyl acetate and ethylformate) of this group are also the isomers with the smallest enthalpies of formation.^{94,95}

Table 3.11: $\Delta_f H^0$ for isomers with 11 atoms and current astronomical status

Molecule	$\Delta_f H^0$ (kcal/mol)						Astronomical status
	W1U	W2U	G3	G4MP2	G4	Expt	
Dimethyldioxirane	-16.4	-16.4	-26.1	-27.7	-27.7		Not observed
Glycidol	-48.3	-48.3	-58.5	-57.3	-57.3		Not observed
Dioxolane	-61.6	62.1	-71.2	-73.3	-73.3	-72.1±0.5	Not observed
Lactaldehyde	-72.9	-72.9	-82.0	-81.3	-81.3		Not observed
Methyl acetate	-84.8	-84.7	-91.7	-95.1	-95.1	-98.0 ⁹⁷	Observed
Ethylformate	-87.4	-87.4	-94.4	-97.5	-97.5	-95.1	Observed
<i>Propanoic acid</i>	<i>-100.6</i>	<i>-100.5</i>	-108.7	<i>-109.4</i>	<i>-109.4</i>	<i>-</i> <i>108.9±0.5</i>	<i>Not observed</i>

The reason for the delayed astronomical observation of propanoic acid even when it has the lowest enthalpy of formation compared to other isomers of the group is likely to be the same (interstellar H-bonding) as reason for the observed low abundance of acetic acid compared to methyl formate. Different interstellar formation routes for propanoic acid compared to the observed isomers may also account for its non-astronomical detection. Figure 11, structures A and B show the optimized structures of propanoic acid and ethylformate respectively. H1 in structure A is the acidic H atom which can easily take part in interstellar H-bonding on the surface of the dust grains causing a greater part of propanoic acid to be attached to the surface of the interstellar dust grains, resulting in the low abundance and the subsequent difficulty in the astronomical observation of propanoic acid compared to ethylformate. A recent study⁹⁶ (discussed in chapter 4 of this Thesis) on interstellar hydrogen bonding has shown that propanoic acid is more strongly bonded to the surface of the interstellar dust as compared to other isomers of the group, thus a greater portion of it is attached to the surface of the dust grains thereby reducing its overall abundance and delaying its successful astronomical detection.

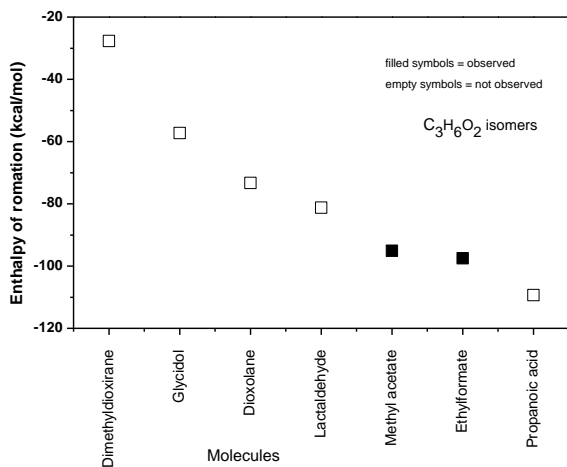


Figure 3.10: Plot showing the $\Delta_f H^\ominus$ for molecules with 11 atoms.

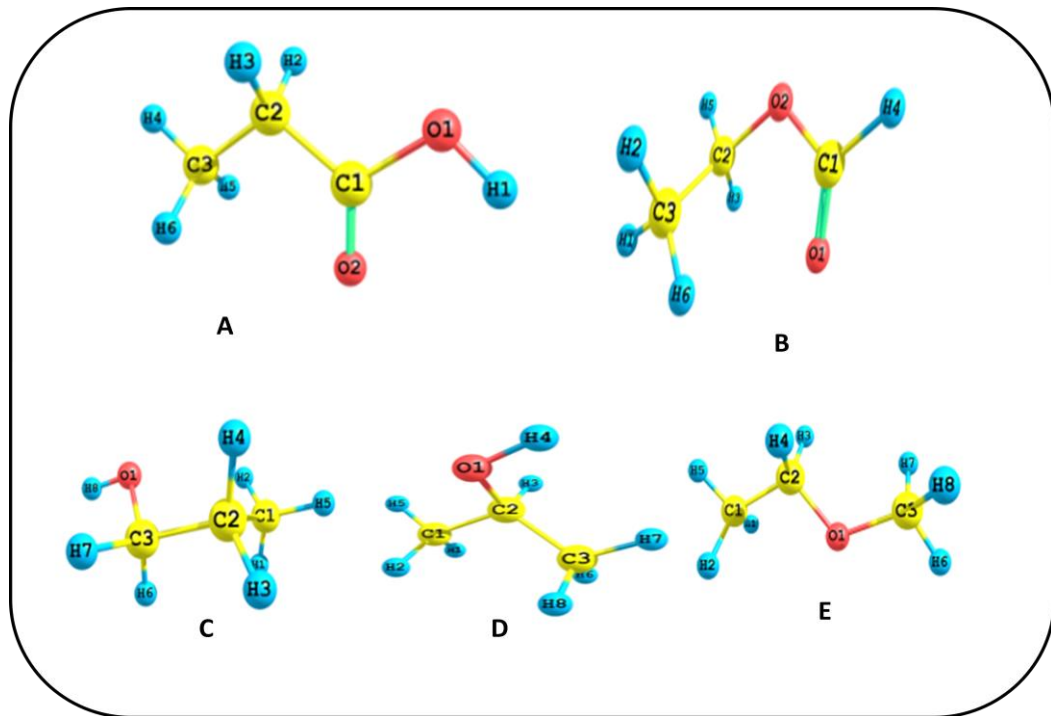


Figure 3.11: Optimized structures of propanoic acid (A), ethylformate (B), propanol (C), propan-2-ol (D) and ethyl methyl ether (E) at G4 level of theory.

3.2.10 Isomers with 12 atoms: Despite the size of the molecule (3 to 12 atoms in this study), the G4 and G4MP2 compound models are consistently reliable in predicting thermochemical properties of molecules to a very good accuracy. The zero-point corrected standard enthalpies of formation of propanol and propan-2-ol attest to this as shown in Table 3.12 as compared to the W1U and W2U methods. The enthalpies of formation and the current astronomical status

of different isomeric groups with 12 atoms considered in this study are summarised in Table 3.12 and Figure 3.12.

Table 3.12: $\Delta_f H^0$ for isomers with 12 atoms and current astronomical status

Molecule	$\Delta_f H^0$ (kcal/mol)						Astronomical status
	W1U	W2U	G3	G4MP2	G4	Expt	
<i>Ethyl methyl ether</i>	-47.2	-47.1	-52.8	-57.4	-57.4	-	<i>Observed</i>
Propanol	-53.7	-53.4	-61.3	-61.9	-61.9	-60.2±0.7	Not observed
Propan-2-ol	-57.2	-57.2	-65.3	65.6	-65.6	-65.2	Not observed
2-azabicyclo(2.1.0)pentane	67.4	67.4	59.8	57.1	57.1		Not observed
N-methyl propargylamine	61.6	61.6	57.2	54.5	54.5		Not observed
3-butyn-1-amine	54.2	54.2	60.8	48.4	48.4		Not observed
N-methyl-1-propyn-1-amine	54.4	53.9	53.0	46.6	46.6		Not observed
N-vinylazardidine	54.8	54.9	51.1	45.9	45.9		Not observed
2,3-butadiene-1-amine	49.7	49.7	47.8	43.3	43.3		Not observed
But-1-en-1-imine	35.6	35.7	34.6	27.8	27.8		Not observed
2,2-dimethylethylenimine	34.1	34.2	38.4	25.7	25.7		Not observed
3-pyrroline	34.5	34.6	28.5	25.4	25.4		Not observed
2-aminobutadiene	30.3	30.4	27.6	24.4	24.4		Not observed
2-isocyanopropane	33.2	33.5	21.7	24.4	24.4		Not observed
Propyl cyanide	13.8	13.8	7.7	5.6	5.6		Observed
Isopropyl cyanide	13.6	13.6	6.7	5.2	5.2	7.4	Observed

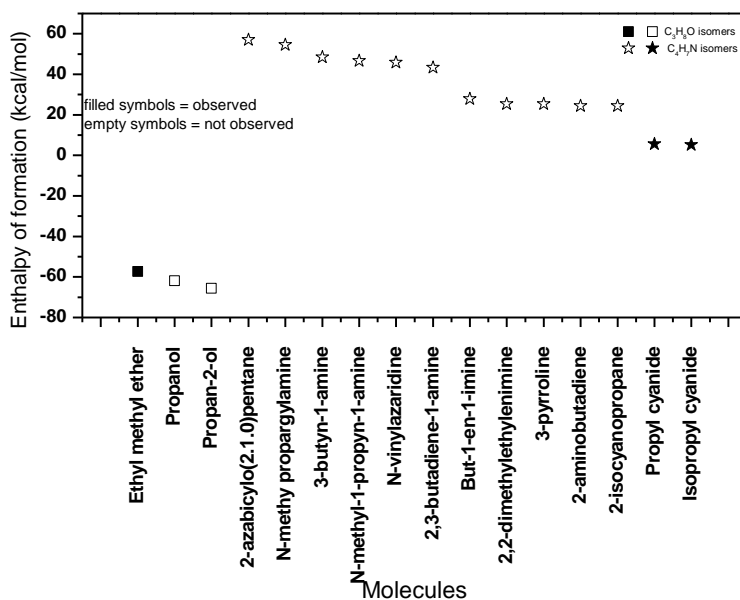


Figure 3.12: Plot showing the $\Delta_f H^\circ$ for molecules with 12 atoms

In the C_3H_8O isomeric group, only ethyl methyl ether with the highest enthalpy of formation has been astronomically observed⁹⁸ while the experimentally/theoretically predicted most stable isomers, propan-1-ol and propan-2-ol are yet to be astronomically observed. The recently observed branched alkyl molecule in the ISM; isopropyl cyanide falls into the C_4H_7N isomeric group. Propyl cyanide and its branched chain counterpart, isopropyl cyanide are the only astronomically observed isomers of this group.^{95,99} These astronomical observations show the direct link between the stability of related molecules and their interstellar abundances, and how this link influences astronomical observations. In accordance with the ESA relationship, the observed species are also the isomers with the smallest enthalpies of formation in the C_4H_7N isomeric group.

The delayed astronomical observations of propan-1-ol and propan-2-ol compared to ethyl methyl ether is likely due to the effect of interstellar hydrogen bonding⁹⁶. The propensity of alcohols to form stronger hydrogen bonds than ethers is well known (Figure 11, structures C, D, and E). Ketones are generally more stable than their corresponding aldehydes because the aldehydic H atom is more acidic and so more reactive.

The low enthalpy of formation estimated for isopropyl cyanide at the G4 level of theory as compared to other isomers of the group suggests the possibility for the astronomical observation of more branched molecules in the ISM from other isomeric groups.

3.3 Immediate Consequences of ESA Relationship

Our knowledge of the young interdisciplinary science of astrochemistry lying at the interface of chemistry, physics, astronomy and astrophysics is still imperfect; this can be seen in the

inabilities and difficulties in convincingly accounting for most of the happenings and observations in this field. The growth in the body of knowledge in this field demands bringing new ideas, insights and innovations to bear in addressing some of the challenges in this field.

The energy of a molecule is of course directly related to its stability. But in this study, this stability has further been shown to be directly linked to the interstellar abundances of related molecular species (isomers in this case) thus influencing their astronomical observations. Thus, the Energy, Stability and (interstellar) Abundance (ESA) are uniquely related. But how does this ESA relationship contribute to knowledge in this field in accounting for some of the observations among interstellar molecules which form a greater research area in astrochemistry and related fields; astronomy, astrobiology and astrophysics. The immediate consequences/impacts/roles of this ESA relationship in addressing some of the whys and wherefores among interstellar molecules are briefly summarised below:

3.3.1 Where are Cyclic Interstellar Molecules? With over 200 different interstellar species so far observed in the interstellar space, only 10 (with the unconfirmed claimed observation of 2H-azirine) are cyclic: c-SiC₂, c-C₃H, c-C₃H₂, c-H₂C₃O, c-C₂H₄O, 2H-azirine, benzene, C₆₀, C₇₀ and C₆₀⁺.^{60, 67, 81, 100-104} More than 10% of all the molecules considered in this study are cyclic; oxirene (Table 4), 2H-azirine, 1H-azirine, cyclopropenone (Table 5), ethylene oxide (Table 6), 1,2-dioxetane, 1,3-dioxetane, cyclopropanone, 2-cyclopropenol, 1-cyclopropenol (Table 7), cyclopropanimine, 1-azetine, 1-azabicyclo(1.1.0)butane, (Table 8), oxetane, cyclopropanol (Table 9), dioxolane, dimethyldioxirane and glycidol (Table 10). From the results, it is evident that the cyclic molecules are among the isomers with the highest enthalpies of formation and in many cases, they indeed have the highest enthalpies of formation. This explains their less stability and less abundance, subsequently resulting in the difficulty of their astronomical observation in contrast to their linear counterparts. This is a clear application of the relationship; energy, stability and abundance among interstellar molecules in addressing an important issue associated with interstellar molecules.

3.3.2 What are the possible candidates for astronomical observation? Only in the cases of AlNC/AlCN and MgCN/MgNC, the isocyanide has lower enthalpy of formation than the cyanide. The difference in enthalpy of formation for the AlNC/AlCN is 7.3 kcal mol⁻¹ according to the best theoretical estimate and 5.4 kcal mol⁻¹ based on experiments and AlCN is yet to be observed. Interestingly, the difference in enthalpies of formation between MgNC/MgCN is much lower (2-3 kcal mol⁻¹) and both have been observed. This is similar to the enthalpy difference between NaCN/NaN₂ and we predict that NaN₂ may be observed in the near future. Curiously, the largest difference between the calculated and experimental enthalpy of formation happens to be for NaCN. It is suspected that the experimental value may have some error.

With respect to larger isomeric species, possible candidates for astronomical observations can easily be predicted following the ESA relationship discussed here. Among others, the five

molecules; methylene ketene, methyl ketene, propanoic acid, propanol and propan-2-ol which have the lowest enthalpy of formation values in their respective isomeric group but are yet to be astronomically observed. These are potential candidates for astronomical observation, though their delayed astronomical observation could be due to the effect of interstellar hydrogen bonding discussed in chapter four of this Thesis.

3.3.3 Why are more Interstellar Cyanides than isocyanides? Cyanide and isocyanide molecules account for about 20% of all the known interstellar molecules. In Tables 3.3-3.10 and 3.12, some of the cyanide/isocyanide pairs among interstellar molecules with their corresponding zero-point corrected enthalpies of formation and their current astronomical status are listed. In particular, the 12 astromolecules considered in this work having 3 atoms turn out to be five cyanide/isocyanide pairs and the only two anions considered in this work ONC^- and OCN^- . In general, the cyanides have lower enthalpy of formation and they have all been observed. Clearly, the ESA relationship can explain the abundance of cyanide over isocyanide and also the exception in AlNC/AlCN . As a test of this fact, of the 24 pairs of cyanide/isocyanide species considered here, the isocyanide species are only astronomically observed in 9 pairs while the cyanide species have been astronomically observed in 21 pairs. This is a direct proof of the ESA relationship existing among interstellar molecules.

Among other whys and wherefores existing in interstellar chemistry, this relationship can also be used in addressing the issue of unsuccessful astronomical searches and Why are some of the Proposed Interstellar Formation Routes not Plausible.

3.4 ESA Relationship Summary: Among the different compound models employed in estimating accurate enthalpies of formation for known and potential astromolecules, the Gaussian G4 and G4MP2 methods are consistently the best in predicting accurate enthalpies of formation that are in good agreement with the available experimental values. From the results, the relationship; energy, stability and (interstellar) abundance is found to exist among interstellar molecules. From the relationship, interstellar abundances of related species are directly proportional to their stabilities. This influences the astronomical observations of some related molecular species at the expense of others. Some of the immediate consequences of this relationship in addressing some of the whys and wherefores among interstellar molecules such as “where are cyclic interstellar molecules? Why are more interstellar cyanides than isocyanide? What are the possible candidates for astronomical observation? Why are some of the proposed interstellar formation routes not plausible?” etc, have been highlighted. The few exceptions are well rationalized on the grounds of interstellar hydrogen bonding, different formation routes for isomeric species, and sensitivity of astronomical instruments. It is hoped to be a useful tool in the fields of astrochemistry, astronomy, astrophysics and other related disciplines.

3.5 Other Applications of the ESA Relationship

Apart from the few immediate consequences of the ESA relationship briefly summarized above, a number of whys and wherefores in interstellar chemistry have been addressed with the help of the ESA relationship. These are discussed in the following studies.

3.6 Is ESA Relationship The Tool In Searching For Interstellar Heterocycles?

3.6.1 Introduction: Despite the broad overlap of the different branches in chemical sciences which has hampered the clear division of these branches, heterocycles have emerged as a unique division in organic chemistry with vast applications and importance in diverse areas. Simply put, these are compounds containing at least one atom of carbon and at least one element other than carbon (which could be oxygen, sulphur or nitrogen), within a ring structure. Generally, organic ring compounds are known to play fundamental roles in terrestrial biochemistry and are believed to have been important ingredients in the earth's prebiotic chemistry. From the astrobiology and prebiotic chemistry perspectives, heterocycles are fundamental building blocks of biological systems as formation subunits of deoxyribonucleic acid (DNA) and ribonucleic acid (RNA). Medically, they are constituents of most drugs currently used as anti-HIV, antifungal, antimicrobial, antimalarial, antidiabetic, herbicidal, fungicidal, antibiotic, antidepressant, and antitumor agents.^{105,106} Industrially, they are used as dyes, brightening, information storage and analytical agents. Heterocycles are also useful in other research areas such as polymer chemistry (as conjugated polymers), inorganic and supra molecular chemistry (as coordination compounds).

The presence of these molecules in carbonaceous chondrites suggests that molecules of biological interest could be formed in non-terrestrial environment through abiotic pathway. It is well known that many of the molecules found in meteorites originated in the interstellar or circumstellar medium. That the heterocycles have been detected in the meteorites is a further confirmatory test of their presence in ISM. Polymerization of small molecules such as ethyne (C_2H_2) and the incorporation of N-atoms via the substitution of ethyne by cyanic acid is considered as a possible formation route for the N-heterocycles. Both ethyne and cyanic acid are well known interstellar molecules with good abundance; hence the above formation route is very plausible.^{33,107-111} Molecular formation processes in ISM are known to be affected by thermodynamics with kinetics also playing important role; this fact is well shown to be true by the ESA relationship existing among interstellar molecules. According to the ESA relationship, the lower the enthalpy of formation of a molecule, the higher its stability and the higher the stability of a molecule, the higher its interstellar abundance which can result in the astronomical observation of such molecule with ease compared to its counterpart with higher enthalpy of formation.¹¹¹ Isomerism is playing a vital role in interstellar chemistry; astronomical observation of an isomer is always a pointer to the presence of other isomers though not yet detected, since isomers are believed to have a common precursor for their formation.⁷ The concept of isomerism can therefore be used to demystify some astronomical issues.

Seven heterocycles furan, imidazole, pyridine, pyrimidine, pyrrole, quinoline and isoquinoline are currently listed as non-detected interstellar molecules¹¹³ as a result of the unsuccessful astronomical searches for these molecules in different astronomical sources. The searches only yielded upper limits in the range of 4×10^{12} to $2.8 \times 10^{21} \text{ cm}^{-2}$ determined for their column densities in all the cases without any successful detection. This has resulted in questions like; were these heterocycles the best candidates for astronomical searches? Are there isomers that would have been better options for astronomical searches? In order to address these questions, we have considered 67 isomers from the six isomeric groups where these 7 heterocycles belong. High level quantum chemical calculations have been applied to determine accurate enthalpies of formation for each of these isomers.

3.6.2 Computational details: The details of the computational methods applied here are the same as described in section 3.1.0. The standard enthalpies of formations for the different systems are calculated as described in section 3.1.1 above.

3.6.3 Results and Discussion

The reported enthalpies of formation in this study are in kcal/mol and at 298.15K. The results obtained from the 6 different isomeric groups where these 7 heterocycles belong are presented (in tables and figures) and discussed accordingly.

C₃H₄N₂ Isomers: Table 3.13 presents the optimized structures and enthalpies of formation for the 13 isomers of the C₃H₄N₂ isomeric group in decreasing order of enthalpy of formation. Figure 3.13 shows the optimized structures of the different isomers of the C₃H₄N₂ isomeric group. This isomeric group consists of important biological molecules; the imidazole ring structure occurs in fundamental biological molecules such as histidine (an amino acid) and purines; imidazolium and pyrazolium-based ionic surface are now receiving attention of researches as good materials for biosensing; pyrazole and its derivatives are important constituents of many drugs because of their muscle relaxing, antidiabetic, analgesic, anti-inflammatory, and other biological activities¹¹⁴⁻¹¹⁶.

As important as the C₃H₄N₂ isomers are, only imidazole has been astronomically searched for.^{114, 117} In accordance with the ESA relationship, among the isomers of C₃H₄N₂ isomeric group, imidazole has least enthalpy of formation (Table 3.13) as compared to other isomers of the group and as such it is expected to be the most stable isomer of the group and probably the most abundant isomer of the C₃H₄N₂ group in the interstellar medium (ISM). The astronomical search of imidazole in the Sgr B2 molecular cloud only lead to an upper limit of the order of 10^{15} cm^{-2} determined for its column density in Sgr B2.¹¹⁷ Irvine et al.¹¹⁴ reported the upper limit in the range of 0.6 to $100 \times 10^{13} \text{ cm}^{-2}$ for the column density of imidazole in different astronomical sources. Both searches could not yield any successful detection of imidazole in ISM. In comparison to other isomers of the group, imidazole remains the most potent candidates for astronomical observation being the most stable and probably the most abundant isomer of the group in ISM. With the range of upper limit so far determined for its column density, its astronomical observation will require highly sensitive astronomical

instruments, more precise transition frequencies and appropriate choice of astronomical sources.

Table 3.13: $\Delta_f H^0$ for $C_3H_4N_2$ isomers

Molecule	$\Delta_f H^0$ (kcal/mol)
Diazocyclopropane	91.7
Pyrazolium	87.0
1-Azaridinecarbonitrile	65.8
3H-Pyrazole	63.3
2-Azaridinecarbonitrile	62.0
4H-Pyrazole	59.3
Imidazolium	53.8
Methylamino acetonitrile	50.6
3-iminopropanenitrile	44.3
2-aminoacrylonitrile	43.5
Pyrazole	37.0
3-aminoacrylonitrile	35.8
Imidazole	26.6

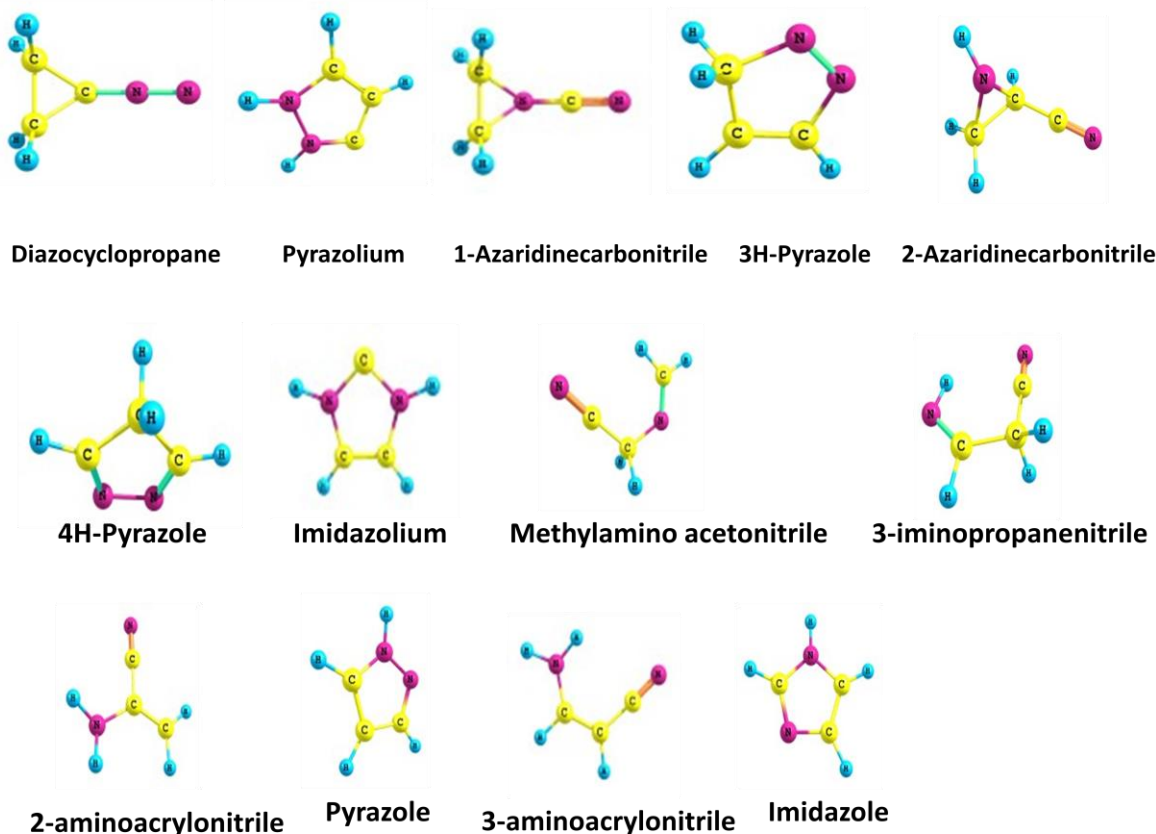


Figure 3.13: Optimized Structures of $C_3H_4N_2$ isomers

Figure 3.14 shows the plot of the enthalpy of formation for the various isomers of $C_3H_4N_2$ with the astronomically searched isomer indicated with green while the ones with no report regarding their astronomical searches are indicated with red. It is crystal clear from the plot

that the only astronomically searched isomer is also the isomer with the least enthalpy of formation, making it the best choice for astronomical observation. This shows the direct application of the ESA relationship as a tool in searching for interstellar molecules.

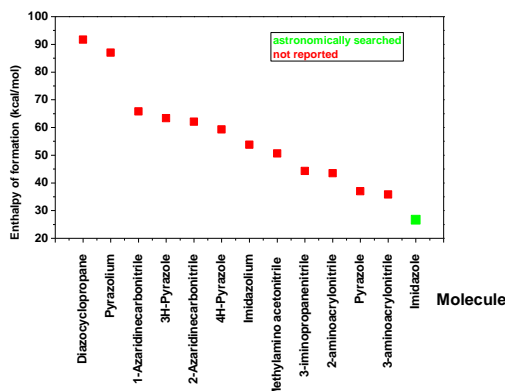


Figure 3.14: Plot showing the $\Delta_f H^\circ$ for $C_3H_4N_2$ isomers

C_5H_5N Isomers: Azafulvene is an inseparable partner in pyrrole chemistry, having been postulated as an intermediate in the nucleophilic substitution reaction at the 2-pyrrolylmethyl position. The structure of 1-cyanobicyclo[1.1.0]butane makes it a choice monomer in polymer chemistry. Pyridine has a long-familiar history of applications in the biological and chemical systems¹¹⁸⁻¹²⁰. Broadly speaking, all the isomers of the C_5H_5N (Table 3.14 and Figure 3.15) group have important applications in diverse areas. However, when it comes to astronomical observations, other parameters are very crucial. These include energy, stability and interstellar abundance which are the components of the ESA relationship. Three different sets of scientists have reported unsuccessful searches for pyridine from different astronomical sources^{121,122}. Upper limits in the range of 7.3×10^{12} to $2.5 \times 10^{15} \text{ cm}^{-2}$ have been determined for the column abundance of pyridine in the different astronomical sources searched.

The optimized structures and enthalpies of formation for the different isomers of C_5H_5N isomeric group are shown in Figure 3.15 and Table 3.14 while Figure 3.16 depicts the plot of the enthalpies of formation for these isomers. The wide difference between the enthalpy of formation of the most stable isomer, pyridine, which is also the only astronomically searched isomer (indicated with green) and the other isomers with no report regarding their astronomical searches (indicated with red) is well pictured in Figure 3.16.

Table 3.14: $\Delta_f H^\circ$ for C_5H_5N isomers

Molecule	$\Delta_f H^\circ$ (kcal/mol)
1-cyanobicyclo[1.1.0]butane	84.2
4-cyano-1-butyne	77.4
2,4-cyclopentadiene-1-imine	61.2
2-methylene-3-butenenitrile	58.2
Azafulvene	56.1
1-cyano-1,3-butadiene	55.5
Pyridine	28.7

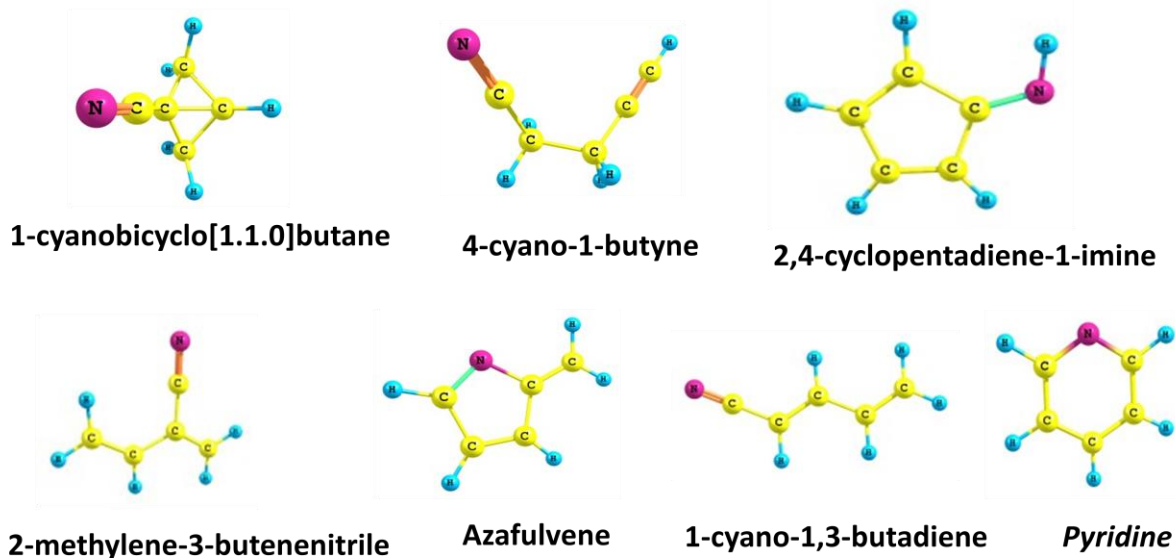


Figure 3.15: Optimized Structures of C_5H_5N isomers

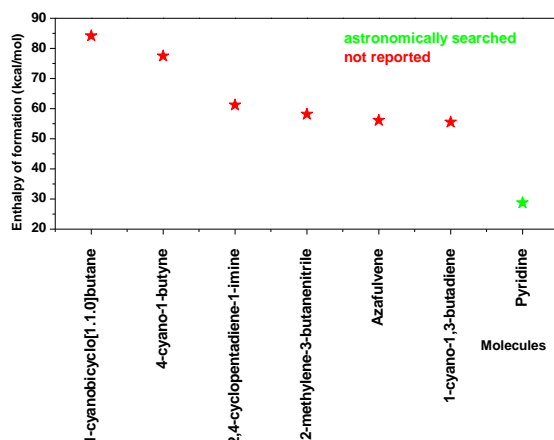


Figure 3.16: Plot showing the $\Delta_f H^\circ$ for C_5H_5N isomers

In conformity with the ESA relationship, pyridine is the only isomer of the group that has been astronomically searched. Pyridine is undisputedly the best candidate for astronomical

observation in comparison with other isomers of this group. It has the least enthalpy of formation; hence it is more stable and probably more abundant in ISM than other isomers of the group. The successful astronomical observation of pyridine is a function time with the current rapid development in astronomical and spectroscopic equipments that will culminate into better sensitivity of astronomical instruments and more accurate rest frequencies.

C₄H₄N₂ Isomers: The enthalpy of formation calculated with the G4 method employed in this study for the different isomers of the C₄H₄H₂ isomeric group and their optimized structures are presented in Table 3.15. In Figure 3.17, the optimized structures of the different isomers are shown. Despite the importance of all the isomers of this group, only pyrimidine has been astronomically searched for in different molecular clouds. The choice for the astronomical search of pyrimidine at the expense of other is easily understood from the ESA relationship. Pyrimidine has the smallest enthalpy of formation as compared to other isomers of the group and as such it is expected to be more stable and probably more abundant in the interstellar space than other isomers of the group.

Figure 3.18 nicely displays the enthalpy of formation of these isomers with the astronomically searched isomer which is also the isomer with the smallest enthalpy of formation indicated with green while others are indicated with red.

Table 3.15: $\Delta_f H^0$ for C₄H₄N₂ isomers

Molecule	$\Delta_f H^0$ (kcal/mol)
1,2-diisocyanoethane	92.4
1,3-butadiene-1,4-diimine	88.0
4-amino-2-butynenitrile	83.0
Iminopyrrole	62.3
2-methylene-2H-imidazole	60.1
Pyridazine	59.0
1,1-dicyanoethane	54.7
Pyrazine	41.0
Pyrimidine	37.1

The astronomical searches for pyrimidine in different molecular clouds yielded upper limits of 1.7×10^{14} cm⁻² for Sgr B2(N), 2.4×10^{14} cm⁻² for Orion KL and 3.4×10^{14} cm⁻² for W51 e1/e2 as column abundance determined for pyrimidine in the respective molecular clouds without any successful detection^{123,124}. Among all the isomers of this group, pyrimidine remains the most possible molecule for astronomical observation in the nearest future.

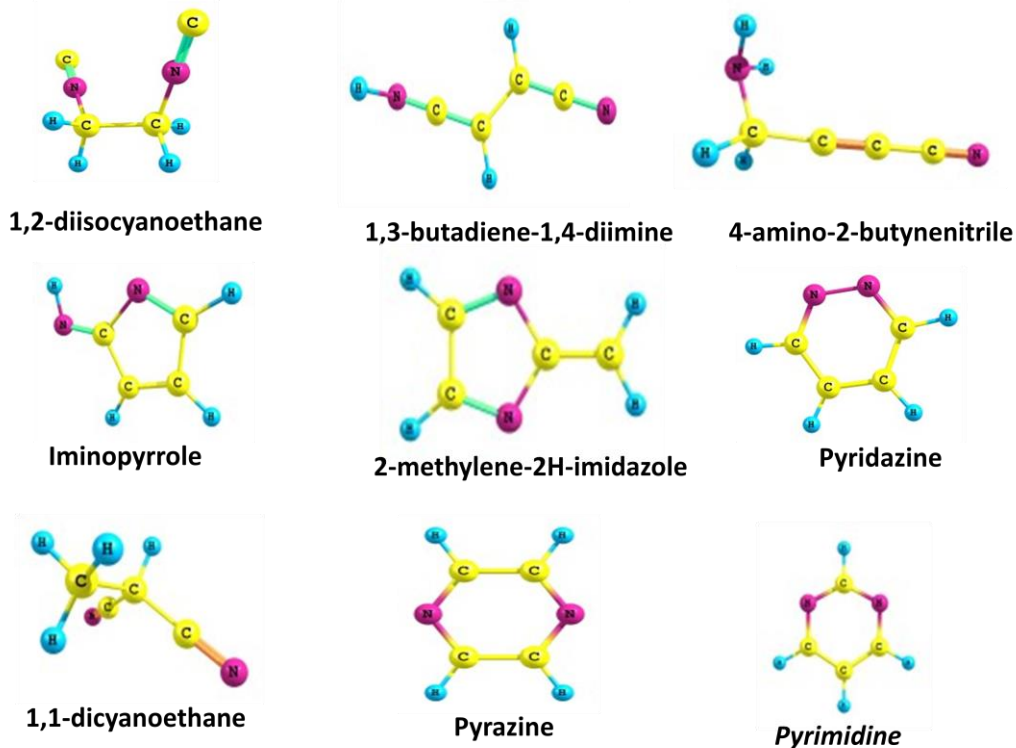


Figure 3.17: Optimized Structures of $\text{C}_4\text{H}_4\text{N}_2$ isomers

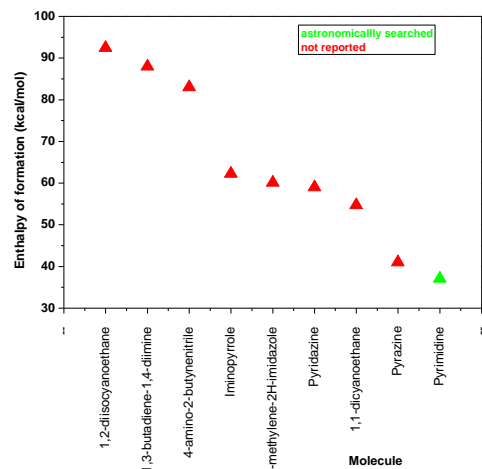


Figure 3.18: Plot showing the $\Delta_f H^\circ$ for $\text{C}_4\text{H}_4\text{N}_2$ isomers

$\text{C}_4\text{H}_5\text{N}$ isomers: Eleven isomers of the $\text{C}_4\text{H}_5\text{N}$ isomeric group with their corresponding optimized structures and enthalpies of formation calculated with the G4 method are shown in Table 3.16. Figure 3.19 pictured the optimized structures of these isomeric species. These isomers are widely studied in different research areas because of their various applications.

Most of them are extensively used in organic synthesis, e.g, pyrrole, ally cyanide etc. Ally cyanide is a good cross-linking agent in some polymers. It has also been proposed as an additive in propylene carbonate-based electrolytes for graphite anode to prevent exfoliation of the anode via film-forming. In biological systems, ally cyanide has been shown to induce antioxidant and detoxification enzymes¹²⁵⁻¹²⁸. As much as these isomers are important in various aspects, when it comes to astronomical searches, other parameters emerge as the priority. These are the energy, stability and interstellar abundance as described in the ESA relationship.

Table 3.16: $\Delta_f H^\ominus$ for C₄H₅N isomers

Molecule	$\Delta_f H^\ominus$ (kcal/mol)
2-vinyl-2H-azirene	78.6
Isocyanocyclopropane	65.3
Ally isocyanide	62.0
N-vinylethyleneimine	61.0
Cyanocyclopropane	43.6
2H-pyrrole	40.1
3H-pyrrole	40.0
Ally cyanide	39.7
2-cyanopropene	34.0
2-butenenitrile	32.8
Pyrrole	24.1

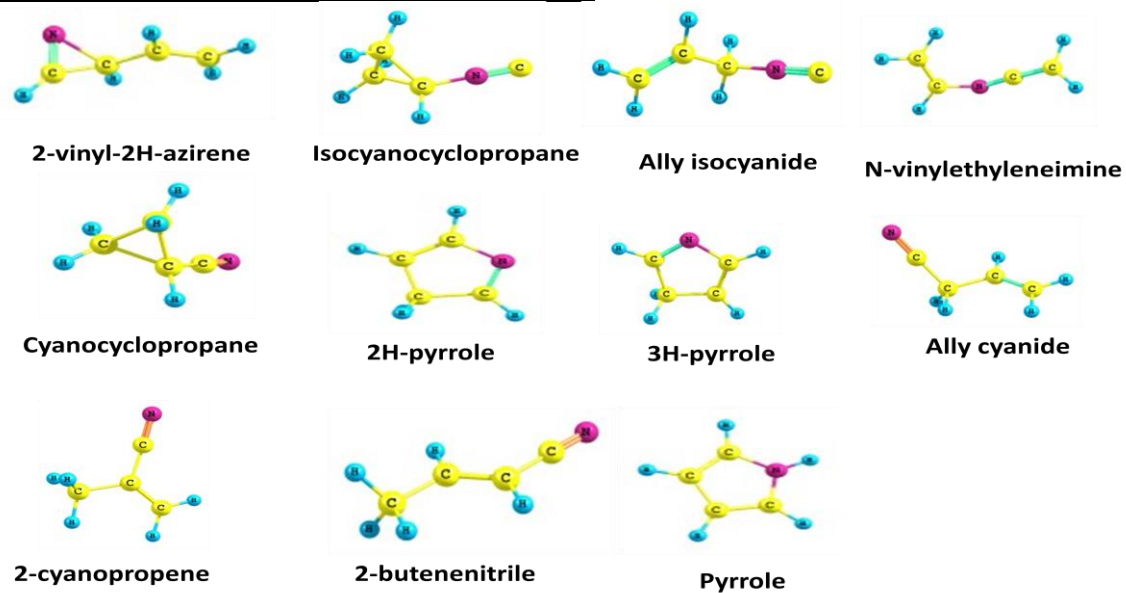


Figure 3.19: Optimized Structures of C₄H₅N isomers

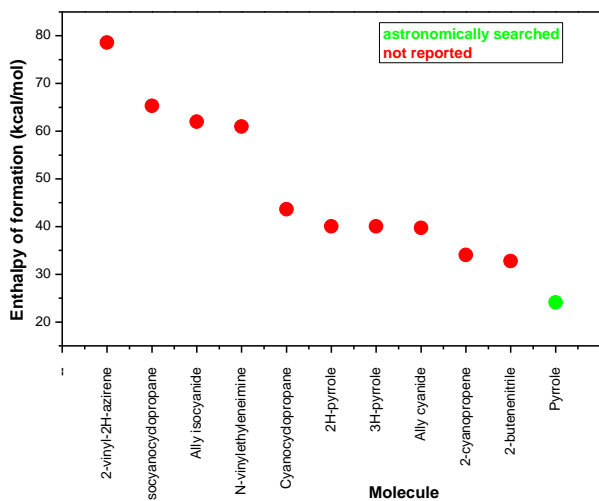


Figure 3.20: Plot showing the $\Delta_f H^\circ$ for C_4H_5N isomers

Just as in the previous cases discussed above, the only astronomically searched isomer of this group; pyrrole is also the isomer with the smallest enthalpy of formation as compared to other isomers of the group. Astronomical searches for pyrrole have been reported by two groups of scientists¹²⁹⁻¹³⁰, with the upper limits in the range of 3 to $10 * 10^{13} \text{ cm}^{-2}$ for Sgr B2 and $4 * 10^{12} \text{ cm}^{-2}$ for TMC determined for the column density of pyrrole in the respective astronomical sources without any successful detection of pyrrole. In the plot of the enthalpy of formation of these isomers (Figure 3.20), the astronomically searched isomer; pyrrole (indicated with green), is conspicuously different from the other isomers (indicated with red) in terms of the magnitude of the enthalpy of formation. Among all the isomers of this group, pyrrole still remains as the most potent candidate for astronomical observation being the most stable and probably the most abundant isomer of the group in ISM.

C_9H_7N Isomers: Unlike in the previous cases where only one isomer has been astronomically searched for from each isomeric group, in the C_9H_7N isomeric group, 2 isomers have been astronomically searched. *Will this group still follow the ESA relationship?* Table 3.17 gives the enthalpies of formation for the 13 isomers of the C_9H_7N isomeric group. These isomers are well studied for their diverse applications in several fields. Figure 3.21 depicts the optimized structures of the same isomers. With respect to astronomical searches, the trend is the same as those discussed above. Quinoline and its closest chemically related isomer, isoquinoline are the only two isomers of this group that have been astronomically searched. As listed in Table 5, these two isomers are also the isomers with the smallest enthalpies of formation in comparison with other isomers of the group and as such are expected to be the most stable and probably the most abundant isomers of the group in ISM. Charnley et al.,¹²³ reported unsuccessful astronomical searches for quinoline and isoquinoline in three different astronomical sources with upper limits in the range of $1.9 * 10^{13}$ to $1.2 * 10^{18}$

cm^{-2} for quinoline and $2.9*10^{13}$ to $2.8*10^{21}\text{cm}^{-2}$ for isoquinoline determined for their column densities in the different molecular clouds searched. Figure 3.22 shows the plot of the enthalpies of formation of these isomers.

Table 3.17: $\Delta_f H^0$ for $\text{C}_9\text{H}_7\text{N}$ isomers

Molecule	$\Delta_f H^0$ (kcal/mol)
3,4-diethynyl-1-methyl-1H-pyrrole	136.3
2,5-diethynyl-1-methyl-1H-pyrrole	133.4
3-phenyl-2-propyn-1-imine	98.3
1-isocyano-2-vinyl-benzene	89.3
1-isocyano-4-vinyl-benzene	87.0
Bicyclo[4.2.0]1,3,5-triene-7-carbonitrile	82.3
Atroponitrile	68.9
3-vinylbenzonitrile	67.4
4-vinylbenzonitrile	66.9
3-methylene-3H-indole	66.6
Cyanostyrene	66.5
Isoquinoline	46.0
Quinoline	44.8

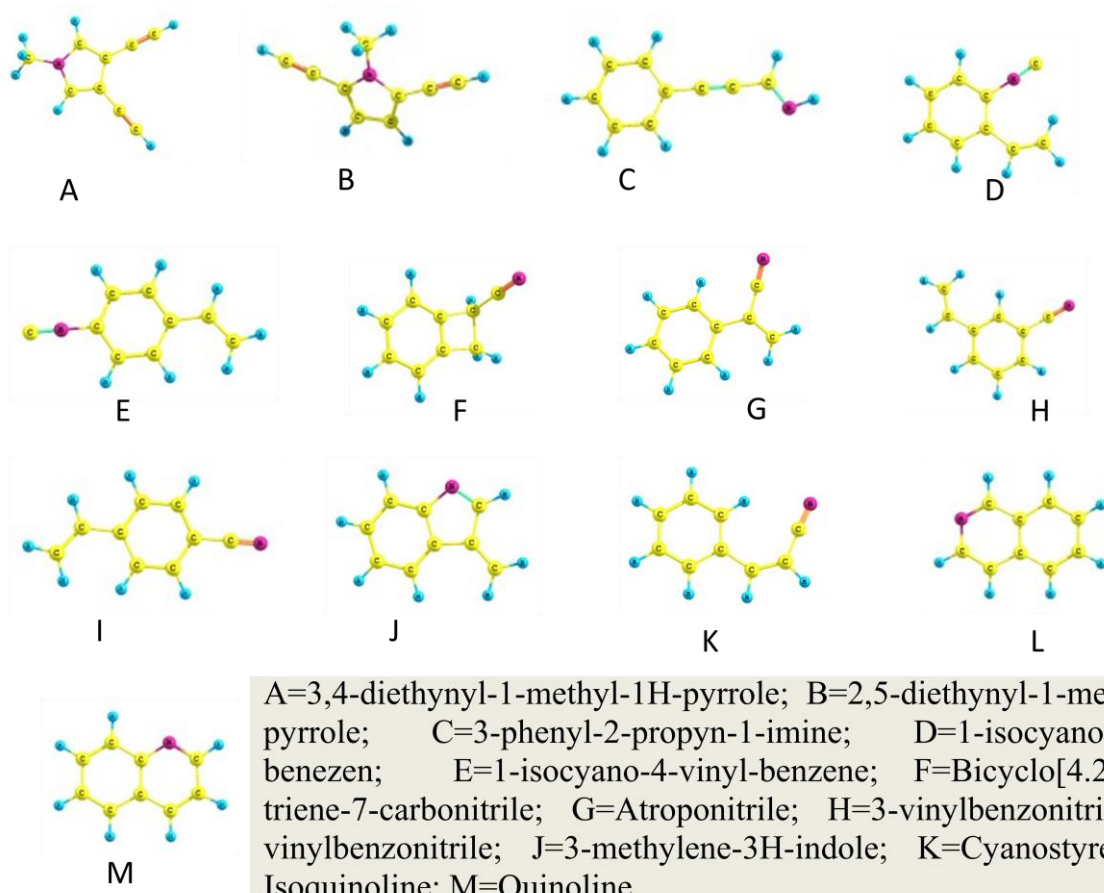


Figure 3.21: Optimized Structures of $\text{C}_9\text{H}_7\text{N}$ isomers

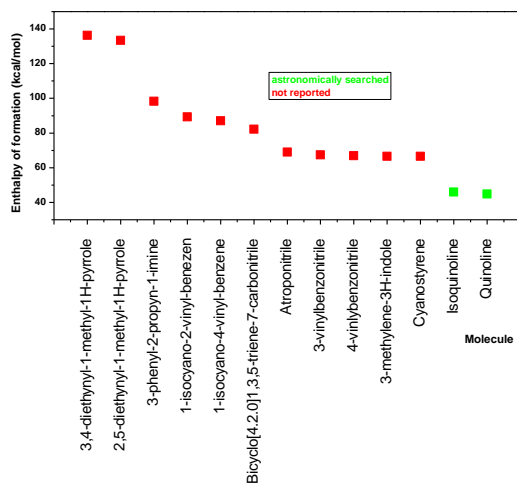


Figure 3.22: Plot showing the $\Delta_f H^0$ for C₉H₇N Isomers

Though yet to be successfully observed in ISM, quinoline and isoquinoline remain the most likely isomers for astronomical observation from this group of isomers. They will probably require more sensitive astronomical tools, accurate rest frequencies and excellent choice of astronomical sources for their observations.

C₄H₄O Isomers: All our discussions so far (under subsection 3.6.3) have been on one type of heterocycles; the N-heterocycles. It will be good to see if the ESA relationship is also used as a tool in searching for other heterocycles not only N-heterocycles as seen thus far. The C₄H₄O isomeric group contains oxygen rather than nitrogen as in the previous groups. The enthalpies of formation for 14 isomers of this group calculated with the G4 method and the optimized structures of these isomers are presented in Table 3.18 and Figure 3.23 respectively.

The trend is exactly the same as discussed for the N-heterocycles. Furan is the only astronomically searched isomer of this group, it is also the isomer with the smallest enthalpy of formation with marked difference in magnitude even with the next isomer; vinylketene. This is well pictured in Figure 6. Furan's stability and its expected interstellar abundance in comparison with other isomers of the group warranted its astronomical searches. Dezafra et al.,¹⁵ and Kutner et al.,¹²⁹ have reported unsuccessful searches for furan in different astronomical sources. The upper limits determined for the column density of furan in Orion A and Sgb B2 are 7×10^{13} cm⁻² and 2×10^{16} cm⁻² respectively. Furan remains a sure candidate for astronomical observation as compared to every other isomer of the C₄H₄O group. Figure 3.24 nicely depicts the plot of the standard enthalpies of formation for the C₄H₄O isomers with the astronomically searched isomer, furan indicated in green while others are shown in red.

Table 3.18: $\Delta_f H^\circ$ for C₄H₄O Isomers

Molecule	$\Delta_f H^\circ$ (kcal/mol)
Ethynyloxy ethene	46.8
Cyclopropene-1-carbaldehyde	39.8
2-Cyclopropene-1-carbaldehyde	38.8
1-buten-3-yn-2-ol	30.7
But-3-ynal	24.5
2-methyl-2-cyclopropenemethanone	21.0
Cyclopropylienemethanone	19.3
3-butyn-2-one	18.2
2-butynal	17.2
1,2-butadienal	13.3
2,3-butadienal	13.1
2-cyclobutene-1-one	9.2
Vinylketene	3.6
Furan	-9.3

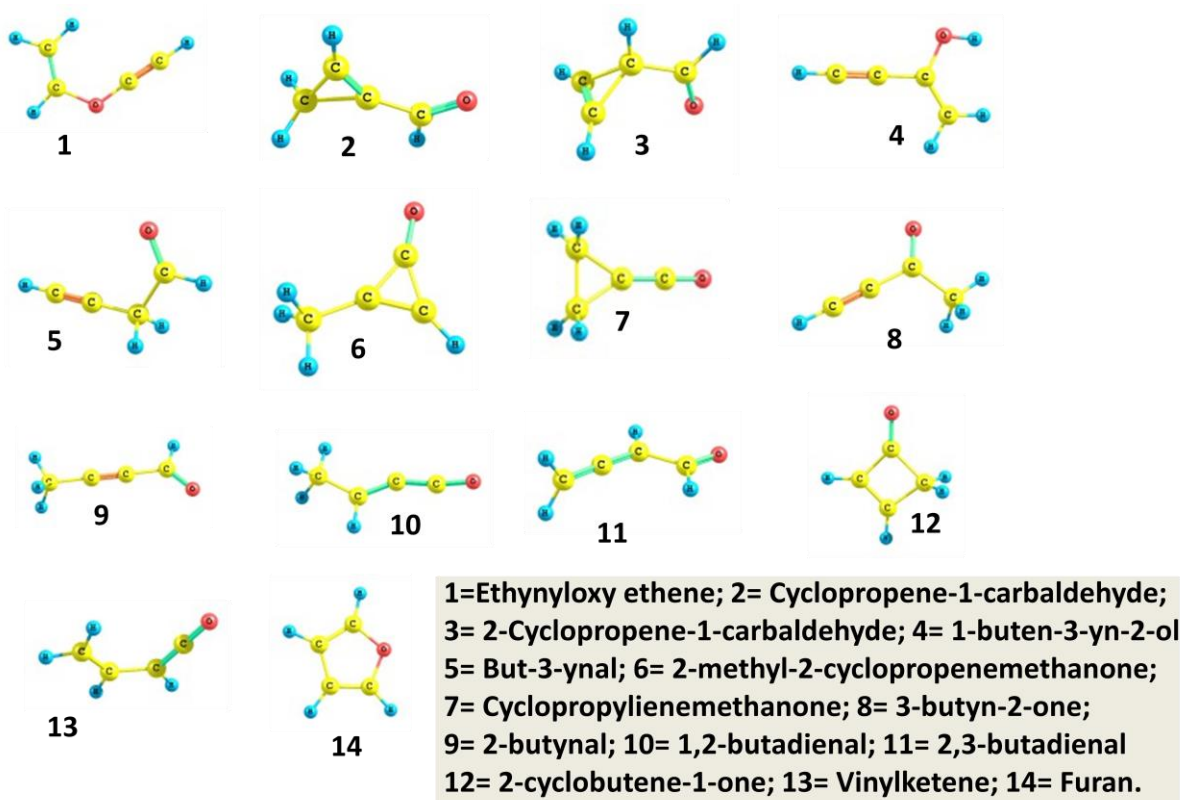


Figure 3.23: Optimized Structures of C₄H₄O isomers

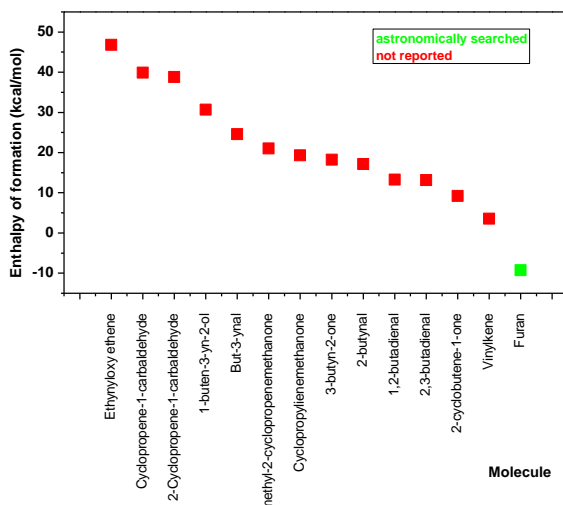


Figure 3.24: Plot showing the $\Delta_f H^\circ$ for C₄H₄O Isomers

3.7 Summary on the Searches for Interstellar Heterocycles with ESA Relationship as the Tool: All the heterocyclic molecules that have so far been searched for in different astronomical sources have been examined in relation to their isomers using high level chemical quantum calculation. There has not been any successful astronomical observation of any of these molecules; they remain the best candidates for astronomical observation in their respective groups. This is because; all the heterocycles so far searched for are the ones with the smallest enthalpy of formation in their respective isomeric groups and as such are the most stable and probably the most abundant in ISM. Their delayed successful astronomical observation could be due to several factors; low resistant to photodissociation, large partition function, low abundance in ISM, etc. The astronomical observation of these molecules will demand more sensitive astronomical equipments, precise transition frequencies, proper choice of astronomical sources, among others. The consistency of the choice of these heterocycles for astronomical searches in each of the groups in accordance with the ESA relationship has led to the question; *Is ESA relationship the tool in searching for interstellar heterocycles?*

3.8. C₅H₉N Isomers: Pointers to Possible Branched Chain Interstellar Molecules

3.8.1 Introduction: Each unique astronomical observation of a molecule does more than just informing us about its presence, the physics and chemistry from where it was observed rather it also serves as a pointer to other possible molecules in ISM, for example the observations of the O-containing molecules and their corresponding S-analogues do not only re-emphasize the relationship between O and S as elements in the same group rather it can easily be seen that for every known O-containing molecule in ISM, the S-analogue is also present even when it is yet to be astronomically observed. The positive impact of the recent development and advances in astronomical and spectroscopic techniques is setting the pace for a better understanding of the science (physics, and chemistry) of the interstellar space and in probing deep into the interior molecular clouds. That about 200 different molecular species have been detected largely via their rotational transitions in the microwave, millimeter-wave, and terahertz region evidently proves a good examination of the interstellar and circumstellar media.

The difficulty in detecting molecules in space increases with the complexity of the molecules. There is a steady decrease in the number of these molecules as the number of atoms increase. The diatomic species account for the largest number of individual molecules. The complex molecules (those with six 6 atoms and above) account for about one third of all the known interstellar circumstellar molecules. Molecular ions (both anions and cations) have been detected in different astronomical sources. They include; CN⁻, C₃N⁻, C₅N⁻, C₄H⁺, C₆H⁺, C₈H⁺, CO⁺, CH⁺, SO⁺, CF⁺, HCO⁺, H₃⁺, HOC⁺ among others.^{19, 131-142} Their detections have initiated studies on ion-molecule chemistry as the basis for the formation of circumstellar and interstellar molecules in the gas phase.¹⁴³ The interstellar and circumstellar carbon chain molecules such as C_n, HC_nN and C_nX (X=N, O, Si, S, H, P, H⁻, N⁻) for a unique class of molecules which account for about 20% of all the known interstellar and circumstellar molecules. They are highly unsaturated and are linked to the formation and destruction of carbonaceous compounds such as the polycyclic aromatic hydrocarbons. The metal containing interstellar and circumstellar molecules such as AlF, AlO, SiH, FeO, MgCN, NaCN, KCl, NaCl, SiO, etc, are good probes of astrophysical phenomena; they also furnish with crucial information on the molecular depletion into dust grains.¹⁴⁴

Though different classes and types of molecules have been observed in space, there was no astronomical observation of a branched chain molecule until recently. Isopropyl cyanide was observed in the Sagittarius B2 complex molecular via its rotational transitions.⁹⁹ From the Energy, Stability and interstellar Abundance (ESA) relationship existing among interstellar/circumstellar molecules which has been firmly established as discussed in the studies above, interstellar formation processes have been shown to be partially thermodynamically controlled. In accordance with the ESA relationship, the astronomical detection of isopropyl cyanide; the first branched molecule in interstellar medium (ISM)

came longer than expected being the most stable isomer of the C_4H_7N isomeric group as shown in Table 3.19 and Figure 3.25. Propyl cyanide; the second most stable isomer of the C_4H_7N isomeric group was observed few years before the branched chain.⁹⁴ Lack of accurate rotational transitions due to the different conformations in which isopropyl cyanide may occur delayed its observation. Available experimental enthalpies of formation for these isomers are indicated in square brackets in Table 3.19 (Hall, Baldt, 1993; NIST)⁹⁷.

Table 3.19: Δ_fH^\ominus for C_4H_7N isomers and current astronomical status

Molecule	Δ_fH^\ominus (kcal/mol)	Astronomical status
2-azabicyclo(2.1.0)pentane	57.1	Not observed
N-methyl propargylamine	54.5	Not observed
3-butyn-1-amine	48.4	Not observed
N-methyl-1-propyn-1-amine	46.6	Not observed
N-vinylazaridine	45.9	Not observed
2,3-butadiene-1-amine	43.3	Not observed
But-1-en-1-imine	27.8	Not observed
2,2-dimethylethylenimine	25.7	Not observed
3-pyrroline	25.4	Not observed
2-aminobutadiene	24.4	Not observed
2-isocyanopropane	24.4	Not observed
Propyl cyanide	5.6 [7.4]	Observed
Isopropyl cyanide	5.2[5.4]	Observed

Edited from Table 3.12.

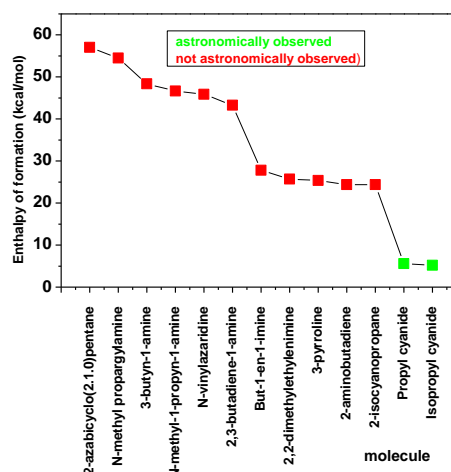


Figure 3.25: Plot showing the Δ_fH^\ominus for C_4H_7N isomers

With no amino acid yet to be successfully detected in interstellar or circumstellar medium, about 80 of them have already been identified in meteorites found on earth.¹⁴⁵ The origin of these chemical compounds or their precursors found in meteorites has been traced to the interstellar or circumstellar medium¹⁴⁶; thus suggesting the detection of more complex molecules in the interstellar and circumstellar media than what have been detected so far. This paints a picture of a link between the interstellar medium and the molecular composition of meteorites. Most of the amino acids identified in meteorites are branched amino acids.^{146,147} The observation of a branched chain molecule; isopropyl cyanide in the interstellar medium further stresses the possibility of this link between the interstellar medium and the molecular composition of meteorites. However, in order to firmly establish this link, the observation of more branched chain molecules in the interstellar and circumstellar media is required. In the light of this, the C₅H₉N isomeric group; where the next higher member of the alkyl cyanide series belong is examined to see if the branched chain molecules in group could be the possible candidates for astronomical observation as in the case of the C₄H₇N isomeric group.

3.8.2 Computational Details: All the calculations here were performed with the Gaussian 09 suite of programs.¹⁰ In order to estimate accurate enthalpies of formation for all the molecules in the C₅H₉N isomeric group that are in good agreement with experimental values (where available), the Gaussian 4 (G4) composite method was employed. In arriving at an accurate total energy for a given molecule, the G4 composite method performs a sequence of well-defined ab initio molecular calculations.¹² Each fully optimized structure was verified to be a stationary point (having non-negative frequency) by harmonic vibrational frequency calculations. In estimating the enthalpy of formation for these molecules from the optimized geometries, the procedures stated in sections 3.1.0 and 3.1.1 are followed.

3.8.3 Results and Discussion: In this section, the results of the high level quantum chemical simulations are presented and discussed. For the four most stable isomers which are good candidates for astronomical searches, information on the available spectroscopic data (from literature) necessary for astronomical observation is given. In Table 3.20, 16 possible isomers of the C₅H₉N isomeric group with their corresponding enthalpy of formation value ($\Delta_f H^\circ$), and dipole moment are presented in ascending order of $\Delta_f H^\circ$. The enthalpies of formation of these molecules range from -0.8 (the most stable isomer; tert-butylnitrile) to 52.1(the least stable isomer; 3-dimethyl amino-1-propyne). All values are reported in kcal/mol. Figure 3.26 shows the optimized structures of these isomers. Available experimental enthalpies of formation for these isomers are indicated in square brackets in Table 3.20.⁹⁷

In column 3 of Table 3.20, the dipole moments obtained with the G4 composite method for the molecules under consideration are presented. This is necessary because of the large dependence of radio-astronomical observation on the dipole moment of the molecule. The

rotational transitions which have been used to detect about 80% of all the known interstellar and circumstellar molecules can only be measured for molecules with permanent dipole moments. The dipole moment also contributes to the intensities of rotational transitions. These intensities scale with the square of the dipole moment, hence, the higher the dipole moment, the higher the intensity of the lines. From the knowledge of Boltzmann distribution and the low temperature of the molecular clouds, it connotes that majority of the molecules in the clouds are in their vibrational and electronic ground states (not excited states). Whereas rotational excited states can be populated at 10-100k and decay by spontaneous emission, infrared emission can be observed if molecules are occasionally excited by high energy photons emitted by hot stars in the vicinity of the cloud which is a rare event. Interestingly, all the molecules considered here have non-zero permanent electric dipole moment ranging from 0.366 (for 1,2,3,6-tetrahydropyridine) to 4.628 Debye (for n-butyronitrile) which implies that their rotational spectra can be measured; thus providing the necessary tool for their astronomical searches.

Table 3.20: $\Delta_f H^\circ$, structures and dipole moments for C_5H_9N isomers

Molecule	$\Delta_f H^\circ$ (kcal/mol)	Dipole moment (Debye)			
		μ_A	μ_B	μ_C	μ
Tert-butylnitrile	-0.8[-0.8]	4.425	-0.0003	0.0003	4.425
Isobutyl cyanide	-0.5	-4.213	-1.201	0.636	4.427
n-butyronitrile	0.5	4.246	1.841	-0.001	4.628
2-methylbutanenitrile	0.6[0.6±0.3]	4.256	1.466	0.545	4.534
2-methyl-1-pyrroline	1.9	-0.109	2.290	0.0001	2.292
Cyclopent-3-en-1-amine	7.3	1.436	-0.759	0.0001	1.625
2,3,4,5-tetrahydropyridine	15.0	1.415	-1.918	0.0001	2.384
Tert-butylisonitrile	17.3	3.786	0.0001	0.0009	3.786
2-isocyanobutane	20.0	3.581	1.334	0.492	3.853
n-butylisocyanide	21.5	3.570	1.621	-0.0001	3.921
1,2,3,6-tetrahydropyridine	24.7	0.120	-0.345	0.000	0.366
3-methylene cyclobutanamine	32.6	1.019	-0.0002	1.312	1.661
2-methyl-3-butyn-2-amine	39.7	0.694	0.001	-0.016	0.695
4-pentyn-1-amine	43.7	1.065	0.950	1.116	1.811
1-ethyl-2-methyleneazardine	44.6	-0.750	0.272	1.191	1.434
3-dimethyl amino-1-propyne	52.1	-0.759	-0.075	0.759	1.077

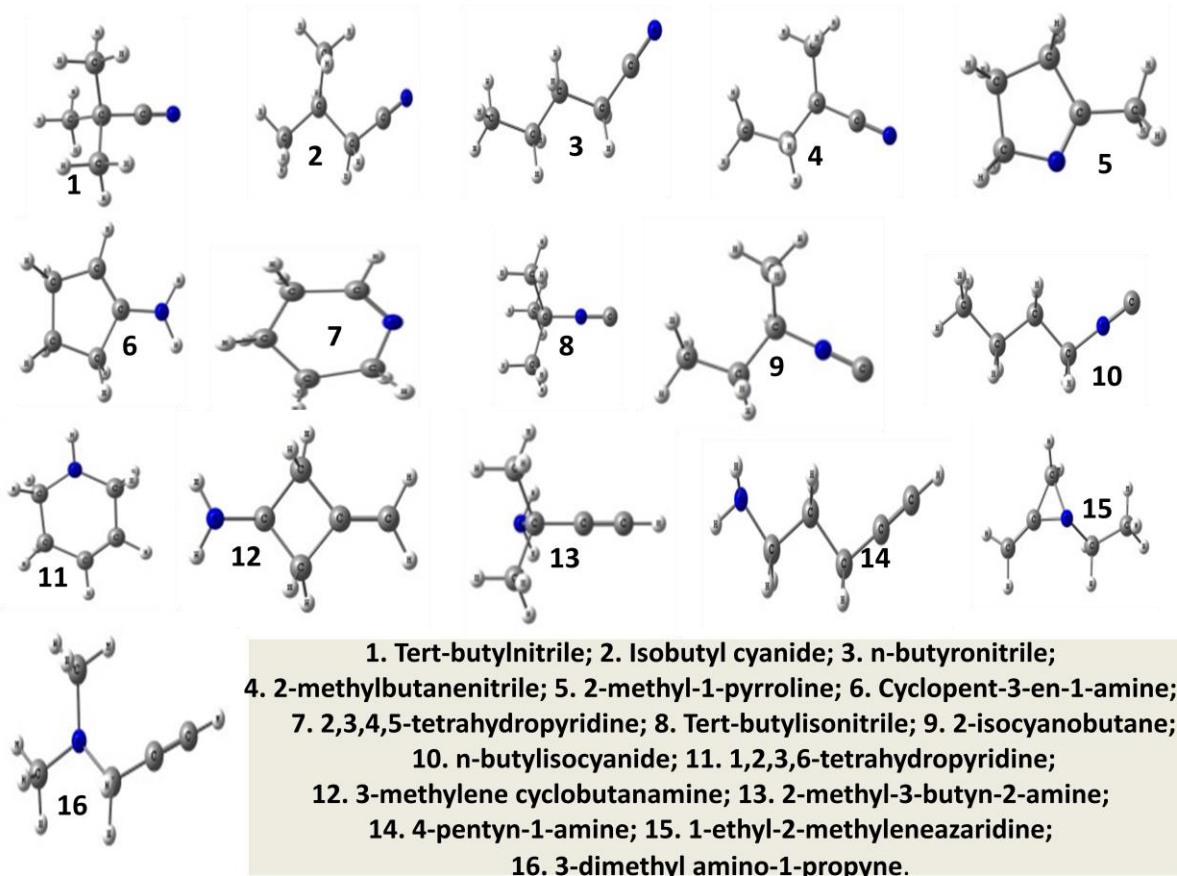


Figure 3.26: Optimized structures of the C_5H_9N isomers.

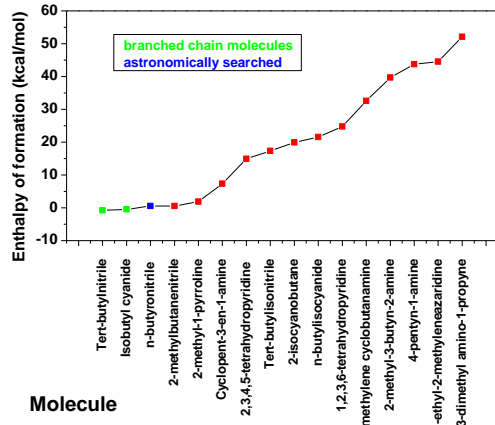


Figure 3.27: Plot showing the Δ_fH° for C_5H_9N isomers.

Figure 3.27 depicts the plot of the Δ_fH° for the C_5H_9N isomers. The two most stable isomers of this group; tert-butylnitrile and isobutyl cyanide are indicated with green while others are shown with red.

Table 3.19 and Figure 3.25 are the enthalpies of formation and the current astronomical status for the C₄H₇N isomers. The two astronomically observed isomers (indicated with green in Fig.3.25) of this group are the most stable isomers (with the smallest enthalpies of formation) as compared to other isomers of the group. The relationship between Energy, Stability and interstellar Abundance (ESA) existing among interstellar and circumstellar molecules is well established. This relationship influences the astronomical observation of some similar molecules (like isomers from the same isomeric group) at the expense of others. From the results of the high level quantum chemical simulations performed on the C₅H₉N isomers presented in Table 3.20 and Figure 3.27, it is crystal clear that the most stable isomer of the group is tert-butylnitrile; a branched chain molecule with a dipole moment of 4.425 Debye and a negative enthalpy of formation (-0.8 kcal/mol). The enthalpy of formation estimated with the G4 composite method (-0.8 kcal/mol) is in excellent agreement with the experimentally measured value of -0.8 kcal/mol reported in the NIST website.²³ The microwave spectrum of this molecule was measured more than five decades ago.¹⁴⁸ From the measured rotational constants, more rest frequencies in the range of interest for astronomical search can be predicted. The astronomical searches of this isomer is yet to be reported anywhere in literature to the best of our knowledge. However, it remains the best candidate for astronomical observation among all the isomers of the C₅H₉N isomeric group being the most stable isomer of the group and as such it is expected to be more abundant as compared to other isomers of the group; thus it could be detected in the interstellar or circumstellar medium. The second most stable isomer of the C₅H₉N isomeric group is isobutyl cyanide; an important intermediate in the pharmaceutical industry and a key starting in the production of diazinon; an organo-phosphorus pesticide.¹⁴⁹ It has a dipole moment of 4.427 Debye similar to that of tert-butylnitrile. The rotational frequencies of this molecule are not known and as such there has not been any report of its astronomical search. With its stability and high dipole moment, it remains a potential candidate for astronomical observation pending the availability of accurate rotational frequencies.

From Table 3.20 and Figure 3.27, the third most stable isomer of the C₅H₉N isomeric group is n-butyl cyanide; the next largest unbranched alkyl cyanide after n-propyl cyanide that was detected in the interstellar medium 5 years ago.⁹⁴ The rotational spectrum of this molecule in the range of 5 to 22 GHz has been measured.¹⁵⁰ This measurement has been extended to the shorter millimeter wavelengths to aid its astronomical searches. The radio-astronomical searches for n-butyl cyanide in the Sagittarius B2(N) molecular cloud yielded only upper limits of its column density without any successful detection.¹⁵¹ This is the only isomer of the C₅H₉N isomeric group that has been astronomically searched for though it is not the most stable molecule of the group (indicated with blue in Figure 3.27). The upper limit obtained for n-butyl cyanide points to the possibility of a successful detection for the most stable isomers; tert-butylnitrile and isobutyl cyanide (branched chain molecules) which are likely to be more abundant in space as compared to the n-butyl cyanide. The next most stable isomer after the linear isomer; n-butyl cyanide is 2-methylbutanenitrile which is very similar to the linear isomer in terms of energy and dipole moment. However, the rotational transitions of this molecule which could warrant its astronomical searches are not known. There is a drastic decrease in stability and dipole moment of the other isomers after 2-methylbutanenitrile thus

making their observations less feasible. The stability of the cyanide more than their corresponding isocyanide which accounts for the high number of known interstellar and circumstellar cyanide molecules as compared to the isocyanides as discussed in the ESA relationship is also noted here among the molecules under consideration with tert-butylnitrile (-0.8 kcal/mol) being more stable than tert-butylisonitrile (17.3 kcal/mol); n-butyronitrile (0.5 kcal/mol) being more stable than n-butylicyanide (19.9 kcal/mol) etc. The cyclic isomers are always found to be less stable than their corresponding straight or branched chain counterparts in majority of the groups, resulting in few numbers of known cyclic molecules in space. This is also observed here.

3.8.4 Summary on C₅H₉N Isomers as Pointers to Possible Branched Chain Interstellar Molecules: The aim of this work has been in examining the best candidate for astronomical observations among the C₅H₉N isomers by searching for the isomer that will probably have the highest abundance in the interstellar space which can thus be detectable as compared to others following the ESA relationship discussed in our previous studies. From the results of our high level quantum chemical simulations, the most stable isomer of the C₅H₉N isomeric group is tert-butylnitrile; a branched chain molecule followed by Isobutyl cyanide; another branched chain molecule. The only isomer of this group that has been astronomically searched for with only upper limit of column density determined is the linear isomer; n-butyl cyanide which ranks third on the energy scale among other isomers of the group; thus, not the most stable isomer and probably not the most abundant isomer of the group in the interstellar medium. The upper limits of column density determined for n-butyl cyanide, the high stability and dipole moments of tert-butylnitrile and isobutyl cyanide suggest these branched chain molecules as the most probable candidates' astronomical observations with accurate rotational transitions, appropriate choice of astronomical source and sensitive radio telescope array like ALMA.

3.9

Is C-C-O Bonding Backbone Truly Elusive?

3.9.1 Introduction: Though there is yet to be a consensus on how interstellar molecules especially the complex ones; those with 6 atoms and above, are formed. A careful observation of these molecules reveals some common basic chemistry properties among them which serve as pointers to the formation of some of the interstellar molecules. Among others, isomerism, successive hydrogen addition and periodic trends are prominent basic chemistry among interstellar molecules. Successive hydrogen addition is now considered as a possible formation route for some interstellar molecules especially when the molecules (the larger and the smaller ones) are chemically and spatially related i.e easily seen or detected in the same

spectral region. Typical examples are the molecular aldehyde hydrogen-addition sequence of propynal, propenal and propanal; glycolaldehyde and ethylene glycol where the larger molecules are believed to be formed from the smaller ones via two successive hydrogen addition.^{7,74} All the molecules in these examples have been astronomically observed from the same molecular showing that they are chemically and spatially related. An instance of the periodic trend is conspicuously seen in the interstellar chemistry of sulphur and oxygen. Of the 18 known S-containing interstellar molecules, 16 have the corresponding O-compounds analogues and the abundances of some of these S-compounds are also consistent with the cosmic ratio of sulphur and oxygen. The case of isomerism as a pointer to the formation route of some interstellar molecules is more pronounced than those cited above as about 40% of all the known interstellar molecules have isomeric counterparts. The preponderance of isomerism among interstellar molecule interstellar molecules suggests a common precursor for the formation of isomeric species. Isomerism has now become an instrument that can be used in elucidating some happenings among interstellar molecules and interstellar chemistry.

Studies have shown the importance of thermodynamics in interstellar formation processes.^{112, 152} According to the energy, stability and abundance (ESA) relationship, the lower the enthalpy of formation of a molecule, the higher its stability and the higher the stability of a molecule, the higher its interstellar abundance which can result in the astronomical observation of such molecule with ease compared to its counterpart with larger enthalpy of formation.¹¹² The number of unsuccessful searches for interstellar molecules has made it a necessity for astronomers and astrophysicists to always analyse the possibility, address the necessary "whys and wherefores" about the presence and abundance of a particular molecule before embarking on its astronomical search. The motivation and the expected benefit of such search to the scientific community are always clarified. Such was the case of interstellar acetic acid, CH_3COOH . As one of the expected benefits for its astronomical observation to the field of astrophysics and other related disciplines, Mehringer et al.¹⁵³ said "*CH₃COOH is important for astrochemical studies because it contains the elusive C-C-O backbone; interstellar molecules with this structure appear to have less potential for formation than their counterparts with C-O-C backbone structure*". This sub chapter re-examines this statement by considering some isomeric species (with at least one species as a known interstellar molecule) with these backbones. High level quantum chemical calculations are applied in calculating accurate enthalpies of formation for these molecules.

3.9.2 Computational methods: The details of the computational methods applied here are the same as described in section 3.1.0. The standard enthalpies of formations for the different systems are calculated as described in section 3.1.1 above.

3.9.3 Results and Discussion

For most of the molecules considered in this study, their experimentally measured enthalpies of formation are known; these values were taken from the NIST website and are reported in the table (as expt) alongside the theoretically calculated values. In majority of the molecules, the G4 method employed in this study is able to estimate the enthalpies of formation to chemical accuracy (i.e, the difference between the theoretically calculated values and the

experimentally measured values is within ± 1 kcal/mol). The results from each isomeric group considered in this study are presented and discussed below.

C₂H₂O isomers: The enthalpies of formation (in descending order of magnitude), bonding backbone and the current astronomical observation for the C₂H₂O isomers are shown in Table 1. The theoretically calculated and the experimentally measured enthalpy of formation of ketene are in good agreement (± 1 kcal/mol). Of the three isomers of this group, only ketene has been astronomically observed.¹⁵⁴ Ketene has the smallest enthalpy of formation has compared to other isomers of the group showing the dominant role of thermodynamics in the formation process of interstellar molecules.

Table 3.21: C₂H₂O isomers, enthalpies of formation and astronomical status

Molecule	Structure	Backbone	Enthalpy of formation		Astronomical status
			Calc.	Expt.	
Oxirene		C-O-C	66.3		Not observed
Ethynol		C-C-O	23.2	9.9 ^{182,*}	Not observed
Ketene		C-C-O	-15.6	-14.8	Observed

*The reported enthalpy of formation for ethynol is very different from the calculated value. This experimental value was obtained from the fragmentation of diketene and the neutral molecule with a mass of 42 that has this enthalpy of formation is only assumed to be an isomer of ketene; ethynol. From available literature, there is dearth of information regarding the enthalpy of formation of ethynol that would have been used to compare with this value.

Ketene has the C-C-O backbone, the next stable isomer, ethynol, also has the same backbone. The only isomer of the group with the C-O-C backbone (oxirene) is also the least stable isomer of the group and probably the least abundant isomer of the group in ISM in comparison with other isomers of the group. As a result of its less stability and the expected low abundance, oxirene with the C-O-C backbone has less potential of formation as compared to other isomers of the group. This is in contrast to the saying of Mehringer et al.¹⁵³

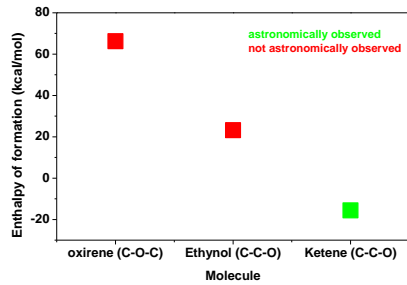


Figure 3.28: Plot of the enthalpy of formation for $\text{C}_2\text{H}_2\text{O}$ isomers.

Figure 3.28 depicts the plot of the $\text{C}_2\text{H}_2\text{O}$ isomers (with the backbone in bracket) against their enthalpies of formation. It is very conspicuous from the plot that the only astronomically observed isomer (indicated with green) of this group has the C-C-O backbone and it is the isomer with the smallest enthalpy of formation.

$\text{C}_2\text{H}_4\text{O}$ Isomers: The four known isomers of the $\text{C}_2\text{H}_4\text{O}$ family, their corresponding enthalpies of formation (in descending order of magnitude) and astronomical status are presented in Table 3.22 below. The enthalpies of formation obtained experimentally and theoretically are in good agreement. Of the four isomers of the group, three have the C-C-O backbone while one has the C-O-C backbone. All the isomers of this group have been detected in ISM.^{64-66, 155} Acetaldehyde (with the C-C-O bonding backbone) which has the smallest enthalpy of formation among all the isomers, was the first isomer of the group to be observed in ISM, indicating the prevalence of thermodynamics as the dominant factor in the formation processes of interstellar molecule. With respect to the enthalpy of formation of these isomers, the only isomer with the C-O-C backbone, ethylene oxide, has the highest enthalpy of formation and by extension is less stable, less abundant in ISM and as such will have less potential of formation as compared to other isomers of the group with the C-C-O bonding backbone as opposed to the words of Mehringer et al.¹⁵³

Figure 3.29 displays the enthalpy of formation of the $\text{C}_2\text{H}_4\text{O}$ isomers. It is crystal clear from the plot that the molecules with the smallest enthalpies of formation are those with the C-C-O backbone not the C-O-O backbone. Hence, the molecules with the C-C-O backbone in this group have higher potential of formation in ISM because they are more stable and more abundant as compared to ethylene oxide with the C-O-C backbone.

Table 3.22: $\text{C}_2\text{H}_4\text{O}$ isomers, enthalpies of formation and astronomical status

Molecule	Structure	Backbone	Enthalpy of formation		Astronomical status
			Calc.	Expt.	
Ethylene oxide		C-O-C	-14.6	-12.6	Observed
Vinyl alcohol (anti) (VAA)		C-C-O	-28.5	-29.9 ± 2.0	Observed
Vinyl alcohol (syn) (VAS)		C-C-O	-30.2	-30.6	Observed
Acetaldehyde		C-C-O	-42.4	-40.8 ± 0.4	Observed

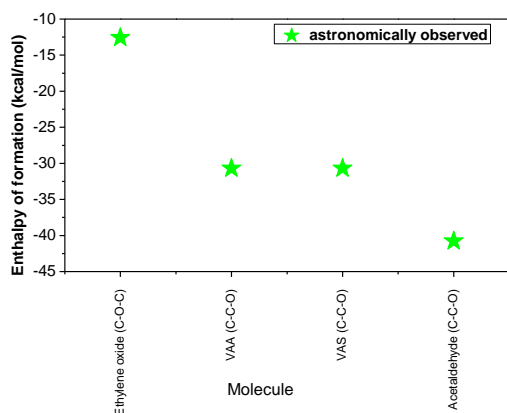


Figure 3.29: Plot of the enthalpy of formation for $\text{C}_2\text{H}_4\text{O}$ isomers.

$\text{C}_2\text{H}_4\text{O}_2$ isomers: Table 3.23 shows the isomers of the $\text{C}_2\text{H}_4\text{O}_2$ family, enthalpies of formation and astronomical status. Of the five isomers of this group, three have the C-C-O backbone while the remaining two have the C-O-C backbone. Three isomers of this group have been astronomically observed^{153,156,73}, of which two; acetic acid and glycolaldehyde have the C-C-O backbone while methyl formate is the only astronomically observed isomer of this group with the C-O-C backbone. From both the experimentally measured and theoretically calculated enthalpies of formation values, acetic acid is more stable than methyl formate and as such, it is expected to be more abundant than methyl formate in ISM. The

high abundance of methyl formate in ISM has given it a name “interstellar weed”. The high abundance of methyl formate in ISM compared to acetic acid is due to interstellar hydrogen bonding on the surface of the interstellar dust grains which causes a greater part of acetic acid to be attached to the surface of the grains thereby reducing its abundance. The acidic hydrogen in the COOH group of acetic acid is lacking in methyl formate, hence the effect of interstellar hydrogen bonding is not pronounced in methyl formate resulting in its high abundance as compared to acetic acid.

Table 3.23: $\text{C}_2\text{H}_4\text{O}_2$ isomers, enthalpies of formation and astronomical status

Molecule	Structure	Backbone	Enthalpy of formation		Astronomical status
			Calc	Expt	
1,2-dioxetane		C-C-O	-0.7		Not observed
1,3-dioxetane		C-O-C	-50.9		Not observed
Glycolaldehyde		C-C-O	-70.5		Observed
Methyl formate		C-O-C	-86.1	-86.5	Observed
Acetic acid		C-C-O	-103.7	-103.5 ± 0.7	Observed

Reactions on the surface of the interstellar dust grains are more dominant for the formation processes of interstellar molecules than gas phase reaction. These reactions on the surface of the interstellar dust grains serve as platform for interstellar hydrogen bonding.

Figure 3.30 pictured the plot of the $\text{C}_2\text{H}_4\text{O}_2$ isomers against their enthalpies of formation. As in the previous cases, the most stable isomer, acetic acid, is the isomer with the C-C-O backbone.

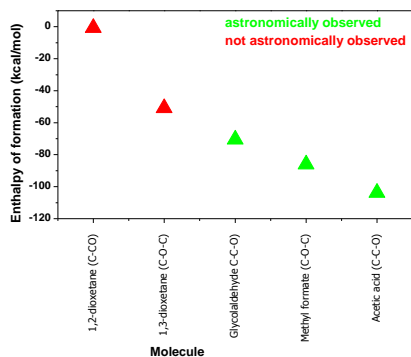


Figure 3.30: Plot of the enthalpy of formation for C₂H₄O₂ isomers.

C₂H₆O isomers: There are two isomers; dimethyl ether and ethanol, with the empirical formula C₂H₆O. Both isomers have been astronomically observed via their rotational transition spectra.⁸³⁻⁸⁵ Their enthalpies of formation and astronomical status are shown in Table 3.24. The experimentally measured and theoretically calculated enthalpies of formation of these isomers are in excellent agreement. Ethanol is more stable than dimethyl ether and as such, it should be more abundant in ISM than dimethyl ether. In accordance with the previous cases, the most stable isomer (isomer with the smallest enthalpy of formation), which is probably the most abundant in ISM with high potential of formation, has the C-C-O backbone not the C-O-C backbone as opposed to the statement of Mehringer et al.¹⁵³

Table 3.24: C₂H₆O isomers, enthalpies of formation and astronomical status

Molecule	Structure	Backbone	Enthalpy of formation		Astronomical status
			Calc	Expt	
Dimethyl ether		C-O-C	-45.1	-44.0±0.1	Observed
Ethanol		C-C-O	-56.7	-56.2	Observed

Fourteen molecules (from four isomeric groups) with C-C-O and C-O-C have been considered in this study, of these 14 molecules, 10 have been astronomically observed, of the astronomically observed molecules, 7 have the C-C-O backbone while 3 have the C-O-C backbone showing that molecules with the C-C-O backbone do not have less potential of formation in ISM as believed by Mehringer et al.¹⁵³

3.9.4 Summary on C-C-O Bonding Backbone: That molecules with the C-C-O backbone have less potential of formation in ISM compared to their counterparts with the C-O-C backbone has been shown to be wrong. In all the cases considered here, the most stable isomer and by extension the molecule with higher abundance in ISM which also has a higher potential of formation is the isomer with the C-C-O backbone in all the isomeric groups examined. Despite the fact that in all the cases considered here, molecules with the C-C-O backbone are found to be most stable and probably most abundant in ISM, bonding backbone alone is not enough to make conclusions regarding the formation processes of molecules in ISM. However, one factor stands out. From our previous study, the present results and available data in literature, interstellar formation processes are shown to be partially thermodynamically controlled.

3.10 Partition Function And Astronomical Observation Of Molecules: Is There A Link?

3.10.1 Introduction: The interstellar medium (ISM) which was seen as an empty vacuum dotted with stars and other celestial bodies by popular opinion in time past is now regarded as the largest chemical reservoir in the universe. This is as a result of the diverse kinds of molecules such as the different carbon chains, highly reactive ions, different organic species, high molecular isomers and the "non-terrestrial" molecules which are very unfamiliar in the terrestrial laboratory; that have been uniquely detected and the ones that are expected and are believed to be present though yet to be detected.^{2,157} The advances in the field of astrophysics, astrochemistry and related fields are the direct results in the improvements in astronomical instruments, spectroscopic tools and the concerted efforts of the laboratory spectroscopists, astrophysicists and the astronomers. From the observation of a few diatomic species; CH, CN and CH⁺ in the 1940s,^{158,140} the first alcohols; CH₃OH and CH₃CH₂OH in the 1970s,^{83,159} to the observation of the first branched chain molecule in 2014.⁹⁹ Till date, about 200 different interstellar and circumstellar molecules have been uniquely detected from different astronomical sources largely through their rotational transition spectra. There is high hope for the observations of more complex molecules in ISM including the "non-terrestrial ones" with the increased advances in these fields.

Of all the known interstellar and circumstellar molecules, only about 10 (including the fullerenes and excluding the unconfirmed claimed observation of 2H-azirine) are cyclic; c-SiC₂, c-SiC₃, c-C₃H, c-C₃H₂, c-H₂C₃O, c-C₂H₄O, benzene, C₆₀, C₇₀ and C₆₀⁺.^{81,100-104,155, 160,161} The few number of known cyclic interstellar and circumstellar molecules and their unsuccessful searches have resulted in a number of questions. In the searches for interstellar ethylene oxide, Dicken etc al.¹¹ said "*The question remains of whether cyclic molecules are chemically less abundant than their related linear species in the ISM, or whether their emission in any one transition is weaker because of a larger partition function, so astronomical detections are more difficult*". Amino acids are important biological molecules. Among these molecules, glycine is the simplest amino acids. Different groups have sought for interstellar glycine from several astronomical sources using different observational

facilities with no successful detection of interstellar glycine till date. The difficulties in detecting glycine and other amino acids have been linked to large molecular partition function of these molecules among other factors.¹⁶²⁻¹⁶⁷

Studies have shown that interstellar formation processes are partially thermodynamically controlled as discussed in the previous sections. Interstellar isomerism is one of the most pronounced features among interstellar and circumstellar molecules. These isomers are believed to have common precursors for their formation routes and as such have equal chances of been detected in the ISM but this is not the case as some of the isomers are detected while others are not. Astronomical detection of some isomers at the expense of others is accounted for on the basis of thermodynamics which controlled the interstellar formation processes. The aim of this letter is to examine, the link between partition and the astronomical detection of molecules in ISM. Different isomeric groups with at least one isomer detected from each group are considered. Isomers are considered based on the reason stated above. All the isomeric groups considered here are also subjected to thermodynamic test by determining the accurate enthalpies of formation of each isomeric species. The details of the high level chemical simulations employed in determining the partition function and the enthalpies of formation all the systems considered in this letter are described in the next section.

3.10.2 Methodology: The GAUSSIAN 09 suite of programs¹⁰ in is employed for all the quantum chemical calculations reported here. The computation of partition function with this program is briefly summarised. The equations used in calculating the different partition functions by the program are described in details in the book by McQuarrie and Simon¹⁶⁸; and in the white paper on 'thermochemistry in GAUSSIAN'¹⁶⁹. For all the systems considered here, the equations are applicable to ideal gases because the particles are assumed to be non-interacting. The error introduced by this assumption depends on the level of the non-ideality of the system under consideration. This error can easily be mitigated in the present case since the systems under consideration are all isomers with many properties in common. The equation used in computing the translational partition function is given as

$$q_t = \left(\frac{2\pi m k_B T}{h^2} \right)^{3/2} \frac{k_B T}{P}. \quad \text{equ. 1.}$$

Where q_t = translational partition function; m = mass of the molecule; K_B = Boltzmann constant; T = temperature; h =Plank's constant; P = pressure. For the electronic partition function, the usual equation for computing it is give as

$$q_e = \omega_0 e^{-\epsilon_0/k_B T} + \omega_1 e^{-\epsilon_1/k_B T} + \omega_2 e^{-\epsilon_2/k_B T} + \dots \quad \text{equ. 2.}$$

Where ω is the degeneracy of the energy level, and ϵ_n is the energy of the n -th level as described in the white paper. The first electronic excitation energy is assumed to be much greater than $K_B T$. Also, the first and higher excited states are assumed to be inaccessible at any temperature. The energy of the ground state is set to zero. Putting these assumptions together, equation 2 reduces to

$$q_e = \omega_0 \quad \text{equ. 3.}$$

This equation is simply the electronic spin multiplicity of the molecule under considerations. Equations 4 and 5 are used in computing the rotational partition function for linear molecules and nonlinear polyatomic molecules respectively.

$$q_r = \frac{1}{\sigma_r} \left(\frac{T}{\Theta_r} \right) \quad \text{equ. 4}$$

$$q_r = \frac{\pi^{1/2}}{\sigma_r} \left(\frac{T^{3/2}}{(\Theta_{r,x} \Theta_{r,y} \Theta_{r,z})^{1/2}} \right) \quad \text{equ. 5}$$

The parameter σ_r in equations 4 and 5 is called the symmetry number which is the number of indistinguishable orientations of the molecule. The quantity $\Theta_r, \Theta_{r,(xyz)}$ is the characteristic temperature for rotation (in the x, y or z plane) defined as follows; $\Theta_r = h^2/8\pi^2Ik_B$ where I is the moment of inertia.

For all the calculations reported here, only equilibrium structures were considered with no imaginary frequency. Hence, the vibrational partition function is computed considering real modes only. The zero-point energy is included in the computing the vibrational partition function; therefore, the first vibrational level is chosen to be the zero of the energy ($V=0$) and the partition function for each vibrational level is given as

$$q_{v,K} = \frac{1}{1 - e^{-\Theta_{v,K}/T}} \quad \text{equ. 6}$$

while the overall vibrational partition function is given as

$$q_v = \prod_K \frac{1}{1 - e^{-\Theta_{v,K}/T}} \quad \text{equ. 7.}$$

Where K is the index of vibrational modes and $\Theta_{v,K}$ is the characteristic temperature for vibration K . Partition function increases with temperature and vice versa. Hence, computing the partition function at different temperatures will give no extra information with respect to the aim of this work. Therefore, the reported values of partition functions in this work are computed at the standard temperature of 298.15K. The Gaussian 4 (G4) composite method was employed in computing the partition functions and the enthalpies of formation for all the systems considered in this study.^{12,13,170} Details on the estimation of enthalpies of formation are as reported in the previous sections; 3.1.0 and 3.1.1. The choice of this level of theory is from experience as discussed in other studies above. This level of theory is known to predict thermodynamic parameters that are in good agreement with experimental values where available.

3.10.3 Results and Discussion

Results from the high level quantum chemical simulations with the Gaussian G4 composite method obtained for all the systems considered in this work are presented and discussed here. The different isomeric groups are grouped according to the number of atoms making up each group ranging from 3 to 12. The molecular partition functions (q) are reported in terms of logarithm to base 10[$\text{Log}_{10}(q)$] while the enthalpy of formation of the molecules are reported in kcal/mol. The current astronomical status for these molecules is based on the available literature presently available for these molecules as much as we know.

Isomers with 3 atoms: The partition function, enthalpy of formation and the current astronomical status of the 10 species from 5 isomeric groups with 3 atoms considered in this study are presented in Table 3.25. These species have even number of electrons resulting in a spin multiplicity of 1, thus the electronic partition function for each of these molecules is zero (since $\log_{10} 1=0$). Of the 120 molecules considered in this study, only C₃H (both cyclic and linear) has odd number of electrons resulting in a spin multiplicity of 2 and a non-zero electronic partition function. Hence, the total partition function for all the molecules considered here is only the contribution from translational, rotational and vibrational partition functions except for the C₃H systems with extra contribution from the electronic partition function. From Table 3.25, one molecule has been detected from each of the isomeric groups except for the CHN case where both HCN and HNC have been detected.^{16-18,25,26,171} From the partition function, in all the cases where only one molecule has been detected from the isomeric group, the detected molecule has a higher partition function as compared to the molecule that has not been detected in contrast to the idea that larger molecular partition function hampers the astronomical detection of molecules. The enthalpy of formation shows a reverse trend, the detected molecules with higher molecular partition functions have lower enthalpies of formation as compared the ones that have not been detected from each group (with the exception of l-C₂Si that has not been detected; see explanation below).

Table 3.25: Molecular partition function, enthalpy of formation and current astronomical status of isomers with 3 atoms

Molecule	Partition function [Log ₁₀ (q)]					$\Delta_f H^\circ$ (kcal/mol)	Astronomical status
	Qt	qe	Qr	qv	Total q		
l-C ₂ Si	7.2	0.0	3.0	11.0	21.2	159.8	Not detected
c-C ₂ Si	7.2	0.0	4.0	11.6	22.8	160.5	Detected
OCN ⁻	7.0	0.0	2.7	9.8	19.5	-40.7	Detected
ONC ⁻	7.0	0.0	0.8	7.8	15.6	-23.6	Not detected
HCN	6.7	0.0	2.1	8.9	17.7	32.2	Detected
HNC	6.7	0.0	1.9	8.7	17.3	45.6	Detected
AlNC	7.2	0.0	3.0	11.1	21.3	65.8	Detected
AlCN	7.2	0.0	2.9	10.4	20.5	73.1	Not detected
NaCN	7.1	0.0	4.2	11.6	22.9	34.5	Detected
NaN ₂	7.1	0.0	3.8	11.0	21.9	37.0	Not detected

The astronomical detection of the molecules with lower enthalpies of formation as compared to the ones with higher enthalpies of formation implies that the molecules with lower enthalpies of formation which of course are more stable are probably more abundant in the interstellar space (since they are less reactive as compared to their counterparts with higher enthalpies of formation which are less stable, very reactive and thus less abundant) and thus can easily be astronomically detected irrespective of their molecular partition functions. The energy, stability and abundance (ESA) relationship existing among interstellar and circumstellar molecules is well established as shown in other studies earlier discussed above. In analogy with C₃, the C₂Si system has long been thought to be linear even as ab initio method predicts the linear form of C₂Si to be the most stable isomer. As it is often said; “theory guides, experiment decides”, the eventual detection of silicon dicarbide via a laboratory experiment which demonstrated that C₂Si has a compact ring with C_{2v} symmetry rather than a linear structure as earlier assumed.¹⁷² Thus, there are no experimental data which could warrant the astronomical searches for the linear silicon dicarbide even when it is predicted to be the most stable isomer.

Isomers with 4 atoms: Table 3.26 shows the partition function, enthalpy of formation and the current astronomical status of 10 molecules from 4 isomeric groups with 4 atoms examined in this study. In accordance with the condition for choosing these isomeric groups, at least one isomer has been uniquely detected from each isomeric group. Cyclic C₃Si is the only isomer of the C₃Si isomeric group that has been detected despite its larger partition function compared to the linear C₃Si.¹⁷³ The reason for this could easily be seen from the high stability (low enthalpy of formation) of c-C₃Si probably resulting in its high abundance and possible astronomical detection as compared to the linear counterpart. This same explanation also applies to the C₂HN isomeric group where HCCN with lower enthalpy of formation has been detected and HCNC with higher enthalpy of formation has not been detected.³⁷ Regardless of the near similarity in the partition function of both isomers, the dominant factor for the astronomical detection of HCCN at the expense of HCNC is the abundance of HCCN which can be traced to its stability as shown in its low enthalpy of formation as compared to HCNC. The astronomical detection of more than one isomeric species in the C₃H and CHNO isomeric groups gives ample opportunity to demonstrate the fact that the thermodynamically most stable isomer is also the most abundant isomer in the interstellar medium which account for why such isomers are easily detected at the expense of other.

The column density reported for l-C₃H which is the most stable isomer of the group is 2.8*10¹³ cm⁻² while that of c-C₃H is 6*10₁₂ cm⁻².^{160,174} In the CHNO group, HNCO, HOCH and HCNO have all been detected. The reported abundance ratio of HNCO/HCNO is 40-70 in the molecular group and greater than 1000 in the hot core region.³³⁻³⁶ It is interesting to note that in many of the case where more than one isomer from the same isomeric group has been detected, the most stable isomer which is probably the most abundant isomer is mostly detected first before the other isomers, thus implying the importance of the interstellar abundance of a molecule in its detection. The linear C₃H was detected before the cyclic; HNCO was detected more than three decades before the other isomers could be detected. The partition function of HOCH that has not been detected is similar to those of HNCO and

HOCN that have been detected. The non-detection of HONC can thus not be linked to its partition function as its isomers with similar partition functions have been detected.

Table 3.26: Molecular partition function, enthalpy of formation and current astronomical status of isomers with 4 atoms

Molecule	Partition function [$\log_{10}(q)$]					$\Delta_f H^\circ$ (kcal/mol)	Astronomical status
	Qt	qe	qr	qv	Total q		
c-C ₃ Si	7.3	0.0	4.4	12.0	23.7	211.8	Detected
l-C ₃ Si	7.3	0.0	3.4	11.4	22.1	221.7	Not detected
l-C ₃ H	6.9	0.3	2.7	10.2	20.1	168.8	Detected
c-C ₃ H	6.9	0.3	3.7	11.0	21.9	338.8	Detected
HCCN	7.0	0.0	3.5	10.7	21.2	122.6	Detected
HCNC	7.0	0.0	3.5	10.7	21.2	133.5	Not detected
HNCO	7.1	0.0	3.4	10.5	21.0	-33.4	Detected
HOCN	7.1	0.0	3.5	10.6	21.2	-4.4	Detected
HCNO	7.1	0.0	0.1	7.6	14.8	34.1	Detected
HONC	7.1	0.0	3.5	10.8	21.4	52.8	Not detected

Isomers with 5 atoms: 15molecular species from 5 isomeric groups comprising of 5 atoms each are presented in Table 3.27 alongside their partition function, enthalpy of formation and their current astronomical status. In the C₃H₂ isomeric group where both the linear and the cyclic isomers have been detected, the linear isomer which is shown to be the most stable isomer is found to be at least 1% more abundant than the cyclic isomer from the reported column density in TMC-1.^{102,175} Ketene is the only astronomically detected isomer of the H₂C₂O isomeric group.¹⁵⁴ Ketene has a higher partition function than ethynol that has not been detected. Thermodynamically, ketene is found to be far more stable than both ethynol and oxirene that have not been detected. Thus, the detection of ketene and the non-detection of its isomers do not show any correlation with their partition function rather there is a direct correlation between interstellar abundance and astronomical detection. In the CH₂N₂ isomeric group, where the three isomers have very similar partition function; the astronomically detected isomer of the group; NH₂CN has partition function that is in-between the highest (NH₂NC) and the lowest (CH₂N);⁴⁵ showing that there is no relationship between the astronomical detection of NH₂CN and its partition function.

Table 3.27: Molecular partition function, enthalpy of formation and current astronomical status of isomers with 5 atoms

Molecule	Partition function [Log10(q)]					ΔfHO (kcal/mol)	Astronomical status
	Qt	qe	qr	Qv	Total q		
I-C3H2	7.0	0.0	2.5	9.6	19.1	152.6	Detected
c-C3H2	7.0	0.0	3.5	10.5	21.	183.0	Detected
Ketene	7.0	0.0	3.7	10.8	21.5	-15.6	Detected
Ethynol	7.0	0.0	3.5	10.8	21.3	23.2	Not detected
Oxirene	7.0	0.0	3.9	11.2	22.1	66.3	Not detected
NH2CN	7.0	0.0	3.7	10.8	21.5	29.2	Detected
CH2NN	7.0	0.0	3.7	10.8	21.5	55.6	Not detected
NH2NC	7.0	0.0	3.7	10.9	21.6	72.7	Not detected
HCCCN	7.2	0.0	1.2	8.6	17.0	88.3	Detected
HCCNC	7.2	0.0	1.3	8.7	17.0	112.4	Detected
HNCCC	7.2	0.0	3.7	11.4	22.3	133.7	Detected
CC(H)CN	7.2	0.0	4.2	11.9	23.3	138.8	Not detected
HCNCC	7.2	0.0	1.7	9.4	18.3	160.9	Not detected
HCOCN	7.2	0.0	4.3	11.8	23.3	10.6	Detected
HCONC	7.2	0.0	4.3	12.0	23.5	21.4	Not detected

However, the enthalpy of formation of the astronomically detected isomer as compared to its isomers answers the question why it has been detected. This same argument applies for the C₂HNO group where one isomer has been detected notwithstanding the similarity in their partition function.¹⁷⁶ In the C₃HN isomeric group; of the 5 isomers, 3 have been astronomically detected, thus giving yet another opportunity to show the link between thermodynamic stability, interstellar abundance and astronomical detection. The reported abundance ratio of HC₃N/HC₂NC is of the order of 20 to 60 clouds while that of HC₃N/HNC₃ is of the order 160 to 450 in the molecular clouds.^{46,42,43} The most stable isomer of the C₃HN isomeric group; HC₃N was astronomically observed decades before the other isomers as noted in previous case. While there is no clear-cut link between the astronomical observation and partition function as shown from the computed partition function of these molecules presented in the table, the relationship between astronomical detection and interstellar abundance (from thermodynamic stability) is well-defined.

Isomers with 6 atoms: In this subsection, we present 14 complex species from 4 isomeric groups with 6 comprising of 6 atoms each. Table 3.28 shows the partition function, enthalpy of formation and the astronomical status of these species. The C₂H₃N isomeric group is one of the very few interstellar isomeric groups with three astronomically observed isomers. This group also possesses another interesting feature by containing two cyclic isomers; making it a good case to test the effect of partition function in the astronomical detection of cyclic molecules.

Table 3.28: Molecular partition function, enthalpy of formation and current astronomical status of isomers with 6 atoms

Molecule	Partition function [$\text{Log}_{10}(q)$]					$\Delta_f H^\circ$ (kcal/mol)	Astronomical status
	Qt	qe	qr	qv	Total q		
Methylene ketene	7.2	0.0	4.2	11.8	23.2	24.8	Not detected
Propynal	7.2	0.0	4.3	11.9	23.4	32.1	Detected
Cyclopropenone	7.2	0.0	4.3	11.6	23.1	35.5	Detected
		0.0					
Methyl cyanide	7.0	0.0	3.9	11.0	21.9	15.8	Detected
Methyl isocyanide	7.0	0.0	3.8	11.1	21.9	38.8	Detected
Ketenimine	7.0	0.0	3.8	10.9	21.7	38.9	Detected
Ethynamine	7.0	0.0	3.7	11.0	21.7	58.1	Not detected
2H-azirine	7.0	0.0	3.9	10.9	21.8	62.4	Not detected
1H-azirine	7.0	0.0	3.9	11.0	21.9	96.7	Not detected
		0.0					
Formamide	7.1	0.0	4.0	11.4	22.5	-47.3	Detected
Hydroxymethylimine	7.1	0.0	4.0	11.1	22.2	-34.7	Not detected
Nitrosomethane	7.1	0.0	4.0	11.4	22.5	13.5	Not detected
		0.0					
HC ₄ N	7.3	0.0	4.6	12.7	24.6	163.6	Detected
HC ₃ NC	7.3	0.0	4.6	12.7	24.6	181.1	Not detected

The partition function of the C₂H₃N isomers ranges from 21.7 to 21.9 with the cyclic isomers falling in-between the range as opposed to the idea that cyclic molecules have larger partition function. While the isomer with least partition function; ethynamine has not been detected, the one with the highest partition function; methyl isocyanide has been detected; still pointing the fact that there is no correlation between the partition function and the astronomical observation of isomeric species. The astronomical detections of these isomers are thermodynamically controlled as shown from the enthalpies of formation of these isomers (Table 3.28). That there is a direct relationship between the stability of a molecule and its interstellar abundance which influences astronomical detection is conspicuously observed from the three isomers that have been detected in the C₂H₃N group. The abundance ration of CH₃CN/CH₃NC is about 50 while that of CH₃CN/CH₂CNH is about 100 in different astronomical sources which is a direct reflection of the their thermodynamic stabilities.^{6,28,52,53,55,177}

In the CH₃NO and C₄HN groups, isomer has been detected from each group.^{54,57} Though there is no correlation between the partition function and the detected isomers as the isomers with the least partition function in each group has not been detected; the relationship between thermodynamic stability and astronomical detection is well observed as the detected molecule in each isomeric group are also the most stable in their respective group. In the C₂H₃O isomeric group, propynal and cyclopropenone (with the highest and the lowest partition function respectively) have been detected.^{100,47} Methylene ketene and methyl ketene are proposed as potential candidates for astronomical detection on the grounds that they are found to be most stable isomers in their respective groups; they are less affected by

interstellar hydrogen bonding on the surface of the interstellar dust grains as compared to their isomers and the simplest ketene molecule has been detected.

Isomers with 7 atoms: $\text{C}_2\text{H}_4\text{O}$ and $\text{C}_3\text{H}_3\text{N}$ are the isomeric groups with 7 atoms considered in the present study. The partition function, enthalpy of formation and astronomical status of the molecules belonging to these groups are presented in Table 3.29. All the known isomers of the $\text{C}_2\text{H}_4\text{O}$ group have been astronomically observed.^{155,64-66} In contrast to the idea that cyclic molecules have larger partition function, ethylene oxide; the only cyclic isomer of the $\text{C}_2\text{H}_4\text{O}$ group is the isomer with the least partition function as compared to other isomers of the group.

Table 3.29: Molecular partition function, enthalpy of formation and current astronomical status of isomers with 7 atoms

Molecule	Partition function [$\text{Log}_{10}(q)$]					$\Delta_f\text{H}^\text{O}$ (kcal/mol)	Astronomical status
	Qt	qe	qr	qv	Total q		
Acetaldehyde	7.1	0.0	4.1	11.5	22.7	-42.4	Detected
Vinyl alcohol (syn)	7.1	0.0	4.1	11.2	22.4	-30.2	Detected
Vinyl alcohol (anti)	7.1	0.0	4.0	11.3	22.4	-28.5	Detected
Ethylene oxide	7.1	0.0	4.0	11.1	22.2	-14.6	Detected
Acrylonitrile	7.2	0.0	4.4	11.9	23.5	43.3	Detected
Isocyanoethene	7.2	0.0	4.4	11.9	23.5	63.2	Not detected

As a fact that the thermodynamically most stable isomer is also the most abundant isomer in the interstellar space, the reported abundance ratios of acetaldehyde/ethylene oxide and acetaldehyde/vinyl alcohol range from 2 to 10 in different astronomical sources.^{66,68,178} Acetaldehyde; the most stable and the most abundant isomer of the group was the first isomer of the group to be astronomically observed as seen in previous cases. This implies the ease in the astronomical detection of an abundant species as compared to the less abundant species. Acrylonitrile is the only astronomically detected isomer of the $\text{C}_3\text{H}_3\text{N}$ group.⁷¹ The near similarity in the partition function of acrylonitrile and its isocyanide does not lead to the detection of both isomers. The detection of acrylonitrile and the non-detection of isocyanoethene could be understood from the thermodynamic stabilities not as a function of their partition function.

Isomers with 8 atoms: Among the interstellar molecules with 8 atoms, 19 molecules from three isomeric groups are examined in this study. Table 3.30 shows their partition function, enthalpy of formation and current astronomical status. Of the 19 molecules considered, 6 are cyclic. These cyclic molecules are seen to have the least partition function in their respective groups as shown in the table.

The $\text{C}_2\text{H}_4\text{O}_2$ isomeric group is yet another interstellar isomeric group with three astronomically detected isomers which are also the most stable isomers of the group. The

detected molecules have the higher total partition functions as compared to the non-detected ones supporting the fact that there is no correlation between partition function and the astronomical detection of these species. The reported abundance ration of acetic acid/methyl formate rages from 0.01 to 0.1 while that of acetic acid/glycolaldehyde is approximately 0.05.^{74,153,179,180} This is the reverse of what has been observed in the previous cases where the most stable isomer is found to be the most abundant isomer in the interstellar space. Why is this sudden change in the trend? Reactions that occur on the surface of the interstellar dust grains are seen as the dominant process by which interstellar molecules are formed. Water molecule which is the main composition of the interstellar dust grains has been shown to form hydrogen bonding with the molecules that are formed on the surface of the interstellar dust grains thereby reducing the abundance of these molecules. Interstellar hydrogen bonding is discussed in chapter 4 of this Thesis.

Table 3.30: Molecular partition function, enthalpy of formation and current astronomical status of isomers with 8 atoms

Molecule	Partition function [$\text{Log}_{10}(q)$]					$\Delta_f\text{H}^\text{O}$ (kcal/mol)	Astronomical status
	Qt	qe	qr	qv	Total q		
Acetic acid	7.3	0.0	4.6	12.5	24.4	-103.7	Detected
Methylformate	7.3	0.0	4.5	12.4	24.2	-86.1	Detected
Glycolaldehyde	7.3	0.0	4.6	12.4	24.3	-70.5	Detected
1,3-dioxetane	7.3	0.0	4.4	11.9	23.6	-50.9	Not detected
1,2-dioxetane	7.3	0.0	4.4	12.1	23.8	-0.7	Not detected
Methyl ketene	7.2	0.0	4.5	12.3	24.0	-18.1	Not detected
Propenal	7.2	0.0	4.5	12.2	23.9	-15.8	Detected
Cyclopropanone	7.2	0.0	4.5	11.9	23.6	0.7	Not detected
Propynol	7.2	0.0	4.3	13.0	24.5	12.7	Not detected
Propargyl alcohol	7.2	0.0	4.5	12.3	24.0	17.2	Not detected
Methoxyethyne	7.2	0.0	4.4	12.3	23.9	23.9	Not detected
1-cyclopropenol	7.2	0.0	4.5	11.9	23.6	25.9	Not detected
2-cyclopropenol	7.2	0.0	4.4	12.0	23.6	27.4	Not detected
Epoxypropene	7.2	0.0	4.5	12.5	24.2	47.7	Not detected
CH ₃ CCCN	7.3	0.0	4.5	12.7	24.5	73.1	Detected
CH ₂ CCHCN	7.3	0.0	4.8	12.7	24.8	76.2	Detected
HCCCH ₂ CN	7.3	0.0	4.8	12.8	25.0	86.1	Not detected
CH ₃ CCNC	7.3	0.0	4.5	12.6	24.4	98.6	Not detected
CH ₂ CCHNC	7.3	0.0	4.8	12.8	24.9	98.7	Not detected

Subjecting the three isomers of the C₂H₄O₂ group that have been astronomically detected to interstellar hydrogen bonding with water shows that acetic acid is more strongly bonded to the surface of the interstellar dust grains followed by glycolaldehyde while methyl formate is the least. Thus the abundance of acetic acid is drastically reduced as compared to those of glycolaldehyde and methyl formate. The non-detection of methyl ketene; the most

stable isomer of the C_3H_4O group and the need for its astronomical search has been discussed (subsection 3.4). With the exception of methyl ketene, the only detected isomer of the C_3H_4O group is propenal which is thermodynamically the most stable isomer and probably the most abundant isomer.¹⁸⁰ The low partition function of the cyclic molecules in this group notwithstanding; none of the cyclic molecules of this group has been detected simply due to low thermodynamic stability resulting in a possible low interstellar abundance. In the C_4H_3N isomeric group, the trend is as discussed above as the detected isomers are the ones with the least enthalpy of formation regardless of their partition function.^{56,180,181}

Isomers with 9 atoms: Two isomeric groups; C_3H_5N and C_2H_5ON making up a total 15 molecular species are investigated under isomers with nine atoms. Table 7 highlight these molecules, their partition function and their corresponding enthalpy of formation. Cyanoethane and acetamide are the astronomically detected isomers from their respective groups.^{61,87} The detection of these molecules is not surprising as they are the most thermodynamically stable isomers in their respective groups, thus they are expected to be the most abundant species in the interstellar medium in comparison to other isomers from their respective groups. In the C_3H_5N isomeric group, the partition function ranges from 23.1 to 24.1 with the cyclic molecules having both the lowest (1-Azetine) and the highest [1-azabicyclo(1.1.0)butane]. In the C_2H_5ON group, as opposed to the idea that larger partition function influences the astronomical detection of molecules, the only detected isomer of the group is the isomer with the largest partition function while the one with lowest partition function is a cyclic molecule that has not been detected.

Table 3.31: Molecular partition function, enthalpy of formation and current astronomical status of isomers with 9 atoms

Molecule	Partition function [$\log_{10}(q)$]					Δ_fH° (kcal/mol)	Astronomical status
	qt	qe	qr	qv	Total q		
Cyanoethane	7.2	0.0	4.6	12.3	24.1	11.0	Detected
Isocyanoethane	7.2	0.0	4.5	12.3	24.0	31.8	Not detected
Propylenimine	7.2	0.0	4.5	12.3	24.0	32.9	Not detected
2-propen-1-imine	7.2	0.0	4.5	12.3	24.0	36.2	Not detected
N-methylene ethenamine	7.2	0.0	4.5	12.1	23.8	36.9	Not detected
1-Azetine	7.2	0.0	4.4	11.7	23.3	43.2	Not detected
Cyclopropanimine	7.2	0.0	4.5	11.9	23.6	48.2	Not detected
Methylene azaridine	7.2	0.0	4.5	11.9	23.6	54.8	Not detected
Propargylamine	7.2	0.0	4.5	12.3	24.0	56.1	Not detected
1- azabicyclo(1.1.0)butane	7.2	0.0	4.3	11.6	23.1	64.4	Not detected
Acetamide	7.2	0.0	4.6	12.9	24.7	-61.9	Detected
N-methylformamide	7.2	0.0	4.5	12.5	24.2	-52.2	Not detected
Nitrosoethane	7.2	0.0	4.6	12.5	24.3	2.8	Not detected
1-aziridinol	7.2	0.0	4.5	12.3	24.0	16.01	Not detected
Cyanoethoxyamide	7.2	0.0	4.5	12.3	24.0	72.5	Not detected

Isomers with 10 atoms: Three isomeric groups of interstellar complexes with 10 atoms making up a total of 14 species chosen in the present investigation are shown in Table 3.32 with their corresponding partition function and enthalpy of formation.

Table 3.32: Molecular partition function, enthalpy of formation and current astronomical status of isomers with 10 atoms

Molecule	Partition function [$\text{Log}_{10}(q)$]					ΔH^O (kcal/mol)	Astronomical status
	Qt	qe	qr	qv	Total q		
Propanone	7.2	0.0	4.3	12.7	24.2	-55.0	Detected
Propanal	7.2	0.0	4.6	12.7	24.5	-47.0	Detected
Propen-2-ol	7.2	0.0	4.6	12.3	24.1	-41.2	Not detected
1-propen-1-ol	7.2	0.0	4.6	12.7	24.5	-36.4	Not detected
Methoxyethene	7.2	0.0	4.6	12.3	24.1	-29.4	Not detected
2-propene-1-ol	7.2	0.0	4.6	12.5	12.3	-27.9	Not detected
1,2-epoxypropane	7.2	0.0	4.5	12.3	24.0	-25.0	Not detected
Cyclopropanol	7.2	0.0	4.5	12.1	23.8	-23.8	Not detected
Oxetane	7.2	0.0	4.4	12.3	23.9	-21.8	Not detected
Ethylene glycol	7.3	0.0	4.6	12.8	24.7	-87.5	Detected
Ethylhydroperoxide	7.3	0.0	4.6	12.8	24.7	-41.7	Not detected
Dimethane peroxide	7.3	0.0	4.5	13.9	25.7	-35.9	Not detected
$\text{CH}_3(\text{CC})_2\text{CN}$	7.5	0.0	4.9	14.2	26.6	125.3	Detected
$\text{CH}_3(\text{CC})_2\text{NC}$	7.5	0.0	4.9	14.2	26.6	150.6	Not detected

In the $\text{C}_3\text{H}_6\text{O}$ group where propanone and propanal have been detected,^{74,89} propanal is the isomer with the largest partition function while the one with the lowest partition function is a cyclic molecule (1,2-epoxypropane) that has not been astronomically observed. Thus, showing lack of correlation between partition function and the astronomical detection of these isomers. In the $\text{C}_2\text{H}_6\text{O}_2$ group, the only detected isomer; ethylene glycol⁹⁰ has partition function which is in-between the largest (dimethane peroxide) and the lowest (ethylhydroperoxide) while in the $\text{C}_6\text{H}_3\text{N}$ group, the only detected molecule; $\text{CH}_3(\text{CC})_2\text{CN}$ ⁹² has very similar partition function to its isocyanide counterpart that has not been detected. These all support the fact that in the astronomical detection of isomers or other related species, partition function is not a determining factor. Regardless of the lack of a well-defined relationship between partition function and the astronomical detection of the molecules discussed in this subsection, one unique relationship stands and that is the fact that all the detected molecules in the three isomeric groups considered here are the thermodynamically most stable molecules in their respective groups. Thus, supporting thermodynamics as the dominant controlling factor in the astronomical detection of these molecules.

Isomers with 11 atoms: Among the few known interstellar molecules with 11 atoms, the $\text{C}_3\text{H}_6\text{O}_2$ isomeric group is the only one with two known interstellar molecules; hence the reason for been chosen here. The partition function, enthalpy of formation and the current astronomical status of these molecules are presented in Table 3.33.

Table 3.33: Molecular partition function, enthalpy of formation and current astronomical status of isomers with 11 atoms

Molecule	Partition function [$\text{Log}_{10}(q)$]					$\Delta_f H^\circ$ (kcal/mol)	Astronomical status
	Qt	Qe	qr	qv	Total q		
Propanoic acid	7.4	0.0	4.9	13.6	25.9	-109.4	Not detected
Ethylformate	7.4	0.0	4.9	13.3	25.6	-97.5	Detected
Methyl acetate	7.4	0.0	4.9	13.5	25.8	-95.1	Detected
Lactaldehyde	7.4	0.0	4.9	13.5	25.8	-81.3	Not detected
Dioxolane	7.4	0.0	4.7	13.0	25.1	-73.3	Not detected
Glycidol	7.4	0.0	4.9	13.1	25.4	-57.3	Not detected
Dimethyldioxirane	7.4	0.0	4.8	13.0	25.2	-27.7	Not detected

As in the previous cases, there is no correlation between the detected molecules and partition function as the detected molecules are neither the molecules with the largest nor the lowest partition function. As discussed earlier, interstellar hydrogen bonding is known to affect the astronomical detection of molecules. From Table 3.33, the thermodynamically most stable isomer which is probably the most abundant isomer of the group; propanoic acid is yet to be astronomically observed. The delay in the astronomical detection of propanoic acid has been shown to be largely due to interstellar hydrogen bonding (as discussed in chapter 4). Propanoic acid is my strongly bonded to the surface of the interstellar dust grains thereby reducing its interstellar abundance as compared to both ethylformate and methyl acetate which have been detected. With the exception of propanoic acid whose delayed detection has been accounted on the basis of interstellar hydrogen bonding, the two detected isomers of this group are the thermodynamically most stable and by extension the most abundant isomers in the interstellar medium. The order of detection and the reported column densities of these isomers are in accordance with their thermodynamic stability. Ethylformateformate was first detected⁷⁵ followed by methyl acetate .⁷⁶ The reported column density for ethylformate and methyl acetate are $5.4 \times 10^{16} \text{ cm}^{-2}$ and $4.2 \pm 0.5 \times 10^{15} \text{ cm}^{-2}$ respectively.⁹⁴⁻⁹⁵

Isomer with 12 atoms: As much as we know, there are four interstellar molecules with 12 atoms; benzene, ethyl methyl ether, n-propyl cyanide and isopropyl cyanide.^{81,94,98,99} The choice of the C_6H_6 isomeric group for consideration here is very appropriate. This is because the only cyclic molecule with 12 atoms (benzene) belongs to this group, and the limited number of known interstellar/circumstellar cyclic molecules has often been linked to their large molecular partition function. The partition function, enthalpy of formation and astronomical status of the 10 most stable isomers of the C_6H_6 group are shown in Table 3.34.

The Gaussian G4 compound model is well known for predicting energies that are good agreement with experiment values (where such values are available). This is well demonstrated in the previous examples. As an example in the present study, the experimentally determined standard enthalpy of formation of benzene reported in the NIST website is 19.1kcal/mol while the theoretically predicted value is at the G4 level employed in this study 18.8kcal/mol which in excellent agreement with the experimental value. The partition function of the C_6H_6 isomers ranges from 23.4 to 27.7 with benzene having the least partition function. The astronomical detection of benzene cannot be linked to its low partition

function as this has been to not to be true from all the cases discussed in the previous subsections. However, benzene is seen to be extremely stable in comparison with its isomers with the next isomer (fulvene) having an enthalpy of formation that is almost thrice that of benzene. Thus, the high thermodynamic stability of benzene implies a high interstellar abundance for benzene, hence its astronomical detection in comparison with its isomers.

In line with the condition for choosing the isomeric groups, the glycine isomeric group is not included since there has not been any successful detection of any of the isomers. However, from the available evidences in all the cases examined in this study, it can be inferred that the unsuccessful detection of glycine and other amino acids is not a function of their partition function. Rather, other factors like their interstellar formation routes, abundances, dipole moment etc should be considered.

Table 3.34: Molecular partition function, enthalpy of formation and current astronomical status of isomers with 12 atoms

Molecule	Partition function [$\text{Log}_{10}(q)$]					$\Delta_f H^\circ$ (kcal/mol)	Astronomical status
	qt	Qe	Qr	qv	Total q		
Benzene	7.4	0.0	4.2	11.8	23.4	18.8	Detected
Fulvene	7.4	0.0	5.0	12.9	25.3	53.0	Not detected
3,4-dimethylenecyclopropene	7.4	0.0	5.1	13.1	25.6	80.8	Not detected
1,5-hexadiene-3-yne	7.4	0.0	4.8	13.9	26.1	81.1	Not detected
2,4-hexadiyne	7.4	0.0	4.9	14.9	27.2	84.0	Not detected
1,2,3,4-hexateraene	7.4	0.0	5.1	14.0	26.5	90.5	Not detected
1,3-hexadiyne	7.4	0.0	5.1	14.0	26.5	92.0	Not detected
Trimethylenecyclopropane	7.4	0.0	5.2	13.4	26.0	98.6	Not detected
1,4-hexadiyne	7.4	0.0	5.2	15.1	27.7	101.1	Not detected
1,5-hexadiyne	7.4	0.0	5.1	13.9	26.4	104.6	Not detected

3.10.4 Summary on Partition Function and Astronomical Observation Of Molecules: A detailed investigation of the relationship between molecular partition function and astronomical detection of molecules has been carried out with 120 different molecules from 30 isomeric groups with at least one astronomically detected molecule from each isomeric group with atoms ranging from 3 to 12. High level quantum chemical simulations using the Guassian G4 compound model method has been used to determine the partition function and the zero-point standard enthalpy of formation of all the systems considered in this study. From the results, it is crystal clear that in all the isomeric groups considered that there is no direct correlation between partition function and the astronomical detection of an isomer at the expenses of others. However, the enthalpy of formation and the reported data in literature on the column density of the astronomically detected molecules show a direct relationship between thermodynamic stability and interstellar abundance as in all the cases, the astronomically most stable isomers are also the ones that have been detected. The reported column densities also support the fact that the more stable isomers are also the more abundant isomers in the interstellar medium. It is sufficient therefore to say that astronomical processes are thermodynamically controlled.

3.11 ESA Relationship and Other Related Studies

On the completion of this project, we learned about the Minimum Energy Principle (MEP) study by Lattelais et al.,¹⁸⁵ where the authors used the energy difference between the two known interstellar isomers from each of the 14 isomeric groups they examined to show that the most stable isomer is always the most abundant. ESA relationship proposed here has expanded MEP significantly as MEP was limited to 14 known isomers in the interstellar space.

Work presented in the Thesis is comprehensive considering 130 molecules from 31 isomeric groups with atoms ranging from 3 to 12 are considered. All possible isomers both the astronomically observed and the ones that are yet to be observed are examined in the ESA relationship while in the MEP only two known isomers from each group are considered.

ESA relationship uses standard enthalpies of formation calculated with 5 different methods (this data on its own represents an important contribution to the scientific community) in which the results are in good agreement with available experimental values while the MEP uses only the relative energy difference between the two isomers.

The deviations from the ESA relationship are well accounted for. The first report on the existence and effects of interstellar hydrogen bonding results from such deviations.

Numerous applications of the ESA relationship in accounting for some of the "*whys and wherefores*" in interstellar chemistry are well reported in this work. Apart from the immediate consequences of the relationship discussed in the chapter, other studies employing the ESA relationship are presented which addressed a number of questions in the field.

ESA relationship has been shown to be applicable to other related systems such as the linear carbon chains discussed in Chapter 5 of this Thesis. It's not only limited to isomeric species like the MEP.

The MEP has been criticised due to the unsuccessful searches^{186,187} for propadienone which is the most stable isomer of the H₂C₃O group. However, in the ESA relationship, the possible reason for this has been highlighted "*Methylene ketene (propadienone), as the name suggests, is an unsaturated ketone. However, the chemistry of ketenes resembles that of carboxylic acid anhydrides which makes ketenes remarkably reactive. The high reactivity of ketenes can affect their abundances in the ISM thereby making their astronomical observations difficult.*"

The argument of Klempner¹⁸⁸ that if energy were decisive, there would be essentially no molecule of the second-most abundant molecular species in the Universe, CO, following its reaction with H₂ (CO + 3H₂ → CH₄ + H₂O) does not hold here as the ESA relationship

examines isomeric or related molecular species. Besides, the said reaction ($\text{CO} + 3\text{H}_2 \rightarrow \text{CH}_4 + \text{H}_2\text{O}$) is only hypothetical.

3.12 Conclusions on Interstellar Isomers: Energy, Stability and Abundance (ESA) Relationship among Interstellar Molecules

In this chapter, the Energy, Stability and Abundance (ESA) relationship existing among interstellar molecular species has been firmly established using accurate thermochemical parameters obtained with the composite models and reported observational data. From the relationship, “*Interstellar abundances of related (isomers) species are directly proportional to their stabilities in the absence of the effect of interstellar hydrogen bonding*”. This also shows that interstellar formation processes are partially thermodynamically controlled. The immediate consequences of the ESA relationship in addressing some of the questions in interstellar chemistry have been briefly summarized. Based on the ESA relationship, other whys and wherefores in interstellar chemistry are discussed in details. From ESA relationship, though there has not been any successful astronomical observation of any heterocycle, the ones so far searched remain the best candidates for astronomical observation in their respective isomeric groups. The observation of the first branched chain molecule in ISM is in agreement with the ESA relationship and the $\text{C}_5\text{H}_9\text{N}$ isomers have been shown to contain potential branched chain interstellar molecules. That molecules with the C-C-O backbone have less potential of formation in ISM as compared to their counterparts with the C-O-C backbone has been demonstrated not to be true following the ESA relationship. A detailed investigation on the relationship between molecular partition function and astronomical detection isomeric species (related molecules) shows that there is no direct correlation between the two rather there is a direct link between the thermodynamic stability of the isomeric species (related molecules) and their interstellar abundances which influences the astronomical observation of some isomers at the expense of others.

3.13 References

1. Thaddeus, P., Guélin, M., Linke, R. A. *Astrophys J.*, 1971, 246, 41
2. Herbst, E. *Chem. Soc. Rev.*, 2001, 30, 168
3. Etim, E. E., Arunan, E. *Planex Newsletter*, 2015, 5(2),16
4. Crawford, T. D., Stanton, J. F., Saeh, J. C., Schaefer, H. F. *J. Am. Chem. Soc.*, 1999, 121, 1902
5. Wlodarczak, G. *J. Mol. Struct.*, 1995, 347, 131
6. Remijan, A. J., Hollis, J. M., Lovas, F. J., Plusquellic, D. F., Jewell, P. R. *Astrophys J.*, 2005, 632, 333
7. Hollis, J. M., in *Proc. IAU Symposium No. 231*, 2005. (Eds) Lis, D. C., Blake, G. A., Herbst, E.
8. Tielens, A. G. G.M. *Rev. Mod. Phys.*, 2013, 85,1021
9. Hudson, R. L., Moore, M. H. *Icarus*, 2004, 172, 466
10. Frisch, M. J., Trucks, G. W., Schlegel, H. B., Scuseria, G. E., Robb, M. A., Cheeseman, J. R., Scalmani, G., Barone, V., Mennucci, B., Petersson, G. A., Gaussian 09, revision D.01, Gaussian, Inc., Wallingford, CT, 2009.
11. Martin, J. M. L, de Oliveira, G. *J Chem Phys*, 1999, 111, 1843
12. Curtiss, L. A., Redfern, P. C., Raghavachari, K. *J Chem Phys*, 2007, 126, 084108
13. Curtiss, L. A., Redfern, P. C., Raghavachari, K. *J Chem Phys*, 2007, 127, 124105

14. Curtiss, L. A., Raghavachari, K., Redfern, P. C., Pople, J. A. *J Chem Phys*, 1997, 106, 1063-1079.

15. <http://webbook.nist.gov/chemistry/> Accesed in May, 2016.

16. Zuckerman, B., Morris, M., Palmer, P., Turner, B. E. *Astrophys J*, 1972, 173,125-129.

17. Blackman, G. L., Brown, R. D., Godfrey, P. D., Gunn, H. I. *Nature*, 1976, 261:395.

18. Turner, B. E., Steimle, T. C., Meerts, L. *Astrophys J*. 1994, 426,97.

19. Ziurys, L. M., Apponi, A. J., Guélin, M., Cernicharo, J. *Astrophys J*, 1995, 445,47

20. Kawaguchi, K., Kagi, E., Hirano, T., Takano, S., Saito, S. *Astrophys J*, 1993, 406, 39

21. Guélin, M., Cernicharo, J., Kahane, C., Gomez-Gonzales, J. *Astron Astrophys* 1986, 157, L17

22. Guelin, M., Lucas, R., Cernicharo, J. *Astron Astrophys*, 1993, 280,19-22.

23. Guélin, M., Muller, S., Cernicharo, J., Apponi, A. J., McCarthy, M. C., Gottlieb, C. A., Thaddeus, P. *Astron Astrophys*, 2000, 369, L 9

24. Guélin, M., Muller, S., Cernicharo, J., McCarthy, M. C., Thaddeus, P. *Astron Astrophys*, 2004, 426, L49

25. Ziurys, L. M., Savage, C., Highberger, J. L., Apponi, A. J., Guélin, M., Cernicharo, J. *Astrophys J*, 2002, 564, 45

26. Soifer, B. T., Puetter, R. C., Russell, R. W., Willner, S. P., Harvey, P. M., Gillett, F. C. *Astrophys J*, 1979, 232, 53

27. Tennekes, P. P., Harju, J., Juvela, M., Tóth, L. V. *Astron Astrophys*, 2006,456, 1037

28. Irvine, W. M., Schloerb, F. P. *Astrophys J*, 1984, 282, 516

29. DeYonker, N. J., Ho, D. S., Wilson, A. K., Cundari, T. R. *J Phys Chem A*, 2007, 111, 10776

30. Meloni, G., and Gingerich, K. A. *J Chem Phys*, 1999, 111, 969

31. Bradorth, S. E., Kim, E. H., Arnold, D. W., Neumark, D. M. *Chem Phys*, 1993, 98, 800

32. Poppinger, D., Radom, L., Pople, J Am Chem Soc, 1977, 99, (24), 7806

33. Snyder, L. E., Buhl, D. *Astrophys J*, 1972, 177, 619

34. Brunken, S., Gottlieb, C. A., McCarthy, M. C., Thaddeus, P. *Astrophys J*, 2009, 697, 880

35. Brunken, S., Belloche, A., Martin, S., Verheyen, L., Menten, K. M. *Astron Astrophys*, 2010, 516, A109

36. Marcelino, N., Cernicharo, J., Tercero, B., Roueff, E. *Astrophys J*, 2009, 690, 27

37. Guélin, M., Cernicharo, J. *Astron Astrophys*, 1991, 244, L21

38. Halfen, D. T., Ziurys, L. M., Brünken, S., Gottlieb, C. A., McCarthy, M. C., Thaddeus, P. *Astrophys J*, 2009, 702, 124

39. Frerking, M. A., Linke, R. A., Thaddeus, P. *Astrophys J*, 1979, 234, 143

40. Poutsma, J. C., Upshaw, S. D., Squires, R. R., Wenthold, P. G. *J Phys Chem A*, 2002, 106, 1067

41. <http://chemister.ru/Database/properties-en.php?dbid=1id=3123> Accessed in May 2016.

42. Kawaguchi, K., Ohishi, M., Ishikawa, S. I., Kaifu, N. *Astrophys J*, 1992, 386, 51

43. Kawaguchi, K., Takano, S., Ohishi, M., Ishikawa, S. I., Miyazawa, K., Kaifu, N., Yamashita, K., Yamamoto, S., Saito, S., Ohshima, Y., Endo, Y. *Astrophys J*, 1992, 396, 49

44. Remijan, A. J., Hollis, J. M., Lovas, F. J., Stork, W. D., Jewell, P. R., Meier, D. S. *Astrophys J*, 2008, 675, L85

45. Turner, B. E., Liszt, H. S., Kaifu, N., Kisliakov, A. G. *Astrophys J*, 1975, 201, 149

46. Turner, B. E. *Astrophys J*, 1971, 163, 35

47. Irvine, W. M., Friberg, P., Hjalmarson, Å., Ishikawa, S., Kaifu, N., Kawaguchi, K., Madden, S. C., Matthews, H. E., Ohishi, M., Saito, S., Suzuki, H., Thaddeus, P., Turner, B. E., Yamamoto, S., Ziurys, L. M. *Astrophys J*, 1988, 334, 107

48. Irvine, W. M., Brown, R. D., Craig, D. M., Friberg, P., Godfrey, P. D., Kaifu, N., Matthews, H. E., Ohishi, M., Suzuki, H., Takeo H. *Astrophys J*, 1988, 335,89

49. Pardo, J. R., Cernicharo, J., Goicoechea, J. R., Guélin, M., Ramos, A. *Astrophys J*, 661, 250-261.

50. Gensheimer, P. D. *Astron Astrophys Sup*, 1997, 251, 199

51. Sablier, M., Fujii, T. *Chem. Rev*, 2002, 102,2855

52. Solomon, P. M., Jefferts, K. B., Penzias, A. A., Wilson, R. W. *Astrophys J*, 1971, 168, 107

43. Cernicharo, J., Kahane, C., Guélin, M., Gomez-Gonzalez, J. *Astron Astrophys*, 1988, 189, 1

54. Cernicharo, J., Guélin, M., Pardo, J. R. *Astrophys J*, 2004, 615, 145

55. Lovas, F. J., Hollis, J. M., Remijan, A. J., Jewell, P. R. *Astrophys J*, 2006, 645,137

56. Lovas, F. J., Remijan, A. J., Hollis, J. M., Jewell, P. R., Snyder, L. E. *Astrophys J*, 2006, 637, 37

57. Rubin, R. H., Swenson, G. W., Solomonm, Jr. R. C., Flygare, H. L. *Astrophys J*, 1971, 169, 39

58. Charnley, S. B., P. Ehrenfreund, P., Kuan, Y. J. *Spectrochim Acta A*, 2001, 57, 685

59. http://www.astrochymist.org/astrochymist_nondetections.html Accessed May 2016.

60. Turner, B. E. 1991. *Astrophys JS* 76, 617

61. Hollis, J. M., Lovas, F. J., Anthony J., Remijan A. J., Jewell, P. R., Ilyushin, V. V., Kleiner, I. *Astrophys J*, 2006, 643, 25

62. Emel'yanenko, V. M., Verevkin, S. P., Varfolomeev, M. A. *J. Chem. Eng. Data* 2011, 56, 4183

63. <https://www.chemeo.com/cid/27-566-4/Propynal,%20dimethylacetal.pdf> Accessed May 2016

64. Fourikis, N., Sinclair, M. W., Robinson, B. J., Godfrey, P. D., Brown, R. D. *Aust J Phys*, 1974, 27, 425

65. Gilmore, W., Morris, M., Palmer, P., Johnson, D. R., Lovas, F.J., Turner, B. E., Zuckerman, B. *Astrophys J*, 1976, 204,43

66. Turner, B. E., Apponi, A. J. *Astrophys J*, 2001, 561, 207

67. Dickens, J. E., Irvine, W. M., Ohishi, M., Ikeda, M., Ishikawa, S.. Nummelin, A., Hjalmarson, A. *Astrophys J*, 1997, 489,753

68. Nummelin, A., Dickens, J. E., Bergman, P., Hjalmarson, A., Irvine, W. M., Ikeda, M., Ohishi, M. *Astrophys JS*, 1998, 117:427

69. Nummelin, A., Bergman, P., Hjalmarson, Å., Friberg, P., Irvine, W. M., Millar, T. J., Ohishi, M., Saito, S. *Astron Astrophys*, 1998, 337, 275

70. Ikeda, M., Ohishi, M., Dickens, J. E., Bergman, P., Hjalmarson, A., Irvine, W. M. *Astrophys J*, 2001, 560, 792

71. Gardner, F. F. Winnewisser, G. *Astrophys J*, 1975, 195, L127

72. Guélin, M., Cernicharo, J., Travers, M. J., McCarthy, C.M. C., Gottlieb, C. A., Thaddeua, P., Ohishi, M.., Saito, S., Yamamoto, S. *Astron Astrophys*, 1997, 317, L1

73. Hollis, J. M., Lovas, F. J., Jewell, P. R. *Astrophys J*, 2000, 540, 107

74. Hollis, J. M., Jewell, P. R., Lovas, F. J., Remijan, A., Møllendal, H. *Astrophys J*, 2004, 610, 21

75. Brotén, N. W., MacLeod, J. M., Avery, L. W., Irvine, W. M., Höglund, B., Friberg, P., Hjalmarson, P. *Astrophys J*, 1984, 276, 25

76. Langer, W. D., Velusamy, T., Kuiper, T. B. H., Peng, R., McCarthy,M. C., Travers, M. J., Kovács, A., Gottlieb, C. A., Thaddeus,P. *Astrophys J*, 1997, 480, 63

77. Churchwell, E., Winnewisser, G. *Astron Astrophys.*, 1975, 45,229

78. Brown, R. D., Crofts, J. G., Godfrey, P. D., Gardner, F. F., Robinson, B. J., Whiteoak, J. B. *Astrophys J*, 1975, 197:L29

79. Belloche, A., Menten, K. M., C. Comito, C.,Müller,H. S. P., Schilke,P., Ott, J., Thorwirth,S., Hieret, C. *Astron Astrophys.*, 2008, 482,179

80. Loomis, R. A., Zaleski, D. P., Steber, A. L., et al., *Astrophys JL*, 2013, 765, L9.

81. Cernicharo, J., Heras, A. M., Tielens, A. G. G. M., Pardo, J. R., Herpin, F., Guélin, M., Waters, L. B. F. M. *Astrophys J*, 2001, 546, L123

82. Remijan, A. J., Snyder, L. E.,McGuire, B. A., et al., *Astrophys J.*, 2014,783:77

83. Zuckerman, B., Turner, B. E., Johnson, D. R., et al., *Astrophys J.*, 1975, 196, 99

84. Pearson, J. C., Sastry, K. V. L. N., Herbst, E., De Lucia, F. C. *Astrophys J*, 1997, 480, 420

85. Snyder, L. E., Buhl, D., Schwartz, P. R., Clark,F. O., Johnson, D.R., Lovas F. J., Giguere, P. T. *Astrophys J.*, 1974, 191, 79

86. White, G. J., Araki, M., Greaves, J. S., Ohishi, M., Higginbottom, N. S. *Astron Astrophys*, 2003, 407: 589

87. Johnson, D. R., Lovas, F. J., Gottlieb, C. A., Gottlieb, E. W., Litvak, M. M., Guélin, M., Thaddeus, P. *Astrophys J.*, 1977, 370

88. Cioslowski, J., Schimeczek, M., Liu, G., Stoyanov, V. J. *CP*, 2000, 113, 9377

89. Combes, F., Gerin, M., Wooten, A., Włodarczak, G., Clauisset, F., Encrenaz, P. I. *Astron Astrophys.*, 1987, 180,L13

90. Hollis, J. M., Lovas, F. J., Jewell, P. R., Coudert, L. H. *Astrophys J*, 2002. 571, 59

91. Snyder, L. E., Lovas, F. J., Mehnninger, D. M., Miao, N. Y., Kuan, Y.-J., Hollis, J. M., Jewell, P. R. *Astrophys J*, 2002,578, 245

92. Snyder, L. E., Hollis, J. M., Jewell, P. R., Lovas, F. J., Remijan, A. *Astrophys J*, 2006, 647,412

93. <https://pqr.pitt.edu/mol/YOXHCYXIAVIFCZ-UHFFFAOYSA-N#> Accessed in May 2016.

94. Belloche, A., Garrod, R. T., Müller, H. S. P., Menten, K. M., Comito, C., Schilke, P. *Astron Astrophys.*, 2009, 499, 215

95. Tercero, B., Kleiner, I., Cernicharo, J., Nguyen, H. V. L., López, A., Muñoz Caro, G. M. *Astrophys JL.*, 2013, 770, 13

96. Etim, E. E., Arunan, E. Manuscript to be submitted.

97. Hall, Jr, H. K., Baldt, J. H. *J Am Chem Soc*, 1971, 93, 140

98. Fuchs, G. W., Fuchs, U., Giesen, T. F., Wyrowski, F. 2005. *Astron Astrophys*, 2005, 444, 521

99. Belloche, A., Garrod, R. T., Müller, H. S. P., Menten, K. M. *Science*, 2014, 345, 1584

100. Hollis, J. M., Remijan, A. J., Jewell, P. R., Lovas, F. J. *Astrophys J*, 2006, 642, 933

101. Thaddeus, P., Cummins, S. E., Linke, R. A. *Astrophys J*, 1984, 283, 45

102. Thaddeus, P., Vrtilek, J. M., Gottlieb, C. A. *Astrophys J*, 1985, 299, 63

103. Cami, J., Bernard-Salas, J., Peeters, E., Malek, S. E. *Science*, 2010, 329:1180

104. Berné, O., Mulas, G., Joblin, C. *Astron Astrophys*, 2013, 550:L4

105. Dua, R., Shrivastava, S., S.K. Sonwane, S.K., Srivastava, S.K. *Advances in Biological Research*, 2011, 5(3): 120

106. Valverde, M.G., Torroba, T. *Molecules*, 2005, 10: 318

107. Ricca, A., Bauschlicher, C.W., Bakes, E.L.O. *Icarus*, 2001, 154, 516

108. Ridgway, S. T., Hall, D. B., Wojslaw, J. M., Kleinmann, S. G., Weinberger, D. A. *Astrophys J*, 1976, 464:345

109. Botta, O., Bada, J. L. *Surv Geophys*, 2002, 23, 411

110. Nuevo, M., Milam, S. N., Sandford, S. A. *Astrobiology*, 2012, 12 (4):295

111. Lacy, J. H., Evans II, N. J., Achtermann, J. M et al. *Astrophys J*, 1989, 342:L43

112. Etim, E. E., Arunan, E. Submitted.

113. http://www.astrochymist.org/astrochymist_nondetections.html accessed in Dec, 2014

114. Irvine, W. M., Ellder, J., Hjalmarson, A., et al. *Astron Astrophys*, 1981, 97:192

115. Noe, F F., Fowden, F. *Nature*, 1959 184: 69

116. Ratel, M., Provencher-Girard, A., Zhao, S. S., et al. *Anal. Chem*, 2013, 85(12):5770.

117. Dezafra, R. L., Thaddeus, P., Kutner, M., et al. *Astrophys JL*, 1971, 10:1

118. Setsune, J., Tanabe, A., Watanabe, J., Maeda, S. *Org. Biomol. Chem.*, 2006, 4, 2247

119. Linnell, R. *J. Organic Chem*, 1960, 25 (2): 290

120. Pearson, R. G., Williams, F. V. *J Am Chem Soc*, 1953, 75 (13): 3073

121. Batchelor, R. A., Brooks, J. W., Godfrey, P. D., Brown, R. D. *Aust. J. Phys.*, 1973, 26:557

122. Simon, M. N. *Simon, M. Astrophys J*, 1973, 184: 757

123. Charnley, S. B., Kuan, Y., Huang, H., et al. *Adv Space Res*, 2005, 36: 137

124. Kuan, Y., Yan, C., Charnley, S. B., et al. *Mon Not R Astron Soc*, 2003, 345, 650

125. Segall, J., Zare, R. N. *J Chem Phys*, 1988, 89 (9), 5704

126. Deniau, G., Lecayon, G., Viel, P., Hennico, G., Delhalle, J. *Langmuir*, 1992, 8(1), 267

127. Tanii, H., Higashi, T., Nishimura, F., Higuchi, Y., Saijoh, K. *Med Sci Monitor*, 2008, 14(10), 189

128. Tanii, H., Takayasu, T., Higashi, T., Leng, S., Saijoh, K. *Food Chem Toxicol*, 2004, 42, 453

129. Kutner, M. L., Machnik, D. E., Tucker, K. D., Dickman, R. L. *Astrophys J*, 1980, 242:541

130. Myers, P. C., Thaddeus, P., Linke, R. A. *Astrophys J*, 1980, 241:155.

131. Agúndez, M., Cernicharo, J., Guélin, M., et al. *Astron Astrophys*, 2010, 517:L2.

132. Thaddeus, P., C. A. Gottlieb, C. A., Gupta, H. et al. *Astrophys J*, 2008, 677:1132

133. Cernicharo, J., Guélin, M., Agúndez, M., McCarthy, M. C., . Thaddeus, P. *Astrophys J*, 2008, 688:L83

134. Cernicharo, J., Guélin, M., Agúndez, M., et al. *Astron Astrophys*, 2007, 467:L37

135. McCarthy, M. C., Gottlieb, C. A., Gupta, H., Thaddeus, P. *Astrophys J*, 2006, 652:L141

136. Brünken, S., Gupta, H., Gottlieb, C. A., McCarthy, M. C., Thaddeus, P. *Astrophys J*, 2007, 664:L43

137. Buhl, D. Synder, L. E. *Nature*, 1970, 228:267

138. Latter, W. B., Walker, C. K., Maloney, P. R. *Astrophys J*, 1993, 419:L97-L100

139. Turner, B. E. *Astrophys J*, 1992, 396,L107

140. Adams, W. S. *Astrophys J*, 1941, 93, 11

141. Neufeld, D. A., Schilke, P., Menten, K. M., et al. *Astron Astrophys*, 2006, 454:L37

142. Geballe, T. R., Oka, T. *Nature*, 1996, 384:334

143. Herbst, E., Klemperer, W. *Astrophys J*, 1973, 185: 505

144. Bachiller, R. *Annu Rev Astro Astr*, 1996, 34, 111

145. Elsila, E., Dworkin, J. P., Bernstein, M. P., Martin, M. P., Sandford, S. A. *Astrophys J*, 2007, 660, 911

146. Botta, O., Bada, J. L. *Surv Geophys*, 2002, 411–467

147. Cronin, J. R., Pizzarello, S. *Adv Space Res*, 1983, 3, 5

148. Nugent, L. J., Mann, D. E., Lide, D. R. Jr. 1962. *J Chem Phys*, 36, 965

149. Dutta, B., De, R., Pal, C., Chowdhury, J. *Spectrochim Acta A*, 2012, 96, 837

150. Bohn, R. K., Pardus, J. L., August, J., et al. *J Mol Struct*, 1997, 413, 293

151. Ordu, M. H., Müller, H. S. P., Walters, A., et al. *Astron Astrophys*, 2012, 541, A121.

152. Dickens, J. E., Irvine, W. M., Nummelin, A., et al. *Spectrochimica Acta Part A*, 2001, 57:643

153. Mehringer, D. M., Snyder, L. E., Miao, Y., Lovas, F. *Astrophys J*, 1997, 480, 71

154. Turner, B. E. *Astrophys J*, 1977, 213,L75

155. Dickens, J. E., Irvine, W. M., Ohishi, M. et al. *Astrophys J*, 1997, 489,753

156. Churchwell, E. *Winnewisser, G. 1975. Astron Astrophys* 45,229

157. Thaddeus, P., Guélin, M. *Linke, R. A. 1971. Astrophys J* 246, 41

158. McKellar, A. *Publ Astron Soc Pac*, 1950, 52:187

159. Ball, J. A., Gottlieb, C. A., Lilley, A. E. Radford, H. E. 1970. *Astrophys J* 162:L203

160. Yamamoto, S., Saito, S., Ohishi, M., et al. 1987. *Astrophys J*, 322, 55

161. Charnley, S. B., P. Ehrenfreund, P. Kuan, Y. J. *Spectrochim Acta A*, 2001, 57, 685

162. Kuan, Y.-J., Charnley, S. B. C. Huang, H.-C., Tseng, W.-L. Kisiel, Z. *Astrophys J*, 2003, 593,848

163. Snyder, L. E., Lovas, F. J., Hollis, J. M. et al. *Astrophys J*, 2005, 619:914

164. Jones, P. A., Cunningham, M. R., Godfrey, P. D. Cragg, D, M. *MNRAS*, 2007, 374,579

165. Cunningham, M. R., Jones, P. A., Godfrey, P. D., et al. *MNRAS*, 2007, 376, 1201

166. Largo, L., Redondo, P., Rayón, V. M., Largo, A, Barrientos, C. *Astron Astrophys*, 2010, 516, A79.

167. Combes, F., Nguyen Q.-R., Wlodarczak, G. *Astron Astrophys*, 1996, 308, 618.

168. McQuarrie, D. A. Simon, J. D. *Molecular Thermodynamics*. 2004, Viva Books, India.

169. Ochterski, J. W. *Thermochemistry in Gaussian*. 2000, Gaussian Inc.

170. Curtiss, L. A.,Raghavachari, K., Redfern, P. C., Rassolov, V.Pople, J. A. *J Chem Phys*,1998, 109, 7764.

171. Snyder, L. E. Buhl, D. *Astrophys J*, 1971, 163:L47

172. Michalopoulos, D. L., Geusic, M. E., Langridge-Smith, P. R. R. Smalley, R. E. *J Chem Phys*, 1984, 80, 3556

173. Apponi, A. J., McCarthy, M. C., Gottlieb, C. A. Thaddeus, P. *Astrophys J*, 1999, 516,L103

174. Thaddeus, P., Gottlieb, C. A., Hjalmarson, A., et al. *Astrophys J*, 1985, 294,L49

175. Cernicharo, J., Gottlieb, C. A., Guélin, M., et al. *Astrophys J*, 1991, 368:L39

176. Remijan, A. J., Hollis, J. M., Lovas, F. J., et al. *Astrophys J*, 2008, 675, 85

177. Cernicharo, J., Cox, P., Fosse, D. Gusten, R. *Astron Astrophys*, 1999, 351, 341

178. Ikeda, M., Ohishi, M., Nummelin, A., et al. *Astrophys J*, 2001, 550, 792

179. Hollis, J. M., Vogel, S. N., Snyder, L. E., Jewell, P. R. Lovas, F. J. *Astrophys J*, 2001, 554, L81

180. Remijan, A., Snyder, L. E., Liu, S. -Y., Mehringer, D.,Kuan, Y, -Y. *Astrophys J*, 2002, 576, 264

181. Broten, N. W., MacLeod, J. M., L. W. Avery, L. W., et al. *Astrophys J*,1984, 276, 25

182. Orlov, V.M., Krivoruchko, A.A., Misharev, A.D., Takhistov, V.V. B. *Acad. Sci USSR. Ch+*, 1986, 2404-2405

183. Kercher, J. P., Fogleman, E. A., Koizumi, H., SztRray, B., Baer, T. *J. Phys. Chem. A* 2005, 109, 939

184. Schuurman, M. S., Muir, S. R., Allen, W. D., Schaefer III, H. F. *J. Chem. Phys.* 2004, 120 (24), 11586

185. Lattelais, M., Pauzat, F., Ellinger, Y., Ceccarelli, C. *Astrophys J*, 2009, 696, L133

186. Loomis, R. A., McGuire, B. A., Shingledecker, C., Johnson, C. H., Blair, S., Robertson, A., Remijan, A. *J. Astrophys J*, 2015, 799,34.

187. Loison, J. C., Agúndez, M., Marcelino, N., Wakelam, V., Hickson, K. M., Cernicharo, J. Gerin, M., Roueff, E.,Guélin, M. *Mon Not R Astron Soc*, 2016, 456, 4101.

188. Klemperer, W. *Annu. Rev. Phys. Chem.* 2011, 62,173.

Interstellar Hydrogen Bonding: Detecting Weakly Bound Complexes in Space

Preamble: The celebration of the centenary of the chemical bond "**100 years of the chemical bond**" stands tall among the key scientific events of the year 2016. The importance of the chemical bond in chemistry and in science generally cannot be overemphasized. Intermolecular interactions or non-covalent interactions are very vital in the elucidation of structures and properties of many biological systems. Among the different intermolecular interactions, hydrogen bond is the most celebrated of it all because of its overwhelming impacts in different systems and phenomena. In this chapter, the existent and effect of *hydrogen bonding* in the interstellar medium are reported for the first time. Other detailed studies utilizing the existence and effects of hydrogen bonding in the interstellar medium are also presented.

4.0 Introduction: Gas phase chemical reactions and reactions that occur on the surfaces of interstellar dust particles are the dominant processes by which molecules can be synthesized from the precursor atoms and ions. Of these two processes, reactions that occur on the surfaces of interstellar dust particles have been invoked for the formation of molecular hydrogen; as well as for the synthesis of larger interstellar molecules¹. Dust grains and ice play an indisputable role in the astrophysics of the interstellar medium. Whereas in the thin space between the stars gas phase reactions relying on three-body collisions are very rare, molecules and atoms residing on the solid surfaces can roam around the surfaces until a reaction occurs, thus forming new species. These surfaces therefore serve as reaction sites for chemical processes that would either be very slow or not occur at all. From spectroscopic observations, the composition of the interstellar ice is dominated by water which accounts for 60-70% of the ice in most lines of sight. Other spectroscopically observed species include methanol, carbon monoxide and carbon dioxide, as well as smaller abundances of other species.²⁻⁸ The composition of the interstellar ice causes most of the molecules formed on the surface of the interstellar dust to form hydrogen bonding with the components of the ice most predominantly, water. This causes a greater part of these molecules to be attached to the surface of the interstellar dust grains, thus reducing its interstellar abundance.

Weak intermolecular interactions are very vital in the elucidation of structures and properties of many important biological molecules like water, DNA, protein etc. Among these weak intermolecular interactions, hydrogen bonding is well recognized, studied and understood to a great extent because of its overwhelming impacts in different systems and phenomena. It is responsible for the unique properties of water essential to life; it serves as a vital force in determining the basic structure of large biomolecules such as DNA, RNA, proteins etc⁹. The binding energy of the hydrogen bonded complex gives information about the strength of the bonding. This binding energy can be determined both experimentally and theoretically. With the advances in quantum chemical calculations, on a careful choice of method (level of theory) and basis set, it is now possible to theoretically estimate binding energy that is in good agreement with the experimentally measured value.

As useful as the DFT method is, it has a number of drawbacks (especially for large systems); insufficient description of van der Waals interaction, inaccurate estimation of polarizabilities of large π -conjugate molecules. It has also been shown to underestimate the binding energy of complexes in comparison with the MP2 to MP4(SQD) methods. This underestimation is said to arise from the insufficient description of electron correlation effects. However, the density functional dispersion correction methods like DFT-D1, DFT-D2, DFT-D3, etc., aim to overcome these drawbacks.¹³⁶⁻¹³⁸ Among the available ab initio methods, the Møller-Plesset second order method (MP2) has been shown to be effective and accurate in investigating hydrogen-bonded systems; the use of the smallest augmented correlation consistent basis set (aug-cc-pVDZ) for hydrogen-bonded complexes is strongly recommended^{9,10,11,12,13}.

Interstellar formation processes have been shown to be partially thermodynamically controlled¹. We have demonstrated this fact by considering several groups of isomers and different interstellar carbon chains¹. A direct relationship between Energy, Stability and interstellar Abundance (ESA) was observed. However, we noticed some deviations from the thermodynamically controlled processes among some of the groups considered; the conspicuous abundance of a less stable isomer (methyl formate) over the most stable one (acetic acid) and the non-detection of some of the most stable isomers whose less stable counterparts have been detected. In the present studies, we aim to account for these deviations, the difficulty in the astronomical observation of sugars and to propose suitable candidates for astronomical observation within the range of our molecules under consideration. For the present study, 20 interstellar molecules (known and possible) which are suitable in achieving the aims of the present study stated above are considered. The strength of their hydrogen bonded complexes with water is investigated by estimating their binding energies at different levels of theory and basis sets. After describing the computational methods used here, the results obtained are presented and discussed.

4.1 Computational details: All the calculations reported in this work are performed using the Gaussian 09 suite of programs¹⁴. The geometry optimization of all the monomers, water and the corresponding hydrogen bonded complexes have been carried out using the Møller-Plesset second order perturbation theory; MP2(full) with the 6-311++G** and aug-cc-pVDZ basis sets, the G4 composite method and the Weizmann theory (W1U)^{11,15,16,17,18,19}. The Gaussian G4 theory and the Weizmann theory are compound models that offer high accurate predictions at less computational cost. Diffuse functions in the basis sets allow the orbitals to occupy a larger region of space while the polarization functions give additional flexibility to the description of molecular orbitals^{20,21}. Harmonic vibrational frequencies were performed on all the systems (monomers, water molecule and complexes) to characterize their stationary nature with equilibrium structures having no imaginary frequency. The binding energy between water molecule and each interstellar molecule (known and possible) considered here is calculated as the energy of the complex minus the energies of the isolated monomers. It is defined by the following expression:

$$\Delta E(\text{binding energy}) = E(\text{complex}) - [E(\text{water molecule}) + E(\text{interstellar molecule})].$$

The reported binding energies have been corrected for the basis set superposition error (BSSE) using the counterpoise method developed by Boys and Bernardi²².

4.2 Result and Discussion

Binding energies for the different hydrogen bonded complexes with water have been estimated at different levels of theory and basis sets. The full geometry parameters for water and all the complexes studied in this work are reported in the supporting information. The results presented here are from the most stable structures of all the systems considered. After a brief description of the geometry parameters for water which is the central molecule for this

study, the discussion will be presented in the subsections in accordance with the aims of this work.

The theoretically calculated geometrical parameters and vibrational frequencies of the water monomer at the different levels of theory and basis sets are listed in Table 4.1. The corresponding experimental values from literature are included in the table (as exptl). The OH bond length predicted by the MP(full)/6-311++H** is exactly as the experimentally measured value. The OH bond length estimated by other methods employed here are in good agreement with the experimental value. The reported values of 103.9° and 104.5°^{23, 24} for the bond angle are exactly the same as estimated by the MP2(full)/aug-cc-pVDZ and W1U methods respectively.

Table 4.1. Optimized geometry (Å, deg) parameters of the water monomer

Parameters	Method				
	MP2(full)6-311++G**	MP2(full)/aug-cc-pVDZ	G4	W1U	exptl
H ₂ -O ₁	0.959	0.966	0.962	0.961	0.959 ^a
H ₃ -O ₁	0.959	0.966	0.962	0.961	0.959 ^a
H ₃ -O ₁ -H ₂	103.5	103.9	103.7	104.5	103.9 ^a (104.5 ^{b,c})

a²³, b²⁴, c²⁵

4.2.1 Deviations from thermodynamically controlled processes: The high abundance of methyl formate in different molecular cloud has earned it the name 'interstellar weed'. In the C₂H₄O₂ isomeric group, acetic acid is unarguably the most stable isomer while methyl formate ranks second with an energy difference of more than 15 kcal/mol from both the theoretically predicted and the experimentally measured enthalpy of formation value¹. The third most stable isomer on that list is glycolaldehyde. These three isomers have all been detected from different astronomical sources via their rotational transition spectra^{26, 27, 28}. As expected from the ESA relationship, the most stable isomer of this group, acetic acid is expected to be more abundant but this is not the case. Methyl formate (which is not the most stable isomer of the group) is found to be conspicuously more abundant than both acetic acid and glycolaldehyde in all the molecular clouds where they have been detected. The two known stable isomers of the C₂H₆O isomeric group; ethanol and dimethyl ether were first detected in the Sagittarius B2 complex and Orion nebula respectively in the 1970s^{29,30,31}. Ethanol is found to be more stable than dimethyl ether with an energy difference of about 12 kcal/mol from the experimentally reported enthalpy of formation. As such, ethanol should be more abundant than dimethyl ether in the interstellar space. However, the abundance ratio of ethanol and dimethyl ether ranges from 0.3 to 3.0^{32,33,34} with ethanol being more abundant than dimethyl ether in some astronomical observations and the reverse being the case from some other astronomical observations.

Tables 4.2 and 4.3 respectively present the binding energies of the hydrogen bonded complexes of the $\text{C}_2\text{H}_4\text{O}_2$ and $\text{C}_2\text{H}_6\text{O}$ isomers with water at different levels of theory and basis sets considered in this study. Figure 4.1 shows the optimized geometries of these complexes at the MP2(full)/6-311++H** level of theory. The optimized geometry parameters including vibrational frequencies for these complexes at all the levels of theory (and basis sets) considered in this study are presented in Tables S2 to S6 of the supporting information respectively. In all the cases, there is an elongation of one of the O-H bonds of water monomer which takes part in the hydrogen bond formation from the original 0.959 \AA for the water monomer to 0.968, 0.965, 0.970, 0.968, and 0.969 \AA for acetic acid, glycolaldehyde, methyl formate, ethanol and dimethyl ether-water complexes respectively at the MP2(full)/6-311++G** level showing the evidence of hydrogen bond formation in all the systems considered.

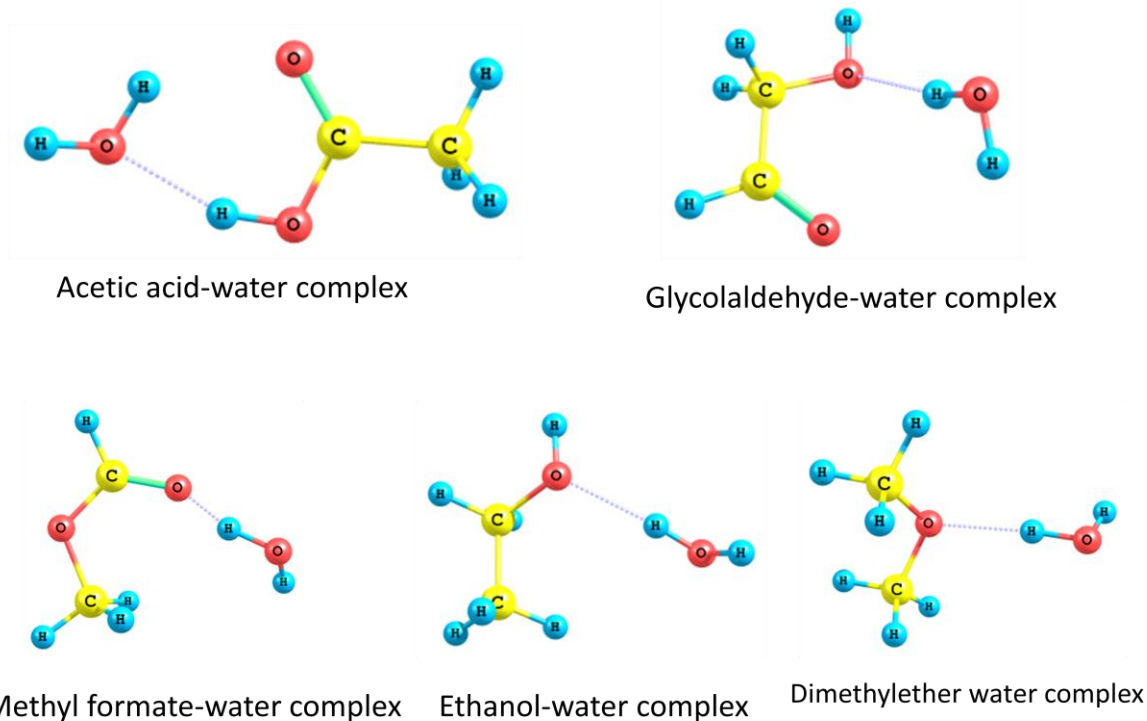


Figure 4.1. Optimized structures of the hydrogen bonded $\text{C}_2\text{H}_4\text{O}_2$ and $\text{C}_2\text{H}_6\text{O}$ isomer complexes with water.

From the binding energies in Table 4.2, acetic acid-water complex is more strongly bonded followed by glycolaldehyde-water complex while methyl formate-water complex is the least bonded complex. There is an inverse correlation between the binding strength of the complex and the interstellar abundance of the molecule that is forming the hydrogen bond with water. Methyl formate is more abundant than both acetic acid and glycolaldehyde; glycolaldehyde in turn is more abundant than acetic acid in the different molecular clouds where they have been detected ^{26,35,36,37,38, 39}. Thus, the higher the binding strength of a complex with water, the lower the interstellar abundance of the molecule as compared to its counterparts with lower binding strength. This is because the more strongly the molecule is bonded to the surface of the interstellar dust grains; the more a greater part of it is being attached to the surface of the

interstellar dust grains thereby reducing its abundance. Ethanol is more strongly bonded to the surface of the interstellar dust grains as evident in binding energy of the ethanol-water complex as compared to the dimethyl ether-water complex (Table 3). From the above analogy, dimethyl ether should be more abundant than ethanol and this has been observed in a few cases. The high abundance of ethanol over dimethyl ether in many cases points to gas phase reactions as the dominant formation processes in such cases where the effect of hydrogen bonding is drastically reduced, thus the abundance of ethanol is not affected as in the case of interstellar dust grains formation process.

Table 4.2: Binding energies for $C_2H_4O_2$ isomer complexes with water

Method	BE (kcal/mol)		
	Acetic acid- H_2O	Glycolaldehyde- H_2O	Methyl formate- H_2O
MP2(full)/6-311++G**	-6.9	-5.5	-3.25
MP2(full)/aug-cc-pVDZ	-9.5	-5.9	-5.5
G4	-9.6	-5.3	-4.3
W1U	-9.3	-5.6	-4.8

Table 4.3: Binding energies for C_2H_6O isomer complexes with water

Method	BE (kcal/mol)	
	Ethanol- H_2O	Dimethyl ether- H_2O
MP2(full)/6-311++G**	-5.1	-5.0
MP2(full)/aug-cc-pVDZ	-5.5	-5.4
G4	-4.8	-4.5
W1U	-5.2	-5.1

4.2.2 Delayed observation of the most stable isomers: In many of the known interstellar isomeric species, the most stable isomer which is probably the most abundant isomer in the interstellar medium has always been the first isomer to be detected. HCN was detected before HNC, MgNC before MgCN, HNCS before HSCN, HC_3N before HC_2NC and HNC_3 , methyl cyanide before methyl isocyanide and ketenimine, acetaldehyde before vinyl alcohol and ethylene oxide, this trend goes on and on.^{1, 40-48}

Propanoic acid ($C_3H_6O_2$ isomeric species) and propan-2-ol and propanol(C_3H_8O isomeric species) are the most stable isomers in their respective isomeric groups. Whereas other less stable isomers have been observed in these groups but none of these most stable isomers have been observed. The binding energies of the hydrogen bonded complexes with water formed by these isomers (most stable and the astronomically observed) are shown in Tables 4.4 ($C_3H_6O_2$ isomers) and 4.5 (C_3H_8O isomers). Ethyl formate and methyl acetate from the $C_3H_6O_2$ isomeric group have been detected in the interstellar space^{49,50} while ethyl methyl ether is the only astronomically observed isomer of the C_3H_8O group⁵¹. Figure 4.2 shows the optimized geometries of the $C_3H_6O_2$ and C_3H_8O isomeric species considered here.

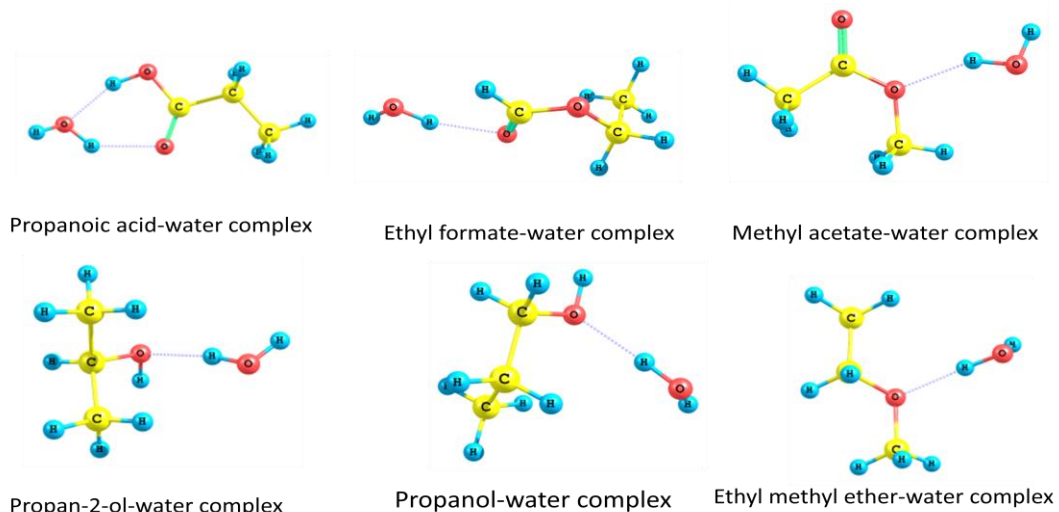


Figure 4.2: Optimized structures of the hydrogen bonded $\text{C}_3\text{H}_6\text{O}_2$ and $\text{C}_3\text{H}_8\text{O}$ isomer complexes with water.

In Tables S7 to S12 of the supporting information, the optimized geometry parameters including vibrational frequencies for $\text{C}_3\text{H}_6\text{O}_2$ and $\text{C}_3\text{H}_8\text{O}$ isomer complexes with water at all the levels of theory (and basis sets) considered in this study are presented accordingly as they appear in Figure 2. At the MP2(full)/6-311++G** level, the O-H bond distance of the water monomer that is forming complex with the interstellar molecule is extended from the normal bond length (0.959\AA) into the range of 0.965 to 0.969\AA for the hydrogen bonded complexes shown in Figure 4.2. Propanoic acid is the most stable isomer of the $\text{C}_3\text{H}_6\text{O}_2$ isomeric group followed by ethyl formate while methyl acetate comes third in the energy scale¹. From the binding energies presented in Table 4, propanoic-water complex is more strongly bonded to the surface of the interstellar dust grains as compared to the ethyl formate-water and methyl acetate-water complexes. This clearly shows that a greater portion of propanoic acid is attached to the surface of the interstellar dust grains via hydrogen bonding thereby reducing its available interstellar abundance thus the delay in its astronomical detection. In the $\text{C}_3\text{H}_8\text{O}$ isomeric group, propan-2-ol is the most stable, followed by propanol while ethyl methyl ether is the least stable isomer of the group¹. As it is evident in Table 4.5, the isomers that have not been observed are more strongly bonded to the surface of the interstellar dust grains than the only observed isomer of the group. This accounts for the delay in the astronomical observations of these isomers as their abundances are reduced due to this interstellar hydrogen bonding as discussed in the previous cases.

Table 4.4: Binding energies for $\text{C}_3\text{H}_6\text{O}_2$ isomer complexes with water

Method	BE (kcal/mol)		
	Propanoic acid - H_2O	Methyl acetate- H_2O	Ethyl formate - H_2O
MP2(full)/6-311++G**	-8.4	-4.8	-4.5
MP2(full)/aug-cc-pVDZ	-9.5	-5.0	-5.0
G4	-9.5	-4.7	-4.3
W1U	-8.3	-4.9	-4.9

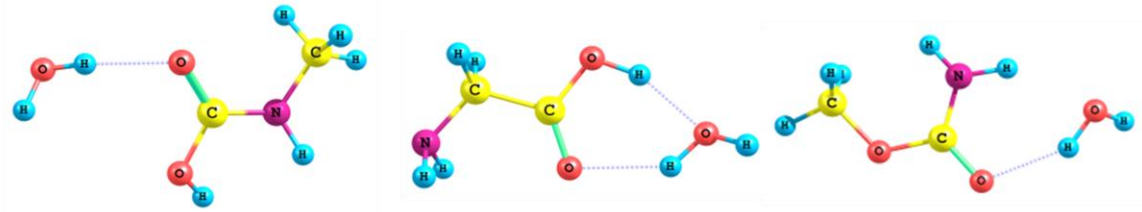
Table 4.5: Binding energies for C₃H₈O isomer complexes with water

Method	BE (kcal/mol)		
	Propan-2-ol-H ₂ O	Propanol-H ₂ O	Ethyl methyl ether-H ₂ O
MP2(full)/6-311++G**	-5.4	-5.2	-5.0
MP2(full)/aug-cc-pVDZ	-5.9	-5.7	-5.4
G4	-5.0	-4.8	-4.7
W1U	-5.5	-5.3	-5.2

4. 2. 3 Unsuccessful observations: Amino acids

Amino acids are water-soluble organic molecules containing both the amine (-NH₂) and the carboxyl (-COOH) groups. Interestingly, from the functional groups alone, the amino acids contain the four most important biogenic elements; carbon, hydrogen, oxygen and nitrogen. The class of amino acids in which both the functional groups are attached to the same carbon atom called the α -carbon atom, are of utmost biological importance being the building blocks of proteins. As a result of this, the search for amino acid in the interstellar medium has been the subject of interest. In particular, glycine; the simplest member of the α -amino acids has attracted the attention of researchers globally. All the searches for glycine in the interstellar medium have not yielded any successful detection of this molecule ^{52, 53, 54, 55}. Though there has not been any successful detection of the amino acid in the interstellar medium, about 80 of them have been identified in meteorites found on Earth and the origin of these compounds found in meteorites are often traced to the interstellar medium; thus linking the interstellar medium and the chemical composition of the meteorites ^{56,57}.

Glycine belongs to the C₂H₅NO₂ isomeric group. The three most stable isomers of this group are methyl carbamic acid, glycine and methyl carbamate respectively. Figure 4.3 shows the optimized structures of these isomers complexes with water while Table 6 gives the binding energies of these complexes. Tables S13 to S15 of the supporting information contain the optimized geometry parameters and vibrational frequencies of glycine, methyl carbamic acid and methyl carbamate-water complexes respectively at all the levels of theory considered in this study. The elongation of the O-H bond length of water is also observed as in the previous cases. From Table 6, the most stable isomer of the C₂H₅NO₂ group; methyl carbamic acid is found to be more strongly bonded to the surface of the interstellar dust grains followed by glycine (the second most stable isomer of the group) and lastly by methyl carbamate. Though methyl carbamic acid has not been searched for possibly because of the lack of its rotational transitions the other two isomers have been searched for in different astronomical sources. Whereas there has been no successful detection of glycine, but methyl carbamate has been tentatively observed in the molecular cloud ⁵⁸. The high bonding strength of glycine to the surface of the interstellar dust grains can easily be seen as having a direct effect on its abundance (reduction in abundance) thus contributing to its unsuccessful astronomical observations.



Methyl carbamic acid-water complex Glycine-water complex Methyl carbamate-water complex

Figure 4.3: Optimized structures of the hydrogen bonded $\text{C}_2\text{H}_5\text{NO}_2$ isomer complexes with water.

Table 4.6: Binding energies for $\text{C}_2\text{H}_5\text{NO}_2$ isomer complexes with water

Method	BE (kcal/mol)		
	Methyl carbamic acid- H_2O	Glycine- H_2O	Methyl carbamate- H_2O
MP2(full)/6-311++G**	-8.3	-4.8	-3.1
MP2(full)/aug-cc-pVDZ	-9.4	-5.1	-3.4
G4	-8.5	-5.1	-3.1
W1U	-9.2	-5.2	-3.3

4.2.4 What could be searched for? Ketenes!!!

As discussed under the delayed observation of the most stable isomers; the most stable isomer is mostly observed before the other less stable isomers. The ketenes (ketene, methylene ketene and methyl ketene) are found to be the most stable isomers in their respective isomeric groups¹, in each of these groups the other less stable isomers have been detected whereas ketene has only been detected in only one group ($\text{C}_2\text{H}_2\text{O}$ isomeric group). The most stable isomer that is expected to be the most abundant may be affected by interstellar hydrogen bonding thereby reducing its abundance, thus making its astronomical observation difficult. In testing the effect of interstellar hydrogen bonding among the ketenes, we subject ketenes and the observed isomer in each group to form hydrogen bonded complex with water.

Figure 4.4 shows the optimized structures of the $\text{C}_2\text{H}_2\text{O}$, $\text{C}_3\text{H}_2\text{O}$ and $\text{C}_3\text{H}_4\text{O}$ complexes with water considered in this study. Tables 4.7 to 4.9 contain the binding energies of the $\text{C}_3\text{H}_4\text{O}$, $\text{C}_3\text{H}_2\text{O}$ and $\text{C}_2\text{H}_2\text{O}$ complexes with water respectively. In the supporting information, Tables S16 to S21 show the optimized geometry parameters and vibrational frequencies of these isomer complexes with water at all the levels of theory considered in this study. The table (S16 to S21) are presented in the same order in which these complexes appear in Figure 4. The formation of hydrogen bond between the water monomer and the interstellar molecule is observed in all the cases via the elongation of one of the O-H bonds of water monomer which takes part in the hydrogen bond formation from the original 0.959 \AA for the water monomer to 0.966, 0.961, 0.965, 0.961, 0.960 and 0.961 \AA for propenal, methyl ketene, propynal, methylene ketene, ethynol and ketene-water complexes respectively at the MP2(full)/6-311++G** level. In ketene-water complex where the water molecule acts as hydrogen bond

acceptor rather than donor as in the previous cases, there is an elongation of both the O-H bonds of the water monomer. This is pictured in Figure 4.4.

From the binding energies of $\text{C}_2\text{H}_2\text{O}$, $\text{C}_3\text{H}_2\text{O}$ and $\text{C}_3\text{H}_4\text{O}$ complexes with water presented in Tables 4.7 to 4.9 respectively, it is crystal clear that the ketenes are less strongly bonded to the surface of the interstellar dust grains as compared to their respective isomers that have been astronomically observed^{60, 61}. That ketenes are thermodynamically the most stable isomers in their respective isomeric groups, they are not affected by interstellar hydrogen bonding as compared to their isomers that have been detected and that a ketene molecule been astronomically detected in the interstellar medium⁶¹, we therefore propose other ketene molecules as potential candidates for astronomical observations especially methyl and methylene ketenes considered in this study.

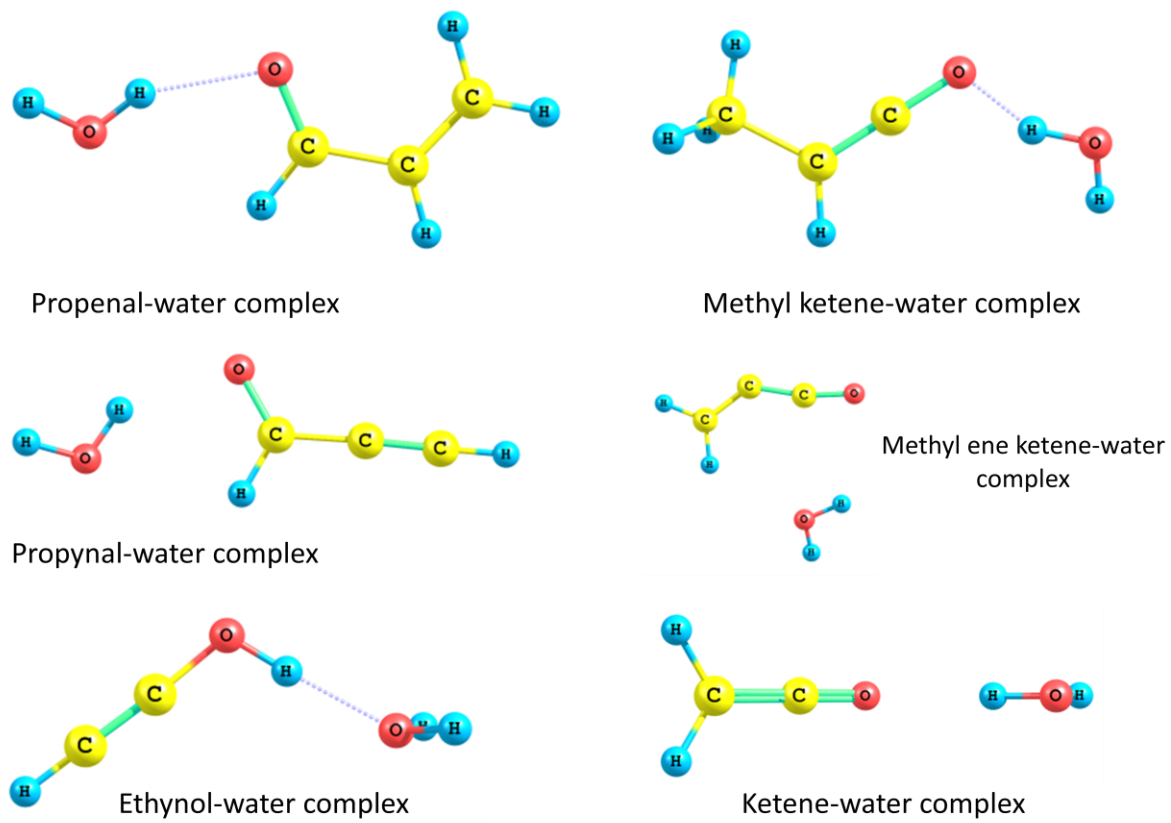


Figure 4.4: Optimized structures of the hydrogen bonded $\text{C}_2\text{H}_2\text{O}$, $\text{C}_3\text{H}_2\text{O}$ and $\text{C}_3\text{H}_4\text{O}$ complexes with water.

Table 4.7: Binding energies for propenal and methyl ketene-water complexes

Method	BE (kcal/mol)	
	Propenal- H_2O	Methyl ketene- H_2O
MP2(full)/6-311++G**	-4.6	-2.1
MP2(full)/aug-cc-pVDZ	-5.2	-2.8
G4	-4.38	-2.4
W1U	-5.0	-2.6

Table 4.8: Binding energies for propynal and methylene ketene-water complexes

Method	BE (kcal/mol)	
	Propynal-H ₂ O	Methylene ketene-H ₂ O
MP2(full)/6-311++G**	-4.2	-2.6
MP2(full)/aug-cc-pVDZ	-4.8	-3.0
G4	-4.1	-2.0
W1U	-5.1	-2.2

Table 4.9: Binding energies for ethynol and ketene-water complexes

Method	BE (kcal/mol)	
	Ethynol-H ₂ O	Ketene-H ₂ O
MP2(full)/6-311++G**	-7.65	-1.8
MP2(full)/aug-cc-pVDZ	-8.41	-2.0
G4	-8.8	-1.9
W1U	-8.7	-2.2

It is worth mentioning here that a ketenyl radical; HCCO has recently been detected in ISM in line with our prediction.⁶²

4.2.5: Interstellar Aldehydes and their Corresponding Reduced Alcohols: Interstellar Propanol?

There is a well defined trend of aldehydes and their corresponding reduced alcohols among the known interstellar molecules; methanal and methanol; ethenone and vinyl alcohol; ethanal and ethanol; glycolaldehyde and ethylene glycol which are believed to be formed via successive hydrogen additions as depicted in Figure 4.5.

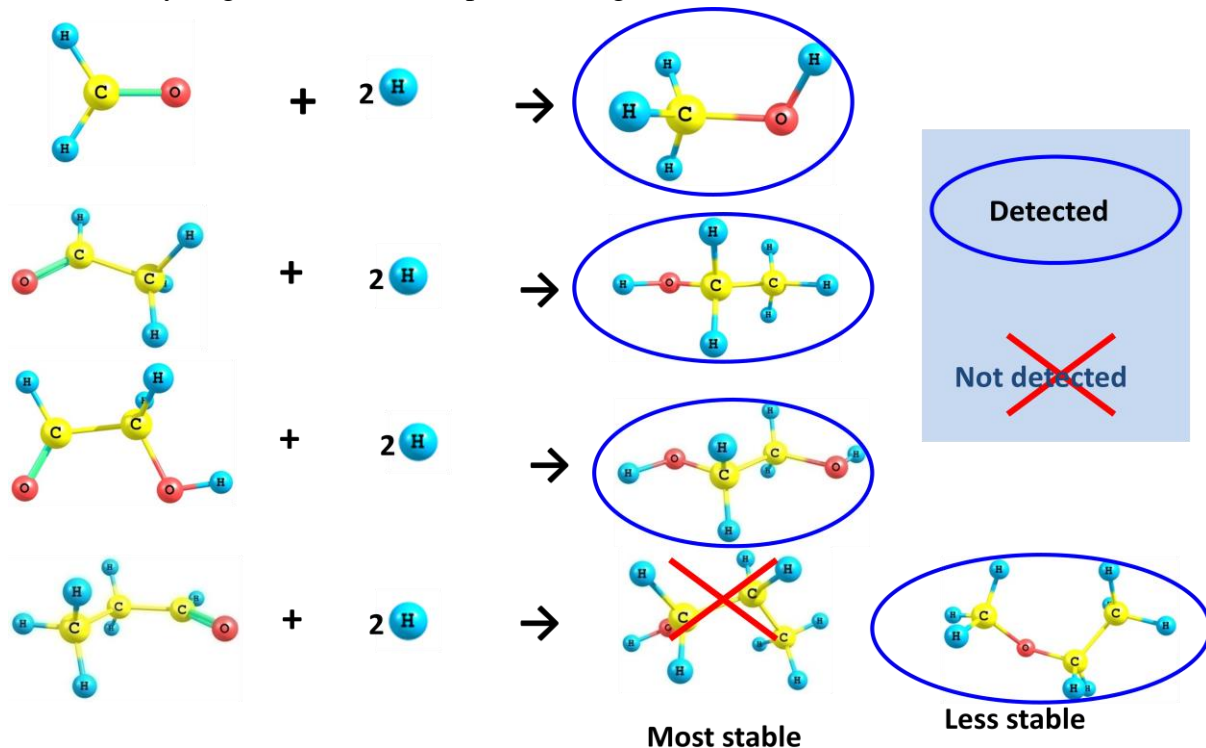


Figure 4.5: Successive hydrogen additions for the formation of alcohols.

But the reduced alcohol of propanal which is propanol has not been observed, however, its isomer; ethyl methyl ether is a known interstellar molecule. What could be responsible for the non or delayed detection of propanol?

Kinetically and with the respect to the formation route, the unquestionable high abundance of hydrogen, the energy sources within some of the molecular clouds and the ease at which it reacts make successive hydrogen addition a highly plausible route for the formation of alcohols from their corresponding reduced aldehydes via two successive hydrogen additions. In terms of stability, the observed alcohols are thermodynamically favorable as compared to their isomers. Regarding the formation process, the hydrogen addition reactions are believed to proceed on the surface of the interstellar grains which leads to the effect of interstellar hydrogen bonding. As shown in Table 4.5, propanol and propan-2-ol are found to be more strongly attached to the surface of the interstellar dust grains which affects its overall gas phase abundance as compared to its isomer; ethyl methyl ether which has been observed.

4.2.6 Detecting Weakly Bound complexes in the ISM?

From the foregoing discussions, the existence of weakly bound complexes in the interstellar medium is well established. But these weakly bound complexes that are formed in ISM, are they detectable? The interstellar molecular species are observed in the gas phase (both the ones that are formed on the surface of the interstellar dust grains and those that are gas phase products). During the warm-up phase associated with formation of stars, the molecular species that are formed on the surface of the interstellar dust grains will be desorbed. The desorbed species will enter the gas phase where they are normally detected; co-desorption of these molecules and water in the form of weakly bound complexes or clusters is highly possible. Also, the conditions in the terrestrial laboratories where weakly bound complexes are observed are similar to the conditions in ISM. In addition, the high binding energies of the complexes as shown in Table 4.1 to 4.8 imply that these complexes are detectable in ISM. Thus, it suffices to say that weakly bound complexes are present and detectable in the interstellar medium.

Figure 4.6 paints a picture of the effect of interstellar hydrogen bonding. It shows how the interstellar molecules are getting bonded to the water molecule on the surface on the interstellar dust grains, thus causing a greater part of these interstellar molecules to be attached to the surface of the interstellar dust grains. This leads in the low abundances observed for these molecules and the unsuccessful observations of others.

The use of different high level quantum ab initio methods in computing the binding energies of these complexes test the reliability and consistency of the results in all the cases considered.

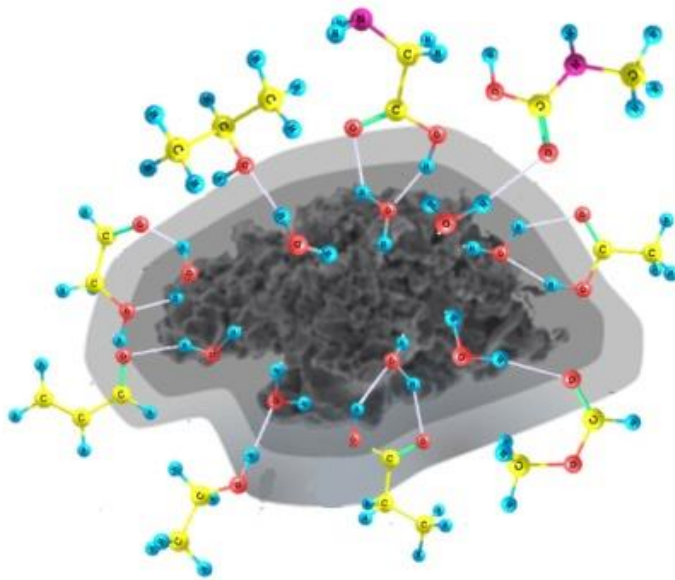


Figure 4.6: Schematic picture of the effect of interstellar hydrogen bonding.

4.2 7. Summary on Interstellar Hydrogen Bonding: The present study reports the first extensive study of the existence and effects of interstellar hydrogen bonding. The binding energies of the hydrogen bonded complexes of interstellar molecules with water obtained from high level quantum chemical simulations show a direct relationship between the binding energies and the interstellar abundances of the molecules. From the relationship, the higher the binding energy of the interstellar molecule bonded with water, the lower its interstellar abundance as compared to its counterparts with lower binding energies. This is because the stronger the molecule is being bonded to the surface of the interstellar dust grains; the more a greater portion of it is being attached to the surface of the interstellar dust grains, thereby reducing its abundance. Available interstellar observations data confirms this. Interstellar hydrogen bonding accounts for the deviations from thermodynamically controlled processes, the delay in detecting the most stable isomers whose less stable counterparts have been detected, the difficulty in observing amino acids (e.g glycine). From this and our previous studies, we propose methyl and methylene ketenes as potential candidates for astronomical observations. The acids are more strongly bonded to the surface of the interstellar dust grains than their corresponding isomers in all the cases observed here. Could this point to the detectability of acid-water complexes in the interstellar medium soon? Apart from water and other major components of the interstellar ice, the formation of hydrogen bonded complexes between these components and other molecules suggests the presence of other minor components in the interstellar ice like acetic acid and other strongly hydrogen bonded molecules. This is worth investigating.

4.3 Other Aspect of Interstellar Hydrogen Bonding

From the foregoing, the existence and effect of hydrogen bonding in the interstellar medium and among interstellar molecular species have been well established. Just as hydrogen bonding; the most celebrated weak interaction plays significant roles in a number of systems and processes in the terrestrial planet, such should also be envisaged for hydrogen bonding in ISM. In the following sections, a study employing the existence and effect of interstellar hydrogen bonding in elucidating some of the happenings and observation in interstellar chemistry and related areas is presented and discussed. Furthermore, in chapter 6, another application of the existence and effect of interstellar hydrogen bonding is discussed in one of the studies involving interstellar heterocycles.

4.4 Interstellar chemistry of sulphur and oxygen containing species: S/O abundance ratio, interstellar hydrogen bonding and detectable analogues

4.4.1 Introduction: The astrophysicists and astronomers are largely concerned with discovering new molecules in the ISM and not so much with the understanding of the chemistry and physics of these molecules. Understanding the chemistry of these molecules discovered by astrophysicists and astronomers has given birth to astrochemistry; a young interdisciplinary field which blends in chemistry into astronomy and astrophysics. In as much as we are still trying to understand the chemistry and physics of these molecules, some of the features are very glaring to be observed by all and sundry. The dominance of organic molecules, isomerism, successive hydrogen addition, periodic trends etc, are some of these notable features among these interstellar and circumstellar molecules. The dominance of organic molecules among these molecular species is very obvious with a greater percentage of these molecules found to contain the four most important biogenic elements; C, H, N and O. Slightly above 200 different molecular species have been detected from different astronomical sources⁶³. About 132 of these species contain at least an atom of H, same number also contain at least an atom of C, 64 of these molecular species contain at least an atom of N while not fewer than 59 contain an atom of O. The high abundances of these elements among the interstellar and circumstellar species can be seen as a direct reflection of their cosmic abundances. With the exceptions of the nobel gases and the unusual abundance of Fe, these four elements (H, O, C, and N) have the highest cosmic abundances.

As discussed in chapter three of this Thesis, isomerism among these molecular species has emerged as one of the important tools in exploring the basic chemistry of these species. This can be understood from the fact about 40% of all interstellar and circumstellar species have isomeric counterparts and these isomers are believed to have a common precursor for their formation routes; thus, the detection of one isomer gives an insight about the presence and the detectability of others. That most of these isomers are easily observed from the same

astronomical sources strongly supports the fact that they have a common precursor for their formation process. In the C₂H₃N isomeric group, methyl cyanide, methyl isocyanide and ketenimine have all been observed from the same astronomical source.⁶⁴⁻⁶⁶ In the C₂H₄O₂ isomeric group, acetic acid, methyl formate and glycolaldehyde have also been observed from the same molecular cloud.^{26,28,67,68} This trend is common among isomers; HCN and HNC, MgCN and MgNC, SiCN and SiNC, etc.^{40,41,68-71} Successive hydrogen addition is considered as a possible route for the formation of alcohol from their corresponding aldehydes; methanol from formaldehyde, ethanol from acetaldehyde and ethylene glycol from glycolaldehyde. Also, these molecules are commonly detected from the same spectral region. Laboratory experiments under interstellar medium conditions have demonstrated how small molecules grow into larger ones via successive hydrogen addition.⁷²

Periodic trends are another observable features of interstellar and circumstellar molecules. Elements from the same group are found to have corresponding molecules as known interstellar and circumstellar molecules as seen in the cases of C and Si; N and P; O and S; F and Cl; among others. Among these trends, those of O and S are very conspicuous. Of the 19 known S-containing molecules, 16 have the corresponding O-analogues as known interstellar and circumstellar molecules. Interestingly, 12 of the S- and their corresponding O-analogues were first detected from the same astronomical sources suggesting a common link in their formation processes. The abundance ratio of these molecules with respect to their cosmic or elemental abundance is also an interesting feature. According to Linke et al.⁷³ "***methyl mercaptan is apparently a fairly good example of the rule that the ratio of an interstellar sulphur molecule to its oxygen analogue is close to the cosmic S/O ratio***". This "rule" of course, is far from being true in many cases even for molecules observed from the same source. It thus requires an in depth investigation. Reactions that occur on the surfaces of the interstellar dust grains are the dominant processes for the formation of interstellar molecules. The composition of the interstellar dust grains which create the surface for these reactions also serve as a platform for hydrogen bonding between the water molecule (the most abundant component of the interstellar dust grains) and the molecules that are formed on these surfaces. This interstellar hydrogen bonding thus reduces the abundance of molecules that are formed on the surface of the dust grains since a greater portion of these molecules are attached to surface of the interstellar dust grains. This poses a serious exception to interstellar formation processes that have been shown to be partially thermodynamically controlled as discussed in chapter 3 of this Thesis.

In the present work, the effect interstellar hydrogen bonding on the variation of the S/O abundance ratio with respect to the cosmic S/O ratio is examined using high level quantum chemical simulations. The binding energy between water molecule on the surface of the dust grains and the O or S-containing molecule gives insight about the level to which the interstellar abundance of such molecule is affected. There are 59 O-containing and 19 S-containing interstellar species, for 16 that are S and O analogues, there is no order regarding their astronomical observations i.e in some cases, the O-containing was observed before the S-containing and vice versa. Thus, the observation of one always gives information about the presence and the possible detectability of the other. In the light of this, the known molecules

from this S/O group whose corresponding analogues are not yet observed are examined for their possible detectability. These species are subjected to the effect of interstellar hydrogen bonding. Their binding energies with water on the surface of the interstellar dust grains are determined. From the ratio of the binding energies of these systems, the S/O abundance ratio is predicted for the unknown systems. For the O-containing molecules where two or more isomers are observed, standard enthalpies of formation are computed for both the O and corresponding S-analogues to guide the preference for astronomical searches for the S-analogues since the most stable isomer is more probably the most abundant in the interstellar medium except where the effect of hydrogen is well pronounced as in the case of methyl formate and acetic acid. After describing the methodology employed in this work, the results obtained are presented and discussed before the concluding remarks.

4.4.2 Computational details: The quantum chemical calculations reported in this work are carried out using the Gaussian 09 suite of programs.¹⁴ The binding energy (B. E) between the water molecule on the surface of the interstellar dust grains and molecule of interest (O or S-containing) is determined using the super molecular approach which is defined as:

$$B.E(\text{complex}) = E(\text{complex}) - [E(\text{water molecule}) + E(\text{heterocycle molecule})].$$

To obtain high accurate values for the binding energy, the MP2(full) with the 6-311++G** basis set is used in examining the effect of interstellar hydrogen bonding. By definition, the standard enthalpy of formation ($\Delta_f H^0$) of any molecule is the enthalpy change of the reaction by which it is formed from its constituent's elements. Among the different composite quantum chemical methods that are now used to accurately predict thermochemistry data, the G4 method has been found to be found to be very effective in predicting enthalpy of formation values to chemical accuracy in many molecules as discussed in the previous chapter.^{11,14,17-19} Details regarding the steps in calculating zero point corrected standard enthalpy of formation have been well described in chapter 3 of this Thesis. The values reported in this work are calculated from the optimized geometries of the systems at the levels of theory mentioned above. The structures are found to be stationary with no imaginary frequency through harmonic vibrational frequency calculations.

4.4.3 Results and discussion: The known S-containing molecules and their corresponding O-analogues are discussed with respect to the observed S/O abundance ratio followed by the detectability of the unknown analogues of these species. Table 4.10 shows all the known S-containing interstellar species in a chronological order with their corresponding O-analogues (where available); the binding energies (B. E) of these species with an isolated water molecule on the surface of the interstellar dust grains computed at the MP2(full)/6-311++G** level discussed above are presented in columns 2 and 4 respectively for S and O-species, the S/O ratio is from the observed abundances of these species taken from the references in column 6. The magnitude of the binding energy shows the extent to which the molecule (S or O-containing) is bonded to the surface of the interstellar dust grains. The higher the magnitude of the B. E, the more strongly bonded is the molecule and vice versa. This also implies that as molecule is strongly bonded to the surface of the interstellar dust grains, a greater portion of it is attached to the surface of the dust grains, thus reducing its overall

abundance. When the S-containing species is more strongly bonded as compared to the O-analogue, the S/O abundance ratio becomes much more smaller than the S/O cosmic ratio of 0.024 (1/42)^{44,73} and the reverse becomes the case when O-analogue is more strongly bonded as compared to the S-analogue. When the ratio of the binding energy of an S-containing species and its O-analogue approaches unity, the observed S/O ratio also approaches the cosmic S/O ratio. Because in this case there is little or no much pronounced effect of interstellar hydrogen bonding which affect the interstellar abundance of these species. The major exception to this trends is observed with the components of the interstellar ices; H₂O, CH₃OH and H₂CO which are thus more abundant than their corresponding S-analogues irrespective of the effect of interstellar hydrogen bonding. Figure 4.7 and Table 4.11 summarize the observed trends in Table 4.10. With the few exceptions observed above, S/O abundance ratio of all the known S-containing species and their corresponding O-analogues follows the same trend as displayed in Table 4.11. As the B. E S/O ratio approaches unity, the observed S/O ratio approaches the cosmic S/O ratio as in the cases of HNCS/HNCO and C₃S/C₃O. When this ratio is above unity, the observed S/O ratio becomes much less than the cosmic S/O ratio e.g CS/CO, SO/O₂, NS/NO, C₂S/C₂O and HSCN/HOCN and the reverse is observed when the ratio is less than unity, e.g OCS/CO₂, SiS/SiO, HCS⁺/HCO⁺, CH₃CH₂SH/CH₃CH₂OH. In summary, the B.E O/S ratio is inversely proportional to the observed variation of S/O abundance ratio with the cosmic S/O ratio.

Table 4.10: S and O-containing species, their B.E with water and S/O ratio

S-containing molecule	B. E (kcal/mol) with water	O-analogue	B. E (kcal/mol) with water	S/O ratio	Refs
CS (1971)	-2.0	CO (1970)	-0.9	0.013	74,75
OCS (1971)	-1.5	CO ₂ (1989)	-2.9	0.032	76,77
H ₂ S (1972)	-2.3	H ₂ O (1969)	-4.7	<<0.001	78,79
H ₂ CS (1973)	-2.6	H ₂ CO (1969)	-4.1	≈0.025	80
SO (1973)	-3.1	O ₂ (2011)	-0.3	0.015	81,82
SO₂ (1975)	-2.1	O₃ (not observed)	-0.5	NA	
SiS (1975)	-3.7	SiO (1971)	-6.8	≈1	83,84
NS (1975)	0.3	NO (1978)	-0.1	0.005	85,86
CH ₃ SH (1979)	-2.0	CH ₃ OH (1970)	-4.4	≈0.023	73,87
HNCS (1979)	-7.5	HNCO (1972)	-9.1	0.025	44,88
HCS ⁺ (1981)	-12.5	HCO ⁺ (1970)	-39.8	≈0.191	75,89
C ₂ S (1987)	-2.6	C ₂ O (1991)	-2.5	0.010	90,91
C ₃ S (1987)	-2.6	C ₃ O (1985)	-2.6	0.028	92,93
SO⁺ (1992)	-18.6	O₂⁺ (not observed)	-50.3	NA	
HSCN (2009)	-98.7	HOCN (2009)	-37.2	4.5E-3	94,88
SH ⁺ (2011)	-73.3	OH ⁺ (2010)	-69.3	0.029	95,96
SH (2012)	-1.4	OH (1963)	-2.9	0.023	97,98
CH ₃ CH ₂ SH (2014)	-1.7	CH ₃ CH ₂ OH (1975)	-4.3	0.286	30,99
C₅S (2014)	-1.9	C₅O (not observed)	-3.0	NA	

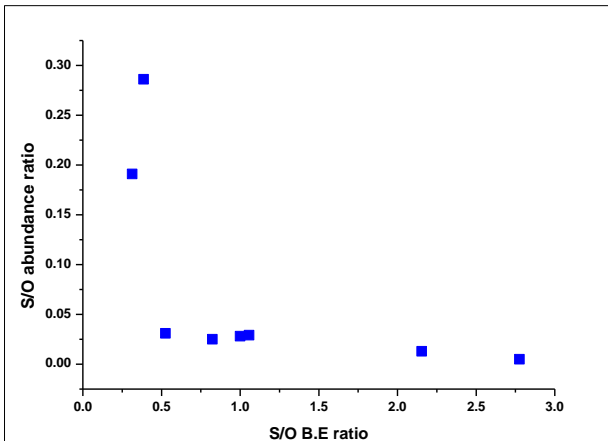


Fig 4.7: Correlation between B.E and S/O abundance ratio.

Table 4.11: Deviation from cosmic S/O ratio as a function of binding energy (B.E)

S/O B.E >1	S/O B. E ≈1	S/O B. E <1
S/O ratio < cosmic S/O ratio	S/O ratio ≈ cosmic S/O ratio	S/O ratio > cosmic S/O ratio

Known O-containing species and detectable S-analogues: As previously mentioned, there are at least 59 known O-containing interstellar and circumstellar molecules of which 16 have the corresponding S-analogues as known astro-molecules leaving us with over 40 O-containing species without the corresponding S-analogues. In assessing the detectability of these S-analogues of known O-containing molecules, the binding energies of these species (both S- and O-containing species) with water on the surface of the interstellar dust grains have been computed. These values are presented in Table 4.12. The reported column densities for the known O-containing molecules are shown on column 2 with the source of the data on column 3 of the same table (refs). Column 7 shows the ratio of the binding energy of the S and O-containing species, from this ratio, the S/O abundance ratio is predicted (column 8) following the observations made in the preceding section (see table 4.11). That the S-containing molecular species are less bonded to the surface of the interstellar dust grains compared to their respective O-analogues as it is observed in over 80% of the systems here (Table 4.12) is a good omen with respect to the detectability of these species because their overall interstellar abundance will be less affected by the effect of interstellar hydrogen bond unlike their O-analogues. However, with respect to the role that the ratio of an interstellar sulphur molecule to its oxygen analogue is close to the cosmic S/O ratio, there will be much deviation from this role since the degree to which the S-containing species is affected by the effect of hydrogen bonding on the surface of the dust grains is much different from those of the corresponding O-analogues. As a result of this, S/O abundance ratio would be expected to be much higher than the cosmic S/O ratio as shown in column 8 of

Table 4.10 for majority of the cases and in very few cases the ratio will tend toward the cosmic S/O ratio except where other processes play a role.

Table 4.12: Parameters for Known O- and detectable S-containing molecules

O-containing molecule	Column density (cm ⁻²)	Refs	B. E (kcal/mol) with water	S-analogue	B. E (kcal/mol) with water	B. E. S/O ratio	Estimated S/O abundance ratio
CO ⁺	≈E12	¹⁰⁰	-58.5	CS ⁺	-13.6	0.2	>S/O*
FeO	9E11	¹⁰¹	10.3	FeS	-3.6	0.3	>S/O*
PO	≈2.8E15	¹⁰²	-10.2	PS	-1.2	0.1	>S/O*
OH ⁺	2.4E15	⁹⁵	-69.3	SH ⁺	-73.3	1.1	≈ S/O*
TiO	6.99E14	¹⁰³	-3.9	TiS	-2.4	0.6	>S/O*
NO ⁺	2.2E12	¹⁰⁴	-20.7	NS ⁺	-21.5	1.0	≈ S/O*
AlO	≈2E15	¹⁰⁵	-0.03	AlS	-15.0	556.7	< S/O*
N ₂ O	≈E15	¹⁰⁶	-2.2	N ₂ S	-1.9	0.8	≈S/O*
HCO	≈E11	¹⁰⁷	-27.2	HCS	-7.5	0.3	>S/O*
HNO	6E11-3.2E14	¹⁰⁸	-72.4	HNS	-35.8	0.5	> S/O*
HOC ⁺	≈3E12	¹⁰⁹	-72.9	HSC ⁺	-127.0	1.7	< S/O*
OCN ⁻	-	¹¹⁰	-11.9	SCN ⁻	-9.0	0.8	> S/O*
H ₂ O ⁺	7.2E12, 2.3E13, 1.1E15	¹¹¹	-45.6	H ₂ S ⁺	-19.1	0.4	>S/O*
TiO ₂	7.5E14	¹⁰³	-32.5	TiOS	-15.6	0.5	> S/O*
HO ₂	2.8E12	¹¹²	-2.1	HSO	-2.7	1.3	≈ S/O*
AlOH	≈E17	¹¹³	-4.0	AlSH	-21.9	5.4	< S/O*
H ₃ O ⁺	3E14	¹¹⁴	-30.6	H ₃ S ⁺	-17.7	0.6	> S/O*
HOCO ⁺	-	¹¹⁵	-34.0	HOCS ⁺	-45.8	1.3	≈ S/O*
HCNO	≈8.9E12	¹¹⁶	-1.9	HCNS	-1.1	0.6	> S/O*
HOOH	8E12	¹¹⁷	-5.9	HOSH	-2.7	0.5	>S/O*
HCOOH	≈5E13	¹¹⁸	-4.3	HCSOH	-0.4	0.1	> S/O*
H ₂ C ₂ O	≈E14	⁶¹	-2.2	H ₂ C ₂ S	-0.5	0.2	> S/O*
H ₂ COH ⁺	E12-E14	¹¹⁹	-25.4	H ₂ CSH ⁺	-15.1	0.6	> S/O*
CNCHO	1-17E14	¹²⁰	-4.7	CNCHS	-4.2	0.9	≈ S/O*
CH ₃ O	7E11	¹²¹	-3.2	CH ₃ S	-2.2	0.7	> S/O*
H ₂ NCO ⁺	6-14E11	¹²²	-21.4	H ₂ NCS ⁺	-17.9	0.8	≈ S/O*
H ₂ NCHO	2.2E16	¹²³	-5.5	H ₂ NCHS	-4.2	0.8	> S/O*
HC ₂ CHO	1.5E12	¹²⁴	-4.1	HC ₂ CHS	-2.9	0.7	> S/O*
c-H ₂ C ₃ O	≈E13	¹²⁵	-6.1	c-H ₂ C ₃ S	-5.6	0.9	≈ S/O*
CH ₃ CHO	≈1.5E14	¹²⁶	-4.7	CH ₃ CHS	-2.5	0.5	> S/O*
c-C ₂ H ₄ O	3.3E14	⁴⁸	-4.5	c-C ₂ H ₄ S	-2.9	0.7	> S/O*
CH ₂ CHOH	2.4E13	⁴⁷	-6.1	CH ₂ CHSH	-2.6	0.4	
CH ₃ COOH	7.3E15	²⁶	-7.9	CH ₃ CSOH	-7.0	0.9	≈ S/O*
HCOOCH ₃	≈1.9E17	¹²⁷	-5.0	HCSOCH ₃	-2.4	0.5	> S/O*

HOCH ₂ CHO	2.8E16	¹²⁷	-5.4	HSCH ₂ CHO	-4.3	0.8	> S/O*
CH ₂ CHCHO	-	¹²⁸	-5.2	CH ₂ CHCHS	-2.8	0.5	> S/O*
(NH ₂) ₂ CO	≈E15	¹²⁹	-7.4	(NH ₂) ₂ CS	-6.7	0.9	≈ S/O*
CH ₃ OCH ₃	<18E14	³¹	-4.4	CH ₃ SCH ₃	-2.5	0.6	> S/O*
CH ₃ CONH ₂	1.8E14	¹³⁰	-5.9	CH ₃ CSNH ₂	-3.9	0.7	> S/O*
(CH ₃) ₂ CO	2.9E16	¹³¹	-5.1	(CH ₃) ₂ CS	-6.7	1.3	≈ S/O*
HOCH ₂ CH ₂ OH	3.2E14	¹³²	-4.1	HOCH ₂ CH ₂ SH	-2.1	0.5	> S/O*
CH ₃ CH ₂ CHO	-	³¹	-4.6	CH ₃ CH ₂ CHS	-3.3	0.7	> S/O*
C ₂ H ₅ OCHO	5.4E16	¹³³	-4.9	C ₂ H ₅ OCHS	-14.8	3.0	< S/O*
CH ₃ COOCH ₃	4.2E15	¹³⁴	-4.8	CH ₃ CSOCH ₃	-4.0	0.8	> S/O*
C ₂ H ₅ OCH ₃	2E14	¹³⁵	-4.2	C ₂ H ₅ SCH ₃	-2.5	0.6	> S/O*

Where S/O* is the cosmic abundance ratio.

Interstellar formation processes have been shown to be partially thermodynamically controlled in many cases. Except with a pronounced effect of interstellar hydrogen bonding, the most stable isomer has always been observed to be the most abundant isomer in the interstellar space. Thus, the most stable isomer is easily observed as compared to other isomers of the group. Figure 4.8 pictures this concept. It shows the how the interstellar abundance (column density) of two isomers each from the CHNO and CHNS groups varies with the stability (enthalpy of formation) where the most stable isomer (with lower enthalpy of formation) is found to be the most abundant in both cases.

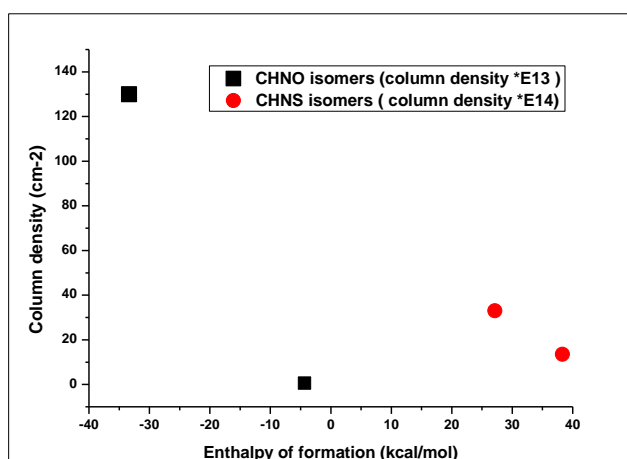


Fig. 4.8: Dependence of column density on enthalpy of formation for CHNO and CHNS systems.

Table 4.13: Enthalpy of formation for O-containing isomers and their detectable S-analogues

Molecule	Enthalpy of formation (kcal/mol)	
	X = O	X = S
3-atoms		
HXC ⁺	234.4	340.7
HCX ⁺	198.6	246.6
4-atoms		
HCNX	34.1	61.2
HXCN	-4.4	38.3
HNCX	-33.4	27.1
7-atoms		
c-H ₂ CH ₂ CX	-14.6	19.1
H ₂ CCHXH (anti)	-28.5	19.4
H ₂ CCHXH (syn)	-30.2	19.4
H ₃ CCHX	-42.4	16.4
8-atoms		
HXH ₂ CCHX	-70.5	32.0
H ₃ CXCHX	-89.4	20.7
H ₃ C(X)XH	-103.7	18.6
9-atoms		
(CH ₃) ₂ X	-49.0	-10.7
C ₂ H ₅ XH	-56.7	-11.9
11 atoms		
H ₃ COC(O)CH ₃	-95.1	12.1
H ₃ CH ₂ CXCHX	-97.5	12.5

Searching for the most stable isomer is thus a step toward successful observation and the successful detection of an isomer reaffirms the presences of other isomers since they are believed to have a common precursor for their formation routes. In view of this, for known O-containing molecules with at least two isomers, the standard enthalpies of formation for these isomers and their S-analogues have been determined as a guide for preference in the astronomical searches for these isomers. Table 4.13 presents the enthalpy of formation for O-containing isomers and their detectable S-analogues. As would be expected, the trend of the stability for O and S-species is the same. From the parameters presented in Table 4.11 coupled with the advancements in astronomical and spectroscopic equipments, that all the S-analogues of known O-containing interstellar molecular species would not be considered as exaggeration. They are detectable.

Known S-species and overdue detectable O-analogue: Without any exception, an interstellar O-containing molecular species is more abundant than its S-analogue (Table 4.10). So for every known S-species, the O-analogue is not only present in detectable abundance, it can be said to have even been overdue for astronomical detection because for sure the O-species are more abundant than their S-analogue and as such could be detected with less difficulty as compared to its S-analogue. Table 4.14 lists the parameters for known

S-containing interstellar species and their detectable O-analogues. The high abundances reported for these S-containing species (column 2) strongly support the detectability of their O-analogues.

Table 4.14: Parameters for Known S- and detectable O-containing molecules

S-containing molecule	Column density (cm ⁻²)	Refs	B. E (kcal/mol) with water	O-analogue	B. E (kcal/mol) with water	B. E. S/O ratio	Estimated S/O abundance ratio
SO ₂	<3.5E16	¹	-2.1	O ₃	-0.5	4.2	<S/O*
SO ⁺	5E12	²	-18.6	O ₂ ⁺	-50.3	0.4	>S/O*
C ₅ S	2-14E12	³	-1.9	C ₅ O	-3.0	0.6	>S/O*

Where S/O* is the cosmic abundance ratio.¹Snyder et al. 1975; ²Turner, 1992; ³Agúndez et al. 2014.

4.4.4 Summary on Interstellar chemistry of sulphur and oxygen containing species: The deviation of the observed S/O abundance from the the rule that the ratio of an interstellar sulphur molecule to its oxygen analogue is close to the cosmic S/O ratio and the possibility of detecting other analogues of the known S- and O-containing species have been examined in this study. The effect of hydrogen bonding on the surface of the interstellar dust grains where these molecules are believed to be formed plays a vital role in the observed S/O abundance ratio. From the binding energy of these species with the water molecule on the surface of the dust grains, the more the molecules are strongly bonded to the surface of the dust grains the more their abundances are reduced. As the ratio of the binding energy of S and O-species (B. E of S/O) with water approaches unity, the S/O abundance ratio approaches cosmic S/O ratio. When this ratio is less than one, the observed S/O abundance ratio becomes much higher than the cosmic S/O ratio and vice versa except for the species that are major components of the interstellar ice. With respect to the detectability of the unknown analogues of these species, every known O-species is an indication of the presence and detectability of the S-analogue. This has been shown to be true in many cases where the S-analogues of known O-species are successfully observed following the detection of the O-analogues. That these S-containing species are less bonded to the surface of the interstellar dust grains as compared to their O-analogues firmly support the high abundances and the detectability of these species. For the known S-species whose O-analogues are yet to be observed, the O-analogues are not only present in detectable abundance, it can be said to have even been overdue for astronomical detection since the O-species without any exception are more abundant than their S-analogue and as such they could be detected with less difficulty as compared to its S-analogues that are already known.

4.5 Conclusions on Interstellar Hydrogen Bonding: Detecting Weakly Bound Complexes in Space

In this chapter, the existence and effects of interstellar hydrogen bonding have been reported for the first time. It has been shown to be responsible for the deviations from thermodynamically controlled processes, delayed observation of the most stable isomers, unsuccessful observations of amino acids among other happening in interstellar chemistry and related areas. On the prediction that ketenes are the right candidates for astronomical searches among their respective isomers, a ketenyl radical; HCCO has recently been detected in line with this prediction. The deviation from the role rule that the ratio of an interstellar sulphur molecule to its oxygen analogue is close to the cosmic S/O ratio is well accounted for on the basis of hydrogen bonding on the surface of the dust grains. As the ratio of the binding energy of S and O-species (B. E of S/O) with water approaches unity, the S/O abundance ratio approaches cosmic S/O ratio. The more this ratio deviates from unity, the more the S/O abundance deviates from the cosmic S/O ratio. Detecting weakly bound complexes in ISM? Obviously, this has not been a major interest in the field so far but the detectability of weakly bound complexes in ISM is very possible as discussed in this chapter. Following the conditions in which these complexes are observed in the terrestrial laboratory as compared to the ISM conditions; it suffices to say that weakly bound complexes present and are detectable in ISM. They could even account for some of the 'U' lines. Let's bring down the complexes.

4.6 References

1. Etim, E. E.; Arunan, E. 2016. Submitted
2. Tielens, A. G. G.M. Rev Mod Phys, 2013, 85,1021
3. Fraser, H. J.; McCoustra., M. R. S.; Williams, D. A. Astron Geophys, 2002, 43, (2), 10
4. Draine, B. T. Annu Rev Astron Astr, 2003, 41,241
5. van Dishoeck, E. F. Annu Rev Astron Astr, 2004, 42, 119
6. Gibb, E., Nummelin, A., Irvine, W. M., Whittet, D. C. B., Bergman, P. Astrophys J, 2000, 545, 309
7. Gibb, E. L., Whittet, D. C. B., Boogert, A. C. A., Tielens, A. G. G. M. Astrophys JS, 2004, 151, 35
8. Whittet, D. C. B. Dust in the Galactic Environment, Institute of Physics Publishing, Bristol, 2003.
9. Park, Y. C., Lee, J. S. Bull. Korean Chem. Soc, 2007, 28 (3), 386
10. Ikeda, A., Nakao, Y., Sato, H., Sakaki, S. J Phys Chem A, 2007, 111, 7124
11. Møller, C., Plesset, M. S. Phys Rev, 1943, 46, 618
12. Head-Gordon, M.; Pople, J. A.; Frisch, M. J Chem Phys Lett, 1988, 153 (6), 503
13. Frisch, M. J., Head-Gordon, M., Pople, J. A. Chem Phys Lett, 1990, 166, 281
14. Frisch, M. J., Trucks, G. W., Schlegel, H. B., Scuseria, G. E., Robb, M. A., Cheeseman, J. R., Scalmani, G., Barone, V., Mennucci, B., Petersson, G. A., Gaussian 09, revision D.01;Gaussian, Inc., Wallingford, CT, 2009.
15. Martin, J. M. L.; de Oliveira, G. J Chem Phys, 1999, 111, 1843
16. Parthiban, S Martin, J. M. L. J Chem Phys, 2001, 114, 6014
17. Curtiss, L. A., Raghavachari, K., Redfern, P. C., Rassolov, V., Pople, J. A. J Chem Phys, 1998, 109, 7764
18. Curtiss, L. A., Redfern, P. C., Raghavachari, K. J Chem Phys, 2007, 126, 084108
19. Curtiss, L. A., Redfern, P. C., Raghavachari, K. J Chem Phys, 2007, 127, 124105

20. Chandrasekhar, J., Andrade, J. G., Schleyer, P. V. R. *J Am Chem Soc*, 1981, 103, 5609

21. Hariharan, P.C., Pople, J. A. *Theor. Chim. Acta*, 1973, 28, 213

22. Boys, S. F., Bernardi, F. *Mol Phys*, 1970, 19, 553

23. Cook, R. L., de Lucia, F. C., Helminger, P. *J Mol. Spectrosc*, 53, 62

24. Benedict, W. S., Gailan, N., Plyler, E. K. *J Chem Phys*, 1956, 24, 1139.

25. Popkie, H., Kistenmacher, H., Clementi, E. *J Chem Phys*, 1973, 59, 1325

26. Mehringer, D. M., Snyder, L. E., Miao, Y., Lovas, F. *Astrophys J.*, 1997, 480, 71

27. Churchwell, E., Winnewisser, G. *Astron Astrophys*, 1975, 45, 229

28. Hollis, J. M., Lovas, F. J., Jewell, P. R. *Astrophys J.*, 2000, 540, 107

29. Zuckerman, B., Turner, B. E., Johnson, D. R., et al. *Astrophys J.*, 1975, 196:99

30. Pearson, J. C., Sastry, K. V. L. N., Herbst, E., De Lucia, F. C. *Astrophys J*, 1997, 480, 420

31. Snyder, L. E., Buhl, D., Schwartz, P. R., Clark, F. A., Johnson, D. R., Lovas F. J.; Giguere, P. T. *Astrophys J* 1974, 191, 79

32. Nummelin, A., Bergman, P., Hjalmarson, Å., Friberg, P., Irvine, W. M., Millar, T. J., Ohishi, M., Saito, S. *Astrophys JS*, 1998, 117, 427

33. Ikeda, M., Ohishi, M., Dickens, J. E., Bergman, P., Hjalmarson, A., Irvine, W. M. *Astrophys J*, 2001, 560, 792

34. White, G. J., Araki, M., Greaves, J. S., Ohishi, M., Higginbottom, N. S. *Astron Astrophys*, 2003, 407, 589

35. Remijan, A., Snyder, L. E., Liu, S. Y., Mehringer, D., Kuan, Y. J. *Astrophys J*, 2002, 576, 264

36. Remijan, A., Snyder, L. E., Friedel, D. N., Liu, S. Y., Shah, R. Y. *Astrophys J*, 2003, 590, 314.

37. Hollis, J. M., Vogel, S. N., Snyder, L. E., Jewell, P. R., Lovas, F. J. *Astrophys J*, 2001, 554 L81

38. Hollis, J. M., Jewell, P. R., Lovas, F. J., Remijan, A. *Astrophys J*, 2004, 613 L45

39. Cazaux, S., Tielens, A. G. G. M., Ceccarelli, C., Castets, A., Wakelam, V., Caux, E., Parise, B., teyssier, D. *Astrophys J*, 2003, 593, L51

40. Zuckerman, B., Morris, M., Palmer, P., Turner, B. E. *Astrophys J*, 1972, 173, 125

41. Ziurys, L. M., Apponi, A. J., Guélin, M., Cernicharo, J. *Astrophys J*, 1995, 445, L47

42. Kawaguchi, K., Kagi, E., Hirano, T., Takano, S., Saito, S. *Astrophys J* 1993, 406, 39

43. Halfen, D. T., Ziurys, L. M., Brünken, S., Gottlieb, C. A., McCarthy, M. C., Thaddeus, P. *Astrophys J*, 2009, 702, 124

44. Frerking, M. A., Linke, R. A., Thaddeus, P. *Astrophys J*, 1979, 234, 143

45. Fourikis, N., Sinclair, M. W., Robinson, B. J., Godfrey, P. D., Brown, R. D. *Aut J Phys* 1974, 27, 425

46. Gilmore, W., Morris, M., Palmer, P., Johnson, D. R., Lovas, F.J., Turner, B. E., Zuckerman, B. *Astrophys J*, 1976, 204, 43

47. Turner, B. E., Apponi, A. J. *Astrophys J*, 2001, 561, 207

48. Dickens, J. E., Irvine, W. M., Ohishi, M., Ikeda, M., Ishikawa, S., Nummelin, A., Hjalmarson, A. *Astrophys J*, 1997, 489, 753

49. Belloche, A., Garrod, R. T., Müller, H. S. P., Menten, K. M., Comito, C., Schilke, P. *Astron Astrophys*, 2009, 499, 215

50. Tercero, B., Kleiner, I., Cernicharo, J., Nguyen, H. V. L., López, A., Muñoz Caro, G. M. *Astrophys J Lett*, 2013, 770, L13

51. Fuchs, G. W., Fuchs, U., Giesen, T. F., Wyrowski, F. *Astron Astrophys*, 2005, 444, 521

52. Kuan, Y.-J., Charnley, S. B., Huang, H.-C., Tseng, W.-L., Kisiel, Z. *Astrophys J*, 2003, 593, 848

53. Snyder, L. E., Lovas, F. J., Hollis, J. M., Friedel, D. N., Jewell, P. R., Remijan, A., Ilyushin, V. V., Alekseev, E. A., Dyubko, S. F. *Astrophys J*, 2005, 619, 914

54. Jones, P. A., Cunningham, M. R., Godfrey, P. D., Cragg, D. M. *Mon Not R Astron Soc*, 2007, 374, 579

55. Cunningham, M. R., Jones, P. A., Godfrey, Mon Not R Astron Soc, 2007, 376, 1201

56. Elsila, E., Dworkin, J. P., Bernstein, M. P., Martin, M. P., Sandford, S. A. *Astrophys J*, 2007, 660, 911

57. Botta, O., Bada, J. L. *Surv Geophys*, 2002, 23, 411

58. Demyk, K., Wlodarczak, G., Dartois, E. in *Semaine de l'Astrohysique Francaise*, (Eds) Combes, F., Barret, D., Contini, T., Meynadier, F., Pagani, L. SF2A-2004 (Les Ulis: EDP-Sciences), p. 493, 2004.

59. Hollis, J. M., Jewell, P. R., Lovas, F. J., Remijan, A., Møllendal, H. *Astrophys J* 2004, 610, 21

60. Irvine, W. M., Brown, R. D., Craig, D. M., Friberg, P., Godfrey, P.D., Kaifu, N., Matthews, H. E., Ohishi, M., Suzuki, H., Takeo, H. *Astrophys J*, 1988, 335, 89

61. Turner, B. E. *Astrophys J*, 1977, 213, 75

62. Agúndez, M., Cernicharo, J., and Guélin, M. *Astron Astrophys*, 2015, 577, L5

63. Etim, E. E., Arunan, E. *Planex Newsletter*, 2015, 5(2), 16

64. Solomon, P. M., Jefferts, K. B., Penzias, A. A., Wilson, R. W. *Astrophys J*, 1971, 168, L107

65. Cernicharo, J., Kahane, C., Guélin, M., Gomez-Gonzalez, J. *Astron Astrophys*, 1988, 189, L1

66. Lovas, F. J., Hollis, J. M., Remijan, A. J., Jewell, P. R. *Astrophys J*, 2006, 645, L137

67. Brown, R. D., Crofts, J. G., Godfrey, P. D., et al. *Astrophys J*, 1975, 197, L29

68. Snyder, L. E., and Buhl, D. *Astrophys J*, 1971, 163, L47

69. Guélin, M., Cernicharo, J., Kahane, C., Gomez-Gonzales, J. *Astron Astrophys*, 1986, 157, 17

70. Guélin, M., Muller, S., Cernicharo, J., et al. *Astron Astrophys*, 2000, 369, 9

71. Guélin, M., Muller, S., Cernicharo, J., McCarthy, M. C., Thaddeus, P. *Astron Astrophys*, 2004, 426, 49

72. Hollis, J. M., Lovas, F. J., Jewell, P. R., Coudert, L. H. *Astrophys J*, 2002, 571, L59

73. Linke, R. A., Frerking, M. A., Thaddeus, P. *Astrophys J*, 1979, 234, L139

74. Smith, A. M., Stecher, T. P. *Astrophys J*, 1971, 164, L43

75. Penzias, A. A., Solomon, P. M., Wilson, R. W., Jefferts, K. B. *Astrophys J*, 1971, 168, L53

76. D'Hendecourt, L. B., de Muizon, M. J. *Astron Astrophys*, 1989, 223, L5

77. Jefferts, K. B., Penzias, A. A., Wilson, R. W., Solomon, P. M. *Astrophys J*, 1971, 168, L111

78. Thaddeus, P., Kutner, M. L., Penzias, A. A., Wilson, W. R., Jefferts, K. B. *Astrophys J*, 1972, 176, L73

79. Coutens, A., Vastel, C., Caux, E., et al. *Astron Astrophys*, 2012, 539, 132

80. Sinclair, M. W., Fourikis, N., Ribes, J. C., et al. *Aut J Phys*, 1973, 26, 85

81. Gottlieb, C. A., Ball, J. *Astrophys J*, 1973, 184, L59

82. Goldsmith, P. F., Liseau, R., Bell, T. A., et al. *Astrophys J*, 2011, 737, 96

83. Morris, M., Gilmore, W., Palmer, P., Turner, B. E., Zuckerman, B. *Astrophys J*, 1975, 199, L47

84. Wilson, R. W., Penzias, A. A., Jefferts, K. B., Kutner, N., Thaddeus, P. *Astrophys J*, 1971, 167, L97

85. Gottlieb, C. A., Ball, J. A., Gottlieb, E. W., Lada, C. J., Penfield, H. *Astrophys J*, 1975, 200, L147

86. Liszt, H. S., Turner, B. E. *Astrophys J*, 1978, 224, L73

87. Gottlieb, C. A.; Ball, J. A., Gottlieb, E. W., Dickinson, D. F. *Astrophys J*, 1979, 227, 422.

88. Halfen, D. T., Ziurys, L. M., Brünken, S., et al. *Astrophys J*, 2009, 702, L124

89. Thaddeus, P., Guélin, M., Linke, R. A. *Astrophys J*, 1981, 246, L41

90. Ohishi, M., Suzuki, H., Ishikawa, S. I., et al. *Astrophys J*, 1991, 380, L39

91. Saito, S., Kawaguchi, K., Yamamoto, S., et al. 1987. *Astrophys J* 317: L115.

92. Yamamoto, S., Saito, S., Kawaguchi, K., Kaifu, N., and Suzuki, H. *Astrophys J*, 1987, 317, L119

93. Brown, R. D., Godfrey, P. D., Cragg, D. M., et al. *Astrophys J*, 1985, 297, 302

94. Brünken, S., Belloche, A., Martín, S., Verheyen, L., and Menten, K. L. *Astron Astrophys*, 2010, 516, A109.

95. Wyrowski, F., Menten, K. M., Güsten, R., Belloche, A. *Astron Astrophys*, 2010, 518, A26.

96. Menten, K. M., Wyrowski, F., Belloche, A., et al. *Astron Astrophys*, 2011, 525, A77

97. Neufeld, D. A., Falgarone, E., Gerin, M., et al. *Astron Astrophys*, 2012, 542, L6

98. Weinreb, S., Barrett, A. H., Meeks, M. L., Henry, J. C. *Nature*, 1963, 200, 829

99. Kolesniková, L., Tercero, B., Cernicharo, J., et al. *Astrophys J*, 2014, 784, L7

100. Latter, W. B., Walker, C. K., Maloney, P. R. *Astrophys J*, 1993, 419, L97

101. Walmsley, C. M., Bachiller, R., Pineau des Forets, G., Schilke, P. *Astrophys J*, 2002, 566, L109

102. Tenenbaum, E. D., Woolf, N. J., Ziurys, L. M. *Astrophys J*, 2007, 666, L29

103. Kamiński, T., Gottlieb, C. A., Menten, K. M., et al. *Astron Astrophys*, 2013, 551, A113

104. Cernicharo, J., Bailleux, S., Alekseev, E., et al. *Astrophys J*, 2014, 795, 40

105. Tenenbaum, E. D., Ziurys, L. M. *Astrophys J*, 2009, 693, L59

106. Ziurys, L. M., Apponi, A. J., Hollis, J. M., and Snyder, L. E. *Astrophys J*, 1994, 436, L181

107. Snyder, L. E., Hollis, J. M., Ulich, B. L. *Astrophys J*, 1976, 208, L91

108. Snyder, L. E., Kuan, Y.-J., Ziurys, L. M., Hollis, J. M. *Astrophys J*, 1993, 403, L17

109. Ziurys, L. M., and Apponi, A. J. *Astrophys J*, 1995, 455, L73

110. Soifer, B. T., Puetter, R. C., Russell, R. W. *Astrophys J*, 1979, 232, L53

111. Ossenkopf, V., Müller, H. S. P., Lis, D. C., et al 2010. *Astron Astrophys*, 2010, 518, L111

112. Parise, B., Bergman, P., and Du, F. *Astron Astrophys*, 2012, 541,L11

113. Tenenbaum, E. D., and Ziurys, L. M. *Astrophys J*, 2010, 712,L93

114. Wootten, A., Boulanger, F., Bogey, M., et al. *Astron Astrophys*, 1986, 166,L15

115. Bogey, M., Demuynck, C., and Destombes, J. L. *Astron Astrophys*, 1984, 138,L11

116. Marcelino, N., Cernicharo, J., Tercero, B., and Roueff, E. *Astrophys J*, 2009, 690, L27

117. Bergman, P., Parise, B., Liseau, R., et al. *Astron Astrophys*, 2011, 531, L8

118. Winnewisser, G., and Churchwell, E. *Astrophys J*, 1975, 200,L33

119. Ohishi, M., Ishikawa, S., Amano, T., et al. *Astrophys J*, 1996, 471,L61

120. Remijan, A. J., Hollis, J. M., Lovas, F. J., et al. *Astrophys J*, 2008, 675, L85

121. Cernicharo, J., Marcelino, N., Roueff, E., et al. *Astrophys J*, 2012, 759, L43

122. Gupta, H., Gottlieb, C. A., Lattanzi, V., Pearson, J. C., and McCarthy, M. C. *Astrophys J*, 2013, 778,L1

123. Rubin, R. H., Swenson, Jr., G. W., Solomon, R. C., Flygare, H. L. *Astrophys J*, 1971, 169,L39

124. Irvine, W. M., Brown, R. D., Craig, D. M., et al. *Astrophys J*, 1988, 335,L89

125. Hollis, J.M., Remijan, A. J., Jewell, P. R., and Lovas, F. J. *Astrophys J*, 2006, 642, 933

126. Gilmore, W., Morris, M., Palmer, P., et al. *Astrophys J*, 1976, 204,43

127. Hollis, J. M., Lovas, F. J., Jewell, P. R. *Astrophys J*, 2000, 540,L107

128. Hollis, J. M., Jewell, P. R., Lovas, F. J., Remijan, A., and Møllendal, H. *Astrophys J*, 2004, 610, L21

129. Remijan, A. J., Snyder, L. E., McGuire, B. A., et al. *Astrophys J*, 2014, 783,77

130. Hollis, J. M., Lovas, F. J., Remijan, A. J., et al. *Astrophys J*, 2006, 643, L25

131. Snyder, L. E., Lovas, F. J., Mehnninger, D. M., et al. *Astrophys J*, 2002, 578,245

132. Hollis, J. M., Lovas, F. J., Jewell, P. R., Coudert, L. H. *Astrophys J*, 2002, 571,L59

133. Belloche, A., Garrod, R. T., Müller, H. S. P., et al. *Astron Astrophys*, 2009, 499,215

134. Tercero, B., Kleiner, I., Cernicharo, J., et al. *Astrophys J*, 2013, 770,L13

135. Fuchs, G. W., U. Fuchs, U., Giesen, T. F., Wyrowski, F. *Astron Astrophys*, 2005, 444, 521

136. Grimme, S. J. *Comput. Chem.*, 2004, 25, 1463

137. Grimme, S. J. *Comput. Chem.*, 2006, 27, 1787

138. Grimme, S. J. *Antony, S. E., Helge, K. J. Chem. Phys.*, 2010,132, 154104

The supporting material for the first part of this chapter on interstellar hydrogen bonding is presented below.

SUPPORTING INFORMATION

Water monomer

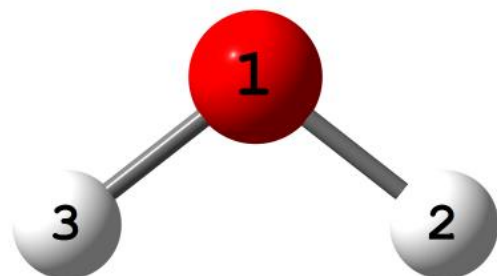


Figure 1 Optimized structure of acetic acid water complex

Table S1.1: Optimized geometry (Å, deg) parameters for water monomer

	Method			
Para met ers	MP2(full) 6- 311++G* *	MP2(full)/a ug-cc- pVDZ	G4	W 1U
H ₂ -	0.959	0.966	0.9	0.9
O ₁			62	61
H ₃ -	0.959	0.966	0.9	0.9
O ₁			62	61
H ₃ -			103	10
O ₁ -	103.5	103.9	.7	4.5
H ₂				
V ₂	1628.6	1623.4	167 1.5	16 39. 4
V ₁	3888.4	3804.2	380 3.5	38 00. 2
V ₃	4006.7	3938.8	390 7.5	39 00. 6

Acetic acid-water complex

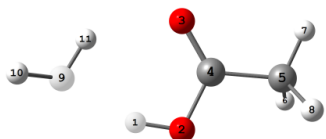


Figure 1 Optimized structure of acetic acid- water complex

Table S2.1: Optimized geometry (Å, deg) parameters for acetic acid-water complex at the MP2(full)/6-311++G** level including vibrational frequencies (cm⁻¹)

R(1-2)	0.981
R(2-4)	1.340
R(3-4)	1.220
R(4-5)	1.502
R(5-6)	1.092
R(5-7)	1.088
R(5-8)	1.092
R(9-10)	0.959
R(9-11)	0.968
A(1-2-4)	107.7
A(2-4-3)	123.7
A(2-4-5)	111.8
A(3-4-5)	124.5
A(4-5-6)	109.3
A(4-5-7)	109.8
A(4-5-8)	109.6
A(6-5-7)	110.1
A(6-5-8)	107.7
A(7-5-8)	110.4
A(10-9-11)	105.7
W1(A)	48.9
W2(A)	85.2
W3(A)	158.7
W4(A)	192.1
W5(A)	264.5
W6(A)	352.4
W7(A)	445.9
W8(A)	563.1
W9(A)	597.9
W10(A)	631.1
W11(A)	892.3
W12(A)	906.2
W13(A)	1034.0
W14(A)	1076.4
W15(A)	1307.1
W16(A)	1406.5
W17(A)	1460.8
W18(A)	1492.4
W19(A)	1494.7

W20(A)	1624.9
W21(A)	1796.6
W22(A)	3106.2
W23(A)	3191.8
W24(A)	3230.7
W25(A)	3529.3
W26(A)	3769.3
W27(A)	3963.6

Table S2.2: Optimized geometry (Å, deg) parameters for acetic acid complex at the MP2(full)/aug-cc-pVDZ level including vibrational frequencies (cm⁻¹)

R(1-2)	0.989
R(2-4)	1.349
R(3-4)	1.231
R(4-5)	1.505
R(5-6)	1.099
R(5-7)	1.095
R(5-8)	1.099
R(9-10)	0.965
R(9-11)	0.978
R(1-9)	1.790
R(3-11)	1.960
A(1-2-4)	107.4
A(2-1-9)	158.2
A(2-4-3)	123.5
A(2-4-5)	112.1
A(3-4-5)	124.5
A(4-3-11)	107.6
A(4-5-6)	109.3
A(4-5-7)	109.7
A(4-5-8)	109.4
A(6-5-7)	110.3
A(6-5-8)	107.6
A(7-5-8)	110.5
A(10-9-11)	105.6
A(10-9-1)	124.9
A(11-9-1)	83.6
A(9-11-3)	139.2
W1(A)	65.1
W2(A)	91.4
W3(A)	170.9
W4(A)	197.4
W5(A)	259.8
W6(A)	365.3
W7(A)	439.7
W8(A)	593.6
W9(A)	611.4

W10(A)	649.3
W11(A)	894.5
W12(A)	913.4
W13(A)	1014.8
W14(A)	1059.6
W15(A)	1293.6
W16(A)	1384.4
W17(A)	1447.8
W18(A)	1468.9
W19(A)	1472.1
W20(A)	1621.6
W21(A)	1762.4
W22(A)	3094.4
W23(A)	3184.4
W24(A)	3226.4
W25(A)	3405.2
W26(A)	3629.5
W27(A)	3886.9

Table S2.3: Optimized geometry (Å, deg) parameters for acetic acid complex at the G4 level including vibrational frequencies (cm⁻¹)

R(1-2)	0.992
R(2-4)	1.332
R(3-4)	1.219
R(4-5)	1.507
R(5-6)	1.094
R(5-7)	1.089
R(5-8)	1.094
R(9-10)	0.963
R(9-11)	0.978
R(1-9)	1.758
R(3-11)	1.920
A(1-2-4)	107.7
A(2-1-9)	158.2
A(2-4-3)	123.7
A(2-4-5)	112.4
A(3-4-5)	123.9
A(4-3-11)	106.6
A(4-5-6)	109.6
A(4-5-7)	109.9
A(4-5-8)	109.9
A(6-5-7)	110.0
A(6-5-8)	107.2
A(7-5-8)	110.2
A(10-9-11)	104.7
A(10-9-1)	111.1
A(11-9-1)	81.8
A(9-11-3)	142.0

Table S2. 4: Optimized geometry (Å, deg) parameters for acetic acid complex at the W1U level including vibrational frequencies (cm-)

R(1-2)	0.989
R(2-4)	1.335
R(3-4)	1.217
R(4-5)	1.502
R(5-6)	1.090
R(5-7)	1.085
R(5-8)	1.090
R(9-10)	0.962
R(9-11)	0.975
R(1-9)	1.779
R(3-11)	1.945
A(1-2-4)	108.2
A(2-1-9)	157.6
A(2-4-3)	123.4
A(2-4-5)	112.6
A(3-4-5)	124.0
A(4-3-11)	107.3
A(4-5-6)	109.5
A(4-5-7)	109.9
A(4-5-8)	109.9
A(6-5-7)	110.0
A(6-5-8)	107.2
A(7-5-8)	110.2
A(10-9-11)	106.0
A(10-9-1)	118.4
A(11-9-1)	82.7
A(9-11-3)	140.7

Glycolaldehyde-water complex

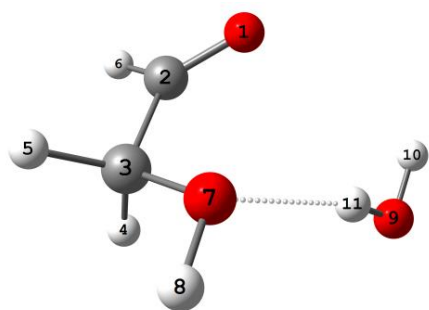


Figure 2: Optimized structure of glycolaldehyde-water complex

Table S3.1: Optimized geometry (Å, deg) parameters for glycolaldehyde-water complex at the MP2(full)/6-311++G** level including vibrational frequencies (cm-)

R(1-2)	1.210
R(2-3)	1.510
R(2-6)	1.109
R(3-4)	1.100
R(3-5)	1.099
R(3-7)	1.411
R(7-8)	0.961
R(9-10)	0.959
R(9-11)	0.965
R(7-11)	1.973
A(1-2-3)	124.6
A(1-2-6)	121.7
A(3-2-6)	113.7
A(2-3-4)	107.0
A(2-3-5)	107.4
A(2-3-7)	109.7
A(4-3-5)	107.8
A(4-3-7)	112.4
A(5-3-7)	112.3
A(3-7-8)	107.9
A(3-7-11)	108.4
A(8-7-11)	115.1
A(10-9-11)	102.5
A(9-11-7)	164.9
W1(A)	25.2
W2(A)	78.3
W3(A)	160.1
W4(A)	181.6
W5(A)	213.5
W6(A)	246.7
W7(A)	275.0
W8(A)	405.4
W9(A)	600.2
W10(A)	731.8
W11(A)	751.7
W12(A)	886.1
W13(A)	1116.9
W14(A)	1150.6
W15(A)	1240.4
W16(A)	1281.9
W17(A)	1427.7
W18(A)	1452.8
W19(A)	1505.1
W20(A)	1675.0
W21(A)	1793.5

W22(A)	2971.1
W23(A)	3044.9
W24(A)	3092.7
W25(A)	3818.7
W26(A)	3899.5
W27(A)	3965.0

Table S3.2: Optimized geometry parameters (\AA , deg) for glycolaldehyde-water complex at the MP2(full)/aug-cc-pVDZ level including vibrational frequencies (cm^{-1})

R(1-2)	1.221
R(2-3)	1.511
R(2-6)	1.116
R(3-4)	1.106
R(3-5)	1.106
R(3-7)	1.424
R(7-8)	0.967
R(9-10)	0.965
R(9-11)	0.972
A(1-2-3)	124.8
A(1-2-6)	121.5
A(3-2-6)	113.8
A(2-3-4)	106.9
A(2-3-5)	107.5
A(2-3-7)	109.7
A(4-3-5)	108.1
A(4-3-7)	112.3
A(5-3-7)	112.1
A(3-7-8)	107.9
A(10-9-11)	103.7
W1(A)	63.5
W2(A)	73.4
W3(A)	138.5
W4(A)	172.8
W5(A)	200.3
W6(A)	244.2
W7(A)	267.6
W8(A)	376.8
W9(A)	599.7
W10(A)	721.6
W11(A)	736.2
W12(A)	882.7
W13(A)	1097.1
W14(A)	1126.1
W15(A)	1225.5
W16(A)	1261.4
W17(A)	1399.3
W18(A)	1435.8
W19(A)	1469.7

W20(A)	1630.2
W21(A)	1762.9
W22(A)	2972.2
W23(A)	3038.9
W24(A)	3092.9
W25(A)	3721.4
W26(A)	3827.9
W27(A)	3897.6

Table S3.3: Optimized geometry (\AA , deg) parameters for glycolaldehyde-water complex at the G4 level including vibrational frequencies (cm^{-1})

R(1-2)	1.201
R(2-3)	1.512
R(2-6)	1.114
R(3-4)	1.102
R(3-5)	1.103
R(3-7)	1.409
R(7-8)	0.962
R(9-10)	0.962
R(9-11)	0.968
A(1-2-3)	125.3
A(1-2-6)	122.0
A(3-2-6)	112.7
A(2-3-4)	106.3
A(2-3-5)	107.5
A(2-3-7)	110.4
A(4-3-5)	107.3
A(4-3-7)	112.7
A(5-3-7)	112.4
A(3-7-8)	108.2
A(10-9-11)	102.6

Table S3.4: Optimized geometry (\AA , deg) parameters for glycolaldehyde-water complex at the W1U level including vibrational frequencies (cm^{-1})

R(1-2)	1.200
R(2-3)	1.507
R(2-6)	1.110
R(3-4)	1.099
R(3-5)	1.099
R(3-7)	1.411
R(7-8)	0.962
R(9-10)	0.961
R(9-11)	0.967
A(1-2-3)	125.4
A(1-2-6)	121.7
A(3-2-6)	113.0
A(2-3-4)	106.5

A(2-3-5)	107.3
A(2-3-7)	110.8
A(4-3-5)	107.3
A(4-3-7)	112.4
A(5-3-7)	112.2
A(3-7-8)	108.8
A(10-9-11)	103.8

A(3-2-10)	151.5
A(6-5-7)	111.2
A(6-5-8)	109.5
A(7-5-8)	111.8
A(10-9-11)	114.0
A(9-10-2)	160.0
W1(A)	11.6
W2(A)	92.9
W3(A)	134.9
W4(A)	153.2
W5(A)	183.3
W6(A)	315.8
W7(A)	322.6
W8(A)	345.1
W9(A)	443.5
W10(A)	784.0
W11(A)	955.3
W12(A)	1047.9
W13(A)	1183.2
W14(A)	1210.5
W15(A)	1279.8
W16(A)	1421.2
W17(A)	1498.0
W18(A)	1511.1
W19(A)	1517.1
W20(A)	1654.3
W21(A)	1775.7
W22(A)	3118.7
W23(A)	3134.3
W24(A)	3218.8
W25(A)	3245.4
W26(A)	3814.0
W27(A)	3975.6

Methyl formate-water complex

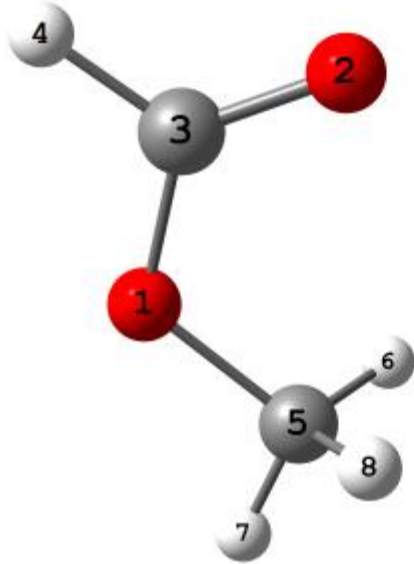


Figure 3: Optimized structure of methyl formate-water complex

Table S4.1: Optimized geometry (Å, deg) parameters for methyl formate-water complex at the MP2(full)/6-311++G** level including vibrational frequencies (cm⁻¹)

R(1-3)	1.323
R(1-5)	1.441
R(2-3)	1.209
R(3-4)	1.097
R(5-6)	1.089
R(5-7)	1.085
R(5-8)	1.089
R(9-10)	0.970
R(9-11)	0.946
R(2-10)	1.200
A(3-1-5)	114.4
A(1-3-2)	123.5
A(1-3-4)	111.5
A(1-5-6)	109.6
A(1-5-7)	105.1
A(1-5-8)	109.7
A(2-3-4)	124.9

Table S4.2: Optimized geometry (Å, deg) parameters for methyl formate-water complex at the MP2(full)/aug-cc-pVDZ level including vibrational frequencies (cm⁻¹)

R(1-3)	1.339
R(1-5)	1.457
R(2-3)	1.222
R(3-4)	1.102
R(5-6)	1.097
R(5-7)	1.094
R(5-8)	1.097
R(9-10)	0.972
R(9-11)	0.964
R(2-10)	1.945
A(3-1-5)	114.6
A(1-3-2)	126.2

A(1-3-4)	109.7
A(1-5-6)	110.1
A(1-5-7)	104.8
A(1-5-8)	110.1
A(2-3-4)	124.1
A(3-2-10)	134.6
A(6-5-7)	111.1
A(6-5-8)	109.6
A(7-5-8)	111.1
A(10-9-11)	104.4
A(9-10-2)	168.2
W1(A)	39.2
W2(A)	98.4
W3(A)	155.6
W4(A)	159.8
W5(A)	203.6
W6(A)	309.9
W7(A)	342.2
W8(A)	349.0
W9(A)	537.1
W10(A)	765.9
W11(A)	926.7
W12(A)	1038.6
W13(A)	1164.8
W14(A)	1186.1
W15(A)	1249.0
W16(A)	1392.0
W17(A)	1456.0
W18(A)	1488.6
W19(A)	1491.3
W20(A)	1647.3
W21(A)	1738.0
W22(A)	3106.5
W23(A)	3143.0
W24(A)	3213.6
W25(A)	3242.9
W26(A)	3708.8
W27(A)	3905.3

R(5-8)	1.092
R(9-10)	0.962
R(9-11)	0.969
A(3-1-5)	115.7
A(1-3-2)	125.3
A(1-3-4)	110.5
A(1-5-6)	110.4
A(1-5-7)	105.7
A(1-5-8)	110.4
A(2-3-4)	124.1
A(6-5-7)	110.7
A(6-5-8)	109.0
A(7-5-8)	110.7
A(10-9-11)	103.7

Table S4.4: Optimized geometry (Å, deg) parameters for methyl formate-water complex at the W1U level including vibrational frequencies (cm⁻¹)

R(1-3)	1.330
R(1-5)	1.443
R(2-3)	1.207
R(3-4)	1.095
R(5-6)	1.088
R(5-7)	1.085
R(5-8)	1.088
R(9-10)	0.961
R(9-11)	0.969
A(3-1-5)	116.2
A(1-3-2)	125.4
A(1-3-4)	110.5
A(1-5-6)	110.3
A(1-5-7)	105.5
A(1-5-8)	110.3
A(2-3-4)	124.1
A(6-5-7)	110.7
A(6-5-8)	109.3
A(7-5-8)	110.7
A(10-9-11)	104.6

Table S4.3: Optimized geometry (Å, deg) parameters for methyl formate-water complex at the G4 level including vibrational frequencies (cm⁻¹)

R(1-3)	1.331
R(1-5)	1.439
R(2-3)	1.208
R(3-4)	1.097
R(5-6)	1.092
R(5-7)	1.089

Ethanol-water complex

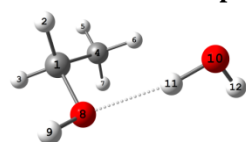


Figure 4: Optimized structure of ethanol-water complex

Table S5.1: Optimized geometry (Å, deg) parameters for ethanol-water complex at the MP2(full)/6-311++G** level including vibrational frequencies (cm⁻¹)

R(1-2)	1.096
R(1-3)	1.096
R(1-4)	1.513
R(1-8)	1.436
R(4-5)	1.093
R(4-6)	1.092
R(4-7)	1.092
R(8-9)	0.961
R(10-11)	0.968
R(10-12)	0.958
R(8-11)	1.898
A(2-1-3)	108.6
A(2-1-4)	110.4
A(2-1-8)	109.9
A(3-1-4)	110.6
A(3-1-8)	109.7
A(4-1-8)	107.7
A(1-4-5)	110.0
A(1-4-6)	110.4
A(1-4-7)	110.2
A(1-8-9)	108.0
A(1-8-11)	112.7
A(5-4-6)	108.8
A(5-4-7)	108.6
A(6-4-7)	108.9
A(9-8-11)	115.7
A(11-10-12)	103.7
A(10-11-8)	172.7
W1(A)	46.1
W2(A)	55.5
W3(A)	120.2
W4(A)	184.2
W5(A)	265.6
W6(A)	305.3
W7(A)	389.4
W8(A)	424.9
W9(A)	692.2
W10(A)	835.1
W11(A)	916.4
W12(A)	1076.0
W13(A)	1114.6
W14(A)	1202.1
W15(A)	1291.2
W16(A)	1328.2
W17(A)	1419.4
W18(A)	1474.6

W19(A)	1505.1
W20(A)	1525.2
W21(A)	1545.4
W22(A)	1670.6
W23(A)	3071.5
W24(A)	3090.4
W25(A)	3121.6
W26(A)	3182.8
W27(A)	3193.2
W28(A)	3758.6
W29(A)	3891.3
W30(A)	3969.4

Table S5.2: Optimized geometry (Å, deg) parameters for ethanol-water complex at the MP2(full)/aug-cc-pVDZ level including vibrational frequencies (cm⁻¹)

R(1-2)	1.103
R(1-3)	1.102
R(1-4)	1.517
R(1-8)	1.450
R(4-5)	1.100
R(4-6)	1.099
R(4-7)	1.099
R(8-9)	0.967
R(10-11)	0.975
R(10-12)	0.964
R(8-11)	1.894
A(2-1-3)	108.8
A(2-1-4)	110.6
A(2-1-8)	109.7
A(3-1-4)	110.9
A(3-1-8)	109.5
A(4-1-8)	107.3
A(1-4-5)	109.8
A(1-4-6)	110.2
A(1-4-7)	110.3
A(1-8-9)	108.0
A(1-8-11)	100.5
A(5-4-6)	108.6
A(5-4-7)	108.7
A(6-4-7)	109.1
A(9-8-11)	106.1
A(11-10-12)	104.6
A(10-11-8)	161.8
W1(A)	53.6
W2(A)	62.1
W3(A)	127.2
W4(A)	188.8
W5(A)	262.5

W6(A)	325.5
W7(A)	392.2
W8(A)	414.8
W9(A)	673.1
W10(A)	819.4
W11(A)	895.0
W12(A)	1061.0
W13(A)	1084.2
W14(A)	1176.2
W15(A)	1271.3
W16(A)	1300.6
W17(A)	1386.2
W18(A)	1442.7
W19(A)	1479.6
W20(A)	1495.8
W21(A)	1518.9
W22(A)	1651.3
W23(A)	3065.3
W24(A)	3079.4
W25(A)	3121.1
W26(A)	3176.2
W27(A)	3186.4
W28(A)	3642.8
W29(A)	3817.8
W30(A)	3898.5

Table S5.3: Optimized geometry (Å, deg) parameters for ethanol-water complex at the G4level including vibrational frequencies (cm⁻¹)

R(1-2)	1.099
R(1-3)	1.100
R(1-4)	1.519
R(1-8)	1.434
R(4-5)	1.094
R(4-6)	1.093
R(4-7)	1.094
R(8-9)	0.962
R(10-11)	0.971
R(10-12)	0.962
R(8-11)	1.925
A(2-1-3)	107.8
A(2-1-4)	110.2
A(2-1-8)	110.4
A(3-1-4)	110.8
A(3-1-8)	109.8
A(4-1-8)	107.9
A(1-4-5)	110.3
A(1-4-6)	109.5
A(1-4-7)	110.5
A(1-8-9)	108.4

A(1-8-11)	106.9
A(5-4-6)	109.1
A(5-4-7)	108.5
A(6-4-7)	108.8
A(9-8-11)	112.0
A(11-10-12)	103.6
A(10-11-8)	166.4

Table S5.4: Optimized geometry (Å, deg) parameters for ethanol-water complex at the W1U level including vibrational frequencies (cm⁻¹)

R(1-2)	1.094
R(1-3)	1.094
R(1-4)	1.514
R(1-8)	1.438
R(4-5)	1.091
R(4-6)	1.090
R(4-7)	1.090
R(8-9)	0.962
R(10-11)	0.970
R(10-12)	0.961
R(8-11)	1.925
A(2-1-3)	108.1
A(2-1-4)	110.4
A(2-1-8)	110.0
A(3-1-4)	110.7
A(3-1-8)	109.6
A(4-1-8)	108.1
A(1-4-5)	110.2
A(1-4-6)	110.3
A(1-4-7)	110.6
A(1-8-9)	109.0
A(1-8-11)	110.4
A(5-4-6)	108.7
A(5-4-7)	108.4
A(6-4-7)	108.7
A(9-8-11)	112.5
A(11-10-12)	104.5
A(10-11-8)	171.1

Dimethyl ether-water complex

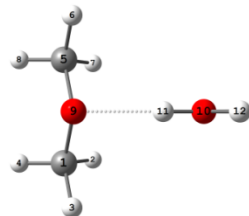


Figure 5: Optimized structure of dimethyl ether-water complex

Table S6.1: Optimized geometry (Å, deg) parameters for ethanol-water complex at the MP2(full)/6-311++G** level including vibrational frequencies (cm⁻¹)

R(1-2)	1.097
R(1-3)	1.090
R(1-4)	1.097
R(1-9)	1.417
R(5-6)	1.090
R(5-7)	1.097
R(5-8)	1.097
R(5-9)	1.417
R(10-11)	0.969
R(10-12)	0.958
R(9-11)	1.861
A(2-1-3)	109.3
A(2-1-4)	109.2
A(2-1-9)	110.8
A(3-1-4)	109.4
A(3-1-9)	107.3
A(4-1-9)	110.7
A(1-9-5)	111.3
A(1-9-11)	112.9
A(6-5-7)	109.3
A(6-5-8)	109.4
A(6-5-9)	107.3
A(7-5-8)	109.2
A(7-5-9)	110.9
A(8-5-9)	110.7
A(5-9-11)	112.6
A(11-10-12)	103.7
A(10-11-9)	172.6
W1(A)	43.4
W2(A)	45.2
W3(A)	125.7
W4(A)	170.7
W5(A)	191.8
W6(A)	266.8
W7(A)	374.9
W8(A)	425.9
W9(A)	696.5
W10(A)	958.7
W11(A)	1137.0
W12(A)	1184.0
W13(A)	1219.0
W14(A)	1219.4
W15(A)	1289.6
W16(A)	1483.7

W17(A)	1503.4
W18(A)	1508.9
W19(A)	1514.0
W20(A)	1519.5
W21(A)	1537.9
W22(A)	1669.2
W23(A)	3045.3
W24(A)	3050.7
W25(A)	3119.2
W26(A)	3124.7
W27(A)	3198.9
W28(A)	3199.4
W29(A)	3731.9
W30(A)	3967.6

Table S6.2: Optimized geometry (Å, deg) parameters for ethanol-water complex at the MP2(full)/aug-cc-pVDZ level including vibrational frequencies (cm⁻¹)

R(1-2)	1.104
R(1-3)	1.097
R(1-4)	1.103
R(1-9)	1.431
R(5-6)	1.097
R(5-7)	1.104
R(5-8)	1.103
R(5-9)	1.431
R(10-11)	0.976
R(10-12)	0.964
R(9-11)	1.866
A(2-1-3)	109.5
A(2-1-4)	109.4
A(2-1-9)	110.7
A(3-1-4)	109.6
A(3-1-9)	107.0
A(4-1-9)	110.5
A(1-9-5)	110.6
A(1-9-11)	102.3
A(6-5-7)	109.5
A(6-5-8)	109.6
A(6-5-9)	107.0
A(7-5-8)	109.4
A(7-5-9)	110.7
A(8-5-9)	110.5
A(5-9-11)	102.3
A(11-10-12)	104.7
A(10-11-9)	160.1
W1(A)	37.3
W2(A)	71.7
W3(A)	111.3

W4(A)	181.1
W5(A)	189.3
W6(A)	275.7
W7(A)	393.0
W8(A)	423.0
W9(A)	672.8
W10(A)	926.5
W11(A)	1103.4
W12(A)	1158.1
W13(A)	1179.3
W14(A)	1191.2
W15(A)	1261.8
W16(A)	1442.7
W17(A)	1473.8
W18(A)	1476.6
W19(A)	1490.5
W20(A)	1491.4
W21(A)	1504.9
W22(A)	1647.3
W23(A)	3038.2
W24(A)	3042.3
W25(A)	3118.4
W26(A)	3124.3
W27(A)	3195.0
W28(A)	3196.2
W29(A)	3625.3
W30(A)	3897.4

Table S6.3: Optimized geometry (\AA , deg) parameters for ethanol-water complex at the G4 level including vibrational frequencies (cm^{-1})

R(1-2)	1.101
R(1-3)	1.092
R(1-4)	1.100
R(1-9)	1.410
R(5-6)	1.091
R(5-7)	1.100
R(5-8)	1.100
R(5-9)	1.415
R(10-11)	0.969
R(10-12)	0.962
R(9-11)	1.939
A(2-1-3)	109.0
A(2-1-4)	108.4
A(2-1-9)	111.5
A(3-1-4)	109.0
A(3-1-9)	107.5
A(4-1-9)	111.4
A(1-9-5)	113.3
A(1-9-11)	137.7

A(6-5-7)	109.1
A(6-5-8)	110.0
A(6-5-9)	106.5
A(7-5-8)	108.5
A(7-5-9)	111.4
A(8-5-9)	111.2
A(5-9-11)	102.0
A(11-10-12)	103.5
A(10-11-9)	153.9

Table S6.4: Optimized geometry (\AA , deg) parameters for ethanol-water complex at the W1U level including vibrational frequencies (cm^{-1})

R(1-2)	1.095
R(1-3)	1.088
R(1-4)	1.095
R(1-9)	1.416
R(5-6)	1.088
R(5-7)	1.095
R(5-8)	1.095
R(5-9)	1.416
R(10-11)	0.970
R(10-12)	0.961
R(9-11)	1.902
A(2-1-3)	109.1
A(2-1-4)	108.8
A(2-1-9)	111.3
A(3-1-4)	109.3
A(3-1-9)	107.2
A(4-1-9)	111.0
A(1-9-5)	113.3
A(1-9-11)	116.7
A(6-5-7)	109.1
A(6-5-8)	109.3
A(6-5-9)	107.2
A(7-5-8)	108.8
A(7-5-9)	111.3
A(8-5-9)	111.0
A(5-9-11)	116.4
A(11-10-12)	104.5
A(10-11-9)	178.7

Propanoic acid-water complex

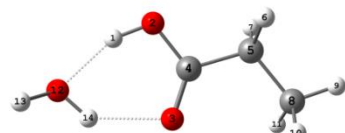


Figure 6: Optimized structure of propanoic acid-water complex

Table S7.1 Optimized geometry (Å, deg) parameters for propanoic acid-water complex at the MP2(full)/6-311++G** level including vibrational frequencies (cm⁻¹)

R(1-2)	0.981
R(2-4)	1.340
R(3-4)	1.220
R(4-5)	1.507
R(5-6)	1.095
R(5-7)	1.095
R(5-8)	1.522
R(8-9)	1.092
R(8-10)	1.092
R(8-11)	1.091
R(12-13)	0.959
R(12-14)	0.968
R(1-12)	1.807
A(1-2-4)	107.6
A(2-1-12)	158.2
A(2-4-3)	123.8
A(2-4-5)	111.9
A(3-4-5)	124.4
A(4-5-6)	107.3
A(4-5-7)	107.0
A(4-5-8)	112.9
A(6-5-7)	105.9
A(6-5-8)	111.7
A(7-5-8)	111.5
A(5-8-9)	110.2
A(5-8-10)	110.9
A(5-8-11)	110.8
A(9-8-10)	108.6
A(9-8-11)	108.6
A(10-8-11)	107.7
A(13-12-14)	105.7
A(13-12-1)	132.8
A(14-12-1)	87.9
W1(A)	28.9
W2(A)	68.8
W3(A)	131.8
W4(A)	186.5
W5(A)	228.3
W6(A)	259.4
W7(A)	277.3
W8(A)	351.1
W9(A)	492.6
W10(A)	564.1
W11(A)	567.5

W12(A)	645.4
W13(A)	819.6
W14(A)	857.5
W15(A)	885.7
W16(A)	1035.0
W17(A)	1120.5
W18(A)	1121.5
W19(A)	1245.9
W20(A)	1296.0
W21(A)	1390.2
W22(A)	1434.5
W23(A)	1462.3
W24(A)	1477.4
W25(A)	1513.4
W26(A)	1520.1
W27(A)	1623.5
W28(A)	1791.0
W29(A)	3095.3
W30(A)	3099.6
W31(A)	3145.5
W32(A)	3184.6
W33(A)	3191.2
W34(A)	3531.4
W35(A)	3766.8
W36(A)	3963.1

Table S7.2 Optimized geometry (Å, deg) parameters for propanoic acid-water complex at the MP2(full)/aug-cc-pVDZ level including vibrational frequencies (cm⁻¹)

R(1-2)	0.989
R(2-4)	1.349
R(3-4)	1.232
R(4-5)	1.510
R(5-6)	1.101
R(5-7)	1.102
R(5-8)	1.527
R(8-9)	1.099
R(8-10)	1.099
R(8-11)	1.098
R(12-13)	0.965
R(12-14)	0.978
R(1-12)	1.793
R(3-14)	1.957
A(1-2-4)	107.4
A(2-1-12)	158.1
A(2-4-3)	123.5
A(2-4-5)	112.1
A(3-4-5)	124.4
A(4-3-14)	107.5

A(4-5-6)	107.1
A(4-5-7)	107.0
A(4-5-8)	112.9
A(6-5-7)	105.9
A(6-5-8)	111.8
A(7-5-8)	111.7
A(5-8-9)	110.2
A(5-8-10)	110.9
A(5-8-11)	110.8
A(9-8-10)	108.5
A(9-8-11)	108.6
A(10-8-11)	107.7
A(13-12-14)	105.6
A(13-12-1)	124.6
A(14-12-1)	83.4
A(12-14-3)	139.6
W1(A)	45.8
W2(A)	74.1
W3(A)	138.9
W4(A)	192.8
W5(A)	221.3
W6(A)	257.1
W7(A)	284.2
W8(A)	366.0
W9(A)	488.0
W10(A)	564.8
W11(A)	627.3
W12(A)	650.4
W13(A)	804.7
W14(A)	847.4
W15(A)	908.9
W16(A)	1020.2
W17(A)	1103.5
W18(A)	1107.9
W19(A)	1227.2
W20(A)	1278.5
W21(A)	1375.9
W22(A)	1405.1
W23(A)	1446.1
W24(A)	1460.1
W25(A)	1488.1
W26(A)	1494.0
W27(A)	1622.1
W28(A)	1756.8
W29(A)	3085.3
W30(A)	3087.8
W31(A)	3137.3
W32(A)	3179.3
W33(A)	3184.5
W34(A)	3406.5

W35(A)	3626.8
W36(A)	3887.0

Table S7.3 Optimized geometry (Å, deg) parameters for propanoic acid-water complex at the G4 level including vibrational frequencies (cm⁻¹)

R(1-2)	0.992
R(2-4)	1.333
R(3-4)	1.219
R(4-5)	1.513
R(5-6)	1.097
R(5-7)	1.097
R(5-8)	1.526
R(8-9)	1.093
R(8-10)	1.093
R(8-11)	1.093
R(12-13)	0.963
R(12-14)	0.978
R(1-12)	1.762
R(3-14)	1.921
A(1-2-4)	107.7
A(2-1-12)	158.2
A(2-4-3)	123.6
A(2-4-5)	112.4
A(3-4-5)	124.0
A(4-3-14)	106.6
A(4-5-6)	107.4
A(4-5-7)	107.2
A(4-5-8)	113.4
A(6-5-7)	105.2
A(6-5-8)	111.7
A(7-5-8)	111.6
A(5-8-9)	110.4
A(5-8-10)	111.0
A(5-8-11)	111.0
A(9-8-10)	108.4
A(9-8-11)	108.5
A(10-8-11)	107.4
A(13-12-14)	104.7
A(13-12-1)	110.9
A(14-12-1)	81.8
A(12-14-3)	142.0

Table S7.4 Optimized geometry (Å, deg) parameters for propanoic acid-water complex at the W1U level including vibrational frequencies (cm⁻¹)

R(1-2)	0.989
R(2-4)	1.335
R(3-4)	1.217
R(4-5)	1.509
R(5-6)	1.093

R(5-7)	1.093
R(5-8)	1.523
R(8-9)	1.090
R(8-10)	1.089
R(8-11)	1.089
R(12-13)	0.962
R(12-14)	0.975
R(1-12)	1.783
R(3-14)	1.945
A(1-2-4)	108.3
A(2-1-12)	157.6
A(2-4-3)	123.3
A(2-4-5)	112.4
A(3-4-5)	124.3
A(4-3-14)	107.4
A(4-5-6)	107.2
A(4-5-7)	107.1
A(4-5-8)	113.8
A(6-5-7)	105.3
A(6-5-8)	111.6
A(7-5-8)	111.5
A(5-8-9)	110.3
A(5-8-10)	111.1
A(5-8-11)	111.1
A(9-8-10)	108.3
A(9-8-11)	108.4
A(10-8-11)	107.4
A(13-12-14)	105.9
A(13-12-1)	118.3
A(14-12-1)	82.6
A(12-14-3)	140.8

R(2-5)	1.448
R(2-8)	1.091
R(2-10)	1.090
R(3-6)	1.093
R(3-7)	1.092
R(3-11)	1.091
R(12-13)	0.958
R(12-14)	0.966
A(4-1-5)	125.7
A(4-1-9)	124.2
A(5-1-9)	110.1
A(1-5-2)	115.7
A(3-2-5)	111.0
A(3-2-8)	111.5
A(3-2-10)	111.6
A(2-3-6)	109.5
A(2-3-7)	110.3
A(2-3-11)	110.8
A(5-2-8)	108.8
A(5-2-10)	104.0
A(8-2-10)	109.6
A(6-3-7)	108.5
A(6-3-11)	108.4
A(7-3-11)	109.2
A(13-12-14)	104.2
W1(A)	29.3
W2(A)	50.0
W3(A)	102.6
W4(A)	122.3
W5(A)	147.1
W6(A)	236.9
W7(A)	270.2
W8(A)	325.3
W9(A)	350.7
W10(A)	471.5
W11(A)	503.5
W12(A)	764.4
W13(A)	833.3
W14(A)	870.2
W15(A)	1043.5
W16(A)	1068.5
W17(A)	1140.0
W18(A)	1201.6
W19(A)	1252.3
W20(A)	1354.4
W21(A)	1410.6
W22(A)	1426.4
W23(A)	1443.5
W24(A)	1505.4
W25(A)	1514.1

Ethyl formate-water complex

Figure 7: Optimized structure of ethyl formate-water complex

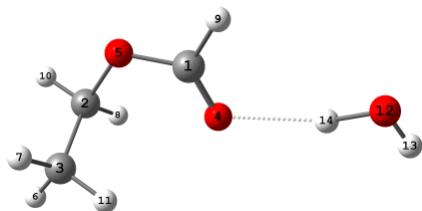


Table S8.1 Optimized geometry (Å, deg) parameters for ethyl formate-water complex at the MP2(full)/6-311++G** level including vibrational frequencies (cm⁻¹)

R(1-4)	1.214
R(1-5)	1.333
R(1-9)	1.096
R(2-3)	1.515

W26(A)	1525.1
W27(A)	1646.6
W28(A)	1762.5
W29(A)	3092.2
W30(A)	3131.3
W31(A)	3142.1
W32(A)	3181.1
W33(A)	3189.7
W34(A)	3209.2
W35(A)	3796.4
W36(A)	3976.0

Table S8.2 Optimized geometry (Å, deg) parameters for ethyl formate-water complex at the MP2(full)/aug-cc-pVDZ level including vibrational frequencies (cm⁻¹)

R(1-4)	1.224
R(1-5)	1.342
R(1-9)	1.102
R(2-3)	1.519
R(2-5)	1.461
R(2-8)	1.098
R(2-10)	1.097
R(3-6)	1.101
R(3-7)	1.099
R(3-11)	1.098
R(12-13)	0.964
R(12-14)	0.973
R(4-14)	1.964
A(4-1-5)	125.6
A(4-1-9)	124.1
A(1-4-14)	99.6
A(5-1-9)	110.3
A(1-5-2)	115.2
A(3-2-5)	110.8
A(3-2-8)	111.8
A(3-2-10)	111.9
A(2-3-6)	109.3
A(2-3-7)	110.5
A(2-3-11)	110.7
A(5-2-8)	108.6
A(5-2-10)	103.7
A(8-2-10)	109.8
A(6-3-7)	108.5
A(6-3-11)	108.4
A(7-3-11)	109.3
A(13-12-14)	104.8
A(12-14-4)	150.7
W1(A)	30.7

W2(A)	58.5
W3(A)	101.5
W4(A)	117.5
W5(A)	154.1
W6(A)	231.5
W7(A)	266.6
W8(A)	345.8
W9(A)	382.0
W10(A)	464.7
W11(A)	534.8
W12(A)	748.6
W13(A)	816.3
W14(A)	849.9
W15(A)	1027.5
W16(A)	1045.4
W17(A)	1124.9
W18(A)	1178.2
W19(A)	1223.5
W20(A)	1323.9
W21(A)	1378.7
W22(A)	1399.5
W23(A)	1410.2
W24(A)	1480.5
W25(A)	1489.2
W26(A)	1498.3
W27(A)	1645.7
W28(A)	1728.0
W29(A)	3079.8
W30(A)	3121.8
W31(A)	3147.2
W32(A)	3173.5
W33(A)	3183.0
W34(A)	3201.9
W35(A)	3692.5
W36(A)	3909.9

Table S8.3 Optimized geometry (Å, deg) parameters for ethyl formate-water complex at the G4 level including vibrational frequencies (cm⁻¹)

R(1-4)	1.209
R(1-5)	1.330
R(1-9)	1.098
R(2-3)	1.520
R(2-5)	1.450
R(2-8)	1.092
R(2-10)	1.092
R(3-6)	1.095
R(3-7)	1.094
R(3-11)	1.092
R(12-13)	0.962

R(12-14)	0.969
A(4-1-5)	125.9
A(4-1-9)	123.7
A(5-1-9)	110.4
A(1-5-2)	116.9
A(3-2-5)	111.3
A(3-2-8)	111.4
A(3-2-10)	111.6
A(2-3-6)	109.6
A(2-3-7)	110.8
A(2-3-11)	110.7
A(5-2-8)	108.6
A(5-2-10)	104.2
A(8-2-10)	109.5
A(6-3-7)	108.3
A(6-3-11)	108.3
A(7-3-11)	109.0
A(13-12-14)	103.7

Table S8.4 Optimized geometry (Å, deg) parameters for ethyl formate-water complex at the W1U level including vibrational frequencies (cm⁻¹)

R(1-4)	1.208
R(1-5)	1.329
R(1-9)	1.095
R(2-3)	1.515
R(2-5)	1.455
R(2-8)	1.088
R(2-10)	1.087
R(3-6)	1.091
R(3-7)	1.090
R(3-11)	1.089
R(12-13)	0.961
R(12-14)	0.969
A(4-1-5)	126.0
A(4-1-9)	123.6
A(5-1-9)	110.3
A(1-5-2)	117.5
A(3-2-5)	111.2
A(3-2-8)	111.6
A(3-2-10)	111.6
A(2-3-6)	109.5
A(2-3-7)	110.9
A(2-3-11)	111.0
A(5-2-8)	108.6
A(5-2-10)	104.0
A(8-2-10)	109.5
A(6-3-7)	108.3
A(6-3-11)	108.2
A(7-3-11)	108.9

A(13-12-14)	104.6
-------------	-------

Methyl Acetate-water complex

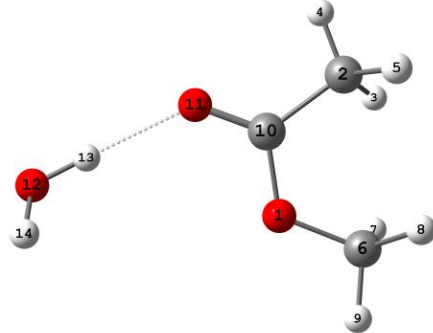


Figure 8: Optimized structure of methyl acetate-water complex

Table S9.1 Optimized geometry (Å, deg) parameters for methyl acetate-water complex at the MP2(full)/6-311++G** level including vibrational frequencies (cm⁻¹)

R(1-6)	1.433
R(1-10)	1.365
R(2-3)	1.093
R(2-4)	1.088
R(2-5)	1.092
R(2-10)	1.509
R(6-7)	1.091
R(6-8)	1.092
R(6-9)	1.089
R(10-11)	1.206
R(12-13)	0.965
R(12-14)	0.959
R(1-13)	1.962
A(6-1-10)	120.7
A(1-6-7)	111.3
A(1-6-8)	110.9
A(1-6-9)	105.1
A(6-1-13)	107.5
A(1-10-2)	117.4
A(1-10-11)	118.3
A(10-1-13)	126.6
A(3-2-4)	109.2
A(3-2-5)	108.0
A(3-2-10)	110.3
A(4-2-5)	109.8
A(4-2-10)	108.0
A(5-2-10)	111.6
A(2-10-11)	124.3

A(7-6-8)	110.4
A(7-6-9)	109.3
A(8-6-9)	109.7
A(13-12-14)	103.8
A(12-13-1)	150.1
W1(A)	23.8
W2(A)	38.9
W3(A)	95.6
W4(A)	130.1
W5(A)	140.0
W6(A)	161.1
W7(A)	231.5
W8(A)	312.6
W9(A)	335.1
W10(A)	486.2
W11(A)	497.8
W12(A)	570.2
W13(A)	584.1
W14(A)	807.2
W15(A)	1017.7
W16(A)	1061.3
W17(A)	1118.7
W18(A)	1189.0
W19(A)	1207.5
W20(A)	1281.8
W21(A)	1413.4
W22(A)	1485.2
W23(A)	1499.5
W24(A)	1509.0
W25(A)	1523.2
W26(A)	1527.9
W27(A)	1653.7
W28(A)	1819.0
W29(A)	3092.0
W30(A)	3101.2
W31(A)	3183.9
W32(A)	3188.5
W33(A)	3220.6
W34(A)	3226.3
W35(A)	3816.5
W36(A)	3974.4

Table S9.2 Optimized geometry (Å, deg) parameters for methyl acetate-water complex at the MP2(full)/aug-cc-pVDZ level including vibrational frequencies (cm⁻¹)

R(1-6)	1.442
R(1-10)	1.365
R(2-3)	1.099
R(2-4)	1.094

R(2-5)	1.099
R(2-10)	1.510
R(6-7)	1.099
R(6-8)	1.099
R(6-9)	1.095
R(10-11)	1.221
R(12-13)	0.973
R(12-14)	0.965
R(11-13)	1.981
A(6-1-10)	119.4
A(1-6-7)	111.2
A(1-6-8)	111.2
A(1-6-9)	105.1
A(1-10-2)	118.3
A(1-10-11)	118.2
A(3-2-4)	109.6
A(3-2-5)	108.0
A(3-2-10)	110.9
A(4-2-5)	109.5
A(4-2-10)	108.0
A(5-2-10)	110.8
A(2-10-11)	123.5
A(7-6-8)	110.3
A(7-6-9)	109.4
A(8-6-9)	109.4
A(10-11-13)	116.5
A(13-12-14)	103.0
A(12-13-11)	175.8
W1(A)	12.0
W2(A)	32.9
W3(A)	57.2
W4(A)	109.8
W5(A)	143.7
W6(A)	149.6
W7(A)	247.2
W8(A)	280.1
W9(A)	333.6
W10(A)	484.3
W11(A)	533.4
W12(A)	577.9
W13(A)	581.6
W14(A)	804.1
W15(A)	1004.8
W16(A)	1046.8
W17(A)	1095.1
W18(A)	1163.7
W19(A)	1184.7
W20(A)	1274.2
W21(A)	1389.6
W22(A)	1453.9

W23(A)	1470.5
W24(A)	1474.7
W25(A)	1495.3
W26(A)	1507.6
W27(A)	1650.0
W28(A)	1771.6
W29(A)	3081.5
W30(A)	3087.9
W31(A)	3173.9
W32(A)	3181.1
W33(A)	3220.0
W34(A)	3223.5
W35(A)	3711.6
W36(A)	3901.0

Table S9.3 Optimized geometry (Å, deg) parameters for methyl acetate-water complex at the G4 level including vibrational frequencies (cm⁻¹)

R(1-6)	1.432
R(1-10)	1.362
R(2-3)	1.094
R(2-4)	1.089
R(2-5)	1.094
R(2-10)	1.514
R(6-7)	1.094
R(6-8)	1.095
R(6-9)	1.090
R(10-11)	1.199
R(12-13)	0.966
R(12-14)	0.962
A(6-1-10)	122.3
A(1-6-7)	111.5
A(1-6-8)	111.4
A(1-6-9)	104.6
A(1-10-2)	117.4
A(1-10-11)	118.4
A(3-2-4)	109.4
A(3-2-5)	107.4
A(3-2-10)	111.2
A(4-2-5)	109.5
A(4-2-10)	108.1
A(5-2-10)	111.3
A(2-10-11)	124.2
A(7-6-8)	109.7
A(7-6-9)	109.7
A(8-6-9)	109.9
A(13-12-14)	103.7

Table S9.4 Optimized geometry (Å, deg) parameters for methyl acetate-water complex at the W1U level including vibrational frequencies (cm⁻¹)

R(1-6)	1.431
R(1-10)	1.353
R(2-3)	1.090
R(2-4)	1.085
R(2-5)	1.091
R(2-10)	1.508
R(6-7)	1.090
R(6-8)	1.090
R(6-9)	1.086
R(10-11)	1.204
R(12-13)	0.968
R(12-14)	0.961
A(6-1-10)	121.5
A(1-6-7)	111.5
A(1-6-8)	111.5
A(1-6-9)	105.6
A(1-10-2)	118.4
A(1-10-11)	118.5
A(3-2-4)	109.4
A(3-2-5)	107.5
A(3-2-10)	111.1
A(4-2-5)	109.4
A(4-2-10)	108.3
A(5-2-10)	111.1
A(2-10-11)	123.2
A(7-6-8)	109.9
A(7-6-9)	109.2
A(8-6-9)	109.2
A(13-12-14)	103.5

Propan-2-ol-water complex

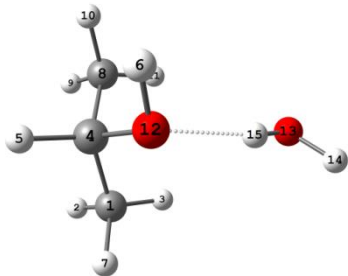


Figure 9: Optimized structure of propan-2-ol-water complex

Table S10.1 Optimized geometry (Å, deg) parameters for propan-2-ol -water complex at the MP2(full)/6-311++G** level including vibrational frequencies (cm⁻¹)

R(1-2)	1.093
R(1-3)	1.094
R(1-4)	1.516
R(1-7)	1.092
R(4-5)	1.098
R(4-8)	1.519
R(4-12)	1.440
R(6-12)	0.962
R(8-9)	1.094
R(8-10)	1.095
R(8-11)	1.093
R(13-14)	0.968
R(13-15)	0.958
R(12-14)	1.896
A(2-1-3)	108.8
A(2-1-4)	110.0
A(2-1-7)	108.8
A(3-1-4)	109.8
A(3-1-7)	108.9
A(4-1-7)	110.6
A(1-4-5)	109.3
A(1-4-8)	112.6
A(1-4-12)	106.4
A(5-4-8)	109.6
A(5-4-12)	108.6
A(8-4-12)	110.3
A(4-8-9)	110.4
A(4-8-10)	111.2
A(4-8-11)	109.9
A(4-12-6)	107.6
A(4-12-14)	112.1
A(6-12-14)	116.2
A(9-8-10)	107.8
A(9-8-11)	108.9
A(10-8-11)	108.6
A(14-13-15)	103.7
A(13-14-12)	171.2

W1(A)	27.0
W2(A)	47.4
W3(A)	115.6
W4(A)	166.6
W5(A)	230.7
W6(A)	282.3
W7(A)	324.6
W8(A)	366.6
W9(A)	375.2
W10(A)	432.1
W11(A)	489.1
W12(A)	673.7
W13(A)	842.9
W14(A)	947.7
W15(A)	968.5
W16(A)	991.7
W17(A)	1121.1
W18(A)	1172.8
W19(A)	1213.2
W20(A)	1299.5
W21(A)	1394.3
W22(A)	1408.4
W23(A)	1430.9
W24(A)	1448.9
W25(A)	1502.6
W26(A)	1504.2
W27(A)	1515.7
W28(A)	1529.8
W29(A)	1667.0
W30(A)	3066.7
W31(A)	3071.5
W32(A)	3083.2
W33(A)	3159.1
W34(A)	3172.9
W35(A)	3179.0
W36(A)	3188.4
W37(A)	3750.7
W38(A)	3872.8
W39(A)	3968.4

Table S10.2 Optimized geometry (Å, deg) parameters for propan-2-ol -water complex at the MP2(full)/aug-cc-pVDZ level including vibrational frequencies (cm⁻¹)

R(1-2)	1.100
R(1-3)	1.100
R(1-4)	1.521
R(1-7)	1.099
R(4-5)	1.105
R(4-8)	1.525

R(4-12)	1.455
R(6-12)	0.968
R(8-9)	1.101
R(8-10)	1.102
R(8-11)	1.100
R(13-14)	0.964
R(13-15)	0.976
R(12-15)	1.891
A(2-1-3)	108.8
A(2-1-4)	110.0
A(2-1-7)	108.6
A(3-1-4)	110.0
A(3-1-7)	109.0
A(4-1-7)	110.5
A(1-4-5)	109.6
A(1-4-8)	112.6
A(1-4-12)	105.9
A(5-4-8)	109.9
A(5-4-12)	108.1
A(8-4-12)	110.7
A(4-8-9)	110.2
A(4-8-10)	111.0
A(4-8-11)	110.1
A(4-12-6)	107.7
A(4-12-15)	106.2
A(6-12-15)	108.2
A(9-8-10)	107.8
A(9-8-11)	109.0
A(10-8-11)	108.7
A(14-13-15)	104.6
A(13-15-12)	166.0
W1(A)	61.5
W2(A)	78.8
W3(A)	157.2
W4(A)	183.4
W5(A)	226.1
W6(A)	277.4
W7(A)	325.6
W8(A)	357.5
W9(A)	390.2
W10(A)	416.3
W11(A)	487.6
W12(A)	676.4
W13(A)	826.4
W14(A)	929.4
W15(A)	950.8
W16(A)	966.8
W17(A)	1105.5
W18(A)	1146.6
W19(A)	1193.2

W20(A)	1278.5
W21(A)	1361.7
W22(A)	1376.2
W23(A)	1406.7
W24(A)	1424.0
W25(A)	1476.9
W26(A)	1483.0
W27(A)	1493.1
W28(A)	1503.7
W29(A)	1650.8
W30(A)	3057.8
W31(A)	3060.4
W32(A)	3072.1
W33(A)	3151.1
W34(A)	3168.0
W35(A)	3172.7
W36(A)	3176.7
W37(A)	3632.2
W38(A)	3800.7
W39(A)	3895.3

Table S10.3 Optimized geometry (Å, deg) parameters for propan-2-ol -water complex at the G4 level including vibrational frequencies (cm⁻¹)

R(1-2)	1.094
R(1-3)	1.094
R(1-4)	1.523
R(1-7)	1.094
R(4-5)	1.101
R(4-8)	1.528
R(4-12)	1.441
R(6-12)	0.963
R(8-9)	1.095
R(8-10)	1.097
R(8-11)	1.094
R(13-14)	0.962
R(13-15)	0.972
R(12-15)	1.928
A(2-1-3)	108.8
A(2-1-4)	110.5
A(2-1-7)	108.6
A(3-1-4)	109.5
A(3-1-7)	108.8
A(4-1-7)	110.5
A(1-4-5)	109.2
A(1-4-8)	112.6
A(1-4-12)	106.2
A(5-4-8)	109.5
A(5-4-12)	108.3
A(8-4-12)	110.9

A(4-8-9)	110.7
A(4-8-10)	111.1
A(4-8-11)	110.0
A(4-12-6)	107.9
A(4-12-15)	105.3
A(6-12-15)	107.1
A(9-8-10)	107.5
A(9-8-11)	108.9
A(10-8-11)	108.6
A(14-13-15)	104.2
A(13-15-12)	163.8

Table S10.4 Optimized geometry (Å, deg) parameters for propan-2-ol-water complex at the W1U level including vibrational frequencies (cm⁻¹)

R(1-2)	1.090
R(1-3)	1.090
R(1-4)	1.518
R(1-7)	1.090
R(4-5)	1.096
R(4-8)	1.523
R(4-12)	1.445
R(6-12)	0.962
R(8-9)	1.091
R(8-10)	1.093
R(8-11)	1.090
R(13-14)	0.961
R(13-15)	0.971
R(12-15)	1.925
A(2-1-3)	108.6
A(2-1-4)	110.4
A(2-1-7)	108.5
A(3-1-4)	110.1
A(3-1-7)	108.7
A(4-1-7)	110.5
A(1-4-5)	109.1
A(1-4-8)	112.9
A(1-4-12)	106.4
A(5-4-8)	109.4
A(5-4-12)	108.0
A(8-4-12)	110.8
A(4-8-9)	110.7
A(4-8-10)	111.0
A(4-8-11)	110.3
A(4-12-6)	108.6
A(4-12-15)	109.0
A(6-12-15)	109.2
A(9-8-10)	107.5
A(9-8-11)	108.7
A(10-8-11)	108.4

A(14-13-15)	104.9
A(13-15-12)	168.2

Propanol-water complex

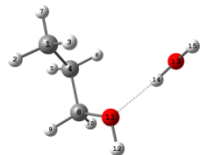


Figure 10: Optimized structure of propanol-water complex

Table S11.1 Optimized geometry (Å, deg) parameters for propanol-water complex at the MP2(full)/6-311++G** level including vibrational frequencies (cm⁻¹)

R(1-2)	1.095
R(1-3)	1.092
R(1-4)	1.526
R(1-7)	1.093
R(4-5)	1.096
R(4-6)	1.094
R(4-8)	1.516
R(8-9)	1.097
R(8-10)	1.096
R(8-11)	1.436
R(11-12)	0.961
R(13-14)	0.968
R(13-15)	0.958
R(11-14)	1.897
A(2-1-3)	108.0
A(2-1-4)	110.8
A(2-1-7)	108.0
A(3-1-4)	110.9
A(3-1-7)	108.2
A(4-1-7)	110.9
A(1-4-5)	110.1
A(1-4-6)	110.4
A(1-4-8)	112.6
A(5-4-6)	107.3
A(5-4-8)	107.6
A(6-4-8)	108.7
A(4-8-9)	110.1
A(4-8-10)	110.3
A(4-8-11)	108.1
A(9-8-10)	108.8
A(9-8-11)	109.6
A(10-8-11)	109.9
A(8-11-12)	107.9
A(8-11-14)	112.3
A(12-11-14)	117.5
A(14-13-15)	103.7

A(13-14-11)	172.0
W1(A)	37.4
W2(A)	60.9
W3(A)	123.5
W4(A)	147.2
W5(A)	187.5
W6(A)	235.7
W7(A)	291.9
W8(A)	335.3
W9(A)	381.5
W10(A)	486.9
W11(A)	675.4
W12(A)	791.9
W13(A)	892.2
W14(A)	938.8
W15(A)	996.7
W16(A)	1105.2
W17(A)	1128.8
W18(A)	1180.3
W19(A)	1263.5
W20(A)	1299.4
W21(A)	1344.3
W22(A)	1398.1
W23(A)	1432.6
W24(A)	1468.6
W25(A)	1500.2
W26(A)	1513.3
W27(A)	1524.1
W28(A)	1534.9
W29(A)	1670.7
W30(A)	3059.1
W31(A)	3079.0
W32(A)	3089.1
W33(A)	3115.5
W34(A)	3144.7
W35(A)	3165.4
W36(A)	3183.0
W37(A)	3755.0
W38(A)	3893.5
W39(A)	3967.9

Table S11.2 Optimized geometry (Å, deg) parameters for propanol -water complex at the MP2(full)/aug-cc-pVDZ level including vibrational frequencies (cm⁻¹)

R(1-2)	1.102
R(1-3)	1.099
R(1-4)	1.531
R(1-7)	1.100
R(4-5)	1.103

R(4-6)	1.101
R(4-8)	1.520
R(8-9)	1.104
R(8-10)	1.103
R(8-11)	1.451
R(11-12)	0.967
R(13-14)	0.975
R(13-15)	0.964
R(11-14)	1.891
A(2-1-3)	108.0
A(2-1-4)	110.8
A(2-1-7)	107.9
A(3-1-4)	110.8
A(3-1-7)	108.2
A(4-1-7)	110.9
A(1-4-5)	110.3
A(1-4-6)	110.7
A(1-4-8)	112.7
A(5-4-6)	107.0
A(5-4-8)	107.5
A(6-4-8)	108.5
A(4-8-9)	110.4
A(4-8-10)	110.5
A(4-8-11)	107.7
A(9-8-10)	109.0
A(9-8-11)	109.5
A(10-8-11)	109.7
A(8-11-12)	108.0
A(8-11-14)	101.2
A(12-11-14)	107.5
A(14-13-15)	104.6
A(13-14-11)	163.0
W1(A)	25.3
W2(A)	57.7
W3(A)	119.9
W4(A)	133.2
W5(A)	202.0
W6(A)	230.9
W7(A)	292.6
W8(A)	334.0
W9(A)	390.4
W10(A)	474.0
W11(A)	667.5
W12(A)	769.2
W13(A)	883.1
W14(A)	921.2
W15(A)	969.5
W16(A)	1091.2
W17(A)	1102.3
W18(A)	1156.5

W19(A)	1242.6
W20(A)	1268.6
W21(A)	1321.1
W22(A)	1367.2
W23(A)	1402.0
W24(A)	1436.2
W25(A)	1472.6
W26(A)	1488.6
W27(A)	1499.3
W28(A)	1510.6
W29(A)	1651.9
W30(A)	3052.0
W31(A)	3067.5
W32(A)	3077.1
W33(A)	3112.8
W34(A)	3134.8
W35(A)	3157.0
W36(A)	3175.6
W37(A)	3642.0
W38(A)	3819.3
W39(A)	3897.8

Table S11.3 Optimized geometry (Å, deg) parameters for propanol -water complex at the G4 level including vibrational frequencies (cm⁻¹)

R(1-2)	1.096
R(1-3)	1.093
R(1-4)	1.531
R(1-7)	1.094
R(4-5)	1.097
R(4-6)	1.096
R(4-8)	1.523
R(8-9)	1.101
R(8-10)	1.099
R(8-11)	1.434
R(11-12)	0.962
R(13-14)	0.971
R(13-15)	0.962
R(11-14)	1.924
A(2-1-3)	107.7
A(2-1-4)	111.3
A(2-1-7)	107.7
A(3-1-4)	110.8
A(3-1-7)	108.1
A(4-1-7)	111.1
A(1-4-5)	110.3
A(1-4-6)	110.4
A(1-4-8)	113.2
A(5-4-6)	107.2
A(5-4-8)	107.9

A(6-4-8)	107.6
A(4-8-9)	110.6
A(4-8-10)	110.0
A(4-8-11)	108.2
A(9-8-10)	108.0
A(9-8-11)	109.7
A(10-8-11)	110.3
A(8-11-12)	108.6
A(8-11-14)	107.2
A(12-11-14)	113.1
A(14-13-15)	103.6
A(13-14-11)	166.3

Table S11.4 Optimized geometry (Å, deg) parameters for propanol -water complex at the W1U level including vibrational frequencies (cm⁻¹)

R(1-2)	1.092
R(1-3)	1.089
R(1-4)	1.528
R(1-7)	1.090
R(4-5)	1.093
R(4-6)	1.092
R(4-8)	1.518
R(8-9)	1.096
R(8-10)	1.094
R(8-11)	1.439
R(11-12)	0.961
R(13-14)	0.970
R(13-15)	0.961
R(11-14)	1.924
A(2-1-3)	107.8
A(2-1-4)	111.2
A(2-1-7)	107.7
A(3-1-4)	111.0
A(3-1-7)	108.0
A(4-1-7)	111.0
A(1-4-5)	110.1
A(1-4-6)	110.3
A(1-4-8)	113.6
A(5-4-6)	106.8
A(5-4-8)	107.7
A(6-4-8)	108.2
A(4-8-9)	110.4
A(4-8-10)	110.1
A(4-8-11)	108.6
A(9-8-10)	108.3
A(9-8-11)	109.5
A(10-8-11)	109.9
A(8-11-12)	109.1
A(8-11-14)	110.8

A(12-11-14)	114.0
A(14-13-15)	104.5
A(13-14-11)	171.2

A(4-1-7)	109.9
A(1-4-5)	110.9
A(1-4-6)	110.9
A(1-4-12)	108.5
A(5-4-6)	108.1
A(5-4-12)	109.3
A(6-4-12)	109.1
A(4-12-8)	111.6
A(4-12-14)	113.9
A(9-8-10)	109.3
A(9-8-11)	109.4
A(9-8-12)	107.2
A(10-8-11)	109.3
A(10-8-12)	110.9
A(11-8-12)	110.7
A(8-12-14)	111.0
A(14-13-15)	103.7
A(13-14-12)	172.2
W1(A)	34.9
W2(A)	51.8
W3(A)	101.3
W4(A)	118.7
W5(A)	169.6
W6(A)	218.9
W7(A)	272.3
W8(A)	301.6
W9(A)	370.5
W10(A)	471.7
W11(A)	690.6
W12(A)	836.5
W13(A)	881.5
W14(A)	1055.2
W15(A)	1133.0
W16(A)	1174.1
W17(A)	1186.1
W18(A)	1218.4
W19(A)	1254.8
W20(A)	1321.9
W21(A)	1411.0
W22(A)	1449.6
W23(A)	1496.3
W24(A)	1504.5
W25(A)	1507.9
W26(A)	1521.8
W27(A)	1527.6
W28(A)	1547.3
W29(A)	1668.3
W30(A)	3037.8
W31(A)	3048.5
W32(A)	3085.6

Ethyl methyl formate

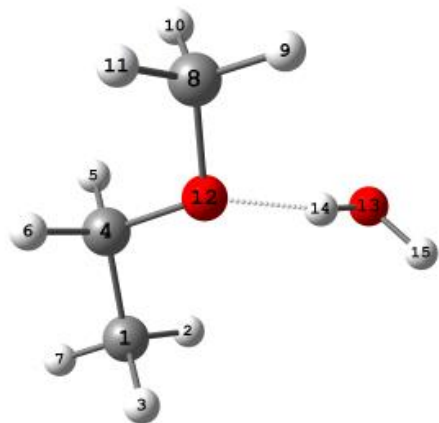


Figure 11: Optimized structure of ethyl methyl formate -water complex

Table S12.1 Optimized geometry (Å, deg) parameters for ethyl methyl formate-water complex at the MP2(full)/6-311++G** level including vibrational frequencies (cm⁻¹)

R(1-2)	1.092
R(1-3)	1.092
R(1-4)	1.514
R(1-7)	1.093
R(4-5)	1.099
R(4-6)	1.099
R(4-12)	1.423
R(8-9)	1.090
R(8-10)	1.097
R(8-11)	1.097
R(8-12)	1.418
R(13-14)	0.969
R(13-15)	0.958
R(12-14)	1.863
A(2-1-3)	109.0
A(2-1-4)	110.4
A(2-1-7)	108.6
A(3-1-4)	110.2
A(3-1-7)	108.6

W33(A)	3089.5
W34(A)	3122.2
W35(A)	3181.4
W36(A)	3190.7
W37(A)	3196.4
W38(A)	3725.6
W39(A)	3965.5

Table S12.2 Optimized geometry (Å, deg) parameters for ethyl methyl formate-water complex at the MP2(full)/aug-cc-pVDZ level including vibrational frequencies (cm⁻¹)

R(1-2)	1.099
R(1-3)	1.099
R(1-4)	1.518
R(1-7)	1.100
R(4-5)	1.106
R(4-6)	1.106
R(4-12)	1.438
R(8-9)	1.097
R(8-10)	1.104
R(8-11)	1.103
R(8-12)	1.431
R(13-14)	0.977
R(13-15)	0.964
R(12-14)	1.861
A(2-1-3)	109.2
A(2-1-4)	110.3
A(2-1-7)	108.5
A(3-1-4)	110.4
A(3-1-7)	108.7
A(4-1-7)	109.7
A(1-4-5)	111.1
A(1-4-6)	111.2
A(1-4-12)	108.3
A(5-4-6)	108.3
A(5-4-12)	109.1
A(6-4-12)	108.8
A(4-12-8)	110.8
A(4-12-14)	100.8
A(9-8-10)	109.5
A(9-8-11)	109.5
A(9-8-12)	107.1
A(10-8-11)	109.4
A(10-8-12)	110.7
A(11-8-12)	110.5
A(8-12-14)	103.0
A(14-13-15)	104.6
A(13-14-12)	161.0
W1(A)	57.9

W2(A)	62.7
W3(A)	114.0
W4(A)	126.1
W5(A)	181.7
W6(A)	223.9
W7(A)	275.5
W8(A)	291.1
W9(A)	399.8
W10(A)	464.4
W11(A)	674.8
W12(A)	821.6
W13(A)	855.5
W14(A)	1037.0
W15(A)	1106.9
W16(A)	1140.6
W17(A)	1160.3
W18(A)	1191.6
W19(A)	1223.8
W20(A)	1296.5
W21(A)	1378.9
W22(A)	1416.5
W23(A)	1459.7
W24(A)	1479.9
W25(A)	1484.2
W26(A)	1493.1
W27(A)	1497.0
W28(A)	1515.8
W29(A)	1650.3
W30(A)	3029.9
W31(A)	3039.3
W32(A)	3078.7
W33(A)	3083.0
W34(A)	3119.8
W35(A)	3174.7
W36(A)	3185.1
W37(A)	3190.5
W38(A)	3613.0
W39(A)	3894.2

Table S12.3 Optimized geometry parameters for ethyl methyl formate-water complex at the G4 level including vibrational frequencies (cm⁻¹)

R(1-2)	1.093
R(1-3)	1.094
R(1-4)	1.519
R(1-7)	1.094
R(4-5)	1.102
R(4-6)	1.102
R(4-12)	1.423
R(8-9)	1.092

R(8-10)	1.100
R(8-11)	1.100
R(8-12)	1.412
R(13-14)	0.970
R(13-15)	0.962
R(12-14)	1.943
A(2-1-3)	108.7
A(2-1-4)	109.9
A(2-1-7)	109.1
A(3-1-4)	110.6
A(3-1-7)	108.4
A(4-1-7)	110.1
A(1-4-5)	110.8
A(1-4-6)	111.2
A(1-4-12)	108.8
A(5-4-6)	107.3
A(5-4-12)	109.6
A(6-4-12)	109.2
A(4-12-8)	113.0
A(4-12-14)	108.6
A(9-8-10)	109.0
A(9-8-11)	109.1
A(9-8-12)	107.5
A(10-8-11)	108.4
A(10-8-12)	111.7
A(11-8-12)	111.2
A(8-12-14)	117.4
A(14-13-15)	103.6
A(13-14-12)	167.9

A(2-1-7)	108.6
A(3-1-4)	110.6
A(3-1-7)	108.3
A(4-1-7)	110.0
A(1-4-5)	110.8
A(1-4-6)	111.0
A(1-4-12)	108.9
A(5-4-6)	107.6
A(5-4-12)	109.4
A(6-4-12)	109.1
A(4-12-8)	113.2
A(4-12-14)	112.4
A(9-8-10)	109.1
A(9-8-11)	109.2
A(9-8-12)	107.4
A(10-8-11)	108.8
A(10-8-12)	111.4
A(11-8-12)	111.0
A(8-12-14)	115.6
A(14-13-15)	104.5
A(13-14-12)	174.3

Glycine-water complex

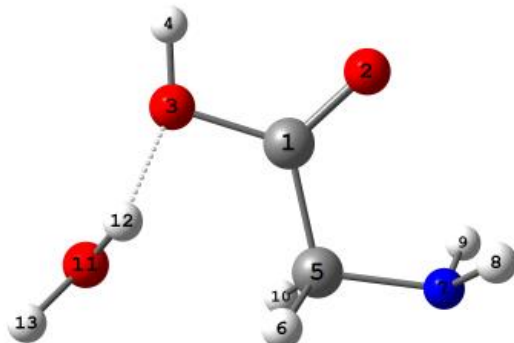


Figure 12: Optimized structure of glycine-water complex

Table S12.4 Optimized geometry parameters for ethyl methyl formate-water complex at the W1U level including vibrational frequencies (cm⁻¹)

R(1-2)	1.090
R(1-3)	1.090
R(1-4)	1.514
R(1-7)	1.091
R(4-5)	1.097
R(4-6)	1.097
R(4-12)	1.426
R(8-9)	1.088
R(8-10)	1.096
R(8-11)	1.095
R(8-12)	1.416
R(13-14)	0.970
R(13-15)	0.961
R(12-14)	1.918
A(2-1-3)	108.6
A(2-1-4)	110.5

Table S13.1 Optimized geometry (Å, deg) parameters for glycine-water complex at the MP2(full)/6-311++G** level including vibrational frequencies (cm⁻¹)

R(1-2)	1.220
R(1-3)	1.337
R(1-5)	1.518
R(3-4)	0.982
R(5-6)	1.094
R(5-7)	1.448
R(5-10)	1.094
R(7-8)	1.014
R(7-9)	1.014
R(11-12)	0.959

R(11-13)	0.968
R(4-11)	1.793
A(2-1-3)	124.4
A(2-1-5)	124.0
A(3-1-5)	111.6
A(1-3-4)	107.8
A(1-5-6)	107.4
A(1-5-7)	115.8
A(1-5-10)	107.3
A(3-4-11)	158.2
A(6-5-7)	109.9
A(6-5-10)	106.1
A(7-5-10)	109.9
A(5-7-8)	109.8
A(5-7-9)	109.7
A(8-7-9)	106.0
A(12-11-13)	105.8
A(12-11-4)	133.1
A(13-11-4)	89.6
W1(A)	43.9
W2(A)	68.4
W3(A)	128.1
W4(A)	189.6
W5(A)	234.3
W6(A)	256.7
W7(A)	282.1
W8(A)	351.8
W9(A)	493.4
W10(A)	551.2
W11(A)	561.2
W12(A)	668.0
W13(A)	863.6
W14(A)	884.3
W15(A)	930.0
W16(A)	955.4
W17(A)	1171.8
W18(A)	1192.1
W19(A)	1251.9
W20(A)	1388.3
W21(A)	1400.9
W22(A)	1463.4
W23(A)	1473.9
W24(A)	1621.5
W25(A)	1678.1
W26(A)	1793.1
W27(A)	3105.7
W28(A)	3157.3
W29(A)	3514.8
W30(A)	3558.0
W31(A)	3647.6

W32(A)	3779.3
W33(A)	3964.0

Table S13.2 Optimized geometry (Å, deg) parameters for glycine-water complex at the MP2(full)/aug-cc-pVDZ level including vibrational frequencies (cm⁻¹)

R(1-2)	1.231
R(1-3)	1.346
R(1-5)	1.521
R(3-4)	0.990
R(5-6)	1.101
R(5-7)	1.455
R(5-10)	1.101
R(7-8)	1.020
R(7-9)	1.020
R(11-12)	0.965
R(11-13)	0.977
R(2-13)	1.980
R(4-11)	1.782
A(2-1-3)	124.1
A(2-1-5)	124.1
A(1-2-13)	107.1
A(3-1-5)	111.8
A(1-3-4)	107.6
A(1-5-6)	107.4
A(1-5-7)	115.8
A(1-5-10)	107.4
A(3-4-11)	157.9
A(6-5-7)	109.9
A(6-5-10)	106.0
A(7-5-10)	109.9
A(5-7-8)	109.4
A(5-7-9)	109.4
A(8-7-9)	105.0
A(12-11-13)	105.6
A(12-11-4)	125.4
A(11-13-2)	137.9
A(13-11-4)	84.8
W1(A)	57.9
W2(A)	72.8
W3(A)	137.5
W4(A)	195.3
W5(A)	223.9
W6(A)	254.9
W7(A)	286.3
W8(A)	363.1
W9(A)	489.9
W10(A)	561.4
W11(A)	623.7

W12(A)	658.6
W13(A)	853.3
W14(A)	907.9
W15(A)	917.7
W16(A)	943.4
W17(A)	1159.1
W18(A)	1180.9
W19(A)	1233.8
W20(A)	1370.8
W21(A)	1382.1
W22(A)	1451.1
W23(A)	1457.8
W24(A)	1619.2
W25(A)	1657.3
W26(A)	1758.7
W27(A)	3093.2
W28(A)	3148.0
W29(A)	3392.3
W30(A)	3513.8
W31(A)	3604.4
W32(A)	3642.3
W33(A)	3887.4

Table S13.3 Optimized geometry (Å, deg) parameters for glycine-water complex at the G4 level including vibrational frequencies (cm⁻¹)

R(1-2)	1.202
R(1-3)	1.366
R(1-5)	1.522
R(3-4)	0.970
R(5-6)	1.096
R(5-7)	1.450
R(5-10)	1.099
R(7-8)	1.016
R(7-9)	1.016
R(11-12)	0.966
R(11-13)	0.962
A(2-1-3)	122.1
A(2-1-5)	126.3
A(3-1-5)	111.6
A(1-3-4)	106.4
A(1-5-6)	107.8
A(1-5-7)	115.1
A(1-5-10)	106.8
A(6-5-7)	111.0
A(6-5-10)	105.7
A(7-5-10)	110.0
A(5-7-8)	109.3
A(5-7-9)	109.3
A(8-7-9)	105.2

A(12-11-13)	104.0
-------------	-------

Table S13.4 Optimized geometry (Å, deg) parameters for glycine-water complex at the W1U level including vibrational frequencies (cm⁻¹)

R(1-2)	1.200
R(1-3)	1.366
R(1-5)	1.519
R(3-4)	0.969
R(5-6)	1.092
R(5-7)	1.447
R(5-10)	1.094
R(7-8)	1.013
R(7-9)	1.013
R(11-12)	0.965
R(11-13)	0.961
A(2-1-3)	122.0
A(2-1-5)	126.4
A(3-1-5)	111.6
A(1-3-4)	107.0
A(1-5-6)	107.9
A(1-5-7)	115.5
A(1-5-10)	106.8
A(6-5-7)	110.5
A(6-5-10)	105.5
A(7-5-10)	110.0
A(5-7-8)	110.2
A(5-7-9)	110.3
A(8-7-9)	106.1
A(12-11-13)	104.9

Methyl carbamic acid-water complex

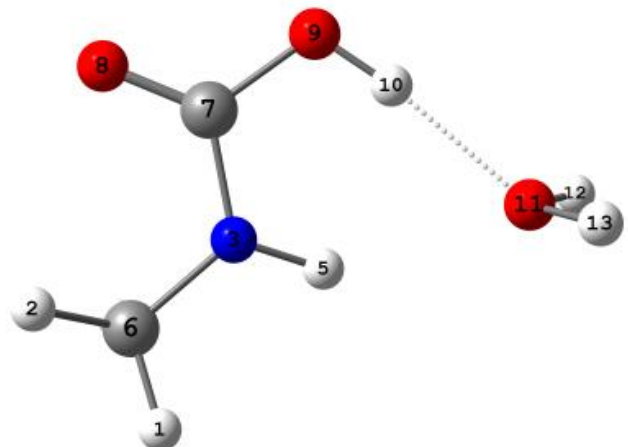


Figure 13: Optimized structure of methyl carbamic acid-water complex

Table S14.1 Optimized geometry (Å, deg) parameters for methyl carbamic acid-water complex at the MP2(full)/6-311++G** level including vibrational frequencies (cm⁻¹)

R(1-6)	1.090
R(2-6)	1.089
R(3-5)	1.009
R(3-6)	1.458
R(3-7)	1.371
R(4-6)	1.093
R(7-8)	1.211
R(7-9)	1.365
R(9-10)	0.963
R(11-12)	0.959
R(11-13)	0.965
A(1-6-2)	109.1
A(1-6-3)	108.4
A(1-6-4)	109.8
A(2-6-3)	108.9
A(2-6-4)	108.6
A(5-3-6)	116.3
A(5-3-7)	116.4
A(6-3-7)	117.9
A(3-6-4)	112.1
A(3-7-8)	124.5
A(3-7-9)	114.8
A(8-7-9)	120.7
A(7-9-10)	109.4
A(12-11-13)	102.0
W1(A)	20.6
W2(A)	42.1
W3(A)	124.2
W4(A)	142.8
W5(A)	151.0
W6(A)	189.1
W7(A)	247.8
W8(A)	285.2
W9(A)	364.9
W10(A)	458.4
W11(A)	517.3
W12(A)	546.6
W13(A)	686.4
W14(A)	764.5
W15(A)	939.5
W16(A)	1127.6
W17(A)	1161.9
W18(A)	1185.3
W19(A)	1228.8
W20(A)	1326.2
W21(A)	1479.4

W22(A)	1504.7
W23(A)	1522.7
W24(A)	1556.8
W25(A)	1676.0
W26(A)	1839.6
W27(A)	3093.5
W28(A)	3184.1
W29(A)	3216.9
W30(A)	3660.1
W31(A)	3828.6
W32(A)	3871.4
W33(A)	3968.2

Table S14.2: Optimized geometry (Å, deg) parameters for methyl carbamic acid-water complex at the MP2(full)aug-cc-pVDZlevel including vibrational frequencies (cm⁻¹)

R(1-6)	1.097
R(2-6)	1.096
R(3-5)	1.013
R(3-6)	1.462
R(3-7)	1.372
R(4-6)	1.100
R(7-8)	1.223
R(7-9)	1.370
R(9-10)	0.969
R(11-12)	0.965
R(11-13)	0.973
R(8-13)	1.947
A(1-6-2)	109.2
A(1-6-3)	108.4
A(1-6-4)	109.8
A(2-6-3)	108.7
A(2-6-4)	108.6
A(5-3-6)	117.3
A(5-3-7)	117.3
A(6-3-7)	118.2
A(3-6-4)	112.0
A(3-7-8)	124.1
A(3-7-9)	115.5
A(8-7-9)	120.3
A(7-8-13)	111.7
A(7-9-10)	110.0
A(12-11-13)	103.6
A(11-13-8)	167.3
W1(A)	11.5
W2(A)	35.3
W3(A)	105.5
W4(A)	118.9
W5(A)	156.9

W6(A)	180.8
W7(A)	278.3
W8(A)	297.9
W9(A)	328.0
W10(A)	431.4
W11(A)	527.2
W12(A)	561.5
W13(A)	670.0
W14(A)	765.9
W15(A)	926.2
W16(A)	1120.0
W17(A)	1146.6
W18(A)	1170.0
W19(A)	1215.4
W20(A)	1323.3
W21(A)	1447.7
W22(A)	1482.1
W23(A)	1501.0
W24(A)	1546.9
W25(A)	1647.1
W26(A)	1799.5
W27(A)	3084.4
W28(A)	3179.0
W29(A)	3212.3
W30(A)	3641.6
W31(A)	3705.8
W32(A)	3801.6
W33(A)	3902.8

Table S14.3: Optimized geometry (Å, deg) parameters for methyl carbamic acid-water complex at the G4 level including vibrational frequencies (cm⁻¹)

R(1-6)	1.093
R(2-6)	1.090
R(3-5)	1.007
R(3-6)	1.455
R(3-7)	1.366
R(4-6)	1.097
R(7-8)	1.209
R(7-9)	1.361
R(9-10)	0.964
R(11-12)	0.962
R(11-13)	0.968
A(1-6-2)	109.4
A(1-6-3)	109.6
A(1-6-4)	109.1
A(2-6-3)	108.0
A(2-6-4)	108.4
A(5-3-6)	117.1
A(5-3-7)	118.4
A(6-3-7)	120.5
A(3-6-4)	112.3
A(3-7-8)	124.4
A(3-7-9)	115.5
A(8-7-9)	120.2
A(7-8-13)	117.8
A(7-9-10)	111.8
A(12-11-13)	103.6
A(11-13-8)	170.2

A(5-3-7)	118.6
A(6-3-7)	120.4
A(3-6-4)	112.3
A(3-7-8)	124.5
A(3-7-9)	115.2
A(8-7-9)	120.3
A(7-9-10)	111.6
A(12-11-13)	101.9

Table S14.4: Optimized geometry (Å, deg) parameters for methyl carbamic acid-water complex at the W1U level including vibrational frequencies (cm⁻¹)

R(1-6)	1.088
R(2-6)	1.086
R(3-5)	1.006
R(3-6)	1.456
R(3-7)	1.363
R(4-6)	1.092
R(7-8)	1.209
R(7-9)	1.362
R(9-10)	0.964
R(11-12)	0.961
R(11-13)	0.968
R(8-13)	1.982
A(1-6-2)	109.1
A(1-6-3)	109.1
A(1-6-4)	109.3
A(2-6-3)	108.7
A(2-6-4)	108.4
A(5-3-6)	117.1
A(5-3-7)	118.4
A(6-3-7)	120.5
A(3-6-4)	112.3
A(3-7-8)	124.4
A(3-7-9)	115.5
A(8-7-9)	120.2
A(7-8-13)	117.8
A(7-9-10)	111.8
A(12-11-13)	103.6
A(11-13-8)	170.2

Methyl carbamate-water complex

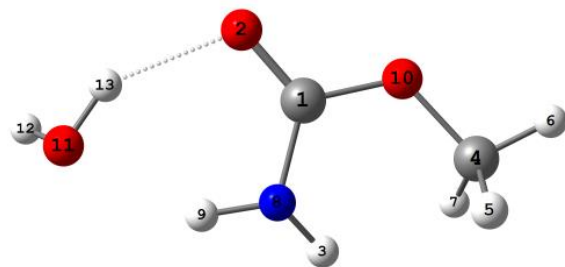


Figure 14: Optimized structure of methyl carbamate-water complex

Table S15.1 Optimized geometry (Å, deg) parameters for methyl carbamate-water complex at the MP2(full)/6-311++G** level including vibrational frequencies (cm⁻¹)

R(1-2)	1.217
R(1-8)	1.371
R(1-10)	1.354
R(3-8)	1.006
R(4-5)	1.093
R(4-6)	1.088
R(4-7)	1.095
R(4-10)	1.425
R(8-9)	1.015
R(11-12)	0.959
R(11-13)	0.971
R(2-13)	1.926
A(2-1-8)	123.9
A(2-1-10)	119.0
A(1-2-13)	109.6
A(8-1-10)	117.0
A(1-8-3)	119.8
A(1-8-9)	113.6
A(1-10-4)	119.4
A(3-8-9)	116.3
A(5-4-6)	109.5
A(5-4-7)	110.3
A(5-4-10)	111.2
A(6-4-7)	108.6
A(6-4-10)	105.5
A(7-4-10)	111.5
A(12-11-13)	105.0
A(11-13-2)	147.0
W1(A)	57.6
W2(A)	116.8
W3(A)	139.3
W4(A)	174.5
W5(A)	225.3
W6(A)	233.0
W7(A)	348.8
W8(A)	364.1

W9(A)	458.6
W10(A)	569.9
W11(A)	588.3
W12(A)	599.9
W13(A)	718.3
W14(A)	784.5
W15(A)	893.8
W16(A)	1132.1
W17(A)	1153.5
W18(A)	1188.5
W19(A)	1229.4
W20(A)	1384.8
W21(A)	1509.5
W22(A)	1520.2
W23(A)	1531.1
W24(A)	1642.2
W25(A)	1658.5
W26(A)	1814.2
W27(A)	3072.6
W28(A)	3162.1
W29(A)	3217.3
W30(A)	3546.4
W31(A)	3712.8
W32(A)	3737.2
W33(A)	3967.5

Table S15.2 Optimized geometry (Å, deg) parameters for methyl carbamate-water complex at the MP2(full)/aug-cc-pVDZ level including vibrational frequencies (cm⁻¹)

R(1-2)	1.230
R(1-8)	1.367
R(1-10)	1.363
R(3-8)	1.008
R(4-5)	1.100
R(4-6)	1.095
R(4-7)	1.102
R(4-10)	1.436
R(8-9)	1.019
R(11-12)	0.964
R(11-13)	0.980
R(2-13)	1.881
A(2-1-8)	123.9
A(2-1-10)	118.7
A(1-2-13)	108.1
A(8-1-10)	117.4
A(1-8-3)	122.2
A(1-8-9)	115.2
A(1-10-4)	118.9
A(3-8-9)	118.9

A(5-4-6)	109.5
A(5-4-7)	110.7
A(5-4-10)	111.0
A(6-4-7)	108.9
A(6-4-10)	105.4
A(7-4-10)	111.2
A(12-11-13)	105.4
A(11-13-2)	150.2
W1(A)	56.6
W2(A)	109.0
W3(A)	145.5
W4(A)	152.0
W5(A)	186.1
W6(A)	219.7
W7(A)	309.2
W8(A)	356.0
W9(A)	404.2
W10(A)	564.8
W11(A)	585.9
W12(A)	647.0
W13(A)	712.2
W14(A)	772.4
W15(A)	880.5
W16(A)	1101.5
W17(A)	1132.1
W18(A)	1166.9
W19(A)	1208.7
W20(A)	1371.2
W21(A)	1477.6
W22(A)	1501.4
W23(A)	1506.3
W24(A)	1627.7
W25(A)	1638.7
W26(A)	1778.8
W27(A)	3062.5
W28(A)	3156.1
W29(A)	3217.5
W30(A)	3515.9
W31(A)	3581.1
W32(A)	3741.5
W33(A)	3897.4

Table S15.3 Optimized geometry parameters for methyl carbamate-water complex at the G4 level including vibrational frequencies (cm⁻¹)

R(1-2)	1.217
R(1-8)	1.361
R(1-10)	1.353
R(3-8)	1.004
R(4-5)	1.098

R(4-6)	1.091
R(4-7)	1.096
R(4-10)	1.422
R(8-9)	1.019
R(11-12)	0.962
R(11-13)	0.978
R(2-13)	1.889
R(9-11)	1.967
A(2-1-8)	123.7
A(2-1-10)	118.5
A(1-2-13)	107.1
A(8-1-10)	117.8
A(1-8-3)	122.0
A(1-8-9)	114.1
A(1-10-4)	120.4
A(3-8-9)	118.9
A(5-4-6)	108.5
A(5-4-7)	109.7
A(5-4-10)	111.7
A(6-4-7)	109.2
A(6-4-10)	106.0
A(7-4-10)	111.6
A(8-9-11)	144.7
A(12-11-13)	103.9
A(12-11-9)	110.2
A(11-13-2)	151.2
A(13-11-9)	78.2

Table S15.4 Optimized geometry (Å, deg) parameters for methyl carbamate-water complex at the W1U level including vibrational frequencies (cm⁻¹)

R(1-2)	1.216
R(1-8)	1.358
R(1-10)	1.353
R(3-8)	1.002
R(4-5)	1.093
R(4-6)	1.086
R(4-7)	1.092
R(4-10)	1.425
R(8-9)	1.015
R(11-12)	0.961
R(11-13)	0.977
R(2-13)	1.890
A(2-1-8)	123.7
A(2-1-10)	118.6
A(1-2-13)	107.9
A(8-1-10)	117.7
A(1-8-3)	122.5
A(1-8-9)	115.1

A(1-10-4)	120.8
A(3-8-9)	119.1
A(5-4-6)	108.7
A(5-4-7)	110.1
A(5-4-10)	111.5
A(6-4-7)	109.2
A(6-4-10)	105.9
A(7-4-10)	111.4
A(12-11-13)	105.2
A(11-13-2)	151.7

Propenal-water complex

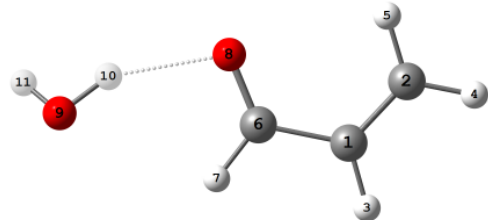


Figure 15: Optimized structure of propenal-water complex

Table S16.1 Optimized geometry (Å, deg) parameters for propenal-water complex at the MP2(full)/6-311++G** level including vibrational frequencies (cm⁻¹)

R(1-2)	1.343
R(1-3)	1.086
R(1-6)	1.482
R(2-4)	1.084
R(2-5)	1.086
R(6-7)	1.104
R(6-8)	1.223
R(9-10)	0.966
R(9-11)	0.958
R(8-10)	1.966
A(2-1-3)	121.4
A(2-1-6)	121.5
A(1-2-4)	121.5
A(1-2-5)	120.1
A(3-1-6)	117.1
A(1-6-7)	116.5
A(1-6-8)	123.8
A(4-2-5)	118.4
A(7-6-8)	119.7

A(6-8-10)	102.1
A(10-9-11)	104.1
A(9-10-8)	153.2
W1(A)	32.4
W2(A)	59.5
W3(A)	111.5
W4(A)	138.8
W5(A)	149.3
W6(A)	307.1
W7(A)	327.1
W8(A)	498.6
W9(A)	538.9
W10(A)	686.0
W11(A)	928.1
W12(A)	958.6
W13(A)	1012.1
W14(A)	1033.3
W15(A)	1073.8
W16(A)	1313.1
W17(A)	1445.8
W18(A)	1458.2
W19(A)	1650.1
W20(A)	1672.6
W21(A)	1740.4
W22(A)	3031.5
W23(A)	3190.6
W24(A)	3225.0
W25(A)	3296.5
W26(A)	3780.3
W27(A)	3974.2

Table S16.2 Optimized geometry (Å, deg) parameters for propenal-water complex at the MP2(full)/aug-cc-pVDZ level including vibrational frequencies (cm⁻¹)

R(1-2)	1.353
R(1-3)	1.093
R(1-6)	1.485
R(2-4)	1.091
R(2-5)	1.093
R(6-7)	1.110
R(6-8)	1.234
R(9-10)	0.974
R(9-11)	0.964
R(8-10)	1.941
A(2-1-3)	121.3
A(2-1-6)	121.5
A(1-2-4)	121.4
A(1-2-5)	120.0
A(3-1-6)	117.2

A(1-6-7)	116.7
A(1-6-8)	123.7
A(4-2-5)	118.6
A(7-6-8)	119.6
A(6-8-10)	100.9
A(10-9-11)	104.7
A(9-10-8)	152.9
W1(A)	42.0
W2(A)	66.7
W3(A)	125.6
W4(A)	154.2
W5(A)	156.7
W6(A)	303.8
W7(A)	389.8
W8(A)	546.7
W9(A)	571.0
W10(A)	676.5
W11(A)	958.9
W12(A)	992.3
W13(A)	1014.2
W14(A)	1028.1
W15(A)	1061.6
W16(A)	1303.4
W17(A)	1425.8
W18(A)	1439.2
W19(A)	1648.7
W20(A)	1667.8
W21(A)	1710.9
W22(A)	3039.1
W23(A)	3191.0
W24(A)	3228.5
W25(A)	3304.0
W26(A)	3673.0
W27(A)	3907.5

Table S16.3 Optimized geometry (Å, deg) parameters for propenal-water complex at the G4 level including vibrational frequencies (cm⁻¹)

R(1-2)	1.335
R(1-3)	1.086
R(1-6)	1.479
R(2-4)	1.084
R(2-5)	1.086
R(6-7)	1.106
R(6-8)	1.217
R(9-10)	0.970
R(9-11)	0.962
R(8-10)	1.968
A(2-1-3)	121.6
A(2-1-6)	121.8

A(1-2-4)	122.2
A(1-2-5)	120.1
A(3-1-6)	116.6
A(1-6-7)	116.4
A(1-6-8)	124.0
A(4-2-5)	117.7
A(7-6-8)	119.6
A(6-8-10)	100.2
A(10-9-11)	103.6
A(9-10-8)	151.2

Table S16.4 Optimized geometry (Å, deg) parameters for propenal-water complex at the W1U level including vibrational frequencies (cm⁻¹)

R(1-2)	1.331
R(1-3)	1.083
R(1-6)	1.477
R(2-4)	1.081
R(2-5)	1.082
R(6-7)	1.103
R(6-8)	1.215
R(9-10)	0.970
R(9-11)	0.961
R(8-10)	1.966
A(2-1-3)	121.3
A(2-1-6)	122.1
A(1-2-4)	121.8
A(1-2-5)	120.3
A(3-1-6)	116.5
A(1-6-7)	116.2
A(1-6-8)	124.2
A(4-2-5)	117.9
A(7-6-8)	119.6
A(6-8-10)	102.7
A(10-9-11)	104.5
A(9-10-8)	155.4

Methyl ketene water complex

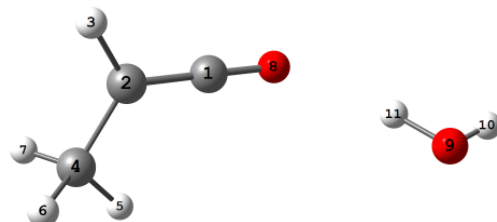


Figure 16: Optimized structure of methyl ketene - water complex

Table S17.1 Optimized geometry (Å, deg) parameters for methyl ketene -water complex at the

MP2(full)/6-311++G** level including vibrational frequencies (cm⁻¹)

R(1-2)	1.318
R(1-8)	1.175
R(2-3)	1.084
R(2-4)	1.511
R(4-5)	1.092
R(4-6)	1.093
R(4-7)	1.093
R(9-10)	0.959
R(9-11)	0.961
A(2-1-8)	179.5
A(1-2-3)	116.0
A(1-2-4)	122.5
A(3-2-4)	121.5
A(2-4-5)	111.0
A(2-4-6)	110.7
A(2-4-7)	110.8
A(5-4-6)	107.8
A(5-4-7)	107.9
A(6-4-7)	108.4
A(10-9-11)	103.6
W1(A)	13.3
W2(A)	30.7
W3(A)	63.8
W4(A)	116.8
W5(A)	137.7
W6(A)	198.8
W7(A)	210.0
W8(A)	350.7
W9(A)	499.0
W10(A)	527.0
W11(A)	651.1
W12(A)	915.6
W13(A)	1065.2
W14(A)	1089.8
W15(A)	1156.0
W16(A)	1409.0
W17(A)	1432.6
W18(A)	1495.4
W19(A)	1531.0
W20(A)	1642.6
W21(A)	2207.5
W22(A)	3083.6
W23(A)	3163.6
W24(A)	3180.5
W25(A)	3243.9
W26(A)	3871.2
W27(A)	3990.9
R(1-2)	1.318

R(1-8)	1.175
R(2-3)	1.084

Table S17.2 Optimized geometry (Å, deg) parameters for methyl ketene -water complex at the MP2(full)/aug-cc-pVDZ level including vibrational frequencies (cm⁻¹)

R(1-2)	1.331
R(1-8)	1.184
R(2-3)	1.091
R(2-4)	1.516
R(4-5)	1.098
R(4-6)	1.100
R(4-7)	1.100
R(9-10)	0.965
R(9-11)	0.967
A(2-1-8)	179.7
A(1-2-3)	115.5
A(1-2-4)	122.4
A(3-2-4)	122.1
A(2-4-5)	110.3
A(2-4-6)	110.7
A(2-4-7)	110.7
A(5-4-6)	108.4
A(5-4-7)	108.4
A(6-4-7)	108.3
A(10-9-11)	104.5
W1(A)	29.5
W2(A)	85.9
W3(A)	104.9
W4(A)	108.3
W5(A)	161.8
W6(A)	204.8
W7(A)	232.9
W8(A)	233.2
W9(A)	501.4
W10(A)	520.6
W11(A)	639.8
W12(A)	907.3
W13(A)	1049.8
W14(A)	1081.2
W15(A)	1148.1
W16(A)	1390.7
W17(A)	1403.7
W18(A)	1481.5
W19(A)	1504.8
W20(A)	1624.9
W21(A)	2168.2
W22(A)	3068.4
W23(A)	3148.9

W24(A)	3186.7
W25(A)	3244.6
W26(A)	3790.2
W27(A)	3927.4

Table S17.3 Optimized geometry (Å, deg) parameters for methyl ketene -water complex at the G4 level including vibrational frequencies (cm⁻¹)

R(1-2)	1.307
R(1-8)	1.171
R(2-3)	1.085
R(2-4)	1.514
R(4-5)	1.092
R(4-6)	1.096
R(4-7)	1.096
R(9-10)	0.963
R(9-11)	0.964
A(2-1-8)	179.9
A(1-2-3)	115.9
A(1-2-4)	123.1
A(3-2-4)	120.9
A(2-4-5)	110.4
A(2-4-6)	110.8
A(2-4-7)	110.9
A(5-4-6)	108.4
A(5-4-7)	108.6
A(6-4-7)	107.7
A(10-9-11)	103.5

Table S17.4 Optimized geometry (Å, deg) parameters for methyl ketene -water complex at the G4 level including vibrational frequencies (cm⁻¹)

R(1-2)	1.305
R(1-8)	1.168
R(2-3)	1.082
R(2-4)	1.510
R(4-5)	1.088
R(4-6)	1.091
R(4-7)	1.091
R(9-10)	0.961
R(9-11)	0.964
A(2-1-8)	179.7
A(1-2-3)	115.7
A(1-2-4)	123.9
A(3-2-4)	120.4
A(2-4-5)	111.4
A(2-4-6)	110.8
A(2-4-7)	110.9
A(5-4-6)	107.8
A(5-4-7)	107.9
A(6-4-7)	107.9

A(10-9-11)	104.3
------------	-------

Propynal-water complex

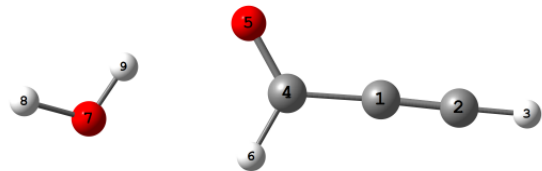


Figure 17: Optimized structure of propynal -water complex

Table S18.1 Optimized geometry (Å, deg) parameters for propynal -water complex at the MP2(full)/6-311++G** level including vibrational frequencies (cm⁻¹)

R(1-2)	1.220
R(1-4)	1.448
R(2-3)	1.066
R(4-5)	1.222
R(4-6)	1.101
R(7-8)	0.958
R(7-9)	0.965
A(2-1-4)	177.8
A(1-2-3)	179.0
A(1-4-5)	122.8
A(1-4-6)	116.3
A(5-4-6)	120.9
A(8-7-9)	104.2
W1(A)	59.8
W2(A)	67.0
W3(A)	142.8
W4(A)	150.5
W5(A)	232.6
W6(A)	298.9
W7(A)	315.8
W8(A)	463.5
W9(A)	627.0
W10(A)	723.2
W11(A)	725.9
W12(A)	979.0
W13(A)	1024.6
W14(A)	1442.9
W15(A)	1642.9
W16(A)	1700.1
W17(A)	2132.5
W18(A)	3071.2
W19(A)	3500.6
W20(A)	3812.0
W21(A)	3976.8

Table S18.2 Optimized geometry (Å, deg) parameters for propynal -water complex at the MP2(full)/aug-cc-pVDZ level including vibrational frequencies (cm⁻¹)

R(1-2)	1.235
R(1-4)	1.455
R(2-3)	1.074
R(4-5)	1.233
R(4-6)	1.107
R(7-8)	0.964
R(7-9)	0.972
A(2-1-4)	175.9
A(1-2-3)	177.7
A(1-4-5)	122.9
A(1-4-6)	116.3
A(5-4-6)	120.8
A(8-7-9)	104.8
W1(A)	60.0
W2(A)	66.6
W3(A)	125.7
W4(A)	146.3
W5(A)	205.9
W6(A)	229.2
W7(A)	365.5
W8(A)	512.9
W9(A)	597.5
W10(A)	618.9
W11(A)	645.4
W12(A)	974.9
W13(A)	1006.8
W14(A)	1414.5
W15(A)	1638.3
W16(A)	1672.2
W17(A)	2116.5
W18(A)	3074.2
W19(A)	3485.2
W20(A)	3705.7
W21(A)	3910.0

Table S18.3 Optimized geometry (Å, deg) parameters for propynal -water complex at the G4 level including vibrational frequencies (cm⁻¹)

R(1-2)	1.204
R(1-4)	1.440
R(2-3)	1.063
R(4-5)	1.215
R(4-6)	1.104
R(7-8)	0.962
R(7-9)	0.969
A(2-1-4)	177.7
A(1-2-3)	179.2

A(1-4-5)	123.5
A(1-4-6)	115.8
A(5-4-6)	120.7
A(8-7-9)	103.8

Table S18.4 Optimized geometry (Å, deg) parameters for propynal -water complex at the W1U level including vibrational frequencies (cm⁻¹)

R(1-2)	1.201
R(1-4)	1.440
R(2-3)	1.062
R(4-5)	1.213
R(4-6)	1.101
R(7-8)	0.961
R(7-9)	0.968
A(2-1-4)	177.4
A(1-2-3)	179.0
A(1-4-5)	123.4
A(1-4-6)	115.7
A(5-4-6)	120.8
A(8-7-9)	104.6

Methylene ketene-water complex

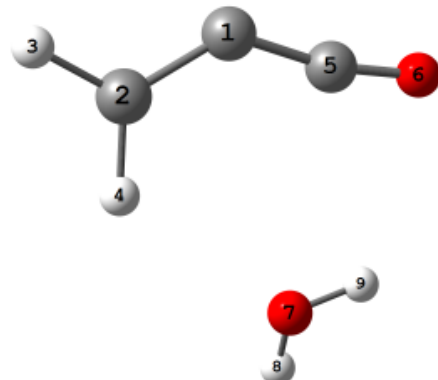


Figure 18: Optimized structure of methylene ketene -water complex

Table S19.1 Optimized geometry (Å, deg) parameters for methylene ketene -water complex at the MP2(full)/6-311++G** level including vibrational frequencies (cm⁻¹)

R(1-2)	1.343
R(1-5)	1.318
R(2-3)	1.088
R(2-4)	1.090
R(5-6)	1.174
R(7-8)	0.960
R(7-9)	0.961
A(2-1-5)	133.4

A(1-2-3)	120.9
A(1-2-4)	121.6
A(1-5-6)	168.7
A(3-2-4)	117.5
A(8-7-9)	103.6
W1(A)	57.4
W2(A)	85.6
W3(A)	102.2
W4(A)	128.0
W5(A)	167.1
W6(A)	204.7
W7(A)	230.8
W8(A)	300.3
W9(A)	551.6
W10(A)	722.7
W11(A)	960.8
W12(A)	1017.0
W13(A)	1103.7
W14(A)	1488.1
W15(A)	1642.0
W16(A)	1695.9
W17(A)	2193.7
W18(A)	3138.5
W19(A)	3234.8
W20(A)	3871.1
W21(A)	3988.3

Table S19.2 Optimized geometry (Å, deg) parameters for methylene ketene-water complex at the MP2(full)/aug-cc-pVDZ level including vibrational frequencies (cm⁻¹)

R(1-2)	1.354
R(1-5)	1.333
R(2-3)	1.095
R(2-4)	1.097
R(5-6)	1.184
R(7-8)	0.965
R(7-9)	0.967
A(2-1-5)	132.0
A(1-2-3)	120.7
A(1-2-4)	121.6
A(1-5-6)	168.0
A(3-2-4)	117.7
A(8-7-9)	104.2
W1(A)	61.0
W2(A)	104.7
W3(A)	115.2
W4(A)	140.1
W5(A)	212.8
W6(A)	221.1

W7(A)	235.3
W8(A)	302.3
W9(A)	546.0
W10(A)	724.3
W11(A)	958.1
W12(A)	1037.7
W13(A)	1089.2
W14(A)	1468.8
W15(A)	1628.8
W16(A)	1678.2
W17(A)	2151.7
W18(A)	3139.2
W19(A)	3243.8
W20(A)	3785.9
W21(A)	3921.4

Table S19.3 Optimized geometry (Å, deg) parameters for methylene ketene -water complex at the G4 level including vibrational frequencies (cm⁻¹)

R(1-2)	1.323
R(1-5)	1.289
R(2-3)	1.090
R(2-4)	1.091
R(5-6)	1.173
R(7-8)	0.963
R(7-9)	0.963
A(2-1-5)	150.4
A(1-2-3)	121.5
A(1-2-4)	121.5
A(1-5-6)	170.8
A(3-2-4)	117.1
A(8-7-9)	103.7

Table S19.4 Optimized geometry (Å, deg) parameters for methylene ketene -water complex at the W1U level including vibrational frequencies (cm⁻¹)

R(1-2)	1.321
R(1-5)	1.287
R(2-3)	1.087
R(2-4)	1.089
R(5-6)	1.171
R(7-8)	0.962
R(7-9)	0.962
A(2-1-5)	152.3
A(1-2-3)	121.0
A(1-2-4)	122.9
A(1-5-6)	171.0
A(3-2-4)	116.1
A(8-7-9)	104.8

Ethynol-water complex

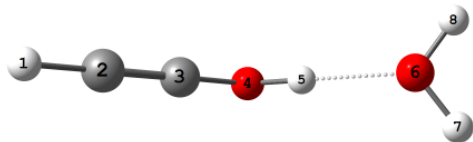


Figure 19: Optimized structure of ethynol -water complex

Table S20.1 Optimized geometry (Å, deg) parameters for ethynol-water complex at the MP2(full)/6-311++G** level including vibrational frequencies (cm⁻¹)

R(1-2)	1.061
R(2-3)	1.215
R(3-4)	1.306
R(4-5)	0.978
R(6-7)	0.960
R(6-8)	0.960
R(5-6)	1.745
A(1-2-3)	179.4
A(2-3-4)	176.9
A(3-4-5)	108.9
A(4-5-6)	177.5
A(7-6-8)	105.0
A(7-6-5)	120.8
A(8-6-5)	120.8
W1(A)	33.5
W2(A)	74.4
W3(A)	215.0
W4(A)	251.9
W5(A)	265.4
W6(A)	382.8
W7(A)	425.4
W8(A)	537.2
W9(A)	609.9
W10(A)	810.6
W11(A)	1096.9
W12(A)	1370.0
W13(A)	1641.5
W14(A)	2223.8
W15(A)	3534.9
W16(A)	3574.4
W17(A)	3876.9
W18(A)	3992.7

Table S20.2 Optimized geometry (Å, deg) parameters for ethynol-water complex at the MP2(full)/aug-cc-pVDZ level including vibrational frequencies (cm⁻¹)

R(1-2)	1.071
R(2-3)	1.231
R(3-4)	1.316
R(4-5)	0.988
R(6-7)	0.967
R(6-8)	0.968
R(5-6)	1.745
A(1-2-3)	178.3
A(2-3-4)	178.2
A(3-4-5)	107.2
A(4-5-6)	167.1
A(7-6-8)	104.4
A(7-6-5)	115.5
A(8-6-5)	106.4
W1(A)	28.8
W2(A)	84.7
W3(A)	238.3
W4(A)	270.1
W5(A)	282.0
W6(A)	321.2
W7(A)	394.9
W8(A)	491.7
W9(A)	536.7
W10(A)	749.5
W11(A)	1073.6
W12(A)	1403.0
W13(A)	1628.4
W14(A)	2191.6
W15(A)	3425.6
W16(A)	3509.4
W17(A)	3784.2
W18(A)	3910.7

Table S20.3 Optimized geometry (Å, deg) parameters for ethynol-water complex at the G4 level including vibrational frequencies (cm⁻¹)

R(1-2)	1.060
R(2-3)	1.203
R(3-4)	1.299
R(4-5)	0.988
R(6-7)	0.964
R(6-8)	0.966
R(5-6)	1.755
A(1-2-3)	177.7
A(2-3-4)	179.6
A(3-4-5)	107.4
A(4-5-6)	157.4
A(7-6-8)	104.4
A(7-6-5)	108.1
A(8-6-5)	95.8

Table S20.4 Optimized geometry (Å, deg) parameters for ethynol -water complex at the W1U level including vibrational frequencies (cm⁻¹)

R(1-2)	1.059
R(2-3)	1.199
R(3-4)	1.300
R(4-5)	0.985
R(6-7)	0.962
R(6-8)	0.962
R(5-6)	1.728
A(1-2-3)	179.4
A(2-3-4)	176.6
A(3-4-5)	111.4
A(4-5-6)	176.3
A(7-6-8)	106.0
A(7-6-5)	115.9
A(8-6-5)	115.2

Ketene-water complex

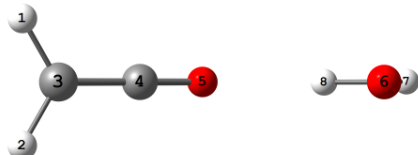


Figure 20: Optimized structure of ethynol-water complex

Table S21.1 Optimized geometry (Å, deg) parameters for ethynol-water complex at the MP2(full)/6-311++G** level including vibrational frequencies (cm⁻¹)

R(1-3)	1.080
R(2-3)	1.080
R(3-4)	1.317
R(4-5)	1.170
R(6-7)	0.959
R(6-8)	0.961
A(1-3-2)	121.8
A(1-3-4)	119.1
A(2-3-4)	119.1
A(3-4-5)	179.7
A(7-6-8)	103.5
W1(A)	23.5
W2(A)	48.3
W3(A)	62.8
W4(A)	114.5
W5(A)	176.5
W6(A)	321.0
W7(A)	440.2

W8(A)	457.9
W9(A)	576.8
W10(A)	983.5
W11(A)	1158.3
W12(A)	1409.6
W13(A)	1640.4
W14(A)	2221.1
W15(A)	3234.3
W16(A)	3346.6
W17(A)	3879.0
W18(A)	3995.2

Table S21.2 Optimized geometry (Å, deg) parameters for ethynol-water complex at the MP2(full)/aug-cc-pVDZ level including vibrational frequencies (cm⁻¹)

R(1-3)	1.087
R(2-3)	1.087
R(3-4)	1.330
R(4-5)	1.180
R(6-7)	0.965
R(6-8)	0.967
A(1-3-2)	122.2
A(1-3-4)	118.9
A(2-3-4)	118.9
A(3-4-5)	179.6
A(7-6-8)	104.1
W1(A)	6.0
W2(A)	53.2
W3(A)	59.8
W4(A)	116.6
W5(A)	185.1
W6(A)	352.0
W7(A)	432.4
W8(A)	504.2
W9(A)	583.6
W10(A)	975.7
W11(A)	1146.8
W12(A)	1398.8
W13(A)	1629.1
W14(A)	2183.9
W15(A)	3232.1
W16(A)	3352.4
W17(A)	3789.1
W18(A)	3925.3

Table S21.3 Optimized geometry (Å, deg) parameters for ethynol-water complex at the G4 level including vibrational frequencies (cm⁻¹)

R(1-3)	1.081
--------	-------

R(2-3)	1.081
R(3-4)	1.305
R(4-5)	1.167
R(6-7)	0.962
R(6-8)	0.964
A(1-3-2)	120.6
A(1-3-4)	119.7
A(2-3-4)	119.7
A(3-4-5)	179.7
A(7-6-8)	103.5

Table S21.4 Optimized geometry (Å, deg) parameters for ethynol -water complex at the W1U level including vibrational frequencies (cm⁻¹)

R(1-3)	1.079
R(2-3)	1.083
R(3-4)	1.306
R(4-5)	1.163
R(6-7)	0.961
R(6-8)	0.961
A(1-3-2)	120.8
A(1-3-4)	119.2
A(2-3-4)	119.9
A(3-4-5)	179.7
A(7-6-8)	105.3

Linear Interstellar Carbon Chains: The Dominant Theme in Interstellar Chemistry

Setting the stage: *Linear carbon chains remain* the dominant theme in interstellar chemistry. These set of molecules account for more than 20% of all the known interstellar and circumstellar molecular species. Of course more of the linear carbon chains are expected to be detected in ISM as nature continues to be in love with the carbon-carbon bond when synthesizing larger molecular species both on earth and in the ISM. This chapter is divided into two main parts. The first part discusses the spectroscopic parameters needed for the astronomical observation of these species. Although the linear carbon chains are molecules of astrophysical importance but are there preferences with respect to astronomical searches; are there some that are more likely to be detected at the expense of others? The second part of this chapter addresses these questions by employing thermodynamics to account for the known linear carbon chains and examine the possible candidates for astronomical searches from the different linear chains.

Accurate Rotational Constants for linear Interstellar Carbon Chains: Achieving Experimental Accuracy

5.0 Introduction: The rapid growth in the field of astrochemistry in the last few decades as a result of the advances in technology, astronomical and spectroscopic instruments and the strong collaborative efforts of laboratory spectroscopists, theoretical chemists, astrophysicist and astronomers have led to the realization that both chemistry and biology are as important as physics in our understanding of the Universe and our place in it. Though molecules constitute a minor component of the total mass of the Universe; their profound effect and influence in the development of the Universe cannot be overemphasized. These have fueled the interest in the study of molecules in space, leading to the unique astronomical detection of over 200 different molecular species in the interstellar medium and circumstellar envelopes.¹⁻³ With hydrogen being the most dominant constituent of the interstellar molecular clouds, the prevalence of highly unsaturated carbon chain molecular species in the interstellar medium (ISM) and the circumstellar shells remains a surprise. Of the over 200 different interstellar and circumstellar molecular species, only about 10 are cyclic: c-SiC₂, c-C₃H, c-C₃H₂, c-H₂C₃O, c-C₂H₄O, 2H-azirine (an unconfirmed claimed observation), benzene, C₆₀, C₇₀ and C₆₀⁺.⁴⁻¹¹, while the rest are straight chain molecules with only one currently known branched chain molecule: isopropyl cyanide¹². Among the straight chain molecules, linear carbon chain molecular species of different classes: C_n, H₂C_n, HC_nN and C_nX (X=N, O, Si, S, H, P, H⁻) are very conspicuous ranging from the simple species to the complex species (with six atoms and above) up to HC₁₁N; the largest known interstellar molecules.¹³⁻²² These set of molecules account for more than 20% of all the known interstellar and circumstellar molecular species.

Linear carbon chains remain the dominant theme in interstellar chemistry. Different studies: modelling, experimental, theoretical and astronomical observations have predicted the detectability of more linear carbon chains. However, the availability of accurate spectroscopic parameters is a core requirement for any successful astronomical detection of a molecule. Despite the fact that molecules have electronic, rotational and vibrational transitions, the rotational transitions are particularly important for the chemical examination of the interstellar medium. Over 80% of all the known molecules in ISM have been detected via their rotational transitions,³ because at the low temperatures of the interstellar medium, excited rotational levels are populated unlike the vibrational transitions that rely on occasional excitation by high energy photons emitted by hot stars in the vicinity of the molecular clouds. In spite of the advancement in spectroscopic instrumentations, probing the rotational spectra of some of these carbon chain radicals and ions experimentally is still a difficult task as revealed by the dearth of experimental data for some of these important linear carbon chains.

Among the different classes of carbon chain molecules; the cyanopolyyynes, HC_{2n+1}N, are well known constituents of different interstellar molecular clouds with successive members up to n=5 already observed in the interstellar space while HC₂N and HC₄N have also been observed from the HC_{2n}N chain²³⁻³⁰. The astronomical detection of these molecules and of

course for every other astromolecule rely on the availability of accurate rotational transitions as already mentioned above except for the microwave inactive chains like HC_nH , C_n , etc., which are observed through their infrared vibrational transitions. The unstable nature of some of the carbon chain molecules under terrestrial conditions makes the laboratory measurement of their rotational microwave spectra difficult.

The application of Fourier transform microwave spectroscopy (FTMS) to supersonic molecular beams brought a partial relieve to this problem. Spectra of large interstellar molecules which are very complex at room temperature become simpler and are easily observed in the molecular beam with temperature as low as 1 K. Electri discharge nozzles are used in the laboratory to synthesis these molecular species. The different microwave spectroscopy groups have played a pivotal role in providing accurate rotational transitions for the astronomical observation of the different interstellar molecules³¹⁻³³. However, the battle is not yet won. A number of molecular species that are believed not only to be present in ISM but also to be playing important role in the formation process of other molecular species are yet to be experimentally probed because of their unstable nature. This of course hinders their astronomical observation. Focusing here on the HC_nN chains, their isocyanide and deuterated analogues; the HC_{2n+1}N have been experimentally probed up to $n=8$; the HC_{2n}N chains are known for $n=1,2,3$ and 4 and few of the deuterated analogues of HC_nN are known.^{13,23-33} But for the $\text{HC}_{2n+1}\text{NC}$ chains, there is no available literature regarding their laboratory measured rotational transitions. The difficulty in probing the rotational transitions of the isocyanide analogues of HC_nN is directly due to their unstable nature as compared to the cyanides.

The HC_{2n+1}N chains are thought to be formed from their protonated analogues; $\text{HC}_{2n+1}\text{NH}^+$ via the dissociative recombination of the cations with an electron³⁴⁻³⁶. These protonated species are not only helpful as major players in interstellar chemical reactions; they are also useful probes for their neutral non-polar analogues (that easily evade astronomical detection) and for chemical modeling of interstellar chemical processes. As important as these protonated species are, only HCNH^+ and HC_3NH^+ have been astronomically observed^{35,36} and these are also the only members of the $\text{HC}_{2n+1}\text{NH}^+$ chain with experimentally known rotational transitions which invariably implies that the astronomical observation of the higher members of the chain await the availability of their accurate rotational transitions. But the highly unstable nature of these ions makes it difficult to have enough concentration of these ions in the gas phase required for the measurement of their rotational transitions.

Theoretical predictions of spectroscopic parameters have been instrumental for probing molecules both in the terrestrial laboratory and in ISM. Of course, theoretical tools have been shown to be effective in guiding successful astronomical detection of molecules with no laboratory measured transitions. That a number of molecules such as HNC , HCO^+ , HOC^+ , N_2H^+ , C_3N , HCNH^+ , C_2H , etc., were first detected in ISM before their identification in the terrestrial laboratory attests to this fact^{35,37-42}. But the accuracy of these predictions depends on a number of factors: the theoretical method, geometry of the molecule, parameters of interest, etc. Thus, finding the appropriate method(s) for accurate predictions of spectroscopic parameters for different classes of molecules of interest in astrochemistry remains a great challenge.

For linear molecules like the HC_nN , HC_nNH^+ chains in which all the atoms are arranged in a straight line; the rotational constant, B and the moment of inertia, I are inversely proportional to each other and are related as follows:

$$B \text{ (Hz)} = h/8\pi^2 I \dots \text{ (equation 1)}$$

where h is the Planck's constant.

The present work aims at accurate estimation of rotational constants for linear molecules of interest in astrochemistry; HC_nN ($n=1$ to 20), DC_{2n+1}N ($n=0$ to 9), HC_{2n}NC ($n=0$ to 9), C_nO , C_nS , HC_nS , C_nN , C_nH , C_nSi (with $n=1$ to 20), C_{2n}H^- , $\text{C}_{2n-1}\text{N}^-$, $\text{CH}_3(\text{CC})_n\text{H}$ (with $n=1$ to 10), and $\text{CH}_3(\text{C}\equiv\text{C})_n\text{CN}$ ($n=0$ to 9) by the use of the simple relationship above (equation 1) alongside few experimentally known rotational constant. Details of the methodology employed are described in the next section after which the obtained results are presented and discussed.

5. 1 Methodology

The basic approach employed in this work for estimating accurate rotational constant for the linear molecules is by calculating the moments of inertia of the different molecular systems using the optimized geometries obtained at Hartree Fock (HF) level with the 6-311++G** basis set without any experimentally measured bond length. The difference; ΔI between the calculated moments of inertia; I_{cal} and the experimental moments of inertia I_{exp} obtained using equation 1 is fitted into a polynomial. The corrected moments of inertia, I_{cor} for the chain of interest; say ${}^nI_{\text{cor}}$ is obtained as the sum of the calculated moment of inertia (${}^nI_{\text{cal}}$) and the solution of the polynomial (σ_n) corresponding to the chain length of interest.

All quantum chemical calculations are carried out using the Gaussian 09 suite of programs⁴³. Equilibrium rotational constants are calculated for all the linear molecules using the Hartree Fock method with the 6-311++G** basis set to monitor the trend in the difference between the experimental (where available) rotational constants and the calculated (those obtained using I_{cor}) rotational constants. The diffuse functions in the basis set allow the orbitals to occupy a larger region of space while the polarization functions give additional flexibility to the description of molecular orbitals⁴⁴⁻⁴⁷. In all the computational calculations, only stable structures with no imaginary frequency are used. The specific assumption(s) on the geometries for the different linear carbon chains systems investigated in this study and the obtained results are presented and discussed in the next section.

5.2 Results and Discussion

The results obtained for the different linear chain carbon systems HC_nN ($n = 1$ to 20), DC_{2n+1}N ($n = 0$ to 9), HC_{2n}NC ($n = 0$ to 9), C_nO , C_nS , HC_nS , C_nN , C_nH , C_nSi (with $n = 1$ to 20), C_{2n}H^- , $\text{C}_{2n-1}\text{N}^-$, $\text{CH}_3(\text{CC})_n\text{H}$ (with $n = 1$ to 10), and $\text{CH}_3(\text{C}\equiv\text{C})_n\text{CN}$ ($n = 0$ to 9) based on the methodology described above are discussed for each set of carbon chains.

5.2.1 HC_{2n+1}N linear carbon chains: Experimentally, the HC_{2n+1}N linear carbon chains are known up to $n=8$.⁴⁸⁻⁵⁴ Table 5.1 shows the experimental moments of inertia, I_{exp} for all the known members of the chain calculated from equation 1 using the experimental rotational constant, the calculated moments of inertia; I_{cal} estimated from the optimized geometry at the Hartree Fock level with the 6-311++G** basis set and the difference between the two sets of moments of inertia. The moments of inertia are reported in Atomic units, AU, (amu \AA^2). The alternating single and triple bond in the $\text{H}-(\text{C}\equiv\text{C})_n-\text{CN}$ chain is assumed to be consistent irrespective of n .

Assuming that the HC_{2n+1}N chains are only known up to $n=3$, the 4 data points corresponding to ΔI for HCN , HC_3N , HC_5N and HC_7N are fitted into a polynomial to predict the higher members of the chain. Table 5.2 shows the corrected moments of inertia; I_{cor} for the higher members of the chain from $n=4$ to 9, the rotational constants calculated from these corrected moments of inertia, the difference between the calculated and the experimentally measured rotational constant (where available).

From Table 5.2, the difference between experimentally measured rotational and the calculated rotational constants (using I_{cor}) ranges from 0.007266 MHz (7.266 KHz) to 0.010958 MHz (10.958 KHz) in all the chains with known experimental constants. This surprisingly high accuracy which is within experimental accuracy for the calculated rotational constants with experimentally measured values signals the same level of accuracy for the HC_{19}N with no experimental value and for higher members of the chain that can be calculated via this approach. HC_{11}N remains the longest carbon chain interstellar molecules. With the availability of accurate rotational constants for higher members of the chain, their astronomical observation is a function of time.

The reported accuracy of 10 KHz and below in this study is far from the reach of the currently known ab initio, DFT and other computational methods. Among the available computational methods, the coupled cluster method with single and double excitation operators plus a perturbative treatment of the effects of connected triple substitutions, CCSD(T) is highly regarded as the "gold standard" for obtaining accurate spectroscopic parameters. The reported rotational constants for these HC_{2n+1}N chains and their protonated analogues at the CCSD(T) level have accuracy in the range of 0.5 to 1 MHz (500 to 1000 KHz) and above⁵⁵⁻⁵⁷. Thus, the approach employed in this study does not only offer highly accurate predictions of the rotational constant but it is very inexpensive as compared to the CCSD(T) calculations which require so much computational resources and time.

In Table 5.3, the equilibrium rotational constants (B_{eHF}^*) for the HC_{2n+1}N chains calculated at the HF level with the 6-311++G** basis set are reported. The difference (ΔB^{++}) between these B_{eHF}^* values and those calculated from the corrected moments of inertia serves as another way of monitoring the accuracy of the calculated rotational constants for the chains with no experimentally measured values. The difference between the B_{eHF}^* and B_{exp} values represented as ΔB^{++} is compared to the ΔB^+ for systems with known experimental values. From Table 5.3, the difference between the HF/6-311++G** rotational constants and the

experimentally measured constants or those calculated in this work shows a steady decrease as the change length increases. Thus, the longer the chain, the more the equilibrium rotational constant approaches the experimental ground state rotational constant. For the HC_{19}N with no experimental rotational, the difference between the HF/6-311++G** equilibrium rotational constant and the calculated rotational constant further shows the accuracy of the calculated rotational constant of 37.063306 MHz for HC_{19}N .

Table 5.1: Experimental rotational constants and moments of inertia for $\text{H-(C}\equiv\text{C)}_n\text{-CN}$ linear carbon chains

n	B_{exp} (MHz)	I_{exp} (AU)	I_{cal} (AU)	ΔI (AU)
0	44,315.970 ⁴⁸	40.724072	38.925480	1.798592
1	4,459.058 ⁴⁹	396.725377	389.500620	7.224767
2	1,331.3313 ⁵⁰	1,355.580500	1,338.952580	16.627918
3	564.00112 ⁵¹	3,199.863768	3,168.715820	31.147948
4	290.518322 ⁵²	6,212.092706	6,160.400920	51.691786
5	169.06295 ⁵²	10,674.880270	10,595.534230	79.346045
6	106.97258 ⁵³	16,870.928500	16,756.046540	114.881956
7	71.950133 ⁵⁴	25,083.021720	24,924.410960	158.610757
8	50.70323 ⁵⁴	35,593.920720	35,380.555370	213.365347

Table 5.2: Calculated parameters for $\text{H-(C}\equiv\text{C)}_n\text{-CN}$ linear carbon chains

n	σ (AU)	I_{cor} (AU)	B_{exp} (MHz)	B_{cal} (MHz)	ΔB (MHz)
4	51.914	6212.31492	290.518322 ⁴⁹	290.507930	0.0104
5	80.038	10,675.57223	169.062950 ⁴⁹	169.051992	0.0110
6	116.465	16,872.51154	106.972580 ⁵⁰	106.962544	0.0100
7	162.284	25,086.69494	71.950133 ⁵¹	71.939598	0.0105
8	218.467	35,599.02237	50.703230 ⁵¹	50.695964	0.0073
9	285.631	48,693.08631	-	37.063306	

Table 5.3: Equilibrium rotational constants for $\text{H-(C}\equiv\text{C)}_n\text{-CN}$ linear carbon chains obtained from HF/6-311++G**

n	B_{eHF}^* (MHz)	ΔB^+ (MHz)	ΔB^{++} (MHz)
0	46,364.0020	2,048.032	-
1	4,633.4750	84.4170	-
2	1,347.8750	16.5437	-
3	569.5500	5.5489	-
4	292.9580	2.4397	2.4501
5	170.3290	1.2660	1.2770
6	107.7060	0.7334	0.7435
7	72.4080	0.4579	0.4684
8	51.0090	0.3058	0.3130
9	37.2820	-	0.2187

*Equilibrium rotational constant, B obtained from HF/6-311++G**; $\Delta B^+ = B_{\text{exp}} - B_{\text{eHF}}$; $\Delta B^{++} = B_{\text{cal}} - B_{\text{eHF}}$.

5.2.2 $DC_{2n+1}N$ linear carbon chains: Among the known isotopologues of interstellar and circumstellar molecules, deuterated molecules are the most detected of all interstellar and circumstellar isotopologues. In one way, this could be understood from the overwhelming high abundance of hydrogen in interstellar space but in another way, it is quite amazing considering the cosmic D/H ratio which is only of the order of 10^{-5} . The D/H ratio on earth (1.6×10^{-4}) is about 10 times higher than the cosmic ratio. The $DC_{2n+1}N$ chains are deuterated isotopologues of the $HC_{2n+1}N$ linear carbon chains discussed above. These deuterated isotopologues have been detected experimentally up to $n=5$ and the first three members of the chain; DCN, DC_3N and DC_5N have been astronomically detected^{58-62, 50, 52}. As in the case of the $HC_{2n+1}N$ linear carbon chains, the alternating triple and single bond in $DC_{2n+1}N$ is assumed to be consistent, the chain length notwithstanding.

Table 5.4 shows the moments of inertia obtained from the experimental rotational constants, those obtained from the optimized geometry at the HF level with the 6-311++G** basis set and the difference between these sets of moments of inertia, ΔI . On the assumption that the $DC_{2n+1}N$ chains are only known experimentally up to $n=3$, the ΔI values corresponding to these chains are utilized in predicting the rotational constants for higher members of the chain. Fitting these ΔI values into a polynomial, the corrected moments of inertia (I_{cor}) are obtained and these are used to predict the rotational constants for higher members of the chains as presented in Table 5.5.

As shown in Table 5.5, the accuracy of the predicted rotational constants for DC_9N and $DC_{11}N$ that are experimentally known ranges from 0.010142 to 0.011071 MHz which within experimental accuracy from astrophysical, spectroscopic and chemical perspectives. The accurate rotational constants predicted for the chains with known experimental values inform the aimed accurate predictions for the chains with no experimental rotational constants. Thus, the predicted rotational constants $DC_{13}N$, $DC_{15}N$, $DC_{17}N$ and $DC_{19}N$ (Table 5.5) are expected to have an accuracy of about 0.010 MHz which is suitable for the astronomical searches of these potential interstellar molecules and for other applications that demand highly accurate rotational constants for these carbon chains. Table 5.6 shows the difference between the Hartree Fock equilibrium rotational constants and the experimental; and calculated rotational constants.

Table 5.4: Experimental rotational constants and moments of inertia for $DC_{2n+1}N$ linear carbon chains

n	B_{exp} (MHz)	I_{exp} (AU)	I_{cal} (AU)	ΔI (AU)
0	$36,207.500^{58}$	49.844003	47.830680	2.013324
1	$4,221.580858^{59}$	427.500221	419.842050	7.658171
2	$1,271.0570^{50}$	1,419.862956	1,402.51086	17.352096
3	545.31530^{52}	3,309.510994	3,277.28086	32.230134
4	282.918520^{52}	6,378.962922	6,325.77860	53.184322
5	165.40690^{52}	10,910.831100	10,829.508420	81.322682

Table 5.5: Calculated parameters for DC_{2n+1}N linear carbon chains

n	σ (AU)	I_{cor} (AU)	B_{exp} (MHz)	B_{cal} (MHz)	ΔB (MHz)
4	53.413000	6,379.191900	282.918520 ⁴⁹	282.908378	0.0101
5	82.053000	10,911.561420	165.406900 ⁴⁹	165.393829	0.0111
6	118.199000	17,188.692830	-	104.994997	-
7	162.792000	25,493.712320	-	70.791053	-
8	218.344000	36,109.733710	-	49.978955	-
9	285.084000	49,319.9094	-	36.59256	-

Table 5.6: Equilibrium rotational constants for DC_{2n+1}N linear carbon chains obtained from HF/6-311++G**

n	B_{eHF}^* (MHz)	ΔB^+ (MHz)	ΔB^{++} (MHz)
0	37,731.8750	1,524.3750	-
1	4,298.6190	77.0381	-
2	1,286.7930	15.7360	-
3	550.6820	5.3668	-
4	285.2990	2.3805	2.3906
5	166.6490	1.2421	1.2552
6	105.7220	-	0.7270
7	71.2460	-	0.4549
8	50.2830	-	0.3040
9	36.805000	-	0.2124

*Ground state rotational constant, B obtained from HF/6-311++G**; $^+B_{\text{exp}} - B_{\text{eHF}}$; $^{++}B_{\text{cal}} - B_{\text{eHF}}$.

5.2 3 HC_{2n}N linear chains: The HC_{2n}N linear carbon chains are the even numbered chains of the HC_nN chains which are known to be less stable than the corresponding odd numbered chains. This unstable nature of the HC_{2n}N linear carbon chains influences both their laboratory and astronomical detections. Whereas the odd numbered chains have been detected up to HC₁₇N experimentally, HC₈N is highest known member of the chain in the terrestrial laboratory. Astronomically, the first two members (HC₂N and HC₄N) of the HC_{2n}N linear carbon chains have been detected.^{29,30,33,63-65}

In Table 5.7, the moments of inertia; calculated from the experimental rotational constants and the optimized geometries at the HF/6-311++G** level are presented together with the difference between the two sets of moments of inertia. The bonding in HC_{2n}N is cumulenic in nature (repeated double bonds) and this is assumed to be consistent irrespective of the chain length. By fitting the difference in the moments of inertia (ΔI) into a polynomial, rotational constants are estimated for higher members of the chain. The first three ΔI values are fitted into a quadratic polynomial to predict the rotational constant for the next higher member; HC₈N which is experimentally known. At each stage, the new ΔI value calculated from I_{cor} and I_{cal} is added into the data point to predict the next higher member of the chain. This

steady increase in the data point has a positive effect on the accuracy of the predicted rotational constants.

Table 5.7: Experimental rotational constants and moments of inertia for HC_{2n}N linear carbon chains

n	B_{exp} (MHz)	I_{exp} (AU)	I_{cal} (AU)	ΔI (AU)
1	10,986.407300 ⁶³	164.269055	159.39502	4.874035
2	2,302.398020 ³³	783.849649	771.225680	12.623969
3	841.307280 ⁶⁴	2,145.145765	2,115.711820	29.433945
4	398.547430 ⁶⁵	4,528.260912	4,473.070310	55.190602

Table 5.8 shows the estimated rotational constants for the HC_{2n}N linear chains from $n=4$ to 10 obtained from the corrected moments of inertia. These predicted rotational constants are estimated to have accuracy of about 10 kHz. If only the first three data points (ΔI values) could predict HC_8N to an accuracy of less than 10 kHz, then an accuracy of 10 kHz for these chains is reasonable. Though the HC_{2n}N chains are difficult to be detected in the terrestrial laboratory; their presence in interstellar space is undoubtable and with HC_2N and HC_4N already observed; higher members of the chain remain potential candidates for astronomical observation with the availability of accurate spectroscopic constants as presented in this study. Table 5.9 contains the equilibrium rotational constants for the HC_{2n}N chains obtained at the Hartree Fock level with the 6-311++G** basis set. The trend in the difference between the $B_{\text{exp}} - B_{\text{eHF}}$ and the $B_{\text{cal}} - B_{\text{eHF}}$ is as observed in the previous cases.

Table 5.8: Calculated parameters for HC_{2n}N linear carbon chains

n	σ (AU)	I_{cor} (AU)	B_{exp} (MHz)	B_{cal} (MHz)	ΔB (MHz)
4	55.3010	4,528.371310	398.547430	398.537714	0.0097
5	89.9640	8,213.93122	-	219.715347	-
6	130.1380	13,481.4737	-	133.867171	-
7	172.8910	20,608.463890	-	87.572114	-
8	213.1510	29876.641290	-	60.405945	-
9	243.7150	41,555.044690	-	43.429787	-
10	262.1570	55,932.671810	-	32.266056	-

Table 5.9: Equilibrium rotational constants for HC_{2n}N linear carbon chains obtained from HF/6-311++G**

n	B_{eHF}^* (MHz)	ΔB^+ (MHz)	ΔB^{++} (MHz)
1	11,322.4440	336.036700	-
2	2,340.0950	37.696980	-
3	853.0180	11.710720	-
4	403.4680	4.920570	4.9303
5	222.1460	-	2.4306
6	135.1720	-	1.3048
7	88.3130	-	0.7409

8	60.8400	-	0.4340
9	43.6860	-	0.2562
10	32.4180	-	0.1519

*Ground state rotational constant, B obtained from HF/6-311++G**; ${}^+B_{exp} - B_{eHF}$; ${}^{++}B_{cal} - B_{eHF}$.

5.2.4 $HC_{2n}NC$ linear carbon chains: The $HC_{2n}NC$ are the isocyanide analogues of the $HC_{2n+1}N$ chains. Of course these isocyanides are less stable than their corresponding cyanides. HNC and HC_2NC are known interstellar molecules. In the terrestrial laboratory, the $HC_{2n}NC$ linear chains are known up to $n=3$.^{66,67,68} As the chain increases, the difficulty in probing these molecules in the laboratory becomes higher. As in the case of $HC_{2n}N$, the middle carbon atoms are assumed to be cumulenic in nature irrespective of the chain length.

Fitting the four ΔI values (Table 5.10) into a polynomial, the calculated moments of inertia for the higher members of the chain are corrected and these corrected moments of inertia are used in predicting accurate rotational for the higher members of the chain with no experimental rotational constant. As in all the cases shown above, these predicted rotational constants (Table 5.11) are expected to be highly accurate with an uncertainty in the range of 10kHz which is extremely good for their astronomical observation. As a way of monitoring the accuracy of the calculated rotational constants, equilibrium rotational constants, B_{eHF} calculated for $HC_{2n}NC$ linear carbon chains from $n=4$ are computational estimated at the HF level with the 6-311++G** basis set (Table 5.12). The trend in the difference between the $B_{exp} - B_{eHF}$ and the $B_{cal} - B_{eHF}$ is consistently decreasing as the chain length increases as noted in the previous cases.

Table 5.10: Experimental rotational constants and moments of inertia for $HC_{2n}NC$ linear carbon chains

n	B_{exp} (MHz)	I_{exp} (AU)	I_{cal} (AU)	ΔI (AU)
0	$45,331.7860^{66}$	39.81150774	38.464090	1.347418
1	$4,967.8370^{67}$	363.2821989	356.381930	6.900269
2	$1,401.18227^{68}$	1,285.251059	1,271.293380	13.957679
3	582.5203^{68}	3098.135377	3066.792210	31.343167

Table 5.11: Calculated parameters for $HC_{2n}NC$ linear carbon chains

n	σ (AU)	I_{cor} (AU)	B_{cal} (MHz)
4	67.8740	6,092.211070	296.2351
5	132.3670	10,557.082510	170.9494
6	233.4930	16,784.697150	107.5221
7	381.5990	25,066.011260	71.9990
8	550.2360	35,656.870290	50.6137
9	739.2430	48,838.354140	36.9531

Table 5.12: Equilibrium rotational constants for HC_{2n}NC linear carbon chains obtained from HF/6-311++G**

n	$B_{\text{eHF}}^*(\text{MHz})$	$\Delta B^+(\text{MHz})$	$\Delta B^{++}(\text{MHz})$
0	46,920.1540	1,588.3680	-
1	5,064.0650	96.2280	-
2	1,419.6100	18.4277	-
3	588.4780	5.9577	-
4	299.5750	-	3.3399
5	173.1200	-	2.1706
6	109.0390	-	1.5168
7	73.11200	-	1.11304
8	51.4070	-	0.7933
9	37.5210	-	0.5679

*Ground state rotational constant, B obtained from HF/6-311++G**; ${}^+B_{\text{exp}}$ -BeHF; ${}^{++}B_{\text{cal}}$ -BeHF.

5.2.5 $\text{CH}_3(\text{C}\equiv\text{C})_n\text{CN}$ Linear Carbon Chains: Methylcyanopolyyynes, $\text{CH}_3(\text{C}\equiv\text{C})_n\text{CN}$ are the methyl analogues of the cyanopolyyynes with alternating single and triple bond terminated by a methyl group at one end and cyano group at the other end. The first three members; CH_3CN , $\text{CH}_3\text{C}_3\text{N}$ and $\text{CH}_3\text{C}_5\text{N}$ of the methylcyanopolyyynes have been detected in interstellar space.^{72,73,74} With the chemical and structural similarities between the methylcyanopolyyynes and the cyanopolyyynes which have been astronomically observed up to HC_{11}N , the higher members of the methylcyanopolyyynes remain potential interstellar molecules. As presented in Table 5.13, the methylcyanopolyyynes have been experimentally detected up to $\text{CH}_3(\text{C}\equiv\text{C})_5\text{CN}$, thus making available 6 ΔI values which are more than enough for the accurate prediction of the higher member of this family.

Fitting the first four ΔI values into a polynomial, accurate rotational constants are predicted from the corrected moments of inertia for the higher members of the chain (both the experimentally known and the once that are not yet probed in the terrestrial laboratory). For the experimentally known chains; $\text{CH}_3\text{C}_{11}\text{N}$ and $\text{CH}_3\text{C}_9\text{N}$, an accuracy of 7.321 and 8.348 kHz (in that order) are obtained from the calculations which are far better than what the high level ab initio methods can offer. The obtained accuracy here is well within experimental accuracy. Table 5.14 contains the predicted rotational constants for higher members of the $\text{CH}_3(\text{C}\equiv\text{C})_n\text{CN}$ linear chains. These predicted rotational constants are expected to be very accurate and are thus, excellent tools for the astronomical searches and possible observation of these potential astromolecules. Table 5.15 shows the equilibrium rotational constants, B_{eHF} for these methylcyanopolyyynes obtained at the Hartree Fock level with the 6-311++G** basis set. The difference between the B_{exp} -BeHF and the B_{cal} -BeHF shows a consistent decrease as the chain length increase as noted in previous cases. This further confirms the accuracy of the predicted rotational constants.

Table 5.13: Experimental rotational constants and moments of inertia for $\text{CH}_3(\text{C}\equiv\text{C})_n\text{CN}$ linear carbon chains

n	B_{exp} (MHz)	I_{exp} (AU)	I_{cal} (AU)	ΔI (AU)
0	9,198.899299 ⁶⁹	196.189423	192.90344	3.285983
1	2,065.738360 ⁷⁰	873.647304	863.24750	10.399804
2	778.039740 ⁷¹	2,319.581708	2,297.224160	22.357548
3	374.721270 ⁷¹	4,816.184438	4,776.212190	39.972248
4	208.736990 ⁷¹	8,645.936444	8581.576680	64.359764
5	128.072300 ⁷¹	14,091.468250	13,995.01182	97.456432

Table 5.14: Calculated parameters for $\text{CH}_3(\text{C}\equiv\text{C})_n\text{CN}$ linear carbon chains

n	σ (AU)	I_{cor} (AU)	B_{exp} (MHz)	B_{cal} (MHz)	ΔB (MHz)
4	64.014000	8,645.590680	208.7370	208.7453	0.0083
5	95.651000	14,090.66282	128.0723	128.0796	0.0073
6	135.383000	21,432.606850	-	84.2047	-
7	192.273000	30,962.477570	-	58.2875	-
8	282.913000	42,988.231240	-	41.9819	-
9	320.600000	57,669.951710	-	31.2941	-

Table 5.15: Equilibrium rotational constants for $\text{CH}_3(\text{C}\equiv\text{C})_n\text{CN}$ linear carbon chains obtained from HF/6-311++G**

n	B_{eHF}^* (MHz)	ΔB^+ (MHz)	ΔB^{++} (MHz)
0	9,355.6700	156.7707	-
1	2,090.6400	24.9927	-
2	785.6200	7.5803	-
3	377.8600	3.13873	-
4	210.3000	1.5630	1.5547
5	128.9500		0.8704
6	84.7400	-	0.5353
7	58.6500	-	0.3625
8	42.2600	-	0.2781
9	31.4700	-	0.1759

*Ground state rotational constant, B obtained from HF/6-311++G**; ⁺ B_{exp} -BeHF; ⁺⁺ B_{cal} -BeHF.

5.2.6 C_nO , C_nS and HC_nS Interstellar Linear Carbon Chains: The C_nO linear carbon chains are of significant importance in interstellar chemistry. CO, the simplest member of the chain is considered as one of the major reservoirs of elemental carbon in the interstellar medium.^{1,2} Among the linear carbon chains, CO, C_2O and C_3O are known astromolecules⁷⁵⁻⁷⁷ with the higher members of the chains (especially the odd numbered carbon chains)

considered as potential candidates for astronomical detection. Experimentally, the C_nO linear chains have been probed in the laboratory up to $n=9$.⁷⁸⁻⁷⁹

Using equation 1 and the experimental rotational constants B_{exp} , moments of inertia, I_{exp} , are calculated for the C_nO linear carbon chains with known experimental constants, these are shown in Table 5.16. The calculated moments of inertia; I_{cal} obtained from the optimized geometry at the Hartree Fock level with the 6-311++G** basis set and the difference between the two sets of moments of inertia are also displayed in the same table. The cumulene-type configuration is assumed for the $C_{2n}O$ linear carbons chains and while the polyyne-type structure is assumed for the $C_{2n-1}O$ linear carbon chains irrespective of the chain length.

Suppose the C_nO and $C_{2n-1}O$ chains are only known up to $n=4$, the 4 data points corresponding to the different ΔI in Table 5.16 are fitted into a polynomial to predict the higher members of the chain. Table 5.17 shows the corrected moments of inertia, I_{cor} , for the higher members of the chains obtained using equation 2, the rotational constants calculated from these corrected moments of inertia, the difference between the calculated and the experimentally measured rotational constant (where available). As shown in Table 5.17, the difference between the experimental and calculated (using I_{cor}) rotational constant for C_9O is 0.02079 MHz (20.79 kHz). This amazingly high accuracy for the calculated rotational constant for C_9O with known experimental is an indication for the anticipated high level of accuracy for the high higher members of the chain from $C_{10}O$ to $C_{20}O$ with no experimental rotational constants. The obtained accuracy is of course within experimental accuracy. Thus, with the calculated rotational constants for the higher members of the C_nO linear chains, these chains could be probed from both the interstellar medium and the terrestrial laboratory.

In order to further monitor the accuracy of the predicted rotational constants, the difference between the equilibrium rotational constants computed at the Hartree Fock level with the 6-311++G** basis set and the experimental or the calculated rotational (using I_{cor}) constants are shown in Table 5.18. From Table 5.18, there is steady decrease in the difference between the Hartree Fock value and the experimental or calculated value as the chain length increases.

Table 5.16: Experimental rotational constants and moments of inertia for C_nO linear carbon chains

n	B_{exp} (MHz)	I_{exp} (AU)	I_{cal} (AU)	ΔI (AU)
1	57,635.9687 ⁷⁹	31.312508	29.912800	1.399708
2	11,545.5970 ⁷⁸	156.321987	151.21517	5.097816
3	4,810.88638 ⁷⁹	375.133937	366.30044	8.833497
4	2,351.2620 ⁷⁸	767.556635	51.616750	15.939885
5	1,366.8471 ⁷⁹	1,320.357458	1,294.404430	25.953028
6	849.7571 ⁷⁸	2,123.814876	2,085.224900	38.589976
7	572.9410 ⁷⁹	3,149.934449	3,091.790520	58.143926
8	400.6410 ⁷⁸	4,504.598254	4,426.367140	78.231114
9	293.7361 ⁷⁹	6,144.041157	6,033.725040	110.316117

Table 5.17: Calculated parameters for C_nO linear carbon chains

n	σ (AU)	I_{cor} (AU)	B_{exp} (MHz)	B_{cal} (MHz)	ΔB (MHz)
9	110.751	6,144.847604	293.715320	293.7361	0.0208
10	139.940	8,189.987520	-	220.3577	-
11	189.204	10,586.892250	-	170.4680	-
12	229.036	13,460.94659	-	134.0713	-
13	298.867	16,762.948420	-	107.6616	-
14	350.642	20,597.531570	-	87.6186	-
15	445.122	24,970.197750	-	72.2752	-
16	509.936	29,879.441590	-	60.4003	-
17	633.351	35,542.375510	-	50.7768	-
18	712.096	41,589.259090	-	43.3941	-
19	868.936	48,805.79185	-	36.9777	-
20	962.300	56,006.273190	-	32.2236	-

Table 5.18: Equilibrium rotational constants for C_nO linear carbon chains obtained from HF/6-311++G**

n	B_{eHF}^* (MHz)	ΔB^+ (MHz)	ΔB^{++} (MHz)
1	60,333.3330	2,679.3643	-
2	11,934.9220	389.3250	-
3	4,926.9430	116.0556	-
4	2,401.1460	49.8840	-
5	1,394.2640	27.4169	-
6	865.4900	15.7329	-
7	583.7200	10.7789	-
8	407.7250	7.0840	-
9	299.1090	5.3729	5.3937
10	224.1900	-	3.8323
11	173.5700	-	3.1020
12	136.3920	-	2.3207
13	109.6160	-	1.9543
14	89.1360	-	1.5174
15	73.5870	-	1.3118
16	61.4490	-	1.0487
17	51.6980	-	0.9212
18	44.1500	-	0.7559
19	37.6480	-	0.6703
20	32.7870	-	0.5633

*Equilibrium rotational constant, B obtained from HF/6-311++G**; $\Delta B^+ = B_{exp} - B_{eHF}$;

$\Delta B^{++} = B_{cal} - B_{eHF}$.

The C_nS linear carbon chains are the isoelectronic analogues of the C_nO chains discussed above. The intensity of the rotational lines scales with the square of the dipole moments. The C_nS carbon chains are found to be highly polar with large dipole moments making them good

candidates for both astronomical and laboratory detections. So far, CS, C₂S, C₃S, and C₅S have been astronomically observed.⁸⁰⁻⁸⁴ From a recent study on the different interstellar carbon chains, the odd numbered carbon chains in C_nS are found to have higher potential for astronomical observation as compared to their corresponding even numbered chains.⁸⁵ The first nine members of the C_nS linear carbon chains have been experimentally probed.^{82,85-87}

Following the same assumptions as in the case of the C_nO linear carbon chains, the experimental values of the first four members of the C_{2n}S and C_{2n-1}S carbon chains are utilized in predicting accurate rotational constants for other members of the series. In Table 5.19, the experimental rotational constants, B_{exp}, experimental moments of inertia, I_{exp}, moments of inertia obtained from the optimized structures at the HF/6-311++G** level, I_{cal}, and the difference (ΔI) in the two sets of moments of inertia are presented. Using the same approach employed in the case of the C_nO series, accurate rotational constants are estimated for C₉S to C₂₀S and these are shown in Table 5.20. C₉S serves as a good test for the accuracy of the predicted rotational transitions. The predicted rotational constant of 222.725727MHz for C₉S is in excellent agreement with the experimental value of 222.72006MHz. The difference in the rotational constant of C₉S between the experimental and the calculated value is 0.005667MHz (5.667 KHz). This high level of accuracy is of course rare even among the highly expensive quantum chemical methods. This level of accuracy is within experimental accuracy and experimental uncertainty. Thus, the accuracy of the predicted rotational constants for C_nS linear carbon chains with no experimental values cannot be overemphasized. Table 5.21 and Figure 5.7 show the difference between equilibrium rotational constants at the HF/6-311++G** level and the experimental or calculated (using the approach discussed in this work) rotational constants.

Table 5.19: Experimental rotational constants and moments of inertia for C_nS linear carbon chains

n	B _{exp} (MHz)	I _{exp} (AU)	I _{cal} (AU)	ΔI (AU)
1	24,495.5746 ⁸⁶	73.675624	71.580640	2.094984
2	6,477.7495 ⁸⁷	278.603972	273.989230	4.614724
3	2,890.3800 ⁸²	624.390824	613.268140	11.122684
4	1,519.2062 ⁸⁵	1,187.940616	1,169.62609	18.314526
5	922.7033 ⁸⁵	1,955.912317	1921.640340	34.271976
6	597.1245 ⁸⁵	3,022.362638	2,974.624100	47.738538
7	414.4280 ⁸⁵	4,354.7409320	4,278.224560	76.516372
8	297.8100 ⁸⁵	6,059.993785	5,967.808650	92.185135
9	222.7201 ⁸⁵	8,103.117200	7,960.14401	142.973190

Table 5.20: Calculated parameters for C_nS linear carbon chains

n	σ (AU)	I_{cor} (AU)	B_{exp} (MHz)	B_{cal} (MHz)	ΔB (MHz)
9	142.767000	8,102.911010	222.720	222.7257	0.0057
10	151.065000	10,576.262270	-	170.6394	-
11	238.065000	13,483.182640	-	133.8502	-
12	223.532000	16,846.38704	-	107.1284	-
13	367.351000	20,782.11915	-	86.8404	-
14	308.949000	25,145.549640	-	71.7712	-
15	535.593000	30,309.683950	-	59.5429	-
16	406.620000	35,746.99145	-	50.4861	-
17	747.75900	42,411.965040	-	42.5523	-
18	515.849000	48,929.797250	-	36.8840	-
19	1,008.817000	57,413.578500	-	31.4338	-
20	635.940000	64,961.815	-	27.7813	-

Table 5.21: Equilibrium rotational constants for C_nS linear carbon chains obtained from HF/6-311++G**

n	B_{eHF}^* (MHz)	ΔB^+ (MHz)	ΔB^{++} (MHz)
1	25,212.7000	717.1254	-
2	6,586.9060	109.1565	-
3	2,942.8260	52.4460	-
4	1,543.0070	23.8008	-
5	939.1670	16.4637	-
6	606.7120	9.5875	-
7	421.8430	7.4150	-
8	302.4130	4.6030	-
9	226.7220	4.0019	3.9963
10	173.1120	-	2.4726
11	136.2560	-	2.4058
12	108.5690	-	1.4406
13	88.4030	-	1.5626
14	72.6640	-	0.8928
15	60.6140	-	1.0711
16	51.0670	-	0.5809
17	43.3160	-	0.7637
18	37.2770	-	0.3930
19	31.9960	-	0.5622
20	28.0560	-	0.2746

*Equilibrium rotational constant, B obtained from HF/6-311++G**; $\Delta B^+ = B_{exp} - B_{eHF}$;

$\Delta B^{++} = B_{cal} - B_{eHF}$.

With the unquestionable high abundance of molecular hydrogen in space and the prevalence of S-bearing molecules in different astronomical sources, it is obvious to consider the hydrogenated molecular species of the form HC_nS as important candidates for astronomical detection though no member of the group is yet to be astronomically detected. While their oxygen analogues HC_nO ($n=1$ to 4) have been shown to be bent molecules; the HC_nS chains have been probed experimentally to be linear chain molecules in their most stable form except for the HCS which is not linear.⁸⁸ The HC_2S to HC_8S linear chains have been detected in the terrestrial laboratory.^{82,85,89} Treating the odd numbered and the even numbered carbon chains in the HC_nS series differently with respect to their geometries, the first 3 members of each series with experimental rotational constants (odd and even numbered carbon chains) are used in predicting accurate rotational constants for higher members of the series. Table 5.22 contains the experimental rotational constants, B_{exp} and the difference, ΔI between the experimental, I_{exp} and calculated, I_{cal} (at the 6-311++G** level) moments of inertia.

With only three experimental rotational constants, a very high accurate prediction is obtained for C_8S with the difference between the experimental value and the calculated value of 0.031067MHz (31.067 kHz). This thus, gives a green light for the expected high level of accuracy for the higher members of the HC_nS series with no experimental rotational constants reported in Table 5.23. The steady decrease in the difference between the equilibrium rotational constants at the 6-311++G** level and the experimental or calculated rotational constants noted in the previous cases is also observed in the HC_nS series as depicted in Table 5.24.

Table 5.22: Experimental rotational constants and moments of inertia for HC_nS linear carbon chains

n	B_{exp} (MHz)	I_{exp} (AU)	I_{cal} (AU)	ΔI (AU)
2	5,875.5672 ⁸⁹	307.157875	307.615950	-0.458075
3	2,688.4362 ⁸⁸	671.292385	686.540650	-15.248265
4	1,435.3255 ⁸⁸	1,257.364095	1,264.873340	-7.509244
5	876.3669 ⁸⁵	2,059.327786	2,089.743100	-30.415314
6	572.1202 ⁸⁵	3,154.453818	3181.283090	-26.829272
7	398.1861 ⁸⁵	4,532.369582	4,592.025390	-59.655808
8	287.2333 ⁸⁵	6,283.138343	6,342.237000	-59.098657

Table 5.23: Calculated parameters for HC_nS linear carbon chains

n	σ (AU)	I_{cor} (AU)	B_{exp} (MHz)	B_{cal} (MHz)	ΔB (MHz)
8	-58.419	6,283.818	287.233330	287.2023	0.0311
9	-109.954	8,377.924150	-	215.4145	-
10	-93.654	10,938.703620	-	164.9854	-
11	-160.360	13,881.146510	-	130.0128	-
12	-165.111	17,371.32025	-	103.8912	-
13	-231.778	21,328.78289	-	84.6146	-
14	-240.251	25,900.8126	-	69.6784	-
15	-317.228	31,006.132680	-	58.2055	-
16	-331.043	36,799.43224	-	49.0422	-
17	-416.498	43,193.643180	-	41.7822	-
18	-438.165	50,351.994820	-	35.8422	-
19	-530.176	58,059.141570	-	31.0843	-
20	-562.295	66,841.131670	-	27.0002	-

Table 5.24: Equilibrium rotational constants for HC_nS linear carbon chains obtained from HF/6-311++G**

n	B_{eHF}^* (MHz)	ΔB^+ (MHz)	ΔB^{++} (MHz)
2	5,866.8650	8.7022	-
3	2,628.7490	59.6872	-
4	1,426.8160	8.5095	-
5	863.6190	12.7479	-
6	567.3000	4.8202	-
7	393.0160	5.1701	-
8	284.5590	2.67433	2.6433
9	212.8010	-	2.6135
10	163.5850	-	1.4004
11	128.5280	-	1.4848
12	102.9130	-	0.9782
13	83.7050	-	0.9096
14	69.0280	-	0.6504
15	57.6160	-	0.5895
16	48.6050	-	0.4372
17	41.3830	-	0.3993
18	35.5330	-	0.3092
19	30.8030	-	0.2813
20	26.7750	-	0.2252

*Equilibrium rotational constant, B obtained from HF/6-311++G**; $\Delta B^+ = B_{\text{exp}} - B_{\text{eHF}}$;

$\Delta B^{++} = B_{\text{cal}} - B_{\text{eHF}}$.

5.2.7 $C_{2n}H^-$ and C_nN^- Linear Carbon Chains: Although ions are known to play significant roles in interstellar chemistry processes, only a few of them have been astronomically observed. Availability of accurate rotational transitions remains one of the primary requirements for the astronomical searches for molecules. Unlike the neutral molecules, having enough concentration of ions in gas phase to probe their rotational spectra is difficult. This of course is one of the reasons for the limited number of known ions among interstellar and circumstellar molecules. Thus, the astronomical detection of ions relying in matching of laboratory measured rotational transitions with emission or absorption lines from the ISM using radio telescope can be seen as a biased procedure as it places a limit to the ions that can be detected in ISM (only those with laboratory measured transitions). The six currently known interstellar anions; C_4H^- , C_6H^- , C_8H^- ; CN^- , C_3N^- , C_5N^- belong to the $C_{2n}H$ and $C_{2n-1}N$ series of linear carbon chains.⁹⁰⁻⁹⁶ And there is a tentative observation of C_2H^- .⁹⁶ Though the anions have long been predicted to be detectable in the interstellar medium, their successful astronomical observation followed their successful laboratory detection. Higher members of $C_{2n}H^-$ and $C_{2n-1}N^-$ series have been shown to be potential candidates for astronomical observation but as much as we know, their rotational spectra have not been experimentally probed thus no successful astronomical searches could be carried out.

Using the first four members of the $C_{2n}H^-$ and the first three members of the $C_{2n-1}N^-$ with experimental rotational constants, accurate rotational constants are predicted for higher members of these chains following the approach employed in this work. Tables 5.25 and 5.28 contain the experimental rotational constants, B_{exp} and the difference, ΔI between the experimental, I_{exp} and the calculated, I_{cal} moments of inertia for the $C_{2n}H^-$ and $C_{2n-1}N^-$ linear carbon chains respectively. The rotational constants calculated for the higher members of these series are shown in Tables 5.26 and 5.29 respectively for $C_{2n}H^-$ and $C_{2n-1}N^-$ linear carbon chains. The same steady decrease in the difference between the equilibrium rotational constants at the HF/6-311++G** level and the experimental or calculated rotational constants is observed for the $C_{2n}H^-$ and $C_{2n-1}N^-$ linear carbon chains as presented in Tables 5.27 and 5.30 respectively. With the accurate rotational constants reported for the higher members of the $C_{2n}H^-$ and $C_{2n-1}N^-$ linear carbon chains, these anions can now be probed both in the terrestrial laboratory and in the interstellar medium.

Table 5.25: Experimental rotational constants and moments of inertia for $C_{2n}H^-$ linear carbon chains

n	B_{exp} (MHz)	I_{exp} (AU)	I_{cal} (AU)	ΔI (AU)
1	41,639.2370 ⁹¹	43.341974	41.964190	1.377784
2	4,654.9449 ⁹⁷	387.700991	381.887610	5.813381
3	1,376.8630 ⁹⁰	1,310.752613	1,296.7841100	13.968503
4	583.3401 ⁹⁷	3,093.781184	3,067.024190	26.756994

Table 5.26: Calculated parameters for $C_{2n}H^-$ linear carbon chains

n	σ (AU)	I_{cor} (AU)	B_{cal} (MHz)
5	39.718	6,013.66896	300.1040
6	69.786	10,369.20931	174.0467
7	101.906	16,427.773970	109.8583
8	142.300	24,477.881840	73.7289
9	191.880	34,802.983100	51.8555
10	251.558	47,684.451950	37.8473

Table 5.27: Equilibrium rotational constants for C_nH^- linear carbon chains obtained from HF/6-311++G**

n	B_{eHF}^* (MHz)	ΔB^+ (MHz)	ΔB^{++} (MHz)
1	43,006.7010	1,367.4640	-
2	4,675.8440	70.8991	-
3	1,391.7050	14.8420	-
4	588.4340	5.09386	-
5	302.1020		1.9979
6	175.22600		1.1793
7	110.5440		0.6857
8	74.1600		0.4311
9	52.1430		0.2875
10	38.0480		0.2007

*Equilibrium rotational constant, B obtained from HF/6-311++G**; $\Delta B^+ = B_{exp} - B_{eHF}$;
 $\Delta B^{++} = B_{cal} - B_{eHF}$.

Table 5.28: Experimental rotational constants and moments of inertia for $C_{2n-1}N^-$ linear carbon chains

N	B_{exp} (MHz)	I_{exp} (AU)	I_{cal} (AU)	ΔI (AU)
1	56,132.7504 ⁹⁸	32.151048	30.824170	1.326878
2	4,851.6218 ⁹⁵	371.984217	364.641250	7.342967
3	1,388.8600 ⁹⁹	11,299.430287	1,282.311310	17.118977

Table 5.29: Calculated parameters for $C_{2n-1}N^-$ linear carbon chains

n	σ (AU)	I_{cor} (AU)	B_{cal} (MHz)
4	30.654	3,095.739410	582.9711
5	47.950	6,043.031360	298.6459
6	69.006	10,423.800330	173.1352
7	93.822	16,521.635620	109.2341
8	122.398	24,618.845120	73.3067
9	154.734	34,998.38202	51.5660
10	190.830	47,942.50352	37.6436

Table 5.30: Equilibrium rotational constants for C_nN^- linear carbon chains obtained from HF/6-311++G**

n	B_{eHF}^* (MHz)	ΔB^+ (MHz)	ΔB^{++} (MHz)
1	58,549.5550	2,416.8046	-
2	4,949.3610	97.7392	-
3	1,407.4130	18.5530	-
4	588.8060	-	5.8348
5	301.0370	-	2.3911
6	174.2890	-	1.1538
7	109.8580	-	0.6238
8	73.6730	-	0.3663
9	51.7950	-	0.2290
10	37.7940	-	0.1504

*Equilibrium rotational constant, B obtained from HF/6-311++G**; $\Delta B^+ = B_{exp} - B_{eHF}$;

$\Delta B^{++} = B_{cal} - B_{eHF}$.

5.2.8 C_nH and C_nN Linear Carbon Chains: The use of Fourier transform microwave spectrometer with a pulsed discharge nozzle has reduced the difficulty in probing molecular species in the gas phase especially for the radicals that are a bit stable. The C_nH chains as long as $C_{14}H$ have now been probed in the terrestrial laboratory via the advanced instrumentation in microwave technique.¹⁰⁰⁻¹⁰⁴ The high cosmic abundance of elemental hydrogen and the unique chemistry of carbon have resulted in the dominance of interstellar and circumstellar molecules containing hydrogen and carbon among other elements. The first eight members of the C_nH linear carbon chains have been observed from different astronomical sources.

Following the same assumption applied in the case of the C_nO linear carbon chains, the first four members from $C_{2n}H$ and $C_{2n-1}H$ linear carbon chains are used in predicting accurate

rotational constants for higher members of these chains. Experimental rotational constants; B_{exp} , experimental and calculated moments of inertia and the difference in the moment of inertia are shown in Table 5.31. The calculated rotational constants for C_9H to $C_{20}H$ are presented in Table 5.32. For the C_nH radicals with known experimental rotational constants (C_9H to $C_{14}H$), the difference between the experimental and the calculated rotational constants ranges from 0.0199760 (19.976 KHz) to 0.0948339 MHz (94.8339 KHz). From Table 5.32, this value keeps decreasing (increasing in accuracy) as the chain length increases for the respective odd and even numbered carbon chains, thus for the $C_{15}H$ to $C_{20}H$ with no experimental rotational constants, the accuracy of the calculated rotational constant will be better than the above range (0.0199760 to 0.0948339 MHz). Table 5.33 demonstrates the steady decrease in the difference between the equilibrium rotational constant at 6-311++G** level and the experimental or calculated rotational constants as the chain length increases.

Table 5.31: Experimental rotational constants and moments of inertia for C_nH linear carbon chains

n	B_{exp} (MHz)	I_{exp} (AU)	I_{cal} (AU)	ΔI (AU)
1	$425,476.8520^{101}$	4.241657	4.078380	0.163277
2	$43,674.5420^{101}$	41.322168	44.186490	-2.864322
3	$11,186.3350^{101}$	161.333158	161.902020	-0.568862
4	$4,758.6557^{101}$	379.251382	385.401660	-6.150278
5	$2,395.1265^{102}$	753.499554	759.167110	-5.667556
6	$1,391.1860^{101}$	1,297.257699	1,309.511170	-12.253471
7	875.4841^{103}	2,061.404275	2,079.866310	-18.462035
8	587.2638^{102}	3,073.110682	3,099.824110	-26.713428
9	413.2576^{104}	4,367.074659	4,409.676360	-42.601701
10	301.4099^{105}	5,987.615633	6,040.789210	-53.173577
11	226.9002^{105}	7,953.833233	8,023.910050	-79.076817
12	174.7840^{105}	10,325.476540	10,418.456730	-92.980192
13	137.7100^{105}	13,105.270130	13,237.442690	-132.172559
14	110.2417^{105}	16,370.63903	16,530.586210	-159.947176

Table 5.32: Calculated parameters for C_nH linear carbon chains

n	σ (AU)	I_{cor} (AU)	B_{exp} (MHz)	B_{cal} (MHz)	ΔB (MHz)
9	-42.217	4,367.459360	413.257590	413.221189	0.0364
10	-55.057	5,985.732210	301.409920	301.504759	0.09483
11	-80.332	7,952.57805	226.900250	226.936062	0.03581
12	-96.761	10,321.695730	174.784000	174.847892	0.0640
13	-128.879	13,108.563690	137.710000	137.675400	0.0346
14	-162.913	16,367.673210	110.241680	110.261656	0.0120
15	-191.868	20,107.628640	-	89.753335	-
16	-255.954	24,363.73695	-	74.074299	-
17	-343.437	29,169.191560	-	61.870989	-
18	-499.355	34,514.64785	-	52.288719	-
19	-696.482	40,465.035820	-	44.599657	-
20	-859.070	47,128.77166	-	38.293524	-

Table 5.33: Equilibrium rotational constants for C_nH linear carbon chains obtained from HF/6-311++G**

n	B_{eHF}^* (MHz)	ΔB^+ (MHz)	ΔB^{++} (MHz)
1	442,513.7220	-17,036.8720	-
2	40,843.7300	2,830.8120	-
3	11,147.1200	39.2150	-
4	4,682.7540	75.9017	-
5	2,377.2650	17.8615	-
6	1,378.1790	13.0070	-
7	867.7200	7.7640	-
8	582.2080	5.0583	-
9	409.2680	3.9896	-
10	298.7590	2.6509	-
11	224.6680	2.2322	-
12	173.2240	1.5599	-
13	136.3350	1.3750	-
14	109.1750	1.0667	-
15	88.9050	-	0.8483
16	73.3040	-	0.7703
17	61.1510	-	0.7120
18	51.5430	-	0.7457
19	43.8450	-	0.7546
20	37.6080	-	0.6855

*Equilibrium rotational constant, B obtained from HF/6-311++G**; $\Delta B^+ = B_{exp} - B_{eHF}$;
 $\Delta B^{++} = B_{cal} - B_{eHF}$.

The C_nN linear carbon chains are the nitrogen analogues of the C_nH discussed above. Whereas the first 8 members of the C_nH linear carbon chains have been astronomically observed, only four members of the C_nN linear carbon chains have been detected in the interstellar medium.¹⁰⁵⁻¹⁰⁸ This is partly due to the lack of spectroscopic parameters for these radicals. For instance, C_3N was first observed in space before been detected in the terrestrial laboratory; though C_2N and C_5N were long thought to be detectable, their successful astronomical observation came soon after their rotational spectra were probed in the laboratory. And currently, there is dearth of information regarding the spectroscopic parameters of higher members of these linear carbon chains beyond C_6N . Thus, for successful astronomical observation of the higher members of these radicals, availability of accurate rotational transitions is a primary requirement. In line with the argument in the C_nH linear carbon chains, the first three members of the $C_{2n}N$ and $C_{2n-1}N$ linear carbon chains are utilized in estimating accurate rotational constant for the higher members of these chains.

Table 5.34 displays the experimental and calculated parameters for the first six members of the group. The calculated rotational constants for the higher members of the C_nN chains with no experimental rotational constants are contained in Table 5.35. These calculated rotational

constants are expected to be very accurate as observed in previous cases, thus, could be useful for both the terrestrial and astronomical detection of these radicals. Table 5.36 illustrates the trend in the difference between the equilibrium rotational constants at the HF/6-311++G** level and the experimental or calculated rotational constants.

Table 5.34: Experimental rotational constants and moments of inertia for C_nN linear carbon chains

n	B_{exp} (MHz)	I_{exp} (AU)	I_{cal} (AU)	ΔI (AU)
1	$56,693.1000^{109}$	31.833270	30.751070	1.082200
2	$11,931.0713^{110}$	151.262758	150.427800	0.834958
3	$4,947.6208^{111}$	364.766586	364.038760	0.727826
4	$2,422.6963^{112}$	744.924879	747.671880	-2.747001
5	$1,403.0798^{113}$	1,286.260936	1,301.999970	-15.739034
6	873.1122^{112}	2,067.004294	2,080.582550	-13.578256

Table 5.35: Calculated parameters for C_nN linear carbon chains

n	σ (AU)	I_{cor} (AU)	B_{cal} (MHz)
7	-48.319	3,062.045120	589.3861
8	-31.648	4,402.06700	409.9726
9	-97.010	5,984.14131	301.5849
10	-56.972	8,035.03505	224.6072
11	-161.813	10,337.01042	174.5888
12	-129.364	13,250.73829	136.1982
13	-242.728	16,407.885990	109.9914
14	-129.364	20,333.55055	88.7561
15	-339.755	24,477.378280	73.7304
16	-176.432	29,570.17669	61.0320
17	-452.894	34,854.98151	51.7782
18	-230.748	41,242.92198	43.7585
19	-582.145	47,430.11698	38.0502
20	-292.213	55,636.99099	32.4375

Table 5.36: Equilibrium rotational constants for C_nN linear carbon chains obtained from HF/6-311++G**

n	$B_{eHF}^*(\text{MHz})$	$\Delta B^+(\text{MHz})$	$\Delta B^{++}(\text{MHz})$
1	58,688.7320	-1,995.6320	-
2	11,997.3910	-66.3197	-
3	4,957.5520	-9.9312	-
4	2,413.8140	8.8833	-
5	1,386.1300	16.9498	-
6	867.4210	11.6912	-
7	580.2350	-	9.1511
8	407.0490	-	2.9236
9	296.7760	-	4.8089
10	223.0280	-	1.5792
11	171.8980	-	2.6908
12	135.2840	-	0.9142
13	108.3880	-	1.6034
14	88.1950	-	0.5611
15	72.7210	-	1.0094
16	60.6700	-	0.3620
17	51.1140	-	0.6642
18	43.5150	-	0.2435
19	37.3320	-	0.7182
20	32.2680	-	0.1695

*Equilibrium rotational constant, B obtained from HF/6-311++G**; $\Delta B^+ = B_{\text{exp}} - B_{eHF}$;
 $\Delta B^{++} = B_{\text{cal}} - B_{eHF}$.

5.2.9 C_nSi and $CH_3(CC)_nH$ Linear Carbon Chains: The C_nSi linear carbon chains are the isoelectronic analogues of the pure carbon chains, C_n which are microwave inactive, thus, their astronomical observation is only limited to the infrared region while the C_nSi chains can be observed both in the radio and infrared regions. The C_nSi linear carbon chains are known to be highly polar. This factor marks them out as favorable candidates for astronomical detection subject to the availability of accurate spectroscopic parameters. These C_nSi linear carbon chains are calculated to have dipole moments that are almost equal in Debye to the number of atoms in the chain. A number of silicon-bearing molecules; SiS, SiC, c-C₂Si, c-C₃Si, C₄Si, have been detected from different astronomical sources.¹¹⁴⁻¹¹⁸

With four experimental rotational constants available for both the odd and even numbered carbon chains of C_nSi series, the rotational constants for the higher members of these chains are calculated using the method described in this work. In Table 5.37, the experimental rotational constants, and moments of inertia (both experimental, I_{exp} and calculated, I_{cal}) are presented. The calculated rotational constants for the higher members of the C_nSi linear carbon chains are shown in Table 5.38. These values are of course very accurate as noted in all the cases discussed above. Thus, are significant for the laboratory and astronomical

probing of these highly polar molecular species. Table 5.39 represents the difference between the equilibrium rotational constants at the 6-311++G** level and the experimental or calculated rotational constants.

Table 5.37: Experimental rotational constants and moments of inertia for C_nSi linear carbon chains

n	B_{exp} (MHz)	I_{exp} (AU)	I_{cal} (AU)	ΔI (AU)
1	20,297.5820 ¹¹⁴	88.91338629	79.91338629	9.751086
3	2,747.7085 ¹¹⁵	656.8115755	645.391820	11.419755
4	1,533.7721 ¹¹⁶	1,176.659033	1,156.01110	20.647933
5	920.8954 ¹¹⁵	1,959.75216	1,925.56741	34.184750
6	611.2510 ¹¹⁵	2,952.513272	2,901.804820	50.708452
7	421.0834 ¹¹⁵	4,285.912836	4,212.264660	73.648176
8	306.2609 ¹¹⁵	5,892.775761	5,795.59919	97.176571

Table 5.38: Calculated parameters for C_nSi linear carbon chains

n	σ (AU)	I_{cor} (AU)	B_{cal} (MHz)
9	125.319	7,907.64728	228.2255
10	160.074	10,277.7866	175.5949
11	184.926	13,096.028	137.8072
12	239.306	16,394.7688	110.0794
13	248.023	20,122.33609	89.6877
14	335.050	24,549.16943	73.5148
15	310.212	29,256.212	61.6870
16	447.262	35,053.7132	51.4846
17	367.095	42,031.30104	42.9377
18	575.960	48,186.54273	37.4529
19	414.274	54,939.38802	32.8494
20	721.162	64,232.09771	28.0970

Table 5.39: Equilibrium rotational constants for C_nSi linear carbon chains obtained from HF/6-311++G**

n	B_{eHF}^* (MHz)	ΔB^+ (MHz)	ΔB^{++} (MHz)
1	22,797.9870	-2500.4050	-
3	2,796.3500	-48.6415	-
4	1,561.1800	-22.4079	-
5	937.2520	-16.3566	-
6	621.9370	-10.6860	-
7	428.4490	-7.3656	-
8	311.3990	-5.1381	-
9	231.9020	-	-3.6765
10	178.3730	-	-2.7781
11	139.8710	-	-2.0638
12	111.7100	-	-1.6306
13	90.8070	-	-1.1193
14	74.5320	-	-1.0172
15	62.3480	-	-0.6610
16	52.1500	-	-0.6654
17	43.3160	-	-0.3783
18	37.9060	-	-0.4531
19	33.0990	-	-0.2496
20	28.4160	-	-0.3190

*Equilibrium rotational constant, B obtained from HF/6-311++G**; $\Delta B^+ = B_{exp} - B_{eHF}$;
 $\Delta B^{++} = B_{cal} - B_{eHF}$.

The $CH_3(CC)_nH$ linear carbon chains are the methyl analogues of the C_nH linear chains earlier discussed and they are also closely related to the cyanopolyyynes which have been detected from different astronomical sources. Fortunately, the first three members of the $CH_3(CC)_nH$ linear carbon chains have been detected in space.¹¹⁹⁻¹²¹ Thus, with the availability of accurate rotational transitions, the successful astronomical detection of the higher members of these chains is a matter of time. Experimentally, the first seven members of these chains have been probed and in this study, this number is extended to ten. Table 5.40 contains the experimental parameters and the calculated moments of inertia for the $CH_3(CC)_nH$ linear carbon chains obtained from the optimized geometries at the HF/6-311++G** level.

Assuming only the first four members of these chains are experimentally known, these experimental parameters are used in estimating accurate rotational constants for other members of the series following the methodology in this work. Table 5.41 has the calculated rotational constants for the $CH_3(CC)_nH$ linear carbon chains from n=5 to 10. For $CH_3(CC)_5H$, $CH_3(CC)_6H$ and $CH_3(CC)_7H$ with experimentally measured rotational constants, the difference between the experimental and calculated rotational constants ranges from 0.003872 (3.872 kHz) to 0.006597 MHz (6.597 kHz). This is unarguably very accurate with respect to any high level ab initio quantum method. The predicted rotational constant for

$\text{CH}_3(\text{CC})_8\text{H}$, $\text{CH}_3(\text{CC})_9\text{H}$ and $\text{CH}_3(\text{CC})_{10}\text{H}$ are obviously very accurate. In Table 5.42, the trend in the difference between the equilibrium rotational constants and the experimental or calculated rotational constants is displayed.

Table 5.40: Experimental rotational constants and moments of inertia for $\text{CH}_3(\text{CC})_n\text{H}$ linear carbon chains

n	B_{exp} (MHz)	I_{exp} (AU)	I_{cal} (AU)	ΔI (AU)
1	8,545.84 ¹²²	211.181902	208.682290	2.499612
2	2,035.74706 ¹²³	886.518165	878.431350	8.086815
3	778.2445 ¹²⁴	2,318.971415	2,300.599270	18.372144
4	376.71252 ¹²⁵	4,790.726756	4,756.40500	34.321756
5	210.23883 ¹²⁵	8,584.174241	8,527.187050	56.987191
6	129.07609 ¹²⁶	13,981.882690	13,894.270140	87.612546
7	84.8622 ¹²⁶	21,266.55624	21,140.05797	126.498268

Table 5.41: Calculated parameters for $\text{CH}_3(\text{CC})_n\text{H}$ linear carbon chains

n	σ (AU)	I_{cor} (AU)	B_{exp} (MHz)	B_{cal} (MHz)	ΔB (MHz)
5	56.798	8,583.98505	210.23883	210.243464	0.004634
6	86.898	13,981.16814	129.07609	129.082687	0.006597
7	125.528	21,265.58597	84.8622	84.866072	0.003872
8	173.648	30,715.64748	-	58.755940	-
9	232.218	42,626.55084	-	42.338090	-
10	302.198	57,269.58275	-	31.512832	-

Table 5.42: Equilibrium rotational constants for $\text{CH}_3(\text{CC})_n\text{H}$ linear carbon chains obtained from HF/6-311++G**

n	B_{eHF}^* (MHz)	ΔB^+ (MHz)	ΔB^{++} (MHz)
1	8,648.270	-102.43	-
2	2,054.500	-18.75294	-
3	784.47	-6.2255	-
4	379.43	-2.71748	-
5	211.65	-	-1.406536
6	129.89	-	-0.807313
7	85.370	-	-0.503928
8	59.09	-	-0.33406
9	42.57	-	-0.231910
10	31.6800	-	-0.167168

*Equilibrium rotational constant, B obtained from HF/6-311++G**; $\Delta B^+ = B_{\text{exp}} - B_{\text{eHF}}$;

$\Delta B^{++} = B_{\text{cal}} - B_{\text{eHF}}$.

5.3 Astrophysical Implications: Towards 'U' Lines Reduction

Unidentified signal lines ('U' lines) are major components of every astronomical survey. It is almost certain that one will have "U" lines in every survey. Assigning these lines remains a great challenge in molecular astrophysics. These lines are left unassigned in most cases when they are not matching the available transitions. Figures 5.1a to 5.1d show different parts of the 3 mm line survey of IRC +10216 with the assigned and unassigned lines.⁸⁴ The unassigned lines; 'U' lines are indicated in red with an oval shape for emphasis. Though, it is practically difficult to do away with these lines whose origin could be diverse in most cases but the availability of more accurate rotational transitions is a step in the right direction towards reducing the numerous unassigned signal lines. Among the unidentified lines lie transitions corresponding to known and unknown interstellar molecules; their isotopologues and even weakly bound complexes which could also survive under the conditions of the interstellar medium though they have not been searched for. The reported rotational constants in this study could be utilized in predicting rotational transitions for the different carbon chains examined in this study. These transitions could certainly correspond to the some known interstellar and circumstellar molecules (among the unidentified lines) and possibly to new molecules whose spectra are yet to be probed experimentally.

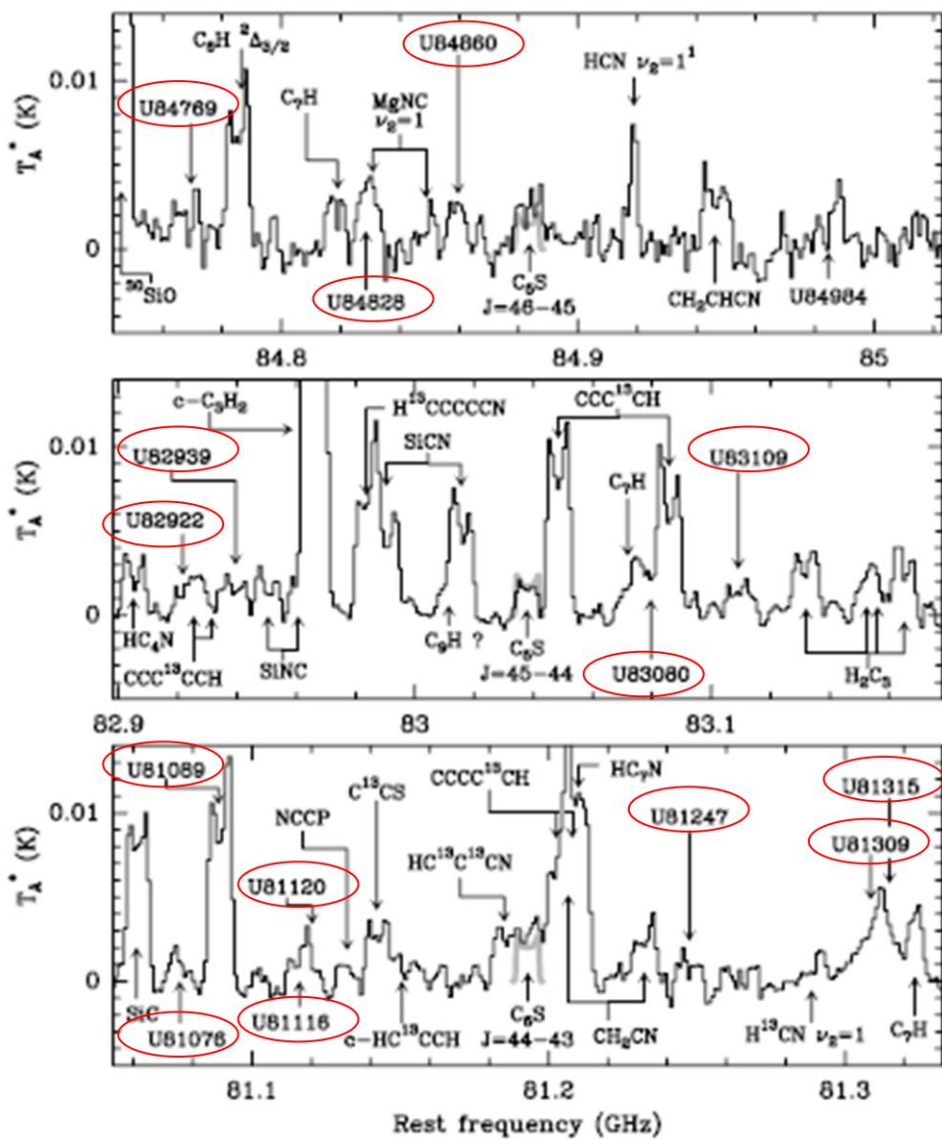


Fig. 5.1a: Parts of the 3 mm line survey of IRC +10216 showing the assigned and unassigned lines ('U' lines in red oval shape). Edited with permission from Agúndez et al.,⁸⁴.

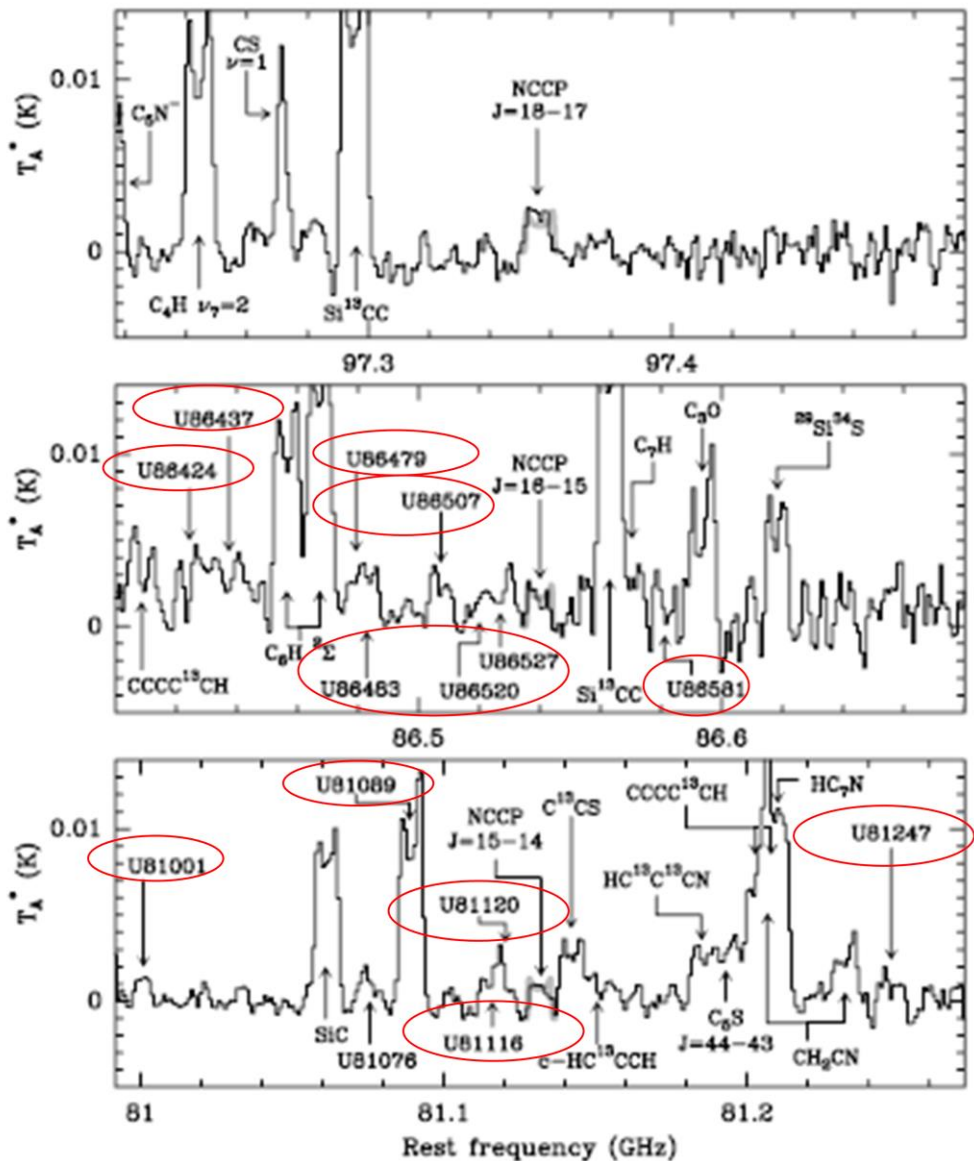


Fig. 5.1b: Parts of the 3 mm line survey of IRC +10216 showing the assigned and unassigned lines ('U' lines in red oval shape). Edited with permission from Agúndez et al.,⁸⁴.

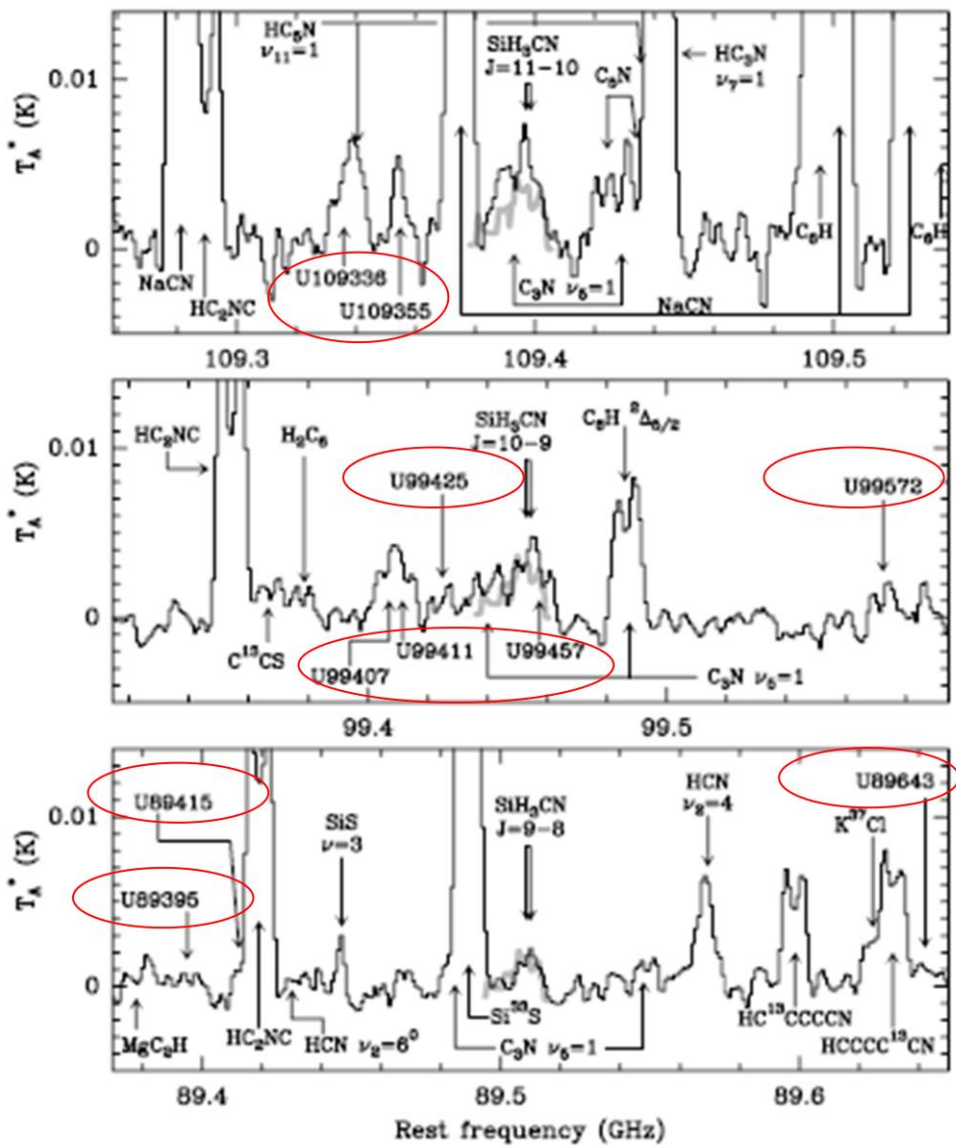


Fig. 5.1c: Parts of the 3 mm line survey of IRC +10216 showing the assigned and unassigned lines ('U' lines in red oval shape). Edited with permission from Agúndez et al.,⁸⁴.

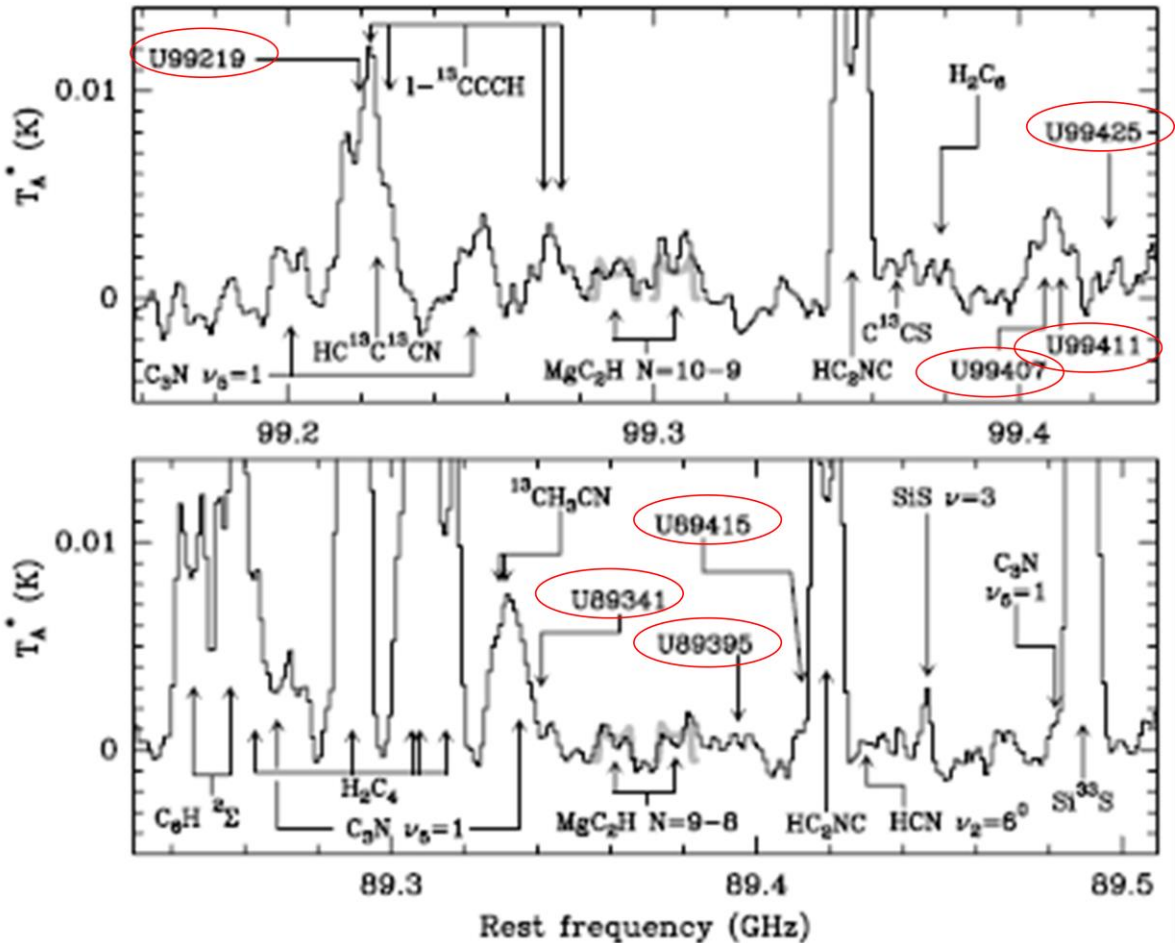


Fig. 5.1d: Parts of the 3 mm line survey of IRC +10216 showing the assigned and unassigned lines ('U' lines in red oval shape). Edited with permission from Agúndez et al.,⁸⁴.

5.4 Summary on Accurate Rotational Constants for linear Interstellar Carbon Chains:

By fitting three or four experimental constants, accurate rotational constants have been calculated for higher members of the different carbon chains; C_nH , C_nH^+ , C_nN , C_nN^- , C_nO , C_nS , HC_nS , C_nSi , $CH_3(CC)_nH$, HC_nN , $DC_{2n+1}N$, $HC_{2n}NC$, and $CH_3(C\equiv C)_nCN$ considered in this study by employing a straightforward and less expensive approach. The results show excellent accuracy of few KHz which is within experimental accuracy in all the systems considered. This level of accuracy is far better than what most of the high level ab initio quantum methods including the gold standard; CCSD(T) can offer. This high level of accuracy is certainly what is required for the astronomical observation of these carbon chains and in the laboratory detection of the same. From the numerous unidentified lines from different astronomical surveys, transitions corresponding to known and new linear carbon chains could be found using the reported rotational constants in this study. The observed ratio between the predicted rotational constants and the equilibrium rotational constants at the Hartree Fock level with the 6-311++G** basis set gives an insight of what could be expected for systems with no experimental rotational constants.

Linear Interstellar Carbon Chains: Is Thermodynamics the key?

5. 5 Introduction: As more and more interstellar and circumstellar molecules are observed, our understanding of the chemistry of these molecules is either strengthened or challenged depending on whether the new molecules fall within or outside the boundaries of their expected basic chemistry. These observations also put a constraint on the different chemical models. The fields of astronomy, astrophysics, astrochemistry and astrobiology have witnessed dramatic changes in the last few decades as a result of the advances in science and technology. In addressing the chemical origin of life and for the proper understanding of the solar system, there has been a constant and consistent searching for molecules in the interstellar and circumstellar media resulting in unique observation of about 200 different molecular species till date. The year 2014 saw unparalleled observations of nine new interstellar and circumstellar molecules including the first branched chain molecule in space, namely, isopropyl cyanide, an important biological molecule; urea, the sulphur analogue (ethyl mercaptan) of the well known interstellar alcohol; ethanol, among others and the confirmation of many others.^{12,14,17,132,146,153}

Almost on a regular basis, carbon chain molecules such as C_n , H_2C_n , HC_nN and C_nX ($X=N$, O , Si , S , H , P , H^- , N^-) are astronomically observed. Till date, the largest claimed straight chain interstellar molecule is the cyanopolyne, $HC_{11}N$; a carbon chain molecule. Among the carbon chains, there seems to be no easily understood trend or pattern within the observed molecules. In the C_nN and C_nN^- chains, with the exception of C_2N , only the odd number carbon chains are observed from $n=1$ to $n=6$.^{105,106,107,95,15,99,17} Whereas in the C_nH chains, both odd and even number chains are observed between 1 and 8 but in the C_nH^- , only even number chains are observed.^{158,42,140,9,129,92,157,19,143,9021,128} Among the cyanopolyne chains, between carbon 6 and 12, only odd number chains are observed^{23-28,30,142} while in the C_nSi group, all the molecules between carbon 1 and 4 have been observed.^{8,114,116,117} This type confusing trend of different interstellar chains is present among all the groups. As observed among the interstellar isomers¹³⁷, observations of interstellar carbon chain can also be seen as having a number of “whys and wherefores”. Addressing these “whys and wherefores” has been a serious concern to a number of research groups.

The energy, stability and abundance (ESA) relationship existing among interstellar and circumstellar molecules is well established¹³⁷. According to the relationship, “***Interstellar abundances of related species are directly proportional to their stabilities in the absence of the effect of interstellar hydrogen bonding***”. The ESA relationship accounts for the astronomical observation of some isomers at the expense of others; the reason for more known interstellar/circumstellar cyanide molecules than their corresponding isocyanides; why there are more linear molecules than cyclic molecules and other whys and wherefores among interstellar and circumstellar molecules¹³⁷. This relationship is discussed in details in chapter 3 of this Thesis. As part of our interest in understanding the basic chemistry of interstellar and circumstellar molecules, the present work focuses on the interstellar and circumstellar carbon chains; C_n , H_2C_n , HC_nN and C_nX ($X=N$, O , Si , S , H , P , H^- , N^-). High level quantum

chemical calculations are applied to accurately determine the enthalpies of formation of these molecules. The possible candidates for astronomical observation among the carbon chain molecules are considered.

5.6 Computational Details: The results of the quantum chemical calculations reported in this work were obtained using Gaussian 09 suite of programs⁴³. In order to estimate accurate enthalpies of formation that are in good agreement with the experimental values (where available) for the different carbon chains considered in this work, the G4 composite method was employed^{135,136}. The choice of the G4 composite method is borne out of experience as it has been shown to compute enthalpies of formation to chemical accuracy¹³⁷. The geometries of these molecules were optimized at the G4 level, harmonic vibrational frequency calculations were used to characterize the stationary nature of all the structures with equilibrium species possessing only real frequencies. The reported zero-point corrected standard enthalpies of formation of the carbon chains were calculated from the optimized geometries. The enthalpies of formations were calculated from atomization energies. Details of the computational analysis are same as described in chapter 3 of this Thesis.

5.7 Results and Discussion: The results of the quantum chemical simulations at the G4 level of theory obtained for all the carbon chain molecules are presented and discussed in this subsection. In all the cases, the reported zero-point corrected standard enthalpies of formation ($\Delta_f H^\circ$) are in kcal/mol.

5.7.1 C_n Chains: Apart from their importance in astrophysics, astrochemistry, and astrobiology, pure carbon chain molecules such as C_2 , C_3 , and C_5 are of great interest in combustion chemistry, flames and propellants. Table 1 shows enthalpy of formation and current astronomical status of carbon chain (C_n) molecules considered in this study. Rotational spectroscopy has been the dominant tool in the chemical examination of interstellar and circumstellar media with about 90% of all known interstellar and circumstellar molecules observed via their rotational transitions. However, the application of rotational spectroscopy in this field is hampered by the fact that it is only limited to molecules with permanent dipole moment. The C_n chain molecules have no permanent dipole moment; hence their pure rotational transitions cannot be measured. All the known interstellar C_n chain molecules have been observed in the infrared region through their vibrational transitions.

From Table 5.43, there is a steady increase in the enthalpy of formation of the C_n chains as the chain length increases. With the exception of C_4 which is yet to be observed all the lower members of the chains with lower enthalpies of formation have all been detected^{155,145,16,127}. In accordance with the ESA relationship, the lower members of the chains with lower enthalpies of formation are more stable, more abundant and probably more abundant than the higher members of the chains with higher enthalpies of formation thus they are easily observed than the higher members of the chains. Figure 5.2 shows the plot of the enthalpy of formation of the C_n chain molecules estimated at the G4 level. That lower members of the

chains remain the most likely candidates for astronomical observation as compared to the higher members of the chains.

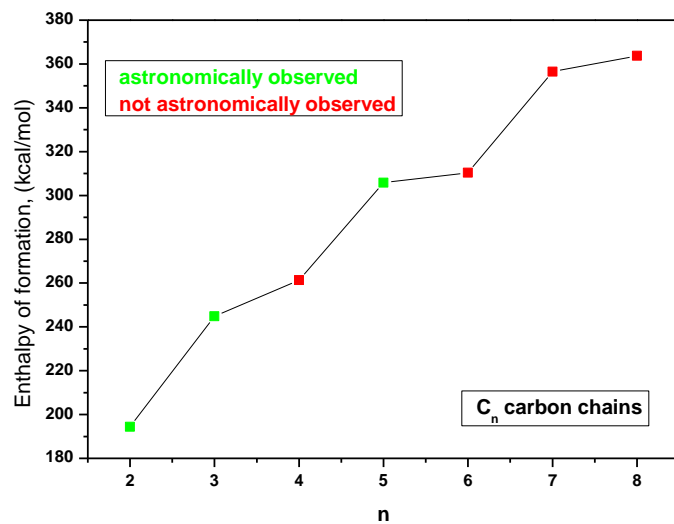


Figure 5.2: Plot showing the $\Delta_f H^\circ$ for C_n chain molecules

Table 5.43: $\Delta_f H^\circ$ for C_n chains and current astronomical status

n	$\Delta_f H^\circ$ (kcal/mol)	Astronomical status
2	194.4	Observed
3	244.8	Observed
4	261.3	Not observed
5	305.8	Observed
6	310.4	Not observed
7	356.5	Not observed
8	363.7	Not observed

5.7.2 C_nO Chains: The C_nO group presents an interesting set of carbon chain molecules containing two (carbon and oxygen) of the four most important biological elements. Unlike the C_n chains that lack permanent dipole moment, the C_nO chains all possess permanent dipole moment, hence, all the known interstellar/circumstellar C_nO molecules have been observed via their rotational transition spectra. The enthalpy of formation and current astronomical status for all the C_nO molecules considered in this study are presented in Table 5.44 while Fig. 5.3 depicts the plot of the enthalpy of formation for these molecules.

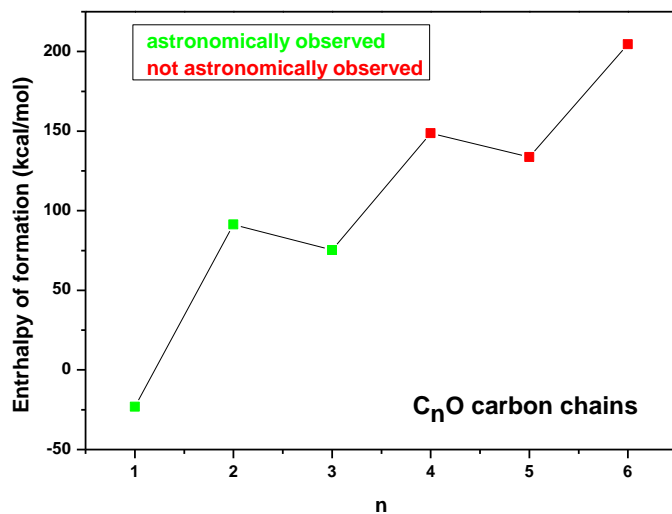


Figure 5.3: Plot showing the $\Delta_f H^\circ$ for $C_n O$ chain molecules

Table 5.44: $\Delta_f H^\circ$ for $C_n O$ chains and current astronomical status

n	$\Delta_f H^\circ$ (kcal/mol)	Astronomical status
1	-23.1	Observed
2	91.4	Observed
3	75.3	Observed
4	148.6	Not observed
5	133.8	Not observed
6	204.5	Not observed

Of the six molecules considered in the $C_n O$ group, the first three ($n=1$ to 3) have been astronomically observed^{75,76,150}. The trend of the enthalpy of formation is the same as in the case of the C_n chain molecules. The odd number carbon chain molecules are found to be more stable (lower enthalpy of formation value) than their corresponding even number carbon chain molecules. The interstellar chemistry of oxygen and sulphur is well established as discussed in chapter 4 of this Thesis, with over 80% of all the known S-containing interstellar molecules having their corresponding O-containing molecules as known interstellar molecules. Also, in most of the cases, the abundance of S-compound relative to its O-analogue is approximately equal to the cosmic S/O ratio^{149,139}. The high probability of $C_5 O$ as an interstellar molecule stems from two important facts; $C_5 O$ has lower enthalpy of formation as compared with $C_4 O$ and $C_6 O$, it is therefore more stable and probably more abundant in ISM, thus can easily be observed as compared to $C_4 O$ and $C_6 O$. Secondly, $C_5 S$, the sulphur analogue of $C_5 O$ has recently been observed¹⁴ and O-containing molecules are known to be more abundant in ISM than their corresponding S-analogue. Hence astronomical observation of $C_5 S$ is a clear indication of the presence of $C_5 O$ in detectable abundance in ISM.

5.7.3 C_nS Chains: IRC+10216, the carbon-star envelope has emerged as one of the richest sources of molecules with over eighty different molecular species so far observed in it. Alongside other molecular clouds, all the known C_nS molecules were observed in IRC+10216. As discussed in the previous section, the interstellar chemistry of oxygen and sulphur is very similar in many ways. Of the four (CS, C₂S, C₃S, C₅S) observed molecules in the C_nS group^{80,81,82,130,14} (CS, C₂S, C₃S) three have the corresponding O-analogues as known interstellar molecules. Whereas C₅S has been astronomically observed, C₄S and C₆S are not. The reason behind this can easily be understood from its enthalpy of formation value (Table 5.45) as compared to those of C₄S and C₆S. This is still in accordance with the ESA relationship. As shown in Table 5.45 and Figure 5.4, all the odd number C_nS chains have lower enthalpy of formation than their corresponding even number C_nS chains, hence they are more stable, more abundant and can thus be more easily observed than the even number counterparts.

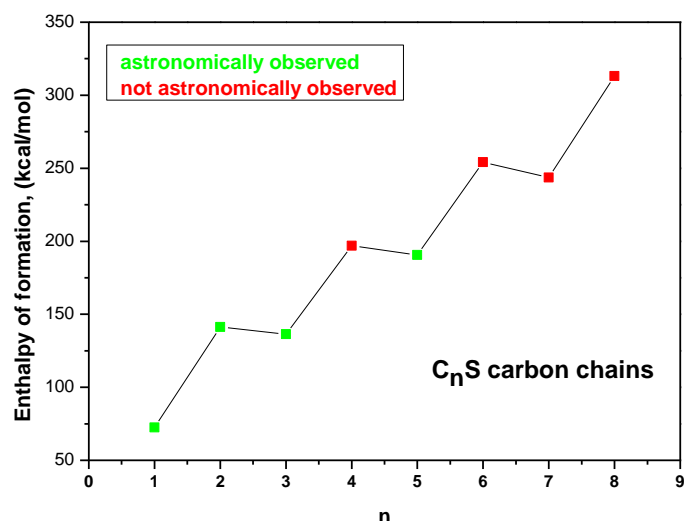


Figure 5.4: Plot showing the $\Delta_f H^\circ$ for C_nS chain molecules

Table 5.45: $\Delta_f H^\circ$ for C_nS chains and current astronomical status

n	$\Delta_f H^\circ$ (kcal/mol)	Astronomical status
1	72.40	Observed
2	141.3	Observed
3	136.3	Observed
4	197.0	Not observed
5	190.7	Observed
6	254.2	Not observed
7	243.7	Not observed
8	313.2	Not observed

5.7.4 C_nN Chains: The long carbon chain radicals like C_nN have long been thought to be present in the interstellar and circumstellar media in detectable abundance and supposed to play an important role in astrophysics. A number of fundamental interstellar molecules were first detected in space before being observed in the gas phase in the terrestrial laboratory, these include HCO⁺, C₂H, HNC, HN₂⁺³⁸ among others, thus most of them were termed "non-terrestrial". Cyanoethynyl radical, C₃N is one of such molecules whose identification was guided by the ESR spectrum of a related species, C₄H (butadiynyl radical). The astronomical observations of C₂N and C₅N were hindered by lack of accurate spectroscopic data. Their astronomical observations became possible immediately after their laboratory microwave spectra were measured.^{17,105-107} Table 5.46 and Figure 5.5 indicate a constant gradual increase in the enthalpy of formation of the C_nN chain molecules as the chain length increases which accounts for why the lower chains have all been observed except for the C₄N.

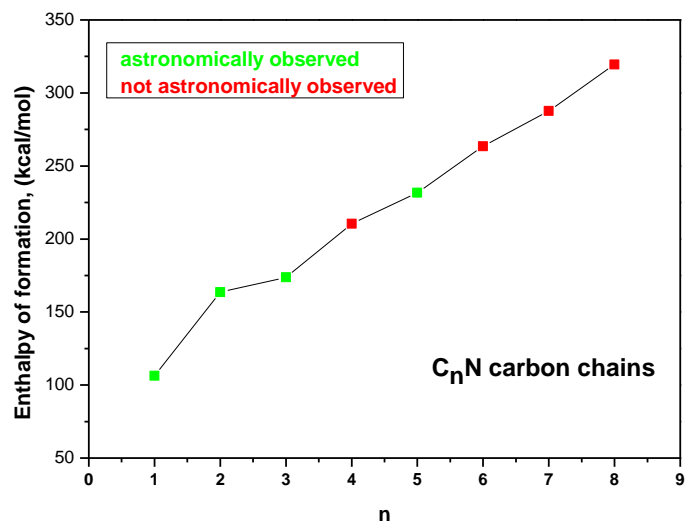


Figure 5.5: Plot showing the $\Delta_f H^\circ$ for C_nN chain molecules

Table 5.46: $\Delta_f H^\circ$ for C_nN chains and current astronomical status

n	$\Delta_f H^\circ$ (kcal/mol)	Astronomical status
1	106.4	Observed
2	163.5	Observed
3	173.7	Observed
4	210.5	Not observed
5	231.7	Observed
6	263.5	Not observed
7	287.7	Not observed
8	319.4	Not observed

5.7 .5 C_nSi Chains: Every unique astronomical observation of molecule(s) in the interstellar or circumstellar medium has always been a concerted effort between the laboratory spectroscopists and the astrophysicists. The successful detection (after a number of failed attempts) of SiC in IRC+10216 came immediately after the successful measurements of its laboratory spectrum.¹¹⁴ Whether cyclic molecules are chemically less abundant than their related linear species in the interstellar or circumstellar medium has been the question for decades now, due to the fact that of about 200 known interstellar and circumstellar molecules, less than 10 are cyclic. However, of the 4 known C_nSi molecules, 2 are cyclic. The ground state geometry of SiC₂ was shown to have a compact symmetric (C_{2v}) ring against the earlier belief that SiC₂ is linear. The proper elucidation of its ground-state geometry became instrumental for its astronomical observation⁸. Figure 5.6 shows the most stable geometry for the SiC₃ molecule which is the rhomboidal isomer. The experimentally determined bond lengths of c-SiC₃ by method of isotopic substitution measurement¹¹⁷ and the theoretically calculated bond lengths at the G4 level are in good agreements as shown in Figure 5A and 5B respectively.

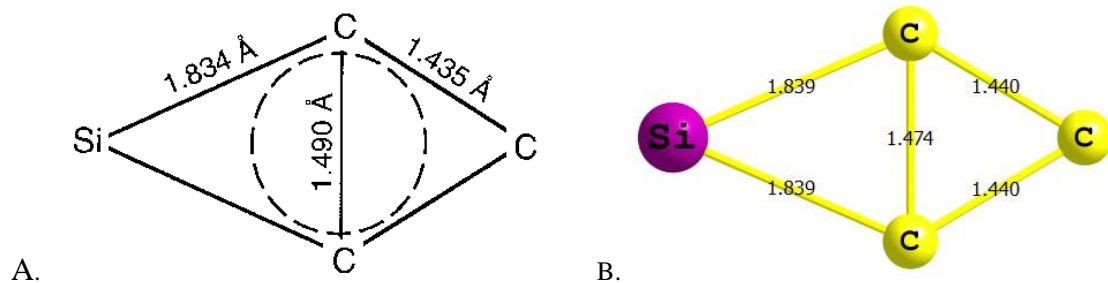


Figure 5.6: Experimental (A) and theoretical geometry (B) of c-SiC₃ molecule

Table 5.47 and Figure 5.7 show the enthalpies of formation for all the C_nSi molecules considered in this study, there is a steady increase in the enthalpy of formation value as the carbon chain increases except for the c-C₂Si. The observed molecules are also the most stable molecules^{114,8,117,116}. The detection of more silicon-carbon molecules in IRC+10216 in particular (where all C_nSi chains have been observed) and other astronomical sources await laboratory spectra of such molecules.

Table 5.47: $\Delta_f H^\circ$ for C_nSi chains and current astronomical status

n	$\Delta_f H^\circ$ (kcal/mol)	Astronomical status
1	177.1	Observed (IRC+10216)
c-C ₂ Si	152.0	Observed (IRC+10216)
c-C ₃ Si	228.8	Observe (IRC+10216)
4	216.9	Observed (IRC+10216)
5	269.7	Not observed
6	277.6	Not observed

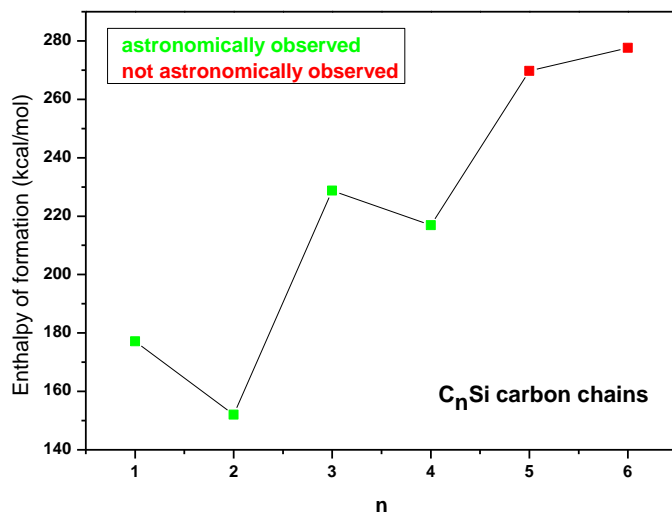


Figure 5.7: Plot showing the $\Delta_f H^\circ$ for C_nSi chain molecules

5.7.6 HC_nN Chains: The largest claimed interstellar linear molecule; the cyanopolyne, $HC_{11}N$ belongs to the HC_nN chains. The enthalpies of formation of these molecules follow a unique trend with the odd number carbon chains being more stable than its preceding and the next even number carbon chains as shown in Table 5.48. For instance, HC_3N is more stable than both HC_2N and HC_4N ; HC_5N is more stable than both HC_4N and HC_6N , etc. Figure 5.8 depicts the zigzag pattern of the enthalpies of formation of the HC_nN chains. Of the 8 molecules belonging to the HC_nN carbon chain that have been detected in interstellar and circumstellar medi^{23-28,30,38} only two (HC_2N and HC_4N) are even number carbon chains while the remaining 6 are odd number carbon chains (HCN , HC_3N , HC_5N , HC_7N , HC_9N , $HC_{11}N$). The reason for the observation of more odd number HC_nN chains can be understood from their enthalpy of formation values in comparison to the even number HC_nN chains. The odd number HC_nN are more stable, more abundant and thus can be more easily observed as compared to the even number HC_nN chains. From this analogy, $HC_{13}N$ is a more probable candidate for astronomical observation than both $HC_{12}N$ and $HC_{14}N$. Accurate laboratory rest frequencies of $HC_{13}N$ will be crucial for its astronomical searches and possible detection.

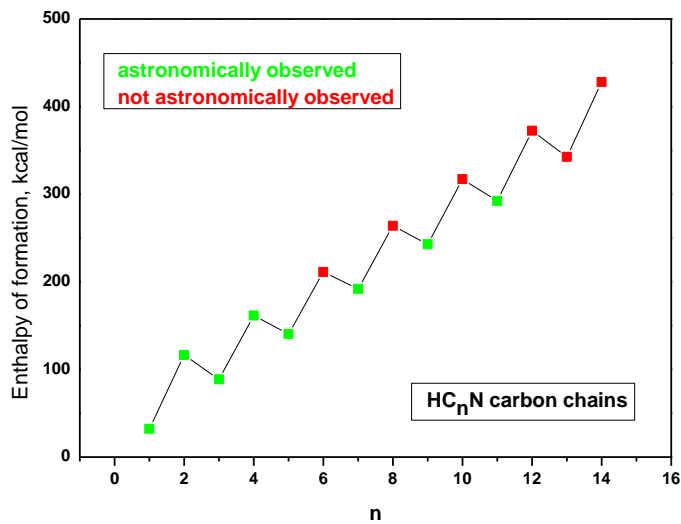


Figure 5.8: Plot showing the $\Delta_f H^\circ$ for HC_nN chain molecules

Table 5.48: $\Delta_f H^\circ$ for HC_nN chains and current astronomical status

n	$\Delta_f H^\circ$ (kcal/mol)	Astronomical status
1	32.2	Observed
2	116.6	Observed
3	88.7	Observed
4	161.6	Observed
5	140.6	Observed
6	211.1	Not observed
7	191.8	Observed
8	263.9	Not observed
9	242.9	Observed
10	317.2	Not observed
11	292.2	Observed
12	372.5	Not observed
13	342.6	Not observed
14	428.0	Not observed

5.7.7 C_nH Chains: Discoveries of cyanopolynes set the pace for the recognition of long chain molecules in space, such as C_nH , C_nH^- etc. The acetylenic chain (C_nH) radical from $n=1$ to $n = 8$ have all been observed in space^{158,42,9,140,129,156,19,143}. The steady increase in the enthalpy of formation of these chains as the carbon chain increases is shown in Table 5.49 and Figure 5.9. Most of the C_nH radicals could be termed as "non-terrestrial" as they were first observed in space using results from quantum chemical calculations prior to being

studied in the laboratory. They are believed to grow steadily in the recombination phase of interstellar medium¹⁵⁶. In the carbon rich astronomical sources such as TMC and IRC+10216 where all the known C_nH chains radicals have been detected, successive members of the C_nH chains ($n > 8$) are more likely to exist.

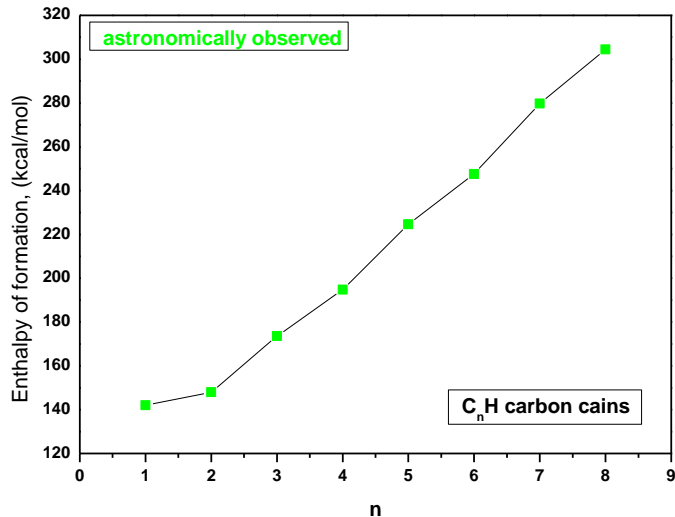


Figure 5.9: Plot showing the Δ_fH° for C_nH chain molecules

Table 5.49: Δ_fH° for C_nH chains and current astronomical status

n	Δ_fH° (kcal/mol)	Astronomical status
1	142.0	Observed
2	148.0	Observed
3	173.6	Observed
4	194.8	Observed
5	224.7	Observed
6	247.6	Observed
7	279.7	Observed
8	304.5	Observed

5.7.8 C_nP Chains: Just like sulphur and oxygen, phosphorus (the 18th most cosmically abundant element) and nitrogen are in the same group in the periodic table. Whereas the similarity between the interstellar chemistry of sulphur and oxygen is well established with almost all S-containing interstellar molecules having the O-analogue as a known interstellar molecule, this is not the case in terms of the interstellar chemistry of N-containing molecules and the P-analogue with only very few known P-containing molecules as compared with the large number of N-containing interstellar/circumstellar molecules. This is due to the cosmic ratio of phosphorus and nitrogen as compared with the cosmic ration of sulphur and oxygen. Table 5.50 and Figure 5.10 display the enthalpy of formation for all the C_nP chains considered in this study. The only two astronomically observed molecules in this group; CP and C_2P ^{141,144} are also the most stable and probably the most abundant in space, thus they are

detectable. Likewise the C_nH chains, there is a corresponding increase in the enthalpy of formation value for every successive increase in the carbon chain.

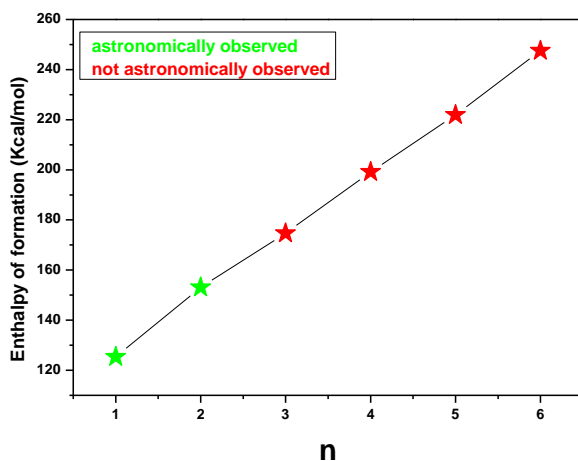


Figure 5.10: Plot showing the $\Delta_f H^\ominus$ for C_nP chain molecules

Table 5.50: $\Delta_f H^\ominus$ for C_nP chains and current astronomical status

n	$\Delta_f H^\ominus$ (kcal/mol)	Astronomical status
1	125.3	Observed
2	153.1	Observed
3	174.7	Not observed
4	199.1	Not observed
5	221.9	Not observed
6	247.6	Not observed

5.7.9 H_2C_n Chains: Interstellar acetylene is a well known starting material in the formation processes of many interstellar and circumstellar species^{154,147}. For the molecules with the empirical formula, H_2C_3 , both the linear and the cyclic isomers have been observed in the Taurus molecular cloud, i.e., TMC-1^{131,159}. The cyclic isomer is now recognized as a common feature of many molecular clouds/astronomical sources. The polyacetylenic chains C_4H_2 and C_6H_2 have been observed in the proto–planetary nebula CRL 618 via their infrared vibrational spectra.²⁰ The first three carbon chains in the H_2C_n group have been astronomically observed as shown in Table 5.51 and Figure 5.11, the next most likely observable member of this group is not H_2C_5 , neither is it H_2C_7 , rather it is the H_2C_6 . This is simply because of its stability and probably its interstellar abundance in comparison to H_2C_5 and H_2C_7 . The even number carbon chains in H_2C_n are stable than their corresponding odd number carbon counterparts, thus accounting for the astronomical observation of more even carbon chains than the odd number carbon chains in this group.

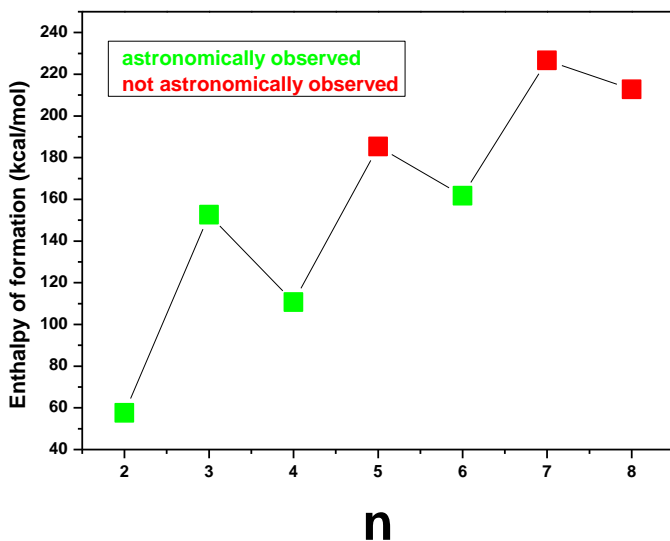


Figure 5.11: Plot showing the Δ_fH° for H_2C_n chain molecules

Table 5.51: Δ_fH° for H_2C_n chains and current astronomical status

n	Δ_fH° (kcal/mol)	Astronomical status
2	57.6	Observed
3(linear)	152.6	Observed
3 (cyclic)	183.0	Observed
4	110.7	Observed
5	185.3	Not observed
6	161.7	Observed
7	226.7	Not observed
8	212.7	Not observed

5.7.10 C_nN^- Chains: Among the ion molecules in interstellar and circumstellar media, the positive ions are known for long and observed while the negative ions are only known for less than a decade. Of the eight C_nN^- chains considered here, only three have been astronomically observed; CN^- C_3N^- and C_5N^- .^{95,99,15} The observed molecules (odd number carbon chains) are found to be more stable than the others. CN^- is more than C_2N^- ; C_3N^- is more stable than both C_2N^- and C_4N^- ; C_5N^- is more stable than both C_4N^- and C_6N^- (Table 5.52). Figure 5.12 depicts the plot of the enthalpy of formation of these molecules which shows a zigzag pattern as noted in the case of the HC_nN chains. Following the order of their astronomical observations, C_7N^- can be considered as the next probable candidate for astronomical observation as it is more stable than both the C_7N^- and the C_8N^- ; thus could be more abundant and easily detectable in space.

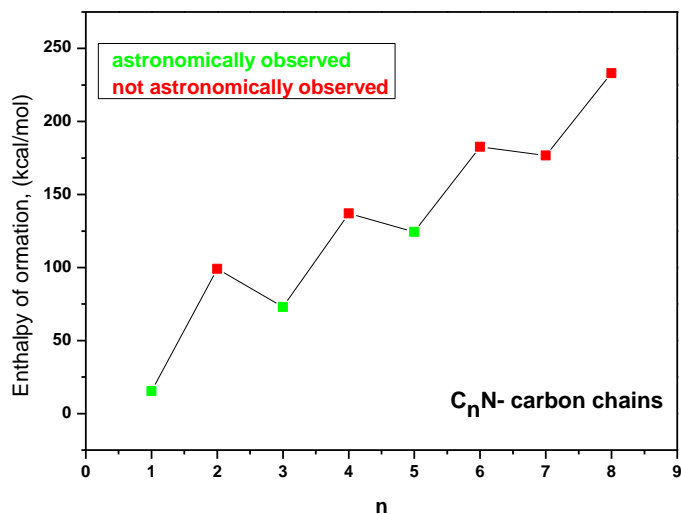


Fig. 5.12. Plot showing the $\Delta_f H^\circ$ for C_nN^- chain molecules

Table 5.52: $\Delta_f H^\circ$ for C_nN^- chains and current astronomical status

n	$\Delta_f H^\circ$ (kcal/mol)	Astronomical status
1	15.5	observed
2	99.2	Not observed
3	72.9	Observed
4	137.1	Not observed
5	124.4	Observed
6	182.6	Not observed
7	176.7	Not observed
8	233.0	Not observed

5.7.11 C_nH⁻ Chains: Molecular anions have long been predicted to be detectable in astronomical sources, and are currently estimated by chemical formation models to be in high abundance than can be compared to their neutral counterparts. The first known interstellar molecular anion, C₆H⁻ was shown to be the carrier of the unidentified series of lines IRC+10216 via laboratory measurements of its rotational spectrum. The astronomical observations of C₄H⁻ and C₈H⁻ came immediately after the successful measurements of their rotational spectra^{92,90,21}. Theoretically estimated enthalpy of formation for the C_nH⁻ (n=1 to 10) chains using the G4 composite method is presented in Table 5.53, the same is also displayed in Figure 5.13. The even number carbon chains are more stable than the preceding and the next odd number carbon chains; C₂H⁻ is more stable than CH⁻ and C₃H, C₄H⁻ is more stable than C₃H⁻ and C₅H⁻, and so on. The rotational spectrum of C₂H⁻ is known¹²⁸, its astronomical observation is a function of time. The three astronomically detected C_nH⁻ are all odd number carbon chains; these are the most stable and thus the most abundant in space which accounts for their observation as compared to the preceding and the next even number chains in each case which have not been observed.

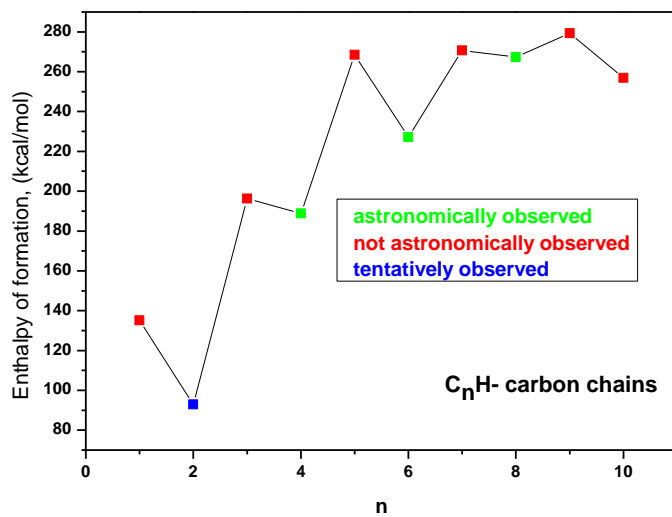


Figure 5.13: Plot showing the Δ_fH° for C_nH^- chain molecules

Table 5.53: Δ_fH° for C_nH^- chains and current astronomical status

n	Δ_fH° (kcal/mol)	Astronomical status
1	135.1	Not observed
2	92.9	Tentatively observed
3	196.3	Not observed
4	188.8	Observed
5	268.5	Not observed
6	227.1	Observed
7	270.7	Not observed
8	267.4	Observed
9	279.3	not observed
10	257.0	not observed

Table 5.54 gives the summary of all the different carbon chains that have been considered in this study, it is obvious from the table that in each group, the number of the odd and even number carbon chains observed depend on the trend of the enthalpy of formation of the molecules in that group. The odd number carbon chains are found to be more stable than their corresponding even number carbon chains in most of the group (Figure 5.14); this has resulted in the observation of more interstellar odd number ($\approx 60\%$) carbon chains than the even number carbon chains.

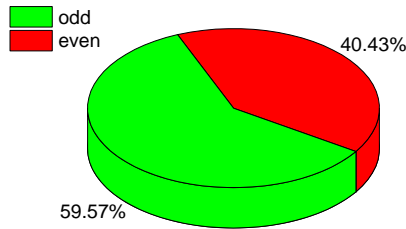


Figure 5.14: Percentage of detected odd and even number carbon chains

Table 5.54: Carbon chains that have been considered in this study

Chain	Total number considered	Odd observed	Even observed
C_n	7	2	1
C_nO	6	2	1
C_nS	8	3	1
C_nN	8	3	1
C_nSi	6	2	2
HC_nN	14	6	2
C_nH	8	4	4
C_nP	6	1	1
C_nN^-	8	3	0
C_nH^-	10	0	3
H_2C_nN	8	2	3
Total	89	27	19

5.8 Effect of Kinetics on the Formation of Carbon Chains

The effect of kinetics in the formation of carbon chain species both in the terrestrial laboratory and in the interstellar medium cannot be overemphasized. Though there is hardly a consensus as to how any molecule (especially the complex ones with six atoms and above) is formed in the interstellar medium, but C_2 addition is the widely claimed route for the formation of the linear carbon chains. In the terrestrial laboratory, unsaturated molecules like acetylene, diacetylene, etc., are used as the source of the C_2 in producing the carbon chains while in the interstellar medium, acetylene which produces the C_2 is generally accepted as the starting material for the formation of these carbon chains^{9,159,53,133,134}. With respect to the carbon chains discussed here, it is obvious that the effect of kinetics is dominated by thermodynamics in almost all the different chains. For instance, in the C_nO chains where the odd numbered carbon chains are more stable than their progressive even numbered chains, C_2 addition to the lower chains to form the higher chains clearly favours the odd numbered chains as compared to their corresponding even numbered chains. A C_2 addition to CO to

form C_3O has a lower barrier as compared to C_2 addition to C_2O to form C_4O , which could account for the delayed observation of C_4O . This is also applicable to the C_nS chains, a C_2 addition to C_3S to form C_5S (astronomically observed) is more favourable than a C_2 addition to C_2S to form C_4S (yet to be observed). And this goes on to the higher members of the chains. Also, in the HC_nN and C_nN^- chains, C_2 addition to form higher members of the chains favours the odd numbered carbon chains as compared to the even numbered chains which explains the trends in the astronomical observation of these species. In the C_nSi , H_2C_n , and C_nH^- chains where the even numbered carbon chains are more stable than their corresponding odd numbered chains, it is crystal clear that C_2 addition to the lower members of the chains obviously favours the even numbered carbon chains as compared to their odd numbered counterparts. For instance, a C_2 addition to HC_5N to form HC_7N is more favourable than C_2 addition to HC_4N to form HC_6N which has not been detected. The effect of kinetics in the formation of these species is predominantly influenced by thermodynamics even for the chains with a linear increase in the enthalpy of formation like the C_nH , C_nP , C_nN and C_n chains. Thus, it suffices to say that the formation of the carbon chains is partially thermodynamically controlled.

5.9 Summary on Linear Interstellar Carbon Chains and Thermodynamics: A comprehensive investigation of different interstellar carbon chain molecules; C_n , H_2C_n , HC_nN and C_nX ($X=N, O, Si, S, H, P, H^-, N^-$) with a total of 88 species have been carried out using high level quantum chemical simulation to determine their accurate enthalpies of formation of these molecules. From the results, in all the groups considered, the most stable molecules which are probably the most abundant in interstellar and circumstellar media are the molecules that have been astronomically observed. This serves as a revalidation of the ESA relationship among interstellar/circumstellar molecules and its importance in elucidating the whys and wherefores among these molecules. This further stresses the significance of thermodynamics as a key parameter in astrophysical/astronomical processes. The next possible candidate for astronomical observations in each of the carbon chain groups considered is proposed. The effect of kinetics in the formation of these molecular species is shown to be predominantly influenced by thermodynamics.

5.10 Conclusions on Linear Interstellar Carbon Chains: The Dominant Theme in Interstellar Chemistry

This chapter discusses one of the most interesting, important and fascinating classes of interstellar molecular species- "***the linear interstellar carbon chains***". After setting the stage, accurate spectroscopic parameters which are the indispensable tools for the astronomical observation of these molecular species are obtained via an inexpensive, combined experimental and theoretical approach. The obtained accuracy of few kHz is within the expected experimental accuracy. With the availability of the spectroscopic parameters; thermodynamics is utilized in accounting for the known systems and in examining the right

candidates for astronomical searches. These molecular species are shown to also obey the ESA relationship observed for the isomeric species discussed in chapter three of this work. The effect of kinetics on the formation processes of these molecular species is well controlled by thermodynamics as discussed in this chapter. Finally, the application of these studies in reducing the 'U' lines and probing new molecular species has been briefly summarized.

5.11 References

1. Fraser, H. J., McCoustra, M. R. S., Williams, D. A. *Astron Geophys*, 2002, 43 (2) 2.10-2.18.
2. Tielens, A. G. G. M. *Rev. Mod Phys.*, 2013, 85, 1021
3. Etim, E. E., Arunan, E. *Planex*, 2015, 5, 16
4. Turner, B. E. 1991. *Astrophys J Suppl S.*, 76, 617
5. Dickens, J. E., Irvine, W. M., Ohishi, M., Ikeda, M., Ishikawa, S., Nummelin, A., Hjalmarson, A. *Astrophys J*, 1997, 489, 753
6. Loomis, R. A., Zaleski, D. P., Steber, A. L., et al., *Astrophys J Lett*, 2013, 765, L9
7. Hollis, J. M., Remijan, A. J., Jewell, P. R., Lovas, F. J. *Astrophys J*, 2006, 642, 933
8. Thaddeus, P., Cummins, S. E., Linke, R. A. *Astrophys J*, 1984, 283, 45-48.
9. Thaddeus, P., Vrtilek, J. M., Gottlieb, C. A. *Astrophys J*, 1985, 299, 63
10. Cami, J., Bernard-Salas, J., Peeters, E., Malek, S. E. *Science*, 2010, 329, 1180
11. Berné, O., Mulas, G., Joblin, C. *Astron Astrophys*, 2013, 550, L4.
12. Belloche, A., Garrod, R. T., Müller, H. S. P., Menten, K. M. *Science*, 2014, 345, 1584-1587.
13. Bell, M. B., Feldman, P. A., Travers, M. J., McCarthy, M. C., Gottlieb, C. A., Thaddeus, P. *Astrophys J*, 1997, 483, L61
14. Agúndez, M., Cernicharo, J., Guélin, M. *Astron Astrophys*, 2014, 570, A45
15. Agúndez, M., Cernicharo, J., Guélin, M., et al. *Astron Astrophys*, 2010, 517, L2.
16. Cernicharo, J., Goicoechea, J. R., Caux, E. *Astrophys J*, 2000, 534, L199
17. Anderson, J. K., Ziurys, L. M. *Astrophys J*, 2014, 795, L1
18. Ohishi, M., Kaifu, N., Kawaguchi, K., et al. *Astrophys J*, 1989, 345, L83
19. Cernicharo, J., Guélin, M. *Astron Astrophys*, 1996, 309, L27
20. Cernicharo, J., Heras, A. M., Tielens, A. G. G. M., et al. *Astrophys J*, 2001, 546, L123
21. Brünken, S., Gupta, H., Gottlieb, C. A., McCarthy, M. C., Thaddeus, P. *Astrophys J*, 2007, 664, L43
22. Halfen, D. T., Clouthier, D. J., Ziurys, L. M. *Astrophys J*, 2008, 677, L101
23. Snyder, L. E., Buhl, D. *Astrophys J*, 1971, 163, L47
24. Turner, B. E. *Astrophys J*, 1971, L35-L39.
25. Avery, L. W., Broten, N. W., MacLeod, J. M., Oka, T., Kroto, H. W. *Astrophys J*, 1976, 205, L173
26. Kroto, H. W., Kirby, C., Walton, D. R. M., et al. *Astrophys J*, 1978, 219, L133-L137.
27. Broten, N. W., Oka, T., Avery, L. W., MacLeod, J. M., Kroto, H. W. *Astrophys J*, 1978, 223, L105
28. Bell, M. B., Feldman, P. A., Travers, M. J., McCarthy, M. C., Gottlieb, C. A., Thaddeus, P. *Astrophys J*, 1997, 483, L61
29. Guelin, M., Cernicharo, J. *Astron Astrophys*, 1991, 244, L21
30. Cernicharo, J., Guelin, M., Pardo, J. R. *Astrophys J*, 2004, 615, L145.
31. Travers, M. J., McCarthy, M. C., Kalmus, P., Gottlieb, C. A., Thaddeus, P. *Astrophys J*, 1996, 472, L61
32. McCarthy, M. C., Grabow, J. -U., Travers, M. J., Chen, W., Gottlieb, C. A., Thaddeus, P. *Astrophys J*, 1998, 494, L231
33. Tang, J., Sumiyoshi, Y., Endo, Y. *Chem. Phys. Lett.*, 1999, 315, 69
34. Botschwina, P. *A Chem. Phys. Lett.*, 1987, 139, 255
35. Ziurys, L. M., Turner, B. E. *Astrophys J*, 1986, 302, L31
36. Kawaguchi, K., Kasai, Y., Ishikawa, S. -I., Ohishi, M., Kaifu, N., Amano, T. *Astrophys J*, 1994, 420, L95
37. Green, S., Montgomery, Jr., J. A., Thaddeus, P. *Astrophys J*, 1974, 193, L89

38. Guélin, M., Thaddeus, P. *Astrophys J*, 1977, 212,L81

39. Buhl, D., Snyder, L. E. *Nature*, 1970, 228,267.

40. Woods, R. C., Gudeman, C. S., Dickman, R. L., et al. *Astrophys J*, 1983, 270,583.

41. Zuckerman, B., Morris, M., Palmer, P., Turner, B. E. *Astrophys J*, 1972, 173,L125.

42. Tucker, K. D., Kutner, M. L., Thaddeus, P. *Astrophys J*, 1974, 193,L115

43. Frisch, M. J., Trucks, G. W., Schlegel, H. B., Scuseria, G. E., Robb, M. A., Cheeseman, J. R., Scalmani, G., Barone, V., Mennucci, B., Petersson, G. A., Gaussian 09, revision D.01, Gaussian, Inc., Wallingford, CT, 2009.

44. Pople, J. A., Nesbet, R. K. *J. Chem. Phys.*, 1954, 22, 571.

45. McWeeny, R., Dierksen, G. *J. Chem. Phys.*, 1968, 49, 4852

46. Chandrasekhar, J., Andrade, J. G., Schleyer, P. V. R. *J Am Chem Soc*, 1981, 103, 5609

47. Hariharan, P.C., Pople, J. A. *Theor. Chim. Acta*, 1973, 28, 213

48. Simmons, J. W., Anderson, W. E., Gordy, W. *Phys. Rev.* 77, 1950, 77.

49. De Zafra, R. L. *Astrophys J*, 1971, 170, 165

50. Alexander, A. J., Kroto, H. W., Walton, D. R. M. *J Mol Spectrosc.*, 1976, 62,175

51. Kroto, H. W., Kirby, C., Walton, D. R. M., et al. *Astrophys J*,1978, 219,L133

52. McCarthy, M. C., Levine, E. S., Apponi, A. J., Thaddeus, P. *J Mol Spectrosc.*, 2000, 203, 75

53. McCarthy, M. C., Travers, M J., KovaCs, A., Gottlieb,C. A., Thaddeus, P. *Astrophys JSuppl S.*, 1997, 113,105

54. McCarthy,M. C., Grabow,J. -U., Travers,M. J., Chen,W., Gottlieb, C. A. Thaddeus, P. *Astrophys J*, 1998, 494,L231-L234.

55. Botschwina, P., Heyl, A., Oswald, M., Hirano, T. *Spectrochim Acta A*, 1997, 53,1079

56. Botschwina, P., Horn, M., Markey, K., Oswald, R. *Mol Phys*, 1997, 92 (3),381

57. Heyl, A., Botschwina, P., Hirano, T. *J Chem Phys*, 1997, 107, 9702

58. Nethercot, Jr., A. H., Klein, J. A., Townes, C. H. *Phys. Rev.* 1952, 86, 798

59. Spahn, H., Mu"ller , H. S. P., Giesena, T. F., Grabow, J. -U., Harding, M. E., Gauss, J., Schlemmer, S. *Chem Phys*, 2008, 346, 132

60. Macleod, J. M., Avery, L. W., Broten, N. W. *Astrophys J*, 1981, 251, L33

61. Howe, D. A., Millar, T. J., Schike, P., Walmsley, C. M. *Mont. Not. R. Astron. Soc.* 1994, 267, 59

62. Turner, B. E., Zuckerman, B. *Astrophys J*, 1987, 225, L75

63. Saito, S., Endo, Y., Hirota, E. *J Chem Phys*, 1984, 80, 1427.

64. Gordon, V. D., McCarthy, M. C., Apponi, A. J., Thaddeus, P. *Astrophys J*, 2000, 540,286

65. McCarthy, M. C., Thaddeus, P. *J. Mol. Spec.*, 2005, 232,351

66. Saykally, R. J., Szanto, P. G., Anderson, T. G., Woods, R. C. *Astrophys J*, 1976, 204,L143

67. Kruger, M., Dreizler, H., Preugschat,D.,Lentz, D. *Angew Chem Int Edit.* 1991, 30(12), 1644

68. Botschwina, P., Heyl, A. *J. Chem.Phys.*, 1998, 109,3108

69. Bester, M., Tanimoto, M., Vowinkel, B., Winnewisser, G., Yamada, K. Z. *Naturforschung*, 1983, 38a, 64

70. Boucher, J. Burie, A. Bauer, A. Dubrulle, J. Demaison. *J. Phys. Chem. Ref. Data*, 1980, 9(3), 659

71. Chen, W., Grabow, J., Travers, M. J., Munrow, M. R., Novick, S. E., McCarthy, M. C., Thaddeus, P. *J Mol Spectrosc*, 1998, 192, 1

72. Snyder, L. E., Hollis, J. H., Jewell, P. R., Lovas, F. J., Remijan, A. *Astrophys J*, 2006, 647,412

73. Broten, N. W., MacLeod, J. M., Avery, L. W., Irvine, W. M., Höglund, B., Friberg, P., Hjalmarson, A. *Astrophys J*, 1984, 276,L25

74. Solomon, P. M., Jefferts, K. B., Penzias, A. A., Wilson, R. W. *Astrophys J*, 1971, 168,L107

75. Smith, A. M., Stecher, T. P. *Astrophys J*, 1971, 164,L43

76. Ohishi, M., Suzuki, H., Ishikawa, S. -I, et al.. *Astrophys J*, 1991, 380, L39

77. Matthews, H. E., Irvine, W. M., Friberg, P., Brown, R. D., Godfrey, P. D. *Nature*, 1984, 310,125.

78. Ohshima, Y., Endo, Y., Ogata, T. *J Chem Phys*, 1995,102, 1493

79. Ogata, T, Ohshima, Y., Endo, Yasuki. *J. Am. Chem. Soc*, 1995, 117, 3593

80. Penzias, A. A., Solomon, P. M., Wilson, R. W., Jefferts, K. B. *Astrophys J*, 1971, 168,L53

81. Saito, S., Kawaguchi, K., Yamamoto, S., Ohishi, M., Suzuki, H., Kaifu, N. *Astrophys J*, 1987, 317,L115

82. Yamamoto, S., Saito, S., Kawaguchi, K., Kaifu, N., Suzuki, H. *Astrophys J*, 1987, 317,L119.

83. Cernicharo, J., Gottlieb, C. A., Guélin, M., Thaddeus, P., Vrtilek, J. M. *Astrophys J*, 1989, 341,L25

84. Agúndez, M., Cernicharo, J., Guélin, M. *Astron Astrophys*, 2014, 570,A45

85. Gordon, V. D., McCarthy, M. C., Apponi, A. J., Thaddeus, P. *Astrophys J, Suppl S*, 2001, 134, 311

86. Lovas, F. J., Krupenie, P. H. *J. Phys.Chem. Ref. Data.*, 1974, 3, 245

87. Saito, S., Kawaguchi, K., Yamamoto, S., Ohishi, M., Suzuki, H., Kaifu, N. *Astrophys J*, 1987, 317,L115

88. Hirahara, Y., Ohshima, Y., Endo, Y. *J Chem. Phys.*, 1994, 101, 7342

89. Vrtilek, J. M., Gottlieb, C. A., Gottlieb, E. W., Wang, W., and Thaddeus, P. *Astrophys J Lett*, 1992, 398, L73

90. McCarthy, M. C., Gottlieb, C. A., Gupta, H., Thaddeus, P. *Astrophys J*, 2006, 652, L141

91. Brünken, S., Gupta, H., Gottlieb, C. A., McCarthy, M. C., Thaddeus, P. *Astrophys J*, 2007, 664, L43

92. Cernicharo, J., Guélin, M., Agúndez, M., Kawaguchi, K., McCarthy, M., Thaddeus, P. *Astron Astrophys*, 2007, 467,L37

93. Cernicharo, J., Guélin, M., Agúndez, M., McCarthy, M. C., Thaddeus, P. *Astrophys J*, 2008, 688, L83

94. Remijan, A. J., Hollis, J. M., Lovas, F. J., et al. *Astrophys J*, 2007, 664, L47

95. Thaddeus, P., Gottlieb, C. A., Gupta, H., et al. *Astrophys J*, 2008, 677,1132

96. Agúndez, M., Cernicharo, J., Guélin, M., et al. *Astron Astrophys*, 2010, 517, L2

97. Gupta, H., Brünken, S., Tamassia, F., Gottlieb, C. A., McCarthy, M. C., Thaddeus, P. *Astrophys J*, 2007, 655, L57

98. Gottlieb, C. A., Brünken, S., McCarthy, M. C., Thaddeus, P. *J. Chem. Phys.*, 2007, 126, 191101

99. Cernicharo, J., Guélin, M., Agúndez, M., McCarthy, M. C., Thaddeus, P. *Astrophys J*, 2008, 688, L83

100. Lovas, F. J., Suenram, R. D. *J. Phys. Chem. Ref. Data.*, 1989, 18(3), 1245

101. McCarthy, M. C., Chen, W., Apponi, A. J., Gottlieb, C. J., and Thaddeus, P. *Astrophys J*, 1999, 520, 158

102. McCarthy, M. C., and Thaddeus, P. *2005. J Chem Phys*, 122, 174308

103. McCarthy, M. C., Travers, M. J., Kalmus, P., Gottlieb, C. A., and Thaddeus, P. *Astrophys J*, 1996, 467, L125

104. Gottlieb, C. A., McCarthy, M. C., Travers, M. J., Grabow, J. -U., and Thaddeus, P. *J Chem Phys*, 1998, 109, 5433

105. Jefferts, K. B., Penzias, A. A., Wilson, R. W. 1970. *Astrophys J*, 1970, 161,L87

106. Frerking, M. A., Linke, R. A., Thaddeus, P. *Astrophys J*, 1979, 234,L143

107. Guélin, M., Neininger, N., Cernicharo, J. *Astron Astrophys*, 1998, 355,L1

108. Anderson, J. K. Ziurys, L. M. *Astrophys J*, 2014, 795,L1

109. Lovas, F. J., Tienmann, E. J. *Phys.Chem. Ref. Data*, 1974, 3, 609

110. Anderson, J. K., Halfen, D. T., Ziurys, L. M. *J Mol Spectrosc*, 2015, 307, 1

111. Gottlieb, C. A., Gottlieb, E. W., Thaddeus, P., Kawamura, H. *Astrophys J*, 1983, 275, 916

112. McCarthy, M. C., Fuchs, F. W., Winnewisser, G., Thaddeus, P. *J. Chem. Phys.*, 2003, 118(8),3549

113. Kasai, Y., Sumiyoshi, Y., Endo, Y., Kawaguchi, K. *Astrophys J*, 1997, 477 ,L65

114. Cernicharo, J., Gottlieb, C. A., Guélin, M., Thaddeus, P., Vrtilek, J. M. *Astrophys J*, 1989, 341,L25

115. McCarthy, M. C., Apponi, A. J., Gottlieb, C. A., Thaddeus, P. *Astrophys J*, 2000, 538,766

116. Ohishi, M., Kaifu, N., Kawaguchi, K., et al. *Astrophys J*, 1989, 345,L83

117. Apponi, A. J., McCarthy, M. C., Gottlieb, C. A., Thaddeus, P. *Astrophys J*, 1999, 516, L103

118. Thaddeus, P., Cummins, S. E., Linke, R. A. *Astrophys J*, 1984, 283,L45

119. Buhl, D., and Snyder, L. E. in *Molecules in the Galactic Environment* (Eds) Gordon, M. A., and Snyder, L. E. Wiley-Interscience, New York, 1973, Pp,187-195.

120. Walmsley, C. M., Jewell, P. R., Snyder, L. E., and Winnewisser, G. 1984. *Astron Astrophys*, 1984, 134,L11

121. Remijan, A. J., Hollis, J. M., Snyder, L. E., Jewell, P. R., and Lovas, F. J. *Astrophys J*, 2006, 643,L37

122. Trambarulo, R., and Gordy, W. 1950. *J Chem Phys.*, 1995, 18, 1613

123. Bester, M., Yamada, K., Winnewisser, G., Joentgen, W., Altenbach, H.-J., Vogel, E. *Astron Astrophys*, 1984, 137, L20

124. Alexander, A. J., kroto, H. W., Maier, M., Walton, D. R. M. *J Mol Spectrosc*, 1978, 70 (1), 84

125. Travers, M. J., Chen, W., Grabow, J.-U., McCarthy, M. C., Thaddeus, P. *J. Mol. Spectrosc.*, 1998, 192, 12

126. Chen, W., McCarthy, M. C., Novick, S. E. Thaddeus, P. J. Mol. Spectrosc., 1998, 196, 335

127. Bernath, P. F., Hinkle, K. H., Keady, J. J. 1989. Science, 1989, 244,562

128. Bru"nken, S., Gottlieb, C. A., Gupta, H., McCarthy, M. C., Thaddeus, P. Astron Astrophys, 2007, 464, L33.

129. Cernicharo, J., Kahane, C., Gómez-González, J., Guélin, M. Astron Astrophys, 1986, 164, L1

130. Cernicharo, J., Kahane, C., Guélin, M., Hein, H. Astron Astrophys, 1987, 181,L9

131. Cernicharo, J., Gottlieb, C. A., Guélin, M. Astrophys J, 1991, 368,L39

132. Cernicharo, J., Bailleux, S., Alekseev, E., et al. Astrophys J, 2014, 795,40

133. Cherchneff, I., Glassgold, A. E., Mamon, G. A. Astrophys J, 1993, 410,188

134. Cherchneff, I., and Glassgold, A. E. Astrophys J, 1993, 419, L41

135. Curtiss, L. A., Redfern, P. C., Raghavachari, K. J Chem Phys, 2007, 126, 084108

136. Curtiss, L. A., Redfern, P. C., Raghavachari, K. J Chem Phys, 2007, 127, 124105

137. Etim, E. E., Arunan, E. 2016. Submitted .

138. Freija De Vleeschouwer et al. ,Org Lett, 2007, 9 (14) 2721

139. Frerking, M. A., Linke, R. A., Thaddeus, P. Astrophys J, 1979, 234,L143

140. Guélin, M., Green, S., Thaddeus, P. Astrophys J, 1978, 224,L27

141. Guélin, M., Cernicharo, J., Paubert, G., Turner, B. E. Astron Astrophys, 1990, 230,L9

142. Guélin, M., Cernicharo, J. Astron Astrophys, 1991, 244,L21

143. Guélin, M., Cernicharo, J., Travers, M. J., et al. Astron Astrophys, 1997, 317,L1

144. Halfen, D. T., Clouthier, D. J., Ziurys, L. M. Astrophys J, 2008, 677,L101

145. Hinkle, K. H., Keady, J. J., Bernath, P. F. Science, 1988, 241,1319

146. Kolesniková, L., Tercero, B., Cernicharo, J., et al. Astrophys J, 2014, 784,L7

147. Lacy, J. H., Evans II, N. J., Achtermann, J. M., et al. Astrophys J, 1989, 342,L43

148. Leung, C.M., Herbst, E., Huebner, W.F. Astrophys J, 1984, 56, 231.

149. Linke, R. A., M. A. Frerking, M. A., Thaddeus, P. Astrophys J, 1979, 234,L139

150. Matthews, H. E., Irvine, W. M., Friberg, P., Brown, R. D., Godfrey, P. D. Nature, 1984, 310,125

151. McElroy, D., Walsh, C., Markwick, A. J., Cordiner, M. A., Smith, K., Millar, T. J. Astron Astrophys, 2013, 550, A36

152. Parr, R. G., Pearson, R. G. J Am. Chem. Soc 1983, 105, 7512

153. Remijan, A. J., Snyder, L. E. , McGuire, B. A., et al. Astrophys J, 2014, 783,77

154. Ridgway, S. T., Hall, D. N. B., Wojslaw, R. S., Kleinmann, S. G., Weinberger, D. A. Nature, 1976, 464,345

155. Souza, S. P., Lutz, B. L. Astrophys J, 1977, 216,L49

156. Suzuki, H. Astrophys J, 1983, 272, 579

157. Suzuki, H., Ohishi, M., Kaifu, N., et al. 1986. Publ Astron Soc JPN. 38,911

158. Swings, P., Rosenfeld, L. Astrophys J, 1937,86,483-486

159. Thaddeus, P., Vrtilek, J. M., Gottlieb, C. A. Astrophys J, 1985, 299,L63

160. Thaddeus, P., McCarthy, M. C., Travers, M. J., Gottlieb, C. A., Chen, W. Faraday Discuss, 1998, 109, 121.

161. Woodall, J., Agndez, M., Markwick-Kemper, A.J., Millar, T.J. Astron Astrophys, 2007, 466, 1197

Interstellar Ions and Isotopologues: Known and Potential

Preamble: Two unique classes of interstellar molecular species; *Interstellar Ions and Isotopologues* are investigated in this chapter. The ions play significant role in the formation process of interstellar molecular species because of their reactive nature and the ease at which they go into reaction with other species. The isotopologues serve as the most appropriate tools for testing ion-molecule processes for the formation and destruction of many interstellar species. Two different studies on interstellar ions are presented in the first part (from section 6.0 to section 6.6) of this chapter while the second part (beginning from section 6.7) has the same number of studies discussing interstellar isotopologues.

Interstellar Protonated Molecular Species

6.0 Introduction: About 10% of all the known interstellar and circumstellar species molecular species are cations. Almost 80% of these cations are protonated species whose neutral analogues are also known molecular species in the interstellar medium (ISM). The unambiguously high cosmic abundance of hydrogen makes it the primary reactant for most of the chemical processes in ISM. Ion-molecule reactions are the dominant gas phase chemistry processes in ISM, the ionized forms of hydrogen; H^+ and H_3^+ are at the root of the ion-molecule reactions which occur with very little or no activation barrier. The high abundance of H_3^+ in the molecular clouds thus implies that any neutral molecular species in ISM can be protonated. The protonated species are natural precursors for the neutral species^{1,2}. Thus there is a direct link between a protonated species and its neutral analogue whether such species have been astronomically observed or yet to be observed. The protonated interstellar species are not only useful in modelling interstellar cloud chemistry, they also signal the presence and abundance of non-polar neutral species that are difficult to detect via rotational transitions due to their lack of permanent dipole moment. For instance, the N_2H^+ and $HOCO^+$ were long detected before their neutral analogues; N_2 and CO_2 respectively. The observations of these protonated species further confirms the presence and detectability of the neutral analogues thus leading to the enhanced searches for these neutral species that finally led to their successful astronomical observations³⁻⁶.

Dissociative recombination process in which a positive molecular ion combines with an electron giving rise to neutral species remains one of the main formation routes for interstellar molecular species as a result of the prevailing conditions in ISM. Isomerism is one of the outstanding characteristics among the interstellar molecular species with about 40% of all the interstellar molecular species (excluding the diatomics and some special species that cannot form isomers) having their isomeric counterparts. These isomeric species are believed to have a common precursor for their formation routes. The large number of metastable isomers among the known interstellar species simply implies that these isomers are formed together via dissociative recombination reactions. Thus for every neutral isomeric species, there also exist its protonated analogue.^{7,8}

The binding of a proton to a neutral molecule can occur in more than one position in the molecular structure; this results in different protonated species and proton affinities (PAs) corresponding to the same neutral species. The magnitude of the PA furnishes us with the strength of the stability of the protonated species. A higher PA value simply entails that the proton is strongly bonded to the neutral molecule which implies a higher stability for the protonated species. Of course there is a direct relationship between the stability of a molecular species and its interstellar abundance which influences astronomical observations. It is well known that the most stable species is also the most abundant species in ISM in comparison with its less stable analogues except where other factors like interstellar hydrogen bonding, different formation routes, etc dominate. Therefore, for a neutral molecule giving rise to two different protonated species with different PAs, the protonated species

corresponding to the highest PA is the most stable compared to the other with the lower PA. The most stable protonated species is thus more abundant and as such easily detectable as compared to its counterpart with lower PA. This is because the species with lower PA can easily transfer its proton and return to its neutral form unlike its isomer that results from a higher PA value for the same neutral species which prefers to remain protonated. The low stability of the protonated species with low PA also implies high reactivity of the protonated species which reduces its interstellar abundance, thus making its astronomical observation a bit difficult. That the protonated species with the highest PA is more stable, more abundant and easily observed astronomically as compared to its analogue with lower PA can easily be proven to be true when both species (with lower and higher PAs) have been astronomically observed. HCO^+ and HOC^+ are both protonated analogues of CO, the reported column densities for these species observed from the same astronomical source illustrates the above fact with the HCO^+ with higher PA being over 10 times more abundant than HOC^+ with lower PA. Also, HCO^+ was observed over a decade before the HOC^+ ; thus showing the ease of observing the most stable species as compared to the less stable which is probably less abundant.⁹⁻¹¹

The present work aims at computing accurate PA for neutral interstellar molecular species using high level ab initio quantum chemical calculations. Over 100 neutral species have been considered majority of which are giving rise to two protonated species from the same neutral species. The results of this investigation are to address the whys and wherefores regarding the astronomical observations of protonated interstellar species. The most stable protonated species which is probably the most abundant species in ISM and as such a better candidate for astronomical observation is highlighted in each case. Comparison is made between the PAs of neutral species whose protonated analogues have been astronomically observed and those with protonated analogues yet to be observed. The computational methods and the procedures are briefly summarised followed by the presentation of the obtained results and the discussion of the same.

6.1 Computational Details

All the quantum chemical calculations reported here have been carried out using the GAUSSIAN 09 suit of programs¹². The PAs for few of the neutral species considered in this study are experimentally known. Computational methods that can compute the PAs to very high accuracy for the neutral species with experimentally known PAs can by extension be able to predict accurate PAs values for those species without experimentally reported PAs. In order to obtain highly accurate PAs for all the systems considered here, different high level ab initio methods have been employed. The Møller-Plesset second order perturbation theory; MP2(full) and the Coupled Cluster method with Single and Double excitations (CCSD) are used with the Dunning correlation-consistent polarized valence double zeta (cc-pVDZ) basis set which is designed to converge smoothly towards the complete basis set limit.¹³⁻¹⁶ In addition to the above methods, 2 compound models; the Gaussian 4 theory (G4) and the Weizmann theory (W2U) are also utilized in predicting accurate PAs for all the systems under consideration. These compound models offer high accuracy results at less

computational cost. They consist of different component calculations whose results are then combined in a predefined manner. Both Hartree-Fock and Post-SCF methods are combined in the process.¹⁷⁻²¹ All the neutral species and their possible protonated analogues were optimized with the different methods mentioned above. For the calculation of the PA for each of the systems, only stable equilibrium structures are considered. This was verified via harmonic frequencies calculations with the equilibrium geometries having only real frequencies with no imaginary frequencies. PA is calculated as the difference in energy (electronic energy) between a neutral species and its protonated analogue. Zero point correction to energies are included in all the calculations reported here. All the values reported here are expressed in kcal/mol.

6.2.0 Results and Discussion

The results obtained based on the methods described in the preceding section are presented and discussed in this section under two sub-sections. Neutral interstellar species with their corresponding astronomically detected protonated analogues are presented and discussed followed by known interstellar neutral species whose protonated analogues are yet to be astronomically observed.

6.2.1 Neutral Species and Their Corresponding Known Protonated Analogues

Table 6.1 presents the proton affinities (in kcal/mol) for neutral species and their corresponding protonated analogues. The experimentally determined proton affinities reported in literature^{161,162} are shown alongside the ones calculated in this work. The calculated values are in good agreement with the reported experimental values for most of the molecules. The reported column densities for these species are listed in the table with the source for the data listed on the last column in the table. For neutral species with experimentally known proton affinities, the reported values are in good agreement with those predicted from the ab initio methods (Table 6.1) employed in this study. The reported proton affinity for N₂, CO (protonated as HCO⁺), H₂, H₂O, HCN (protonated as HCNH⁺) and HCl (protonated as H₂Cl⁺) are 118.4, 141.0, 101.4, 166.7, 171.0 and 134.9 kcal/mol respectively²². Of the 14 different neutral species listed in Table 6.1, six (CO, CS, HCl, HCN, HC₃N and HNCO) can be well protonated from 2 different positions on the molecular structure, thus furnishing us with two protonated species and two proton affinities corresponding to each of the six neutral species as shown in the Table. Of these 6 cases, one protonated species each has been detected in 5 cases while in the case of CO, both HCO⁺ and HOC⁺ have been astronomically observed. These situations provide ample opportunity to examine the effect of different proton affinity from the same neutral species and how this effect influences the astronomical observation of the resulting protonated species. In CS, HCN, HCl, HC₃N and HNCO, the astronomically detected protonated analogues; HCS⁺, HCNH⁺, H₂Cl⁺, HC₃NH⁺ and H₂NCO⁺ respectively are those giving rise to the highest proton affinity (PA) in their respective cases. The high PA of these systems enhance their stability; thus these protonated species prefer to remain in their protonated form rather than transferring a proton to another system and returning to their neutral form. The high stability of these systems in comparison with their counterparts that give rise to lower PA values is a good omen with respect to

astronomical observation. There is of course a direct relationship between stability of a molecule and its interstellar abundance which influences astronomical observation.

This relationship is well illustrated in the CO case where both HCO^+ and HOC^+ have been astronomically observed. HCO^+ results from a higher PA as compared to HOC^+ (Table 6.1). Thus, HCO^+ is more stable than HOC^+ . That the protonated species from a higher PA is more stable and also more abundant in ISM as compared from its counterpart from the same neutral species with lower PA is practically proven from the reported column densities for these protonated species with the most stable species; HCO^+ ($3.6 \times 10^{13} \text{ cm}^{-2}$) being over 10 times more abundant than the less stable species ($2.6 \times 10^{12} \text{ cm}^{-2}$).^{5,10,11} As mentioned earlier, the most stable protonated species, HCO^+ was astronomically observed over a decade before the less stable analogue.^{9,10,11} This emphasises the fact that the most stable species which is also the abundant species is astronomically more easily detectable as compared to the less abundant species. Thus, for the CS, HCN, HCl, HC_3N and HNCO systems where only the most stable abundant species in ISM have been detected; the detection of other less stable protonated species is a function of time as they await more sensitive astronomical instruments.

Figure 6.1 pictures the relationship between PA and astronomical detection of protonated species. With the exception of CO where both protonated analogues have been astronomically observed with the most stable species (HCO^+) being the most abundant and the first to be astronomically observed; in all other cases, the observed protonated species are those giving rise to the highest PA value in their respective neutral species. For these neutral species with two possible protonated analogues from each neutral species, standard enthalpy of formation ($\Delta_f H^\circ$) has been computed for the resulting protonated species using the G4 compound model. These values are indicated in parenthesis along each protonated species in Table 6.1. This further supports the dominance of thermodynamics in interstellar chemical processes as demonstrated in Chapter 3 of this Thesis. It is obvious that a neutral special is more stable than its protonated analogue(s). This factor plays a major role in the detection of more neutral molecules than their corresponding protonated analogues simply because of the high interstellar abundances of the neutral species as compared to their protonated analogues. The reported column densities of the neutral species and their protonated analogues presented in Table 1 attest to this fact as the neutral molecules are found to be more abundant than their corresponding protonated analogues in all the cases.

Table 6.1 Known protonated species and their corresponding neutral analogues

Neutral molecule	Proton affinity (kcal/mol)					Column Density (cm ⁻²)	Protonated Form ($\Delta_f H^\circ$ in kcal/mol)	Column Density (cm ⁻²)	Ref
	MP2/cc-pVDZ	CCS D/cc-pVDZ	G4	W2U	Experimental value				
N ₂	118.1	119.8	118.5	116.7	118.0	>3.8*10 ¹³	N ₂ H ⁺	2.7-6.6*10 ¹³ (3*10 ¹³)	3,4,
CO	144.6	142.6	142.9	140.2	142.0	7.6*10¹⁵, 3.5*10¹⁷	HCO ⁺ (198.6)	3.64*10 ¹³	5,11,23
	98.9	104.9	107.6	103.6	-	7.6*10¹⁵, 3.5*10¹⁷	HOC⁺(234.3)	2.6*10¹²	5
CS	191.2	189.5	190.4	189.4	175.0	\approx 10 ¹⁴	HCS ⁺ (246.6)	1-3*10 ¹²	6,24
	93.4	96.6	96.2	118.0	-	\approx 10 ¹⁴	HSC⁺(340.7)	Not observed	
H ₂	98.8	99.3	97.0	98.6	100.9	10 ²⁴	H ₃ ⁺	4-6*10 ¹⁴	25
OH	146.5	148.0	145.2	141.5	141.8	1.5-5*10 ¹⁴	H ₂ O ⁺	7.2*10 ¹² , 2.3*10 ¹³ , 1.1*10 ¹⁵	26,27
HCl	133.7	135.8	133.2	133.5	133.1	0.5-2*10 ¹⁶ , 2.7*10 ¹¹	H ₂ Cl ⁺ (212.1)	1.7*10 ¹³	28,29,30
	77.8	79.1	77.8	78.0	-	0.5-2*10¹⁶, 2.7*10¹¹	HClH⁺(266.5)	Not observed	
H ₂ O	169.4	170.4	170.3	165.8	165.2	<6.1*10 ¹⁸	H ₃ O ⁺	10 ¹⁵	31,32
HCN	167.6	170.4	172.6	169.5	170.4	\approx 4*10 ¹⁵ , 6.1-8.8*10 ¹⁸	HCNH ⁺ (224.2)	\approx 4*10 ¹⁴	23
	87.3	103.7	105.8	102.7	-	\approx 4*10 ¹⁵ , 6.1-8.8*10 ¹⁸	H₂CN⁺(291.1)	Not observed	
CO ₂	117.9	120.2	122.2	119.0	129.2	2.0*10 ¹⁷ , 9.3*10¹⁶, 9.5*10¹⁶	HOCO ⁺	1.2*10¹²- 2.8*10¹⁴	5,34
H ₂ CO	169.9	173.4	172.8	169.6	170.4	1.6*10¹⁵, 3.5*10¹⁵, 3.0*10¹⁶	H ₂ COH ⁺	2.3*10 ¹³ , 5.0*10¹⁴	37
HC ₃ N	176.5	178.2	185.2	181.7	184.6	2.1*10 ¹⁶ , 6.0*10 ¹³ , 1.71*10 ¹⁴	HC ₃ NH ⁺ (267.5)	1*10 ¹² , 1.6*10 ¹⁴	3,38
	132.5	144.4	150.2	146.5	-	2.1*10¹⁶, 6.0*10¹³, 1.71*10¹⁴	HC₃NH⁺(303.5)	Not observed	
NH ₂ D	208.9	210.3	207.6	204.3	-	3.2 \pm 1.2*10 ¹⁴	NH ₃ D ⁺	1.1 \pm 0.2*10 ₁₂	36
C ₃	178.6	180.0	181.2	177.7	183.3	6*10 ¹⁵ , 2*10 ¹⁷	HC ₃ ⁺	4.8 \pm 0.9*10 ₁₁	39,40
HNCO	182.3	185.9	179.7	175.8	180.0	1*10 ¹⁵ ,	H₂NCO⁺(156.2)	6-14*10 ¹¹	41
	146.3	149.4	150.7	147.3	-	1*10¹⁵,	HNCOH⁺(185.1)	Not observed	

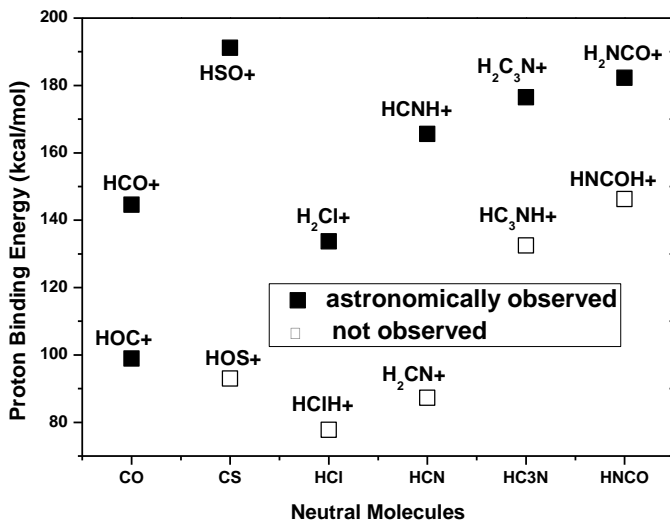


Figure 6.1: Relationship between PA and astronomical observation of protonated species.

6.2.2 Neutral Species and Their Corresponding Detectable Protonated Analogues

With respect to the number of atoms, the diatomics constitute the highest number of known interstellar species with over 30 of them uniquely detected from different astronomical sources. The dominance of diatomics among interstellar molecular species is also reflected among the protonated species with seven of them (Table 6.1) having their corresponding neutral analogues as diatomics. Table 6.2 shows the proton affinities (PAs) for all the diatomics considered in this study and their corresponding protonated analogues. The reported proton affinities^{161,162} for NO (127.1 kcal/mol), and SiO (185.9 kcal/mol) compare well with the caucted values shown in Table 6.2 while those of SiS (149.9 kcal/mol), HF (115.7 kcal/mol) and PO (163.0 kcal/mol) differ to an extent from the calculated values. About half of all the diatomics considered here are uniquely protonated from two different positions in the molecular structure thus resulting in two different protonated species and two different PA values corresponding to a single neutral species. The protonated species corresponding to the highest PA for each of these neutral species are highlighted with bold type face in the table. These are the most stable and probably the most abundant species in ISM, thus, they remain the best candidates for astronomical searches as compared to their analogues that result from a lower PA value of the same neutral molecule.

Table 6.2: Proton affinity for known neutral species with 2 atoms

Neutral molecule	Proton affinity (kcal/mol)				Protonated form
	MP2/cc-pVDZ	CCSD/cc-pVDZ	G4	W2U	
CSi	206.7	214.8	220.4	220.0	HCSi⁺
	148.7	158.4	160.5	158.8	HSiC ⁺
NO	126.3	129.7	128.7	126.8	HNO⁺
	111.1	114.9	113.5	111.2	HON ⁺
NS	157.1	173.5	172.1	170.8	HNS⁺
	131.4	142.3	138.8	137.4	HSN ⁺
SO	165.2	167.9	168.1	166.8	HSO⁺
	159.9	166.4	163.3	160.3	HOS ⁺
AlCl	176.4	174.9	176.8	177.4	HAICl⁺
	168.7	172.0	165.4	166.3	AlClH ⁺
AlF	174.1	176.6	166.2	166.5	AlFH⁺
	167.4	164.9	168.9	166.9	HAiF ⁺
PN	185.6	191.4	194.0	192.6	HNP⁺
	109.7	107.1	103.8	191.4	HPN ⁺
SiO	188.7	195.8	193.9	192.4	HOSi⁺
	132.9	129.2	129.3	127.5	HSiO ⁺
CP	190.6	189.1	193.0	192.3	HCP ⁺
NaCl	211.9	214.4	205.0	205.4	NaClH ⁺
SiN	187.8	178.8	206.4	205.6	HNSi ⁺
SiS	164.7	170.3	168.9	169.2	HSSi⁺
	153.4	153.2	153.5	153.4	HSiS ⁺
NH	172.0	169.8	168.9	166.2	NH ₂ ⁺
C ₂	84.5	101.2	117.2	115.6	HC ₂ ⁺
CN	155.2	149.9	150.4	148.2	HNC⁺
	136.7	132.7	134.3	131.5	HCN ⁺
HF	106.1	106.2	110.0	103.6	H ₂ F ⁺
FeO	193.6	OFR	OFR	OFR	FeOH ⁺
CH	178.6	175.5	178.0	175.9	CH ₂ ⁺
SH	164.7	166.9	163.5	163.7	SH ₂ ⁺
O ₂	122.9	128.4	127.7	125.0	HO ₂ ⁺
PO	168.5	174.7	170.8	168.2	HOP⁺
	136.3	146.5	145.7	143.6	HPO ⁺
SiH	180.7	178.6	181.0	180.9	SiH ₂ ⁺
AlO	237.5	219.9	217.7	217.4	HOAl⁺
	174.9	167.2	161.9	156.0	HAiO ⁺
TiO	186.8	177.7	OFR	OFR	HTiO ⁺

OFR=Out of range of the methods.

In comparison with the diatomics species whose protonated analogues have been observed, the high PA values estimated for these diatomics with the different ab initio methods strongly signal the detectability of the protonated analogues of these diatomics in astronomical sources. At the MP2 level of theory with the cc-pVDZ basis set, the PA for the diatomics ranges 98.8 to 146.5 kcal/mol (Table 6.1), with the exceptions of NO, CN, C₂, HF, O₂, PO,

NS (protonated as HSN^+), PN (protonated as HPN^+), and SiO (protonated as HSiO^+); the PA for these neutral diatomic species are all higher than the range for those neutral species with known protonated analogues. This implies the presence (in high abundance) and detectability of the protonated analogues of these neutral species in ISM, as a result of the high PA values, these protonated species will prefer to remain in their protonated form, thus their astronomical observation is highly feasible.

Among the interstellar molecules with three atoms, H_2O , HCN, CO_2 and C_3 have their corresponding protonated analogues^{5,31-34,39,40}. PAs have been calculated for 23 interstellar molecular neutral species with 3 atoms (Table 6.3). The experimental proton affinities^{161,162} for HNC (184.6 kcal/mol), SO_2 (160.7 kcal/mol), N_2O (131.4 kcal/mol), NH_2 (187.0 kcal/mol), and C_2O (185.2 kcal/mol) are in good agreement with the calculated values presented in Table 6.3 except for those of H_2S (168.5 kcal/mol) and HCO (152.0 kcal/mol). With the exceptions of H_2S , NH_2 , c-SiC₂ and CH_2 , each of the triatomic species considered in this study has two protonated analogues; the best candidates for astronomical searches in each of these cases are highlighted as in Table 6.2 with bold type face. From Table 6.1, with the exception of CS, all the protonated species are from neutral molecules that are composed of the four most important biogenic elements; C, H, N, and O. From an astronomical perspective, this can easily be traced to the high cosmic abundances of these elements. However, some of the diatomic and triatomic interstellar molecules contain other elements (like Al, Si, P, Mg, Ti, Fe, Cl, F, etc) outside the four listed above. The high PAs of these neutral species as shown in Tables 6.2 and 6.3 imply that protonated molecular species are not only limited to C, N, O, S and H containing molecular species.

H_2CO , NH_2D and HNCO are the only tetra-atomic interstellar molecules with known protonated analogues as much as we know. Rotational spectroscopy has remained an indispensable tool in the chemical examination of the interstellar space with over 80% of all the known interstellar and circumstellar molecules detected via their rotational transition spectra with its only limitation being the fact only molecules with permanent dipole moment can be probed by it. Ammonia; NH_3 has a very high PA and as such its protonated analogue, NH_4^+ should have been a good candidate for astronomical searches, however, NH_4^+ is a spherical top molecule with no permanent dipole moment; thus its rotational spectrum cannot be probed but its deuterated analogue, NH_2D^+ has a small dipole moment which allows the experimental determination of its spectrum that led to its successful astronomical detection.⁴² The PAs of the different interstellar neutral molecules with 4 atoms considered in this study are shown in Table 6.4 with their corresponding protonated analogues. The values of 181.6 kcal/mol, 180.0 kcal/mol and 181.2 kcal/mol reported^{161,162} for the proton affinities of H_2CS , HNCO and HCNO respectively are in good agreement with the calculated values in Table 6.4. Just like all the neutral species with known protonated analogues, all the tetra-atomic species considered here are C, H, O, N and S containing species. With the exceptions of HSCN, H_2CN and HOCN, the PAs for all the neutral molecules listed in Table 6.4 are within the range of those (in Table 1) whose protonated analogues have been astronomically observed.

Table 6.3: Proton affinity for known neutral species with 3 atoms

Neutral molecule	Proton affinity (kcal/mol)				Protonated form
	MP2/cc-pVDZ	CCSD/cc-pVDZ	G4	W2U	
H ₂ S	140.4	141.4	139.3	139.4	H ₃ S ⁺
HNC	187.8	186.5	186.6	183.8	HNCH⁺
	131.3	139.6	136.7	132.9	H ₂ NC ⁺
SO ₂	156.6	162.5	155.1	151.0	HOSO⁺
	66.8	75.2	54.6	44.5	HSO ₂ ⁺
MgCN	150.0	153.8	210.5	208.0	MgCNH⁺
	143.1	139.1	140.2	138.9	HMgCN ⁺
MgNC	224.1	224.1	221.1	220.2	MgNCH⁺
	129.7	148.3	150.4	148.9	HMgNC ⁺
N ₂ O	132.8	143.9	137.1	135.1	N₂OH⁺
	136.0	134.5	136.8	134.7	HN ₂ O ⁺
NH ₂	190.0	190.7	187.8	185.7	NH ₃ ⁺
OCS	149.2	154.6	148.9	148.1	HSCO⁺
	142.8	146.0	145.6	144.3	HOCS ⁺
HCO	173.8	185.1	182.3	177.4	H₂CO⁺
	132.9	135.8	140.2	135.9	HCOH ⁺
C ₂ H	195.0	186.0	192.4	188.1	HC₂H⁺
	146.9	146.7	151.6	147.1	C ₂ H ₂ ⁺
C ₂ O	177.9	175.8	181.5	178.6	HC₂O⁺
	126.8	135.7	134.6	130.7	C ₂ OH ⁺
C ₂ S	201.0	199.4	205.3	203.3	HC₂S⁺
	150.5	158.1	156.9	155.1	C ₂ SH ⁺
AlNC	216.8	215.9	210.7	209.6	AlNCH⁺
	169.6	169.6	173.7	171.9	HAINC ⁺
HNO	243.7	244.1	237.6	232.9	H₂NO⁺
	113.0	117.4	121.3	118.3	HNOH ⁺
SiCN	204.2	644.0	192.0	190.1	SiCNH⁺
	125.8	131.3	136.1	134.1	HSiCN ⁺
SiNC	200.7	202.9	202.2	200.8	SiNCH⁺
	165.5	164.8	169.1	167.3	HSiNC ⁺
c-SiC ₂	151.8	151.0	154.9	152.4	c-HSiC ₂ ⁺
HCP	155.5	167.0	167.6	166.6	H₂CP⁺
	124.6	126.2	126.0	124.3	HCPH ⁺
CCP	219.1	211.6	214.6	212.7	HCCP⁺
	103.3	110.8	111.1	108.4	CCPH ⁺
AlOH	200.1	202.8	194.2	192.1	AlOH₂⁺
	185.3	183.2	186.3	185.0	HAI OH ⁺
HO ₂	136.5	137.2	136.4	133.2	H₂O₂⁺
	90.0	159.3	159.2	155.5	HO ₂ H ⁺
TiO ₂	229.5	233.7	OFR	OFR	HPTiO ⁺
CH ₂	210.6	207.7	210.3	207.4	CH ₃ ⁺

OFR=Out of range of the methods.

With the exceptions of H₂CO, H₂CN and H₂CS with one and only one unique protonated analogues each, every other tetra-atomic molecule reported in Table 6.4 has two detectable protonated analogues. However, the protonated species that gives rise to the highest PA in

each case remains the best candidate for astronomical searches as discussed before; these most stable and probably most abundant protonated species in ISM are highlighted in the table as in the previous cases.

Table 6.4: Proton affinity for known neutral species with 4 atoms

Neutral molecule	Proton affinity (kcal/mol)				Protonated form
	MP2/cc-pVDZ	CCSD/cc-pVDZ	G4	W2U	
H ₂ CS	180.7	184.7	184.3	183.8	H ₂ CSH ⁺
HNCO	176.7	179.7	175.2	171.6	H₂NCO⁺
	140.7	143.2	146.2	143.1	HNCOH ⁺
HNCS	185.8	189.5	185.5	183.7	H₂NCS⁺
	175.4	180.9	174.6	173.7	HNCSH ⁺
C₃S	222.9	222.8	220.2	218.0	HC₃S
	136.3	147.9	144.9	142.6	C ₃ SH ⁺
H ₂ CN	175.8	174.0	176.2	173.3	H ₂ CNH ⁺
C₃H	210.1	201.1	208.1	204.3	HC₃H⁺
	170.9	170.9	172.1	167.7	H ₂ C ₃ ⁺
HC₂N	217.3	215.9	211.9	208.0	H₂C₂N⁺
	188.7	191.0	190.9	186.9	HC ₂ NH ⁺
C₃N	182.9	179.0	194.0	189.4	HC₃N⁺
	186.3	174.5	179.8	176.4	C ₃ NH ⁺
C₃O	210.4	210.0	207.0	203.7	HC₃O⁺
	119.9	127.2	129.5	125.6	C ₃ OH ⁺
HCNO	170.4	180.7	174.2	171.4	HCNOH⁺
	161.1	172.7	167.8	164.2	H ₂ CNO ⁺
HSCN	180.6	182.8	187.7	185.0	HSCNH⁺
	145.4	147.5	146.3	145.2	H ₂ SCN ⁺
HOCH	181.5	183.2	188.0	184.5	HOCHN⁺
	125.4	127.4	126.4	122.9	H ₂ OCN ⁺

As much as we know, there are no reported interstellar protonated molecular species corresponding to neutral molecules with five atoms and above. Do protonated species of these neutral molecules exist in ISM or are they detectable? We do think they exist and should be detectable. Of course the phenomenon of isomerism among interstellar molecular species becomes more pronounced for larger interstellar molecules; for instance, out of the 12 known interstellar molecules with 8 atoms⁴³⁻⁵⁴, 7 have their corresponding isomeric counterparts as known interstellar molecules. As pointed out, the large number of metastable isomeric species among the known interstellar molecules entails that these isomers are formed together through dissociative recombination process. Hence, for every isomeric species, its protonated analogue is present and astronomically detectable. Also, the high abundance of the potent Bronsted acid, H₃⁺ in ISM implies that every interstellar molecule is subject to protonation. Therefore, protonated species corresponding to neutral species with 5 atoms and above are likely to be present and detectable in ISM though none is yet to be detected presently. Still in support of the astronomical detectability of these protonated species are the high PAs calculated for the neutral species with 5 atoms and above considered in this study. Tables 6.5, 6.6, 6.7 and 6.8 contain the PAs for neutral species with 5, 6, 7 and 8

atoms respectively and their corresponding protonated analogues. The reported experimental values^{161,162} of 198.3 kcal/mol and 177.3 kcal/mol for the proton affinities of CH₂CO and HCOOH compare well with the calculated values shown in Table 6.5.

The high PAs for these species buttress the fact that the corresponding protonated species are relatively stable as compared to those that have been detected. As in the previous cases, most of these neutral species have two different protonated analogues. The computed PAs are thus used to distinguish the most stable protonated analogues from the less stable ones in their respective neutral molecules. The most stable protonated species which obviously are expected to be the most abundant in ISM are highlighted in the tables (6.5-6.8) with bold type face. These stable protonated species remain the priority for astronomical searches as compared to the less stable analogues.

Table 6.5: Proton affinity for known neutral species with 5 atoms

Neutral molecule	Proton affinity (kcal/mol)				Protonated form
	MP2/cc-pVDZ	CCSD/cc-pVDZ	G4	W2U	
CH ₂ NH	208.5	210.8	210.8	207.7	CH ₂ NH ₂ ⁺
NH ₂ CN	191.5	193.4	199.6	195.6	NH ₂ CN ⁺
	170.3	171.9	167.2	163.7	NH ₃ CN ⁺
CH ₂ CO	201.2	202.6	197.0	192.8	CH ₃ CO ⁺
	130.8	157.3	144.5	141.1	CH ₂ COH ⁺
HCOOH	179.2	182.4	182.7	178.3	HCO(H)OH ⁺
	164.4	163.9	161.8	158.8	HCOOH ₂ ⁺
HC ₂ NC	189.7	186.7	191.4	187.8	HC ₂ NCH ⁺
	151.8	162.1	166.8	162.1	H ₂ C ₂ NC ⁺
HNCCC	234.0	234.0	230.9	227.2	HNC ₃ H ⁺
	160.7	170.6	168.6	163.9	H ₂ NC ₃ ⁺
CH ₂ CN	184.5	181.7	186.6	183.1	CH ₂ CN ⁺
	130.7	132.7	137.8	134.1	CH ₃ CN ⁺
C ₄ Si	240.9	245.5	240.5	238.5	HC ₄ Si ⁺
	147.0	150.4	150.7	147.0	C ₄ SiH ⁺
C ₄ H	228.1	213.2	218.5	214.6	HC ₄ H ⁺
	182.3	179.3	181.5	176.7	H ₂ C ₄ ⁺
HC(O)CN	168.2	171.3	173.3	169.7	HC(O)CNH ⁺
	155.2	158.3	161.6	157.9	HC(OH)CN ⁺

In all the systems examined in this study, it suffices to say that the protonated analogue of every known interstellar or circumstellar species is detectable. However, one of the primary requirements for astronomical searches is the availability of accurate rotational transitions for the molecular species under consideration. Most of the protonated species that are shown to be present and detectable in ISM from this study could be described as "non-terrestrial" molecules as a number of them are yet to be probed in the terrestrial laboratory. But theoretically predicted rotational transitions have been instrumental in the astronomical observation of some molecular species such as HNC, HCO⁺, HOC⁺, N₂H⁺, C₃N, HCNH⁺, C₂H, etc^{3,6,11,23,33,55,56} and in guiding laboratory measurement of rotational spectra of molecules. In the same vein, accurate rotational transitions, theoretically predicted for these protonated species could be useful for astronomical searches.

Table 6.6: Proton affinity for known neutral species with 6 atoms

Neutral molecule	Proton affinity (kcal/mol)				Protonated form
	MP2/cc-pVDZ	CCSD/ cc-pVDZ	G4	W2U	
CH ₃ OH	181.8	183.4	183.5	180.1	CH ₃ OH ₂ ⁺
CH ₃ SH	184.5	186.8	186.2	185.7	CH ₃ SH ₂ ⁺
CH ₃ CN	184.0	186.5	191.8	188.4	CH ₃ CNH ⁺
	103.8	103.5	105.3	103.6	CH ₄ CN ⁺
CH ₃ NC	201.8	200.7	202.5	199.7	CH ₃ NCH ⁺
	103.2	106.0	109.7	107.4	CH ₄ NC ⁺
HC(O)NH ₂	188.4	190.5	185.1	180.8	HC(O)NH ₃ ⁺
HC ₂ CHO	151.5	157.6	163.9	158.8	H ₂ C ₂ CHO ⁺
HC ₄ N	221.4	221.1	217.7	213.3	H ₂ C ₄ N ⁺
	195.5	197.5	201.4	197.0	HC ₄ NH ⁺
C ₅ N	226.5	206.0	211.4	207.8	HC ₅ N ⁺
	179.3	172.9	178.3	178.4	C ₅ NH ⁺
C ₅ H	235.0	218.8	224.9	221.1	HC ₅ H ⁺
	189.7	186.3	189.9	185.1	H ₂ C ₅ ⁺
H ₂ CCNH	217.8	218.0	214.9	210.7	H ₃ CCNH ⁺
	196.9	201.9	202.1	198.2	H ₂ CCNH ₂ ⁺
C ₅ S	227.1	241.1	234.6	232.1	HC ₅ S ⁺
	151.7	167.1	162.3	159.6	C ₅ SH ⁺

The experimental values^{161,162} of 180.3 kcal/mol, 184.8 kcal/mol and 186.2 kcal/mol reported for CH₃OH, CH₃SH and CH₃CN respectively are in good agreement with the calculated values shown in Table 6.6. From literature^{161,162} the values 183.7 kcal/mol, 189.7 kcal/mol,

187.3 and 187.0 kcal/mol reported for the proton affinities of CH_3CHO , CH_2CHCN , CH_3COOH and HCOOCH_3 respectively are within the range of the calculated proton affinities for these molecules shown in Tables 6.7 and 6.8.

Table 6.7: Proton affinity for known neutral species with 7 atoms

Neutral molecule	Proton affinity (kcal/mol)				Protonated Form
	MP2/cc-pVDZ	CCSD/cc-pVDZ	G4	W2U	
CH_3CHO	183.5	186.6	189.1	185.6	CH_3CHOH^+
$\text{c-C}_2\text{H}_4\text{O}$	168.1	171.4	172.9	170.2	$\text{c-C}_2\text{H}_4\text{OH}^+$
$\text{CH}_2\text{CH(OH)}$ (anti)	199.4	201.9	203.0	197.4	$\text{CH}_3\text{CH(OH)}^+$
	173.1	175.6	176.6	172.4	$\text{CH}_2\text{CH(OH}_2^+$
$\text{CH}_2\text{CH(OH)}$ (syn)	196.9	199.8	201.0	195.5	$\text{CH}_3\text{CH(OH)}^+$
	171.0	173.9	175.0	171.2	$\text{CH}_2\text{CH(OH}_2^+$
CH_2CHCN	184.5	187.5	194.2	190.3	$\text{CH}_2\text{CHCNH}^+$
	143.6	147.5	154.2	149.9	CH_3CHCN^+
HC_5N	183.4	183.0	194.6	190.3	HC_5N^+
	152.8	164.3	174.0	169.3	$\text{H}_2\text{C}_5\text{N}^+$
C_6H	252.8	228.3	231.9	227.9	HC_6H^+
	197.7	191.0	195.2	189.9	H_2C_6^+

Table 6.8: Proton affinity for known neutral species with 8 atoms

Neutral molecule	Proton affinity (kcal/mol)				Protonated Form
	MP2/cc-pVDZ	CCSD/cc-pVDZ	G4	W2U	
CH_2CHCHO	190.2	192.8	197.7	193.6	$\text{CH}_2\text{CHCHOH}^+$
	157.5	158.0	156.5	156.7	$\text{CH}_3\text{CHCHO}^+$
CH_2CCHCN	188.2	191.3	199.2	195.2	$\text{CH}_2\text{CCHCNH}^+$
	154.0	157.3	160.9	156.9	$\text{CH}_3\text{CCHCN}^+$
C_7H	252.7	229.4	236.3	232.2	HC_7H^+
	220.9	192.9	200.9	195.4	H_2C_7^+
CH_3NH_2	218.4	219.8	218.1	214.8	CH_3NH_3^+
CH_3COOH	189.2	192.4	194.4	189.6	$\text{CH}_3\text{CO(OH)H}^+$
HCOOCH_3	187.8	191.1	191.9	188.0	HCO(H)OCH_3^+
HOCH_2CHO	184.3	187.4	190.7	187.0	$\text{HOCH}_2\text{CHOH}^+$

6.3 Summary on Interstellar Protonated Molecular Species: This study extensively demonstrates the influence of proton affinity (PA) in astronomical observation of protonated species in ISM and accounts for the astronomical observations of the known protonated species over their closest analogues. Proton affinities have been computed for over 100

neutral interstellar species of which majority of them are protonated at two different positions on the molecular structure; thus, resulting in two protonated species and two different value of PA corresponding to the same neutral species. The protonated species resulting from the neutral species with higher PA is shown to be more stable, more abundant in ISM and thus easily detectable as compared to its counterpart resulting from a lower PA with the same neutral species. The protonated species giving rise to a lower PA is less stable, and very reactive in ISM. This high reactivity of this protonated species drastically reduces its interstellar abundance thereby making its astronomical observation difficult. This species also has a very high tendency of transferring a proton to another species and returning to its neutral form. The reverse is the case for its analogue resulting from a higher PA. Based on the above observations, the most probable protonated species for astronomical observation have been highlighted in all the cases considered. The PAs computed for most of the species considered in this study whose protonated analogues are yet to be astronomically observed as compared to those that have been astronomically observed strongly supports the possible astronomical observations of these protonated species, provided their accurate rotational transitions are available. That interstellar formation processes are partially thermodynamically controlled is again demonstrated in this study as the detected protonated species are the thermodynamically most stable species as compared to their closest isomers that have not been observed and where both isomers observed, of course, the most stable is found to be the most abundant species.

Detectable Interstellar Anions: Examining the Key Factors

6.4. Introduction: The existence of positive molecular ions in the interstellar medium (ISM) has long been known. The discovery of CH^+ in ISM came after soon the discoveries of the first two molecular species in ISM; CN and CH.⁵⁷⁻⁵⁹ The astronomical observation of positive ions has been highly successful and encouraging. With over 200 currently known interstellar molecular species, about 10% are positive ions.⁶⁰ These ions play a major role in the ion-molecule reactions in ISM which are the dominant gas phase chemistry processes in ISM.² The existence and possible astronomical observation of the anions started coming into the limelight in the 1970s when they were predicted on the basis of ion-molecule chemical models.⁶¹⁻⁶³ Though theoretical predictions may take time, in most cases they always come true. In this case, it took about three decades for the first anion; C_6H^- to be astronomically observed.⁶⁴ Currently, six anions; C_4H^- , C_6H^- , C_8H^- ; CN^- , C_3N^- , C_5N^- have been uniquely detected from different astronomical sources⁶³⁻⁶⁹ with a tentative observation of C_2H^- .⁶⁹

The formation of anions via the electron radiative attachment process depends largely on the electron affinity (EA) of the neutral molecule. The EA shows the strength to which the electron is bonded to the neutral molecule. The higher the EA, the more stable the corresponding anion because a high amount of energy is required for the electron detachment process. The more stable an anion is as compared to its corresponding neutral analogue, the

higher the possibility of its astronomical detection. The rate coefficient for the associative attachment of an electron to a neutral molecule increases with an increase in EA^{62,63,68}. According to Herbst⁶², "the most abundant interstellar molecular negative ions stem from neutral free radicals with estimated large (>2eV) electron affinities". The dipole moment of the neutral molecule is yet another important factor in the electron radiative attachment process. For highly polar neutral molecules with dipole moment >2-2.5D, long-lived dipole-bound states (which are electronic states close to the detachment threshold) have been shown to exist and to possibly facilitate anion formation process. For neutral species with large dipole moment, there is a significant enhancement in the cross sections for the electron attachment process^{65,70}. Electron capture and the formation of the temporary negative ion which are the initial steps in the electron radiative attachment process are also influenced by the dipole moment and the existence of dipole bound state⁷¹. High EA and large dipole moment of a neutral species are thus, the key factors influencing the formation and interstellar abundance of their corresponding anion. All the known interstellar anions are in accordance with these factors as their corresponding neutral analogues possess high EAs and large dipole moments. Therefore, potential interstellar anions should be species whose corresponding neutral analogues have high EAs and large dipole moment among other factors.

Interestingly, the known anions are all interstellar carbon chain species belonging to the C_nH⁻ and C_nN⁻ chains. The interstellar carbon chains; C_n, HC_nN, H₂C_n, and C_nX (X= N, O, S, H, Si, P, H⁻, N⁻) accounts for more than 20% of all the known interstellar molecular species. Fortunately, electron radiative attachment process becomes more efficient as the size of the carbon chain increases, thus favouring the formation of large chains. For small carbon chains C_n, highly efficient electron attachment dominates on reaching a critical size of about 6 atoms^{64,72-74}. Thus, the different interstellar carbon chains remain the potential source of detectable interstellar anions. In the present study, over 80 different interstellar carbon chain molecular species are examined with the aim of identifying highly potential interstellar anions based on the factors discussed above. Electron affinities are theoretically calculated for all the neutral molecules considered in this study, dipole moments are also estimated for both the neutral molecules and their corresponding anions.

6.5 Computational Method: The geometries of all the neutral molecules and their corresponding anions are optimized using the Møller-Plesset second order perturbation theory; MP2(full)¹³, the full option includes inner shell electrons. The 6-311++G** basis set is used; this allows the orbitals to change size and shape and to also occupy a large region of space; p and d functions are added to hydrogen and heavy atoms respectively. The diffuse functions are added to both hydrogen and heavy atoms^{75,76}. All computations are carried out using GAUSSIAN 09 suit if programs¹². Electron affinity is calculated as the energy (sum of electronic and zero-point energies) difference between a neutral molecule and its corresponding anion. The electron affinity is expressed in electron volt (eV) while the dipole moment is expressed in Debye (D).

6.6 Results and discussion

The neutral carbon chains with corresponding anions are presented and discussed followed by the neutral chains with potential interstellar anions.

6.6.1 Carbon Chains with Corresponding Known Interstellar Anions

C_nN Carbon Chains

Among the C_nN neutral interstellar carbon chains, CN, C₂N, C₃N and C₅N have been astronomically detected ^{76,77,78,79}. Of these known interstellar C_nN neutral species, CN, C₃N and C₅N have their corresponding anions as known interstellar anions^{66,68,69}. Table 6.9 contains electron affinity for the C_nN (n from 1 to 10) chains calculated at the MP2(full)/6-311++G** level. The dipole moment for these neutral molecules and their corresponding anions computed with the same are also shown in the table. The experimental electron affinities¹⁶¹ of C₄N (3.1 eV) and C₆N (3.4 eV) are in good agreement with the values shown in Table 6.9. The anions are significantly more stable than their corresponding neutral analogues as shown in the large positive EA values. The EAs for the C_nN chains are quite high ranging from 2 to 10eV; this increases the chances for the astronomical observation of their corresponding anions since a huge amount of energy will be required for the electron detachment process, thus the anions corresponding to these neutral molecules prefer to remain in their anionic form. Rotational line intensity scales with the square of the dipole moment of the molecule, the larger the dipole moment of a molecule, the higher its rotational line strength which of course is a good requirement for probing a molecule. The large dipole moment for most of these anions is a good omen regarding their observation both in the laboratory and in the ISM. As a prove of the effect of EA in the astronomical observation of anions, the CN, C₃N and C₅N whose corresponding anions have been astronomically detected have higher EAs as compared to their C₂N, C₄N and C₆N chains respectively. The dipole moments of the C_{2n-1}N chains are also higher than those of C_{2n}N (from n=1 to 3) chains except for the C₅N in which the MP2(full)/6-311++G** has predicted its dipole moment to be low.

Table 6.9: Electron affinity (eV) for C_nN chains and dipole moment for both C_nN and C_nN⁻ chains

n	EA (eV)	Dipole moment (D)	C _n N ⁻ dipole moment (D)
1	4.5	2.3	0.3
2	2.0	0.8	1.6
3	5.4	3.1	2.4
4	3.5	0.5	2.4
5	6.5	0.2	4.2
6	3.9	0.9	3.5
7	7.9	0.1	6.1
8	5.7	0.3	5.0
9	10.0	0.1	8.2
10	6.7	0.3	6.7

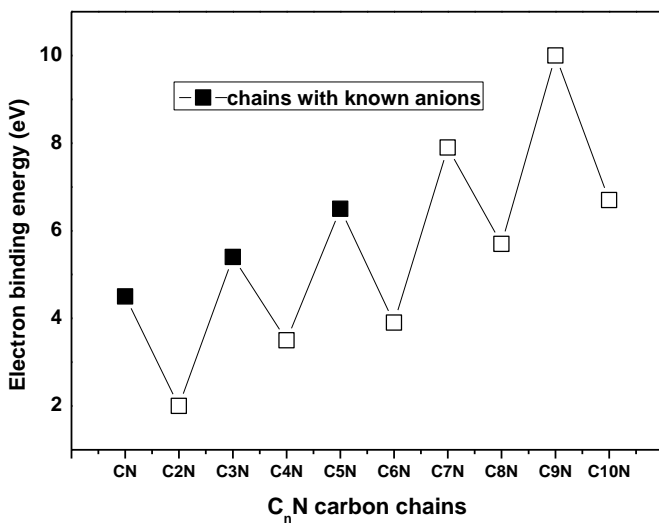


Figure 6.2: Plot showing electron affinity for C_nN carbon chains

Figure 6.2 shows the plot of the EAs for the C_nN chains with the odd numbered carbon chains found to possess higher EAs (from 4.5eV and above) than their corresponding even numbered carbon chains in all the cases. Though the C_7N and the C_9N are yet to be observed in ISM, it is crystal clear that their corresponding anions are potential interstellar molecules considering the high EAs of the neutral species and the large dipole moment of the anions.

C_nH Chains

The electron affinities for the C_nH ($n=1$ to 10) chains considered in this study are presented in Table 6.10 with their dipole moments and those of their corresponding anions. The experimental value¹⁶³ of 3.0 eV for the electron affinity of CH compares well with the calculated value shown in Table 6.10. Unlike in the previous case where all the anions are found to be more stable than their corresponding neutral species, the CH is found to be more stable than its corresponding anion; CH^- as reflected in the negative electron affinity. The neutral C_nH chains from $n=1$ to $n=8$ are all known interstellar molecules^{49,59,68,80-84}. Of these neutral molecules, C_4H , C_6H , and C_8H have their corresponding anions as known interstellar molecules^{63-65,67} and there is a tentative observation of C_2H^- reported by Ag'undez *et al.* and references therein⁶⁹. Thus, almost all the known $C_{2n}H$ neutral species have their corresponding anions as known interstellar molecular species. The astronomical observation of the $C_{2n}H^-$ anions ($n=1$ to 4) without any observation of the corresponding $C_{2n-1}H^-$ anions explains the effects of electron affinities and dipole moment as the key factors that influence the astronomical observation of anions. The $C_{2n}H^-$ systems are found to be more stable than their corresponding $C_{2n-1}H^-$ systems as depicted in the electron affinity. The high stability of the $C_{2n}H^-$ systems implies high interstellar abundance which favours the astronomical observation of these systems as compared to their corresponding $C_{2n-1}H^-$ systems. The $C_{2n}H$ and $C_{2n}H^-$ chains have larger dipole moments as compared to their corresponding $C_{2n-1}H$ and

$C_{2n-1}H^-$ chains respectively. The reported dipole moment for C_4H^- (6.2D), C_6H^- (8.2D) and C_8H^- (11.9D)⁶⁵ are in good agreement with those calculated in this study.

Table 6.10: Electron affinity (eV) for C_nH chains and dipole moment for both C_nH and C_nH^- chains

n	EA (eV)	Dipole moment (D)	C_nH^- dipole moment (D)
1	-0.4	1.7	2.1
2	3.3	0.7	3.4
3	1.1	3.4	4.2
4	4.5	4.1	6.1
5	2.8	4.2	6.2
6	5.6	4.7	8.8
7	4.1	4.6	8.4
8	6.7	4.9	11.7
9	5.2	4.8	10.8
10	7.8	5.1	14.6

Figure 6.3 shows the plot of the electron affinities for the C_nH systems with the even numbered carbon chains being more stable than their corresponding odd numbered chains. Between the C_9H^- and the $C_{10}H^-$, the latter remains a potential candidate for astronomical observation though its neutral analogue ($C_{10}H$) is yet to be observed and there is no information regarding the rotational spectra of these molecules that could warrant their astronomical searches.

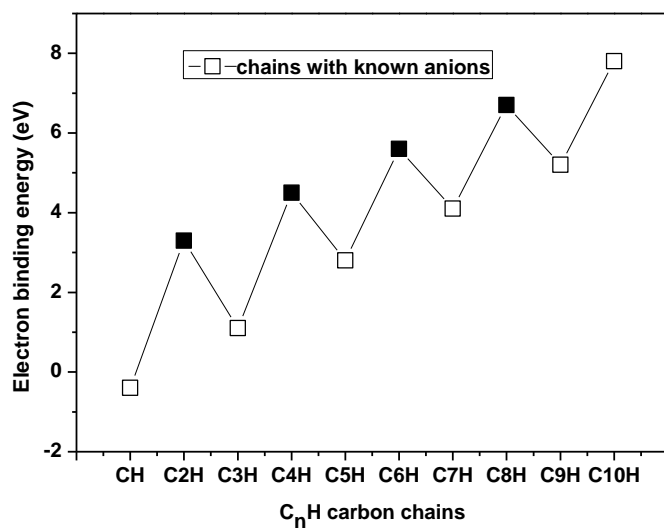


Figure 6.3: Plot showing electron affinity for C_nH carbon chains

6.6.2 Carbon Chains with Potential Interstellar Anions

The six known interstellar anions are from the C_nH^- and C_nN^- chains discussed above. Of course, interstellar anions are not only limited to these chains. There are certainly other

interstellar carbon chains with detectable anions. These chains are examined in these subsections.

C_nO and C_nS Chains

The C_nO and C_nS chains are isoelectronic and there exist some unique similarities between the interstellar chemistry of O and S-containing molecules. 16 of the 19 known S-containing interstellar molecules have their corresponding O-containing molecules as known astromolecules. With the exception of the effect of interstellar hydrogen bonding, the interstellar abundance of these molecules also reflects the cosmic O/S ratio. In the C_nO chains, CO, C₂O, and C₃O have been astronomically observed while in the C_nS chains, CS, C₂S, C₃S, and C₅S have been detected from different astronomical sources^{23,24,85-90}. Tables 6.11 and 6.12 respectively show the electron affinities for the C_nO and C_nS (n=1 to 10) chains examined in this study. The dipole moments of these species together with those of their corresponding anions are also presented in the respective tables. The anions corresponding to both CO and CS are less stable than their corresponding neutral species, thus, resulting in the negative electron affinity value. In both the C_nO and C_nS chains, the even numbered chains are more stable than the odd numbered chains except for C₁₀S. The high electron affinities for the C_{2n}O (n=1 to 5) and C_{2n}S (n=1 to 4) chains coupled with their large dipole moments strongly put their corresponding anions in the forefront as potential interstellar molecules. Figure 6.4 and 6.5 represent the plots of electron affinities for the C_{2n}O and C_{2n}S carbon chains respectively. These plots depict the variation of the electron affinities between the even and the odd numbered carbon chains.

Table 6.11: Electron affinity (eV) for C_nO chains and dipole moment for both C_nO and C_nO⁻ chains

n	EA (eV)	Dipole moment (D)	C_nO⁻ dipole moment (D)
1	-1.9	0.4	2.8
2	3.0	0.7	3.3
3	0.2	1.6	3.5
4	3.0	1.6	4.7
5	0.7	2.8	5.1
6	3.3	2.6	5.1
7	0.3	4.0	9.5
8	3.4	3.7	6.6
9	1.0	5.2	4.7
10	2.8	4.9	6.1

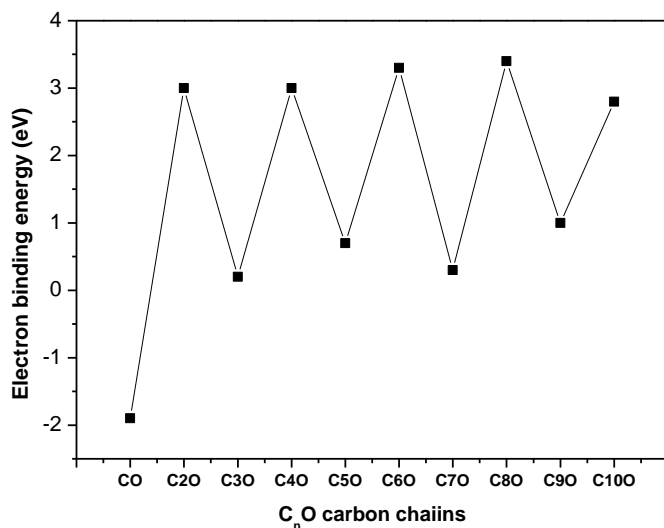


Figure 6.4: Plot showing electron affinity for C_nO carbon chains

Table 6.12: Electron affinity (eV) for C_nS chains and dipole moment for both C_nS and C_nS^- chains

n	EA (eV)	Dipole moment (D)	C_nS^- dipole moment (D)
1	-0.6	1.5	2.2
2	3.1	2.2	4.0
3	0.7	3.1	4.4
4	3.2	3.2	4.8
5	0.7	4.3	2.5
6	3.4	4.2	6.3
7	1.1	5.6	4.8
8	3.3	5.3	7.9
9	0.9	6.9	6.7
10	0.4	6.5	6.0

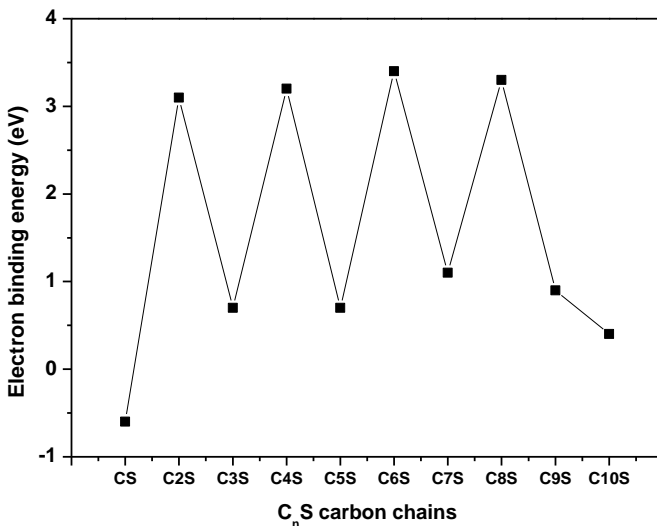


Figure 6.5: Plot showing electron affinity for C_nS carbon chains

C_n and C_nSi Chains

The C_n and C_nSi Chains are another set of isoelectronic chains among interstellar molecules. In the C_n chains, C_2 , C_3 , and C_5 have been astronomically detected^{39,91-93}. The non-permanent dipole moment of these molecules implies that they are only probed in ISM via their infrared vibrational transitions. The C_nSi chains have the advantage of having non-zero permanent dipole moments, thus they can be detected in ISM through their rotational transitions which is a more common event as compared to astronomical observation through infrared emission which relies on the occasional excitation of the molecules by high energy photons emitted by hot stars in the vicinity of the molecular cloud. The C_nSi chains from $n=1$ to $n=4$ have all been observed from IRC+10216.⁹⁴⁻⁹⁷ However, only CSi and C_4Si are linear interstellar molecules while for the C_2Si and C_3Si , only the cyclic isomers have been observed. The CSi is experimentally found to have a compact symmetric (C_{2v}) ring not a linear geometry in analogy to C_3 while the cyclic C_3Si has been shown to be more stable than the linear C_3Si ; hence the reason for its astronomical observation.

Tables 6.13 and 6.14 contain the electron affinities theoretically determined for the C_n and C_nSi chains. The experiential value of 3.3 eV reported¹⁶³ for the electron affinity of C_2 is in good agreement with the calculated value shown in Table 6.13. The dipole moment for the C_nSi chains and their corresponding anions are shown in Table 6.15. In both chains, the anions are found to be more stable than their corresponding neutral molecules with no negative electron affinity. In the C_n chains, even numbered carbon chains are more stable than the odd numbered carbon chains as shown in the table. Thus, the C_{2n}^- anions are likely detectable anions via vibrational transitions. In the C_nSi chains, the odd numbered chains possess electron affinities in the range of 2.6 to 3.1 eV which is reasonably high for a possible successful astronomical observation of their corresponding anions. The dipole moments of C_nSi and C_nSi^- chains are large enough for possible probing of their spectra. Figures 6.6 and 6.7 are the plot of the electron affinities for the C_n and C_nSi chains considered in this study.

Table 6.13: Electron affinity (eV) for pure C_n chains

n	EA (eV)
2	3.1
3	1.5
4	4.3
5	1.9
6	4.3
7	2.0
8	4.2
9	0.3
10	1.5
11	1.4
12	3.7

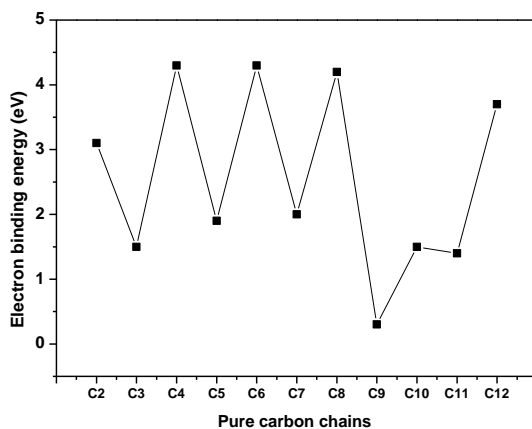


Figure 6.6: Plot showing electron affinity for C_n pure carbon chains

Table 6.14: Electron affinity (eV) for C_nSi chains and dipole moment for both C_nSi and C_nSi^- chains

n	EA (eV)	Dipole moment (D)	C_nSi^- dipole moment (D)
1	2.9	2.2	2.2
2	1.1	4.7	4.0
3	3.1	4.7	4.7
4	1.2	7.0	7.7
5	3.1	6.8	7.3
6	0.6	9.2	12.9
7	2.9	9.7	2.9
8	0.8	11.1	5.4
9	2.6	11.0	12.5
10	0.4	13.0	6.6

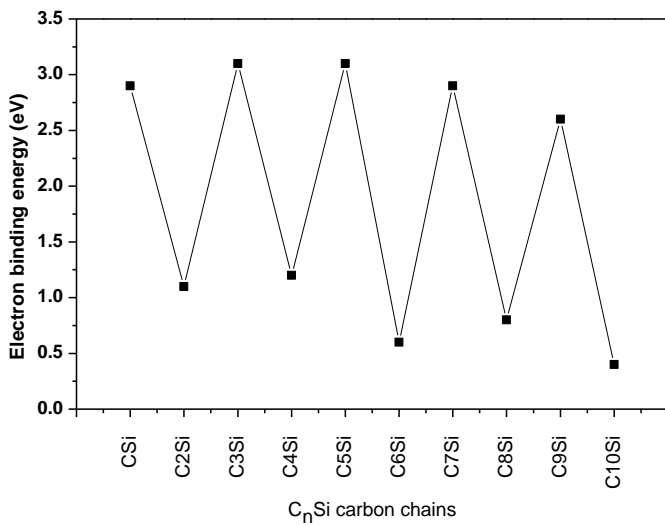


Figure 6.7: Plot showing electron affinity for C_nSi pure carbon chains

C_nP Chains

There are very few known P-containing interstellar molecules; PN, CP, HCP, PO, C₂P, PH₃ and NC₂P as compared to its isoelectronic analogue; N with over 60 known N-containing interstellar molecules⁶⁰. In the C_nP chains, on CP and C₂P have been astronomically observed^{98,99}. In Table 6.15, the electron affinity of the neutral C_nP (n=1 to 10) chains examined in this work are listed with the dipole moments of the both the C_nP and C_nP⁻ chains. The anions are significantly more stable than their corresponding neutral molecules. If we go by the key factors; electron affinity and dipole moment, influencing the formation, abundance and astronomical observation of anions, then all the corresponding anions of all the C_nP chains considered in this study are astronomically detectable. Figure 6.8 depicts the plot of the electron affinities for these chains, with the exception of C₂P, all the C_nP chains have electron affinity of 3.5eV and above. Both the C_nP chains and their corresponding anions also have large dipole moments.

Table 6.15: Electron affinity (eV) for C_nP chains and dipole moment for both C_nP and C_nP⁻ chains

n	EA (eV)	Dipole moment (D)	C _n P ⁻ dipole moment (D)
1	3.5	0.1	2.7
2	2.3	2.9	3.4
3	5.5	0.3	5.2
4	4.3	3.4	5.2
5	6.5	3.8	7.8
6	8.2	3.8	7.2
7	7.5	4.2	10.5
8	9.0	4.1	9.4
9	8.6	4.4	13.3
10	4.3	7.6	12.3

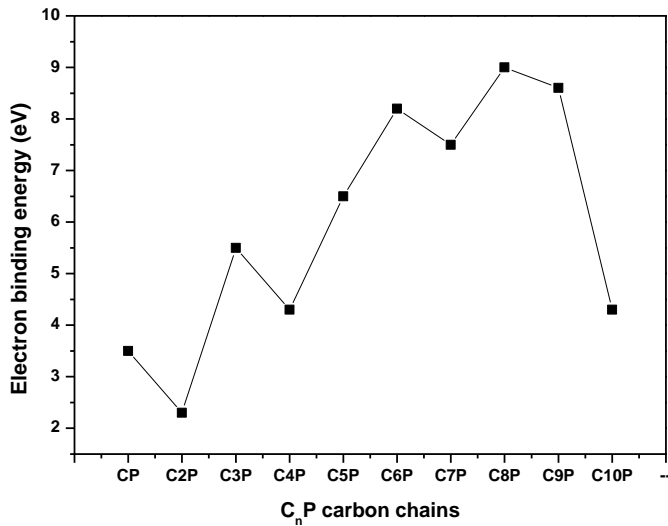


Figure 6.8: Plot showing electron affinity for C_nP carbon chains

HC_nN Chains

Table 8 contains electron affinities for the HC_nN ($n=1$ to 11) chains obtained by ab initio quantum chemical calculations and the dipole moment for these neutral molecules and their corresponding anions. Interstellar chemical processes are partially thermodynamically controlled. In the HC_nN chains, 8 neutral molecules have been astronomically observed $^{100-1087}$, out of these known HC_nN neutral molecules, only HC_2N and HC_4N are even numbered carbon chains. This is thermodynamically understood as the odd numbered carbon chains are more stable than their preceding and the next even numbered carbon chains. With respect to their corresponding anions, the odd numbered neutral HC_nN molecules are more stable than their corresponding anions as reflected in the negative electron affinity values for these molecules (Table 6.16).

Table 6.16: Electron affinity (eV) for C_nP chains and dipole moment for both C_nP and C_nP^- chains

n	EA (eV)	Dipole moment (D)	HC_nN^- dipole moment (D)
1	-0.9	3.3	10.2
2	2.3	3.6	1.9
3	-1.0	4.3	2.6
4	2.3	4.8	2.9
5	-0.3	5.0	3.8
6	2.2	5.7	4.0
7	-0.2	5.6	4.5
8	1.8	6.4	4.9
9	-0.5	6.2	5.3
10	1.2	7.0	5.0
11	-1.0	6.6	4.9

The even numbered HC_nN anions are more stable than their corresponding neutral HC_nN molecules. Thus, in line with the aim of the present study, the even numbered HC_nN^- anions are more probable candidates for astronomical searches and for possible detection. Figure 8 shows the plot of the electron affinity for these chains.

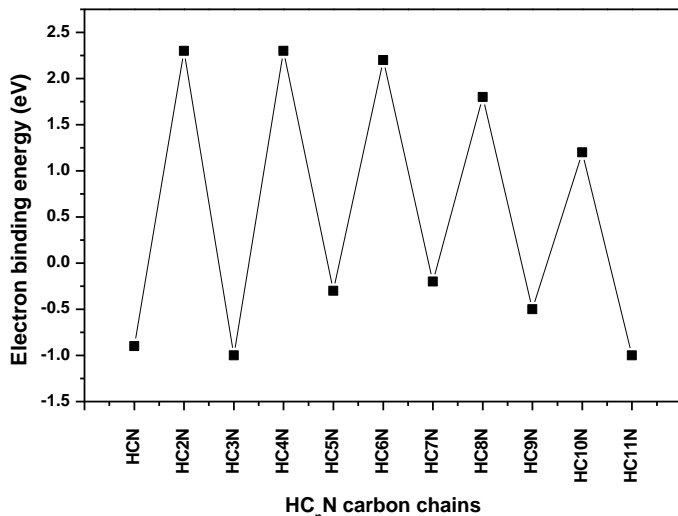


Figure 6.9: Plot showing electron affinity for HC_nN carbon chains

6.6.3 Summary on Detectable Interstellar Anions: High electron affinity (EA) and large dipole moment of neutral molecules have been shown to be the dominant factors influencing the formation and abundance of the corresponding anion species in ISM. Possible detectable anions in the ISM have been extensively investigated in this study. Over 80 neutral molecular comprising of carbon chain molecules (including those that are yet to be astronomically observed) have been examined with the aim of identifying possible detectable anions corresponding to these neutral molecules on the basis of electron affinity and dipole moment which have been theoretically calculated. Within the range of the EA and dipole moment of neutral interstellar species whose corresponding anions have been detected in ISM, a large number of neutral species considered here show a very high possibility for the astronomical observation of their corresponding anions. The C_{2n}O^- , C_{2n}S^- , $\text{C}_{2n-1}\text{Si}^-$, HC_{2n}N^- , C_2P^- , and C_{2n} are outstanding candidates including the higher the higher members of the C_{2n}H^- and $\text{C}_{2n-1}\text{N}^-$ groups whose lower members have been observed. The astronomical observation of members of the C_{2n}^- chains will imply the dominance of the EA over the effect of dipole moment in the formation and abundance of interstellar anions. Availability of accurate rotational transitions (or vibrational transitions for those species without permanent dipole moment) remains a major requirement for the astronomical observations of these molecules.

Deuterated Interstellar and Circumstellar Molecules: D/H Ratio and Dominant Formation Processes

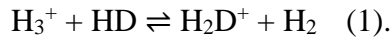
6.7 Introduction: In the early part of the 20th century, space was considered as chemically barren. The discoveries of NH₃, H₂O, H₂CO, CO, CH₃OH, etc in the 1960's and early 1970's in quick succession from different astronomical sources caused the idea to die a natural death^{35,108-111}. These discoveries ignited a strong interest among researchers on what molecules could be seen in space and what could be learned from these molecules. Today, over 200 different molecular species have been detected from different astronomical sources⁶⁰. These molecules are not only opening up a new research field; molecular astrophysics/astrochemistry, but have also increased the body of knowledge and interest in other related fields. That these molecules are excellent probes of the physical conditions in space is one of the driving forces for increased interest in astronomy. The field of astrobiology thrives on the discoveries of biologically related molecules in space.

Among these interstellar and circumstellar molecules, various isotopologues of H, C, N, O and S containing species have also been detected. Deuterated molecules are the most detected isotopologues of all interstellar and circumstellar isotopologues. This is quite amazing considering the cosmic D/H ratio which is only of the order of 10⁻⁵. Studies of deuterated molecules from both astronomical observation and theoretical modeling serve as the most appropriate test of ion-molecule processes for the formation and destruction of many interstellar species¹¹²⁻¹¹⁵. The origin of deuterium in the interstellar space is traced to the Big Bang. It is believed to have been produced in large quantities as part of the primordial Big Bang Nucleosynthesis¹¹⁶. Despite the low D/H ratio ($\approx 10^{-5}$), the reported D/H ratios for different deuterated molecules detected from different astronomical sources are far higher than the cosmic or elemental D/H ratio. D/H ratio ranging from 0.04 to 0.18 is reported for CH₃CCD; 0.054 for CH₂DCCH; 0.001-0.03 for D₂CO; ≈ 0.003 for NH₂D; 8×10^{-4} for ND₃; 0.0007-1.0 for DCN; >0.003-0.05 for HDO^{36,76,113-115,117-121}. These high D/H ratios are reported for all known deuterated molecules notwithstanding the low cosmic D/H ratio. The observed D/H ratios for different deuterated molecules set a high expectation for many other deuterated isotopologues of interstellar and circumstellar molecules to be detectable.

Accounting for the high D/H ratios has been a major concern of many studies for decades including models and space observatory missions; for instance the Far Ultraviolet Spectroscopic Explorer (FUSE)¹¹⁶ among others. While the models are still trying to account for the high ratios reported for singly deuterated molecules on the bases of ion-molecule chemistry, deuterium fractionation processes, cold grain surface processes and some gas-phase processes^{113,118,122}. D/H ratios for multiple deuterated species were predicted by various models to be very low such that their astronomical detection was not in view. According to Turner¹¹⁵ "*An overall prediction of ion-molecule chemistry is that while many species may be singly deuterated in detectable quantities, none will be doubly or multiply deuterated to similar degree*". The detection of D₂CO with D₂CO/H₂CO ratio of ≈ 0.003 led to the

conclusion that gas-phase chemistry cannot account for the observed high D₂CO/H₂CO ratio^{115,122}.

HD is the main reservoir of deuterium in the interstellar medium and it is also one of the earliest detected deuterated molecules¹²³. Deuterium fractionation is a temperature dependent process; the main reaction for this process is



The forward reaction is exothermic at the low temperature of the molecular clouds, thereby allowing the redistribution of deuterium resulting in the enhanced D/H ratio while at high temperature, the reverse reaction becomes favourable, thus, destroying the H₂D⁺ and suppressing the deuterium enhancement; the reverse reaction is said to require an additional energy of about 232k which is not easily achievable considering the conditions in the molecular clouds, thus the forward reaction keeps thriving^{119,124-126}. In accordance with Le Châtelier's principle, as the H₂D⁺ ion is being depleted via successive reactions with neutral molecules; the forward reaction is further enhanced. The depletion of H₂D⁺ results in the transfer and subsequent incorporation of deuterium in the newly species. The dependence on temperature by fractionation process has been reported for a number of systems. In the N₂D⁺/N₂H⁺ system, major fractionation occurs before 15k (with maximum at 13k) while at above 15k, deuterium fractionation drops drastically as the temperature approaches 30k^{119,125-128}.

Thermodynamically, the most conspicuous difference between a molecule and its deuterated analogue is in the zero point energy (ZPE) with the deuterated molecule having a lower ZPE. From the ZPE difference between a molecule and its deuterated analogue; the Boltzmann factor (E/kT) for a particular system (say DX/HX) can be determined using the determined using the temperature of the molecular cloud/rotational temperature from which DX was observed. The calculated Boltzmann factor gives insight about the nature or level of fractionation leading to the formation of DX. Boltzmann factor of 1 (or ≈ 1) implies no major fractionation, thus, the cosmic ratio of D/H ($\approx 10^{-5}$) will be expected for such system while for larger values of Boltzmann factor, notable and major fractionation will occur which will result in very high D/H ratio above the cosmic ratio. The present work aims at determining the Boltzmann factor D/H systems of all H-containing interstellar/circumstellar molecules using the ZPE of the H-and their corresponding D-analogues computed from high level quantum chemical simulations. The results obtained are used in accounting for the observed D/H ratios of the known deuterated molecules and in setting the pace of what should be expected for others depending on the prevailing conditions that will lead to their formation. The dominant formation processes for deuterated molecules and the possibility of more deuterated molecules are also discussed within the limit of the results obtained. The methodology employed in this work is briefly discussed in the next section while the results obtained based on the discussed methodology are presented and discussed after the methodology.

6.7.1 Methodology: Advances in computational and theoretical methods have made it possible to study systems, reactions and predict parameters which would have been either impossible or very difficult to study experimentally. For the present work, the GAUSSIAN 09 suit of programs¹² is employed for all computational quantum chemical calculations reported here. Achieving high accurate results at less computational cost is a major consideration for every computational study. In this regard, the compound models are the best candidates. Among these compound models, the G4 method has proven to be very reliable in predicting thermodynamic parameters to very high accuracy^{20,21}. The high accuracy of the G4 method coupled with our previous experience on the use of this method (as discussed in chapter 3) made it the right choice for the present work. The ZPE is obtained from the optimized structures of all the systems under consideration, all the structures are found to be stable with no imaginary frequency as shown from the frequency calculations. For all the known deuterated molecules, the reported temperature or rotational temperature of the molecular cloud from which they are detected are used in computing the Boltzmann factor while for the D/H systems whose D-analogues are not yet detected; a range of temperature is used in computing the Boltzmann factor.

6.8 Results and Discussion: Of the over 200 known interstellar and circumstellar molecules, 132 of them contain at least an atom of H as much as we know. This is not surprising with atoms of H making up about 89% of the gas in the interstellar medium (ISM) and molecular hydrogen (H_2) being the most abundant molecules species in ISM. All of these H-containing and their corresponding deuterated analogues are considered in this study. Over 20 deuterated molecules have been detected from different astronomical sources. 22 of these molecules with reported D/H ratio and the excitation temperature in the astronomical source where they are detected are examined. In Table 6.17, the ZPE, the excitation temperature (indicated as source temp), Boltzmann factor, E/kT (obtained by dividing the value of ΔT in column 3 by the source temp. in column 4), D/H ratio and reference (ref) to the reported values are presented. These molecules are arranged in ascending order of the number of atoms and are discussed in the same manner together with the ones presented in subsequent tables.

For H-containing interstellar and circumstellar species whose deuterated analogues are not known, four sets of temperature; 10, 100, 500 and 1000k have been adopted in determining the Boltzmann factor for such systems. This temperature range spans from what could be expected in the cold molecular clouds ($\approx 10k$) as reported for most species in Table 6.17 to those in the very hot cores. Table 6.18 shows the diatomic H-containing molecules and their corresponding D-analogues; their ZPE and the Boltzmann factor for the four sets of temperature considered. There are 14 H-containing known interstellar/circumstellar species of which 5 (CH^+ , OH^+ , SH^+ , HCl^+ , ArH^+) are ions. The contain some of the rare species among interstellar molecules; the only known noble gas, Ar- and Li-containing species are in this group. HD is the only known deuterated species among the diatomic species¹²³. This is not surprising considering the abundance of H_2 with respect to other diatomic species. The Boltzmann factor for the HD/ H_2 system is almost unity (1.010-0.903) using the reported temperature at the source from which HD was observed while the D/H ratio is 10^{-6} , a value

that is close to the cosmic D/H ratio ($\approx 10^{-5}$). Thus, at high temperature no major deuterium fractionation occurs, hence the D/H ratio would likely reflect the cosmic or elemental D/H ratio as observed here.

Table 6.17: Known D-molecules, their excitation temperature, Boltzmann factor (E/kT) and D/H ratio

Molecule	ZPE (kcal/mol)	* ΔT (k)	Source Temp. (k)	E/kT	D/H ratio	Ref.
H ₂	6.4	-				
HD	5.5	430.1	423- 473	1.0-0.9	10^{-6}	123
H ₂ O	13.4	-				
HDO	11.6	906.3	100	9.1	0.014-0.058	129
D ₂ O	9.8	1838.2	100	18.4	1.7×10^{-3} (D ₂ O/HDO) 5×10^{-5} (D ₂ O/H ₂ O)	130
N ₂ H ⁺	10.4	-				
N ₂ D ⁺	8.6	874.4	<20 >20	<43.7 >43.7	0.3-0.8 <0.04	114
H ₃ ⁺	12.8					
H ₂ D ⁺	11.7	582.9	18	32.4	<0.003	139
HCO ⁺	10.3	-				
DCO ⁺	8.6	857.7	<20 >20	<42.9 >42.9	0.04-3.4 <0.01-0.6	114
C ₂ H	8.0	-				
C ₂ D	6.7	671.3	20	33.6	0.01	140
HCN	10.4	-				
DCN	8.6	898.1	<20 >20	<44.9 >44.9	7×10^{-4} -0.018 ≈ 1.0	114
HNC	9.3	-				
DNC	7.684	807.4	<20 >20	<40.4 >40.4	0.7-1.3 0.006-0.24	114
H ₂ S	9.5	-				
HDS	8.1	661.6	20	33.1	0.1	140
D ₂ S	6.8	1343.0	12	(56.8) 111.9	0.011(D ₂ S/HDS)	136
H ₂ CS	15.5	-				
HDCS	13.7	902.2	≈ 10	90.2	0.300	131
D ₂ CS	11.9	1819.2	≈ 10	181.9	0.111 (D ₂ CS/H ₂ CS) 0.333 (D ₂ CS/HDCS)	141
NH ₃	21.6	-				
NH ₂ D	19.7	954.9	10.8-14.6	65.4-88.4	0.04-0.33	42
NHD ₂	17.7	1931.6	24	80.5	0.03	137
ND ₃	15.7	2929.8	5-10	293.0-586.0	8×10^{-4}	118
1-C ₃ H	11.5	-				
1-C ₃ D	9.9	812.8	13.9	58.5	0.048	138
H ₂ CS	15.5	-				
HDCS	13.7	902.2	18 50	50.1 18.0	0.02-0.06 0.01-0.03	120,121
D ₂ CS	11.9	1819.2	18 50	101.1 36.4	0.01-0.03 0.001-0.01	120,121

c-C ₃ H ₂	18.5	-				
c-C ₃ HD	16.7	918.9	12.3	74.7	0.071	138
C ₄ H	15.2	-				
C ₄ D	13.5	869.3	10	86.9	0.0043	135
HC ₃ N	16.6	-				
DC ₃ N	14.9	889.2	10	89.9	0.05	133
CH ₃ OH	32.1	-				
CH ₂ DOH	30.1	1011.4	12.3	82.2	0.030	138
CHD ₂ OH	28.1	2015.9	47	42.9	0.060	141
CD ₃ OH	26.1	3030.9	85	35.67	0.014	141
CH ₃ CN	28.4	-				
CH ₂ DCN	26.5	981.4	240	4.1	≥0.005	117
H ₂ C ₄	22.4	-				
HDC ₄	20.7	876.9	12.3	71.3	0.030	138
HC ₅ N	23.3	-				
DC ₅ N	21.5	888.6	10	88.9	0.006-0.016	134
CH ₃ CCH	34.8	-				
CH ₃ CCD	33.0	894.3	10	89.4	0.04-0.18	113
CH ₂ DCCH	32.8	977.3	10	97.7	0.079-0.17	113
HCOOCH ₃	38.9	-				
HCOOCH ₂ D	36.8	1012.7	110	9.2	0.04±0.02	132

*The difference in the ZPE of a molecule and its D-analogue expressed in terms of temperature.

NH₃D⁺ has been detected with a column density of $1.1\pm0.2 \times 10^{12} \text{ cm}^{-2}$.³⁶ The hydrogenated analogue, NH₄⁺ is not detected (it's a spherical top with no permanent dipole moment), hence the D/H ratio cannot be determined.

From Table 6.18, if the deuterium fractionation processes that will lead to the formation of the D-analogues of these diatomics are to occur as part of the low temperature grain surface processes, pronounced deuterium fractionation that will result in D/H ratio higher than the cosmic or elemental D/H ratio is the most probable event. But at temperature close to the range where HD is observed, the Boltzmann factor will tend towards unity signifying no pronounced deuterium fractionation; therefore, D/H ratio close to the cosmic D/H ratio would be expected. That only HD is the only observed D-analogues of the diatomic species could be due to interstellar abundances of these species. Since most of them are radicals/ions, they are not very stable; thus, their D-analogues may not be very abundant.

Table 6.18: Boltzmann factor (E/kT) for D-analogues of H-containing diatomic species and the corresponding ZPE

Molecule	ZPE (kcal/mol)	* ΔT (K)	E/kT (at T=10k)	E/kT (at T=100k)	E/kT (at T=500k)	E/kT (at T=1000k)
H ₂	6.4	-	-	-	-	-
HD	5.5	430.1	43.0	4.3	0.9	0.4
HCl	4.2	-	-	-	-	-
DCl	3.0	600.3	60.0	6.0	1.2	0.6
NH	4.7	-	-	-	-	-
ND	3.4	637.6	63.8	6.4	1.3	0.6
OH	5.3	-	-	-	-	-
OD	3.8	723.4	72.3	7.2	1.4	0.7
OH ⁺	4.4	-	-	-	-	-
OD ⁺	3.2	598.1	59.8	6.0	1.2	0.6
HF	5.9	-	-	-	-	-
DF	4.3	813.8	81.4	8.1	1.6	0.8
LiH	2.0	-	-	-	-	-
LiD	1.5	256.7	25.7	2.6	0.5	0.3
CH	4.0	-	-	-	-	-
CD	2.9	538.1	53.8	5.4	1.1	0.5
CH ⁺	4.0	-	-	-	-	-
CD ⁺	2.9	537.1	53.7	5.4	1.1	0.5
SH	3.8	-	-	-	-	-
SD	2.7	542.5	54.2	5.4	1.1	0.5
SH ⁺	3.6	-	-	-	-	-
SD ⁺	2.6	516.6	51.7	5.2	1.0	0.5
SiH	2.9	-	-	-	-	-
SiD	2.1	407.357	40.7	4.1	0.8	0.4
HCl ⁺	3.8	-	-	-	-	-
DCl ⁺	2.7	537.1	53.7	5.4	1.1	0.5
ArH ⁺	3.8	-	-	-	-	-
ArD ⁺	2.7	540.6	54.1	5.4	1.1	0.5

*The difference in the ZPE of a molecule and its D-analogue expressed in terms of temperature.

The triatomic species constitute the highest number of known deuterated molecules. Of the 20 H-containing triatomic species presented in Table 6.19, 8 (indicated with bold typeface in Table 6.19) have their corresponding D-analogues as known interstellar/circumstellar species^{114,129,130,136,139,140}. From Table 1, the Boltzmann factor for these detected deuterated species ranges from 9 to 97.054 with reported excitation or molecular cloud temperature in the range of 5 to 100k. Under these conditions, major deuterium fractionation which will culminate in D/H ratio far higher than the cosmic D/H ratio should be expected and this is evident from the results. For the singly deuterated species, the D/H ratio ranges from 7×10^{-4} to ≈ 1 and 5×10^{-5} to 0.011 for the doubly deuterated species. These trends are anticipated for other triatomic species if they are observed under similar conditions.

Table 6.19: Boltzmann factor (E/kT) for D-analogues of H-containing triatomic species and the corresponding ZPE

Molecule	ZPE (kcal/mol)	*ΔT(K)	E/kT (at T=10k)	E/kT (at T=100k)	E/kT (at T=500k)	E/kT (at T=1000k)
H₂O	13.4	-	-	-	-	-
HDO	11.6	906.3	90.6	9.1	1.8	0.9
D₂O	9.8	1838.2	183.8	18.4	3.7	1.8
H ₂ O ⁺	11.7	-	-	-	-	-
HDO ⁺	10.1	786.6	78.7	7.9	1.6	0.8
H₂S	9.5	-	-	-	-	-
HDS	8.1	661.6	66.2	6.6	1.3	0.7
D₂S	6.8	1343.0	134.3	13.4	2.7	1.3
HCN	10.4	-	-	-	-	-
DCN	8.6	898.1	89.8	9.0	1.8	0.9
HNC	9.3	-	-	-	-	-
DNC	7.7	807.4	80.7	8.1	1.6	0.8
NH ₂	11.9	-	-	-	-	-
NDH	10.3	797.0	79.7	8.0	1.6	0.8
CH ₂	11.6	-	-	-	-	-
CHD	10.1	759.8	76.0	7.6	1.5	0.8
HCO	8.9	-	-	-	-	-
DCO	7.3	798.3	79.8	8.0	1.6	0.8
HCO⁺	10.3	-	-	-	-	-
DCO⁺	8.6	857.7	85.8	8.6	1.7	0.8
HOC ⁺	8.4	-	-	-	-	-
DOC ⁺	6.9	753.1	75.3	7.5	1.5	0.7
HCS ⁺	9.2	-	-	-	-	-
DCS ⁺	7.4	902.5	90.2	9.0	1.8	0.9
H₃⁺	12.8	-	-	-	-	-
H₂D⁺	11.7	582.9	58.3	5.8	1.2	0.6
H ₂ Cl	4.6	-	-	-	-	-
HDCl	3.3	634.4	63.4	6.3	1.3	0.6
H ₂ Cl ⁺	7.2	-	-	-	-	-
HDCl ⁺	6.2	515.7	51.6	5.2	1.0	0.5
AlOH	6.9	-	-	-	-	-
AlOD	5.4	786.6	78.7	7.9	1.6	0.8
HO ₂	7.6	-	-	-	-	-
DO ₂	6.0	791.7	79.2	7.9	1.6	0.8
C₂H	8.0	-	-	-	-	-
C₂D	6.7	671.3	67.1	6.7	1.3	0.7
HNO	9.0	-	-	-	-	-
DNO	7.3	874.7	87.5	8.7	1.7	0.9
HCP	8.9	-	-	-	-	-
DCP	7.1	898.1	89.8	9.0	1.8	0.9
N₂H⁺	10.4	-	-	-	-	-
N₂D⁺	8.6	874.4	87.4	8.7	1.7	0.9

*The difference in the ZPE of a molecule and its D-analogue expressed in terms of temperature.

From Table 6.19, if the fraction processes leading to the formation of these species are to occur at temperature above 500k where the Boltzmann factor will be approaching unity, then D/H ratio in the range of the cosmic D/H ratio will be expected. The observed D/H ratios signal grain surface reactions as the dominant processes leading to the formation of these species. The trends of the D/H ratios noted here are anticipated for other triatomic species if they are formed and observed under similar conditions.

As much as we know, there are currently 20 H-containing tetra-atomic interstellar/circumstellar molecular species (same number as the triatomic species). The ZPE of these species are their corresponding D-analogues together with the Boltzmann factor for all the systems considered here are depicted in Table 4. Of these 20 species, 4 (H_2CS , H_2CO , NH_3 and $\text{I}-\text{HC}_3$) have their deuterated analogues as known molecular species in space^{131,42,137,118,138,120,121}. Ammonia is one of the very few molecules with triply deuterated analogues. The periodic trend between O and S is noted here with the O-containing molecules (H_2CO) having its S-analogue (H_2CS) also deuterated to the same level. This is also the case of H_2O and H_2S in the previous part (Tables 6.17 and 6.19). The reported source temperature (excitation/molecular cloud temperature) where these tri-atomic species are observed ranges from 5 to 50k (Table 6.17). This range is far below the temperature (${}^*\Delta T$ in Table 6.20) at which the Boltzmann factor for these species should be unity. The high values of the Boltzmann factor results in high D/H ratios.

The D/H ratio increase with Boltzmann factor, as the Boltzmann factor approaches unity, the D/H ratio approaches the cosmic D/H ratio (see HD, Table 6.17). Against the predictions of various models which did not envisage the detectability of multiply deuterated species due to the low abundances predicted for them, these species have been detected with very D/H ratios (0.001-0.333 for doubly deuterated species and 8×10^{-4} for triply deuterated ammonia). From the Boltzmann factor and the conditions surrounding the observations of these molecules, these ratios are not surprising. At the reported source temperature for these species, there is no doubt that there is very high level of deuterium fractionation, thus resulting in the high D/H ratios of these species. This temperature range further supports the grain surface processes as the dominant mechanisms for the formation of deuterated molecules. The observed D/H ratio can easily be foreseen for other D-analogues tetra-atomic species if the same conditions here dominate their formation processes.

Table 6.20: Boltzmann factor (E/kT) for D-analogues of H-containing tetra-atomic species and the corresponding ZPE

Molecule	ZPE (kcal/mol)	*ΔT(K)	E/kT (at T=10k)	E/kT (at T=100k)	E/kT (at T=500k)	E/kT (at T=1000k)
NH₃	21.6	-	-	-	-	-
NH₂D	19.7	954.9	95.5	9.5	1.9	0.9
NHD₂	17.7	1931.6	193.2	19.3	3.9	1.9
ND₃	15.7	2929.8	293.0	29.3	5.9	2.9
H₂CO	16.7	-	-	-	-	-
HDCO	14.9	889.2	88.9	8.9	1.8	0.9
D₂CO	13.1	1790.5	179.0	17.9	3.6	1.8
H₂CS	15.5	-	-	-	-	-
HDCS	13.7	902.2	90.2	9.0	1.8	0.9
D₂CS	11.9	1819.2	181.9	18.2	3.6	1.8
HNCO	13.0	-	-	-	-	-
DNCO	11.4	810.6	81.1	8.1	1.6	0.8
HNCS	11.4	-	-	-	-	-
DNCS	9.8	800.2	80.0	8.0	1.6	0.8
H₂CN	15.8	-	-	-	-	-
HDCN	14.1	854.8	85.5	8.5	1.7	0.8
CH₃	18.6	-	-	-	-	-
CH₂D	17.0	813.8	81.4	8.1	1.6	0.8
PH₃	15.0	-	-	-	-	-
PH₂D	13.6	690.9	69.1	6.9	1.4	0.7
MgC₃H	11.1	-	-	-	-	-
MgC₃D	9.3	900.3	90.0	9.0	1.8	0.9
H₂O₂	16.6	-	-	-	-	-
HDO₂	14.6	1032.9	103.3	10.3	2.1	1.0
HSCN	10.6	-	-		-	-
DSCN	9.2	724.1	72.4	7.2	1.4	0.7
HOCH	13.6	-	-	-	-	-
DOCH	11.7	967.2	96.7	9.7	1.9	1.0
HCNO	12.0	-	-	-	-	-
DCNO	10.6	723.8	72.4	7.2	1.4	0.7
HC₂N	11.5	-	-	-	-	-
DC₂N	9.9	819.4	81.9	8.2	1.6	0.8
HCNH⁺	17.6	-	-	-	-	-
DCNH⁺	15.8	890.2	89.0	8.9	1.8	0.9
HOCO⁺	12.7	-	-	-	-	-
DOCO⁺	11.165	752.8	75.3	7.5	1.5	0.7
H₃O⁺	20.6	-	-	-	-	-
H₂DO⁺	18.7	925.5	92.5	9.2	1.8	0.9
I-C₃H	11.5	-	-	-	-	-
I-C₃D	9.9	812.8	81.3	8.1	1.6	0.8
c-C₃H	12.0	-	-	-	-	-
c-C₃D	10.1	921.4	92.1	9.2	1.8	0.9
C₂H₂	16.8	-	-	-	-	-
C₂HD	15.1	887.3	88.7	8.9	1.8	0.9

*The difference in the ZPE of a molecule and its D-analogue expressed in terms of temperature.

Table 6.21: Boltzmann factor (E/kT) for D-analogues of H-containing penta-atomic species and the corresponding ZPE

Molecule	ZPE (kcal/mol)	* ΔT (K)	E/kT (at T=10k)	E/kT (at T=100k)	E/kT (at T=500k)	E/kT (at T=1000k)
CH ₄	28.1	0	0	0	0	0
CH ₃ D	26.3	920.5	92.0	9.2	1.8	0.9
SiH ₄	19.5	0	0	0	0	0
SiH ₃ D	18.2	671.7	67.2	6.7	1.3	0.7
CH ₂ NH	25.0	0	0	0	0	0
CHDNH	23.1	960.9	96.1	9.6	1.9	1.0
NH ₂ CN	21.4	0	0	0	0	0
NHDCN	19.4	1007.6	100.8	10.1	2.0	1.0
CH ₂ CO	19.9	0	0	0	0	0
CHDCO	18.2	870.9	87.1	8.7	1.7	0.9
HCOOH	21.3	0	0	0	0	0
DCOOH	19.1	1070.8	107.1	10.7	2.1	1.1
CH ₄ ⁻	15.1	-	-	-	-	-
CH ₃ D ⁻	13.6	749.0	74.9	7.5	1.5	0.7
HC(O)CN	16.6	-	-	-	-	-
DC(O)CN	14.7	965.6	96.6	9.7	1.9	1.0
HNCNH	18.8	-	-	-	-	-
DHCNH	17.2	820.1	82.0	8.2	1.6	0.8
CH ₃ O	22.8	-	-	-	-	-
CH ₂ DO	20.1	1340.8	134.1	13.4	2.7	1.3
NH ₄ ⁺	31.0	-	-	-	-	-
NH ₃ D ⁺	28.9	1025.3	102.5	10.2	2.0	1.0
HC₃N	16.6	-	-	-	-	-
DC₃N	14.9	889.2	88.9	8.9	1.8	0.9
HC ₂ NC	16.4	-	-	-	-	-
DC ₂ NC	14.6	870.9	87.1	8.7	1.7	0.9
HNC ₃	15.8	-	-	-	-	-
DNC ₃	14.1	834.6	83.5	8.3	1.7	0.8
CH ₂ CN	19.5	-	-	-	-	-
CHDCN	17.7	887.3	88.7	8.9	1.8	0.9
l-C ₃ H ₂	18.5	-	-	-	-	-
l-C ₃ HD	16.8	839.0	83.9	8.4	1.7	0.8
c-C₃H₂	18.5	-	-	-	-	-
c-C₃HD	16.7	918.9	91.9	9.2	1.8	0.9
C₄H	15.2	-	-	-	-	-
C₄D	13.5	869.3	86.9	8.7	1.7	0.9
H ₂ COH ⁺	25.4	-	-	-	-	-
HDCOH ⁺	23.5	974.8	97.5	9.7	1.9	1.0

*The difference in the ZPE of a molecule and its D-analogue expressed in terms of temperature.

Only a handful of all the interstellar and circumstellar molecules are cyclic. Whether this will be the trend among the isotopologues remains to be seen. However, that of the three deuterated species with 5 atoms, one is cyclic is a good omen in this direction. The number of H-containing molecules with 5 atoms is as many (19) as those with 4 and 3 atoms (20 each). These molecules and their corresponding D-analogues are presented in Table 6.21 with the

predicted parameters for the respective systems. DC₄, c-C₃HD and DC₃N are the known D-molecules of these series^{133,135,138}. The D/H ratio for these molecules ranges from 0.0045 to 0.071 far above the cosmic D/H ratio which is consistent with the Boltzmann factors for these molecules that are also far from unity. From Table 6.21, achieving a Boltzmann factor of unity which will suppress deuterium fractionation and lead to the cosmic D/H ratio for these molecules will mean a process or processes occurring at very high temperature (*ΔT). However, it is clear from the present results, that the processes that led to the formation of the observed penta-atomic species are largely cold temperature processes occurring on the surface of the interstellar dust grains surfaces.

Molecules with 6 atoms and above are regarded as complex in interstellar chemistry parlance, as the complexity increases, the number of known molecules decreases as compared to the non-complex molecules (those with 2 to 5 atoms). CH₃OH, CH₃CN and H₂C₄ are the haxa-atomic molecules with known D-analogues out of the 16 H-containing hexa-atomic molecules displayed in Table 6.22. CH₃OH is another molecule after NH₃ with triply deuterated analogue^{134,138,141}. The D/H ratio reported for these molecules ranges from 0.005 to 0.06 with least value corresponding to the least Boltzmann factor (4.061) among all the systems (Table 6.17). The source temperature and the Boltzmann factor for these molecules would not have suggested anything less than high D/H ratio above the cosmic D/H ratio because under these conditions, exchange reactions among D-containing molecules are highly exothermic, thus the deuterium get distributed and redistributed among different species leading to the observed high D/H ratio. From Table 6.22, this range of ratio is expected for other complex (with 6 atoms discussed here) species since most of the main species (H-analogues) are grain surface product except where other formation processes (very high temperature) prevail.

All the known interstellar and circumstellar molecules with seven atoms contain at least an atom of H. Of the 9 species in this series, two of their deuterated analogues have been detected in space. For HC₅N, it is the only possible deuterated analogue of it (DC₅N) that has been detected while for CH₃CCH, two isotopomers of it (CH₃CCD and CH₂DCCH) have been detected^{134,113}. As would be expected, the position of substitution of the D-atom has an effect on the entire system is observed in the two isotopomers. Table 6.23 shows the H-containing hepta-atomic species, their D-analogues; ZPE and the Boltzmann factor. The D/H ratio for DC₅N ranges from 0.006 to 0.016 at the reported source temperature of 10k. The observation of the two isotopomers under the same conditions allows one to test the dependence of the D/H ratio on the Boltzmann factor for similar systems. As in previous cases, D/H ratio increases with increasing value of Boltzmann factor. The source temperature and the Boltzmann factor for these systems rightly support the high D/H ratio reported for these systems, since under these conditions, major deuterium fractionation is expected to occur which is believed to culminate in D/H ratio higher than the cosmic D/H ratio. By all considerations, the dominance of grains surface reactions as the prevailing formation processes for these molecules cannot be ruled out.

Table 6.22: Boltzmann factor (E/kT) for D-analogues of H-containing hexa-atomic species and the corresponding ZPE

Molecule	ZPE (kcal/mol)	* ΔT (K)	E/kT (at T=10k)	E/kT (at T=100k)	E/kT (at T=500k)	E/kT (at T=1000k)
CH₃OH	32.1	-	-	-	-	-
CH₂DOH	30.1	1011.4	101.1	10.1	2.0	1.0
CHD₂OH	28.1	2015.9	201.6	20.2	4.0	2.0
CD₃OH	26.1	3030.9	303.1	30.3	6.1	3.0
CH ₃ SH	28.8	-	-	-	-	-
CH ₂ DSH	26.8	988.42	98.8	9.9	2.0	1.0
C ₂ H ₄	32.0	-	-	-	-	-
C ₂ H ₃ D	30.1	960.9	96.1	9.6	1.9	1.0
H₂C₄	22.4	--	-	-	-	-
HDC₄	20.7	876.9	87.7	8.8	1.7	0.9
HNCHCN	24.9	-	-	-	-	-
DNCHCN	22.8	1058.2	105.8	10.6	2.1	1.1
SiH ₃ CN	20.7	-	-	-	-	-
SiH ₂ DCN	19.3	717.1	71.7	7.2	1.4	0.7
CH₃CN	28.4	-	-	-	-	-
CH₂DCN	26.5	981.4	98.1	9.8	2.0	2.0
CH ₃ NC	28.3	-	-	-	-	-
CH ₂ DNC	26.3	1001.0	100.1	10.0	2.0	1.0
H ₂ CCNH	27.5	-	-	-	-	-
HDCCNH	25.7	911.3	91.1	9.1	1.8	0.9
HC ₄ N	18.3	-	-	-	-	-
DC ₄ N	16.6	862.1	86.2	8.6	1.7	0.9
c-H ₂ C ₃ O	23.8	-	-	-	-	-
c-HDC ₃ O	21.9	922.4	92.2	9.2	1.8	0.9
HCCC(O)H	23.3	-	-	-	-	-
DCCC(O)H	21.5	905.7	90.6	9.1	1.8	0.9
HC(O)NH ₂	28.4	-	-	-	-	-
DC(O)NH ₂	26.5	980.5	98.0	9.8	2.0	2.0
H(CC) ₂ H	23.4	-	-	-	-	-
H(CC) ₂ D	21.7	889.2	88.9	8.9	1.8	0.9
HC ₅	18.2	-	-	-	-	-
DC ₅	16.6	842.5	84.2	8.4	1.7	0.8
HC ₃ NH ⁺	24.2	-	-	-	-	-
DC ₃ NH ⁺	22.4	920.2	92.0	9.2	1.8	0.9

*The difference in the ZPE of a molecule and its D-analogue expressed in terms of temperature.

Table 6.23: Boltzmann factor (E/kT) for D-analogues of H-containing hepta-atomic species and the corresponding ZPE

Molecule	ZPE (kcal/mol)	* ΔT (K)	E/kT (at T=10k)	E/kT (at T=100k)	E/kT (at T=500k)	E/kT (at T=1000k)
CH ₂ CH(OH)	35.3	-	-	-	-	-
CHDCH(OH)	33.3	1008.6	100.9	10.1	2.0	1.0
c-C ₂ H ₄ O	35.9	-	-	-	-	-
c-C ₂ H ₃ D	33.9	1031.3	103.1	10.3	2.1	1.0
HC(O)CH ₃	34.7	-	-	-	-	-
HC(O)CH ₂ D	32.8	967.2	96.7	9.7	1.9	1.0
CH ₂ CH(CN)	31.9	-	-	-	-	-
CHDCH(CN)	29.9	997.2	99.7	10.0	2.0	1.0
CH₃CCH	34.8	-	-	-	-	-
CH₂DCCH	32.8	977.3	97.7	9.8	1.9	1.0
CH₃CCD	33.0	894.3	89.4	8.9	1.8	0.9
CH ₃ NH ₂	40.1	-	-	-	-	-
CH ₂ DNH ₂	38.1	1003.5	100.3	10.0	2.0	1.0
HC₅N	23.3	-	-	-	-	-
DC₅N	21.5	888.6	88.9	8.9	1.8	0.9
HC ₆	21.9	-	-	-	-	-
DC ₆	20.2	871.9	87.2	8.7	1.7	0.9
HC ₆ ⁻	21.2	-	-	-	-	-
DC ₆ ⁻	19.8	737.0	73.7	7.4	1.5	0.7

*The difference in the ZPE of a molecule and its D-analogue expressed in terms of temperature.

There 12 interstellar/circumstellar molecules with 8 atoms (Table 6.24). Fortunately, all of these molecules contain at least an atom of H. HCOOCH₂D is the only D-analogue of these species with atoms¹³². This is probably the largest deuterated molecule detected till date. The detection of HCOOCH₂D can largely be traced to the high abundance of its main isotopologue; methyl formate. The high abundance of methyl formate in many astronomical sources has earned it the name "interstellar weed". It is more abundant than its isomers; acetic acid and glycolaldehyde. Its high abundance in comparison to its isomers has been traced to interstellar hydrogen bonding where its isomers are found to be high bonded to the surface of the interstellar dust grains thereby reducing their abundance while methyl formate is the least affected isomer of the C₂H₄O₂ isomeric group with respect to interstellar hydrogen bonding. The D/H ratio reported for HCOOCH₂D (0.04±0.02) is far above the cosmic D/H ratio, the Boltzmann factor and other conditions surrounding its detection support this ratio.

Table 6.24: Boltzmann factor (E/kT) for D-analogues of H-containing octa-atomic species and the corresponding ZPE

Molecule	ZPE (kcal/mol)	* ΔT	E/kT (at T=10k)	E/kT (at T=100k)	E/kT (at T=500k)	E/kT (at T=1000k)
CH ₃ COOH	38.7	-	-	-	-	-
CH ₃ COOD	36.6	1090.4	109.0	10.9	2.2	1.1
HCOOCH₃	38.9	-	-	-	-	-
HCOOCH₂D	36.8	1012.7	101.3	10.1	2.0	1.0
HOCH ₂ C(O)H	37.9	-	-	-	-	-
HOCH ₂ C(O)D	35.9	1018.41	101.8	10.2	2.0	1.0
H ₃ C ₄ N	34.9	-	-	-	-	-
H ₂ DC ₄ N	32.9	978.9	97.9	9.8	2.0	1.0
CH ₂ CHCHO	38.5	-	-	-	-	-
CH ₂ CDCHO	36.5	1011.1	101.1	10.1	2.0	1.0
CH ₂ C ₂ HCN	34.4	-	-	-	-	-
CHDC ₂ HCN	32.6	954.0	95.4	9.5	1.9	0.9
H ₂ C ₆	29.0	-	-	-	-	-
HDC ₆	27.3	884.5	88.4	8.8	1.8	0.9
CH ₃ CHNH	42.9	-	-	-	-	-
CH ₃ CDNH	41.0	977.3	97.7	9.8	1.9	1.0
(NH ₂) ₂ CO	38.4	-	-	-	-	-
NH ₂ CONHD	36.3	1017.1	101.7	10.2	2.0	1.0
NH ₂ CH ₂ CN	39.7	-	-	-	-	-
NHDCH ₂ CN	37.6	1063.2	106.3	10.6	2.1	1.1
HC ₇	44.5	-	-	-	-	-
DC ₇	23.4	10619.7	1062.0	106.2	21.2	10.6
HC ₆ H	29.5	-	-	-	-	-
DC ₆ H	27.8	878.8	87.9	8.8	1.8	0.9

*The difference in the ZPE of a molecule and its D-analogue expressed in terms of temperature.

In Tables 6.25 to 6.29, we present H-containing interstellar and circumstellar molecules comprising of 9 to 13 atoms. Their deuterated analogues, ZPE and Boltzmann factor are also presented. From available literature, there is currently no known deuterated interstellar or circumstellar species in this series. The discussion in this section will only be limited to what could be expected based on what is known. Interstellar chemistry processes are partially thermodynamically controlled. As it is discussed in the energy, stability and abundance (ESA) relationship, the astronomical detection of a molecule is largely a function of its abundance. The higher the interstellar abundance of a species the higher its chances of being detected as compared to similar species with low abundance. As seen in all the cases of the known D-molecules, the main isotopologue should be highly abundant for the detection of its D-analogue to be anticipated. Despite the abundance of these species, the availability of accurate laboratory measurement of the rotational transitions/rest frequencies of these D-isotopologues is a crucial issue. As in most cases, even when there is overwhelming evidence of the present of the D-analogue in a detectable form, its astronomical search will still be dependent on the availability of accurate laboratory measurements.

Table 6.25: Boltzmann factor (E/kT) for D-analogues of H-containing nona-atomic species and the corresponding ZPE

Molecule	ZPE (kcal/mol)	*ΔT(K)	E/kT (at T=10k)	E/kT (at T=100k)	E/kT (at T=500k)	E/kT (at T=1000k)
(CH ₃) ₂ O	49.9	-	-	-	-	-
CH ₃ OCH ₂ D	47.9	1002.6	100.3	10.0	2.0	1.0
CH ₃ CH ₂ CN	46.5	-	-	-	-	-
CH ₃ CHDCN	44.5	1036.7	103.7	10.4	2.1	1.0
CH ₃ CH ₂ OH	50.0	-	-	-	-	-
CH ₃ CHDOH	48.0	1046.2	104.6	10.5	2.1	1.0
CH ₃ C(O)NH ₂	45.9	-	-	-	-	-
CH ₂ DC(O)NH ₂	44.0	968.5	96.8	9.7	1.9	1.0
CH ₃ CH ₂ SH	46.8	-	-	-	-	-
CH ₃ CHD ₂ SH	44.7	1043.0	104.3	10.4	2.1	1.043
CH ₃ C ₄ H	41.2	-	-	-	-	-
CH ₂ DC ₄ H	39.3	977.3	97.7	9.8	1.9	1.0
HC ₇ N	30.1	-	-	-	-	-
DC ₇ N	28.4	883.9	88.4	8.8	1.8	0.9
CH ₃ CHCH ₂	49.9	-	-	-	-	-
CH ₂ CHCH ₂	48.0	984.6	98.5	9.8	2.0	1.0
HC ₈	29.0	-	-	-	-	-
DC ₈	27.2	875.0	87.5	8.7	1.7	0.9
HC ₈ ⁻	28.3	-	-	-	-	-
DC ₈ ⁻	26.8	744.9	74.5	7.4	1.5	0.7

*The difference in the ZPE of a molecule and its D-analogue expressed in terms of temperature.

Table 6.26: Boltzmann factor (E/kT) for D-analogues of H-containing deca-atomic species and the corresponding ZPE

Molecule	ZPE (kcal/mol)	*ΔT(K)	E/kT (at T=10k)	E/kT (at T=100k)	E/kT (at T=500k)	E/kT (at T=1000k)
(CH ₃) ₂ CO	52.3	-	-	-	-	-
CH ₃ COCH ₂ D	50.3	1002.3	100.2	10.0	2.0	1.0
HOCH ₂ CH ₂ OH	53.1	-	-	-	-	-
HOCH ₂ CHDOH	51.0	1049.0	104.9	10.5	2.1	1.0
CH ₃ CH ₂ CHO	52.8	-	-	-	-	-
CH ₂ DCH ₂ CHO	50.8	1000.7	100.1	10.0	2.0	1.0
CH ₃ C ₄ CN	41.3	-	-	-	-	-
CH ₂ DC ₄ CN	39.4	977.7	97.8	9.8	1.9	1.0

*The difference in the ZPE of a molecule and its D-analogue expressed in terms of temperature.

Table 6.27: Boltzmann factor (E/kT) for D-analogues of H-containing undeca-atomic species and the corresponding ZPE

Molecule	ZPE (kcal/mol)	*ΔT(K)	E/kT (at T=10k)	E/kT (at T=100k)	E/kT (at T=500k)	E/kT (at T=1000k)
HC ₉ N	37.5	-	-	-	-	-
DC ₉ N	35.7	881.7	88.2	8.8	1.8	0.9
CH ₃ C ₆ H	47.6	-	-	-	-	-
CH ₂ DC ₆ H	45.7	977.7	97.8	9.8	1.9	1.0
CH ₃ CH ₂ OCHO	56.8	-	-	-	-	-
CH ₂ DCH ₂ OCHO	54.8	998.5	99.8	10.0	2.0	1.0
CH ₃ OC(O)CH ₃	56.1	-	-	-	-	-
CH ₂ DOC(O)CH ₃	54.1	987.8	98.8	9.9	2.0	1.0

*The difference in the ZPE of a molecule and its D-analogue expressed in terms of temperature.

Table 6.28: Boltzmann factor (E/kT) for D-analogues of H-containing dodeca-atomic species and the corresponding ZPE

Molecule	ZPE (kcal/mol)	*ΔT(K)	E/kT (at T=10k)	E/kT (at T=100k)	E/kT (at T=500k)	E/kT (at T=1000k)
C ₂ H ₅ OCH ₃	67.7	-	-	-	-	-
CH ₂ DCH ₂ OCH ₃	65.7	1001.3	100.1	10.0	2.0	1.0
iso-C ₃ H ₇ CN	64.2	-	-	-	-	-
iso-C ₃ H ₆ DCN	62.2	1012.7	101.3	10.1	2.0	1.0
C ₃ H ₇ CN	64.4	-	-	-	-	-
C ₃ H ₆ DCN	62.4	1002.9	100.3	10.0	2.0	1.0
C ₆ H ₆	62.9	-	-	-	-	-
C ₆ H ₅ D	54.1	4386.2	438.6	43.9	8.8	4.4

*The difference in the ZPE of a molecule and its D-analogue expressed in terms of temperature.

Table 6.29: Boltzmann factor (E/kT) for D-analogues of H-containing trideca-atomic species and the corresponding ZPE

Molecule	ZPE (kcal/mol)	*ΔT(K)	E/kT (at T=10k)	E/kT (at T=100k)	E/kT (at T=500k)	E/kT (at T=1000k)
HC ₁₁ N	42.8	-	-	-	-	-
DC ₁₁ N	41.0	883.5	88.3	8.8	1.8	0.9

*The difference in the ZPE of a molecule and its D-analogue expressed in terms of temperature.

Table 6.30 shows specific examples of Boltzmann factor and D/H ratio for different systems. Figure 6.10 depicts the dependence of D/H ratio on the Boltzmann factor. It is obvious from the figure that the D/H ratio increases as the Boltzmann factor increases. This is traceable to the low temperature processes which dominate the formation of these species in the interstellar medium under which there is a very high enhancement of deuterium fractionation, thus, resulting in very high D/H ratio.

Table 6.30: The dependence of D/H ration on Boltzmann factor

Boltzmann Factor	$\text{CH}_2\text{DCCH}/\text{CH}_3\text{CCH}^{42}$
96.9	0.061
64.6	0.054
48.4	0.051
Boltzmann Factor	$\text{CH}_3\text{CCD}/\text{CH}_3\text{CCH}^{42}$
88.7	0.015
59.1	0.014
44.3	0.013
Boltzmann Factor	$\text{HDCO}/\text{H}_2\text{CO}^{121}$
126.1	0.034
49.1	0.030
17.7	0.010
Boltzmann Factor	$\text{D}_2\text{CO}/\text{H}_2\text{CO}^{121}$
254.0	0.020
98.8	0.010
35.6	0.001

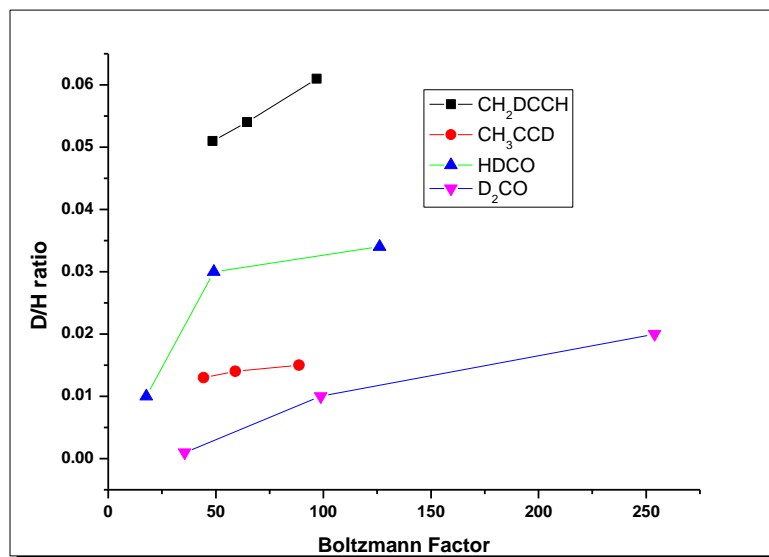


Fig. 6.10: Dependence of D/H ratio on Boltzmann factor

6.9 Summary on Deuterated Interstellar and Circumstellar Molecules: A total of 132 H-containing interstellar and circumstellar molecules and their corresponding deuterated analogues with atoms ranging from 2 to 13 have been examined with the aim of investigating the D/H ratios and the dominant formation processes for the known deuterated molecules and what could be expected for others. The Boltzmann factor computed for each of these systems using the ZPE obtained from high level quantum chemical simulations shows a direct correlation with the D/H ratio reported for various known deuterated molecules. As the Boltzmann factor approaches unity, the D/H ratio also approaches the cosmic D/H ratio while at higher Boltzmann factor, the D/H ratio increases to various orders of magnitude above the cosmic D/H ratio. This implies that at lower temperature (higher Boltzmann factor), the exchange reaction involving deuterium or deuterium fractionation is much pronounced leading to the distribution and redistribution of deuterium among various species, thus resulting in the high D/H ratio while at very high temperature (Boltzmann factor approaching unity), there will be no major fractionation, thus the D/H ratio will probably reflects the cosmic D/H ratio as observed in the case of HD. From this study, it can be concluded that interstellar grain processes are the dominant formation mechanisms for the deuterated molecules rather than gas-phase processes and as such, the high D/H ratios could also be envisaged for the other deuterated molecules that are yet to be detected.

Optimizing the Searches for Interstellar Heterocycles

6.10 Introduction: The interstellar medium (ISM) remains a unique laboratory. Most of the chemical species that exist in it are either too difficult to be found or do not exist at all in the terrestrial laboratory. These molecules thus serve as guides for new chemistry in the terrestrial laboratory. To the astronomers and astrophysicists, these molecules are perfect probes of astrophysical phenomena while to the astrochemists, they provide information to better understand the chemistry and chemical composition of the ISM. Using these molecules to shed more light on the chemical origin of life and how the small chemical species that were present on the early may have given birth to the complex systems and structures that we see today are a major concern to the astrochemists. The importance of these molecules coupled with the curiosity of understanding the solar system and in general the world around have resulted in the unique detection and characterization of over 200 of these molecules largely via their rotational transition spectra^{60,142,143}. Among the known interstellar and circumstellar molecules, isotopologues of H, C, O, N and S-containing molecules have also been detected. Just as H-containing molecules constitute majority of all the known astrophysical molecules, deuterated molecules are the highest known interstellar and circumstellar isotopologues.

Heterocycles are major players in different aspects of terrestrial biology. The nitrogen containing heterocycles are fundamental building blocks for nucleic acid. Their applications in medicine, industry and other areas are well recognized¹⁴⁴⁻¹⁴⁷. Nitrogen heterocycles, amino

acids, carboxylic acids, sugar related compounds, phosphorus compounds, sulphur compounds, amine and amides, aliphatic and aromatic hydrocarbon, and macromolecular materials like polycyclic aromatic hydrocarbons (PAHs) are among the various classes of molecules that have been detected in carbonaceous meteorites¹⁴⁶. The detection of these molecules from carbonaceous meteorites demonstrates their possible formation and survival outside the Earth^{144,146,148,149}. The possible origin of the molecules and/or their precursors has been linked to the interstellar or circumstellar medium. Branched chain molecules are very common among the materials detected in carbonaceous materials, the recent detection of a branched chain molecule in ISM (iso-propyl cyanide) further stresses the link between the interstellar medium and the molecular composition of meteorites. All of these have prompted the astronomical searches for heterocycles.

Seven heterocycles; imidazole, pyridine, pyrimidine, pyrrole, quinoline, isoquinoline and furan that have been searched for from different astronomical sources with upper limits in the range of $4*10^{12}$ to $2.8*10^{21}\text{cm}^{-2}$ determined for their column densities in all the cases without any successful detection¹⁵²⁻¹⁵⁹. Interstellar formation processes are partially thermodynamically controlled. From the energy, stability and abundance (ESA) relationship existing among interstellar and circumstellar molecules, it has been shown that there is a direct link between the stability of a molecule and its interstellar abundance which influences its astronomical observation. For related molecules like isomers which are very common among the known interstellar and circumstellar molecules, it is observed that the higher the stability of an isomer, the higher its interstellar abundance which enhances its astronomical detection as compared to others with low stability. Concerned by the unsuccessful detection of all the heterocycles that have been astronomically searched, these heterocycles alongside their various isomers were subjected to stability check in line with the ESA relationship. Interestingly, it turns out these heterocycles are the best candidates for astronomical searches as they are found to be the most stable isomers in their respective isomeric groups as discussed in chapter 3 of this Thesis.

Processes that occur on the surface of the interstellar dust grains are the dominant processes for the formation of interstellar molecules over the gas phase processes. Due to its chemical composition, the surface of the interstellar dust grains serves as a platform for hydrogen bonding among the molecules that are formed on it. This interstellar hydrogen bonding leads to a reduction in the interstellar abundance of the molecule involved as a greater part of the molecules is attached to the surface of the interstellar dust grains. For instance, acetic acid is more stable than its isomer; methyl formate but in all astronomical sources, methyl formate is found to be highly abundant than acetic acid and the reason for this is trace to interstellar hydrogen in which acetic acid is strongly bonded to the surface of the interstellar dust grains thereby reducing its abundance as compared to methyl formate. This explains the exception in the ESA relationship where the most stable isomer is not the most abundant.

Optimizing the searches for interstellar heterocycles is the aim of the present study. In doing this, a two step approach using ab initio quantum chemical calculations is considered. Firstly, these heterocycles and their isomers are subjected to the effect of interstellar hydrogen

bonding which could affect the interstellar abundance of these heterocycles thus making their astronomical detection difficult. Secondary, a recent study has shown that subjecting large molecules of astrophysical interest like PAHs (which are similar to the heterocycles considered here) to interstellar medium conditions leads to the transformation of these molecules through hydrogenation, oxygenation and hydroxylation to complex organics. As a consequence, these fully hydrogenated molecules lose their spectroscopic signature which in turn contributes to their lack of astronomical detection¹⁶⁰. This thus suggests the searches for the isotopologues of these molecules as a means of mitigating this effect. Based on this, the deuterated isotopologues of these heterocycles are examined. One of the main distinctions between a molecule and its deuterated analogue is the difference in the zero point energy (ZPE). From this difference, the Boltzmann factor which gives insight about the possible formation conditions for the deuterated molecule can be computed. This has been computed for all the heterocycles considered here in order to investigate the nature of deuterium fractionation and the possible detectability of these D-analogues

6.11 Methodology: Mimicking the interstellar laboratory conditions in our terrestrial laboratory could be an extremely difficult task especially when the system of interest involves short-lived species, intermediates and transitions states. However, such conditions and systems can be simulated using computational and theoretical tools. For the present study, Gaussian 09 suit of program is used for all computational simulations¹². In order to obtain high accurate results that could be in good agreement with experimental data (if available) the Møller–Plesset second order perturbation theory; MP2(full) with the 6-311++G** basis set was used in examining the interstellar hydrogen bonding while the G4 compound model was used in obtaining the ZPE for the heterocycles and their corresponding D-analogues. The choice of these methods came from previous experience^{13,19-21}. The optimized structures used for all the results reported here were found to be stable with no imaginary frequency as confirmed by the harmonic vibrational frequency calculations. The binding energy (B. E) of the complex formed between the heterocycles and the water molecule on the surface of the interstellar dust drains is determined using the super molecular approach which is defined as:

$$B.E \text{ (complex)} = E \text{ (complex)} - [E(\text{water molecule}) + E(\text{heterocycle molecule})].$$

The difference in the ZPE between a molecule and its deuterated analogue expressed in terms of temperature (in Kelvin) represents the temperature at which the Boltzmann factor (E/kT) for the system is unity. Considering the temperature range of ≈ 10 to 100k typical of the dense molecular clouds where these heterocycles are believed to be formed, two temperature regimes of 10 and 100k are used in computing the Boltzmann factor for the systems considered here. The dipole moment of a molecule is among the factors considered for an astronomical of a molecule. This is because intensities of rotational transitions of a molecule scale with the square of the dipole moment, thus, the higher the dipole moment, the higher the intensity of the lines. As a result of this, dipole moment of these heterocycles and their corresponding isomers at the MP(full)/6-311++G** level are reported in all the cases considered here.

6.12 Results and Discussion: Since the order of stability of these heterocycles and their isomers is known from previous study, for the effect of interstellar hydrogen bonding, the heterocycles and their three next most stable isomers are considered except in the C₄H₅N and C₉H₇N isomeric groups where the 5 and 6 most stable isomers are examined respectively. The effect of the substitution of deuterium at different positions on the ZPE of the deuterium molecules is also observed. The results for both approaches considered here for optimizing the searches for interstellar heterocycles are presented and discussed for each heterocycle.

6.12.1: Imidazole and Its Isomers: The three next most stable isomers of the C₃H₄N₂ group after imidazole are 3-aminoacrylonitrile, pyrazole and 2-aminoacrylonitrile respectively. The binding energy (B.E) of these isomers with water on the surface of the interstellar dust grains, their enthalpy of formation from previous study and their dipole moment are shown in Table 6.31. From the table, pyrazole is found to be more strongly bonded to the surface of the interstellar dust grains followed by the molecule of interest; imidazole while both 3-aminoacrylonitrile and 2-aminoacrylonitrile are the least bonded isomers. This implies that a reasonable portion of imidazole could be attached to the surface of the interstellar dust grains thereby reducing its overall interstellar abundance and hence, hampering its astronomical observation. Isomers are believed to have common precursors for their formation route, thus a successful detection of an isomer is an indication of the interstellar present of the other isomers not yet detected. This concept of isomerism has been an important search light for interstellar and circumstellar molecules with about 40% of all the known interstellar and circumstellar molecules having known isomeric counterparts. Thus, should the aminoacrylonitriles with high dipole moments, which are less bonded to the surface of the interstellar dust grains, be searched and possible observed from the astronomical sources, this obviously will confirm the present and detectability of imidazole in space.

Table 6.31: C₃H₄N₂ Isomers, Binding Energy with water, ΔH°_f and Dipole moment

Molecule	B. E with H ₂ O (kcal/mol)	* ΔH°_f (kcal/mol)	Dipole moment (Debye)
Imidazole	-5.7	26.6	4.0
3-aminoacrylonitrile	-4.6	35.8	5.5
Pyrazole	-6.2	37.9	2.5
2-aminoacrylonitrile	-3.7	43.5	4.4

*Chapter 3.

Figure 6.11 pictures the optimized structures of the hydrogen bonded C₃H₄N₂ isomer complexes with water considered here. Water molecule has the ability of acting as both hydrogen bond donor and acceptor. Both cases are observed here. It acts as hydrogen bond acceptor in the case of pyrazole-water complex while in the other three complexes, it acts as hydrogen bond donor where the hydrogen atom in water is forming bond with the nitrogen atom of the respective C₃H₄N₂ isomer. There is an elongation of one of the O-H bonds from the original 0.959 Å in the cases where the water molecule acts as hydrogen bond donor while both O-H bonds of water elongate in the case of pyrazole-water complex where it acts as hydrogen bond acceptor. This elongation of the O-H bond(s) of water shows evidence of

hydrogen bond formation between the $C_3H_4N_2$ isomers and the water on the surface of the interstellar dust grains.

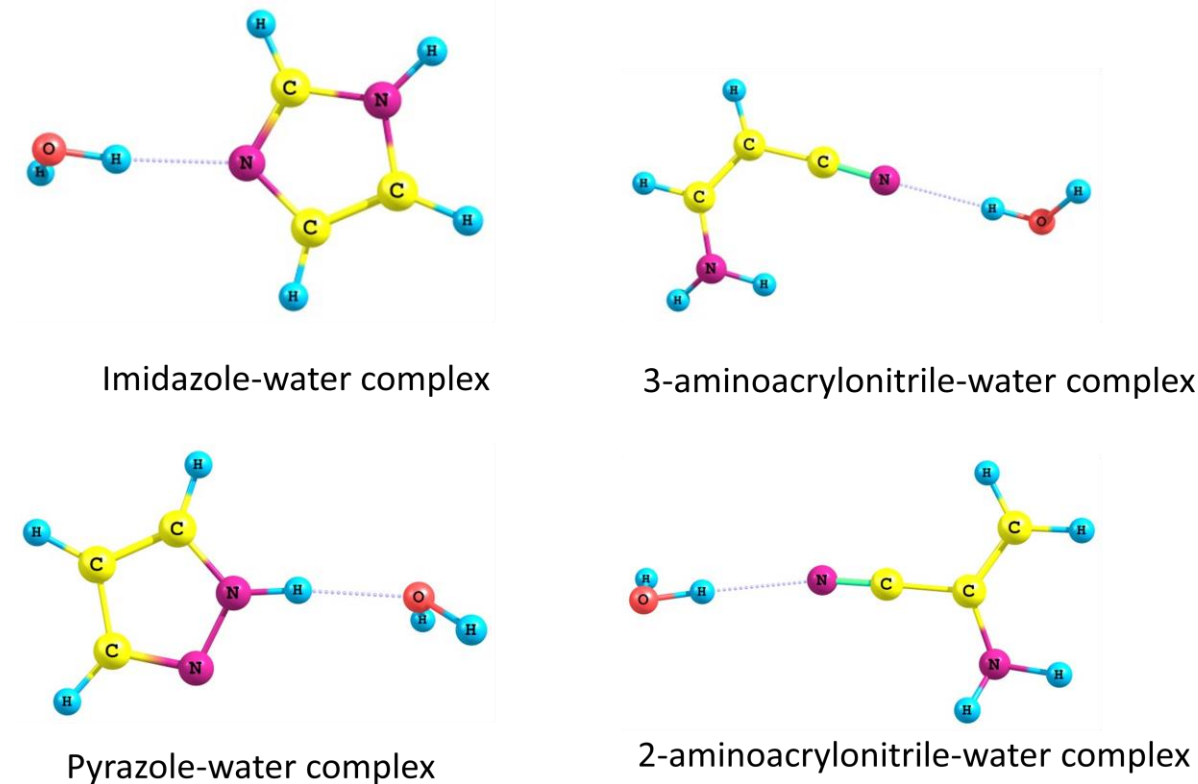


Figure 6.11: Optimized structures of the hydrogen bonded $C_3H_4N_2$ isomer complexes with water

Table 6.32 shows the ZPE of imidazole and its deuterated analogues, the Boltzmann factor (E/kT) at the two temperature regimes and the temperature (${}^*\Delta T$) where the Boltzmann factor is unity. The number(s) in bracket in the first column of Table 2 represents the position of substitution of the deuterium atom on the imidazole molecule as shown in Figure 6.12. As would be expected, the ZPE of imidazole is much higher than that of its deuterated analogues. The four hydrogen atoms at positions 6, 7, 8 and 9 are all non-identical. Deuterium substitution at these positions also shows non-identical effects resulting in the different in the ZPE. With a Boltzmann factor of one, no major deuterium fractionation is expected to occur, thus the D/H ratio will reflect the cosmic or elemental D/H ratio of $\approx 10^{-5}$. From Table 6.32, it is obvious that having a Boltzmann factor of unity is not achievable within the conditions of the molecular clouds where these molecules are believed to form except they are formed in the hot cores with temperature range of 100 to 1000k. Under the conditions of the molecular clouds, the large value of the Boltzmann factor (E/kT at $T=10$ and 100k) indicates major deuterium fractionation which will result in high abundance of the deuterated analogue of imidazole since the D/H ratio will much higher than the cosmic D/H ratio. This of course signals the possible detectability of this D-analogue.

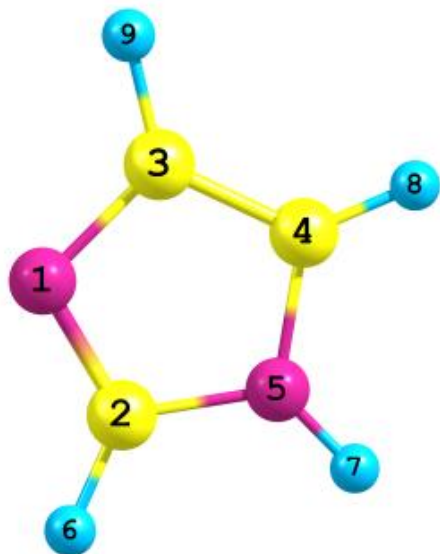


Figure 6.12: Optimized structure of imidazole

Table 6.32: ZPE and Boltzmann factor (E/kT) for Imidazole and its D-analogues

Molecule	ZPE (kcal/mol)	* ΔT (K)	E/kT (at T=10k)	E/kT(at T=100k)
Imidazole	44.6	-	-	-
C ₃ H ₃ D(6)N ₂	42.6	1026.6	102.7	10.3
C ₃ H ₃ D(7)N ₂	42.5	1075.2	107.5	10.7
C ₃ H ₃ D(8)N ₂	42.6	1004.8	100.5	10.0
C ₃ H ₃ D(9)N ₂	42.4	1139.0	113.9	11.4
C ₃ H ₂ D ₂ (6,7)N ₂	40.5	2102.1	210.2	21.0
C ₃ HD ₃ (6,7,8)N ₂	38.5	3108.2	310.8	31.1
C ₃ D ₄ N ₂	36.4	4136.1	413.6	41.4

*The difference in the ZPE of a molecule and its D-analogue expressed in terms of temperature.

6.12.2: Pyridine and Its Isomers: As shown in Table 6.33, pyridine is by far the most stable isomer of the C₅H₅N isomeric group. The other stable isomers after pyridine are also listed in the table. The astronomical searches for pyridine by different groups gave only the upper limits of its column density in the range of 7.3*10¹² to 2.5*10¹⁵ cm⁻² without any successful detection^{154,155,156}. As much as we know, there is no report on the astronomical search for other members of this isomeric group. Figure 6.13 shows the optimized structures of the hydrogen bonded these isomers complexes with water molecule on the surface of the interstellar dust grains. After azafulvene, the next most affected molecule by the effect of interstellar hydrogen bonding is our molecule of interest; pyridine suggesting that a portion of it is probably attached to the surface of the interstellar dust grains thereby reducing the chances of its successful astronomical detection. The low dipole moment of pyridine in comparison to its isomers is also an issue of concern. Though 2-methylene-3-butanenitrile and 1-cyano-1,3-butadiene are thermodynamically less stable than pyridine but the less effect of interstellar hydrogen bonding on them and their high dipole moment are good factors that should warrant their astronomical searches. Their successful observations will not only add to

the list of known interstellar and circumstellar molecules but will obviously increase the hope of detecting pyridine. As shown in Figure 3, in all the cases the water molecule acts as hydrogen bond donor with an elongation of one of its hydrogen bonds from the original 0.959 Å in the monomer to 0.972 Å, 0.964 Å, 0.973 Å and 0.964 Å respectively in the pyridine, 1-cyano-1,3-butadiene, azafulvene and 2-methylene-3-butanenitrile-water complexes confirming the formation of the bond.

Table 6.33: C_5H_5N isomers, Binding Energy with water, ΔH°_f and Dipole moment

Molecule	$^*\Delta H^\circ_f$ (kcal/mol)	B. E with H_2O (kcal/mol)	Dipole moment (Debye)
Pyridine	28.7	-4.7	2.4
1-cyano-1,3-butadiene	55.5	-4.2	5.3
Azafulvene	56.1	-5.6	2.2
2-methylene-3-butanenitrile	58.2	-3.8	4.2

*Chapter 3

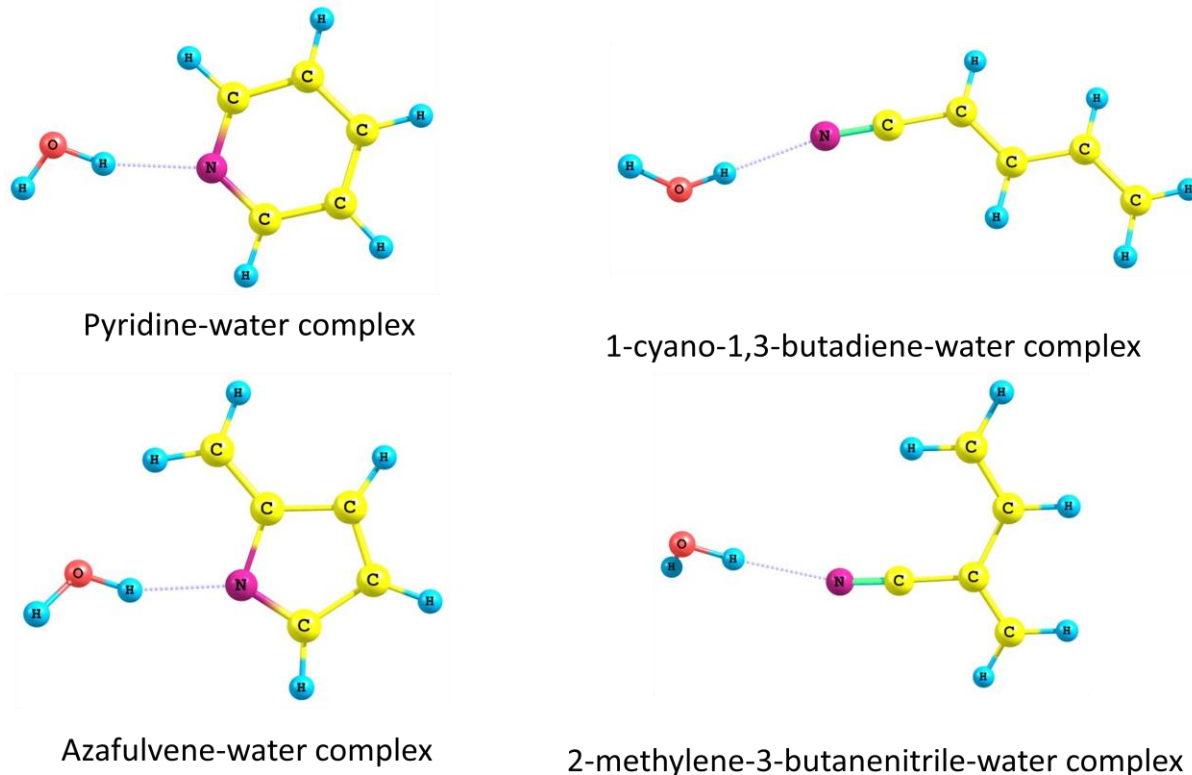


Figure 6.13: Optimized structures of the hydrogen bonded C_5H_5N isomer complexes with water

Table 6.34 shows the ZPE of pyridine and its D-analogues, the Boltzmann factor (E/kT) at 10 and 100k; and the temperature where the Boltzmann factor is unity ($^*\Delta T$). The number(s) in bracket is (are) s defined before. Unlike in the previous case where a pronounced difference in the ZPE was observed for singly substituted deuterium at different positions, such trend is not observed in the case of D-pyridine isotopomers. Deuterium fractionation is a temperature dependent process (EtimArunan 2015). That a Boltzmann factor of unity is far from being

achieved under conditions of the dense molecular clouds where these molecules are expected to be formed is a good omen. Since major deuterium fractionation occurs under the conditions where these molecules are formed, it thus implies that a high D/H ratio above the cosmic D/H ratio will be the result of such fractionation. Such high D/H ratio should of course prompt the astronomical search for D-pyridine.

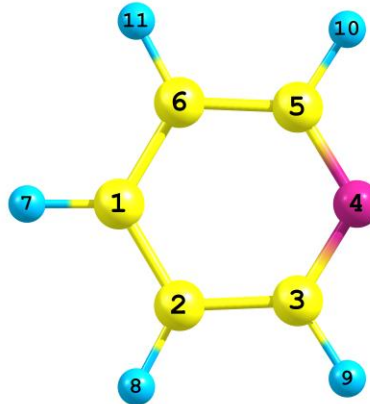


Figure 6.14: Optimized structure of Pyridine

Table 6.44: ZPE and Boltzmann factor (E/kT) for Pyridine and its D-analogues

Molecule	ZPE (kcal/mol)	* ΔT (K)	E/kT (at T=10k)	E/kT(at T=100k)
Pyridine	55.6	-	-	-
C ₅ H ₄ D(7)N	53.6	1031.3	103.1	10.3
C ₅ H ₄ D(8)N	53.6	1031.3	103.1	10.3
C ₅ H ₄ D(9)N	53.6	1045.5	104.5	10.4
C ₅ H ₃ D ₂ (8,9)N	51.5	2075.0	207.5	20.7
C ₅ H ₂ D ₃ (7,8,9)N	49.5	3107.0	310.7	31.1
C ₅ HD ₄ (7,8,9,10)N	47.4	4153.1	415.3	41.5
C ₅ D ₅ N	45.3	5183.5	518.3	51.8

*The difference in the ZPE of a molecule and its D-analogue expressed in terms of temperature.

6.12.3: Pyrimidine and Its Isomers: Table 6.35 shows the binding energy (B. E) of the C₄H₄N₂ isomers with water and their dipole moment. The zero-point corrected standard enthalpy of formation of these isomers from previous work is also included in the table. Pyrimidine is the most stable isomer of the C₄H₄N₂ isomeric group. This has led to its astronomical searches with the column density of 7*10¹⁴, 2.4*10¹⁴, and 3.4*10¹⁴ cm⁻² determined for its upper limits in SgrB2(N), Orion KL and W51 e1/e2 respectively¹⁵⁷ without any successful detection from any of the astronomical sources. With respect to interstellar hydrogen bonding, pyridazine and pyrimidine are the most bonded isomers of the C₄H₄N₂ isomeric group to the surface of the interstellar dust grains. Thus suggests a possible reduction in the overall abundance of pyrimidine since a portion of it is strongly attached to the surface of the interstellar dust grains. Among these isomers, 1,1-dicyanoethane is the least affected by interstellar hydrogen bonding. This factor coupled with its high dipole moment and the high number of known cyanide molecules from interstellar space makes it a suitable

candidate for astronomical search with a high expectation for possible observation. Figure 6.15 pictures the optimized structures of the hydrogen bonded complexes of these isomers with water. In the pyridazine-water complex where the two O-H bonds of the water monomer are taking part in the complex formation, there is an elongation of both bond lengths from the original 0.959 Å to 0.962 Å for each of the O-H bonds of the water monomer while in the cases of pyrimidine, pyrazine and 1,1-dicyanoethane-complexes, one of the O-H bonds elongates to 0.969 Å, 0.969 Å and 0.963 Å in that order.

Table 6.35: $C_4H_4N_2$ Isomers, Binding Energy with water, ΔH°_f and Dipole moment

Molecule	B. E with H_2O (kcal/mol)	$^*\Delta H^\circ_f$ (kcal/mol)	Dipole moment (Debye)
Pyrimidine	-4.5	37.1	2.5
Pyrazine	-3.9	41.0	0.0
1,1-dicyanoethane	-3.3	54.7	4.7
Pyridazine	-4.8	59.0	4.6

*Chapter 3.

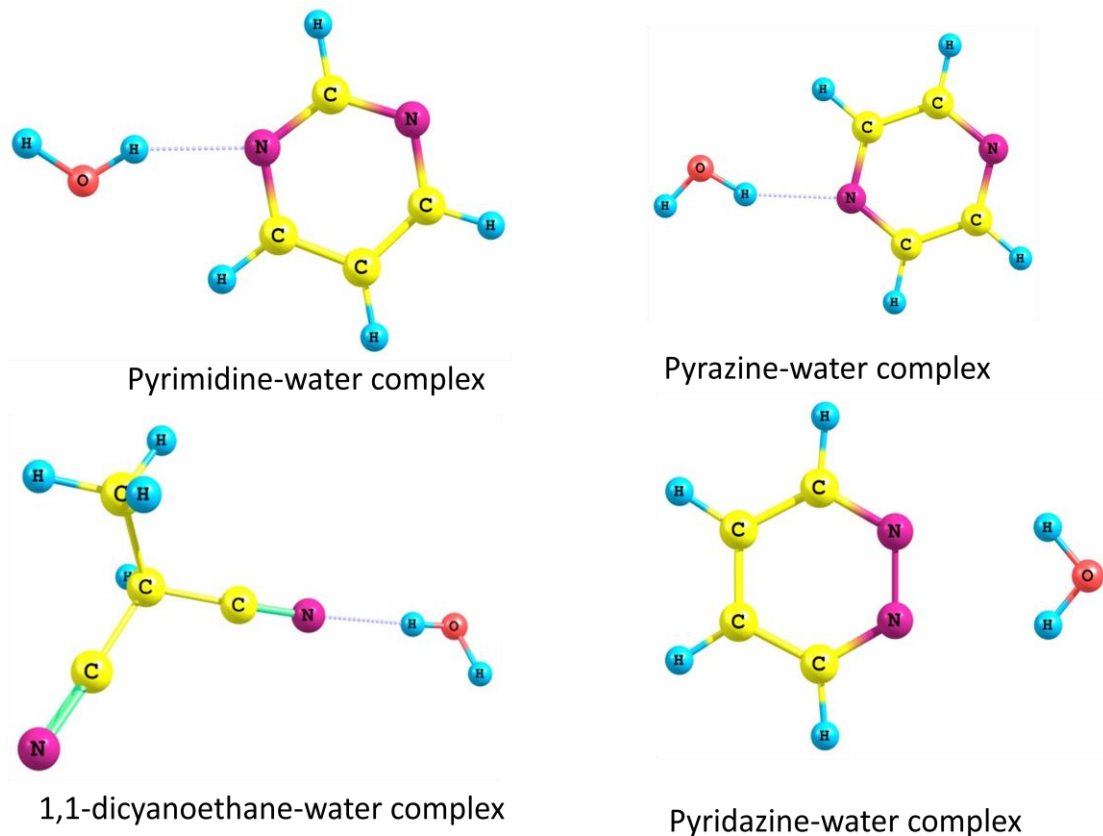


Figure 6.15: Optimized structures of the hydrogen bonded $C_4H_4N_2$ isomer complexes with water

Figure 6.16 is the structure of pyrimidine showing the numbering of the atoms as guide for the deuterium substitution at different positions as presented in Table 6.36. The H-atoms at positions 8 and 10 are identical. For the non-identical H-atoms, deuterium substitution at

these positions leads in different values of ZPE which results in the different values of the Boltzmann factor for the singly deuterated pyrimidine. This implies different D/H ratio for these species in the interstellar space. From Table 6, major deuterium fractionation is expected to be observed for these D-analogues of pyrimidine since the prevailing conditions in the molecular clouds make it impossible to achieve a Boltzmann factor of unity. The high Boltzmann factor at the low temperature of the molecular clouds will thus favor high abundance of these deuterated molecules, thus their successful observation can be envisaged.

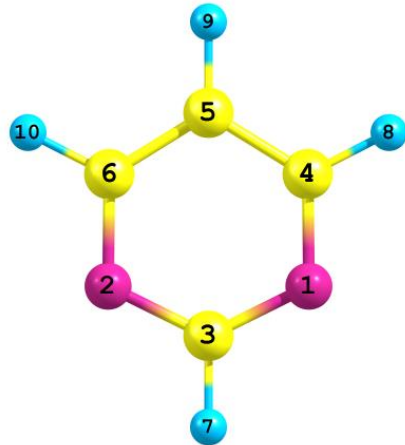


Figure 6.16. Optimized structure of pyrimidine

Table 6.36: ZPE and Boltzmann factor (E/kT) for Pyrimidine and its D-analogues

Molecule	ZPE (kcal/mol)	* ΔT (K)	E/kT (at T=10k)	E/kT(at T=100k)
Pyrimidine	48.3	-	-	-
$\text{C}_4\text{H}_3\text{D}(7)\text{N}_2$	46.2	1059.1	105.9	10.6
$\text{C}_4\text{H}_3\text{D}(8)\text{N}_2$	46.2	1043.0	104.3	10.4
$\text{C}_4\text{H}_3\text{D}(9)\text{N}_2$	46.2	1026.0	102.6	10.3
$\text{C}_4\text{H}_2\text{D}_2(7,8)\text{N}_2$	44.1	2102.5	210.2	21.0
$\text{C}_4\text{H}_2\text{D}_3(7,8,9)\text{N}_2$	42.1	3128.7	312.9	31.3
$\text{C}_4\text{D}_4\text{N}_2$	40.08	4172.4	417.2	41.7

*The difference in the ZPE of a molecule and its D-analogue expressed in terms of temperature.

6.12.4: Pyrrole and Its Isomers: Unlike in the previous cases where only the most stable isomer is the there only molecule that has been astronomically searched for, in the $\text{C}_4\text{H}_5\text{N}$ isomeric group, both the most stable isomer (pyrrole) and a less stable isomer;ally isocyanide have been astronomically searched from different molecular clouds with only upper limits determined for both without any successful detection. The dipole moment, binding energy (B. E) of the complex formed between these isomers and water are captured in Table 6.37 including the zero-point corrected standard enthalpy of formation of these isomers from previous study. The astronomical search of more than one isomer from this group provides an excellent opportunity to practically test the effect of interstellar hydrogen bonding discussed here. Pyrrole (24.094kcal/mol) is extremely more stable as compared to allyl isocyanide (61.986 kcal/mol). However, with respect to the effect of interstellar hydrogen bonding, pyrrole is the most bonded isomer of the $\text{C}_4\text{H}_5\text{N}$ isomeric group to the surface of the

interstellar dust grains while ally isocyanide is the second least affected isomer as regards this effect. The column density determined for pyrrole ranges from 3 to 10×10^{13} cm $^{-2}$ while for ally isocyanide, 1.1 to 3.3×10^{14} cm $^{-2}$ is reported as its range of column density^{143,156}. The high column density reported for ally isocyanide clearly shows that a large portion of pyrrole is strongly attached to the surface of the interstellar dust grains thus reducing its overall abundance. Considering 2-cyanopropene which is less bonded to the surface of the interstellar dust grains than every other isomer; its thermodynamic stability is almost double that of ally isocyanide while its dipole moment is higher than those of pyrrole and ally isocyanide. These properties of 2-cyanopropene in addition to the reported column density of pyrrole and ally isocyanide put it in a right place for a successful astronomical observation. Figure 7 depicts the optimized structures of the hydrogen bonded C₄H₅Nisomer complexes with water with the water monomer acting as hydrogen bond donor in all the complexes here with an elongation of the O-H bond.

Table 6.37: C₄H₅NIsomers, Binding Energy with water, $\Delta H^{\circ f}$ and Dipole moment

Molecule	B. E with H ₂ O (kcal/mol)	* $\Delta H^{\circ f}$ (kcal/mol)	Dipole moment (Debye)
Pyrrole	-4.6	24.1	1.9
2-butenenitrile	-4.2	32.8	5.2
2-cyanopropene	-3.1	34.0	4.4
Ally cyanide	-4.0	39.7	4.3
Ally isocyanide	-3.2	62.0	3.6

*Chapter 3.

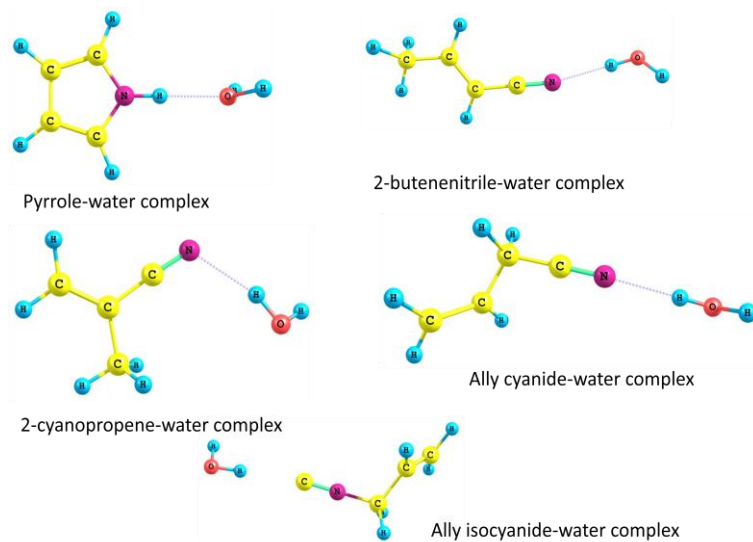


Figure 6.17: Optimized structures of the hydrogen bonded C₄H₅Nisomer complexes with water

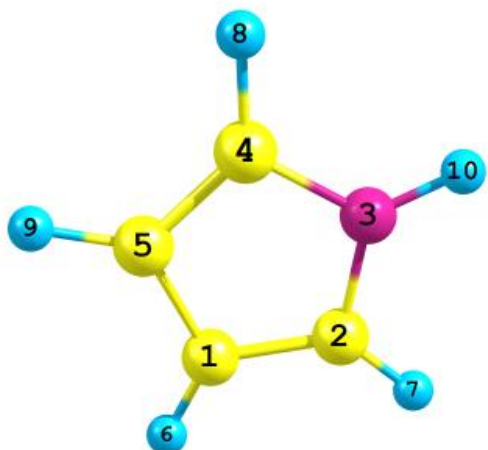


Figure 6.18: Optimized structure of pyrrole

The non-identical H-atoms in pyrrole (Figure 6.18) show similar effect on deuteration. Deuterium substitution at positions 7 and 10 results in exactly the same ZPE as it is also noted for substitution at positions 6 and 9 (Table 8). The large Boltzmann factor makes it clear that deuteratedpyrrole occurs under the same conditions as its main isotopologue (low temperature interstellar cloud conditions). Under these conditions, pronounced deuterium fractionation from its reservoir will lead to an enhanced D/H ratio far above the cosmic D/H ratio which increases the probability of its astronomical observation.

Table 6.38: ZPE and Boltzmann factor (E/kT) for Pyrrole and its D-analogues

Molecule	ZPE (kcal/mol)	* ΔT (K)	E/kT (at T=10k)	E/kT(at T=100k)
Pyrrole	51.7	-	-	-
C ₄ H ₄ D(10)N	49.6	1085.0	108.5	10.8
C ₄ H ₄ D(7)N	49.6	1085.0	108.5	10.8
C ₄ H ₄ D(8)N	49.7	1012.4	101.2	10.1
C ₄ H ₄ D(6)N	49.7	1012.7	101.3	10.1
C ₄ H ₄ D(9)N	49.7	1012.7	101.3	10.1
C ₄ H ₃ D ₂ (6,7)N	47.7	2021.6	202.2	20.2
C ₄ H ₂ D ₃ (6,7,8)N	45.7	3031.2	303.1	30.3
C ₄ HD ₄ (6,7,8,9)N	43.7	4041.0	404.1	40.4
C ₄ D ₅ N	41.5	5124.2	512.4	51.2

*The difference in the ZPE of a molecule and its D-analogue expressed in terms of temperature.

6.12.5: Quinoline, Isoquinoline and their Isomers: Table 6.39 shows the six most stable isomer of the C₉H₇N isomeric group. Unsuccessful astronomical searched have been reported for the two most stable isomers of the group; quinoline and isoquinoline¹⁵⁶. The strong attachments of heterocycles to the surface of the interstellar dust grains as compared to their respective isomers observed in the previous cases is not left out here. As shown in Table 9, quinoline is the most strongly bonded isomer of the group to the surface of the interstellar dust grains while its closest counterpart; isoquinoline ranks third. This effect affects the interstellar abundance of these heterocycles thus influencing their successful detection.

Figure 9 displays the optimized structures of the hydrogen bonded C_9H_7N isomer complexes with water. The elongation of the O-H bond from its original length signifies bond formation.

Table 6.39: C_9H_7N Isomers, Binding Energy with water, ΔH°_f and Dipole moment

Molecule	B. E with H_2O (kcal/mol)	$*\Delta H^\circ_f$ (kcal/mol)	Dipole moment (Debye)
Quinoline	-4.2	44.1	2.3
Isoquinoline	-3.9	46.0	2.7
Cyanostyrene	-3.3	66.5	4.7
3-methylene-3H-indole	-4.0	66.6	2.9
4-vinylbenzonitrile	-3.6	66.9	5.4
3-vinylbenzonitrile	-3.4	67.4	5.1

*Chapter 3.

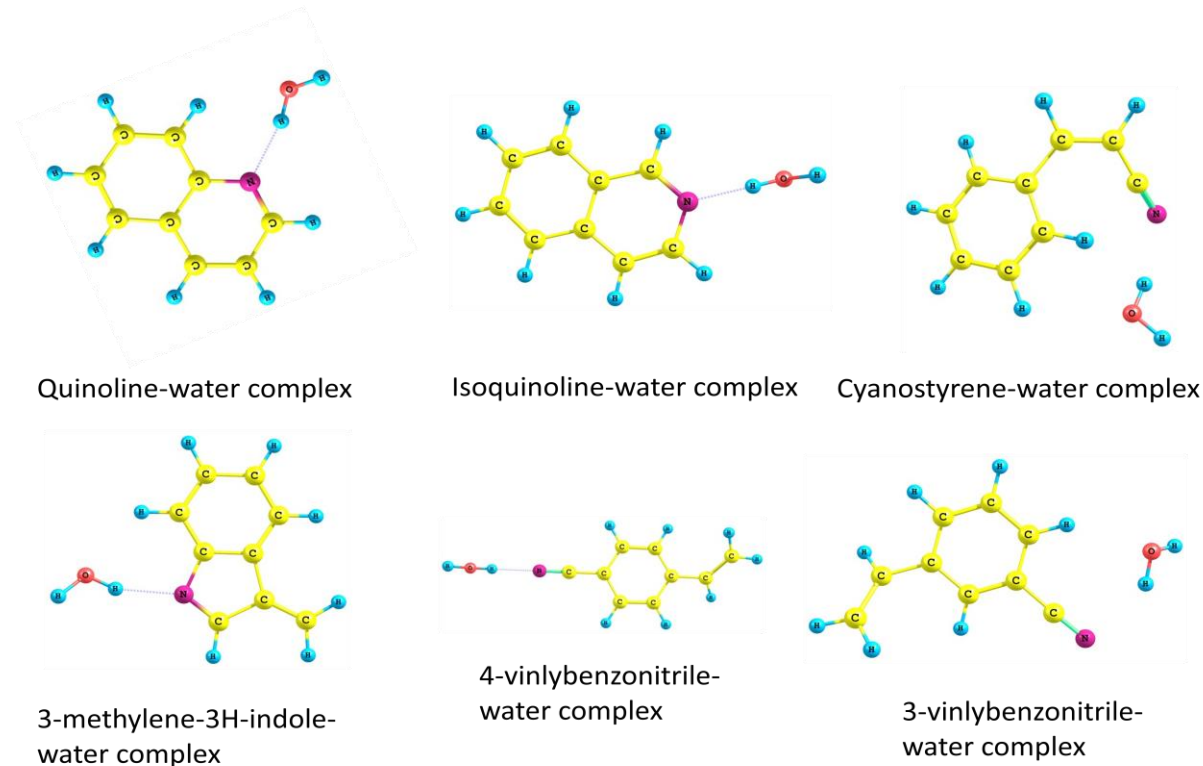


Figure 6.19: Optimized structures of the hydrogen bonded C_9H_7N isomer complexes with water

Quinoline and isoquinoline belong to the nitrogen containing PAHs. The non-detection of fully hydrogenated PAHs and related compounds from the interstellar ice grains is partly linked to the loose of spectroscopic signature of these molecules due their transformations to more complex organics¹⁶⁰. This places an important demand on the astronomical searches for the deuterated analogue of these molecules. The numbering in Figures 6.20 and 6.21 is as defined before. The Boltzmann factor shown in Tables 6.40 and 6.41 support major deuterium fractionation for the formation of the D-analogues of quinoline and isoquinoline. This implies the possible present of these deuterated molecules in detectable amount.

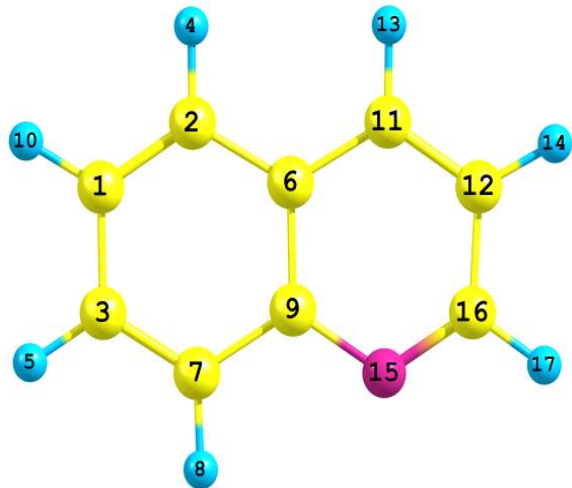


Figure 6.20: Optimized structure of quinoline

Table: 6.40: ZPE and Boltzmann factor (E/kT) for Quinoline and its D-analogues

Molecule	ZPE(kcal/mol)	* ΔT (K)	E/kT (at T=10k)	E/kT(at T=100k)
Quinoline	84.9	-	-	-
C ₉ H ₆ D(17)N	82.9	1045.2	104.5	10.4
C ₉ H ₆ D(14)N	80.1	2429.6	243.0	24.3
C ₉ H ₆ D(13)N	82.9	1028.5	102.8	10.3
C ₉ H ₆ D(8)N	82.9	1030.1	103.0	10.3
C ₉ H ₅ D ₂ (14,17)N	80.8	2076.3	207.6	20.8
C ₉ H ₅ D ₂ (5,10)N	80.8	2066.1	206.6	20.7
C ₉ H ₄ D ₃ (13,14,17)N	78.8	3107.6	310.8	31.1
C ₉ D ₇ N	70.6	7238.6	723.9	72.4

*The difference in the ZPE of a molecule and its D-analogue expressed in terms of temperature.

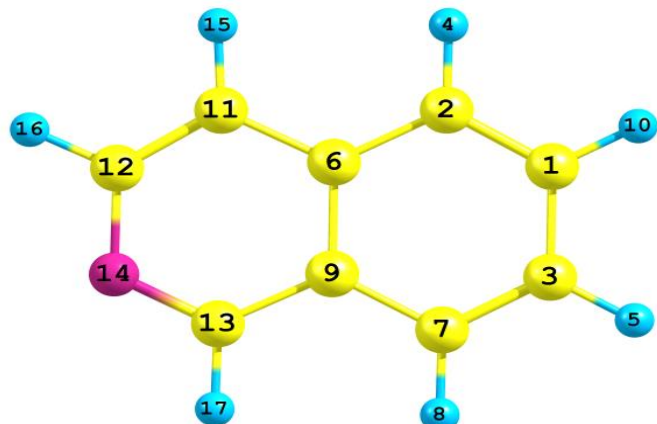


Figure 6.21: Optimized structure of isoquinoline

Table 6.41: ZPE and Boltzmann factor (E/kT) for Isoquinoline and its D-analogues

Molecule	ZPE(kcal/mol)	*ΔT(K)	E/kT (at T=10k)	E/kT(at T=100k)
Isoquinoline	85.0	-	-	-
C ₉ H ₆ D(17)N	82.9	1040.2	104.0	10.4
C ₉ H ₆ D(16)N	82.9	1045.9	104.6	10.5
C ₉ H ₆ D(15)N	82.9	1026.0	102.6	10.3
C ₉ H ₆ D(4)N	80.5	2244.2	224.4	22.4
C ₉ H ₅ D ₂ (16,17)N	80.8	2088.9	208.9	20.9
C ₉ H ₄ D ₃ (15,16,17)N	78.8	3117.4	311.7	31.2
C ₉ H ₄ D ₃ (4,8,10)N	78.8	3094.6	3096.5	30.9
C ₉ D ₇ N	70.6	7249.7	725.0	72.5

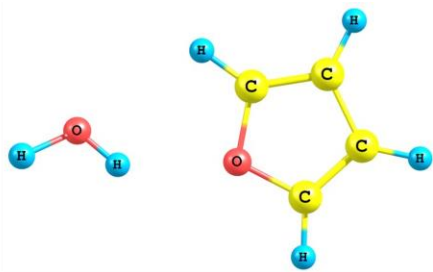
*The difference in the ZPE of a molecule and its D-analogue expressed in terms of temperature.

6.12.6: Furan and Its Isomers: The C₄H₄O isomeric group is the only O-containing group considered in this study. Furan, the most stable isomer of this series is a cyclic molecule with 9 atoms. Though there is no cyclic molecule with 9 atoms among the known interstellar and circumstellar molecules, 10 linear molecules with 9 atoms have so far been detected from different astronomical sources. The detection of furan will be an interesting development, firstly as a heterocyclic molecule and secondly as an addition to the very few known cyclic interstellar and circumstellar molecules. Unlike in the previous cases where the heterocyclic molecule always falls among the top most bonded isomer to the surface of the interstellar dust grains, the trend is reversed here. Furan is the second least affected isomer with respect to interstellar hydrogen bonding as shown by the data in Table 6.42. This suggests that a greater portion of furan is not attached to the surface of the interstellar dust grains, thus its overall abundance is not largely affected. The report on the astronomical searches for furan came in the last 3 to 4 decades^{153,158} with its upper limits of column density determined to be 7*10¹³ cm⁻² and 2*10¹⁶ cm⁻² in Orion A and Sgb B2 respectively. Considering the advances in astronomical instruments and the complex molecules that have been astronomically detected within this period, it suffices to say that a new dedicated search for interstellar furan will probably be successful.

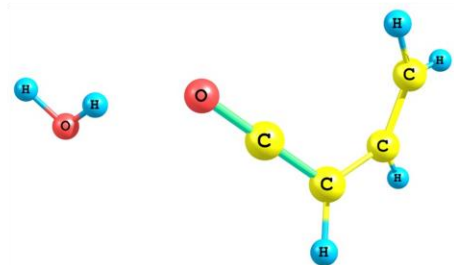
Table 6.42: C₄H₄OIsomers, Binding Energy with water,ΔH^o_f and Dipole moment

Molecule	B.E with H ₂ O (kcal/mol)	*ΔH ^o _f (kcal/mol)	Dipole moment (Debye)
Furan	-2.5	-9.3	0.8
Vinylketene	-1.9	3.6	1.8
2-cyclobutene-1-one	-4.8	9.2	4.2
2,3-butadienal	-4.5	13.1	4.4

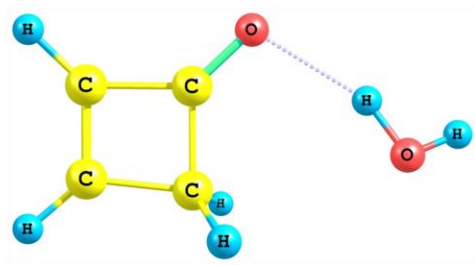
*Chapter 3.



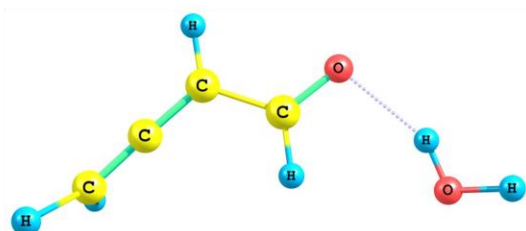
Furan-water complex



Vinylketene-water complex



2-cyclobutene-1-one-water complex



2,3-butadienal-water complex

Figure 6.22: Optimized structures of the hydrogen bonded $\text{C}_4\text{H}_4\text{O}$ isomer complexes with water

Figure 6.22 nicely pictures the optimized structures of the hydrogen bonded $\text{C}_4\text{H}_4\text{O}$ isomer complexes with water monomer on the surface of the interstellar dust grains. In all the cases, the water molecule acts as hydrogen bond donor with an elongation for the O-H bond from its original 0.959 \AA to 0.962 \AA , 0.961 \AA , 0.966 \AA and 0.966 \AA in furan, vinylketene, 2-cyclobutene-1-one and 2,3-butadienal respectively indicating the bond formation. The numbering in Figure 13 stands as earlier defined. As presented in Table 6.43, the parameters for the deuterated analogue of furan follow the same trend as the cases discussed above with major deuterium fractionation being the dominant process for the formation of D-furan.

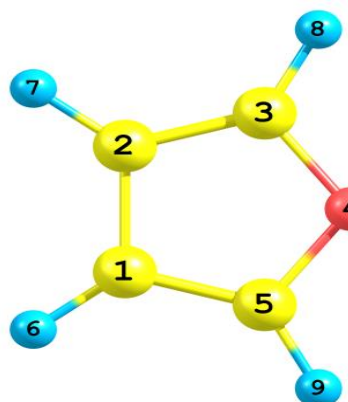


Figure 6.23: Optimized structure of furan

Table 6.43: ZPE and Boltzmann factor (E/kT) for Furan and its D-analogues

Molecule	ZPE(kcal/mol)	* ΔT (K)	E/kT (at T=10k)	E/kT(at T=100k)
Furan	43.8	-	-	-
C ₄ H ₃ D(8)O	41.8	1020.3	102.0	10.2
C ₄ H ₃ D(9)O	41.8	1020.3	102.0	10.2
C ₄ H ₃ D(6)O	41.8	1007.6	100.8	10.1
C ₄ H ₃ D(7)O	41.8	1007.6	100.8	10.1
C ₄ H ₂ D ₂ (8,9)O	39.8	2041.2	204.1	20.4
C ₄ H ₂ D ₂ (6,7)O	39.8	2015.9	201.6	20.2
C ₄ HD ₃ (6,7,8)O	37.8	3037.5	303.7	30.4
C ₄ D ₄ O	35.8	4059.4	405.9	40.6

*The difference in the ZPE of a molecule and its D-analogue expressed in terms of temperature.

6.13: Summary on Optimizing the Searches for Interstellar Heterocycles: Effect of interstellar hydrogen bonding on the astronomical detection of heterocycles and the possible detectability of the deuterated analogues of these heterocycles have been examined as strategies to optimize the astronomical searches for these heterocycles. On the effect of interstellar hydrogen bonding, imidazole, pyridine, pyrimidine, pyrrole, quinoline and isoquinoline are found to be strongly bonded to the surface of the interstellar dust grains as compared to their other stable isomers. This causes a greater portion of these molecules to be attached to the surface of the interstellar dust grains thereby reducing their overall abundance thus influencing their successful astronomical observation. On the basis of this, the other isomers of these heterocycles could be observed despite their low thermodynamic stability. Successful detection of furan remains highly feasible as it is not really affected by this effect. With respect to the detectability of the deuterated analogues of these heterocycles, the Boltzmann factor determined for all the D-analogues of these molecules at the temperature range of the dense molecular cloud are far above unity which implies major deuterium fractionation as the formation process for these D-analogues. This will result in very high D/H ratio far above the cosmic D/H ratio implying a high abundance of the D-analogue which is desirable for their successful detection.

6.14 Conclusions on Interstellar Ions and Isotopologues: Known and Potential

Different studies on interstellar ions and isotopologues are presented in this chapter. From the studies on interstellar protonated species with over 100 molecular species; protonated species resulting from a high proton affinity prefers to remain protonated rather than transferring a proton and returning to its neutral form as compared to its analogue that gives rise to a lower proton affinity from the same neutral species. The studies on detectable interstellar anions account for the known interstellar anions and predict members of the C_{2n}O⁻, C_{2n}S⁻, C_{2n-1}Si⁻, HC_{2n}N⁻, C_nP⁻, and C_{2n} chains as outstanding candidates for astronomical observation including the higher members of the C_{2n}H⁻ and C_{2n-1}N⁻ groups whose lower members have been observed. From high level ab initio quantum chemical calculations; ZPE and Boltzmann factor have been used to explain the observed deuterium enhancement and the possibility of detecting more deuterated species in ISM. Though all the heterocycles that have so far been

searched for in ISM have been shown to be the right candidates for astronomical observation as discussed in the ESA relationship, they have also been shown to be strongly bonded to the surface of the interstellar dust grains thereby reducing their abundances, thus, contributing to their unsuccessful detection except for furan which is less affected by hydrogen bonding. The D-analogues of the heterocycles are shown from the computed Boltzmann factor to be formed under the dense molecular cloud conditions where major deuterium fractionation dominates implying very high D/H ratio above the cosmic D/H ratio which suggests the detectability of these deuterated species.

6.15: References

1. Defrees, D. J., McLean, A. D. *Chem. Phys. Lett.*, 1986, 136, 403
2. Cheikh, F., Pauzat, F., Ellinger, Y. *Chem. Phys.*, 2003, 290, 147-162
3. Turner, B. E. *Astrophys J*, 1971, 163,L35
4. Knauth, D. C., Andersson, B.-G., McCandliss, S. R., Moos, H. W. *Nature*, 2004, 409,636
5. d'Hendecourt, L. B., de Muizon, M. *J. Astron Astrophys*, 1989, 223,L5
6. Thaddeus, P., Guélin, M., Linke, R. A. *Astrophys J*, 1981, 246,L41
7. Herbst, E. *J Phys Conf Ser*, 2005, 4,17
8. Larsson, M., Orel, A. E. 2008. "Dissociative Recombination of Molecular Ions", Cambridge University Press, The Edinburgh Building, Cambridge CB2 8RU, UK, ISBN 978-0-521-82819-2
9. Buhl, D Snyder, L. E. 1970. *Nature*, 1970, 228,267
10. Woods, R. C., Gudeman, C. S., Dickman, R. L., et al., *Astrophys J*, 1983, 270,583
11. Ziurys, L. M., Apponi, A. J. *Astrophys J*, 1995, 455,L73
12. Frisch, M. J., Trucks, G. W., Schlegel, H. B., et al 2009. G09,RevC.01, Gaussian, Inc., Wallingford CT
13. Møller, C., Plesset, M. S. *Phys. Rev.*, 1934, 46 (7), 618
14. Pople, J. A., Krishnan, R., Schlegel, H. B., Binkley, J. S. *Int J Quantum Chem*, 1978,14, 545
15. Scuseria, G. E., Janssen, C. L., Schaefer III, H. F. *J. Chem. Phys.*, 1988,89, 7382
16. Dunning, T. H. *J. Chem. Phys.*, 1989, 90 (2), 1007
17. Martin, J. M. L, de Oliveira, G. *J Chem Phys*, 1999, 111, 1843
18. Parthiban, S Martin, J. M. L. *J Chem Phys*, 2001, 114, 6014
19. Curtiss, L. A., Raghavachari, K., Redfern, P. C., Rassolov, V., Pople, J. A. *J Chem Phys*, 1998, 109, 7764
20. Curtiss, L. A., Redfern, P. C., Raghavachari, K. *J Chem Phys*, 2007, 126, 084108
21. Curtiss, L. A., Redfern, P. C., Raghavachari, K. *J Chem Phys*, 2007, 127, 124105
22. Jolly, W. L. 1991. *Modern Inorganic Chemistry* (2nd Edn.). New York, McGraw-Hill. ISBN 0-07-112651-1
23. Smith, A. M., Stecher, T. O. *Astrophys J*, 1971, 164,L43
24. Penzias, A. A., Solomon, P. M., Wilson, R. W., Jefferts, K. B. *Astrophys J*, 1971, 168,L53
25. Geballe, T. R., Oka, T. *Nature*, 1996, 384,334
26. Weinreb, S., Barrett, A. H., Meeks, M. L., Henry, J. C. *Nature*, 1963, 200,829
27. Ossenkopf, V., Muller, H. S. P., Lis, D. C., et al. *Astron Astrophys*, 2010, 518,L111
28. Blake, G. A., Keene, J., Phillips, T. G. *Astrophys J*, 1985, 295,501
29. Federman, S. R., Cardell, J. A., van Dishoeck, E. F., Lambert, D. L., Black, J. H. *Astrophys J*, 1995, 445,325
30. Lis, D. C., Pearson, J. C., Neufeld, D. A., et al. *Astron Astrophys*, 2010, 521, L9
31. Wootten, A., Boulanger, F., Bogey, M., et al. *Astron Astrophys*, 1986, 166,L15
32. Wootten, A., Mangum, J. G., Turner, B. E., et al. *Gerin, Astrophys J*, 1991, 390,L79
33. Ziurys, L. M., Turner, B. E. *Astrophys J*, 1986, 302,L31
34. Minh, Y. C., Irvine, W. M., Ziurys, L. M. *Astrophys J*, 1988, 334,175
35. Cheung, A.C., Rank, D. M., Townes, C. H., Thornton, D. D., Welch, W. J. *Phys Rev Lett.*, 1968, 25,1701
36. Cernicharo, J., Tercero, B., Fuente, A., et al. *Astrophys J*, 2013, 771,L10
37. Ohishi, M., Ishikawa, S., Amano, T., et al. *Astrophys J*, 1996, 471,L61

38. Kawaguchi, K., Kasai, Y., Ishikawa, S. I., et al. *Astrophys J*, 1994, 420,L95

39. Cernicharo, J., Goicoechea, J. R., Caux, E. *Astrophys J*, 2000, 534,L199

40. Pety, J., Gratier, P., Guzmán, V., et al. *Astron Astrophys*, 2012, 548,A68

41. Gupta, H., Gottlieb, C. A., Lattanzi, V., Pearson, J. C., McCarthy, M. C. *Astrophys J*, 2013, 778,L1

42. Hatchell, J. 2003. *Astron Astrophys*, 403, L25

43. Mehringer, D. M., Snyder, L. E., Miao, Y., Lovas, F. *Astrophys J*, 1997, 480, 71

44. Churchwell, E Winnewisser, G. *Astron Astrophys*, 1975, 45,229

45. Hollis, J. M., Lovas, F. J., P. R. Jewell, P. R. *Astrophys J*, 2000, 540, 107

46. Hollis, J. M., Jewell, P. R., Lovas, F. J., Remijan, A. Møllendal, H. *Astrophys J*, 2004, 610, 21

47. Broten, N. W., MacLeod, J. M., L. W. Avery, L. W., et al. *Astrophys J*, 1984, 276, 25

48. Langer, W. D., Velusamy, T., Kuiper, T. B. H., et al. *Astrophys J*, 1997, 480, 63

49. Guélin, M., Cernicharo, J., Travers, M. J.. *Astron Astrophys*, 1997, 317, 1

50. Lovas, F. J., Remijan, A. J., Hollis, J. M., Jewell, P. R., Snyder, L. E. *Astrophys J*, 2006, 637, L37

51. Belloche, A., Menten, K. M., C. Comito, C., et al. *Astron Astrophys*, 2008, 482,179

52. Loomis, R. A., Zaleski, D. P., A. L. Steber, A. L., et al. *Astrophys J Lett*, 2013, 765,10

53. Cernicharo, J., Heras, A. M., Tielens, A. G. G. M., et al. *Astrophys J*, 2001, 546, 123

54. Remijan, A. J., Snyder, L. E., McGuire, B. A., et al. *Astrophys J*, 2014, 783,77

55. Defrees, D. J., Loew, G. H., McLean. *Astrophys J*, 1982, 254, 405

56. Defrees, D. J., Loew, G. H., McLean. *Astrophys J*, 1982, 257, 376

57. Adams, W. S. *Astrophys J*, 1941, 93,11

58. Douglas A. E., Herzberg, G. *Astrophys J*, 1941, 94,381

59. Swings, P., Rosenfeld, L. 1937. *Astrophys J*, 1937, 86,483

60. Etim, E. E., Arunan, E. *Planex Newsletter*, 2015, 5(2),16

61. Dalgarno, A., McCray, R. A. *Astrophys J*, 1973, 181, 9

62. Herbst, E. *Nature*, 1981, 289, 65

63. Cernicharo, J., Guélin, M., Agúndez, M., et al. *Astron Astrophys*, 2007, 467,L37

64. McCarthy, M. C., Gottlieb, C. A., Gupta, H., Thaddeus. P. *Astrophys J*, 2006, 652, L141

65. Brünken, S., Gupta, H., Gottlieb, C. A., McCarthy, M. C., Thaddeus, P. *Astrophys J*, 2007, 664, L43

66. Cernicharo, J., Guélin, M., Agúndez, M., McCarthy, M. C., Thaddeus, P. *Astrophys J*, 2008, 688, L83

67. Remijan, A. J., Hollis, J. M., Lovas, F. J., et al., . *Astrophys J*, 2007, 664, L47

68. Thaddeus, P., Gottlieb, C. A., Gupta, H., et al. *Astrophys J*, 2008, 677, 1132.

69. Agúndez, M., Cernicharo, J., Guélin, M., et al. *Astron Astrophys*, 2010, 517, L2

70. Güthe, F., Tulej, M., Pachkov, M. V., Maier, J. P. *Astrophys J*, 2001, 555, 466

71. Desfrançois, C., Abdoul-Carime, H., Schermann, J.-P. *Int. J. Mod. Phys. B*, 1996, 10, 1339

72. Lepp, S., Dalgarno, A. *Astrophys J*, 1988, 324, 553

73. Lepp, S., Dalgarno, A. *Astrophys J*, 1988, 335, 769

74. Terzieva, R., Herbst, E. *Int. J. Mass Spectrom.*, 2000, 201, 135

75. Raghavachari, K., Binkley, J. S., Seeger, R., Pople, J. A. *J. Chem. Phys.*, 1980, 72, 650

76. Frisch, M. J., Pople, J. A., Binkley, J. S. *J. Chem. Phys.*, 1984, 80, 3265

77. Anderson, J. K Ziurys, L. M. *Astrophys J*, 2014, 795,L1

78. Friberg, P., Hjalmarson, Å., Irvine, W. M., Guélin, M. *Astrophys J*, 1980, 241,L99

79. Guélin, M., Neininger, N., Cernicharo, J. *Astron Astrophys*, 1998, 355,L1

80. Thaddeus, P., Gottlieb, C. A., A. Hjalmarson, A., et al. *Astrophys J*, 1985, 294,L49

81. Guélin, M., Green, S., Thaddeus, P. *Astrophys J*, 1978,224,L27

82. Cernicharo, J., Guélin, M. *Astron Astrophys*, 1996, 309,L27

83. Cernicharo, J., Kahane, C., Gómez-González, J., Guélin, M. *Astron Astrophys*, 1986, 164, L1

84. Suzuki, H., Ohishi, M., Kaifu, N., et al. 1986. *Publ Astron Soc Jpn*, 1986, 38,911

85. Ohishi, M., Suzuki, H., Ishikawa, S., et al. *Astrophys J*, 1991, 380,L39

86. Matthews, H. E., Irvine, W. M., Friberg, P., Brown, R. D., Godfrey, P. D. *Nature*, 1984, 310,125

87. Saito, S., Kawaguchi, K., Yamamoto, S., et al. *Astrophys J*, 1987, 317,L115

88. Cernicharo, J., Kahane, C., Guélin, M., . Hein, H. *Astron Astrophys*, 1987, 181,L9

89. Yamamoto, S., Saito, S., Kawaguchi, K., Kaifu, N., Suzuki, H. *Astrophys J*, 1987, 317,L119.

90. Agúndez, M., Cernicharo, J., Guélin, M. *Astron Astrophys*, 2014, 570,A45

91. Souza, S. P., Lutz, B. L. *Astrophys J*, 1977, 216,L49

92. Hinkle, K. H., Keady, J. J., Bernath, P. F. *Science*, 1988, 241,1319

93. Bernath, P. F., Hinkle, K. H., Keady, J. J. *Science*, 1989, 244,562

94. Cernicharo, J., Gottlieb, C. A., Guélin, M., Thaddeus, P., Vrtilek, J. M.. *Astrophys J*, 1989, 341,L25

95. Thaddeus, P., Cummins, S. E., Linke, R. A. *Astrophys J*, 1984, 283,L45

96. Apponi, A. J., McCarthy, M. C., Gottlieb, C. A., Thaddeus, P. *Astrophys J*, 1999, 516,L103

97. Ohishi, M., Kaifu, N., Kawaguchi, K., et al. *Astrophys J*, 1989, 345,L83

98. Guélin, M., Cernicharo, J., Paubert, G., Turner, B. E. *Astron Astrophys*, 1990, 230,L9

99. Halfen, D. T., Clouthier, D. J., Ziurys, L. M. *Astrophys J*, 2008, 677,L101

100. Snyder, L. E., Buhl, D. *Astrophys J*, 1971, 163,L47

101. Guélin, M., Cernicharo, J. *Astron Astrophys*, 1991, 244,L21

102. Turner, B. E. *Astrophys J*, 1971, 163,L35

103. Cernicharo, J., Guélin, M., Pardo, J. R.. *Astrophys J*, 2004, 615,L145

104. Avery, L. W., Broten, N. W., McLeod, J. M., Oka, T., Kroto, H. W. *Astrophys J*, 1976, 205,L173

105. Kroto, H. W., Kirby, C., Walton, D. R. M., et al. *Astrophys J*, 1978, 219,L133

106. Bell, M. B. , Feldman, P. A., Travers, M. J., et al. *Astrophys J*, 1997, 483,L61

107. Broten, N. W., Oka, T., Avery, L. W., MacLeod, J. M., Kroto, H. W. *Astrophys J*, 1978, 223,L105

108. Cheung, A. C., Rank, D. M., Townes, C. H., Thornton, D. D., Welch, W. J. *Nature*, 1969, 221

109. Synder, L. E., Buhl, D., Zuckerman, B., Palmer, P. *Phys Rev Lett*, 1969, 22,679

110. Wilson, R. W., Jefferts, K. B., Penzias, A. A. *Astrophys J*, 1970, 161,L43

111. Ball, J. A., Gottlieb, C. A., Lilley, A. E., Radford, H. E. *Astrophys J*, 1970, 162,L203

112. Wlodarczak, G. *J Mol Struct.*, 1995, 347, 131

113. Markwick, A. J., Charnley, S. B., Butner, H. M., Millar, T. J. *Astron Astrophys*, 2005, 627, L117

114. Turner, B. E., Zuckerman, B. *Astrophys J*, 1978, 225,L75

115. Turner, B. E. *Astrophys J*, 1990, 362, L29

116. Lacour, S., Andre, M. K., Sonnentrucker, P., et al. *Astron Astrophys*, 2005, 430, 967

117. Gerin, M., Combes, F., Wlodarczak, G., et al. *Astrophys J*, 1992, 259, L35

118. Lis, D. C., Roueff, E., Gerin, M., et al. *Astrophys J*, 2002, 571, L55

119. Lee, J-E., Bergin, E. A. *Astrophys J*, 2015. 799,104

120. Roberts, H., Fuller, G. A., Millar, T. J., Hatchell, J., Buckle, J. V. *Astron Astrophys*, 2002, 381, 1026

121. Roberts, H., Millar, T. J. 2007, *Astron Astrophys*, 2007, 471, 849

122. Ceccarelli, C. *Planet Space Sci*, 2002, 50, 1267

123. Spitzer, L., Drake, J. F., Jenkins, E. B., et al. *Astrophys J*, 1973, 181, L116

124. Rehder, D. 2010. *Chemistry in Space*. Wiley-VCH Verlag Co. KGaA, Weinheim, Germany

125. Millar T. J., Roberts H., Markwick A. J., and Charnley S. B. 2000. *Philos. Trans. R. Soc. Lond.*, A358, 2535– 2547

126. Tielens A. G. G. M. *Astron Astrophys*, 1983, 119, 177

127. Kong, S., Caselli, P., Tan, J. C., Wakelam, V., Sipila, O. 2015. Submitted, arXiv,1312.0971 [astro-ph.SR]

128. Solomon, P. M., Woolf, N. J. *Astrophys J*, 1973, 180, L89

129. Coutens, A., Vastel, C., Caux, E., et al. *Astron Astrophys*, 2012, 539, 132

130. Butner, H. M., Charnley, S. B., Ceccarelli, C., et al. *Astrophys J*, 2007, 659, L137

131. Marcelino, N., Cernicharo, J., Roueff, E., Gerin, M., Mauersberger, R. *Astrophys J*, 2005, 620, 308

132. Coudert, L. H., Drouin, B. J., Tercero, B., et al. *Astrophys J*, 2013, 779,119

133. Howe, D. A., Millar, T. J., Schike, P., Walmsley, C. M. *Mont. Not. R. Astron. Soc.*, 1994, 267, 59

134. Macleod, J. M., Avery, L. W., Broten, N. W. *Astrophys J*, 1981, 251, L33

135. Turner, B. E. *Astrophys J*, 1989, 347,L39

136. Vastel, C., Phillips, T. G., Ceccarelli, C., Pearson, J. *Astrophys J*, 2003, 593, L97

137. Loinard, L., Castets, A., Ceccarelli, C., Caux, E., A.G.G.M. Tielens, A.G.G.M. *Astrophys J*, 2001, 552, L163

138. Sakai, N., Sakai, T., Hirota, T., Yamamoto, S. *Astrophys J*, 2009, 702, 1025

139. Stark, R., van der Tak, F., van Dishoeck, E. F. *Astrophys J*, 1999, 521, L67

140. van Dishoeck, E., Blake, G. A., Jansen, D. J., Groesbeck, T. D. *Astrophys J*, 1995, 447, 760

141. Praise, B., Castets, A., Herbst, E., et al. *Astron Astrophys*, 2004, 416, 159

142. Mandal, S. K., Roesky, H. W. *Chem. Commun.*, 2010, 46, 6016

143. Haykal, I., Margul`es, L., Huet, T. R., et al. *Astrophys J*, 2013, 777,120

144. Peeters1, Z., Botta, O., Charnley, S. B. *Astron Astrophys*, 2005, 433, 583

145. Dua, R., Shrivastava, S., S.K. Sonwane, S.K., Srivastava, S.K. *Adv Biol Res*, 2011, 5 (3), 120

146. Sephton, M. A. *Phil. Trans. R. Soc. A*, 2005, 363, 2729

147. Valverde, M.G., Torroba, T. *Molecules*, 2005,10, 318-320

148. Gupta, V. P., Tandon, P., Mishra, P. *Adv Space Res*, 2013, 51, 797

149. Martins, Z., Botta, O., Fogel. M. L, et al. *Earth Planet Sc Lett*, 2008, 270, 130

150. Botta, O., Bada, J. L. *Surv Geophys*, 2002, 411

151. Belloche, A.,Garrod, R. T., Müller, H. S. P., Menten, K. M. *Science*, 2014, 345, 158

152. Irvine, W. M., Eller, J., Hjalmarson, A., et al. 1981. *Astron Astrophys*, 97,192

153. Dezafra, R. L., Thaddeus, P., Kutner, M., et al. *Astrophys J*, 1971,10,1

154. Batchelor, R. A., Brooks, J. W., Godfrey, P. D., Brown, R. D. *Aust. J. Phys.*, 1973, 26,557

155. Simon, M. N Simon, M. *Astrophys J*, 1973, 184, 757

156. Charnley, S. B., Kuan, Y., Huang. H., et al. *Adv Space Res*, 2005, 36, 137

157. Kuan, Y., Yan. C., Charnley, S. B., et al. *Mon. Not. R. Soc*, 2003, 345,650

158. Kutner, M. L., Machnik, D. E., Tucker, K. D., Dickman, R. L. *Astrophys J*, 1980, 242,541

159. Myers, P. C., Thaddeus, P., Linke, R. A. *Astrophys J*, 1980, 241,155

160. Gudipati, M. S., Yang, R. *Astrophys J*, 2012, 756, L24.

161. <http://webbook.nist.gov/chemistry/> Accesed in July, 2016.

162. Lias, S. G., Liebman, J. F., and Levi, R. D. *J. Phys. Chem. Ref. Data*, 1984, 13(3),695

163. Ervin, K. M., Lineberger, W.C. *J. Phys. Chem.* 1991, 95, 1167

Benchmark Studies on the Isomerization Enthalpies for Interstellar Molecules

Setting the stage: Because of the prevailing conditions in the interstellar medium (ISM), there is hardly a consensus as to how molecules are formed in ISM but some of the observed chemistry among these molecular species serve as pointers or clues as to how they are formed. With the well established correlation between the relative stabilities of isomers and their interstellar abundances coupled with the prevalence of isomeric species among the interstellar molecular species, isomerization remains a plausible formation route for isomers in the interstellar medium. In this chapter, an extensive investigation on the isomerization enthalpies of 246 molecular species from 65 isomeric groups using the Gaussian-4 theory composite method with atoms ranging from 3 to 12 is presented.

7.0 Introduction: That the interstellar medium (SIM) is chemically rich is not an argument with the discoveries of over 200 different molecular species in this thin space between the stars which was earlier regarded as a vacuum dotted with stars, black hole and other celestial bodies.¹ These molecules are importance in various fields such as atmospheric chemistry, astrochemistry, prebiotic chemistry, astrophysics, astronomy, astrobiology, etc, and in our understanding of the solar system "the world around us" with each successfully detected interstellar molecule telling the story of the chemistry and physics of the environment from where it was detected. They serve as the most important tools for probing deep into the interior of the molecular clouds and the molecular clouds are significant because it is from them that stars and consequently new plants are formed. The symmetric rotors serve as interstellar thermometers while the metal-bearing species provide useful information regarding the depletion of these molecular species into the molecular dust grains. Understanding how the simple molecules that were present on the early earth may have given rise to the complex systems and processes of contemporary biology is one question the biologically related interstellar molecules can be used to address. Molecules also provide the cooling mechanism for the clouds through their emission.¹⁻³

A careful look at the list of the known interstellar and circumstellar molecules reveals some interesting chemistry among these molecular species. Tables 1.2 and 1.3 contain the list of the currently known interstellar and circumstellar species arranged according to the number of atoms making up the molecules.

Some of the chemistry existing among the interstellar molecular species include the dominance of the linear carbon chain species of the form C_n , H_2C_n , HC_nN , $CH_3(CC)_nH$, $CH_3(C\equiv C)_nCN$ and C_nX ($X=N, O, Si, S, H, P, N^-, H^+$) which account for more than 20% of all the known interstellar and circumstellar molecular species; the presence of about 30 alkyl group containing interstellar molecules mostly observed from the same or similar molecular clouds; periodic trends in which elements from the same group appear to form similar compounds with similar properties as in the case of oxygen and sulphur (group 6/16 elements) in which of the 19 S-containing molecules observed in ISM, 16 have the corresponding O-containing molecules uniquely detected in ISM and the abundance of S-compound relative to its O-analogue is approximately equal to the cosmic S/O ratio, 1/42 as seen in methyl mercaptan, thioisocyanic acid, etc, except where the effect of interstellar hydrogen bonding dominates;^{4,5} successive hydrogen addition where larger species are believed to be formed from the smaller unsaturated species via successive hydrogen addition in which both species could be shown to be chemically and spatially related.⁶

Isomerism is yet another prevailing chemistry among the interstellar molecular species. Apart from the diatomics and a few species which cannot form isomers, about 40% of all the known interstellar molecules have isomeric analogues ranging from the isomeric pairs to the isomeric triads which are believed to have a common precursor for their formation process. Table 3.1 lists some of the known isomeric species and their isomeric groups. As discussed in chapter three, thermodynamics has been shown from several studies to be one of the dominant factors controlling the formation processes of these molecular species with the

effects of interstellar hydrogen bonding known to account from the deviations from thermodynamically controlled processes.⁷⁻¹⁰

Because of the conditions (low temperature and pressure) in the interstellar medium, there is hardly a consensus as to how these molecules are formed but some of the chemistry listed above and the effect of thermodynamics serve as clues as to how these molecules could be formed in ISM. Focusing here on isomerization, the prevalence of isomeric species among the known astromolecules coupled with the energy sources in ISM such as the shock waves (which could arise from the interaction of the Earth's magnetic field with the solar wind, molecular outflows during star formation, supernova blasts and galaxies colliding with each other) which provide energy for both the formation and distribution of large interstellar species, place isomerization as one of the most plausible routes for the formation of interstellar molecules.¹¹ As shown in the ESA relationship, the most stable isomers are found to be more abundant than their less stable analogues except where other factors dominate; thus, the isomerization of the most stable isomer (which is probably the most abundant) to the less stable isomers can be a very effective and efficient formation mechanism in ISM. Also, apart from the energy sources in ISM, the high abundance of the most stable isomer can drive the isomerization process irrespective of the energy barrier.

According to the minimum energy principle¹²⁷, isomerization is the most important process in determining the relative abundances of the isomers in ISM. Isomers of the same generic formula are said to have a common intermediate in their formation and destruction routes. After reaching the generic formula, equilibration process is said to occur. This implies an internal isomerization with a low activation barrier, assisted isomerization or catalytic isomerization at the grain/ice surface.¹²⁷

The present work aims at estimating accurate isomerization enthalpies for 246 different molecular species from 65 isomeric groups using the Gaussian 4 theory composite method.¹² The molecules range from the 3 atomic species to those with 12 atoms with at least one known interstellar molecule from each isomeric group (except the CHS, C₂N₂ and C₅O groups with no known species). The results account for the extent and effectiveness of isomerization as a plausible formation route in ISM; and the rationale behind the successful observation of the known species. Among other things, potential candidates for astronomical searches are highlighted and discussed.

7.1 Computational Details: The methodology employed here is the same as described in section 3.1.0 of this Thesis. Only the results from the G4 composite method are used in this chapter.

7.2 Results and Discussion

All the standard enthalpies of formation ($\Delta_f H^\circ$) presented in section 3.2 of this Thesis are utilized in this chapter. The $\Delta_f H^\circ$ of the new molecular species that are not part of section 3.2 are presented in the supporting information after the references in this chapter. The relative

enthalpies for each isomeric group are presented and discussed in this section. The different isomeric groups investigated are grouped according to the number of atoms beginning from 3 to 12.

7.2.1 Isomers with 3 atoms

In Table 7.1, the relative enthalpies or isomerization energies of the 26 molecular species from 13 isomeric groups with 3 atoms are shown alongside the current astronomical status of these species. With the exception of the CHS isomeric group where no isomer has been detected, at least one isomer from each of the remaining 12 groups is a known interstellar molecule.¹⁴⁻³² The isomerization enthalpies range from 0.2 to 37.3 kcal/mol for groups where both isomers have been detected. This range illustrates the effectiveness of the isomerization mechanism as a plausible route for the formation of these molecular species in ISM, it also shows how far or the extent to which the energy sources within the ISM can drive some chemical processes. For the isomeric groups where only one isomer has been detected, the observed range of isomerization barrier suggests that species like NaNC, AlCN, ONC⁻ and even HOC can be formed from their most stable isomers that have been detected already. The high abundances of the stable isomers coupled with the energy sources in ISM imply the possibility of these less stable isomers being formed from their most stable isomers via the isomerization mechanism.

With the exception of C₂N group where only the less stable isomer is been detected, in all other cases where only one isomer is detected, it is the most stable isomer which support the fact that the most stable isomer is probably the most abundant and the most abundant species is easily detected compared to the less stable isomer. Where both isomers have been detected, the most stable isomer is found to be the most abundant except where other processes dominate. CNC is more stable than CCN but the less stable isomer has been detected while the most stable isomer is yet to be astronomically observed. From literature perusal, there is no information regarding the spectroscopic parameters of CNC that would have warranted it astronomical searches. Thus, the detection of CNC awaits the availability of accurate spectroscopic parameters.

The CHS group is included because of the close similarity between the O and S-containing interstellar molecules. The most stable isomer of the CHO group is known and every known O-containing species suggests the presence and detectability of the corresponding S-analogue. Thus, HCS remains a potential interstellar molecule. Ions (both cations and anions) play important role in the formation processes of interstellar molecules. Under the conditions of the ISM, neutral atoms and molecules tend to be unreactive toward molecular hydrogen but in the presence of ions, most of the reactions become very efficient since the ions can easily react without having to overcome the reaction barrier.^{2,33} This can be seen in the case of the CHO⁺ group where HOC⁺ with an isomerization barrier of 37.3 kcal/mol has been detected. Theoretical calculations and laboratory experiment have shown that the isomerization process in the CHO⁺ isomers has essentially no barrier.¹²⁷ Thus, with the

availability of accurate spectroscopic parameters, the HSC^+ and ONC^- ions (where their most stable isomers are already detected) could be successfully detected.

Table 7.1: Isomerization enthalpies for isomers with 3 atoms

Isomeric group	Isomers	Relative $\Delta_f H^\circ$ (kcal/mol)	Astronomical status
CNH	HCN	0.0	Observed ¹⁴
	HNC	13.5	Observed ¹⁵
CNNa	NaCN	0.0	Observed ¹⁶
	NaNC	2.5	Not observed
CNMg	MgNC	0.0	Observed ¹⁷
	MgCN	0.7	Observed ¹⁸⁻²⁰
CNAI	AlNC	0.0	Observed ²¹
	AlCN	7.3	Not observed
CNSi	SiNC	0.0	Observed ²²
	SiCN	0.2	Observed ²³
CHO	HCO	0.0	Observed ²⁴
	HOC	38.2	Not observed
CHP	HCP	0.0	Observed ²⁵
	HPC	75.7	Not observed
C_2N	CNC	0.0	Not observed
	<i>CCN</i>	2.1	<i>Observed</i> ²⁶
C_2P	CCP	0.0	Observed ²⁷
	CPC	85.3	Not observed
CHO^+	HCO^+	0.0	Observed ²⁸
	<i>HOC</i> ⁺	37.3	<i>Observed</i> ²⁹⁻³⁰
CHS^+	HCS^+	0.0	Observed ³¹
	HSC^+	94.1	Not observed
CNO^-	OCN^-	0.0	Observed ³²
	ONC^-	17.1	Not observed
CHS	HCS	0.0	Not observed
	HSC	41.5	Not observed

Isomerization appears to be a favourable route for the cyanide/isocyanide pair. Table 7.1 contains 7 cyanide/isocyanide pairs of which both cyanide and isocyanide have been detected in three groups with an isomerization energy ranging from 0.2 to 13.5 kcal/mol. With the

exception of the ONC^- ion with an isomerization energy of 17.1 kcal/mol; the remaining members of the cyanide/isocyanide pairs have isomerization barriers in range of 0.0 to 7.3 kcal/mol which is well within the range of those already detected. Thus, NaNC , AlCN and CNC are most likely to be formed from their corresponding analogues and could be successfully detected.

7.2.2 Isomers with 4 atoms

For the isomers with 4 atoms, 25 molecular species from 10 isomeric groups are examined. Table 7.2 contains the isomerization energies of these molecular species and their current astronomical status. Thirteen of these molecular species have been detected from different astronomical sources.³⁴⁻⁵¹ In the CHON, CHSN and C_3H groups where more than one isomer has been detected, the isomerization energy ranges from 3.1 to 67.4 kcal/mol. For the remaining 7 isomeric groups with only one known molecular species from each, the isomerization barrier ranges from 21.6 to 49.8 kcal/mol. This range falls within that of the known species, thus, pointing to the possibility of detecting the less stable isomers of these groups that could be formed via isomerization process.

Among the isomers with 4 atoms examined here, there are eight cyanide/isocyanide pairs. In two of these pairs, both cyanide and isocyanide have been detected with an isomerization barrier in the range of 2.8 to 29.0 kcal/mol. For the other cyanide/isocyanide pairs where only the cyanides are observed, the isomerization enthalpy ranges from 18.7 to 24.7 kcal/mol which is below the 29.0 kcal/mol isomerization barrier calculated for the known cyanide/isocyanide pairs. Thus, isomerization remains a plausible mechanism for the formation of the less stable isocyanides from their corresponding cyanides which are probably more abundant.

The C_2N_2 isomeric group is the isoelectronic analogue of the C_2NP isomeric group. Just as there is an interesting chemistry between the O and S-containing interstellar molecular species; such also exist for the N and P-containing species, though it is not well explored as that of O and S. Over 80% of all the known interstellar and circumstellar molecules have been detected via their rotational spectral features because at the low temperature of the ISM, rotational excited states are easily populated. NC_2N (the most stable isomer of the C_2N_2 group) is microwave inactive meaning that it cannot be astronomically detected via radio astronomy. There are reasons to believe the presence and detectability of NC_2N ; its protonated analogue, NC_2NH^+ has been detected.⁵² NCCP, the isoelectronic analogue of NC_2N is also known.⁵¹ Both the protonated analogues of NC_2N and its isoelectronic analogue that have been observed are likely to be less abundant than NC_2N because of the reactive nature of the ion and the less cosmic abundance of P as compared to N. Thus, infrared astronomy of NCCP or radio astronomy of its isotopologues (which are microwave active) are likely to be successful.

Table 7.2: Isomerization enthalpies for isomers with 4 atoms

Isomeric group	Isomers	Relative $\Delta_f H^\circ$ (kcal/mol)	Astronomical status
CHON	Isocyanic acid	0.00	Observed ³⁴
	Cyanic acid	29.0	Observed ^{35,36}
	Fulminic acid	67.4 (0.0)	Observed ³⁷
	Isofulminic acid	86.1 (18.7)	Not observed
CHSN	HNCS	0.0	Observed ³⁸
	HSCN	11.2	Observed ³⁹
	HCNS	40.6 (0.0)	Not observed
	HSNC	43.3 (2.8)	Not observed
C ₃ H	c-C ₃ H	0.0	Observed ⁴⁰
	l-C ₃ H	3.1	Observed ⁴¹
C ₃ N	l-C ₃ N	0.0	Observed ^{42,43}
	C ₂ NC	22.7	Not observed
	c-C ₃ N	28.8	Not observed
C ₂ NH	HC ₂ N	0.0	Observed ⁴⁴
	HCNC	28.0	Not observed
C ₃ O	l-C ₃ O	0.0	Observed ^{45,46}
	c-C ₃ O	21.6	Not observed
C ₃ S	l-C ₃ S	0.0	Observed ^{47,48,49}
	c-C ₃ S	26.3	Not observed
SiC ₃	c-C ₃ Si	0.0	Observed ⁵⁰
	l-C ₃ Si	49.8	Not observed
C ₂ NP	NCCP	0.0	Observed ⁵¹
	CNCP	24.1	Not observed
C ₂ N ₂	NC ₂ N	0.0	Not observed
	CNCN	24.7	Not observed

7.2.3 Isomers with 5 atoms

Isomerization energies for 20 molecular species from 6 isomeric groups are presented in Table 7.3 alongside their current astronomical status. Nine of these species are known astromolecules.⁵³⁻⁶¹ In the C₃HN and C₃H₂ groups where more than one isomer has been detected, the isomerization energy ranges from 13.7 to 45.4 kcal/mol and the isomerization energies for some of the isomers with five atoms whose most stable isomers have been detected fall within this range. These include; ethynol, CH₂NN, NH₂NC, CH₂NC, HCONC and c-C₂NHO. These species can as well be formed from their most stable isomers via isomerization mechanism.

Again, isomerization appears to be a favourable route for the formation of isocyanides from their corresponding cyanides. As shown in Table 7.3, an isomerization enthalpy as high as 45.4 kcal/mol is noted for an isocyanide formation. This strongly supports the formation of other isocyanides from their corresponding cyanides. The barrier for other isocyanides whose corresponding cyanides have been detected ranges from 12.9 to 43.4 kcal/mol which is within the limit of the one that has been observed.

The fact that the most stable isomers are probably the most abundant and they are easily detected in ISM is well demonstrated among these isomers. From table 7.3, all the observed isomers are the most stable ones in their respective isomeric groups as compared to the ones that have not been detected.

Table 7.3: Isomerization enthalpies for isomers with 5 atoms

Isomeric group	Isomers	Relative $\Delta_f H^\circ$ (kcal/mol)	Astronomical status
C_3HN	HCCCN	0.0	Observed ⁵³
	HCCNC	24.1	Observed ⁵⁴
	HNCCC	45.4	Observed⁵⁵
	CC(H)CN	50.5	Not observed
	HCNCC	72.6	Not observed
C_2H_2O	Ketene	0.0	Observed ⁵⁶
	Ethyneol	38.8	Not observed
	Oxirene	81.9	Not observed
C_3H_2	c- C_3H_2	0.0	Observed ⁵⁷
	l- C_3H_2	13.7	Observed ⁵⁸
N_2H_2C	NH_2CN	0.0	Observed ⁵⁹
	CH_2NN	26.3	Not observed
	NH_2NC	43.4	Not observed
C_2H_2N	CH_2CN	0.0	Observed ⁶⁰
	CH_2NC	22.2	Not observed
C_2HNO	CNCHO	0.0	Observed ⁶¹
	HCONC	12.9	Not observed
	c- C_2NHO	30.2	Not observed
	HNCCO	69.2	Not observed
	HC_2NO	83.3	

7.2.4 Isomers with 6 atoms

The isomerization energies and the current astronomical status of the different isomeric species with 6 atoms investigated in this study are presented in Table 7.4. Figures 7.1 to 7.5

display some of the cyclic isomers highlighted in Table 7. One third of all the molecular species presented in Table 7.4 have all been detected from several astronomical sources.⁶²⁻⁷³

Table 7.4: Isomerization enthalpies for isomers with 6 atoms

Isomeric group	Isomers	Relative $\Delta_f H^\circ$ (kcal/mol)	Astronomical status
C_5N	l- C_5N	0.0	Observed ⁶²
	c- C_5N^*	17.4	Not observed
	C_4NC	20.7	Not observed
	c- C_5N^{**}	21.0	Not observed
	c- C_5N^{***}	100.1	Not observed
C_5H	l- C_5H	0.0	Observed ⁶³⁻⁶⁵
	c-C_5H^a	1.0	Not observed
	c- C_5H^b	34.7	Not observed
	c- C_5H^c	60.8	Not observed
C_2H_3N	Methyl cyanide	0.0	Observed ⁶⁶
	Methyl isocyanide	23.0	Observed ⁶⁷
	Ketenimine	23.1	Observed⁶⁸
	Ethynamine	42.3	Not observed
	2H-azirine	46.5	Not observed
	1H-azirine	80.8	Not observed
$SiCH_3N$	SiH ₃ CN	0.0	Observed ⁵¹
	SiH ₃ NC	4.5	Not observed
	c-SiCH ₃ N ^d	33.4	Not observed
	H ₂ SiCNH	46	Not observed
	c-SiCH ₃ N ^e	50.2	Not observed
	H ₂ NCSiH	57.0	Not observed
C_4HN	HC ₄ N	0.0	Observed ⁶⁹
	HC ₃ NC	17.4	Not observed
H_2C_3O	Methylene ketene	0.0	Not observed
	Propynal	7.3	Observed ⁷⁰
	Cyclopropenone	10.6	observed ⁷¹
H_3CON	Formamide	0.0	Observed ⁷²
	Hydroxymethylimine	12.6	Not observed
	Nitrosomethane	60.8	Not observed
C_5S	l- C_5S	0.0	Observed ^{51,73}
	c- $C_5S^{\#}$	26.9	Not observed
	c- $C_5S^{##}$	41.8	Not observed
	c- $C_5S^{###}$	84.1	Not observed
	C_4SC	114.2	Not observed
C_5O	l- C_5O	0.0	Not observed
	c- C_5O^{σ}	28.6	Not observed

	c-C ₅ O ^{σσ}	46.3	Not observed
	c-C ₅ O ^{σσσ}	84.5	Not observed
	C ₄ OC	114.3	Not observed

*Figure 7.1a, **Figure 7.1b, ***Figure 7.1c; ^aFigure 7.2a, ^bFigure 7.2b, ^cFigure 7.2c; [#]Figure 7.3a, ^{##}Figure 7.3b, ^{##}Figure 7.3c; ^dFigure 4a, ^eFigure 7.4b; ^fFigure 7.5a, ^gFigure 7.5b, ^{gg}Figure 7.5c.

In the C₂H₃N and H₂C₃O groups where more than one isomer has been detected, the isomerization enthalpies range from 7.3 to 23.1 kcal/mol. With the exception of some of the cyclic isomers which are highly unstable, most of the unknown isomers (c-C₅N*, C₄NC, c-C₅N**, c-C₅H^a, SiH₃NC, HC₃NC, methylene ketene, hydroxymethylimine) have isomerization enthalpies in the range of the known isomers, suggesting their possible astronomical observation if they could be formed via isomerization as the ones that have been observed.

Ketenimine for instance is reported to be formed from methyl cyanide via tautomerization (i.e, an isomerisation pathway in which the migration of hydrogen atom from the methyl group to the nitrogen atom is accompanied by a rearrangement of bonding electrons) and this process is said to be driven by shock waves that provide the energy for both the formation and distribution of large interstellar species.⁶⁸

The C₅H isomers; l-C₅H and c-C₅H^a are almost identical in energy. If the spectroscopic parameters of c-C₅H^a (Figure 2a) are accurately probed, either experimentally or theoretically; this species (c-C₅H) could be detected in ISM. The four cyanide/isocyanide pairs among the isomers with 6 atoms presented in Table 7.4 have isomerization enthalpies in the range of 4.5 to 23.0 kcal/mol. Interestingly, the C₂H₃N group where methyl cyanide and methyl isocyanide have been detected, has the highest isomerization barrier of 23.0 kcal/mol which implies the possible detection of the other isocyanides with lower barriers (4.5 to 20.7kcal/mol) assuming isomerization as their plausible formation route.

Except for the delayed astronomical observation of methylene ketene, all the observed isomeric species shown in Table 7.4 are in accordance with the ESA relationship with only the most stable isomers been the detected isomers in their various groups. Methylene ketene and methyl ketene have been proposed as potential interstellar molecules for many reasons. The ketenes are found to be more stable than their corresponding isomers (Tables 7.3, 7.4 and 7.6); they are less affected by interstellar hydrogen bonding assuming surface formation processes; ketene and ketenyl radical (H₂C₂O and HC₂O respectively) are known interstellar molecules.^{56,74}

Just as every known O-containing interstellar molecule points to the presence and the detectability of the S-analogue. For every known S-species, the O-analogue is not only present in detectable abundance, it can be said to have even been overdue for astronomical detection. C₅O is the O-analogue of C₅S that has been detected. Thus, it is an important potential interstellar molecule.

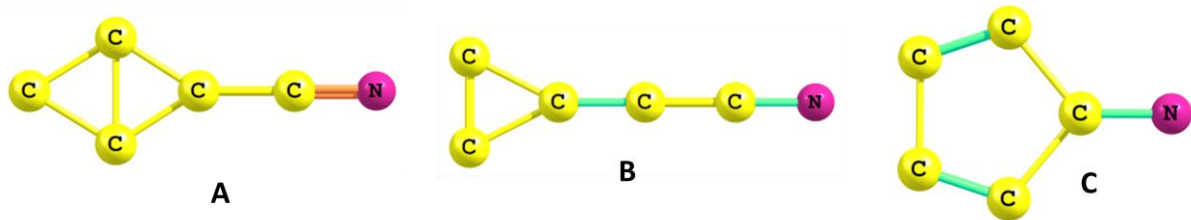


Figure 7.1: Optimized structures of cyclic C₅N isomers.

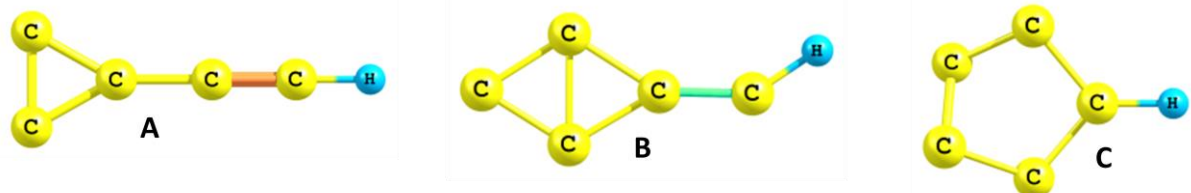


Figure 7.2: Optimized structures of cyclic C₅H isomers.

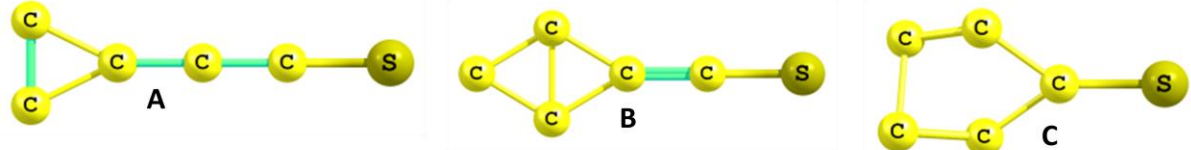


Figure 7.3: Optimized structures of cyclic C₅S isomers.

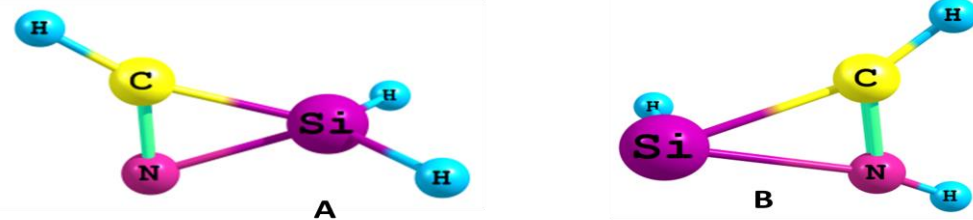


Figure 7.4: Optimized structures of cyclic SiCH₃N isomers.

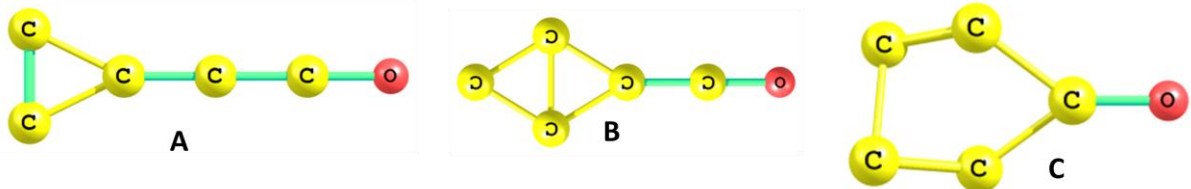


Figure 7.5: Optimized structures of cyclic C₅O isomers.

7.2.5 Isomers with 7 atoms

Table 7.5 shows the isomerization energies and the current astronomical status of different isomeric species with 7 atoms investigated in this study. Of the 22 molecular species in the Table, 7.7 have been astronomically observed.⁷⁵⁻⁸² In the H₄C₂O isomeric group where all the isomers have been detected, the isomerization energies range from 12.2 to 27.8 kcal/mol. All the non-observed isomers in the H₃C₃N and C₃H₄ isomeric groups including, cyanomethanol, iminoacetaldehyde and methyl cyanate (from C₂H₃NO isomeric group) have isomerization

enthalpies in the range calculated for the $\text{H}_4\text{C}_2\text{O}$ isomers which have all been detected. This points to the possibility of detecting these molecules in ISM with isomerization barriers within those of the known interstellar molecules. There is no cyanide/isocyanide pair observed among these systems, however, the isomerization barrier in the range of 19.9 to 27.3 kcal/mol is within the range of those noted for other observed cyanide/isocyanide pairs.

Table 7.8: Isomerization enthalpies for isomers with 7 atoms

Isomeric group	Isomers	Relative $\Delta_f\text{H}^\text{O}$ (kcal/mol)	Astronomical status
$\text{H}_4\text{C}_2\text{O}$	Acetaldehyde	0.0	Observed ^{75,76}
	Vinyl alcohol (syn)	12.2	Observed ⁷⁷
	Vinyl alcohol (anti)	13.9	Observed ⁷⁷
	Ethylene oxide	27.8	Observed ⁷⁸
$\text{H}_3\text{C}_3\text{N}$			
	Acrylonitrile	0.0	Observed ⁷⁹
	Isocyanoethene	19.9	Not observed
C_3H_4	$\text{CH}_3\text{C}_2\text{H}$	0.0	Observed ⁸⁰
	H_2CCCH_2	7.8	Not observed
	c- C_3H_4	23.6	Not observed
$\text{C}_2\text{H}_3\text{NO}$	Methyl isocyanate	0.0	Observed ^{81,82}
	Cyanomethanol	13.6	Not observed
	Iminoacetaldehyde	20.1	Not observed
	Methyl cyanate	27.3	Not observed
	2-Aziridinone	36.0	Not observed
	2-Oxiranimine	40.8	Not observed
	Methyl fulminic acid	56.5	Not observed
	2-Iminoethanol	60.9	Not observed
	Nitrosoethene	69.3	Not observed
	2H-1,2-Oxazete	79.8	Not observed
	Methyl isofulminic acid	84.8	Not observed
	N-Hydroxyacetylenamin	93.6	Not observed
	(Aminooxy)acetylene	94.7	Not observed

As in the previous examples, all the observed isomers are the most stable ones in their respective groups. In the $\text{H}_4\text{C}_2\text{O}$ isomeric group where all the stable isomers have been observed, the most stable isomer; acetaldehyde was first observed before the other isomers. As would be expected, the most stable isomer (acetaldehyde) has been found to be present in high abundance in the different astronomical sources where it has been detected as compared to the abundances of the less stable isomers in the same sources.⁸³⁻⁸⁵

7.2.6 Isomers with 8 atoms

Table 7.6 contains the isomerization energies for 33 isomeric species from 7 groups containing eight atoms each. The astronomical statuses of these species are also shown in the table. Figure 7.6 highlights the cyclic isomers from the $\text{C}_2\text{H}_5\text{N}$ and $\text{CH}_4\text{N}_2\text{O}$ groups. As shown in the table, 10 of these species have been astronomically detected.⁸⁶⁻⁹⁸ The isomerization energies of these species range from 3.1 to 50.0 kcal/mol. Except for 1,2-dioxetane, 1,3-dioxetane and epoxypropene, the isomerization energies for all the unknown isomers with 8 atoms fall within the range (13.0 to 46.9 kcal/mol) of the known isomers (3.1 to 50.0 kcal/mol). Thus, some of the unknown isomers in Table 7.9 could be formed from their most stable isomers (which are probably more abundant) via isomerization process.

The three cyanide/isocyanide pairs among these isomers have isomerization enthalpies ranging from 19.0 to 25.6 kcal/mol. Though no cyanide/isocyanide pair has been detected among these molecular species, the isomerization barrier is within the range of those where the pairs have been detected. CH_3CCNC and $\text{H}_2\text{NCH}_2\text{NC}$ could be formed from their corresponding cyanides that have detected, thus, they could also be detected provided their spectroscopic parameters are accurately known.

Methyl ketene, the most stable isomer of the $\text{H}_4\text{C}_3\text{O}$ group is yet to be astronomically detected. The reasons for its presence and detectability in ISM are same as discussed for methylene ketene (among the isomers with 6 atoms). With the exception of methyl ketene, all the molecular species with 8 atoms examined in this study strictly follow the ESA relationship with only the most stable isomers being the observed isomers in their respective groups.

Table 7.6: Isomerization enthalpies for isomers with 8 atoms

Isomeric group	Isomers	Relative $\Delta_f\text{H}^\circ$ (kcal/mol)	Astronomical status
$\text{C}_4\text{H}_3\text{N}$	CH_3CCCN	0.0	Observed ⁸⁶
	CH_2CCHCN	3.1(0.0)	Observed ^{87,88}
	HCCCH_2CN	13.0	Not observed
	CH_3CCNC	25.6	Not observed
	CH_2CCHNC	25.7 (22.6)	Not observed

C ₂ H ₄ N ₂	H ₂ NCH ₂ CN	0.0	Observed ⁸⁹
	H ₂ NCH ₂ NC	19.0	Not observed
C ₂ H ₄ O ₂	Acetic acid	0.0	Observed ⁹⁰
	Methylformate	17.7	Observed ^{91,92}
	Glycolaldehyde	33.2	Observed ⁹³
	1,3-dioxetane	52.9	Not observed
	1,2-dioxetane	103.0	Not observed
H ₄ C ₃ O	Methyl ketene	0.0	Not observed
	Propenal	2.3	Observed ⁹⁴
	Cyclopropanone	17.3	Not observed
	Propynol	30.8	Not observed
	Propargyl alcohol	35.2	Not observed
	Methoxy ethyne	42.0	Not observed
	1-cyclopropenol	44.0	Not observed
	2-cyclopropenol	45.5	Not observed
	Epoxypropene	65.8	Not observed
H ₂ C ₆	HC ₆ H	0.0	Observed ⁹⁵
	<i>H₂C₆</i>	50.0	<i>Observed⁹⁶</i>
C ₂ H ₅ N	CH ₃ CHNH	0.0	Observed ⁹⁷
	H ₂ CCHNH ₂	2.8	Not observed
	CH3NCH ₂	8.1	Not observed
	c-C ₂ H ₅ N ^m	19.8	Not observed
CH ₄ N ₂ O	H ₂ NCONH ₂	0.0	Observed ⁹⁸
	H ₂ NNHCHO	11.0	Not observed
	HN ₂ CH ₂ OH	35.0	Not observed
	c- CH ₄ N ₂ O ⁿ	42.4	Not observed
	CH ₃ NHNO	43.4	Not observed
	H ₂ NCHNHO	46.9	Not observed

^mFigure 5a; ⁿFigure 5b.

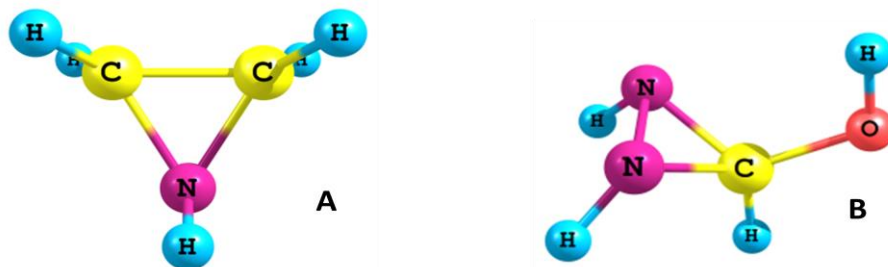


Figure 7.6: Optimized structures of cyclic $\text{C}_2\text{H}_5\text{N}$ (A) and $\text{CH}_4\text{N}_2\text{O}$ (B) isomers.

7.2.7 Isomers with 9 atoms

In Table 7.7, 28 isomeric species from 7 groups are presented with their isomerization enthalpies and current astronomical status. Eight of these species are known interstellar molecular species.⁹⁹⁻¹⁰⁹ Figure 7 shows some of the cyclic molecules with 9 atoms. Among the species shown in Table 10, only ethanol and dimethyl ether from the $\text{C}_2\text{H}_6\text{O}$ group have been observed in more than one isomeric form with an isomerization barrier of 12.6 kcal/mol. CH_3SCH_3 , the S-analogue of dimethyl ether remains a potential candidate for astronomical detection for many reasons; the well established chemistry of S and O-containing interstellar molecules, the high abundance of $\text{CH}_3\text{CH}_2\text{SH}$ (the most stable isomer of the group which can isomerize to CH_3SCH_3) and the low isomerization barrier (1.4 kcal/mol) as compared to that of dimethyl ether (12.6 kcal/mol). Assuming accurate spectroscopic parameters are available, interstellar CH_3SCH_3 will soon become a reality.

Isomerization remains one of plausible formation routes for the formation of the less stable isomers of the different groups here whose most stable isomers have been detected. The isomerization enthalpies for the two cyanide/isocyanide pairs range from 20.8 to 27.1 kcal/mol. Though none of these pairs has been detected, the possibility of their formation from their corresponding cyanides (via isomerization) which could lead to their successful detection cannot be ruled out. HC_6NC is the highest member of the HC_{2n}NC linear chains with experimentally measured rotational transitions that can be used for its astronomical search.¹¹⁰ However, a recent study using a combined experimental and theoretical approach has provided accurate rotational constants for higher members of the HC_{2n}NC linear chains.¹¹¹ HNC remains the only member of this series that has been detected in ISM.¹¹² Without any exception, all the molecular species with 9 atoms examined in this study are in accordance with the ESA relationship with respect to their astronomical observation.

Table 7.7: Isomerization enthalpies for isomers with 9 atoms

Isomeric group	Isomers	Relative $\Delta_f H^\circ$ (kcal/mol)	Astronomical status
C_2H_6O	Ethanol	0.0	Observed ^{99,100}
	Dimethyl ether	12.6	Observed ¹⁰⁰¹
C_2H_6S	CH_3CH_2SH	0.0	Observed ¹⁰²
	CH_3SCH_3	1.4	Not observed
C_2H_5ON	Acetamide	0.0	Observed ¹⁰³
	N-methylformamide	9.7	Not observed
	Nitrosoethane	64.7	Not observed
	1-aziridnol	77.9	Not observed
	Cyanoethoxyamide	134.4	Not observed
C_3H_5N	Cyanoethane	0.0	Observed ¹⁰⁴
	Isocyanoethane	20.8	Not observed
	Propylenimine	22.0	Not observed
	2-propen-1-imine	25.3	Not observed
	N-methylene ethenamine	26.0	Not observed
	1-Azetine	32.2	Not observed
	Cyclopropanimine	37.2	Not observed
	Methylene azaridine	43.8	Not observed
	Propargylamine	45.1	Not observed
C_5H_4	CH_3C_4H	0.0	Observed ¹⁰⁵
	$H_2C_3HC_2H$	5.2	Not observed
	$H_2C_5H_2$	8.1	Not observed
	c- $C_5H_4^x$	26.1	Not observed
	c- $C_5H_4^y$	31.6	Not observed
C_3H_6	CH_3CHCH_2	0.0	Observed ¹⁰⁶
	c- $C_3H_6^z$	8.2	Not observed
C_7HN	HC_7N	0.0	Observed ¹⁰⁷⁻¹⁰⁹
	HC_6NC	27.1	Not observed

^xFigure 7.6a; ^yFigure 7.6b; ^zFigure 7.6c.

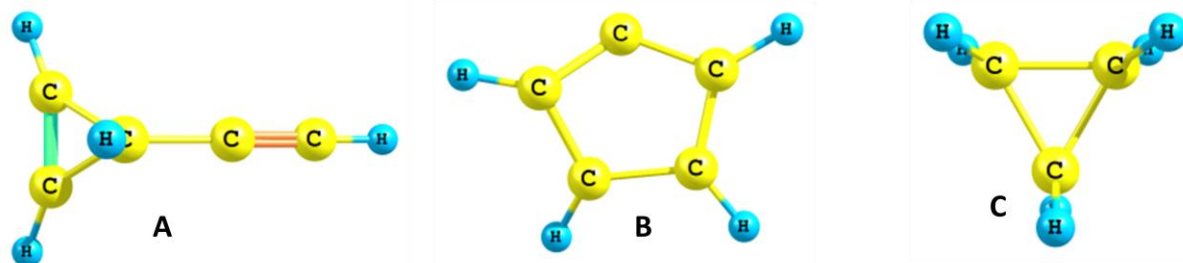


Figure 7.7: Optimized structures of cyclic C_5H_4 (A and B) and C_3H_6 (C) isomers.

7.2.8 Isomers with 10 atoms

Isomerization energies and astronomical statuses for 16 molecular species from three isomeric groups comprising of 10 atoms each are presented in Table 7.8. Of these three groups, only the C_3H_6O group contains isomers (propanone and propanal) that have been detected in more than one isomeric form with an isomerization barrier of 8.1 kcal/mol.^{94,113-116} $CH_3(CC)_2NC$ is the isocyanide analogue of $CH_3(CC)_2CN$ that has been detected. It has an isomerization barrier of 25.3 kcal/mol which is within the range of the known cyanide/isocyanide pairs. However, there is little or no information regarding the rotational spectrum of $CH_3(CC)_2NC$ that could warrant its astronomical search. Thus, the availability of accurate spectroscopic parameters for this species remains the starting point in the steps towards its astronomical detection.

Table 7.8: Isomerization enthalpies for isomers with 10 atoms

Isomeric group	Isomers	Relative Δ_fH° (kcal/mol)	Astronomical status
$C_2H_6O_2$	1,1-Ethanediol	0.0	Not observed
	Ethylene glycol	6.1	Observed ¹¹³
	Methoxy methanol	15.9	Not observed
	Ethyl hydroperoxide	51.9	Not observed
	Dimethane peroxide	57.7	Not observed
C_3H_6O	Propanone	0.0	Observed ^{114,115}
	Propanal	8.1	Observed ⁹⁴
	Propen-2-ol	13.8	Not observed
	1-propen-1-ol	18.6	Not observed
	Methoxy ethene	25.6	Not observed

	2-propene-1-ol	27.1	Not observed
	1,2-epoxypropane	30.0	Not observed
	Cyclopropanol	31.2	Not observed
	Oxetane	33.2	Not observed
C ₆ H ₃ N	CH ₃ (CC) ₂ CN	0.0	Observed ¹¹⁶
	CH ₃ (CC) ₂ NC	25.3	Not observed

1,1-ethanediol; the most stable isomer of the C₂H₆O₂ group has not been detected whereas ethylene glycol, the next stable isomer of the group with an isomerization enthalpy of 6.1 kcal/mol has been detected in good abundance. The delayed astronomical detection of 1,1-ethanediol is directly linked lack of spectroscopic parameters for this molecule. The rotational spectrum of 1,1-ethanediol is yet to be probed either experimentally or theoretically. Once this is done, this molecule could be successfully observed. With the exception of 1,1-ethanediol, the observed isomers with 10 atoms are in accordance with the ESA relationship as in the previous cases.

7.2.9 Isomers with 11 atoms

There are currently four known interstellar molecules (HC₇N, CH₃C₆H, ethyl formate and methyl acetate) containing 11 atoms.¹¹⁷⁻¹²⁰ In Table 7.9, the 9 isomeric species from two groups containing 11 atoms are shown with their isomerization enthalpies and current astronomical status. For the known isomers in the C₃H₆O₂ group, the isomerization energy ranges from 11.8 to 14.3 kcal/mol. The non-detection or delayed detection of propanoic acid (the most stable isomer of the group) has been traced to the effect of interstellar hydrogen bonding on the surface of the dust grains which reduces the overall abundance of this species in the gas phase, thus, influencing its successful astronomical observation.

HC₉N is the second largest member of the cyanopolyyne chain that has been detected in ISM. As seen in other cyanide/isocyanide pairs, the isomerization of HC₉N to HC₈NC with a barrier of 27.2 is achievable. Accurate rotational constant for HC₈NC is now available from a recent study.¹¹¹ Thus, HC₈NC could be astronomically searched. With the delayed detection of propanoic acid accounted for on the basis of interstellar hydrogen bonding, all the observed isomers with 11 atoms also follow the ESA relationship with only the most stable isomer been the detected isomers.

Table 7.9: Isomerization enthalpies for isomers with 11 atoms

Isomeric group	Isomers	Relative $\Delta_f H^\circ$ (kcal/mol)	Astronomical status
$C_3H_6O_2$	Propanoic acid	0.0	Not observed
	Ethylformate	11.8	Observed ¹¹⁷
	Methyl acetate	14.3	Observed ¹¹⁸
	Lactaldehyde	28.1	Not observed
	Dioxolane	36.1	Not observed
	Glycidol	52.1	Not observed
	Dimethyldioxirane	81.7	Not observed
C_9HN	HC_9N	0.0	Observed ¹¹⁹
	HC_8NC	27.2	Not observed

7.2.10 Isomers with 12 atoms

Only very few cyclic molecules are known among the interstellar molecular species.⁸ From the different isomeric groups considered in this study, it is clear that the cyclic isomers are found to be among the less stable isomers in their respective groups as compared to their corresponding straight chain analogues. This low stability affects their interstellar abundances and influences their astronomical observation. The C_6H_6 isomeric group is one of the few groups where the cyclic molecules are found to be the most stable species. All the four currently known interstellar molecules with 12 atoms,^{96,117,121,122} their corresponding isomers, and isomerization enthalpies are presented in Table 7.10.

The only known branched-chain interstellar molecule; isopropyl cyanide is almost equivalent in energy to its linear chain analogue; propyl cyanide with an isomerization barrier of 0.4kcal/mol. Propan-2-ol and propanol (the two most stable isomers of the C_3H_6O group) are yet to be astronomically observed. These species have also been shown to be strongly affected by interstellar hydrogen bonding as compared to ethyl methyl ether that has been detected.⁹ The stability of ethyl methyl ether is also enhanced by the stabilizing effect of the two alkyl substituents while propanol and propan-2-ol have only one alkyl substituent each. With the delayed detection of propan-2-ol and propanol rationalized on the basis of interstellar hydrogen bonding, all the systems investigated here strictly follow the ESA relationship.

Table 7.10: Isomerization enthalpies for isomers with 12 atoms

Isomeric group	Isomers	Relative $\Delta_f H^\circ$ (kcal/mol)	Astronomical status
C_6H_6	Benzene	0.0	Detected ⁹⁶
	Fulvene	34.2	Not detected
	3,4-dimethylenecyclopropene	62.0	Not detected
	1,5-hexadiene-3-yne	62.3	Not detected
	2,4-hexadiyne	65.2	Not detected
	1,2,3,4-hexateraene	71.7	Not detected
	1,3-hexadiyne	73.2	Not detected
	Trimethylenecyclopropane	79.8	Not detected
	1,4-hexadiyne	82.3	Not detected
	1,5-hexadiyne	85.8	Not detected
C_3H_8O	Propan-2-ol	0.0	Not observed
	Propanol	3.7	Not observed
	Ethyl methyl ether	8.2	Observed ¹²¹
C_4H_7N	Isopropyl cyanide	0.0	Observed ¹²²
	Propyl cyanide	0.4	Observed ¹¹⁷
	2-isocyanopropane	18.2	Not observed
	2-aminobutadiene	18.2	Not observed
	3-pyrroline	20.2	Not observed
	2,2-dimethylethylenimine	20.5	Not observed
	But-1-en-1-imine	22.6	Not observed
	2,3-butadiene-1-amine	38.1	Not observed
	N-vinylazardidine	40.1	Not observed
	N-methyl-1-propyn-1-amine	41.4	Not observed
	3-butyn-1-amine	43.2	Not observed
	N-methyl propargylamine	49.3	Not observed
	2-azabicyclo(2.1.0)pentane	51.9	Not observed

7.3 Potential Interstellar Molecules

Knowing the right candidates for astronomical searches is vital in reducing the number of unsuccessful astronomical searches considering the time, energy and resources involved in these projects. From the present study, few molecular species have been identified as potential interstellar molecules. These are briefly summarized below:

Isocyanomethylidyne, CNC: This is the isocyanide analogue of C_2N that has been detected.²⁶ CNC is found to be more stable than its cyanide analogue. Table 7.11 contains the relative energies of CNC and CCN from different quantum chemical calculation methods while Figure 8 shows the optimized geometries of these isomers at the MP2(full)/6-311++G** level with the bond angle in degrees and bond distance in angstroms. As discussed under the isomers with 3 atoms, all the observed species are the most stable ones and these stable species are also found to be more abundant. Where both species have been detected, the most stable is reported to present in high abundance than the less stable. For instance, HCN is found to be more abundant than HNC in different molecular clouds and this is also the case for the MgNC/MgCN abundance ratio measured in the asymptotic giant branch (AGB) stars.^{19,20,123,124} CNC is more stable than CCN which implies that CNC should be present in high abundance in ISM than CCN that has been detected. Thus, CNC remains a potential candidate for astronomical detection. CNC is microwave inactive with a zero dipole moment, thus, infrared astronomy remains the best approach for its astronomical observation.

Table 7.11: Relative energies of CNC and CCN

Method	Relative energy (kcal/mol)	
	CNC	CCN
CCSD/6-311++G**	0.0	1.5
MP2(full)/6-311++G**	0.0	6.2
B3LYP/6-311++G**	0.0	2.0
G4	0.0	3.7

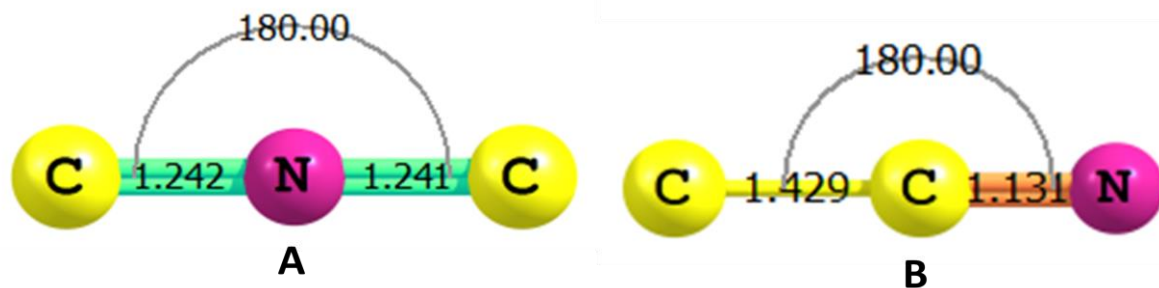


Figure 7.8: Optimized geometries of CNC and CCN at MP2(full)/6-311++G** level.

NCCN: The rationale for the choice of NCCN as a potential interstellar molecule is well discussed under the isomers with 4 atoms.

c-C₅H: With the limited number of known cyclic interstellar molecules, it is always exciting finding rings that are as stable as their corresponding chains. c-C₅H (Figure 7.2a) is the cyclic analogue of C₅H that has been detected. From Table 7.4, the isomerization barrier between the linear chain and this cyclic analogue is just 1 kcal/mol. Table 7.12 shows the relative energies of these species at different quantum chemical calculation methods. While the MP2 methods predicts the cyclic isomer to be more stable than the linear, others methods predict the reverse but the magnitude of the difference in energy is much at the MP2 level as compared to other methods. Figure 7.9 displays the optimized structures of these species. As shown in Table 7.12, c-C₅H is microwave active with a very good dipole moment making its astronomical searches in the radio frequency possible. If the spectroscopic parameters of c-C₅H can be accurately probed, either experimentally or theoretically, the possibility of its astronomical observation is very high.

Table 7.12: Relative energies of linear and cyclic stable isomers of C₅H

Method	Relative energy (kcal/mol)		Dipole moment (Debye)	
	c-C ₅ H	l-C ₅ H	c-C ₅ H	l-C ₅ H
MP2(full)/6-311++G**	0.0	18.7	3.4	4.2
MP2/aug-cc-pVTZ	0.0	17.5	3.4	4.2
G4	10.9	0.0	3.7	4.6
CCSD/6-311++G**	3.0	0.0	3.4	4.6
B3LYP/6-311++G**	10.4	0.0	3.7	5.2
B3LYP/aug-cc-pVTZ	10.3	0.0	3.7	5.2

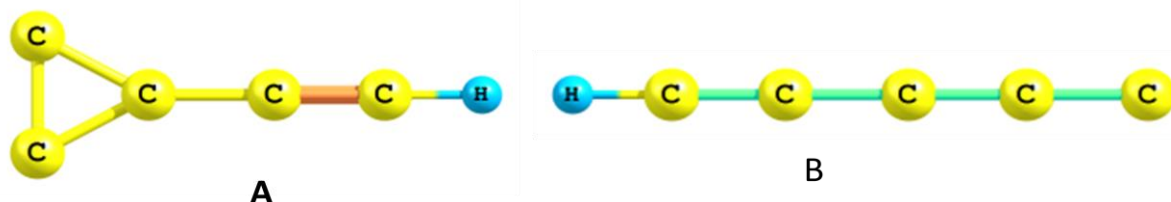


Figure 7.9: Optimized structures of C₅H most stable isomers.

Methylene and Methyl Ketenes: As highlighted in the text, the ketenes are found to be more stable than their corresponding isomers in all the isomeric groups examined in this study (Tables 7.3, 7.4 and 7.6) and as such be present in detectable amounts in ISM. Ketenes have also been shown to be less affected by hydrogen bonding on the surface of the interstellar dust grains as compared to their corresponding isomers. Also, the fact that ketene (H₂C₂O), ketenyl radical (HC₂O) and isomers of ketenes (like propynal, cyclopropenone, and propenal) are known interstellar molecular species further supports the presence and detectability of methyl ketene and methylene ketene in ISM. Thus, methyl ketene and methylene ketene remain potential interstellar molecules pending their astronomical searches. No unsuccessful astronomical search has been reported for any of these ketenes.

C₅O: This is the oxygen analogue of C₅S that is a known interstellar molecule. Without any exception, an interstellar O-containing molecular species is more abundant than its S-analogue. This could simply be traced to the cosmic abundance of O and S. Thus, for every known S-species, the O-analogue is not only present in detectable abundance, it can be said to have even been overdue for astronomical detection because for sure the O-species are more abundant than their S-analogue and as such could be detected with less difficulty as compared to its S-analogue. The column density of 2-14E12 cm⁻² reported for C₅S suggests the high abundance of C₅O in ISM.^{51,73,125} The microwave spectrum of C₅O that could guide its successful astronomical observation is available.¹²⁶ Interstellar C₅O is just a matter of time.

CH₃SCH₃: This is the S-analogue of dimethyl ether; a known interstellar molecule. The interstellar chemistry of S- and O-containing species is well established. Every known O-containing interstellar molecule points to the presence and detectability of the S-analogue. As earlier mentioned, except where the effect of interstellar hydrogen bonding dominates, the ratio of an interstellar sulphur molecule to its oxygen analogue is close to the cosmic S/O ratio. Assuming dimethyl ether is formed from ethanol via isomerization with a barrier of 12.6 kcal/mol, then the isomerization of C₂H₅SH to CH₃SCH₃ is a much feasible process with an isomerization barrier of just 1.4 kcal/mol (nine times lower than that of CH₃OCH₃) compared to that of the O-analogue. Thus, because of the unique chemistry of S- and O-containing interstellar molecules and the low isomerization barrier, CH₃SCH₃ is considered a potential candidate for astronomical observation assuming its spectroscopic parameters are accurately known.

1,1-Ethanediol, Propanoic Acid, Propan-2-ol and Propanol: These molecules are found to be the most stable isomers in their respective groups (Tables 7.8, 7.9 and 7.10). Whereas their less stable isomers have been astronomically detected; successful detection of these most stable isomers is highly feasible. The spectroscopic parameters for propanoic acid, propan-2-ol and propanol are known but those of 1,1-ethanediol are yet to come by. Though the delayed astronomical observations of some of these species have been linked to the effect of interstellar hydrogen bonding; there are high chances for their successful astronomical detection.

7.4 Conclusion: An extensive investigation on the isomerization energies of 246 molecular species from 64 isomeric groups is reported in this study. From the results, isomerization is found to be one of the plausible mechanisms for the formation of molecules in ISM. The high abundances of the most stable isomers coupled with the energy sources in ISM drive the isomerization process even for barrier as high as 67.4 kcal/mol. Specifically, the process is found to be very effective in converting cyanides to their corresponding isocyanides and vice versa. Thus, for every cyanide or isocyanide, the corresponding isocyanide or cyanide could be synthesized via isomerization. Also, from the results, the following potential interstellar molecules; CNC, NCCN, c-C₅H, methylene ketene, methyl Ketene, CH₃SCH₃, C₅O, 1,1-ethanediol, propanoic acid, propan-2-ol and propanol are highlighted and discussed. This study further reaffirms the Energy, Stability and Abundance (ESA) relationship in a larger scale.

7.5 References

1. Etim, E. E., And Arunan, E. Planex Newsletter, 2015, 5(2),16
2. Fraser, H. J., Mccoustra., Williams, D. A. Astron Geophys, 2002, 43 (2), 10
3. Tielens, A. G. G.M. Rev. Mod. Phys., 2013, 85,1021
4. Frerking, M. A., Linke, R. A., Thaddeus, P. *Astrophys J*, 1979, 234,L143
5. Linke, R. A., M. A. Frerking, M. A., Thaddeus, P. *Astrophys J*, 1979,234,L139
6. Hollis, J. M., Jewell, P. R., Lovas, F. J., Remijan, A., And Møllendal, H. *Astrophys J*, 2004, 610,L21
7. Dickens J.E., Irvine W.M., Nummelin, A., et al. *Spectrochim Acta A*, 2001,57, 643
8. Etim, E. E., Arunan. Submitted.
9. Etim, E. E., Arunan, E. Submitted
10. Etim, E. E., Gorai, P., Das, A., Chakrabati, S., Arunan, E.
11. Lovas, F. J., Hollis, J. M., Remijan, A. J., And Jewell, P. R. *Astrophys J*, 2006, 645,L137
12. Curtiss, L. A., Redfern, P. C., Raghavachari, K. *J. Chem. Phys*, 2007, 126, 084108
13. Curtiss, L. A., Raghavachari, K., Redfern, P. C., Rassolov, V., And Pople, J. A. *J. Chem. Phys.*, 1998, 109 ,7764.
14. Zuckerman, B., Morris, M., Palmer, P., Turner, B. E. *Astrophys J*, 1972, 173,125
15. Blackman, G. L., Brown, R. D., Godfrey, P. D., Gunn, H. I. *Nature*, 1976, 261,395
16. Turner, B. E., Steimle, T. C., Meerts, L. *Astrophys J*,1994, 426,97
17. Kawaguchi, K., Kagi, E., Hirano, T., Takano, S., Saito, S. *Astrophys J*,1993, 406, 39
18. Ziurys, L. M., Apponi, A. J., Guélin, M., Cernicharo, J. *Astrophys J*, 1995, 445,47
19. Guélin, M., Cernicharo, J., Kahane, C., Gomez-Gonzales, J. *Astron Astrophys*, 1986, 157, L17
20. Guelin, M., Lucas, R., Cernicharo, J. *Astron Astrophys*, 1993, 280,19.
21. Ziurys, L. M., Savage, C., Highberger, J. L., Apponi, A. J., Guélin, M., Cernicharo, J. *Astrophys J*, 2002, 564, 45
22. Guélin, M., Muller, S., Cernicharo, J., Mccarthy, M. C., Thaddeus, P. *Astron Astrophys*, 2004, 426, L49
23. Guélin, M., Muller, S., Cernicharo, J., Apponi, A. J., Mccarthy, M. C., Gottlieb, C. A., Thaddeus, P. *Astron Astrophys*, 2000, 369, L 9
24. Snyder, L. E., Hollis, J. M., And Ulich, B. L. *Astrophys J*, 1976, 208,L91
25. Agúndez, M., Cernicharo, J., And Guélin, M. *Astrophys J*, 2007, 662,L91
26. Anderson, J. K., And Ziurys, L. M. *Astrophys J*, 2014, 795,L1
27. Halfen, D. T., Clouthier, D. J., And Ziurys, L. M. *Astrophys J*, 2008, 677,L101
28. Buhl, D., And Snyder, L. E. *Nature*, 1970, 228,267
29. Woods, R. C., Gudeman, C. S., Dickman, R. L, Goldsmith, P. F., et al. *Astrophys J*, 1983, 270,583
30. Ziurys, L. M., And Apponi, A. J. *Astrophys J*, 1995, 455,L73
31. Thaddeus, P., Guélin, M., And Linke, R. A. *Astrophys J*, 1971, 246,L41
32. Soifer, B. T., Puetter, R. C., Russell, R. W., Willner, S. P., Harvey, P. M., Gillett, F. *Astrophys J*,1979, 232, 53
33. Shaw, A. M. *Astrochemistry, From Astronomy To Astrobiology*. Wiley, 2006.
34. Snyder, L. E., Buhl, D. *Astrophys J* 1972, 177, 619
35. Brunken, S., Gottlieb, C. A., Mccarthy, M. C., Thaddeus, P. *Astrophys J*, 2009, 697, 880
36. Brunken, S., Belloche, A., Martin, S., Verheyen, L., Menten, K. M. *Astron Astrophys*, 2010, 516, A109
37. Marcelino, N., Cernicharo, J., Tercero, B., Roueff, E. *Astrophys J*, 2009, 690, 27
38. Frerking, M. A., Linke, R. A., Thaddeus, P. *Astrophys J*, 1979, 234, 143
39. Halfen, D. T., Ziurys, L. M., Brünken, S., Gottlieb, C. A., Mccarthy, M. C., Thaddeus, P. *Astrophys J*, 2009, 702,124
40. Thaddeus, P., Gottlieb, C. A., Hjalmarson, A., et al. *Astrophys J*, 1985,294,L49
41. Yamamoto, S., Saito, S., Ohishi, M., Suzuki, S., Ishikawa, S.-I., Kaifu, N., Murakami, A. *Astrophys J*, 1987, 322,L55

42. Guélin, M., And Thaddeus, P. *Astrophys J*, 1977, 212,L81

43. Friberg, P., Hjalmarson, A., Irvine, W. M., And Guélin, M. *Astrophys J*, 1980, 241,L99

44. Guélin, M., Cernicharo, J. *Astron Astrophys*, 1991, 244, L21

45. Matthews, H. E., Irvine, W. M., Friberg, P., Brown, R. D., Godfrey, P. D. *Nature*, 1984, 310,125

46. Brown, R. D., Godfrey, P. D., Cragg, D. M., et al. *Astrophys J*, 1985, 297,302

47. Kaifu, N., Suzuki, H., Ohishi, M., Miyaji, T., Ishikawa, S., Kasuga, T., And Morimoto, M. *Astrophys J*, 1987, 317,L111

48. Yamamoto, S., Saito, S., Kawaguchi, K., Kaifu, N., And Suzuki, H. *Astrophys J*, 1987, 317,L119

49. Cernicharo, J., Kahane, C., Guélin, M., And Hein, H. *Astron Astrophys*, 1987, 181,L9

50. Apponi, A. J., McCarthy, M. C., Gottlieb, C. A., And Thaddeus, P. *Astrophys J*, 1999, 516,L103

51. vAgúndez, M., Cernicharo, J., And Guélin, M. *Astron Astrophys*, 2014, 570,A45

52. Agúndez, M., Cernicharo, J., Vicente, P. De., Et Al. *Astron Astrophys*, 2015, 579,L10

53. Turner, B. E. Detection Of Interstellar Cyanoacetylene. *Astrophys J*, 1971, 163, 35

54. Kawaguchi, K., Ohishi, M., Ishikawa, S. I., Kaifu, N. *Astrophys J*, 1992, 386, 51

55. Kawaguchi, K., Takano, S., Ohishi, M., et al. *Astrophys J*, 1992, 396, 49

56. Turner, B. E. *Astrophys J*, 1977, 213,L75

57. Thaddeus, P., Vrtilek, J. M., And Gottlieb, C. A. *Astrophys J*, 1985, 299,L63

58. Cernicharo, J., Gottlieb, C. A., Guélin, M., Killian, T. C., Thaddeus, P., And Vrtilek, J. M. *Astrophys J*, 1991, 368,L43

59. Turner, B. E., Liszt, H. S., Kaifu, N., Kisliakov, A. *Gastrophys J*, 1975, 201, 149.

60. Irvine, W. M., Friberg, P., Hjalmarson, Å., et al. *Astrophys J*, 1988, 334, 107.

61. Remijan, A. J., Hollis, J. M., Lovas, F. J., Stork, W. D., Jewell, P. R., Meier, D. S. *Astrophys J*, 2008, 675, L85

62. Guélin, M., Neininger, N., And Cernicharo, *Astron Astrophys*, 1998, 355,L1

63. Cernicharo, J., Kahane, C., Gómez-González, J., Guélin, M. *Astron Astrophys*, 1986, 164, L1

64. Cernicharo, J., Kahane, C., Gómez-González, J., Guélin, M. *Astron Astrophys*, 1986, 167,L5

65. Cernicharo, J., Guelin, M., Walmsley, C. M. *Astron Astrophys*, 1987, 172,L5

66. Solomon, P. M., Jefferts, K. B., Penzias, A. A., Wilson, R. W. *Astrophys J*, 1971, 168, 107

67. Cernicharo, J., Kahane, C., Guélin, M., Gomez-Gonzalez, J. *Astron Astrophys*, 1988, 189, 1

68. Lovas, F. J., Hollis, J. M., Remijan, A. J., Jewell, P. *Rastrophys J*, 2006, 645,137

69. Cernicharo, J., Guélin, M., Pardo, J. R. *Astrophys J*, 2004, 615, 145

70. Irvine, W. M., Brown, R. D., Craig, D. M., et al. *Astrophys J*, 1988, 335,89

71. Hollis, J. M., Remijan, A. J., Jewell, P. R., And Lovas, F. J. *Astrophys J*, 2006, 642,933

72. Rubin, R. H., Swenson, G. W., Solomon, Jr. R. C., Flygare, H. L. *Astrophys J*, 1971, 169, 39

73. Bell, M. B., Avery, L. W., And Feldman, P. A. *Astrophys J*, 1993, 417,L37,

74. Agúndez, M., Cernicharo, J., And Guélin, M. *Astron Astrophys*, 2015, 577,L5

75. Fourikis, N., Sinclair, M. W., Robinson, B. J., Godfrey, P. D., Brown, R. D.. *Aust J. Phys*, 1974, 27, 425.

76. Gilmore, W., Morris, M., Palmer, P., Johnson, D. R., Lovas, F.J., Turner, B. E., Zuckerman, B. *Astrophys J*, 1976, 204,43

77. Turner, B. E., Apponi, A. J. *Astrophys J*, 2001, 561, 207

78. Dickens, J. E., Irvine, W. M., Ohishi, M., Ikeda, M., Ishikawa, S., Nummelin, A., Hjalmarson, A. *Astrophys J*, 1997, 489,753

79. Gardner, F. F. *Winnewisser, G. Astrophys J*, 1975, 195, L127

80. Buhl, D., And Snyder, L. E., in *Molecules In The Galactic Environment* (Eds) Gordon, M. A., Snyder, L. E. Wiley- Interscience, New York, 187-195, 1973.

81. Halfen, D. T., Ilyushin, V. V., Ziurys, L. M. *Astrophys J*, 2015, 812,L5

82. Cernicharo, J., Kisiel, Z., Tercero, B., Kolesniková, L., et al. *Astron Astrophys*, 2016, 587,L4

83. Nummelin, A., Dickens, J. E., Bergman, P., et al. *Astrophys J, Suppl S.*, 1998, 117,427

84. Nummelin, A., Bergman, P., Hjalmarson, Å., et al. *Astron Astrophys*, 1998, 337, 275

85. Ikeda, M., Ohishi, M., Dickens, J. E., Bergman, P., Hjalmarson, A., Irvine, W. M.. *Astrophys J*, 2001, 560, 792

86. Broten, N. W., Macleod, J. M., Avery, L. W., Irvine, W. M., Höglund, B., Friberg, P., Hjalmarson, P. *Astrophys J*, 1984, 276, 25

87. Lovas, F. J., Remijan, A. J., Hollis, J. M., Jewell, P. R., And Snyder, L. E *Astrophys J*, 2006 ,637,L37

88. Chin, J. N., Kaiser, R. I., Lemme, C., Henkel, C. *AIP Conf. Proc.*, 2006, 855,149

89. Belloche, A., Menten, K. M., C. Comito, C., Müller, H. S. P., Schilke, P., Ott, J., Thorwirth, S., Hieret, C. *Astron Astrophys.*, 2008, 482,179

90. Mehringer, D. M., Snyder, L. E., Miao, Y., Lovas, F. *Astrophys J*, 1997, 480,L71

91. Churchwell, E., Winnewisser, G. *Astron Astrophys.*, 1975, 45,229.

92. Brown, R. D., Crofts, J. G., Godfrey, P. D., Gardner, F. F., Robinson, B. J., Whiteoak, J. B. *Astrophys J*, 1975, 197,L29

93. Hollis, J. M., Lovas, F. J., Jewell, P. R. *Astrophys J*,2000, 540, 107

94. Hollis, J. M., Jewell, P. R., Lovas, F. J., Remijan, A., Møllendal, H. *Astrophys J*, 2004, 610, 21

95. Langer, W. D., Velusamy, T., Kuiper, T. B. H., et al. *Astrophys J*, 1997, 480, 63

96. Cernicharo, J., Heras, A. M., Tielens, A. G. G. M., et al. *Astrophys J*,2001, 546, L123

97. Loomis, R. A., Zaleski, D. P., Steber, A. L., Neill, J. L., et al. *Astrophys J*,Lett, 2013, 765, L9.

98. Remijan, A. J., Snyder, L. E., Mcguire, B. A., et al. *Astrophys J*, 2014,783,77.

99. Zuckerman, B., Turner, B. E., Johnson, D. R., et al. *Astrophys J*, 1975, 196, 99

100. Pearson, J. C., Sastry, K. V. L. N., Herbst, E., De Lucia, F. C. *Astrophys J*, 1997, 480, 420

101. Snyder, L. E., Buhl, D., Schwartz, P. R., Clark, F. O., Johnson, D.R., Lovas F. J., Giguere, P. T *Astrophys J*, 1974, 191, 79

102. Kolesniková, L., Tercero, B., Cernicharo, J., Alonso, J. L., Daly, A. M., Gordon, B. P., Shipman, S. T. *Astrophys J*, 2014, 784,L7

103. Hollis, J. M., Lovas, F. J., Anthony J., Remijan A. J., Jewell, P. R., Ilyushin, V. V., Kleiner, I *Astrophys J*, 2006, 643, 25.

104. Johnson, D. R., Lovas, F. J., Gottlieb, C. A., Gottlieb, E. W., Litvak, M. M., Guélin, M., *Astrophys J*, 1977, 370

105. Walmsley, C. M., Jewell, P. R., Snyder, L. E., And Winnewisser, G. *Astron Astrophys* , 1984, 134,L11

106. Marcelino, N., Cernicharo, J., Agúndez, M., Roueff, E., Gerin, M., Martín-Pintado, J. *Astrophys J*, 2007. 665,L127

107. Kroto, H. W., Kirby, C., Walton, D. R. M., et al. *Astrophys J*, 1978,219,L133

108. Little, L. T., Macdonald, G. H., Riley, P. W., Matheson, D. N. *Mon Not R Astron Soc.*, 1978, 183,45

109. Winnewisser, G., And Walmsley, C. M. *Astron Astrophys*, 1978, 70,L37

110. Botschwina, P., Heyl, A. J. *Chem.Phys.*, 1998, 109,3108

111. Etim, E. E., And Arunan, E. Submitted.

112. Blackman, G. L., Brown, R. D., Godfrey, P. D., Gunn, H. *Nature*, 1976, 261,395

113. Hollis, J. M., Lovas, F. J., Jewell, P. R., Coudert, L. H. *Astrophys J*, 2002. 571, 59

114. Combes, F., Gerin, M., Wooten, A., Wlodarczak, G., Clausset, F., Encrenaz, P. I. *Astron Astrophys.*, 1987, 180,L13

115. Snyder, L. E., Lovas, F. J., Mehnninger, D. M., Miao, N. Y., Kuan. Y.-J., Hollis, J. M., Jewell, P. R. *Astrophys J*, 2002,578, 245

116. Snyder, L. E., Hollis, J. M., Jewell, P. R., Lovas, F. J., Remijan, A *Astrophys J*, 2006, 647,412

117. Belloche, A., Garrod, R. T., Müller, H. S. P., Menten, K. M., Comito, C., Schilke, P. *Astron Astrophys.*, 2009, 499, 215

118. Tercero, B., Kleiner, I., Cernicharo, J., Nguyen, H. V. L., López, A., Muñoz Caro, G. M. *Astrophys J* Lett.,2013, 770, 13

119. Broten, N. W., Oka, T., Avery, L. W., Macleod, J. M., And Kroto, H. W. *Astrophys J*, 1978, 223,L105

120. Remijan, A. J.,Hollis, J. M., Snyder, L. E., Jewell, P. R., And Lovas, F. J. *Astrophys J*, 2006, 643,L37

121. Fuchs, G. W., Fuchs, U., Giesen, T. F., Wyrowski, F. 2005. *Astron Astrophys*, 2005, 444, 521

122. Belloche, A., Garrod, R. T.,Müller, H. S. P.,Menten, K. M. *Science*, 2014, 345, 1584.

123. Tennekes, P. P., Harju, J., Juvela, M., Tóth, L. V. *Astron Astrophys*, 2006,456, 1037

124. Irvine, W. M., Schloerb, F. P. *Astrophys J*, 1984, 282, 516

125. Etim, E. E., And Arunan, E.

126. Ogata, T., Ohshima, Y., Endo, Yasuki. *J. Am. Chem. Soc.*, 1995, 117, 3593

127. Lattelais, M., Pauzat, F., Ellinger, Y., Ceccarelli, C. *Astrophys J.*, 2009, 696, L133

7.6 Supporting Information

The following tables contain the enthalpies of formation for the 243 molecular species from 64 isomeric groups investigated in this study. The Gaussian 4 theory composite method is used for all the calculations reported here. The tables are arranged according to the number of atoms in each isomeric group beginning with 3 to 13.

Table 1: Standard enthalpies of formation for isomers with 3 atoms

Isomeric group	Isomers	$\Delta_f H^\circ$ (kcal/mol)
CHO	HCO	39.6
	HOC	77.9
CHP	HCP	19.0
	HPC	94.7
C ₂ N	CNC	162.0
	CCN	164.1
C ₂ P	CCP	122.8
	CPC	208.1
CHO ⁺	HCO ⁺	200.4
	HOC⁺	237.7
CHS ⁺	HCS ⁺	244.3
	HSC ⁺	338.4
CHS	HCS	77.7
	HSC	119.2

Table 2: Standard enthalpies of formation for isomers with 4 atoms

Isomeric group	Isomers	$\Delta_f H^\circ$ (kcal/mol)
CHSN	HCNS	67.7
	HSNC	70.5
C ₃ H	c-C ₃ H	171.1
	l-C ₃ H	174.2
C ₃ N	l-C ₃ N	180.4
	C ₂ NC	203.1
	c-C ₃ N	209.2
C ₃ O	l-C ₃ O	81.5
	c-C ₃ O	103.1
C ₃ S	l-C ₃ S	138.8
	c-C ₃ S	165.1
SiC ₃	c-C ₃ Si	171.6
	l-C ₃ Si	221.4
C ₂ NP	NCCP	50.4
	CNCP	74.5
C ₂ N ₂	NC ₂ N	75.3
	CNCN	100.0

Table 3: Standard enthalpies of formation for isomers with 5 atoms

Isomeric group	Isomers	$\Delta_f H^\circ$ (kcal/mol)
C ₃ H ₂	c-C ₃ H ₂	120.9
	l-C ₃ H ₂	134.6
C ₂ HNO	CNCHO	11.0
	HCONC	23.9
	c-C ₂ NHO	41.2
	HNCCO	80.2
	HC ₂ NO	94.3

Table 4: Standard enthalpies of formation for isomers with 6 atoms

Isomeric group	Isomers	$\Delta_f H^\circ$ (kcal/mol)
C ₅ N	l-C ₅ N	236.2
	c-C ₅ N*	253.6
	C ₄ NC	256.9
	c-C ₅ N**	257.2
	c-C ₅ N***	336.6
C ₅ H	l-C ₅ H	225.3
	c-C₅H^a	226.3
	c-C ₅ H ^b	260.0
	c-C ₅ H ^c	286.1
SiCH ₃ N	SiH ₃ CN	35.9
	SiH ₃ NC	40.4
	c-SiCH ₃ N ^d	69.3
	H ₂ SiCNH	81.9
	c-SiCH ₃ N ^e	86.1
	H ₂ NCSiH	92.9
C ₅ S	l-C ₅ S	201.3
	c-C ₅ S [#]	228.2
	c-C ₅ S ^{##}	243.1
	c-C ₅ S ^{###}	285.4
	C ₄ SC	315.5
C ₅ O	l-C ₅ O	144.2
	c-C ₅ O ^σ	172.8
	c-C ₅ O ^{σσ}	190.5
	c-C ₅ O ^{σσσ}	228.7
	C ₄ OC	258.5

Table 5: Standard enthalpies of formation for isomers with 7 atoms

Isomeric group	Isomers	$\Delta_f H^\circ$ (kcal/mol)
C ₃ H ₄	CH ₃ C ₂ H	49.1
	H ₂ CCCH ₂	59.9
	c-C ₃ H ₄	72.7
C ₂ H ₃ NO	Methyl isocyanate	-26.4
	Cyanomethanol	-12.8
	Iminoacetaldehyde	-6.4
	Methyl cyanate	0.84
	2-Aziridinone	9.61
	2-Oxiranimine	14.1

	Methyl fulminic acid	30.1
	2-Iminoethenol	34.4
	Nitrosoethene	42.9
	2H-1,2-Oxazete	53.4
	Methyl isofulminic acid	58.4
	N-Hydroxyacetylenamin	67.1
	(Aminooxy)acetylene	68.3

Table 6: Standard enthalpies of formation for isomers with 8 atoms

Isomeric group	Isomers	$\Delta_f H^\circ$ (kcal/mol)
H ₂ C ₆	HC ₆ H	167.2
	H₂C₆	217.2
C ₂ H ₅ N	CH ₃ CHNH	17.3
	H ₂ CCHNH ₂	20.1
	CH ₃ NCH ₂	25.4
	c-C ₂ H ₅ N ^m	37.1
CH ₄ N ₂ O	H ₂ NCONH ₂	-18.8
	H ₂ NNHCHO	-7.8
	HN ₂ CH ₂ OH	16.2
	c-CH ₄ N ₂ O ⁿ	23.6
	CH ₃ NHNO	24.9
	H ₂ NCHNHO	28.1

Table 7: Standard enthalpies of formation for isomers with 9 atoms

Isomeric group	Isomers	$\Delta_f H^\circ$ (kcal/mol)
C ₅ H ₄	CH ₃ C ₄ H	104.1
	H ₂ C ₃ HC ₂ H	109.3
	H ₂ C ₅ H ₂	112.2
	c-C ₅ H ₄ ^x	130.3
	c-C ₅ H ₄ ^y	135.7
C ₃ H ₆	CH ₃ CHCH ₂	11.6
	c-C ₃ H ₆ ^z	19.8
C ₇ HN	HC ₇ N	201.7
	HC ₆ NC	228.8

Table 8: Standard enthalpies of formation for isomers with 10 atoms

Isomeric group	Isomers	$\Delta_f H^\circ$ (kcal/mol)
$C_2H_6O_2$	1,1-Ethanediol	-93.6
	Methoxy methanol	-77.7

Table 9: Standard enthalpies of formation for isomers with 11 atoms

Isomeric group	Isomers	$\Delta_f H^\circ$ (kcal/mol)
C_9HN	HC_9N	255.7
	HC_8NC	282.9

Table 10: Standard enthalpies of formation for isomers with 12 atoms

Isomeric group	Isomers	$\Delta_f H^\circ$ (kcal/mol)
C_6H_6	Benzene	18.8
	Fulvene	53.0
	3,4-dimethylenecyclopropene	80.8
	1,5-hexadiene-3-yne	81.1
	2,4-hexadiyne	84.0
	1,2,3,4-hexateraene	90.5
	1,3-hexadiyne	92.0
	Trimethylenecyclopropane	98.6
	1,4-hexadiyne	101.1
	1,5-hexadiyne	104.6

Chapter 8

Conclusions and Future Directions

The conclusions drawn from the different studies presented in this Thesis and some of the future directions of these studies are briefly summarized in this chapter.

8.1 Conclusions: As clearly stated in the opening chapter, the focus of the present investigations is mainly on understanding some of the chemistry of the different classes of interstellar and circumstellar molecular species, both the known and potential. In line with this aim, several studies have been carried out on the different classes of interstellar molecular species and some of the conclusions drawn from these studies are summarized below.

Energy, Stability and Abundance (ESA) relationship exists among interstellar molecular species and according to the relationship, “***Interstellar abundances of related species are directly proportional to their stabilities in the absence of the effect of interstellar hydrogen bonding***”.

Among other immediate consequences of the relationship, it addresses the following interstellar chemistry questions:

- ***Where are Cyclic Interstellar Molecules?***
- ***What are the possible candidates for astronomical observation?***
- ***Why are more Interstellar Cyanides than isocyanides?***

Also, from the ESA relationship; though there has not been any successful astronomical observation of any heterocycle, the ones so far searched remain the best candidates for astronomical observation in their respective isomeric groups.

The observation of the first branched chain molecule in ISM is in agreement with the ESA relationship and the C₅H₉N isomers have been shown to contain potential branched chain interstellar molecules.

That molecules with the C-C-O backbone have less potential of formation in ISM as compared to their counterparts with the C-O-C backbone has been demonstrated not to be true following the ESA relationship.

A detailed investigation on the relationship between molecular partition function and astronomical detection isomeric species (related molecules) shows that there is no direct correlation between the two rather there is a direct link between the thermodynamic stability of the isomeric species (related molecules) and their interstellar abundances which influences the astronomical observation of some isomers at the expense of others.

The existence and effect of **Interstellar Hydrogen Bonding** have been reported for the first time in this Thesis. This interstellar hydrogen bonding is shown to be responsible for the following observations among other:

- ***Deviations from thermodynamically controlled processes***

- *Delayed observation of the most stable isomers*
- *Unsuccessful observations of amino acids*

On the prediction that ketenes are the right candidates for astronomical searches among their respective isomers, a ketenyl radical; HCCO has recently been detected in line with this prediction.

The deviation from the role rule that the ratio of an interstellar sulphur molecule to its oxygen analogue is close to the cosmic S/O ratio is well accounted for on the basis of hydrogen bonding on the surface of the dust grains.

On the **Detecting weakly bound complexes in ISM**; this is very possible. Following the conditions in which these complexes are observed in the terrestrial laboratory as compared to the ISM conditions; it suffices to say that weakly bound complexes present and are detectable in ISM. They could even account for some of the 'U' lines.

Accurate spectroscopic parameters within experimental accuracy of few kHz are obtained for higher members of the different linear interstellar carbon chains using an inexpensive combined experimental and theoretical approach. These are the indispensable tools for the astronomical observation of these molecular species.

Thermodynamics is utilized in accounting for the known linear interstellar carbon chains and in examining the right candidates for astronomical searches with the availability of accurate spectroscopic parameters obtained in this study. These molecular species are shown to also obey the ESA relationship.

The effect of kinetics on the formation processes of the linear interstellar carbon chains is shown to be well controlled by thermodynamics.

The spectroscopic tools provided for the different linear interstellar carbon chains could be applied in reducing the 'U' lines and probing new molecular species.

From the studies on interstellar protonated species with over 100 molecular species; protonated species resulting from a high proton affinity prefers to remain protonated rather than transferring a proton and returning to its neutral form as compared to its analogue that gives rise to a lower proton affinity from the same neutral species.

The studies on detectable interstellar anions account for the known interstellar anions and predict members of the $C_{2n}O^-$, $C_{2n}S^-$, $C_{2n-1}Si^-$, $HC_{2n}N^-$, C_nP^- , and C_{2n} chains as outstanding candidates for astronomical observation including the higher members of the $C_{2n}H^-$ and $C_{2n-1}N^-$ groups whose lower members have been observed.

From high level ab initio quantum chemical calculations; ZPE and Boltzmann factor have been used to explain the observed deuterium enhancement and the possibility of detecting more deuterated species in ISM. Though all the heterocycles that have so far been searched for in ISM have been shown to be the right candidates for astronomical observation as discussed in the ESA relationship, they have also been shown to be strongly bonded to the surface of the interstellar dust grains thereby reducing their abundances, thus, contributing to their unsuccessful detection except for furan which is less affected by hydrogen bonding.

The D-analogues of the heterocycles are shown from the computed Boltzmann factor to be formed under the dense molecular cloud conditions where major deuterium fractionation dominates implying very high D/H ratio above the cosmic D/H ratio which suggests the detectability of these deuterated species.

With the well established correlation between the relative stabilities of isomers and their interstellar abundances coupled with the prevalence of isomeric species among the interstellar molecular species, isomerization of the most stable isomer (which is probably the most abundant) to the less stable ones is examined as one of the plausible formation routes for isomers in the interstellar medium. From an extensive investigation on the isomerization enthalpies of 243 molecular species from 64 isomeric groups, the high abundances of the most stable isomers coupled with the energy sources in interstellar medium is shown to drive the isomerization process even for relative enthalpy difference as high as 67.4 kcal/mol.

The cyanides and their corresponding isocyanides pairs appear to be effectively synthesized via this process. CNC, NCCP, c-C₅H, methylene ketene, methyl Ketene, CH₃SCH₃, C₅O, 1,1-ethanediol, propanoic acid, propan-2-ol and propanol are identified and discussed as potential interstellar molecular species.

8.2 Future Directions: The chemistry of interstellar molecular species is reach and ever fascinating. The present work explores some of the basic chemistry of the different classes of these molecular species. Of course there are still more and more interesting chemistry of these molecular species that are could be elucidated. Some of the future directions of interest in this area are briefly summarized.

8.2.1 Bending the linear carbon chains: Potential Interstellar Cyclic Molecules

The idea that the linear carbon chains with ten atoms and below are more stable than their cyclic analogues is not true in all cases. A preliminary work searching for rings that are more stable than their corresponding chains showed some rings that are more stable than their corresponding chains within four carbon atoms. These rings are of outmost importance in interstellar chemistry as they could easily be detected because of their high stability. Interestingly, the corresponding linear chains have not been astronomically observed which could be traced to their low stability and low abundance. Experimentally, these rings can easily be detected as compared to their chains.

What next? This work was done with the compound methods (G4 and G4MP2), MP2 and B3LYP but the results follow two different trends. Hence, firm conclusions cannot be made. The B3LYP; which does not account for the effect of electron correlation, predicts the linear

chains to be more stable than the cyclic chains in all the cases (Tables 8.1-8.3). It also predicts the nature of the rings different from other methods. Calculations at the CCSD(T) level are required in order to make firm conclusions and to search for more stable rings among the various linear carbon chains; C_n , H_2C_n , HC_nN , HC_nO , HC_nS , and C_nX ($X=N, O, Si, S, H, P, H^-, N^-$).

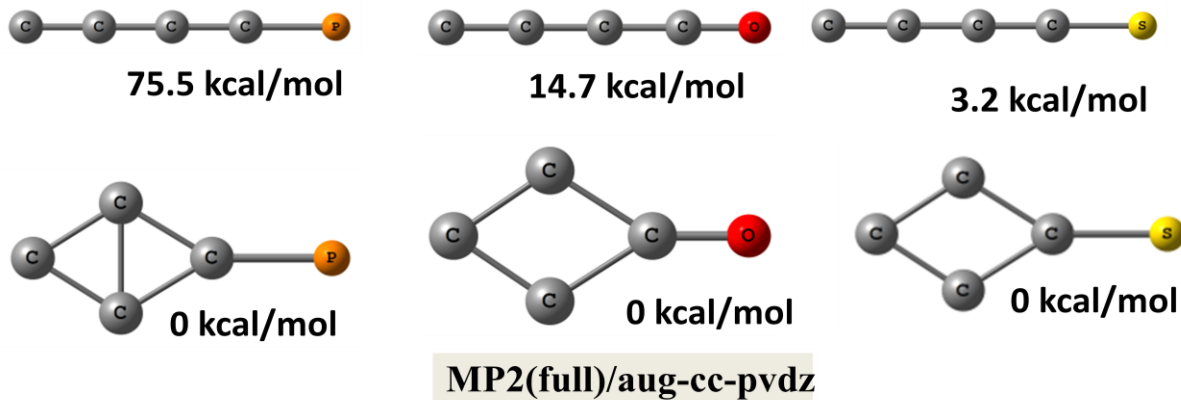


Figure 7.1: Relative energy of cyclic and their corresponding linear carbon chains

Table 8.1: Relative energy for C_4O linear and cyclic isomers

Method	Relative energy (kcal/mol)		Nature of ring
	Ring	Linear chain	
G4	0	3.3	Bicyclic
G4MP2	0	3.6	Bicyclic
MP2(full)/6-311++G**	0	13.5	Monocyclic
MP2(full)/aug-cc-pvdz	0	14.7	Monocyclic
MP2(full)/aug-cc-pvtz	0	11.0	Monocyclic
B3LYP/6-311++G**	0	-8.4	Bicyclic
B3LYP/ aug-cc-pvdz	0	-4.6	Bicyclic
B3LYP/ aug-cc-pvtz	0	-8.2	Bicyclic

Table 8.2: Relative energy for C_4S linear and cyclic isomers

Method	Relative energy (kcal/mol)		Nature of ring
	Ring	Linear chain	
G4	0	-6.8	Bicyclic
G4MP2	0	-6.5	Bicyclic
MP2(full)/6-311++G**	0	2.2	Bicyclic
MP2(full)/aug-cc-pvdz	0	3.2	Monocyclic
B3LYP/6-311++G**	0	-17.7	Bicyclic
B3LYP/ aug-cc-pvdz	0	-14.5	Bicyclic
B3LYP/ aug-cc-pvtz	0	-17.8	Bicyclic

Table 8.3: Relative energy for C4P linear and cyclic isomers

Method	Relative energy (kcal/mol)		Nature of ring
	Ring	Linear chain	
G4	0	-65.8	Monocyclic
G4MP2	0	-64.4	Monocyclic
MP2(full)/6-311++G**	0	15.3	Bicyclic
MP2(full)/aug-cc-pvdz	0	75.5	Bicyclic
B3LYP/6-311++G**	0	-74.4	Monocyclic
B3LYP/ aug-cc-pvdz	0	-71.3	Monocyclic
B3LYP/ aug-cc-pvtz	0	74.7	Monocyclic

8.2.2 Spectroscopy of Linear Interstellar Carbon Chain Isotopologues

As already discussed in this Thesis, the linear carbon chains remain the dominant theme in interstellar chemistry accounting for more than 20% of all the known interstellar molecules. Their continuous astronomical observation depends on the availability of accurate spectroscopic parameters. The unstable nature of some of these linear carbon chains, radicals and ions makes it difficult for the laboratory measurement of their rotational spectra needed for their astronomical observation. Theoretical predictions of spectroscopic parameters have been instrumental for probing molecules both in the terrestrial laboratory and in interstellar medium (ISM). But accurate predictions are not easily archived by most of the commonly used methods. A combined experimental and theoretical approach is reported in this Thesis which has been used to estimate accurate rotational constants within experimental accuracy of few KHz for hundreds of linear carbon chains.

Among the known interstellar and circumstellar molecules, isotopologues of H, C, N, O, and S containing species have also been detected. These isotopologues unlike their corresponding main species do not suffer from opacity problems, thus, they are excellent tools for probing the physical and chemical conditions of ISM. The starting point for their astronomical observation is the availability of accurate spectroscopic parameters. The experimental difficulty noted in the case of the main carbon chains is more pronounced for the isotopologues because of their low natural abundances. Theoretically, the methods that cannot accurately predict for the main carbon chains obviously cannot do so for their corresponding isotopologues. The combined experimental and theoretical approach depends on the availability of at least three experimental rotational constants but there is dearth of information regarding the experimental data for most of the linear carbon chain isotopologues. Thus, this approach cannot be utilized for estimating accurate rotational constants for the isotopologues. But could there be any correlation between the rotational constants of the linear carbon chains and their corresponding isotopologues which could be explored in estimating accurate rotational transitions for the isotopologues. Yes, there exist a correlation between the rotational constants of the linear carbon chains and their corresponding isotopologues as follows:

$$(I_{\text{exp}}/I_{\text{cal}})\text{carbon chain} = (I_{\text{exp}}/I_{\text{cal}})\text{isotopologue}$$

But the accuracy [ΔB (MHz)] of the estimated rotational constants using this correlation is only good for larger system as shown in Tables 8.4-8.7.

What could be done? Accurate theoretical methods preferably the CCSD(T) method is required in order to obtain accurate rotational constants for these isotopologues.

Astrophysical implication of this work: The possibility that most of the 'U' lines associated with the known linear interstellar carbon chains belong to their isotopologues cannot be totally ruled out. With the availability of accurate rotational constants, some of the 'U' lines could be assigned.

Table 8.4: C_nO systems and their isotopologues

System	B_{exp}	B_{cal}	B_{exp}/B_{cal}	New B for iso	ΔB (MHz)
CO	57,635.9687	60,333.333	0.955292	-	-
^{13}CO	55,101.0205	57,673.470	0.955396	55,095.02205	5.99845
$C^{17}O$	56,179.9829	58,805.556	0.955352	56,176.49509	3.48781
$C^{18}O$	54,891.4239	57,453.562	0.955400	54,884.94563	6.47827
C_5O	1,366.84709	1,394.264	0.980336	-	-
$C_5^{18}O$	1,307.59431	1,334.138	0.980104	1,307.903412	0.309102
$^{13}CC_4O$	1,327.22525	1,382.441	0.96006	1,355.256578	28.03133

Table 8.5: C_nH^- systems and their isotopologues

System	B_{exp}	B_{cal}	B_{exp}/B_{cal}	New B for iso	ΔB (MHz)
C_2H^-	41,639.237000	43,006.701	0.968203	-	
$^{13}CCH^-$	40,111.413	41,977.771	0.955539	40,643.02341	531.61041
C_4H^-	4,654.9449	4,725.844	0.984989	-	
C_4D^-	4,324.020	4,388.429	0.985323	4,322.591942	1.428058
C_6H^-	1,376.86298	1,391.705	0.989335	-	
C_6D^-	1,314.47424	1,328.611	0.989360	1,314.441854	0.032386

Table 8.6: C_nSi systems and their isotopologues

System	B_{exp}	B_{cal}	B_{exp}/B_{cal}	New B for iso	ΔB (MHz)
SiC4	1,533.77206	1,561.180	0.982444	-	
29SiC4	1,510.2298	1,537.211	0.982448	1,510.223858	0.005942
30SiC4	1,488.0256	1,514.605	0.982451	1,488.014727	0.010873
Si13CC3	1,532.0511	1,559.540	0.982374	1,532.160852	0.109752
SiC6	611.25102	621.937	0.982818	--	
29SiC6	602.2978	612.831	0.982812	602.301477	0.003677
<i>Si13CC5</i>	608.7851	619.450	0.982783	608.806751	0.021651
30SiC6	593.7901	604.177	0.982808	593.796168	0.006068

Table 8.7: HC_nN systems and their isotopologues

System	B _{exp}	B _{cal}	B _{exp} /B _{cal}	New B for iso	ΔB (MHz)
HCN	44,315.97	46,364.002	0.955827	-	
DCN	36,207.50	37,731.875	0.959600	36,065.149	142.350996
HC3N	4,459.058	4,633.475	0.962357	-	
DC3N	4,221.580858	4,298.619	0.982078	4136.806919	84.773938
HC5N	1,331.3313	1,347.875	0.987726	-	
DC5N	1,271.057	1,286.793	0.987771	1270.9990	0.057985
HC7N	564.00112	569.550	0.990257	-	
DC7N	545.3153	550.682	0.990254	545.316943	0.001643
H13CC6N	551.64401	562.968	0.979885	557.483246	5.839235
HC715N	552.25338	557.740	0.990163	552.306180	0.05280
HC ₉ N	290.518322	292.958	0.991672	-	
DC₉N	282.91852	285.299	0.991656	282.9231042	0.004584
H ¹³ CC ₈ N	285.2948	289.563	0.985260	287.151595	1.856795
HC₉¹⁵N	285.05909	287.712	0.990780	285.316009	0.256919
HC11N	169.06295	170.329	0.992567	-	
DC11N	165.4069	166.649	0.992547	165.410303	0.003403
HC₁₁¹⁵N	166.39526	167.651	0.992510	166.404855	0.009595
H ¹³ CC ₁₀ N	166.28861	168.435	0.987257	167.183028	0.894418
HC13N	106.97258	107.706	0.993190	-	-
DC13N	104.994997	105.722	0.993123	105.00209	0.007093
HC15N	71.950133	72.408	0.993676	-	
DC15N	70.791053	71.246	0.993614	70.795481	0.004428
HC17N	50.70323	51.009	0.994005	-	
DC17N	49.978955	50.283	0.993953	49.981582	0.002627
HC19N	37.063306	37.282	0.994107	-	-
DC19N	36.59256	36.805	0.994228	36.589104	0.003456

Appendix 1: Preliminary Investigations on Isoprene...Ar complex

Appendix 1: Preliminary Investigations on Isoprene...Ar complex

A1.1 Introduction: Apart from the chemical examination of the ISM in which microwave spectroscopy remains a reliable and indispensable tool, understanding the nature of weak interactions is yet another unique application of this tool. Isoprene is a well known organic compound with a huge interest from atmospheric chemistry perspective. Its structure makes it a suitable candidate for studying weak interaction which is the central focus of this ongoing project. The microwave spectrum of isoprene monomer in the frequency range of 20 to 30 GHz is known for decades.¹ The weakly bound complex of this isoprene with argon is investigated in this study. The optimized structure of this complex is shown in Figure A.1.1. Table A.1.1 contains the theoretically predicted rotational constants and the dipole moment components of this complex. Optimization of the guess structure and the prediction of the mentioned parameters are done at the CISD level with the cc-pVDZ basis set using Gaussian 09 software.²⁻⁴

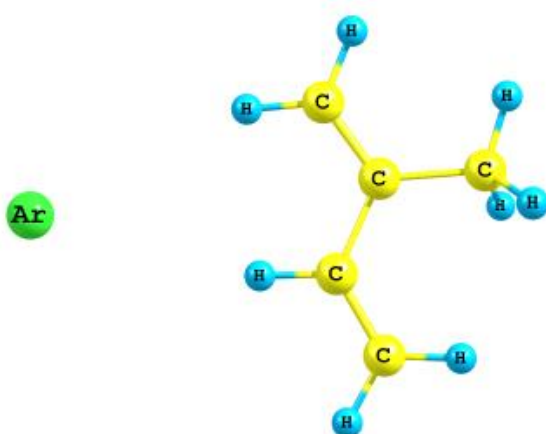


Figure A1.1: Optimized structure for Isoprene...Ar complex

Table A1.1: Rotational constants and dipole moment components along the three principle axes for the isoprene...Ar complex

Parameter	Value
A/MHz	4,166.8
B/MHz	731.1
C/MHz	624.4
$ \mu_a /D$	0.1
$ \mu_b /D$	0.0
$ \mu_c /D$	0.0

A1.2: Search for the Isoprene Monomer and Isoprene...Argon Rotational Spectra

Although the microwave spectrum of isoprene is known in the frequency range mentioned above but in searching for the transitions for the isoprene...argon complex, we began by for the monomer transitions within the frequency range of our spectrometer (as described in chapter two of this Thesis). In searching for both the isoprene monomer and isoprene...argon complex transitions, argon was used as the carrier gas. The gas was bubbled through the isoprene sample. The mixture was expanded from a stagnation pressure of 1.1bar and microwave pulse of 1 μ s time duration was used during the search.

A total of ten (10) transitions in the range of 7 to 14.2GHz were observed which could well fit very well with the theoretically predicted transitions for the monomer. These transitions are shown in Table A.1.2. These transitions were shown to be dependent only on isoprene as they were still observed when helium (instead of argon) was used as the carrier gas.

Two transitions at **9758.263281MHz** and **9920.253516MHz** were observed while searching for the 9749.371343 MHz ($2_{20}-1_{10}$ line) and 9919.220000 MHz ($2_{21}-1_{11}$ line) transitions respectively. These transitions were dependent on both isoprene and argon. With helium as the carrier gas, these lines could not be seen, thus they are transitions corresponding to the isoprene...argon weakly bound complex.

Table A1.2: Observed transitions of isoprene monomer

Frequency (MHz)	Transition		Obs-Cal (MHz)
	J	K ₋₁ K ₊₁ -- J	
7256.4944	2, 1, 1	2, 0, 2	0.0500
9444.4336	2, 0, 2	1, 1, 1	-0.0040
9830.6563	3, 1, 2	2, 2, 1	-0.1007
10035.2930	3, 1, 2	3, 0, 3	-0.0135
11397.1855	1, 1, 1	0, 0, 0	0.0933
12404.3926	4, 2, 2	4, 1, 3	-0.0940
12484.9121	3, 2, 2	3, 1, 2	0.0400
13313.8613	2, 2, 0	2, 1, 1	0.1189
13353.5801	5, 2, 3	5, 1, 4	0.2793
14207.1348	4, 1, 3	4, 0, 4	-0.0654

A1.3 Conclusion: In the preliminary investigations on the weakly bound complex of isoprene...argon, 10 transitions in the frequency range of 7 to 14.2GHz corresponding to the isoprene monomer were observed and assigned. Two transitions corresponding to isoprene...argon weakly bound complex were observed which could not be assigned as at the time of writing this Thesis as more and more of these transitions were required for accurate assignment of the spectrum.

A1.4 References:

1. D. R. Lide Jr, M. Jen, J. Chem. Phys., 1964, 40, 252
2. Frisch, M. J., Trucks, G. W., Schlegel, H. B., et al. Gaussian 09, revision D.01, Gaussian, Inc., Wallingford, CT, 2009.
3. K. Raghavachari, H. B. Schlegel, and J. A. Pople. J. Chem. Phys., 72 (1980) 4654-55

4. K. Raghavachari and J. A. Pople. Int. J. Quantum Chem., 20 (1981) 1067-71.

Appendix 2: Interstellar C₃S: Different Dipole Moment, Different Column Density, Same Astronomical Source

Appendix 2: Interstellar C₃S: Different Dipole Moment, Different Column Density, Same Astronomical Source

A2.1 Introduction: The early astronomical observations witnessed the detection of molecules composed of only four elements; H, C, N and O from the first two rows of the periodic table leading to the earlier conclusion that interstellar molecules are only composed of these four elements. The subsequent astronomical observations of sulphur compounds (from the 1970s) in interstellar medium (ISM) and circumstellar envelopes (CEs) serve as the main exception to this earlier conclusion. The unique astronomical detections of 19 different interstellar sulphur containing molecules, conspicuously established the prevalence of S-compound in interstellar medium and circumstellar envelopes. Table A2.1 gives a chronological list of the known S-containing molecules and their corresponding O-analogues (where available). The year 2014 was astronomically very successful with nine new interstellar molecules so far detected as compared to the yearly average of four molecules.¹⁻⁶ Of the nine molecules so far observed, two are S-containing molecules; ethyl mercaptan (CH₃CH₂SH) and C₅S.

Table A2.1: Chronological listing of interstellar S-containing molecules and their O-analogues

S-containing molecule	O-analogue
CS (1971)	CO (1970)
OCS (1971)	CO ₂ (1989)
H ₂ S (1972)	H ₂ O (1969)
H ₂ CS (1973)	H ₂ CO (1969)
SO (1973)	O ₂ (2011)
SO ₂ (1975)	<i>O₃ not observed</i>
SiS (1975)	SiO (1971)
NS (1975)	NO (1978)
CH ₃ SH (1979)	CH ₃ OH (1970)
HNCS (1979)	HNCO (1972)
HCS ⁺ (1981)	HCO ⁺ (1970)
C ₂ S (1987)	C ₂ O (1991)
C ₃ S (1987)	C ₃ O (1985)
SO ⁺ (1992)	<i>O₂⁺ not observed</i>
HSCN (2009)	HOCN (2009)
SH ⁺ (2011)	OH ⁺ (2010)
SH (2012)	OH (1963)
CH ₃ CH ₂ SH (2014)	CH ₃ CH ₂ OH (1975)
C ₅ S (2014)	<i>C₅O not observed</i>

The close relationship of the chemistry of S and O-containing molecules in ISM can easily be comprehended by the fact that of the 19 S-containing molecules observed in ISM, 16 have the corresponding O-containing molecules uniquely detected in ISM. Notwithstanding the differences which may exist in the interstellar space between the chemistry of sulphur and oxygen, a simple guideline has proven effective in searching for new sulphur containing

molecules in ISM, i.e the abundance of S-compound relative to its O-analogue is approximately equal to the cosmic S/O ratio, 1/42 as seen in methyl mercaptan, thioisocyanic acid, etc⁷⁻⁸; making the relationship between interstellar chemistry of S and O-compounds a simple game of abundance.

Astrophysical and astronomical models give insight into the heart of what is going on, unfolds the existence of phenomena and effects that would otherwise not have been known. With respect to interstellar molecules, these models help in elucidating some of the properties of the known molecules, give insight about the unknown and the ones that are highly plausible for astronomical observations. These models rely greatly on the estimated column densities (or abundances) of the known interstellar and circumstellar molecules⁹. Accurate column density depends on accurate dipole moment. Dipole moment contributes to the intensities of rotational transitions and also affects the reactivity of the molecule. The intensities of rotational transitions scale with the square of the dipole moment, the higher the dipole moment, the higher the intensity of the lines. Dipole moment determination depends on Stark effect measurement. About 80% of all the known interstellar and circumstellar molecules have been detected via their rotational transition spectra. The Fourier transform microwave spectroscopy used in determining the rotational spectra of these molecules is not commonly used in measuring Stark effect due to the unstable nature of some of the molecules generated by discharge. For charged molecules, the electric field causes a frequency shift due to acceleration or deceleration of the ion thereby making Stark effect measurement a nearly impossible task. Theoretically calculated dipole moments are well embraced in estimating the abundances of interstellar and circumstellar molecules due to the difficulty in applying external field to the discharge plasma for Stark effect measurement in the laboratory. This has been shown to be very successful with good agreement between high-level theory and experimental values (where available) indicating that the predictions for other species are likely to be very reliable.^{9,10}

C_3S , the sulphur analogue of C_3O has been experimentally and theoretically shown to be to be a linear molecule with a singlet ground state,¹¹⁻¹³. C_3S has been detected in the interstellar space by three different sets of researchers¹³⁻¹⁵, two of these astronomical observation were made from the same source (IRC+10216) while the other was made from a different source (TMC). Surprisingly, all of these groups used different values of dipole moment in estimating the column abundance of this molecule, thus resulting in different estimates for the column abundance of C_3S even from the same astronomical source in which the values are expected to be approximately same as seen in case of its oxygen analogue, C_3O , where the abundance from the same astronomical source (TMC-1) estimated by different sets of researchers is approximately same ($\approx 1*10^{12} \text{ cm}^{-2}$),^{16,17}. The inconsistent abundance estimated for interstellar C_3S has placed a constraint on the accurate estimate of C_3S abundance in ISM and CEs for application in astronomical and astrophysical models of interstellar and circumstellar molecules. This letter reports accurate theoretically calculated dipole moment for C_3S with excellent agreement with the experimentally measured value ($<\pm 0.1\text{D}$) that can be used in estimating consistent interstellar abundance for C_3S .

A2. 2 Computational details: All the calculations reported here were done using Gaussian 09 suite of programs¹⁸. Different levels of theory ranging from the less expensive to the high level quantum chemical calculation methods were employed in order to estimate accurate dipole moment, These include; the Hartree-Fock (HF), reduced Hartree-Fock (RHF)^{19,20}, three-parameter correlation functional of Lee, Yang, and Parr, (B3LYP)²¹, the second (MP2) and third (MP3) orders order Møller-Plesset perturbation methods^{22,23}, coupled cluster using single and double substitutions (CCSD)²⁴, Weizmann theory (W1U and W2U)^{25,26}, Gaussian methods (G2, G3, G4 and G4MP2)²⁷⁻²⁹, complete basis set (CBS)³⁰, and the configuration integration (CI) method with single (CIS) and double (CISD) substitutions³¹. Taking into cognizance the importance of appropriate choice of basis set, we employed the augmented Dunning's correlation consistent basis sets (pvdz, pvtz, pvqz) and the commonly used 6-31G*, 6-311G* basis sets^{32,33}. The stationary point geometries were fully optimized and confirmed by harmonic vibrational frequency calculations where equilibrium species possess no imaginary frequency.

A2. 3 Results and Discussion

Table A2.2 shows the theoretically calculated dipole moment for C₃S. The values reported in table 1 are in excellent agreement with the experimentally measured value³⁴ (3.704D) with the difference between the theoretically calculated and the experimentally measured values of less than ± 0.01 D. Other values outside this excellent agreement from other levels of theory and basis sets are reported in the supporting information.

Table A2.2: Dipole moment of C₃S from different levels of theory and basis sets.

Method	Dipole moment (in Debye)	Calc.- expt (3.704)
B3LYP/aug-cc-pvdz	3.614	-0.090
B3LYP/aug-cc-pvtz	3.733	0.029
B3LYP/aug-cc-pvqz	3.773	0.069
W1U	3.625	0.079
W2U	3.781	0.077
CI/aug-cc-pvdz	3.737	0.033

The different theoretically calculated values of different moment reported for C₃S (indicated with green) in literature, the value for from the present work (indicated with red) and the experimentally measured value (indicated with red) are depicted in FigureA2.1. From the plot, it is crystal clear that the result from the present work is in excellent agreement with the experimentally measured value as compared with other reported values in literature.

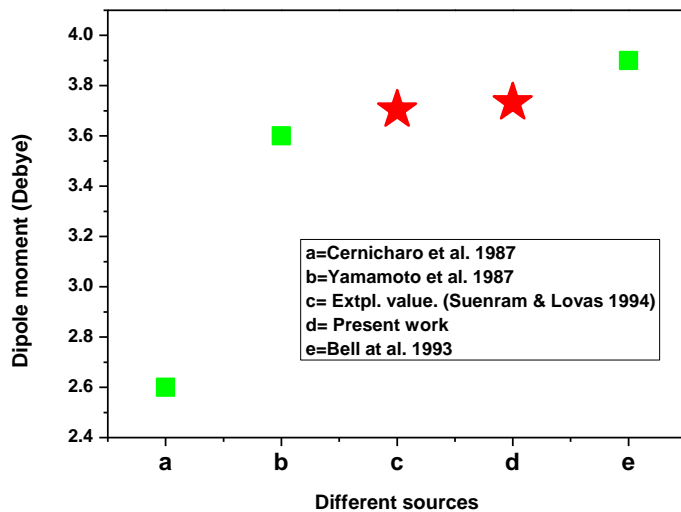


Figure A2.1: Plot of the experimental dipole moment of C₃S in comparison with theoretically calculated values.

The different values of dipole moment reported in literature for C₃S have been used in estimating the column density (abundance) of this molecule from the same and different molecular clouds/astrophysical sources. The reported abundances for interstellar C₃S are tabulated in Table 3. It is normal to expect the interstellar abundance of a molecule from the same source estimated by different groups/scientists to be same or approximately same as seen in the case of the oxygen analogue of C₃S^{16,17} but this is not observed in the reported values for the interstellar abundance of C₃S. The reason beside this is quite simple, the different groups used different values of dipole moment in estimating the column abundance of C₃S thereby resulting in different values even for the same astronomical source (IRC+10216). The values of dipole moment used in estimating the reported column density of C₃S differs from the experimental value in the range of -1.104 to 0.196D.

Table A2.3 depicts the direct link between the dipole moment of a molecule and its column density. The higher the dipole moment of a molecule, the lower its estimated column density and vice versa. Equation 1 below shows the relation used in estimating the column density of the upper state for an optically thin transition (e.g C₃S).

$$N_u = \frac{8\pi k v^2}{h c^3 A_{ul} \eta_{mb}} \int T_A dv \text{ equ. 1}$$

Where: A_{ul} = Einstein coefficient for spontaneous emission; η_{mb} = main beam efficiency of the telescope; T_A = Antenna temperature; k = Boltzmann constant; h = Planck constant; c = Speed of light and v = frequency of the transition.

Table A2.3: Column density of C₃S estimated with different dipole moment values.

Dipole moment (cal.)	Calc.-expt	Column density (in cm ⁻²)	Astronomical source
2.6D	-1.104	1.1 *10 ¹⁴	IRC+10216 ^a
3.9±0.1D	0.196	6.7*10 ¹²	IRC+10216 ^b
3.6D	-0.104	1.3±0.6*10 ¹³	TMC ^c

^aCernicharo et al. 1987; ^bBell et al. 1993; ^cYamamoto et al. 1987

The quantity, A_{ul} , depends on the *dipole moment*, angular momentum of the upper state and the frequency of the transition. Hence, inaccurate value of dipole moment has a direct effect on the final value of the column density of the molecule as seen in the case of C₃S, where three different values of dipole moment have resulted in three different values of column density for the same molecule, the astronomical source notwithstanding. The reported column abundances for C₃S place a serious constraint on the use of these values for astronomical and astrophysical models of interstellar/circumstellar molecules, because different experts could choose to use different reported column density for C₃S since there is no consensus value even for the observation from the same astronomical source, thus leading to likely misleading and non-plausible models.

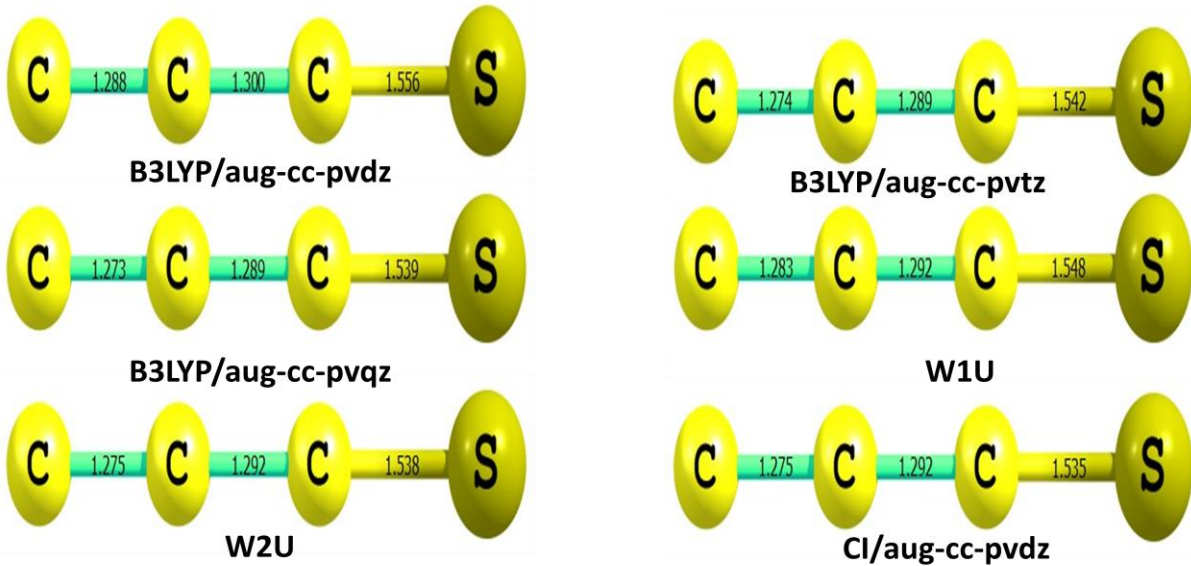


Figure A2.2: Optimized geometry of C₃S from different levels of theory and basis sets.

Figure A2.2 shows the optimized geometry of C₃S with the bond length from the different methods and basis sets that predict the dipole moment in excellent agreement with the experimental value (Table 1). C₃S has been shown to be linear from both experimental measurements and theoretical calculations¹¹⁻¹³; the methods adopted here for the accurate dipole moment determination of C₃S are in excellent agreement with this fact as all the methods also predict linear structure for C₃S. The bond lengths between the carbon atoms

(the first and second carbons; the second and the third carbons) are close to each other in all the cases suggesting a cumulated bond among the carbon atoms rather than an alternating single and triple bonds¹¹.

A2. 4.0 Conclusion: Accurate dipole moment of C₃S has been theoretically calculated with excellent agreement with the experimental value. The different values of dipole moment used in calculating the interstellar abundance of C₃S has been shown to be responsible for the different values obtained for the same molecule even in the same molecular cloud thereby placing a constraint on the use of these values in astrophysical and astronomical models. A recalculation of the column density of C₃S using accurate dipole moment reported in this study is necessary in order to provide accurate and reliable column density for this molecule for the same and different molecular clouds.

A2.5 References

1. Kolesniková, L., Tercero, B., Cernicharo, J., et al. *Astrophys J*, 2014, 784,L7
2. Belloche, A., Garrod, R. T., Müller, H. S. P., Menten, K. M. *Science*, 2014, 345,1584
3. Anderson, J. K., Ziurys, L. M. *Astrophys J*, 2014, 795,L1
4. Remijan, A. J., L. E. Snyder, L. E., B. A. McGuire, B. A., et al. *Astrophys J*, 2014, 783,77
5. Cernicharo, J., Bailleux, S., Alekseev, E., Fuente, A., et al. 2014. *Astrophys J*, 795,40
6. Agúndez, M., Cernicharo, J., Guélin, M. *Astron Astrophys*, 2014, 570,A45
7. Linke, R. A., M. A. Frerking, M. A., Thaddeus, P. *Astrophys J*, 1979, 234,L139
8. Frerking, M. A., Linke, R. A., Thaddeus, P. *Astrophys J*, 1979,234,L143
9. Müller, H. S. P. Woon, D. E. *J. Phys. Chem. A*, 2013, 117, 13868
10. Lovas, F. J., Suenram, R. D., Ogata, T., Yamamoto, S. *Astrophys J*, 1992, 399,325
11. Peeso, D. J., Ewing, D. W., Curtis, T. T. *Chem. Phys. Lett*, 1990, 166,307
12. Saito, S., Kawaguchi, K., Yamamoto, S., et al. *Astrophys J*, 1987, 317,L115
13. Yamamoto, S., Saito, S., Kawaguchi, K., Kaifu, N., Suzuki, H. *Astrophys J*, 1987, 317,L119
14. Cernicharo, J., Kahane, C., Guélin, M., Hein, H. *Astron Astrophys*, 1987, 181,L9
15. Bell, M. B., Avery, L. W., Feldman, P. A. *Astrophys J*, 1993, 417,L37
16. Brown, R. D., Godfrey, P. D., Cragg, D. M., et al. *Astrophys J*, 1985, 297,302
17. Matthews, H. E., Irvine, W. M., Friberg, P., Brown, R. D., Godfrey, P. D. *Nature*, 1984, 310,125
18. Frisch, M. J., Trucks, G. W., Schlegel, H. B., et al 2009. G09,RevC.01, Gaussian, Inc., Wallingford CT
19. Pople, J. A., Nesbet, R. K. *J. Chem. Phys.*, 1954, 22,571
20. Becke, A. D. *J Chem Phys*, 1996, 104,1040
21. Lee, C., Yang, W., Parr, R. G. *Phys. Rev. B*, 1988, 37,785
22. Head-Gordon, M., Pople, J. A., Frisch, M. J. *Chem. Phys. Lett.*, 1988, 153,503
23. Pople, J. A., Seeger, R., Krishnan, R. *Int. J. Quantum Chem.,Suppl.* 1977, Y-11, 149
24. Čížek, J. *J Chem Pjys*, 1966, 45 (11), 4256
25. Martin, J. M. L, de Oliveira, G. *J Chem Phys.*, 1999, 111, 1843
26. Parthiban, S Martin, J. M. L. 2001. *JChPh*, 114, 6014
27. Curtiss, L. A.,Raghavachari, K., Redfern, P. C., Rassolov, V., Pople, J. A. *J Chem Phys* ,1998, 109, 7764
28. Curtiss, L. A., Redfern, P. C., Raghavachari, K. *J Chem Phys*, 2007, 126, 084108
29. Curtiss, L. A., Redfern, P. C., Raghavachari, K. *J Chem Phys*, 2007, 127, 124105
30. Petersson, G. A., Bennett, A., Tensfeldt, T. G., et al. *J Chem Phys* , 1988, 89,2193
31. Foresman, J. B., Head-Gordon, M., Pople, J. A., Frisch, M. J. *J Chem Phys*, 1992,96,135
32. Dunning Jr., T. H. *J Chem Phys*, 1989, 90,1007
33. Ditchfield, R, Hehre, W.J, Pople, J. A. *J Chem Phys* , 1971, 54 (2), 724
33. Suenram, R. D., Lovas, F. J. *Astrophys J*,1994, 429,L89

A2.6 Supporting Information: The dipole moments calculated for C₃S from all the methods employed in this study are shown below (Table A2.4). The values that are in excellent agreement with the experimental value are indicated with red; these values are presented and discussed in Table 2.

Table A2.4: Dipole moment of C₃S from different levels of theory and basis sets.

Method	Dipole moment	Calc.- expt (3.704)
HF/6-31G*	2.645	-1.059
HF/6-311G*	3.128	-0.576
HF/aug-cc-pvdz	3.189	-0.515
HF/aug-cc-pvtz	3.356	-0.348
HF/aug-cc-pvqz	2.818	-0.886
RHF/6-31G*	2.645	-1.059
RHF/6-311G*	3.128	-0.576
B3LYP/6-31G*	3.042	-0.662
B3LYP/6-311G*	3.497	-0.207
B3LYP/aug-cc-pvdz	3.614	-0.090
B3LYP/aug-cc-pvtz	3.733	0.029
B3LYP/aug-cc-pvqz	3.773	0.069
MP2/6-31G*	2.451	-1.253
MP2/6-311G*	2.911	-0.793
MP2/aug-cc-pvdz	2.888	-0.816
MP2/aug-cc-pvtz	3.089	-0.624
MP3/6-31G*	2.611	-1.093
MP3/6-311G*	3.092	-0.612
MP3/aug-cc-pvdz	3.970	0.266
CCSD/6-31G*	3.530	-0.174
CCSD/6-311G*	4.046	0.342
CCSD/aug-cc-pvdz	3.907	0.203
WIU	3.625	0.079
W2U	3.781	0.077
G2	2.412	-1.292
G3	2.412	-1.292
G4MP2	3.214	-0.490
G4	3.214	-0.490
CBS-QB3	3.551	-0.153
CI/6-31G*	3.299	-0.405
CI/6-311G*	3.317	-0.387
CI/aug-cc-pvdz	3.737	0.033
CIS/6-31G*	1.814	-1.89
CIS/aug-cc-pvdz	2.267	-1.437
CISD/6-31G*	3.314	-0.39
CISD/6-311G*	3.831	0.127